

Catalogue of chiral phonon materials

Yue Yang,^{1, 2,*} Zhenyu Xiao,^{3,*} Yu Mao,^{1, 2,*} Zhanghuan Li,⁴ Zhenyang Wang,⁵ Tianqi Deng,^{6, 7}
Yanhao Tang,^{2, 8} Zhi-Da Song,³ Yuan Li,⁴ Huiqiu Yuan,^{1, 2} Ming Shi,^{1, 2} and Yuanfeng Xu^{1, 2, †}

¹*Center for Correlated Matter, Zhejiang University, Hangzhou 310027, China*

²*School of Physics, Zhejiang University, Hangzhou 310027, China*

³*International Center for Quantum Materials,*

School of Physics, Peking University, Beijing 100871, China

⁴*Beijing National Laboratory for Condensed Matter Physics,*

Institute of Physics, Chinese Academy of Sciences, Beijing, China

⁵*College of Computer Science and Technology, Zhejiang University, Hangzhou, China*

⁶*State Key Laboratory of Silicon and Advanced Semiconductor Materials,*

School of Materials Science and Engineering,

Zhejiang University, Hangzhou 310027, China

⁷*Key Laboratory of Power Semiconductor Materials and Devices of Zhejiang Province,
Institute of Advanced Semiconductors, ZJU-Hangzhou Global Scientific and Technological Innovation Center,
Zhejiang University, Hangzhou 311200, China*

⁸*Zhejiang Key Laboratory of Micro-Nano Quantum Chips and Quantum Control,
Zhejiang University, Hangzhou 310027, China*

Chiral phonons—circularly polarized lattice vibrations carrying intrinsic angular momentum—offer unprecedented opportunities for controlling heat flow, manipulating quantum states through spin-phonon coupling, and realizing exotic transport phenomena. Despite their fundamental importance, a universal framework for identifying and classifying these elusive excitations has remained out of reach. Here, we address this challenge by establishing a comprehensive symmetry-based theory that systematically classifies the helicity and the velocity–angular momentum tensor underlying phonon magnetization in thermal transport across all 230 crystallographic space groups. Our approach, grounded in fundamental representations of phononic angular momentum, reveals three distinct classes of crystals: achiral crystals with vanishing angular momentum, chiral crystals with *s*-wave helicity, and achiral crystals exhibiting higher-order helicity patterns beyond the *s*-wave. By performing high-throughput computations and symmetry analysis of the dynamical matrices for 11,614 crystalline compounds, we identified 2,738 materials exhibiting chiral phonon modes and shortlisted the 170 most promising candidates for future experimental investigation. These results are compiled into an open-access [Chiral Phonon Materials Database](#) website, enabling rapid screening for materials with desired chiral phonon properties. Our theoretical framework transcends phonons—it provides a universal paradigm for classifying chiral excitations in crystalline lattices, from magnons to electronic quasiparticles.

I. INTRODUCTION

Chirality, a fundamental property that prevents an object from superimposing on its mirror image[1], pervades nature, from the double helix of DNA[2] to the stereoselectivity in asymmetric catalysis[3, 4] and the topologically protected edge states in quantum Hall systems[5, 6]. In recent years, the chirality of phonons has emerged as a frontier in condensed matter physics due to its profound implications for spintronics, valleytronics, thermal management, and phononic engineering. Chiral phonons[7–12], analogous to circularly polarized electromagnetic waves, manifest themselves as circularly polarized vibrational modes carrying intrinsic angular momentum. In crystalline materials, a chiral phonon with finite

lattice momentum is characterized by its helicity, defined as the scalar product of the unit vector along the lattice momentum and phonon angular momentum. A phonon exhibits positive helicity if its angular momentum aligns with the momentum direction, and negative helicity if they are anti-aligned. See the Supplementary Information (SI) A for definitions of phonon angular momentum and helicity. This chirality not only governs the dynamic coupling between phonons and other quasiparticles (e.g., electron, photon, or magnon) but also dictates selection rules in scattering processes, potentially enabling novel phenomena such as the Einstein-de Haas effect[7, 13–16], spin Seebeck effect[17–22], chiral-induced spin selectivity effect [23–26], thermal Hall effect[27–29], and phononic magnetism[30–37].

Chirality and symmetry are intrinsically interrelated properties in physical systems. In crystalline solids, the geometric chirality of a crystal is determined by its space group: a crystal is chiral if

* These authors contributed equally

† y.xu@zju.edu.cn

its space group lacks any improper rotation operations (i.e., inversion or rotoinversion), whereas an achiral crystal possesses at least one such operation. Within three-dimensional (3D) space, the crystalline structures are classified into 65 chiral space groups (SGs) and 165 achiral SGs. In an achiral crystal, the atomic displacements associated with a phonon mode exhibiting a nontrivial improper-rotation eigenvalue (i.e., an eigenvalue distinct from that corresponding to the identity) can locally break the achiral symmetry, inducing a transient chiral distortion[38]. This symmetry-breaking can be initiated through interactions with photons, magnons, or comparable excitations. In contrast, in a chiral crystal, every phonon mode is inherently chiral, as its dynamic lattice vibrations typically further reduce, or at minimum maintain, the already diminished symmetry present in the structure.

Despite a decade of theoretical predictions and experimental investigations of chiral phonon materials[8, 9, 15, 39–47], they remain exceptionally rare compared to the vast repository of crystalline materials catalogued in structural databases. This scarcity has substantially impeded both fundamental research and practical applications in the field of chiral-phonon materials. Consequently, there exists an urgent need to establish a comprehensive classification methodology for chiral phonon materials and to conduct systematic, high-throughput computational searches to identify promising candidates.

In the present work, we address these challenges by developing a rigorous symmetry-based classification of chiral phonon materials that encompass all 230 space groups, elucidating the precise group-theoretical constraints that govern the emergence and characteristics of chiral phonons. We subsequently implement a high-throughput computational workflow — integrating precomputed and newly generated *ab initio* phonon data — to systematically catalogue chiral phonon materials across 11,614 crystalline compounds. Our results not only establish the theoretical foundations for chiral phonon phenomena but also provide an accessible database of candidate materials with detailed phonon-chirality characterizations, paving the way for future experimental validation and applications.

II. CLASSIFICATION METHODS

In this section, we systematically classify phononic chirality across all 230 space groups by analyzing the symmetry representations of phonon angular momentum, which uniquely characterize circularly polarized lattice vibrations in reciprocal space. We subsequently derive the symmetry representations of

phonon helicity, relevant to Raman scattering experiments, as well as the velocity–angular-momentum tensor that underlies phonon magnetism in thermal transport. The main results are summarized in Fig. 1, with detailed discussions below.

We first investigate the symmetry properties of the phonon angular momentum $\mathbf{J}^{ph}(\mathbf{q})$ in the momentum space. Under inversion symmetry (\mathcal{P}), \mathbf{q} reverses its direction, while \mathbf{J}^{ph} is invariant. In contrast, under time-reversal symmetry (TRS, \mathcal{T}), both \mathbf{q} and \mathbf{J}^{ph} reverse directions. Therefore, in non-magnetic materials with inversion symmetry, the operation \mathcal{PT} requires $\mathbf{J}^{ph}(\mathbf{q}) = -\mathbf{J}^{ph}(\mathbf{q})$, thus $\mathbf{J}^{ph}(\mathbf{q})$ must vanish for any \mathbf{q} [11, 48]. Let G be the point group of the space group \mathcal{G} without inversion \mathcal{P} . In such groups, $\mathbf{J}^{ph}(\mathbf{q})$ is generally non-zero for a generic \mathbf{q} . A proper (improper) spatial rotation \mathcal{R} with $\det(\mathcal{R}) = 1$ (-1) in G requires that

$$\mathbf{J}^{ph}(\mathcal{R}\mathbf{q}) = \det(\mathcal{R})\mathcal{R}\mathbf{J}^{ph}(\mathbf{q}). \quad (1)$$

In addition, TRS requires that $\mathbf{J}^{ph}(\mathbf{q}) = -\mathbf{J}^{ph}(-\mathbf{q})$. Thus, the point group G of a space group does not completely capture the symmetry of $\mathbf{J}^{ph}(\mathbf{q})$ in momentum space. The symmetry should be characterized by $G \times C_i$, where the inversion group C_i in the momentum space is generated by TRS.

For a given \mathbf{q} , the operations in $G \times C_i$ that remain momentum \mathbf{q} invariant up to a translation by a reciprocal lattice vector constitute its little point group $G_{\mathbf{q}}$. Notably, $G_{\mathbf{q}}$ should be isomorphic to the little magnetic group of the associated gray group (i.e., type-II magnetic space group) of the space group \mathcal{G} because of additional TRS. The angular momentum $\mathbf{J}^{ph}(\mathbf{q})$ at \mathbf{q} forms a 3D real representation $\gamma_{G_{\mathbf{q}}}$ of $G_{\mathbf{q}}$, which can be decomposed to a direct sum of irreducible representations (irreps). Refer to SI B for the decompositions. If trivial irreps (i.e., identity representations) appear in the decomposition, the corresponding components of \mathbf{J}^{ph} can be non-zero. Conversely, components associated with non-trivial irreps must vanish.

Next, we investigate the symmetry of helicity h , defined as $h(\mathbf{q}) = \mathbf{e}_q \cdot \mathbf{J}^{ph}(\mathbf{q})$ with \mathbf{e}_q being the unit vector along the wave vector \mathbf{q} . As a product between a polar vector and a pseudovector, h is a pseudoscalar: $h(\mathcal{R}\mathbf{q}) = \det(\mathcal{R})h(\mathbf{q})$ for a rotation \mathcal{R} in G . In addition, h is invariant under TRS: $h(\mathbf{q}) = h(-\mathbf{q})$. Similar to \mathbf{J}^{ph} , if inversion exists in G (referred to as type-I point group), \mathcal{PT} symmetry requires $h(\mathbf{q}) = 0$ for any \mathbf{q} . If there is no improper rotation or inversion in G (referred to as type-II point group), $h(\mathbf{q})$ is invariant under all operations in G , as well as TRS: $h(\mathbf{q})$ forms an *s*-wave-type pattern in the Brillouin zone (BZ). By contrast, if improper rotation exists but inversion

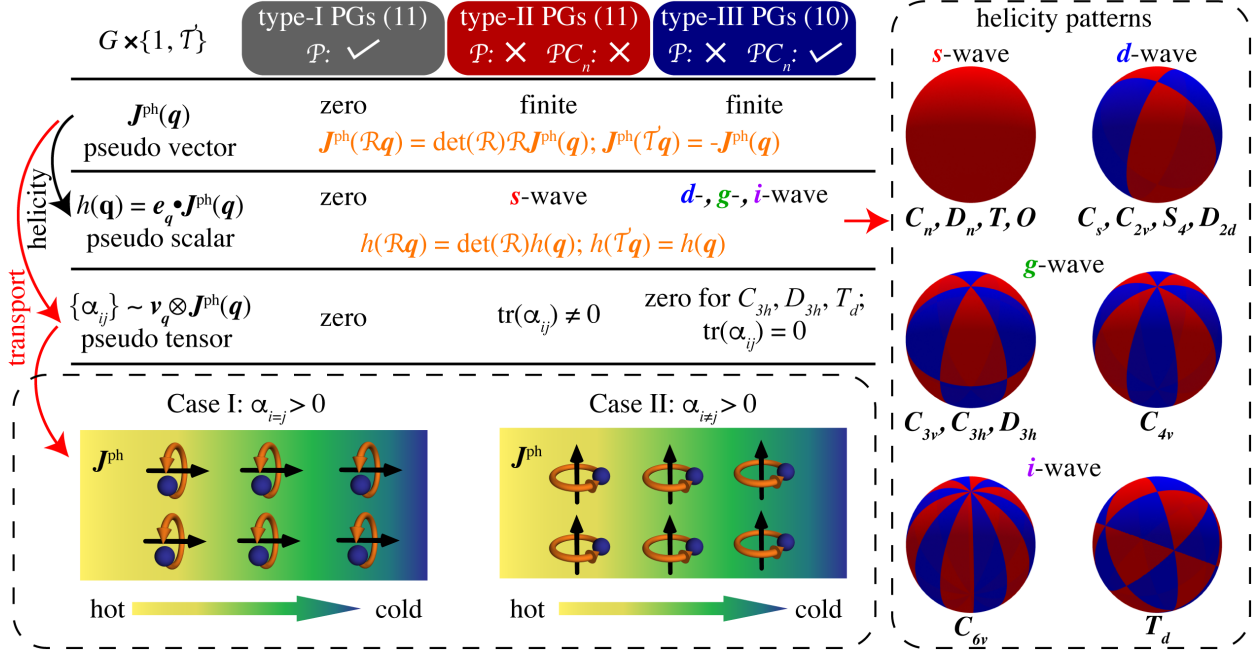


FIG. 1. Summary of the classifications. The 32 PGs (G) of the 230 space groups are categorized into three types: 11 type-I PGs with inversion (\mathcal{P}), 11 type-II PGs lacking \mathcal{P} or any roto-inversion (\mathcal{PC}_n), and 10 type-III PGs without \mathcal{P} but with \mathcal{PC}_n). For each type, we derive symmetry constraints on the phonon angular momentum \mathbf{J}^{ph} , helicity (h), and the velocity-angular momentum tensor ($\mathbf{v} \otimes \mathbf{J}^{ph}$) that determines the phonon magnetization response in thermal transport (α), all based on their transformation properties under point group operations (\mathcal{R}) and time-reversal symmetry (T). Right panel: Helicity patterns around the Brillouin zone center for type-II and type-III PGs. Red and blue regions signify helicity of opposite sign. The polynomials that characterize these helicity patterns are tabulated in SI B. Bottom panel: Schematics of two symmetry-allowed chiral-phonon transport responses. $\alpha_{i=j} > 0$ ($\alpha_{i \neq j} > 0$) carries phonon angular momentum parallel (perpendicular) to the thermal gradient.

is absent (referred to as type-III point group), $h(\mathbf{q})$ should form an alternating pattern (see Fig. 1). The pattern can be *d*-, *g*-, or *i*-wave-like, depending on the symmetry. Helicity can be alternatively defined as $h' = \mathbf{v} \cdot \mathbf{J}^{ph}$ with $\mathbf{v} = \nabla\omega(\mathbf{q})$ being the group velocity of a phonon. Since \mathbf{v} transforms in the same manner as \mathbf{q} under generic operations, h' should exhibit the same symmetry and a similar pattern in the BZ as h .

Finally, we consider the symmetry of the pseudotensor $\mathbf{v} \otimes \mathbf{J}^{ph}$, which governs the temperature-gradient-induced phonon magnetization, $\mathbf{M}_i = \alpha_{ij}\partial_j T$, where $\partial_j T$ is the temperature gradient along the j -th direction and \mathbf{M}_i is magnetization along the i -direction. Within Boltzmann transport theory, the response tensor α_{ij} is proportional to $\sum_p \int \mathbf{J}_i^{ph} \mathbf{v}_j \partial f_B(\omega_p(\mathbf{q})/T) / \partial T d\mathbf{q}$ with p being the phonon band index and $f_B(\cdot)$ being the Bose-Einstein distribution [15, 16]. The nine components of α_{ij} furnish the same symmetry representation as the tensor $\mathbf{v} \otimes \mathbf{J}^{ph}$ at $\mathbf{q} = 0$. Any trivial irrep in its decomposition therefore corresponds to a symmetry-allowed (potentially nonzero) component or a linear

combination of α_{ij} . In all type-I point groups, \mathcal{PT} symmetry forces $\alpha_{ij} = 0$. Among the 21 type-II and type-III point groups, 18 admit at least one trivial irrep and thus support nonzero components of α_{ij} . The three exceptions are C_{3h} , D_{3h} , and T_d , which lack any trivial irrep. See SI B for the full decomposition of the representation of $\mathbf{v} \otimes \mathbf{J}^{ph}$. Moreover, in type-II groups the trace $h' = \text{Tr}(\mathbf{v} \otimes \mathbf{J}^{ph})$ is itself a trivial irrep, guaranteeing at least one nonzero diagonal entry of α . In contrast, for type-III groups, h' transforms as a nontrivial irrep, so all diagonal components of α vanish in the principal-axis frame.

III. HIGH-THROUGHPUT CALCULATIONS

A. Workflow

Using the classification methods outlined above, we performed a high-throughput screening, combined with *ab initio* calculations, to discover chiral phonon materials. The workflow comprises three

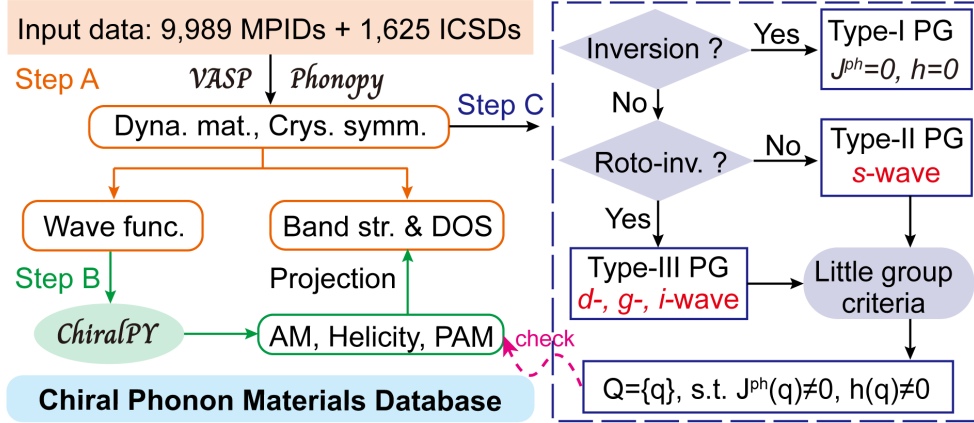


FIG. 2. Workflow of high-throughput calculations and classifications. Dynamical matrices for 9,989 MPID and 1,625 ICSD material entries are obtained from *ab initio* calculations using VASP package [49]. Step A: Crystal symmetry, phonon band structures, density of states, and phonon wave functions are analyzed with *Phonopy* [50]. Step B: Phonon angular momentum (AM), helicity, and pseudo angular momentum (PAM) are calculated using the in-house code *ChiralPY*. Step C: Materials are classified into three categories based on the symmetry analysis from step A—achiral phonons with zero angular momentum (with inversion), chiral phonons with *s*-wave helicity patterns (without inversion or roto-inversion), and chiral phonons with *d*-, *g*-, or *i*-wave helicity patterns (without inversion but with roto-inversion). All the materials’ phonon data were collected to build the *Chiral Phonon Materials Database*.

main steps.

In step A, we assembled two input sets: 9,989 materials (MPIDs) from the *Topological Phonon Database* (TPDB)[51] and 1,625 ICSD entries from the *Topological Materials Database* (TMDB)[52–54]. For the materials in TPDB, the force constants were precomputed and archived in the *Phonondb data on MDR at NIMS*, obviating new *ab initio* work. In contrast, although TMDB catalogues tens of thousands of compounds by electronic topology, it lacks phonon data. We therefore selected 1,625 material entries with fewer than ten atoms per unit cell and performed high-throughput *ab initio* calculations to obtain their force constant matrices. For each compound, we extracted the dynamical matrix, the phonon band structure along high-symmetry paths in the BZ, the phonon density of states, and the corresponding vibrational eigenmodes (*i.e.*, phonon wave functions).

In step B, we developed an in-house code named *ChiralPY* to compute the phonon angular momentum $\mathbf{J}^{ph} = (j_x, j_y, j_z)$, the helicity h , and the pseudo angular momentum (PAM) [8, 11, 46, 55]. PAM is instrumental in characterizing the phase factor that a wave function acquires under (screw-) rotations and is crucial in electron-photon-phonon interactions, where both energy and angular momentum must be conserved [8, 11, 46, 55]. See further computational details on PAM in SI A. Feeding the vibrational eigenmodes from Step A into *ChiralPY*, we then projected \mathbf{J}^{ph} , h , and PAM onto the phonon band structures.

In step C, we perform a symmetry analysis on each material and classified its phonon band structure into three categories based on the methods in Sec. II. Materials with inversion symmetry are described by type-I point groups. In such materials, \mathcal{PT} symmetry enforces zero phonon angular momentum at any momenta, rendering all phonons achiral. If the crystals lack both inversion and roto-inversion symmetry, they fall under a type-II point group, generally allowing nonzero phonon angular momentum at generic momenta—except at the eight TRIM points—while the phonon helicity pattern on the isoenergy surface displays an *s*-wave-like character. The remaining materials lack inversion symmetry but include roto-inversion symmetry, belonging to type-III point groups. Their phonon band structure can be further distinguished as having *d*-, *g*-, or *i*-wave-like helicity pattern. In addition, we cross-checked these symmetry-based classifications against the angular-momentum, helicity, and PAM obtained numerically in Step B to verify consistency with the enforced symmetry constraints.

In polar crystals, we incorporated non-analytical corrections into the dynamical matrix, which gives rise to the characteristic longitudinal-optical versus transverse-optical (LO–TO) mode splitting as $\mathbf{q} \rightarrow \mathbf{0}$ [56]. For an in-depth *ab initio* treatment of these corrections and their implementation, see SI C.

B. Results and statistics

Using the classification method and high-throughput computational framework above, we performed a comprehensive survey of phonon chirality across 11,614 phonon datasets sourced from TPDB (9,989 MPID entries) and TMDB (1,625 ICSD entries). This extensive dataset enables, for the first time, a statistically robust and systematic mapping of chiral phonon activity throughout the landscape of crystal materials. The results yield several notable and foundational insights.

As shown in Fig. 3(a)–(b), our analysis reveals that 8,876 materials (76.43%) exhibit type-I (achiral) phonon spectra with zero phonon angular momentum and helicity at all wavevectors. In sharp contrast, 869 materials (7.48%) are hosted in type-II PGs, which possess only proper rotational symmetries. They display phonon bands that robustly support non-zero angular momentum and *s*-wave helicity patterns throughout much of the BZ, except at the eight TRIM points. An additional 1,869 materials (16.09%) emerge as type-III candidates, combining the absence of inversion with the presence of at least one improper rotation. Notably, these support more intricate chiral phonon textures, giving rise to higher-harmonic helicity patterns—classified here as 1,030 (8.87%) *d*-wave, 463 (3.98%) *g*-wave, and 376 (3.24%) *i*-wave according to the underlying point-group symmetry. For the complete list of chiral phonon materials in type-II and type-III point groups, see SI E. The relative scarcity of chiral (type-II/III) versus achiral (type-I) phonon materials quantitatively demonstrates the strong crystallographic constraints imposed by improper symmetry operations. Our finding also highlights how even subtle deviations from inversion symmetry can unlock entirely new vibrational physics. Importantly, the systematic enumeration establishes a lower bound on the prevalence of chiral phonons in known solid-state materials, underscoring a rich but previously underexplored realm for future research.

Despite differences in the two source databases (TPDB and TMDB), both manifest qualitatively similar statistical trends across the three phonon chirality classes and within type-III subtypes (see Fig. 3(c)–(d)). In TMDB entries, where full phonon spectra are not always available, our symmetry-based analysis nevertheless predicts similar proportions of achiral, *s*-, *d*-, *g*- and *i*-wave chiral phonon materials. This invariance confirms that the encoded phonon chirality is a structural property fundamentally dictated by space-group symmetry—inviting further studies to generalize these predictions to other crystal repositories and synthetic targets.

To maximize the utility of this resource, all com-

puted data—including phonon dispersions, mode-resolved angular momentum and helicity projections, symmetry classifications, and crystallographic information—have been made publicly accessible via the [Chiral Phonon Materials Database \(CPMDB\)](#) developed for this work. Refer to SI D for details about [CPMDB](#). The database’s property-driven search and filtering capabilities empower the community to identify materials matching desired symmetry, chemical, or phononic criteria, accelerating targeted synthesis, characterization, and application efforts. We also highlight 170 compounds with remarkable chiral phonon bands and provide detailed angular momentum and helicity analysis in SI F. With stable crystal structures and simple formulas, these materials are the most promising candidates for future experimental studies.

IV. PROTOTYPE MATERIAL EXAMPLES

To exemplify the diverse chiral phonon behaviors revealed through the high-throughput screening, we showcase four prototypical materials from [CPMDB](#) representing distinct classes of phonon helicity patterns, including LiAlO_2 [mp-3427, SG 92 ($P4_12_12$)] with *s*-wave helicity, AgClO_4 [mp-22993, SG 121 ($I\bar{4}2m$)] with *d*-wave helicity, NaSrP [mp-13275, SG 189 ($P\bar{6}2m$)] with *g*-wave helicity, and ZnSe [mp-380, SG 186 ($P6_3mc$)] with *i*-wave helicity. The phonon band structures for these selected materials, with bands colored by phonon helicity, are shown in Fig. 4(a)–(d). For each prototype material, we calculated its isoenergy surfaces and helicity distributions near the Γ point (Fig. 4(e)–(h)) within a ± 0.2 meV window centered on the energy level indicated in the band structures. These isoenergy surfaces provide a 3D visualization of the helicity patterns and confirm the theoretical predictions outlined in Fig. 1. In LiAlO_2 , the isoenergy surface displays uniform helicity coloring under the PG D_4 , consistent with the *s*-wave pattern. In contrast, AgClO_4 shows four distinct regions of alternating helicity under the PG D_{2h} , confirming its *d*-wave character. NaSrP exhibits a six-fold alternating pattern characteristic of *g*-wave helicity under PG D_{3h} , while ZnSe displays the most complex helicity texture with multiple sign changes consistent with the *i*-wave behavior under PG C_{6v} .

These four prototypes span part of the symmetry-enforced helicity patterns and demonstrate how space-group constraints translate into distinct chiral-phonon textures. These quantitative helicity amplitudes and anisotropies offer concrete targets for polarized Raman, neutron, and ultrafast optical pump-probe experiments.

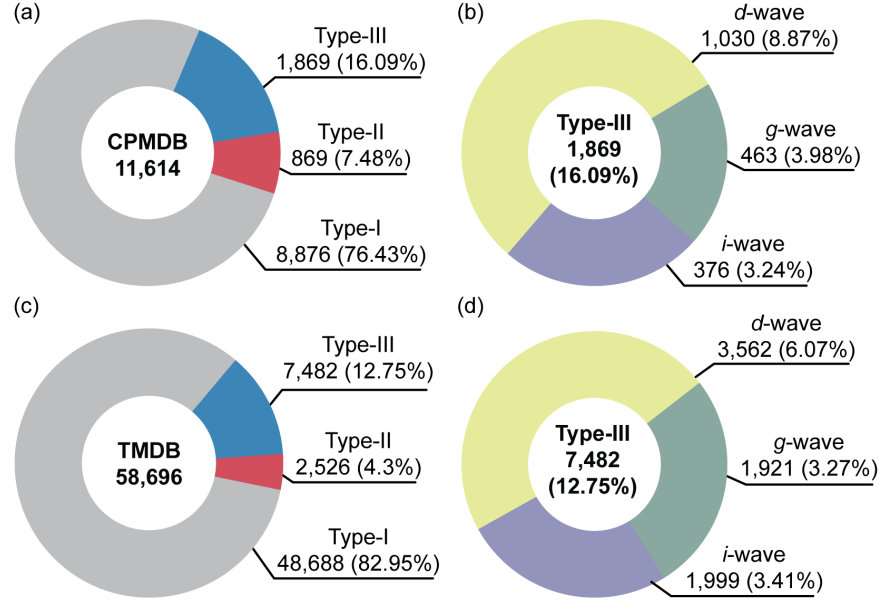


FIG. 3. Statistical overview of chiral phonon materials in the high-throughput classification. (a) Pie chart showing the percentage distribution of all 11,614 surveyed materials in the CPMDB across the three phonon chirality types: type-I (achiral, 76.43%), type-II (s-wave, 7.48%), and type-III (16.09%). (a) Distribution of the 11,614 crystalline compounds classified into type-I (achiral), type-II (s-wave) and type-III chiral phonon categories. (b) Breakdown of the type-III subset into *d*-wave, *g*-wave and *i*-wave helicity patterns, with corresponding material counts and percentages. (c) and (d) are similar with the statistics in (a) and (b), respectively, but for the 58,696 materials in TMDB.

V. DISCUSSIONS

This comprehensive catalogue establishes a robust statistical foundation for chiral phonon materials. By mapping crystallographic point groups to allowed phonon angular momentum textures, we demonstrate that chiral phonons are surprisingly prevalent - they occur in approximately 24% of the 11,614 surveyed crystalline materials. This includes 7.5% exhibiting type-II (s-wave) chirality and 16.1% displaying type-III behavior with complex *d*-, *g*- or *i*-wave helicity patterns. We predict 170 promising candidates across diverse chemistries, from insulators to metals, dramatically expanding the scope of experimental exploration beyond current investigations. Our symmetry-based classification enables chirality predictions without exhaustive phonon calculations, transforming material discovery from an exploratory pursuit to a systematic endeavor. This framework extends naturally to magnetic systems, where spin-phonon coupling breaks time-reversal

symmetry[57–59]. Here, chiral phonons may exhibit odd-parity helicity patterns (e.g., *p*-, *f*-, or *h*-wave), opening entirely new classes of phononic phenomena. Although the catalogue provides an extensive resource, experimental verification remains crucial. Future experiments should focus on direct observation of phonon angular momentum through advanced techniques such as time-resolved Raman spectroscopy, neutron scattering with polarization analysis, and ultrafast phonon interferometry. Such studies would validate our predictions and quantify the magnitude of phonon circular dichroism in these materials.

ACKNOWLEDGMENTS

We thank Tiantian Zhang, Lifa Zhang, Qian Niu, and Xi Dai for the helpful discussion. Funding: This work was supported by the Fundamental Research Funds for the Central Universities (grant no. 226-2024-00200) and the National Natural Science Foundation of China (General Program no. 12374163).

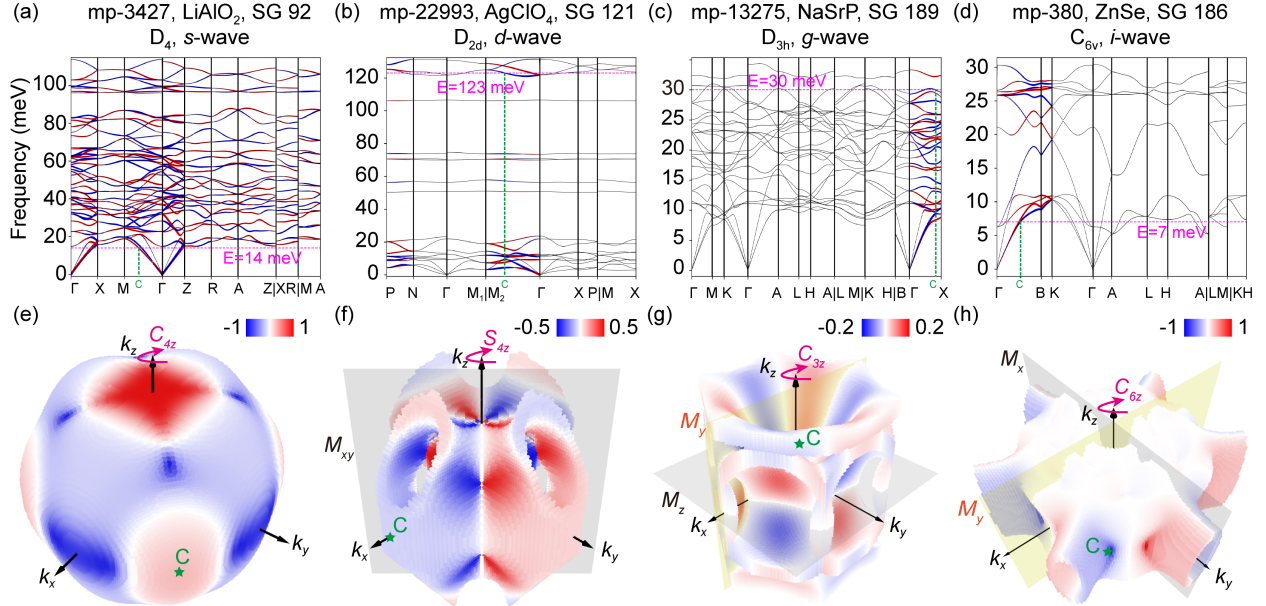


FIG. 4. Phonon band structures and isoenergy surface with helicity projections for four prototypical materials. (a) LiAlO₂ crystallizes in the tetragonal chiral space group (SG) 92 (type-II PG D_4), which contains only proper rotations and lacks both inversion and roto-inversion symmetry. This results in an *s*-wave helicity pattern throughout the Brillouin zone, as shown in (e). (b) AgClO₄ adopts SG 121 (type-III PG D_{2d}), which includes roto-inversion symmetries S_{4z} and M_{xy} but no inversion, leading to a *d*-wave helicity pattern characterized by alternating sign regions enforced by symmetry, seen in the helicity-projected isoenergy surface (f). (c) NaSrP, adopting SG 189, exhibits a type-III PG (D_{3h}) that support a *g*-wave helicity pattern (g). This nontrivial pattern results from the discrete three-fold rotation (C_{3z}) and mirror reflections (M_y and M_z). (d) ZnSe (SG 186; type-III PG C_{6v}) combines six-fold rotation C_{6z} and mirror symmetries (M_x and M_y) to produce an *i*-wave helicity pattern (h), featuring a twelve-fold alternation of sign within the Brillouin zone. The energy of each surface in panels (e)–(h) corresponds to the purple dashed line in panels (a)–(d), respectively. In panels (a)–(d), helicity projection is represented by red (positive) and blue (negative) dots, with dot size proportional to helicity amplitude. The reference point *C* in each isoenergy surface is marked with a green star in panels (e)–(h) and labeled by a green vertical line in panels (a)–(d).

Supplementary Information for "Catalogue of chiral phonon materials"

CONTENTS

I. Introduction	1
II. Classification methods	2
III. High-throughput calculations	3
A. Workflow	3
B. Results and statistics	5
IV. Prototype material examples	5
V. Discussions	6
Acknowledgments	6
A. Concepts and definitions	9
I. Phonon frequencies and lattice vibration modes	9
II. Phonon angular momentum	9
III. Pesudo angular momentum	10
a. Symmetry eigenvalues of phonon modes	10
b. Rotational symmetries, and the pseudo angular momentum	11
B. Representation theory of chiral phonons	11
a. Representations of phonon angular momentum and helicity	11
b. Representations of velocity-angular momentum tensor	15
C. Density functional theory calculations	17
I. Non-analytical correction to the dynamical matrix	17
D. Introduction of the chiral phonon materials database	18
E. List of chiral phonon materials	20
F. Ideal chiral phonon materials	67
References	161

These supplementary appendices detail our methodology and high-throughput results. Section A defines fundamental chiral-phonon concepts, while section B presents their representation theory. Section C describes the *ab initio* methods employed. Section D introduces our open-access database, [Chiral Phonon Materials Database](#). Section E lists all chiral-phonon materials in type-II and type-III point groups, and section F tabulates ideal candidates along with their phonon band structures projected onto angular momentum, helicity, and pseudo-angular momentum.

Appendix A: Concepts and definitions

I. Phonon frequencies and lattice vibration modes

Given a crystalline material, its force constant matrix is defined as the second-order derivative of the total energy with respect to the atomic displacements [56],

$$\mathcal{F}_{\alpha\mu,\beta\nu}(\mathbf{R} - \mathbf{R}') = \frac{\partial^2 E}{\partial u_{\alpha\mu}(\mathbf{R}) \partial u_{\beta\nu}(\mathbf{R}')} |_{u=0} \quad (\text{A1})$$

where \mathbf{R} and \mathbf{R}' represent translations of the Bravais lattice and $u_{\alpha\mu}(\mathbf{R})$ ($u_{\beta\nu}(\mathbf{R}')$) refers to the atomic displacement of the atom labelled as μ (ν) in the unit cell \mathbf{R} (\mathbf{R}') along the α (β) direction, where $\alpha, \beta = x, y, z$. The dynamical matrix is the mass-reduced discrete Fourier transform of the force constant matrix,

$$\mathcal{D}_{\alpha\mu,\beta\nu}(\mathbf{q}) = \frac{1}{N_R \sqrt{M_\mu M_\nu}} \sum_{\mathbf{R}} e^{i\mathbf{q}\cdot\mathbf{R}} \mathcal{F}_{\alpha\mu,\beta\nu}(\mathbf{R}) \quad (\text{A2})$$

where M_μ is the mass of atom μ and whose basis is defined as

$$|u_{\alpha\mu}(\mathbf{q})\rangle = \frac{1}{\sqrt{N_R}} \sum_{\mathbf{R}} e^{-i\mathbf{q}\cdot\mathbf{R}} |u_{\alpha\mu}(\mathbf{R})\rangle = \frac{1}{\sqrt{N_R}} \sum_{\mathbf{R}} e^{-i\mathbf{q}\cdot\mathbf{R}} |u_\alpha(\mathbf{R} + \tau_\mu)\rangle, \quad (\text{A3})$$

and τ_μ is the position of atom μ in the unit cell \mathbf{R} .

For a given \mathbf{q} , the eigenvalues of the dynamical matrix $\mathcal{D}(\mathbf{q})$ give the squares of phonon frequencies $\omega_n^2(\mathbf{q})$ ($n = 1, 2, \dots, 3N$ with N being the number of atoms in one unit cell),

$$\mathcal{D}(\mathbf{q}) |\phi_n^\mathbf{q}\rangle = \omega_n^2(\mathbf{q}) |\phi_n^\mathbf{q}\rangle \quad (\text{A4})$$

Since the dynamical matrix $\mathcal{D}(\mathbf{q})$ is Hermitian, the eigenvalues $\{\omega_n^2(\mathbf{q})\}$ are real. The eigenvector $|\phi_n^\mathbf{q}\rangle = \sum_{\alpha\mu} C_n^{\alpha\mu} |u_{\alpha\mu}(\mathbf{q})\rangle$ characterizes the lattice vibrational mode of frequency $\omega_n(\mathbf{q})$ at \mathbf{q} .

Using the force constant matrices obtained from DFT calculations, the eigenvalue problem in Eq. A4 can be solved with the *phonopy* package [50]. In the high-throughput calculations, we have also computed the phonon band structure along high-symmetry paths and density of states for each material entry.

II. Phonon angular momentum

In general, the (real) Bloch basis defined in Eq. A3 can be converted to a complex basis by the following unitary transformation:

$$|R_{\gamma\mu}(\mathbf{q})\rangle = \frac{\epsilon_{\alpha\beta\gamma}}{\sqrt{2}} (|u_{\alpha\mu}(\mathbf{q})\rangle + i|u_{\beta\mu}(\mathbf{q})\rangle), \quad (\text{A5})$$

$$|L_{\gamma\mu}(\mathbf{q})\rangle = \frac{\epsilon_{\alpha\beta\gamma}}{\sqrt{2}} (|u_{\alpha\mu}(\mathbf{q})\rangle - i|u_{\beta\mu}(\mathbf{q})\rangle) \quad (\text{A6})$$

where $\epsilon_{\alpha\beta\gamma}$ is the Levi-Civita symbol and $\alpha, \beta, \gamma \in \{x, y, z\}$. The states $|R_{\gamma\mu}(\mathbf{q})\rangle$ and $|L_{\gamma\mu}(\mathbf{q})\rangle$ describe, respectively, right-handed and left-handed circularly-polarized vibration modes of atom μ about the γ axis.

The phonon angular momentum operator $\hat{J}^{ph} = (\hat{j}_x, \hat{j}_y, \hat{j}_z)$ in wave vector \mathbf{q} , summed over all atoms in a unit cell, is then defined as [7]

$$\hat{j}_\gamma(\mathbf{q}) = \sum_\mu |R_{\gamma\mu}(\mathbf{q})\rangle \langle R_{\gamma\mu}(\mathbf{q})| - |L_{\gamma\mu}(\mathbf{q})\rangle \langle L_{\gamma\mu}(\mathbf{q})|. \quad (\text{A7})$$

For a phonon normal mode $|\phi_n^{\mathbf{q}}\rangle$ (A4), the expectation value of its angular momentum is

$$j_\gamma(\mathbf{q}) = \langle \phi_n^{\mathbf{q}} | \hat{j}_\gamma(\mathbf{q}) | \phi_n^{\mathbf{q}} \rangle. \quad (\text{A8})$$

Throughout this work we set the reduced Planck constant to unity (i.e., $\hbar \equiv 1$).

III. Pesudo angular momentum

For a crystal with an n -fold rotational symmetry about axis α , denoted C_n^α , the phononic *pseudo-angular momentum* (PAM) [8] is fixed by the phase a wavefunction acquires under this discrete rotation. PAM decomposes into (i) a local spin contribution and (ii) a non-local orbital contribution, capturing, respectively, the intracell and intercell responses to (screw) rotations [8, 11, 46, 55]. Both parts follow directly from the corresponding symmetry eigenvalues. Using the conventions of Ref. [51], we derive the explicit PAM expressions below.

a. Symmetry eigenvalues of phonon modes

Given a space group \mathcal{G} , a general symmetry operator $g \in \mathcal{G}$ is defined as $g = \{\mathcal{R}|\tau\}$ where \mathcal{R} is a symmetry operation of the point group and τ represents a translation. For symmorphic space groups expressed in a primitive basis and with a proper choice of the origin, τ has integer components in all symmetry operations. However, in non-symmorphic space groups, the translation τ of certain symmetry operations takes fractional values. In reciprocal space, the little group of a \mathbf{q} -point is $G_{\mathbf{q}} \subset \mathcal{G}$, whose elements $\tilde{g} = \{\tilde{\mathcal{R}}|\tilde{\tau}\}$ satisfy the following condition,

$$\tilde{\mathcal{R}}\mathbf{q} = \mathbf{q} + \mathbf{G} \quad (\text{A9})$$

where \mathbf{G} are the reciprocal lattice vectors.

In real materials, the dynamical matrix is written in the basis of $|u_{\alpha\mu}(\mathbf{q})\rangle$. When a general symmetry operator $\tilde{g} = \{\tilde{\mathcal{R}}|\tilde{\tau}\}$ acts on $|u_{\alpha\mu}(\mathbf{q})\rangle$, we have,

$$\begin{aligned} \{\tilde{\mathcal{R}}|\tilde{\tau}\} |u_{\alpha\mu}(\mathbf{q})\rangle &= \frac{1}{\sqrt{N_R}} \sum_R e^{-i\mathbf{q}\cdot\mathbf{R}} |u_{\tilde{\mathcal{R}}\alpha}(\tilde{\mathcal{R}}\mathbf{R} + \tilde{\mathcal{R}}\tau_\mu + \tilde{\tau})\rangle \\ &= \frac{1}{\sqrt{N_R}} \sum_R e^{-i(\tilde{\mathcal{R}}\mathbf{q})\cdot\tilde{\mathcal{R}}\mathbf{R}} |u_{\tilde{\mathcal{R}}\alpha}(\tilde{\mathcal{R}}\mathbf{R} + \tilde{\mathcal{R}}\tau_\mu + \tilde{\tau})\rangle \\ &= \frac{1}{\sqrt{N_{R'}}} \sum_{R',\mu'} e^{-i\mathbf{q}[\mathbf{R}' + \tau_{\mu'} - \tilde{\mathcal{R}}\tau_\mu - \tilde{\tau}]} |u_{\tilde{\mathcal{R}}\alpha}(\mathbf{R}' + \tau_{\mu'})\rangle \\ &= \sum_{\mu',\alpha'} \mathcal{O}_{\alpha'\alpha} e^{-i\mathbf{q}[\tau_{\mu'} - \tilde{\mathcal{R}}\tau_\mu - \tilde{\tau}]} \frac{1}{\sqrt{N_{R'}}} \sum_{R'} e^{-i\mathbf{q}\mathbf{R}'} |u_{\alpha'}(\mathbf{R}' + \tau_{\mu'})\rangle \\ &= \sum_{\mu',\alpha'} \mathcal{O}_{\alpha'\alpha} \mathcal{A}_{\mu'\mu} |u_{\alpha'\mu'}(\mathbf{q})\rangle \end{aligned} \quad (\text{A10})$$

where we have taken $\tilde{\mathcal{R}}\mathbf{R} + \tilde{\mathcal{R}}\tau_\mu + \tilde{\tau} = \mathbf{R}' + \tau_{\mu'}$, and $|u_{\alpha'\mu'}(\mathbf{q})\rangle = \frac{1}{\sqrt{N_{R'}}} \sum_{R'} e^{-i\mathbf{q}\mathbf{R}'} |u_{\alpha'}(\mathbf{R}' + \tau_{\mu'})\rangle$. \mathcal{O} and \mathcal{A} are the transformation matrices of the vibrational directions and atomic positions under the operation \tilde{g} ,

respectively. As derived above, the element of \mathcal{A} is expressed as,

$$\mathcal{A}_{\mu'\mu} = \begin{cases} e^{-i\mathbf{q}\cdot[\tau_{\mu'} - (\tilde{\mathcal{R}}\tau_\mu + \tilde{\tau})]}, & \text{when } \tau_{\mu'} = (\tilde{\mathcal{R}}\tau_\mu + \tilde{\tau}) \bmod \mathbf{R} \\ 0, & \text{otherwise.} \end{cases} \quad (\text{A11})$$

The matrix \mathcal{O} is actually the representation of $\tilde{\mathcal{R}}$ under the basis of Cartesian coordinates, *i.e.*, $[\tilde{\mathcal{R}}]_c$. However, in the standard setting of the space group \mathcal{G} , the point group operations $\tilde{\mathcal{R}}$ are expressed in the basis of the lattice of translations given by three vectors $\mathbf{a}_{i=1,2,3}$ which are, in general, not orthogonal. If we represent the symmetry operation in the basis of the lattice as $[\tilde{\mathcal{R}}]_\ell$, the transformation between the two matrices is given by,

$$\mathcal{O} = [\tilde{\mathcal{R}}]_c = U[\tilde{\mathcal{R}}]_\ell U^{-1} \quad (\text{A12})$$

where the transformation matrix is

$$U = \begin{bmatrix} \mathbf{a}_1 \\ \mathbf{a}_2 \\ \mathbf{a}_3 \end{bmatrix}^T, \quad (\text{A13})$$

and $\mathbf{a}_{i=1,2,3}$ are the three lattice vectors expressed in Cartesian coordinates.

b. Rotational symmetries, and the pseudo angular momentum

In three-dimensional crystals, the only admissible discrete rotational symmetries are C_n ($n = 2, 3, 4, 6$), whose eigenvalues take the form $e^{-i\frac{2\pi}{n}l}$ ($l = 0, 1, \dots, n-1$). Consider a phonon-mode eigenstate $|\phi_n^\mathbf{q}\rangle$ whose little group at wavevector \mathbf{q} contains the (screw) rotation $\{C_n \mid \tau\}$. The expectation value of its symmetry operator,

$$e^{-i\frac{2\pi}{n}l^{ph}} = \langle \phi_n^\mathbf{q} | \mathcal{O} \otimes \mathcal{A} | \phi_n^\mathbf{q} \rangle, \quad (\text{A14})$$

yields the phase factor $e^{-2\pi i l^{ph}/n}$, where $\mathcal{O} \otimes \mathcal{A}$ is the matrix representation of $\{C_n \mid \tau\}$ (see Eqs. A10–A13) and l^{ph} is the pseudo angular momentum (PAM) of the mode.

Appendix B: Representation theory of chiral phonons

a. Representations of phonon angular momentum and helicity

TABLE S1: A Map from magnetic point groups (MPGs) to point groups (PGs). The constraint from a MPG on $\mathbf{J}^{ph}(\mathbf{q})$ (time-reversal-odd pseudovector) is identical to the constraint from the corresponding PG on a polar vector v . If v is required to be zero (symmetry-allowed non-zero) along certain directions by the PG, $\mathbf{J}^{ph}(\mathbf{q})$ vanishes (is symmetry-allowed nonzero) along the same directions. An operation in a MPG reads $\mathcal{R} \cdot X$ with \mathcal{R} being a proper ($\det \mathcal{R} = 1$) or improper rotation ($\det \mathcal{R} = -1$) and X being identity 1 or time-reversal \mathcal{T} . The map from MPG to PG is given by $\mathcal{R} \cdot X \rightarrow \det(\mathcal{R})s(X)\mathcal{R}$ with $s(1) = 1$ and $s(\mathcal{T}) = -1$.

No.	MPG	PG	No.	MPG	PG	No.	MPG	PG
1	1.1	1	42	4'22'	42m	83	6/m.1'	6/m
2	1.1'	1̄	43	42'2'	4mm	84	6'/m	6/m
3	1̄.1	1	44	4mm.1	422	85	6/m'	6/m
4	1̄.1'	1̄	45	4mm.1'	4/mmm	86	6'/m'	6̄

5	$\bar{1}'$	$\bar{1}$	46	$4'm'm$	$\bar{4}2m$	87	622.1	622
6	2.1	2	47	$4m'm'$	4mm	88	622.1'	6/mmm
7	$2.1'$	$2/m$	48	$\bar{4}2m.1$	422	89	$6'22'$	$\bar{6}m2$
8	$2'$	m	49	$\bar{4}2m.1'$	$4/mmm$	90	$6'2'2'$	6mm
9	m.1	2	50	$\bar{4}'2'm$	$\bar{4}2m$	91	6mm.1	622
10	$m.1'$	$2/m$	51	$\bar{4}'2m'$	$\bar{4}2m$	92	$6mm.1'$	6/mmm
11	m'	m	52	$\bar{4}2'm'$	4mm	93	$6'mm'$	$\bar{6}m2$
12	$2/m.1$	2	53	$4/mmm.1$	422	94	$6m'm'$	6mm
13	$2/m.1'$	$2/m$	54	$4/mmm.1'$	$4/mmm$	95	$\bar{6}m2.1$	622
14	$2'/m$	$2/m$	55	$4/m'mm$	$4/mmm$	96	$\bar{6}m2.1'$	6/mmm
15	$2/m'$	$2/m$	56	$4'/mm'm$	$\bar{4}2m$	97	$\bar{6}'m'2$	$\bar{6}m2$
16	$2'/m'$	m	57	$4'/m'm'm$	$\bar{4}2m$	98	$\bar{6}'m2'$	$\bar{6}m2$
17	222.1	222	58	$4/mm'm'$	4mm	99	$\bar{6}m'2'$	6mm
18	222.1'	mmmm	59	$4/m'm'm'm'$	$4/mmm$	100	$6/mmm.1$	622
19	$2'2'2$	mm2	60	3.1	3	101	$6/mmm.1'$	6/mmm
20	mm2.1	222	61	3.1'	$\bar{3}$	102	$6/m'mm$	6/mmm
21	mm2.1'	mmmm	62	$\bar{3}.1$	3	103	$6'/mmmm'$	6/mmm
22	$m'm2'$	mm2	63	$\bar{3}.1'$	$\bar{3}$	104	$6'/m'mm'$	$\bar{6}m2$
23	$m'm'2$	mm2	64	$\bar{3}'$	$\bar{3}$	105	$6/mm'm'$	6mm
24	mmmm.1	222	65	32.1	32	106	$6/m'm'm'm'$	6/mmm
25	mmmm.1'	mmmm	66	32.1'	$\bar{3}m$	107	23.1	23
26	$m'mm$	mmmm	67	32'	3m	108	23.1'	$m\bar{3}$
27	$m'm'm$	mm2	68	3m.1	32	109	$m\bar{3}.1$	23
28	$m'm'm'm'$	mmmm	69	3m.1'	$\bar{3}m$	110	$m\bar{3}.1'$	$m\bar{3}$
29	4.1	4	70	$3m'$	3m	111	$m'\bar{3}'$	$m\bar{3}$
30	$4.1'$	$4/m$	71	$\bar{3}m.1$	32	112	432.1	432
31	$4'$	$\bar{4}$	72	$\bar{3}m.1'$	$\bar{3}m$	113	432.1'	$m\bar{3}m$
32	$\bar{4}.1$	4	73	$\bar{3}'m$	$\bar{3}m$	114	$4'32'$	$\bar{4}3m$
33	$\bar{4}.1'$	$4/m$	74	$\bar{3}'m'$	$\bar{3}m$	115	$\bar{4}3m.1$	432
34	$\bar{4}'$	$\bar{4}$	75	$\bar{3}m'$	3m	116	$\bar{4}3m.1'$	$m\bar{3}m$
35	$4/m.1$	4	76	6.1	6	117	$\bar{4}'3m'$	$\bar{4}3m$
36	$4/m.1'$	$4/m$	77	6.1'	$6/m$	118	$m\bar{3}m.1$	432
37	$4'/m$	$\bar{4}$	78	6'	$\bar{6}$	119	$m\bar{3}m.1'$	$m\bar{3}m$
38	$4/m'$	$4/m$	79	$\bar{6}.1$	6	120	$m'\bar{3}'m$	$m\bar{3}m$
39	$4'/m'$	$4/m$	80	$\bar{6}.1'$	$6/m$	121	$m\bar{3}m'$	$\bar{4}3m$
40	422.1	422	81	$\bar{6}'$	$\bar{6}$	122	$m'\bar{3}'m'$	$m\bar{3}m$
41	422.1'	$4/mmm$	82	$6/m.1$	6			

In three-dimensional (3D) crystals, the lattice momentum $\mathbf{q} = (q_x, q_y, q_z)$ is a polar vector, whereas the phonon angular momentum $\mathbf{J}^{ph} = (j_x, j_y, j_z)$ is an axial (pseudo)-vector. As discussed in the main text, time-reversal symmetry (TRS) requires that

$$\mathbf{J}^{ph}(\mathbf{q}) = -\mathbf{J}^{ph}(-\mathbf{q}), \quad (\text{B1})$$

and a spatial rotation \mathcal{R} leads to

$$\mathbf{J}^{ph}(\mathcal{R}\mathbf{q}) = \det(\mathcal{R})\mathcal{R}\mathbf{J}^{ph}(\mathbf{q}). \quad (\text{B2})$$

For type-I point groups, which include inversion symmetry, \mathcal{PT} symmetry requires that $\mathbf{J}^{ph}(\mathbf{q})$ vanishes for all \mathbf{q} . For type-II point groups (lacking both inversion and roto-inversion operations) and type-III point groups (lacking inversion but including roto-inversion operations), $\mathbf{J}^{ph}(\mathbf{q})$ is generally nonzero at generic \mathbf{q} .

Further, the symmetry of \mathbf{J}^{ph} in the Brillouin zone (BZ) is characterized by $G \times C_i$, where G is the point group of the material, and the inversion group C_i in the momentum space is generated by TRS.

Let $M_{\mathbf{q}}$ be the magnetic little group of the associated gray group (i.e., type-II magnetic space group) of the space group \mathcal{G} , which completely capture the symmetry of \mathbf{J}^{ph} at \mathbf{q} . We can construct a corresponding point group $P_{\mathbf{q}}$ such that the constraint from $M_{\mathbf{q}}$ on $\mathbf{J}^{ph}(\mathbf{q})$ (time-reversal-odd pseudovector) is identical to the constraint from $P_{\mathbf{q}}$ on a polar vector v . An operation in $M_{\mathbf{q}}$ can be expressed as $\mathcal{R} \cdot X$ with \mathcal{R} being a proper ($\det \mathcal{R} = 1$) or improper rotation ($\det \mathcal{R} = -1$) and X being identity 1 or time-reversal \mathcal{T} . The map from $M_{\mathbf{q}}$ to $P_{\mathbf{q}}$ is given by $\mathcal{R} \cdot X \rightarrow \det(\mathcal{R})s(X)\mathcal{R}$ with $s(1) = 1$ and $s(\mathcal{T}) = -1$. See the map from 122 magnetic point groups to the point groups in Table S1. v furnishes a 3D representation $\gamma_{P_{\mathbf{q}}}$ of $P_{\mathbf{q}}$, which can be decomposed into irreducible representations (irreps),

$$\gamma_{P_{\mathbf{q}}} = \bigoplus_{i=1}^{n_{P_{\mathbf{q}}}} m(\Gamma_{P_{\mathbf{q}}}^i) \Gamma_{P_{\mathbf{q}}}^i,$$

where $m(\Gamma_{P_{\mathbf{q}}}^i)$ denotes the multiplicity of the irrep $\Gamma_{P_{\mathbf{q}}}^i$. Table S2 lists these decompositions for the polar vector \mathbf{v} (see the column “**Reps. of \mathbf{q}** ”) under all 32 crystallographic point groups (without TRS), using the conventions of the [Bilbao Crystallographic Server](#). If trivial irreps appear in the decomposition, the associated components of v and \mathbf{J}^{ph} are allowed to be non-zero. For example, let us consider $\mathbf{q} = (q_x, q_y, 0)$ within the plane $q_z = 0$ in the SG 2 ($P2$) and SG 6 (Pm). For $P2$, \mathbf{q} is invariant under the combination of \mathcal{T} and π -rotation along the z axis, and hence the magnetic little group is $2'$. Its corresponding point group is m (see Table S1), implying that j_x and j_y are symmetry-allowed nonzero (see Table S2). For Pm , \mathbf{q} is invariant under mirror across the z -axis. The magnetic little group is m , and its corresponding point group of 2 (see Table S1), implying that j_z is symmetry-allowed nonzero (see Table S2).

Phonon helicity is defined as the scalar product between the unit vector along the phonon-momentum direction and its angular momentum: $h = \mathbf{e}_q \cdot \mathbf{J}^{ph}$. Notably, as helicity is invariant under TRS, only considering crystalline symmetry is sufficient to determine whether helicity is nonzero at a certain \mathbf{q} . At a certain \mathbf{q} , it transforms as a one-dimensional real representation that can be deduced from the representations of \mathbf{q} and \mathbf{J}^{ph} . If this representation is trivial, the helicity is symmetry-allowed and can take a non-zero value at that \mathbf{q} . Otherwise, point-group symmetry forces the helicity to vanish. In Table S2, the 32 crystallographic point groups are divided into three categories: (i) type-I PGs, which contain inversion symmetry; (ii) type-II PGs, which contain only proper rotations; (iii) type-III PGs, which lack inversion symmetry but include at least one improper rotation. In type-I and type-III groups, inversion or an improper rotation flips the sign of the helicity operator, so phonon helicity is symmetry-enforced zero for any momentum whose little group falls into either class. In contrast, every symmetry operation in a type-II group is proper and leaves helicity unchanged, making the corresponding representation trivial and therefore symmetry-allowed nonzero.

As discussed above, both angular momentum and helicity vanish throughout the entire BZ, for type-I SGs. In contrast, for type-II SGs, all momenta except the eight time-reversal invariant momenta (TRIM) can have symmetry-allowed nonzero angular momentum and helicity. At the TRIM points, angular momentum either vanishes for one-dimensional phonon modes or exhibit degeneracy, where the sum of the angular momenta of degenerate modes equal zero. Since all symmetry elements in a type-II PG preserve helicity, the helicity pattern in the BZ has an s -wave character. In systems with TRS, the helicity pattern of a type-III PG is described by an even-power polynomial with the same representation as helicity. This leads to d -, g - or i -wave characteristics in the pattern when the polynomial's order is 2, 4, or 6, respectively.

In Table S2, we have summarized the helicity representations for all 32 point groups (PGs) in the absence of TRS, as well as the corresponding characteristics of helicity in the BZ with the presence of TRS. Table S3 lists the lowest even-order polynomials that transform according to the same representation as the phonon helicity in type-III PGs. Fig. S1 presents schematics of the helicity patterns in the 3D Brillouin zone for all 10 type-III PGs.

TABLE S2: Representations of phonon angular momentum and helicity. The 32 point groups (PGs), as well as their corresponding space groups (SGs), are classified into three categories based on the presence of inversion symmetry (Inv.) or improper rotational symmetry (Irot.). For each PG, we list the representations (Reps.) of both the momentum vector $\mathbf{q} = (q_x, q_y, q_z)$ and the angular momentum vector $\mathbf{J}^{ph} = (j_x, j_y, j_z)$. The last two columns provide, respectively, the irreducible representation (irrep) of phonon helicity, $h = e_q \cdot J^{ph}$, in the absence of time-reversal symmetry (TRS), and the anisotropy characteristics of the helicity pattern in the presence of TRS.

Type	PG	SGs	Inv.?	Irot?	Reps. of \mathbf{q}			Reps. of J^{ph}			Rep. of h	anisotropy	
					q_x	q_y	q_z	j_x	j_y	j_z			
Type-I	$C_i (\bar{1})$	2	✓	✗	A _u	A _u	A _u	A _g	A _g	A _g	A _u	\\	
	$C_{2h} (2/m)$	10-15	✓	✓	B _u	B _u	A _u	B _g	B _g	A _g	A _u	\\	
	$D_{2h} (mmm)$	47-74	✓	✓	B _{3u}	B _{2u}	B _{1u}	B _{3g}	B _{2g}	B _{1g}	A _u	\\	
	$C_{3i} (\bar{3})$	147-148	✓	✓	¹ E _u	² E _u	A _u	¹ E _g	² E _g	A _g	A _u	\\	
	$D_{3d} (\bar{3}m)$	162-167	✓	✓	E _u		A _{2u}	E _g		A _{2g}	A _{1u}	\\	
	$C_{4h} (4/m)$	83-88	✓	✓	¹ E _u	² E _u	A _u	¹ E _g	² E _g	A _g	A _u	\\	
	$D_{4h} (4/mmm)$	123-142	✓	✓	E _u		A _{2u}	E _g		A _{2g}	A _{1u}	\\	
	$C_{6h} (6/m)$	175-176	✓	✓	¹ E _{1u}	² E _{1u}	A _u	¹ E _{1g}	² E _{1g}	A _g	A _u	\\	
	$D_{6h} (6/mmm)$	191-194	✓	✓	E _{1u}		A _{2u}	E _{1g}		A _{2g}	A _{1u}	\\	
	$T_h (m\bar{3})$	200-206	✓	✓			T _u			T _g		A _u	\\
Type-II	$O_h (m\bar{3}m)$	221-230	✓	✓			T _{1u}			T _{1g}		A _{1u}	\\
	$C_1 (1)$	1	✗	✗	A	A	A	A	A	A	A	s-wave	
	$C_2 (2)$	3-5	✗	✗	B	B	A	B	B	A	A	s-wave	
	$D_2 (222)$	16-24	✗	✗	B ₃	B ₂	B ₁	B ₃	B ₂	B ₁	A	s-wave	
	$C_3 (3)$	143-146	✗	✗	¹ E ² E		A	¹ E ² E		A	A	s-wave	
	$D_3 (32)$	195-199	✗	✗	E		A ₂	E		A ₂	A ₁	s-wave	
	$C_4 (4)$	75-80	✗	✗	¹ E ² E		A	¹ E ² E		A	A	s-wave	
	$D_4 (422)$	89-98	✗	✗	E		A ₂	E		A ₂	A ₁	s-wave	
	$C_6 (6)$	168-173	✗	✗	¹ E ₁ ² E ₁		A	¹ E ₁ ² E ₁		A	A	s-wave	
	$D_6 (622)$	177-182	✗	✗	E ₁		A ₂	E ₁		A ₂	A ₁	s-wave	
Type-III	$T (23)$	195-197	✗	✗			T			T		A	s-wave
	$O (432)$	207-214	✗	✗			T ₁			T ₁		A ₁	s-wave
	$C_s (m)$	6-9	✗	✓	A'	A'	A''	A''	A''	A'	A''	d-wave	
	$C_{2v} (mm2)$	25-46	✗	✓	B ₁	B ₂	A ₁	B ₂	B ₁	A ₂	A ₂	d-wave	
	$C_{3v} (3m)$	156-161	✗	✓			E	A ₁	E	A ₂	A ₂	g-wave	
	$S_4 (\bar{4})$	81-82	✗	✓	¹ E ² E		B	¹ E ² E		A	B	d-wave	
	$C_{4v} (4mm)$	99-110	✗	✓	E		A ₁	E		A ₂	A ₂	g-wave	
	$D_{2d} (\bar{4}2m)$	111-122	✗	✓			B ₂	E		A ₂	B ₁	d-wave	
	$C_{3h} (\bar{6})$	174	✗	✓	² E ¹ E'		A''	¹ E ^{''2} E ^{''}		A'	A''	g-wave	
	$D_{3h} (\bar{6}m2)$	187-190	✗	✓	E'		A ₂ '	E''		A ₂ '	A ₁ '	g-wave	
	$C_{6v} (6mm)$	183-186	✗	✓	E ₁		A ₁	E ₁		A ₂	A ₂	i-wave	
	$T_d (\bar{4}3m)$	215-220	✗	✓			T ₂			T ₁		A ₂	i-wave

TABLE S3: The lowest-even-order polynomials that transform according to the same representation as the phonon helicity in type-III PGs.

PG	Representation of h	polynomial	order	anisotropy
$C_s (m)$	A''	xz or yz	$l = 2$	d-wave
$C_{2v} (mm2)$	A ₂	xy	$l = 2$	d-wave
$C_{3v} (3m)$	A ₂	$z(x^3 - 3xy^2)$	$l = 4$	g-wave

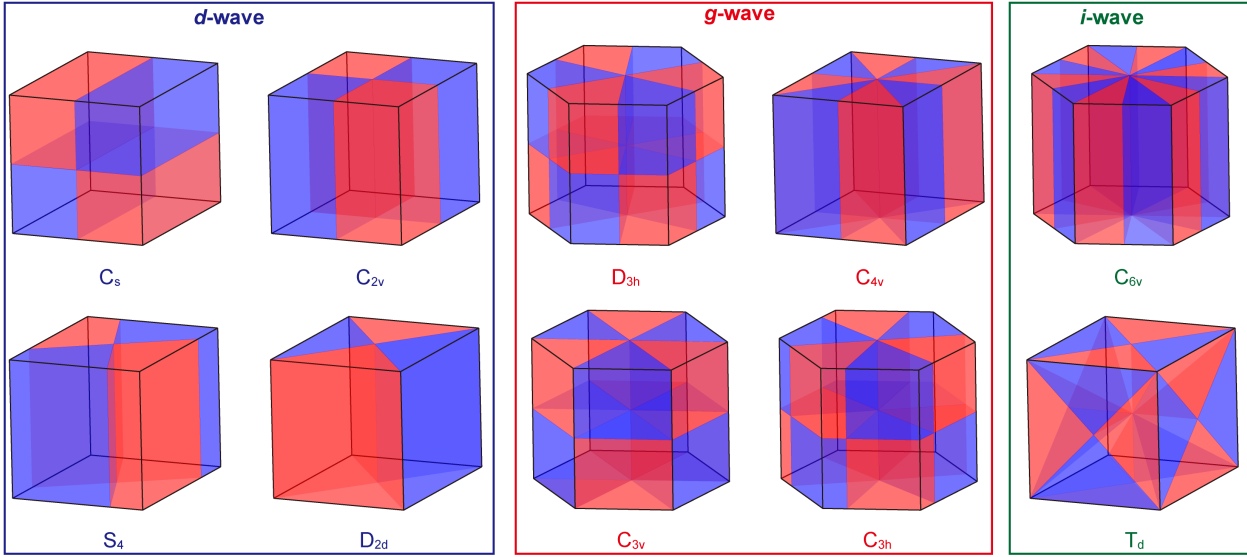


FIG. S1. Schematic of phonon helicity patterns in the 3D Brillouin zone for type-III point groups. The 10 type-III point groups are classified into *d*-, *g*-, or *i*-wave helicity types based on their symmetry. In each pattern, red and blue regions indicate helicities of opposite sign, related by roto-inversion symmetries. The polynomials that characterize these helicity patterns are tabulated in Table S3.

$S_4 (\bar{4})$	B	$xy \text{ or } x^2 - y^2$	$l = 2$	<i>d</i> -wave
$C_{4v} (4mm)$	A ₂	$xy(x^2 - y^2)$	$l = 4$	<i>g</i> -wave
$D_{2d} (\bar{4}2m)$	B ₁	$x^2 - y^2$	$l = 2$	<i>d</i> -wave
$C_{3h} (\bar{6})$	A''	$z(x^3 - 3xy^2) \text{ or } z(y^3 - 3x^2y)$	$l = 4$	<i>g</i> -wave
$D_{3h} (\bar{6}m2)$	A'' ₁	$z(y^3 - 3x^2y)$	$l = 4$	<i>g</i> -wave
$C_{6v} (6mm)$	A ₂	$3x^5y - 10x^3y^3 + 3xy^5$	$l = 6$	<i>i</i> -wave
$T_d (\bar{4}3m)$	A ₂	$x^4y^2 + y^4z^2 + z^4x^2 - x^2y^4 - y^2z^4 - z^2x^4$	$l = 6$	<i>i</i> -wave

b. Representations of velocity-angular momentum tensor

The group velocity of phonons is defined as $\mathbf{v}_n(\mathbf{q}) = \nabla_{\mathbf{q}}\omega_n(\mathbf{q})$, where $\omega_n(\mathbf{q})$ is the phonon frequency at momentum \mathbf{q} of the n -th phonon mode. Here we examine the symmetry properties of the pseudotensor, $\mathbf{v} \otimes \mathbf{J}^{ph}$, which governs the phonon magnetization induced by a temperature gradient [15]. Because \mathbf{v} transforms in the same way as the lattice momentum \mathbf{q} , the symmetry representation of $\mathbf{v} \otimes \mathbf{J}^{ph}$ can be read directly from Table S2. Table S4 presents the reduction of this representation into irreps for all 32 point groups; for each irrep we list the corresponding tensor elements $v_{\alpha}j_{\beta}$.

TABLE S4: Representations of the velocity-angular momentum tensor. For each point group (PG) listed in the first column, the representations of the tensor $\mathbf{v} \otimes \mathbf{J}$ are given as a direct sum of irreps. For each irrep, all associated tensor components are listed and separated by commas. If an irrep is two- or three-dimensional, the corresponding components are grouped within braces. Identity irreps are highlighted in red.

PG	Reps. of $\mathbf{v} \otimes \mathbf{J}$	Irreps and the associated tensor components		
$C_1 (1)$	9A	A	$v_{\alpha}j_{\beta}$ ($\alpha, \beta = x, y, z$)	
$C_2 (2)$	5A \oplus 4B	A	$v_x j_x, v_x j_y, v_y j_x, v_y j_y, v_z j_z$	
		B	$v_x j_z, v_y j_z, v_z j_x, v_z j_y$	

D ₂ (222)	3A \oplus 2B ₁ \oplus 2B ₂ \oplus 2B ₃	A	$v_x j_x, v_y j_y, v_z j_z$
		B ₁	$v_x j_y, v_y j_x$
		B ₂	$v_x j_z, v_z j_x$
		B ₃	$v_y j_z, v_z j_y$
C ₃ (3)	3A \oplus 3 ¹ E ² E	A	$v_x j_x + v_y j_y, v_z j_z, v_x j_y - v_y j_x$
		¹ E ² E	$\{v_x j_z, v_y j_z\}, \{v_z j_x, v_z j_y\}, \{v_x j_y + v_y j_x, v_x j_x - v_y j_y\}$
D ₃ (32)	2A ₁ \oplus A ₂ \oplus 3E	A₁	$v_x j_x + v_y j_y, v_z j_z$
		A ₂	$v_x j_y - v_y j_x$
		E	$\{v_x j_z, v_y j_z\}, \{v_z j_x, v_z j_y\}, \{v_x j_x - v_y j_y, v_x j_y + v_y j_x\}$
C ₄ (4)	3A \oplus 2B \oplus 2 ¹ E ² E	A	$v_x j_x + v_y j_y, v_z j_z, v_x j_y - v_y j_x$
		B	$v_x j_y + v_y j_x, v_x j_x - v_y j_y$
		¹ E ² E	$\{v_x j_z, v_y j_z\}, \{v_z j_x, v_z j_y\}$
D ₄ (422)	2A ₁ \oplus A ₂ \oplus B ₁ \oplus B ₂ \oplus 2E	A₁	$v_x j_x + v_y j_y, v_z j_z$
		A ₂	$v_x j_y - v_y j_x$
		B ₁	$v_x j_x - v_y j_y$
		B ₂	$v_x j_y + v_y j_x$
		E	$\{v_x j_z, v_y j_z\}, \{v_z j_x, v_z j_y\}$
C ₆ (6)	3A \oplus 2 ¹ E ₁ ² E ₁ \oplus ¹ E ₂ ² E ₂	A	$v_x j_x + v_y j_y, v_z j_z, v_x j_y - v_y j_x$
		¹ E ₁ ² E ₁	$\{v_z j_x, v_z j_y\}, \{v_x j_z, v_y j_z\}$
		¹ E ₂ ² E ₂	$\{v_x j_y + v_y j_x, v_x j_x - v_y j_y\}$
D ₆ (622)	2A ₁ \oplus A ₂ \oplus 2E ₁ \oplus E ₂	A₁	$v_x j_x + v_y j_y, v_z j_z$
		A ₂	$v_x j_y - v_y j_x$
		E ₁	$\{v_z j_x, v_z j_y\}, \{v_x j_z, v_y j_z\}$
		E ₂	$\{v_x j_y + v_y j_x, v_x j_x - v_y j_y\}$
T (23)	A \oplus ¹ E ² E \oplus 2T	A	$v_x j_x + v_y j_y + v_z j_z$
		¹ E ² E	$\{2v_z j_z - v_x j_x - v_y j_y, v_x j_x - v_y j_y\}$
		T	$\{v_y j_z + v_z j_y, v_z j_x + v_x j_z, v_x j_y + v_y j_x\}, \{v_y j_z - v_z j_y, v_z j_x - v_x j_z, v_x j_y - v_y j_x\}$
O (432)	A ₁ \oplus E \oplus T ₁ \oplus T ₂	A₁	$v_x j_x + v_y j_y + v_z j_z$
		E	$\{2v_z j_z - v_x j_x - v_y j_y, v_x j_x - v_y j_y\}$
		T ₁	$\{v_y j_z - v_z j_y, v_z j_x - v_x j_z, v_x j_y - v_y j_x\}$
		T ₂	$\{v_y j_z + v_z j_y, v_z j_x + v_x j_z, v_x j_y + v_y j_x\}$
C _s (m)	4A' \oplus 5A''	A'	$v_x j_z, v_y j_z, v_z j_x, v_z j_y$
		A''	$v_x j_x, v_y j_y, v_z j_z, v_x j_y, v_y j_x$
C _{2v} (mm2)	2A ₁ \oplus 3A ₂ \oplus 2B ₁ \oplus 2B ₂	A₁	$v_x j_y, v_y j_x$
		A ₂	$v_x j_x, v_y j_y, v_z j_z$
		B ₁	$v_y j_z, v_z j_y$
		B ₂	$v_x j_z, v_z j_x$
C _{3v} (3m)	A ₁ \oplus 2A ₂ \oplus 3E	A₁	$v_x j_y - v_y j_x$
		A ₂	$v_x j_x + v_y j_y, v_z j_z$
		E	$\{v_x j_z, v_y j_z\}, \{v_z j_x, v_z j_y\}, \{v_x j_y + v_y j_x, v_x j_x - v_y j_y\}$
S ₄ ($\bar{4}$)	2A \oplus 3B \oplus 2 ¹ E ² E	A	$v_x j_x - v_y j_y, v_x j_y + v_y j_x$
		B	$v_x j_x + v_y j_y, v_x j_y - v_y j_x, v_z j_z$
		¹ E ² E	$\{v_x j_z, v_y j_z\}, \{v_z j_x, v_z j_y\}$
C _{4v} (4mm)	A ₁ \oplus 2A ₂ \oplus B ₁ \oplus B ₂ \oplus 2E	A₁	$v_x j_y - v_y j_x$
		A ₂	$v_x j_x + v_y j_y, v_z j_z$
		B ₁	$v_x j_y + v_y j_x$
		B ₂	$v_x j_x - v_y j_y$
		E	$\{v_x j_z, v_y j_z\}, \{v_z j_x, v_z j_y\}$
D _{2d} ($\bar{4}2m$)	A ₁ \oplus A ₂ \oplus 2B ₁ \oplus B ₂ \oplus 2E	A₁	$v_x j_x - v_y j_y$
		A ₂	$v_x j_y + v_y j_x$

		B ₁	$v_x j_x + v_y j_y, v_z j_z$
		B ₂	$v_x j_y - v_y j_x$
		E	$\{v_x j_z, v_y j_z\}, \{v_z j_x, v_z j_y\}$
$C_{3h} (\bar{6})$	$3A'' \oplus 2^1E'^2E' \oplus ^1E''^2E''$	A''	$v_x j_x + v_y j_y, v_x j_y - v_y j_x, v_z j_z$
		${}^1E'^2E'$	$\{v_x j_z, v_y j_z\}, \{v_z j_x, v_z j_y\}$
		${}^1E''^2E''$	$\{v_x j_x - v_y j_y, v_x j_y + v_y j_x\}$
$D_{3h} (\bar{6}m2)$	$2A''_1 \oplus A''_2 \oplus 2E' \oplus E''$	A'' ₁	$v_x j_x + v_y j_y, v_z j_z$
		A'' ₂	$v_x j_y - v_y j_x$
		E'	$\{v_x j_z, v_y j_z\}, \{v_z j_x, v_z j_y\}$
		E''	$\{v_x j_x - v_y j_y, v_x j_y + v_y j_x\}$
$C_{6v} (6mm)$	$A_1 \oplus 2A_2 \oplus 2E_1 \oplus E_2$	A ₁	$v_x j_y - v_y j_x$
		A ₂	$v_x j_x + v_y j_y, v_z j_z$
		E ₁	$\{v_z j_x, v_z j_y\}, \{v_x j_z, v_y j_z\}$
		E ₂	$\{v_x j_y + v_y j_x, v_x j_x - v_y j_y\}$
$T_d (\bar{4}3m)$	$A_2 \oplus E \oplus T_1 \oplus T_2$	A ₂	$v_x j_x + v_y j_y + v_z j_z$
		E	$\{2v_z j_z - v_x j_x - v_y j_y, v_x j_x - v_y j_y\}$
		T ₁	$\{v_y j_z + v_z j_y, v_z j_x + v_x j_z, v_x j_y + v_y j_x\}$
		T ₂	$\{v_y j_z - v_z j_y, v_z j_x - v_x j_z, v_x j_y - v_y j_x\}$

Appendix C: Density functional theory calculations

We performed ab initio calculations for 1,625 ICSD material entries, for which the crystal structures are provided on the [Topological Materials Database](#) website. For each ICSD entry, the crystal structure was first fully relaxed, followed by the calculation of the dynamical matrix. All calculations were carried out within the framework of Density Functional Theory (DFT)[60, 61] using the *Vienna Ab-initio Simulation Package* (VASP)[49, 62] and the finite difference method. Interactions between ion cores and valence electrons were treated with the projector augmented-wave (PAW) method [63]. The exchange-correlation effects were described using the generalized gradient approximation (GGA) with the Perdew-Burke-Ernzerhof (PBE) functional [64]. Dynamical matrices were obtained via the post-processing software Phonopy [65, 66].

I. Non-analytical correction to the dynamical matrix

In polar semiconductors, whose positive and negative ions lie on separate planes, the long range macroscopic electric field induced by long wavelength (with $\mathbf{q} \rightarrow \mathbf{0}$) longitudinal optical (LO) phonons is non-negligible [56]. The coupling between LO phonons and electric fields result in the difference in frequency between LO and transverse optical (TO) phonons at the Brillouin zone centre, namely the LO-TO splitting.

To quantitatively characterize the LO-TO splitting of phonon frequencies, we need an additional non-analytical term correction (NAC) in the dynamical matrix. The origin of this term is the long range dipole-dipole interaction given by [67, 68],

$$\mathcal{D}_{\alpha\mu,\beta\nu}^{NA}(\mathbf{q} \rightarrow \mathbf{0}) = \frac{4\pi e^2}{\Omega \sqrt{M_\mu M_\nu}} \frac{(\mathbf{q} \cdot \mathbf{Z}_\mu^*)_\alpha (\mathbf{q} \cdot \mathbf{Z}_\nu^*)_\beta}{\mathbf{q} \cdot \epsilon_\infty \cdot \mathbf{q}} \quad (C1)$$

where Ω is the volume of one unit cell, and ϵ_∞ is the high frequency static dielectric tensor. Z_μ^* is the Born effective charge tensor of atom μ in one unit cell, which describes the polarization ($\vec{\mathcal{P}}$) induced by the displacement of atom μ (\vec{r}_μ) under the condition of zero electric field ($\vec{E} = 0$) and defined as,

$$Z_{\mu,\alpha\beta}^* = \Omega \frac{\partial \mathcal{P}_\beta}{\partial r_{\mu,\alpha}} |_{\vec{E}=0} \quad (C2)$$

where $\alpha, \beta = x, y, z$.

Hence, the total dynamical matrix for $\mathbf{q} \rightarrow \mathbf{0}$ is expressed as,

$$\mathcal{D}^{Total}(\mathbf{q} \rightarrow \mathbf{0}) = \mathcal{D}(\mathbf{q}) + \mathcal{D}^{NA}(\mathbf{q}) \quad (C3)$$

where $\mathcal{D}(\mathbf{q})$ is the analytical term in Eq. A2. Note that the NAC term is 0 at $\mathbf{q} = \mathbf{0}$.

Appendix D: Introduction of the chiral phonon materials database

The website [Chiral Phonon Materials Database](#) is built to collect all data of phonon materials through the high-throughput calculations mentioned in this article so that it is publicly available and convenient to browse and search for existing information. In this part, a brief overview and guideline of the Chiral Phonon website are provided for possible users.

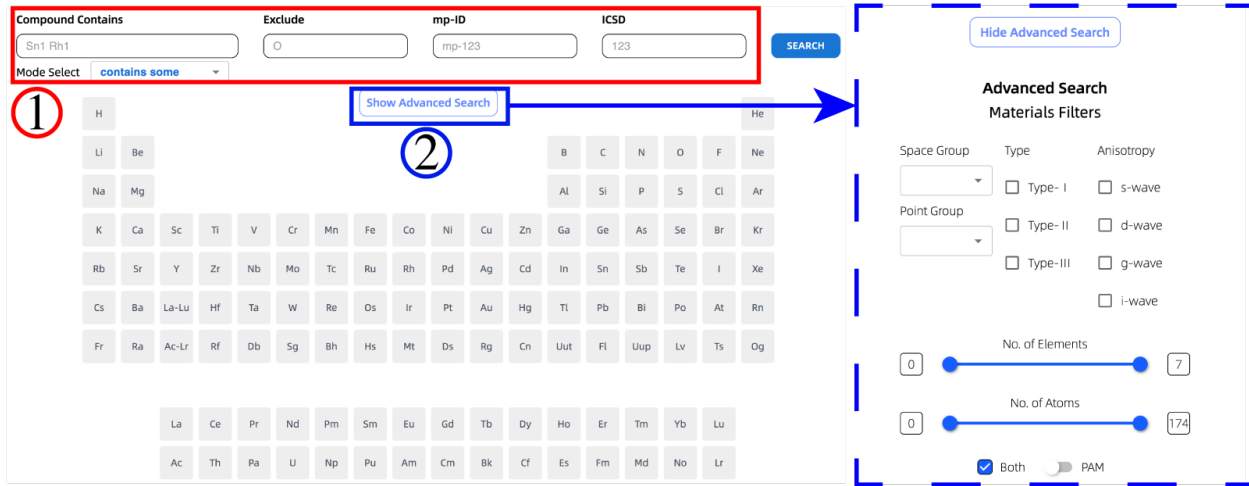


FIG. S2. Homepage of the [Chiral Phonon Materials Database](#). Chiral-phonon materials can be searched in two ways: (1) Basic mode, which lets users query by chemical composition or by identifier (mp-ID or ICSD); (2) Advanced mode, which lets users filter by symmetry characteristics and structural complexity.

As illustrated in Fig. S2, the database supports two search modes. The default basic mode lets users retrieve compounds by element, exact stoichiometric formula, Materials Project ID (MP-ID), or ICSD number. Within this mode, users can choose among four options:

1. Compounds that contain at least one of the specified elements.
2. Compounds that contain every specified element.
3. Compounds composed only of any of the specified elements.
4. Compounds composed exclusively of all the specified elements.

Advanced search mode offers a suite of additional filters for fine-grained results. You can narrow queries by space group, point group and point-group type, helicity-pattern anisotropy, number of distinct elements, atoms per primitive unit cell, and whether a pseudo-angular momentum is defined along any high-symmetry path.

Each compound page (Fig. S3) begins with a summary that lists its mp-ID or ICSD, chemical formula, presence of pseudo-angular momentum along any high-symmetry path, space and point groups (with type), helicity-pattern anisotropy, inclusion of non-analytical correction (NAC) in the phonon calculations, electronic band gap, crystallographic parameters, and a lattice-structure visualization. It also links to the [Topological Phonon Database](#) and [Topological Materials Database](#) and supplies the essential input and output files from the high-throughput workflow. The second part of Fig. S3 includes a table listing every

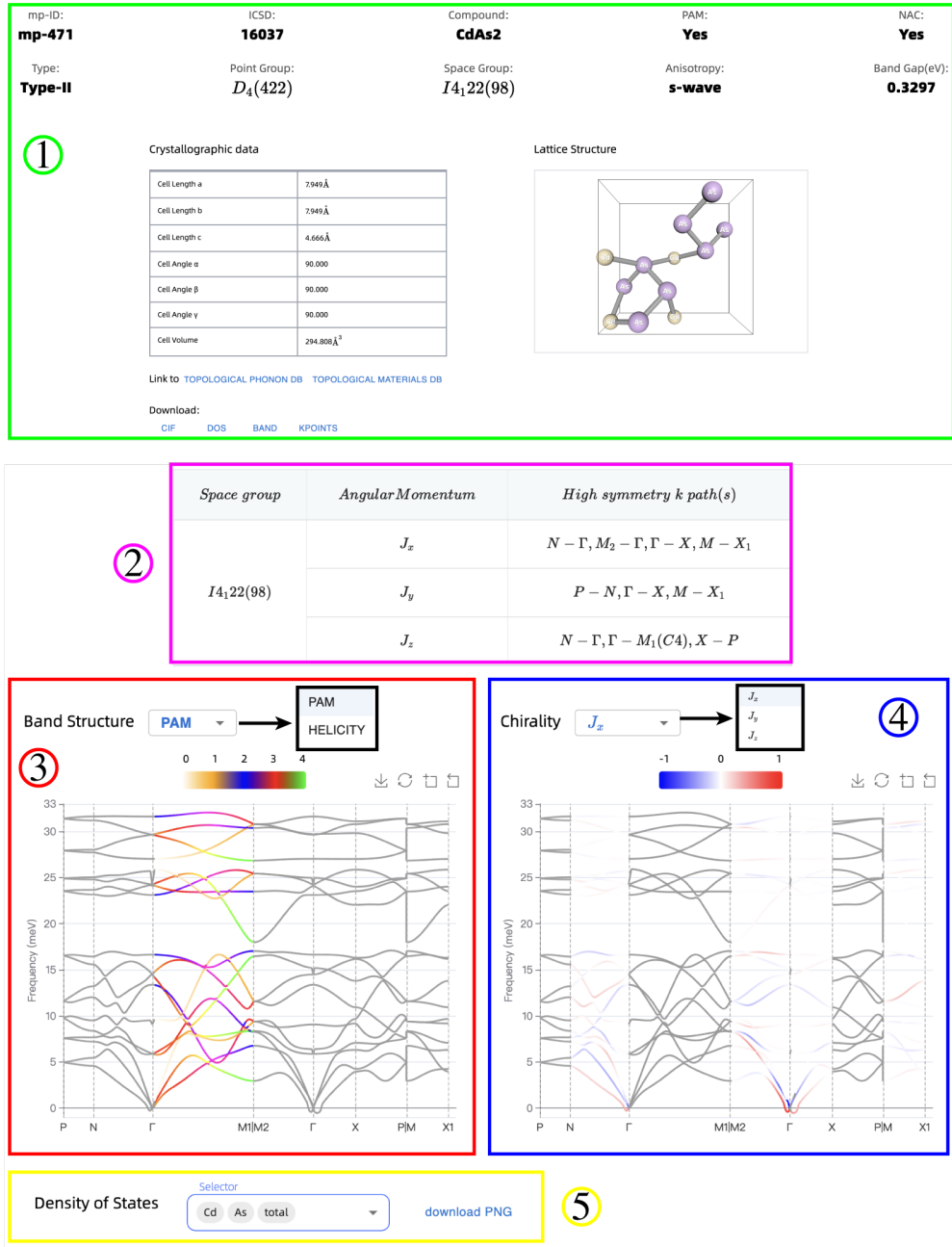


FIG. S3. Basic information and computational results for a specific material entry stored in the [Chiral Phonon Materials Database](#). Part 1, basic information summary of the material entry. Part 2, high-symmetry paths with symmetry-allowed non-zero angular momentum. Part 3, phonon band structure with PAM and helicity projections. Part 4, phonon band structure with angular-momentum projections. Part 5, element-resolved and total phonon density of states.

high-symmetry path with symmetry-allowed non-zero angular momentum. For each angular-momentum component, multiple comma-separated paths may be listed; when a path has PAM defined, its corresponding rotational symmetry is given in brackets. Part 3 of Fig. S3 shows phonon band structure with PAM and helicity projections. PAM ranges are $0 \leq l < 3$ for three-fold (screw) rotations and $0 \leq l < 4$ for four-fold (screw) rotations, while helicity spans $-\hbar \leq h \leq \hbar$. Part 4 of Fig. S3 displays the phonon band structure with angular-momentum projections; each component ranges from $-\hbar$ to \hbar . Part 5 of Fig. S3 presents the

element-resolved and total phonon density of states.

Appendix E: List of chiral phonon materials

Table S5 summarizes all 2,738 chiral phonon materials on the [CPMDB](#), indicating 869 crystallized in type-II point groups and 1,869 in type-III point groups. Regarding phonon helicity anisotropy, 869 materials are *s*-wave, 1,030 are *d*-wave, 463 are *g*-wave, and 376 are *i*-wave. The table also includes the electronic band gap of each material as determined by ab initio calculations.

TABLE S5: Chiral phonon materials of type-II and type-III point groups on the [CPMDB](#). For each material entry, the table provides its identification number (ID)–linked to its [CPMDB](#) page, space group (SG), associated point group (PG), chemical formula, and electronic band gap. If the phonon spectrum contains a negative (imaginary) frequency (NF) issue, NF is set to 1; otherwise, it is 0. The last two columns indicate the type of point group and the anisotropy characteristics of the phonon helicity pattern in the presence of TRS.

#	ID	SG	PG	chem. formula	Band Gap (eV)	NF	Type	Helicity
1	mp-571132	3 (<i>P</i> 2)	C ₂ (2)	LiMg ₁₀ AlH ₂₄	3.717	0	Type-II	<i>s</i> -wave
2	mp-581967	3 (<i>P</i> 2)	C ₂ (2)	Nb ₂ O ₅	1.773	1	Type-II	<i>s</i> -wave
3	mp-695202	3 (<i>P</i> 2)	C ₂ (2)	Mg ₄ Al ₉ Cu(SiO ₄) ₉	1.989	0	Type-II	<i>s</i> -wave
4	mp-756432	3 (<i>P</i> 2)	C ₂ (2)	Li ₂ Ti(TeO ₄) ₃	1.714	1	Type-II	<i>s</i> -wave
5	mp-758389	3 (<i>P</i> 2)	C ₂ (2)	LiNb(TeO ₄) ₃	1.598	0	Type-II	<i>s</i> -wave
6	mp-758894	3 (<i>P</i> 2)	C ₂ (2)	Li ₂ Ti(TeO ₄) ₃	1.774	0	Type-II	<i>s</i> -wave
7	mp-761825	3 (<i>P</i> 2)	C ₂ (2)	LiSb(TeO ₄) ₃	1.659	0	Type-II	<i>s</i> -wave
8	mp-761842	3 (<i>P</i> 2)	C ₂ (2)	Hf ₃ SnO ₈	3.587	0	Type-II	<i>s</i> -wave
9	mp-849223	3 (<i>P</i> 2)	C ₂ (2)	LiNb(TeO ₄) ₃	1.457	0	Type-II	<i>s</i> -wave
10	mp-849732	3 (<i>P</i> 2)	C ₂ (2)	LiSb(TeO ₄) ₃	1.59	0	Type-II	<i>s</i> -wave
11	mp-850190	3 (<i>P</i> 2)	C ₂ (2)	Li ₄ Ti(TeO ₄) ₃	1.641	1	Type-II	<i>s</i> -wave
12	icsd-52501	4 (<i>P</i> 2 ₁)	C ₂ (2)	Te	0	0	Type-II	<i>s</i> -wave
13	icsd-87272	4 (<i>P</i> 2 ₁)	C ₂ (2)	Te	0	1	Type-II	<i>s</i> -wave
14	icsd-659254	4 (<i>P</i> 2 ₁)	C ₂ (2)	Se	0	1	Type-II	<i>s</i> -wave
15	mp-10517	4 (<i>P</i> 2 ₁)	C ₂ (2)	LiScP ₂ O ₇	4.765	0	Type-II	<i>s</i> -wave
16	mp-11634	4 (<i>P</i> 2 ₁)	C ₂ (2)	KSmGeSe ₄	1.663	0	Type-II	<i>s</i> -wave
17	mp-12011	4 (<i>P</i> 2 ₁)	C ₂ (2)	KTbGeS ₄	2.46	0	Type-II	<i>s</i> -wave
18	mp-12012	4 (<i>P</i> 2 ₁)	C ₂ (2)	KPrGeSe ₄	1.633	0	Type-II	<i>s</i> -wave
19	mp-12177	4 (<i>P</i> 2 ₁)	C ₂ (2)	Te ₂ O ₅	1.682	0	Type-II	<i>s</i> -wave
20	mp-12193	4 (<i>P</i> 2 ₁)	C ₂ (2)	Nd ₂ Ti ₂ O ₇	2.963	1	Type-II	<i>s</i> -wave
21	mp-13538	4 (<i>P</i> 2 ₁)	C ₂ (2)	KPrSiSe ₄	2.177	0	Type-II	<i>s</i> -wave
22	mp-13979	4 (<i>P</i> 2 ₁)	C ₂ (2)	Ca ₂ Nb ₂ O ₇	3.011	1	Type-II	<i>s</i> -wave
23	mp-15201	4 (<i>P</i> 2 ₁)	C ₂ (2)	Pr ₂ Ti ₂ O ₇	2.973	1	Type-II	<i>s</i> -wave
24	mp-16773	4 (<i>P</i> 2 ₁)	C ₂ (2)	KTb(PO ₃) ₄	5.33	0	Type-II	<i>s</i> -wave
25	mp-17008	4 (<i>P</i> 2 ₁)	C ₂ (2)	CaTeO ₃	3.299	0	Type-II	<i>s</i> -wave
26	mp-17894	4 (<i>P</i> 2 ₁)	C ₂ (2)	Rb ₃ Sm(PS ₄) ₂	2.186	0	Type-II	<i>s</i> -wave
27	mp-18168	4 (<i>P</i> 2 ₁)	C ₂ (2)	TlZnPO ₄	3.9	0	Type-II	<i>s</i> -wave
28	mp-18463	4 (<i>P</i> 2 ₁)	C ₂ (2)	RbZnPO ₄	3.715	0	Type-II	<i>s</i> -wave
29	mp-18572	4 (<i>P</i> 2 ₁)	C ₂ (2)	KEr(PO ₃) ₄	5.295	0	Type-II	<i>s</i> -wave
30	mp-18578	4 (<i>P</i> 2 ₁)	C ₂ (2)	TlZnAsO ₄	3.147	0	Type-II	<i>s</i> -wave
31	mp-18661	4 (<i>P</i> 2 ₁)	C ₂ (2)	KY(PO ₃) ₄	5.339	0	Type-II	<i>s</i> -wave
32	mp-21097	4 (<i>P</i> 2 ₁)	C ₂ (2)	KLaGeSe ₄	1.622	0	Type-II	<i>s</i> -wave
33	mp-23360	4 (<i>P</i> 2 ₁)	C ₂ (2)	Zn(IO ₃) ₂	3.26	0	Type-II	<i>s</i> -wave
34	mp-23535	4 (<i>P</i> 2 ₁)	C ₂ (2)	K ₂ ZnBr ₄	3.677	0	Type-II	<i>s</i> -wave
35	mp-23544	4 (<i>P</i> 2 ₁)	C ₂ (2)	Bi ₄ Br ₂ O ₅	2.652	0	Type-II	<i>s</i> -wave
36	mp-23719	4 (<i>P</i> 2 ₁)	C ₂ (2)	BeAlH ₅	3.204	0	Type-II	<i>s</i> -wave
37	mp-28348	4 (<i>P</i> 2 ₁)	C ₂ (2)	Ba ₂ As ₂ Se ₅	1.155	0	Type-II	<i>s</i> -wave
38	mp-28759	4 (<i>P</i> 2 ₁)	C ₂ (2)	Al ₇ (TlS ₄) ₃	2.796	0	Type-II	<i>s</i> -wave
39	mp-29187	4 (<i>P</i> 2 ₁)	C ₂ (2)	Co(SiP) ₃	1.263	0	Type-II	<i>s</i> -wave
40	mp-29198	4 (<i>P</i> 2 ₁)	C ₂ (2)	Na ₅ AuSe ₁₂	1.075	0	Type-II	<i>s</i> -wave
41	mp-30130	4 (<i>P</i> 2 ₁)	C ₂ (2)	Bi ₄ I ₂ O ₅	2.362	0	Type-II	<i>s</i> -wave
42	mp-30532	4 (<i>P</i> 2 ₁)	C ₂ (2)	Tl ₂ ZnI ₄	2.937	0	Type-II	<i>s</i> -wave
43	mp-3094	4 (<i>P</i> 2 ₁)	C ₂ (2)	SrAl ₂ O ₄	4.142	0	Type-II	<i>s</i> -wave

44	mp-38322	4 (P_{21})	C ₂ (2)	Mg(IO ₃) ₂	3.484	0	Type-II	s-wave
45	mp-5263	4 (P_{21})	C ₂ (2)	Ca ₄ P ₂ O ₉	4.747	0	Type-II	s-wave
46	mp-542749	4 (P_{21})	C ₂ (2)	K ₂ (MoSe ₆) ₃	0.862	0	Type-II	s-wave
47	mp-553897	4 (P_{21})	C ₂ (2)	Ba ₂ Si ₃ O ₈	4.813	0	Type-II	s-wave
48	mp-554704	4 (P_{21})	C ₂ (2)	TiPHO ₅	2.85	1	Type-II	s-wave
49	mp-555191	4 (P_{21})	C ₂ (2)	La ₃ Si ₂ Cl ₃ O ₇	3.869	0	Type-II	s-wave
50	mp-555202	4 (P_{21})	C ₂ (2)	KTeHOF ₄	5.032	0	Type-II	s-wave
51	mp-555284	4 (P_{21})	C ₂ (2)	Ba ₂ NdAlO ₅	3.691	0	Type-II	s-wave
52	mp-556592	4 (P_{21})	C ₂ (2)	TlBi(PS ₃) ₂	2.031	0	Type-II	s-wave
53	mp-556609	4 (P_{21})	C ₂ (2)	KSB(P ₃) ₂	2.273	0	Type-II	s-wave
54	mp-556806	4 (P_{21})	C ₂ (2)	BaNa ₂ (SiO ₃) ₂	4.173	0	Type-II	s-wave
55	mp-556884	4 (P_{21})	C ₂ (2)	CaSi ₂ (NO) ₂	4.369	0	Type-II	s-wave
56	mp-557082	4 (P_{21})	C ₂ (2)	H ₂ O	5.458	1	Type-II	s-wave
57	mp-557301	4 (P_{21})	C ₂ (2)	K ₂ Ti(Si ₂ O ₅) ₃	3.439	1	Type-II	s-wave
58	mp-557437	4 (P_{21})	C ₂ (2)	KBi(PS ₃) ₂	2.227	0	Type-II	s-wave
59	mp-557728	4 (P_{21})	C ₂ (2)	KCu ₄ AsS ₄	1.288	0	Type-II	s-wave
60	mp-557836	4 (P_{21})	C ₂ (2)	Na ₅ B ₂ P ₃ O ₁₃	5.079	1	Type-II	s-wave
61	mp-558102	4 (P_{21})	C ₂ (2)	KLiSi ₂ O ₅	4.707	0	Type-II	s-wave
62	mp-559043	4 (P_{21})	C ₂ (2)	KLaGeS ₄	2.304	0	Type-II	s-wave
63	mp-559144	4 (P_{21})	C ₂ (2)	GePb ₃ O ₅	2.271	0	Type-II	s-wave
64	mp-559184	4 (P_{21})	C ₂ (2)	Zn ₂ Si ₃ Pb ₄ SO ₁₅	3.607	0	Type-II	s-wave
65	mp-559391	4 (P_{21})	C ₂ (2)	Pr ₃ Si ₂ Cl ₃ O ₇	4.848	0	Type-II	s-wave
66	mp-559768	4 (P_{21})	C ₂ (2)	La ₂ Ti ₂ O ₇	2.917	1	Type-II	s-wave
67	mp-560173	4 (P_{21})	C ₂ (2)	KAlSiO ₄	4.761	0	Type-II	s-wave
68	mp-561022	4 (P_{21})	C ₂ (2)	SrMgF ₄	6.687	1	Type-II	s-wave
69	mp-561303	4 (P_{21})	C ₂ (2)	NaSb(PS ₃) ₂	2.151	0	Type-II	s-wave
70	mp-567472	4 (P_{21})	C ₂ (2)	CuP ₄ I	1.001	0	Type-II	s-wave
71	mp-567594	4 (P_{21})	C ₂ (2)	Cs ₂ HgI ₄	2.066	0	Type-II	s-wave
72	mp-568802	4 (P_{21})	C ₂ (2)	KBi(PS ₃) ₂	1.764	0	Type-II	s-wave
73	mp-5707	4 (P_{21})	C ₂ (2)	CsAsF ₄	4.613	0	Type-II	s-wave
74	mp-608653	4 (P_{21})	C ₂ (2)	As ₂ Pb ₂ S ₅	1.709	1	Type-II	s-wave
75	mp-625359	4 (P_{21})	C ₂ (2)	NdHO ₂	4.159	0	Type-II	s-wave
76	mp-625857	4 (P_{21})	C ₂ (2)	Zn(HO) ₂	3.205	0	Type-II	s-wave
77	mp-626716	4 (P_{21})	C ₂ (2)	KHO	3.619	0	Type-II	s-wave
78	mp-626721	4 (P_{21})	C ₂ (2)	RbHO	3.344	0	Type-II	s-wave
79	mp-634418	4 (P_{21})	C ₂ (2)	NaCaSiHO ₄	4.492	0	Type-II	s-wave
80	mp-6433	4 (P_{21})	C ₂ (2)	KNd(PO ₃) ₄	5.354	0	Type-II	s-wave
81	mp-6481	4 (P_{21})	C ₂ (2)	Na ₂ ZnSi ₃ O ₈	3.947	0	Type-II	s-wave
82	mp-6903	4 (P_{21})	C ₂ (2)	Na ₂ Ca ₄ ZrNbSi ₄ O ₁₇ F	4.04	0	Type-II	s-wave
83	mp-690929	4 (P_{21})	C ₂ (2)	Cs ₄ MgZr ₃ (PO ₄) ₆	3.769	0	Type-II	s-wave
84	mp-696946	4 (P_{21})	C ₂ (2)	BaSn ₂ (HO ₂) ₂	2.102	0	Type-II	s-wave
85	mp-7123	4 (P_{21})	C ₂ (2)	KSB(PS ₃) ₂	1.806	0	Type-II	s-wave
86	mp-7305	4 (P_{21})	C ₂ (2)	SmZrF ₇	5.908	0	Type-II	s-wave
87	mp-752425	4 (P_{21})	C ₂ (2)	Dy ₂ Ti ₂ O ₇	3.057	1	Type-II	s-wave
88	mp-758770	4 (P_{21})	C ₂ (2)	Li ₂ Mg ₃ Ti ₆ O ₁₆	3.332	1	Type-II	s-wave
89	mp-759849	4 (P_{21})	C ₂ (2)	Li ₂ Ti ₆ Zn ₃ O ₁₆	2.893	1	Type-II	s-wave
90	mp-762225	4 (P_{21})	C ₂ (2)	BaCO ₃	4.474	0	Type-II	s-wave
91	mp-768695	4 (P_{21})	C ₂ (2)	Ho ₂ Ti ₂ O ₇	3.066	1	Type-II	s-wave
92	mp-771323	4 (P_{21})	C ₂ (2)	Tm ₂ Ti ₂ O ₇	3.068	1	Type-II	s-wave
93	mp-772758	4 (P_{21})	C ₂ (2)	Sm ₂ Zr ₂ O ₇	3.963	1	Type-II	s-wave
94	mp-772760	4 (P_{21})	C ₂ (2)	Dy ₂ Zr ₂ O ₇	4.075	1	Type-II	s-wave
95	mp-772783	4 (P_{21})	C ₂ (2)	Li ₂ Mg ₃ Ti ₆ O ₁₆	3.303	1	Type-II	s-wave
96	mp-772850	4 (P_{21})	C ₂ (2)	La ₂ Hf ₂ O ₇	4.292	1	Type-II	s-wave
97	mp-775918	4 (P_{21})	C ₂ (2)	LaTiNO ₂	1.214	0	Type-II	s-wave
98	mp-776407	4 (P_{21})	C ₂ (2)	LaTa ₂ NO ₅	2.517	0	Type-II	s-wave
99	mp-778102	4 (P_{21})	C ₂ (2)	BaYF ₅	6.859	0	Type-II	s-wave
100	mp-779763	4 (P_{21})	C ₂ (2)	Tb ₂ Ti ₂ O ₇	3.1	1	Type-II	s-wave
101	mp-8491	4 (P_{21})	C ₂ (2)	LiInP ₂ O ₇	3.973	0	Type-II	s-wave
102	mp-861606	4 (P_{21})	C ₂ (2)	KLaSiSe ₄	2.208	0	Type-II	s-wave

103	mp-861866	4 ($P2_1$)	C ₂ (2)	KNdGeS ₄	2.367	0	Type-II	<i>s</i> -wave
104	mp-861938	4 ($P2_1$)	C ₂ (2)	KLaSiS ₄	2.869	0	Type-II	<i>s</i> -wave
105	mp-867328	4 ($P2_1$)	C ₂ (2)	KYSiS ₄	2.829	0	Type-II	<i>s</i> -wave
106	mp-867334	4 ($P2_1$)	C ₂ (2)	KYGeS ₄	2.418	0	Type-II	<i>s</i> -wave
107	mp-9427	4 ($P2_1$)	C ₂ (2)	NaYP ₂ O ₇	5.281	0	Type-II	<i>s</i> -wave
108	mp-972831	4 ($P2_1$)	C ₂ (2)	SiGeN ₂ O	3.657	0	Type-II	<i>s</i> -wave
109	mp-975577	4 ($P2_1$)	C ₂ (2)	K ₃ La(AsO ₄) ₂	3.882	0	Type-II	<i>s</i> -wave
110	mp-995190	4 ($P2_1$)	C ₂ (2)	KCaSiHO ₄	4.351	0	Type-II	<i>s</i> -wave
111	mp-11131	5 ($C2$)	C ₂ (2)	K ₂ Hg ₃ (GeS ₄) ₂	1.551	0	Type-II	<i>s</i> -wave
112	mp-23349	5 ($C2$)	C ₂ (2)	Bi(BO ₂) ₃	3.844	0	Type-II	<i>s</i> -wave
113	mp-24181	5 ($C2$)	C ₂ (2)	CsGaP ₃ HO ₁₀	4.612	0	Type-II	<i>s</i> -wave
114	mp-27171	5 ($C2$)	C ₂ (2)	Hg ₂ P ₂ S ₇	1.809	0	Type-II	<i>s</i> -wave
115	mp-33318	5 ($C2$)	C ₂ (2)	Ca ₁₁ Al ₁₄ O ₃₂	3.433	0	Type-II	<i>s</i> -wave
116	mp-35799	5 ($C2$)	C ₂ (2)	Hf ₂ Bi ₂ O ₇	2.937	1	Type-II	<i>s</i> -wave
117	mp-36165	5 ($C2$)	C ₂ (2)	Na ₁₀ Zn ₄ O ₉	1.487	0	Type-II	<i>s</i> -wave
118	mp-36641	5 ($C2$)	C ₂ (2)	Cd(Ga ₃ Te ₅) ₂	0.634	0	Type-II	<i>s</i> -wave
119	mp-531826	5 ($C2$)	C ₂ (2)	Li ₂ PtO ₃	1.842	0	Type-II	<i>s</i> -wave
120	mp-545346	5 ($C2$)	C ₂ (2)	LiGaAs ₂ O ₇	2.546	0	Type-II	<i>s</i> -wave
121	mp-546285	5 ($C2$)	C ₂ (2)	NbI ₃ O	0.82	0	Type-II	<i>s</i> -wave
122	mp-547017	5 ($C2$)	C ₂ (2)	LiAlAs ₂ O ₇	3.05	0	Type-II	<i>s</i> -wave
123	mp-549720	5 ($C2$)	C ₂ (2)	NbI ₂ O	0.843	0	Type-II	<i>s</i> -wave
124	mp-550070	5 ($C2$)	C ₂ (2)	NbBr ₂ O	0.904	0	Type-II	<i>s</i> -wave
125	mp-550925	5 ($C2$)	C ₂ (2)	NaScAs ₂ O ₇	3.46	0	Type-II	<i>s</i> -wave
126	mp-551826	5 ($C2$)	C ₂ (2)	NbTlBr ₄ O	1.25	0	Type-II	<i>s</i> -wave
127	mp-552663	5 ($C2$)	C ₂ (2)	LiScAs ₂ O ₇	3.452	1	Type-II	<i>s</i> -wave
128	mp-555966	5 ($C2$)	C ₂ (2)	BaTi ₂ O ₅	2.147	1	Type-II	<i>s</i> -wave
129	mp-556676	5 ($C2$)	C ₂ (2)	Na ₃ Al ₂ (AsO ₄) ₃	3.386	0	Type-II	<i>s</i> -wave
130	mp-556865	5 ($C2$)	C ₂ (2)	NaBe ₂ BO ₃ F ₂	5.939	0	Type-II	<i>s</i> -wave
131	mp-557584	5 ($C2$)	C ₂ (2)	K ₄ Ba(GeO ₃) ₃	3.235	0	Type-II	<i>s</i> -wave
132	mp-557632	5 ($C2$)	C ₂ (2)	K ₂ LiBO ₃	3.583	0	Type-II	<i>s</i> -wave
133	mp-560019	5 ($C2$)	C ₂ (2)	K ₂ Ge ₃ (BO ₅) ₂	3.868	0	Type-II	<i>s</i> -wave
134	mp-560570	5 ($C2$)	C ₂ (2)	Rb ₂ NaAl ₆ F ₂₁	7.004	0	Type-II	<i>s</i> -wave
135	mp-561075	5 ($C2$)	C ₂ (2)	Na ₂ CdSnS ₄	1.925	0	Type-II	<i>s</i> -wave
136	mp-561245	5 ($C2$)	C ₂ (2)	Sr ₈ Si ₂ PtO ₁₄	2.26	1	Type-II	<i>s</i> -wave
137	mp-561412	5 ($C2$)	C ₂ (2)	CaCO ₃	4.973	0	Type-II	<i>s</i> -wave
138	mp-608311	5 ($C2$)	C ₂ (2)	Cs ₂ Li ₃ I ₅	3.826	0	Type-II	<i>s</i> -wave
139	mp-625565	5 ($C2$)	C ₂ (2)	Cd(HO) ₂	1.786	0	Type-II	<i>s</i> -wave
140	mp-626143	5 ($C2$)	C ₂ (2)	Mg(HO) ₂	4.205	1	Type-II	<i>s</i> -wave
141	mp-626644	5 ($C2$)	C ₂ (2)	Ca(HO) ₂	4.219	0	Type-II	<i>s</i> -wave
142	mp-675118	5 ($C2$)	C ₂ (2)	Y ₂ Th ₈ O ₁₉	3.018	1	Type-II	<i>s</i> -wave
143	mp-675750	5 ($C2$)	C ₂ (2)	Ca(Ga ₃ Te ₅) ₂	0.737	0	Type-II	<i>s</i> -wave
144	mp-676110	5 ($C2$)	C ₂ (2)	Tb ₁₄ (PbSe ₈) ₃	1.821	0	Type-II	<i>s</i> -wave
145	mp-676644	5 ($C2$)	C ₂ (2)	Yb(Ga ₃ Te ₅) ₂	1.051	0	Type-II	<i>s</i> -wave
146	mp-677731	5 ($C2$)	C ₂ (2)	Rb ₂ NaNb ₆ (PO ₈) ₃	2.248	1	Type-II	<i>s</i> -wave
147	mp-680676	5 ($C2$)	C ₂ (2)	K ₂ Dy ₄ Cu ₄ S ₉	1.131	0	Type-II	<i>s</i> -wave
148	mp-683957	5 ($C2$)	C ₂ (2)	Nd ₄ CuTe ₅ (ClO ₅) ₃	1.491	1	Type-II	<i>s</i> -wave
149	mp-686004	5 ($C2$)	C ₂ (2)	Li ₃ ScCl ₆	3.677	1	Type-II	<i>s</i> -wave
150	mp-697960	5 ($C2$)	C ₂ (2)	Ba ₂ Na ₂ B ₁₀ H ₂ O ₁₉	4.693	0	Type-II	<i>s</i> -wave
151	mp-7079	5 ($C2$)	C ₂ (2)	CaZrSi ₂ O ₇	4.553	0	Type-II	<i>s</i> -wave
152	mp-7147	5 ($C2$)	C ₂ (2)	KCrP ₂ S ₇	1.129	0	Type-II	<i>s</i> -wave
153	mp-752767	5 ($C2$)	C ₂ (2)	LiAgF ₂	1.863	0	Type-II	<i>s</i> -wave
154	mp-756854	5 ($C2$)	C ₂ (2)	Sr ₂ LiNb ₃ O ₁₀	1.765	1	Type-II	<i>s</i> -wave
155	mp-757001	5 ($C2$)	C ₂ (2)	Y ₁₅ TmO ₂₄	4.143	0	Type-II	<i>s</i> -wave
156	mp-757197	5 ($C2$)	C ₂ (2)	DyY ₃ O ₆	4.022	0	Type-II	<i>s</i> -wave
157	mp-757791	5 ($C2$)	C ₂ (2)	SmY ₁₅ O ₂₄	4.112	0	Type-II	<i>s</i> -wave
158	mp-759638	5 ($C2$)	C ₂ (2)	Y ₅ Tm ₁₁ O ₂₄	4.147	0	Type-II	<i>s</i> -wave
159	mp-759876	5 ($C2$)	C ₂ (2)	Na ₅ SbO ₅	1.654	0	Type-II	<i>s</i> -wave
160	mp-766207	5 ($C2$)	C ₂ (2)	Zr ₆ Nb ₂ O ₁₇	2.052	1	Type-II	<i>s</i> -wave
161	mp-766256	5 ($C2$)	C ₂ (2)	YTmO ₃	4.156	0	Type-II	<i>s</i> -wave

162	mp-770456	5 (<i>C</i> 2)	C ₂ (2)	Li ₆ Ti ₂ O ₇	2.426	0	Type-II	<i>s</i> -wave
163	mp-772968	5 (<i>C</i> 2)	C ₂ (2)	LiTlPHO ₃	3.992	0	Type-II	<i>s</i> -wave
164	mp-849636	5 (<i>C</i> 2)	C ₂ (2)	SrTaNO ₂	1.087	1	Type-II	<i>s</i> -wave
165	mp-867329	5 (<i>C</i> 2)	C ₂ (2)	K ₂ ZnH ₄ (I ₂ O ₇) ₂	3.118	1	Type-II	<i>s</i> -wave
166	mp-40519	6 (<i>Pm</i>)	C _s (m)	Na ₃ Sr ₇ Ta ₃ Ti ₇ O ₃₀	1.794	1	Type-III	<i>d</i> -wave
167	mp-625452	6 (<i>Pm</i>)	C _s (m)	Pr(HO) ₃	3.812	1	Type-III	<i>d</i> -wave
168	mp-674333	6 (<i>Pm</i>)	C _s (m)	Na ₃ PO ₄	3.919	0	Type-III	<i>d</i> -wave
169	mp-695409	6 (<i>Pm</i>)	C _s (m)	Ba ₇ Na ₃ Ti ₇ Nb ₃ O ₃₀	1.114	1	Type-III	<i>d</i> -wave
170	mp-721011	6 (<i>Pm</i>)	C _s (m)	Pr ₂₀ AlSi ₁₉ N ₃₃ Cl ₂ O ₁₉	3.013	0	Type-III	<i>d</i> -wave
171	mp-754505	6 (<i>Pm</i>)	C _s (m)	SrTaNO ₂	0.813	1	Type-III	<i>d</i> -wave
172	mp-755441	6 (<i>Pm</i>)	C _s (m)	SrTaNO ₂	0.982	1	Type-III	<i>d</i> -wave
173	mp-758059	6 (<i>Pm</i>)	C _s (m)	Ba ₇ Pb ₁₇ O ₂₄	2.12	1	Type-III	<i>d</i> -wave
174	mp-758379	6 (<i>Pm</i>)	C _s (m)	Y ₁₁ Ta ₅ O ₂₈	0.986	1	Type-III	<i>d</i> -wave
175	mp-778064	6 (<i>Pm</i>)	C _s (m)	Ga ₃ NO ₃	0.939	1	Type-III	<i>d</i> -wave
176	mp-977164	6 (<i>Pm</i>)	C _s (m)	Li ₃ H ₃ N ₂	1.957	1	Type-III	<i>d</i> -wave
177	mp-13923	7 (<i>Pc</i>)	C _s (m)	SnPS ₃	2.13	0	Type-III	<i>d</i> -wave
178	mp-15144	7 (<i>Pc</i>)	C _s (m)	ZnAg ₂ GeO ₄	0.267	0	Type-III	<i>d</i> -wave
179	mp-15559	7 (<i>Pc</i>)	C _s (m)	KSb ₅ S ₈	1.592	0	Type-III	<i>d</i> -wave
180	mp-23376	7 (<i>Pc</i>)	C _s (m)	GaSeBr ₇	2.22	0	Type-III	<i>d</i> -wave
181	mp-27181	7 (<i>Pc</i>)	C _s (m)	KAuCl ₄	1.426	0	Type-III	<i>d</i> -wave
182	mp-28361	7 (<i>Pc</i>)	C _s (m)	Al ₂ CdCl ₈	3.708	0	Type-III	<i>d</i> -wave
183	mp-29018	7 (<i>Pc</i>)	C _s (m)	ZrSnCl ₆	2.226	1	Type-III	<i>d</i> -wave
184	mp-29193	7 (<i>Pc</i>)	C _s (m)	Nb ₂ Se ₄ O ₁₃	2.427	1	Type-III	<i>d</i> -wave
185	mp-29407	7 (<i>Pc</i>)	C _s (m)	AlTeI ₇	1.885	0	Type-III	<i>d</i> -wave
186	mp-29408	7 (<i>Pc</i>)	C _s (m)	AlSeBr ₇	2.194	0	Type-III	<i>d</i> -wave
187	mp-29703	7 (<i>Pc</i>)	C _s (m)	BaSi ₇ N ₁₀	3.912	0	Type-III	<i>d</i> -wave
188	mp-29895	7 (<i>Pc</i>)	C _s (m)	Rb ₃ Bi ₂ I ₉	2.475	0	Type-III	<i>d</i> -wave
189	mp-30325	7 (<i>Pc</i>)	C _s (m)	In ₂ (Se ₂ O ₅) ₃	3.48	1	Type-III	<i>d</i> -wave
190	mp-31243	7 (<i>Pc</i>)	C _s (m)	BaAs ₂	0.414	0	Type-III	<i>d</i> -wave
191	mp-3267	7 (<i>Pc</i>)	C _s (m)	TlSb ₅ S ₈	1.587	0	Type-III	<i>d</i> -wave
192	mp-3926	7 (<i>Pc</i>)	C _s (m)	NbAg ₇ S ₆	0.911	0	Type-III	<i>d</i> -wave
193	mp-5116	7 (<i>Pc</i>)	C _s (m)	K ₆ Ge ₂ O ₇	3.083	1	Type-III	<i>d</i> -wave
194	mp-532604	7 (<i>Pc</i>)	C _s (m)	Na ₂ Zr ₁₂ B ₂ I ₅ Cl ₂₃	1.272	0	Type-III	<i>d</i> -wave
195	mp-542863	7 (<i>Pc</i>)	C _s (m)	Ca ₇ NbSi ₄ O ₁₇ F	3.551	1	Type-III	<i>d</i> -wave
196	mp-555006	7 (<i>Pc</i>)	C _s (m)	CsGa ₂ P ₅ O ₁₆	4.418	1	Type-III	<i>d</i> -wave
197	mp-555186	7 (<i>Pc</i>)	C _s (m)	Li ₂ ZnSnS ₄	2.176	0	Type-III	<i>d</i> -wave
198	mp-555805	7 (<i>Pc</i>)	C _s (m)	AlS ₂ Cl ₇	2.496	0	Type-III	<i>d</i> -wave
199	mp-556544	7 (<i>Pc</i>)	C _s (m)	LiAlSiO ₄	5.021	0	Type-III	<i>d</i> -wave
200	mp-557705	7 (<i>Pc</i>)	C _s (m)	OsO ₂ F ₃	0.574	0	Type-III	<i>d</i> -wave
201	mp-560228	7 (<i>Pc</i>)	C _s (m)	K ₆ Ti ₂ O ₇	3.455	0	Type-III	<i>d</i> -wave
202	mp-560847	7 (<i>Pc</i>)	C _s (m)	Nb ₂ TlPS ₁₀	1.345	0	Type-III	<i>d</i> -wave
203	mp-570370	7 (<i>Pc</i>)	C _s (m)	SnPSe ₃	1.497	0	Type-III	<i>d</i> -wave
204	mp-570598	7 (<i>Pc</i>)	C _s (m)	SrSi ₇ N ₁₀	3.866	0	Type-III	<i>d</i> -wave
205	mp-625526	7 (<i>Pc</i>)	C _s (m)	Te(HO ₂) ₂	1.72	0	Type-III	<i>d</i> -wave
206	mp-625856	7 (<i>Pc</i>)	C _s (m)	TeHO ₃	2.058	1	Type-III	<i>d</i> -wave
207	mp-6391	7 (<i>Pc</i>)	C _s (m)	Na ₂ ZnSiO ₄	3.174	0	Type-III	<i>d</i> -wave
208	mp-6402	7 (<i>Pc</i>)	C _s (m)	Na ₂ ZnGeO ₄	2.64	0	Type-III	<i>d</i> -wave
209	mp-6406	7 (<i>Pc</i>)	C _s (m)	Na ₂ MgSiO ₄	3.749	0	Type-III	<i>d</i> -wave
210	mp-6708	7 (<i>Pc</i>)	C _s (m)	RbNb ₂ PS ₁₀	1.552	0	Type-III	<i>d</i> -wave
211	mp-674465	7 (<i>Pc</i>)	C _s (m)	K ₂ SrCl ₄	4.988	0	Type-III	<i>d</i> -wave
212	mp-677002	7 (<i>Pc</i>)	C _s (m)	SrZr ₁₂ B ₂ I ₅ Cl ₂₃	1.19	0	Type-III	<i>d</i> -wave
213	mp-696288	7 (<i>Pc</i>)	C _s (m)	LiH ₃ (SeO ₃) ₂	4.32	0	Type-III	<i>d</i> -wave
214	mp-723064	7 (<i>Pc</i>)	C _s (m)	Ti ₃ (BiO ₃) ₄	2.372	1	Type-III	<i>d</i> -wave
215	mp-753460	7 (<i>Pc</i>)	C _s (m)	BaCa ₂ I ₆	3.945	0	Type-III	<i>d</i> -wave
216	mp-756088	7 (<i>Pc</i>)	C _s (m)	SrTaNO ₂	1.707	0	Type-III	<i>d</i> -wave
217	mp-771883	7 (<i>Pc</i>)	C _s (m)	Sr ₃ LaCl ₉	3.675	1	Type-III	<i>d</i> -wave
218	mp-771955	7 (<i>Pc</i>)	C _s (m)	Sr ₃ LaBr ₉	2.984	0	Type-III	<i>d</i> -wave
219	mp-772018	7 (<i>Pc</i>)	C _s (m)	Ba ₃ YI ₉	2.647	0	Type-III	<i>d</i> -wave
220	mp-772024	7 (<i>Pc</i>)	C _s (m)	Ba ₃ LaBr ₉	3.035	0	Type-III	<i>d</i> -wave

221	mp-772034	7 (<i>Pc</i>)	C _s (m)	Ba ₃ LaI ₉	2.252	0	Type-III	<i>d</i> -wave
222	mp-772074	7 (<i>Pc</i>)	C _s (m)	Sr ₃ LaI ₉	2.18	0	Type-III	<i>d</i> -wave
223	mp-777773	7 (<i>Pc</i>)	C _s (m)	LaTa ₂ NO ₅	2.398	0	Type-III	<i>d</i> -wave
224	mp-8070	7 (<i>Pc</i>)	C _s (m)	Li ₂ BeSiO ₄	6.056	0	Type-III	<i>d</i> -wave
225	mp-8184	7 (<i>Pc</i>)	C _s (m)	Li ₂ ZnGeO ₄	3.105	0	Type-III	<i>d</i> -wave
226	mp-9359	7 (<i>Pc</i>)	C _s (m)	ZnSi(AgO ₂) ₂	0.607	0	Type-III	<i>d</i> -wave
227	mp-984519	7 (<i>Pc</i>)	C _s (m)	NaAsSe ₂	1.432	0	Type-III	<i>d</i> -wave
228	mp-27821	8 (<i>Cm</i>)	C _s (m)	Ag ₃ P ₁₁	0.831	0	Type-III	<i>d</i> -wave
229	mp-28456	8 (<i>Cm</i>)	C _s (m)	Sn ₁₅ Os ₃ O ₁₄	1.508	0	Type-III	<i>d</i> -wave
230	mp-28769	8 (<i>Cm</i>)	C _s (m)	K(SnSe ₂) ₂	1.173	0	Type-III	<i>d</i> -wave
231	mp-28790	8 (<i>Cm</i>)	C _s (m)	Al ₁₃ (TlS ₇) ₃	3.119	0	Type-III	<i>d</i> -wave
232	mp-29365	8 (<i>Cm</i>)	C _s (m)	Li ₅ BiO ₅	1.36	1	Type-III	<i>d</i> -wave
233	mp-34038	8 (<i>Cm</i>)	C _s (m)	Li ₆ NCl ₃	1.387	0	Type-III	<i>d</i> -wave
234	mp-35712	8 (<i>Cm</i>)	C _s (m)	Mg(GaO ₂) ₂	2.417	1	Type-III	<i>d</i> -wave
235	mp-39003	8 (<i>Cm</i>)	C _s (m)	Mg ₃ Al ₁₄ O ₂₄	4.312	1	Type-III	<i>d</i> -wave
236	mp-530121	8 (<i>Cm</i>)	C _s (m)	Mg(GaO ₂) ₂	2.295	1	Type-III	<i>d</i> -wave
237	mp-530216	8 (<i>Cm</i>)	C _s (m)	MgAl ₆ O ₁₀	3.403	0	Type-III	<i>d</i> -wave
238	mp-530303	8 (<i>Cm</i>)	C _s (m)	Mg(GaO ₂) ₂	2.473	1	Type-III	<i>d</i> -wave
239	mp-530748	8 (<i>Cm</i>)	C _s (m)	MgAl ₂ O ₄	4.139	0	Type-III	<i>d</i> -wave
240	mp-530826	8 (<i>Cm</i>)	C _s (m)	Mg ₇ Al ₂₂ O ₄₀	3.523	0	Type-III	<i>d</i> -wave
241	mp-531340	8 (<i>Cm</i>)	C _s (m)	MgAl ₂ O ₄	2.849	0	Type-III	<i>d</i> -wave
242	mp-531840	8 (<i>Cm</i>)	C _s (m)	MgAl ₂ O ₄	3.812	1	Type-III	<i>d</i> -wave
243	mp-532405	8 (<i>Cm</i>)	C _s (m)	MgAl ₆ O ₁₀	1.914	1	Type-III	<i>d</i> -wave
244	mp-540574	8 (<i>Cm</i>)	C _s (m)	Cs ₂ Hg ₃ I ₈	1.731	0	Type-III	<i>d</i> -wave
245	mp-550751	8 (<i>Cm</i>)	C _s (m)	BaBeSiO ₄	4.611	1	Type-III	<i>d</i> -wave
246	mp-553374	8 (<i>Cm</i>)	C _s (m)	Cs ₄ Sb ₂ O ₅	2.575	0	Type-III	<i>d</i> -wave
247	mp-559916	8 (<i>Cm</i>)	C _s (m)	Na ₁₇ Al ₅ O ₁₆	2.442	1	Type-III	<i>d</i> -wave
248	mp-561121	8 (<i>Cm</i>)	C _s (m)	CsTi ₃ P ₅ O ₁₉	2.791	1	Type-III	<i>d</i> -wave
249	mp-570756	8 (<i>Cm</i>)	C _s (m)	Cs ₃ Li ₂ Cl ₅	5.089	0	Type-III	<i>d</i> -wave
250	mp-6076	8 (<i>Cm</i>)	C _s (m)	Ca ₄ LaB ₃ O ₁₀	4.303	1	Type-III	<i>d</i> -wave
251	mp-625521	8 (<i>Cm</i>)	C _s (m)	H ₃ BrO	4.417	0	Type-III	<i>d</i> -wave
252	mp-626497	8 (<i>Cm</i>)	C _s (m)	Al(HO) ₃	4.697	0	Type-III	<i>d</i> -wave
253	mp-626550	8 (<i>Cm</i>)	C _s (m)	Ti ₃ H ₂ O ₇	2.873	1	Type-III	<i>d</i> -wave
254	mp-630927	8 (<i>Cm</i>)	C _s (m)	Pb ₄ SeBr ₆	1.978	0	Type-III	<i>d</i> -wave
255	mp-6388	8 (<i>Cm</i>)	C _s (m)	Ca ₄ SmB ₃ O ₁₀	4.398	1	Type-III	<i>d</i> -wave
256	mp-646007	8 (<i>Cm</i>)	C _s (m)	Cs ₂ Tb ₆ Te ₇ N ₂	0.743	0	Type-III	<i>d</i> -wave
257	mp-650619	8 (<i>Cm</i>)	C _s (m)	Cs ₃ Bi ₇ Se ₁₂	0.61	0	Type-III	<i>d</i> -wave
258	mp-662823	8 (<i>Cm</i>)	C _s (m)	In ₁₀ (Pb ₂ S ₇) ₃	1.313	0	Type-III	<i>d</i> -wave
259	mp-6632	8 (<i>Cm</i>)	C _s (m)	Ca ₅ B ₃ O ₉ F	4.237	1	Type-III	<i>d</i> -wave
260	mp-675342	8 (<i>Cm</i>)	C _s (m)	NdPb ₄ F ₁₁	4.438	1	Type-III	<i>d</i> -wave
261	mp-675376	8 (<i>Cm</i>)	C _s (m)	HoAgSe ₂	0.713	0	Type-III	<i>d</i> -wave
262	mp-675488	8 (<i>Cm</i>)	C _s (m)	Li ₆ I ₃ N	2.357	1	Type-III	<i>d</i> -wave
263	mp-675941	8 (<i>Cm</i>)	C _s (m)	Li ₇ IN ₂	1.91	0	Type-III	<i>d</i> -wave
264	mp-676284	8 (<i>Cm</i>)	C _s (m)	YAgSe ₂	0.516	1	Type-III	<i>d</i> -wave
265	mp-676572	8 (<i>Cm</i>)	C _s (m)	NdPb ₆ F ₁₅	4.41	1	Type-III	<i>d</i> -wave
266	mp-676650	8 (<i>Cm</i>)	C _s (m)	Li ₆ Br ₃ N	2.092	1	Type-III	<i>d</i> -wave
267	mp-680679	8 (<i>Cm</i>)	C _s (m)	K ₂ Ho ₄ Cu ₄ S ₉	1.184	0	Type-III	<i>d</i> -wave
268	mp-685982	8 (<i>Cm</i>)	C _s (m)	MgIn ₂ O ₄	1.222	0	Type-III	<i>d</i> -wave
269	mp-695325	8 (<i>Cm</i>)	C _s (m)	Ti ₅ ZnBi ₂ (Pb ₂ O ₉) ₂	1.948	1	Type-III	<i>d</i> -wave
270	mp-720985	8 (<i>Cm</i>)	C _s (m)	CaEr ₁₅ Si ₈ Se ₁₁ ClO ₂₈	2.575	0	Type-III	<i>d</i> -wave
271	mp-733443	8 (<i>Cm</i>)	C _s (m)	Ca ₇ Si ₆ H ₄ CO ₂₃	4.581	1	Type-III	<i>d</i> -wave
272	mp-753048	8 (<i>Cm</i>)	C _s (m)	TiSnO ₄	1.837	0	Type-III	<i>d</i> -wave
273	mp-754668	8 (<i>Cm</i>)	C _s (m)	Hf ₃ N ₂ O ₃	3.262	0	Type-III	<i>d</i> -wave
274	mp-754790	8 (<i>Cm</i>)	C _s (m)	Ti ₃ N ₂ O ₃	1.547	0	Type-III	<i>d</i> -wave
275	mp-755078	8 (<i>Cm</i>)	C _s (m)	Sr ₂ Ti ₆ N ₂ O ₁₁	1.758	1	Type-III	<i>d</i> -wave
276	mp-755132	8 (<i>Cm</i>)	C _s (m)	Zr ₃ N ₂ O ₃	2.683	0	Type-III	<i>d</i> -wave
277	mp-755353	8 (<i>Cm</i>)	C _s (m)	Sr ₂ Ti ₆ N ₂ O ₁₁	1.777	1	Type-III	<i>d</i> -wave
278	mp-755491	8 (<i>Cm</i>)	C _s (m)	Sr ₂ Ti ₆ N ₂ O ₁₁	2.211	1	Type-III	<i>d</i> -wave
279	mp-755505	8 (<i>Cm</i>)	C _s (m)	Li ₂ NbOF ₅	0	0	Type-III	<i>d</i> -wave

280	mp-755526	8 (<i>Cm</i>)	C _s (m)	Ba ₂ Ti ₆ N ₂ O ₁₁	1.978	1	Type-III	<i>d</i> -wave
281	mp-755881	8 (<i>Cm</i>)	C _s (m)	Ba ₂ Ti ₆ N ₂ O ₁₁	1.924	1	Type-III	<i>d</i> -wave
282	mp-755891	8 (<i>Cm</i>)	C _s (m)	CsLiH ₄ SO ₅	4.591	0	Type-III	<i>d</i> -wave
283	mp-757343	8 (<i>Cm</i>)	C _s (m)	Ca ₄ Bi ₆ O ₁₃	1.719	0	Type-III	<i>d</i> -wave
284	mp-757457	8 (<i>Cm</i>)	C _s (m)	LaNb ₃ O ₉	1.785	1	Type-III	<i>d</i> -wave
285	mp-757574	8 (<i>Cm</i>)	C _s (m)	Ba ₈ In ₈ O ₁₉	1.312	0	Type-III	<i>d</i> -wave
286	mp-758243	8 (<i>Cm</i>)	C _s (m)	TiNb ₂ O ₇	1.365	1	Type-III	<i>d</i> -wave
287	mp-761033	8 (<i>Cm</i>)	C _s (m)	Hf ₃ N ₂ O ₃	3.135	0	Type-III	<i>d</i> -wave
288	mp-762351	8 (<i>Cm</i>)	C _s (m)	Li ₄ Ti ₇ O ₁₆	2.453	1	Type-III	<i>d</i> -wave
289	mp-776466	8 (<i>Cm</i>)	C _s (m)	Ba ₂ Ti ₆ N ₂ O ₁₁	2.129	1	Type-III	<i>d</i> -wave
290	mp-776509	8 (<i>Cm</i>)	C _s (m)	Sr ₂ Ti ₆ N ₂ O ₁₁	1.941	1	Type-III	<i>d</i> -wave
291	mp-780772	8 (<i>Cm</i>)	C _s (m)	Ta ₂ O ₅	3.073	1	Type-III	<i>d</i> -wave
292	mp-849335	8 (<i>Cm</i>)	C _s (m)	Ti ₃ N ₂ O ₃	1.641	1	Type-III	<i>d</i> -wave
293	icsd-69758	9 (<i>Cc</i>)	C _s (m)	CuO	0	1	Type-III	<i>d</i> -wave
294	icsd-635377	9 (<i>Cc</i>)	C _s (m)	Ga ₂ Se ₃	1.1684	0	Type-III	<i>d</i> -wave
295	mp-11674	9 (<i>Cc</i>)	C _s (m)	Al ₂ Se ₃	1.8	0	Type-III	<i>d</i> -wave
296	mp-1340	9 (<i>Cc</i>)	C _s (m)	Ga ₂ Se ₃	1.044	0	Type-III	<i>d</i> -wave
297	mp-14535	9 (<i>Cc</i>)	C _s (m)	In(PO ₃) ₃	4.44	1	Type-III	<i>d</i> -wave
298	mp-14659	9 (<i>Cc</i>)	C _s (m)	KAsSe ₂	1.596	0	Type-III	<i>d</i> -wave
299	mp-14935	9 (<i>Cc</i>)	C _s (m)	P ₃ RhO ₉	1.692	1	Type-III	<i>d</i> -wave
300	mp-15560	9 (<i>Cc</i>)	C _s (m)	Ga(PO ₃) ₃	4.992	1	Type-III	<i>d</i> -wave
301	mp-15895	9 (<i>Cc</i>)	C _s (m)	Cu ₂ SiS ₃	1.118	0	Type-III	<i>d</i> -wave
302	mp-16839	9 (<i>Cc</i>)	C _s (m)	Na ₃ WN ₃	1.769	0	Type-III	<i>d</i> -wave
303	mp-16956	9 (<i>Cc</i>)	C _s (m)	Na ₃ Sc ₂ (PO ₄) ₃	4.658	0	Type-III	<i>d</i> -wave
304	mp-17791	9 (<i>Cc</i>)	C _s (m)	Cd ₄ SiSe ₆	0.822	0	Type-III	<i>d</i> -wave
305	mp-17948	9 (<i>Cc</i>)	C _s (m)	Si(Hg ₂ S ₃) ₂	0.439	0	Type-III	<i>d</i> -wave
306	mp-18163	9 (<i>Cc</i>)	C _s (m)	Cd ₄ GeSe ₆	0.756	0	Type-III	<i>d</i> -wave
307	mp-18179	9 (<i>Cc</i>)	C _s (m)	Cd ₄ SiS ₆	1.438	0	Type-III	<i>d</i> -wave
308	mp-18582	9 (<i>Cc</i>)	C _s (m)	Rb ₂ Ti(Si ₂ O ₅) ₃	3.485	1	Type-III	<i>d</i> -wave
309	mp-24120	9 (<i>Cc</i>)	C _s (m)	CaAsH ₅ O ₆	4.055	1	Type-III	<i>d</i> -wave
310	mp-24389	9 (<i>Cc</i>)	C _s (m)	CaPH ₅ O ₆	5.342	1	Type-III	<i>d</i> -wave
311	mp-24469	9 (<i>Cc</i>)	C _s (m)	CaAl ₄ Si ₂ (HO ₆) ₂	4.535	1	Type-III	<i>d</i> -wave
312	mp-2804	9 (<i>Cc</i>)	C _s (m)	LaP ₂	0.556	0	Type-III	<i>d</i> -wave
313	mp-28261	9 (<i>Cc</i>)	C _s (m)	Na ₄ SnO ₃	1.884	0	Type-III	<i>d</i> -wave
314	mp-28922	9 (<i>Cc</i>)	C _s (m)	Ca ₂ Si ₅ N ₈	3.345	0	Type-III	<i>d</i> -wave
315	mp-29163	9 (<i>Cc</i>)	C _s (m)	Ag ₂ TeS ₃	1.3	0	Type-III	<i>d</i> -wave
316	mp-29246	9 (<i>Cc</i>)	C _s (m)	Cd ₂ P ₃ Cl	1.201	0	Type-III	<i>d</i> -wave
317	mp-29299	9 (<i>Cc</i>)	C _s (m)	TeSeO ₄	2.952	0	Type-III	<i>d</i> -wave
318	mp-29815	9 (<i>Cc</i>)	C _s (m)	LaAs ₂	0.597	0	Type-III	<i>d</i> -wave
319	mp-29959	9 (<i>Cc</i>)	C _s (m)	TlBSe ₃	0.915	0	Type-III	<i>d</i> -wave
320	mp-30126	9 (<i>Cc</i>)	C _s (m)	Ba(BS ₂) ₂	2.745	0	Type-III	<i>d</i> -wave
321	mp-32616	9 (<i>Cc</i>)	C _s (m)	Ga ₂ S ₃	1.81	0	Type-III	<i>d</i> -wave
322	mp-36066	9 (<i>Cc</i>)	C _s (m)	PNO	5.072	0	Type-III	<i>d</i> -wave
323	mp-38970	9 (<i>Cc</i>)	C _s (m)	Ga ₂ Te ₃	0.638	0	Type-III	<i>d</i> -wave
324	mp-43068	9 (<i>Cc</i>)	C _s (m)	Na ₃ Al ₃ Si ₃ AgBrO ₁₂	3.335	0	Type-III	<i>d</i> -wave
325	mp-505607	9 (<i>Cc</i>)	C _s (m)	In ₂ Ag ₂ GeSe ₆	0.437	0	Type-III	<i>d</i> -wave
326	mp-5151	9 (<i>Cc</i>)	C _s (m)	Cd ₄ GeS ₆	1.355	0	Type-III	<i>d</i> -wave
327	mp-532091	9 (<i>Cc</i>)	C _s (m)	Na ₂₆ In ₄ O ₁₉	1.278	0	Type-III	<i>d</i> -wave
328	mp-539	9 (<i>Cc</i>)	C _s (m)	Ga ₂ S ₃	1.711	0	Type-III	<i>d</i> -wave
329	mp-540549	9 (<i>Cc</i>)	C _s (m)	Al(PO ₃) ₃	5.805	1	Type-III	<i>d</i> -wave
330	mp-542199	9 (<i>Cc</i>)	C _s (m)	Ag ₄ HgGe ₂ S ₇	0.463	0	Type-III	<i>d</i> -wave
331	mp-542200	9 (<i>Cc</i>)	C _s (m)	CdAg ₄ Ge ₂ S ₇	0.633	0	Type-III	<i>d</i> -wave
332	mp-542545	9 (<i>Cc</i>)	C _s (m)	K ₃ Nb ₂ AsSe ₁₁	1.165	0	Type-III	<i>d</i> -wave
333	mp-554627	9 (<i>Cc</i>)	C _s (m)	Cu ₆ PS ₅ Br	0.818	0	Type-III	<i>d</i> -wave
334	mp-554749	9 (<i>Cc</i>)	C _s (m)	P ₃ IrO ₉	2.249	1	Type-III	<i>d</i> -wave
335	mp-555313	9 (<i>Cc</i>)	C _s (m)	ScBiO ₃	2.69	0	Type-III	<i>d</i> -wave
336	mp-555743	9 (<i>Cc</i>)	C _s (m)	LiZnPO ₄	4.299	0	Type-III	<i>d</i> -wave
337	mp-555874	9 (<i>Cc</i>)	C _s (m)	LiAsS ₂	1.066	0	Type-III	<i>d</i> -wave
338	mp-556489	9 (<i>Cc</i>)	C _s (m)	Ta ₂ SnO ₆	2.285	0	Type-III	<i>d</i> -wave

339	mp-556916	9 (<i>Cc</i>)	C _s (m)	GaAgS ₂	1.02	0	Type-III	<i>d</i> -wave
340	mp-557892	9 (<i>Cc</i>)	C _s (m)	BaLi(BS ₂) ₃	2.86	0	Type-III	<i>d</i> -wave
341	mp-558016	9 (<i>Cc</i>)	C _s (m)	CaMgAsO ₄ F	3.752	0	Type-III	<i>d</i> -wave
342	mp-558219	9 (<i>Cc</i>)	C _s (m)	SrLi(BS ₂) ₃	2.91	0	Type-III	<i>d</i> -wave
343	mp-558277	9 (<i>Cc</i>)	C _s (m)	Tl ₃ (BiO ₃) ₄	2.343	1	Type-III	<i>d</i> -wave
344	mp-558407	9 (<i>Cc</i>)	C _s (m)	In ₂ Si(AgS ₃) ₂	0.991	0	Type-III	<i>d</i> -wave
345	mp-558582	9 (<i>Cc</i>)	C _s (m)	In(PO ₃) ₃	4.378	1	Type-III	<i>d</i> -wave
346	mp-559949	9 (<i>Cc</i>)	C _s (m)	Zn ₃ (BO ₃) ₂	2.718	1	Type-III	<i>d</i> -wave
347	mp-560386	9 (<i>Cc</i>)	C _s (m)	In ₂ Ag ₂ GeS ₆	0.962	0	Type-III	<i>d</i> -wave
348	mp-561013	9 (<i>Cc</i>)	C _s (m)	Ga ₂ PbO ₄	3.532	0	Type-III	<i>d</i> -wave
349	mp-561256	9 (<i>Cc</i>)	C _s (m)	Ba ₂ TiOF ₆	3.9	0	Type-III	<i>d</i> -wave
350	mp-570957	9 (<i>Cc</i>)	C _s (m)	CsSiTe ₃	1.261	0	Type-III	<i>d</i> -wave
351	mp-581517	9 (<i>Cc</i>)	C _s (m)	K ₂ In(PSe ₄) ₂	1.195	0	Type-III	<i>d</i> -wave
352	mp-581868	9 (<i>Cc</i>)	C _s (m)	NaY(IO ₃) ₄	3.307	1	Type-III	<i>d</i> -wave
353	mp-6215	9 (<i>Cc</i>)	C _s (m)	AgHgAsS ₃	1.245	0	Type-III	<i>d</i> -wave
354	mp-625801	9 (<i>Cc</i>)	C _s (m)	Sr(H ₈ O ₅) ₂	3.843	0	Type-III	<i>d</i> -wave
355	mp-625832	9 (<i>Cc</i>)	C _s (m)	Ba(H ₂ O ₃) ₂	2.545	1	Type-III	<i>d</i> -wave
356	mp-640614	9 (<i>Cc</i>)	C _s (m)	In ₂ Si(AgSe ₃) ₂	0.476	0	Type-III	<i>d</i> -wave
357	mp-673633	9 (<i>Cc</i>)	C _s (m)	In ₂ S ₃	1.604	0	Type-III	<i>d</i> -wave
358	mp-674508	9 (<i>Cc</i>)	C _s (m)	RbPbF ₃	3.785	0	Type-III	<i>d</i> -wave
359	mp-674531	9 (<i>Cc</i>)	C _s (m)	Li ₅ GeP ₃	0.521	0	Type-III	<i>d</i> -wave
360	mp-6748	9 (<i>Cc</i>)	C _s (m)	Cs ₂ Ti(Si ₂ O ₅) ₃	3.509	1	Type-III	<i>d</i> -wave
361	mp-680555	9 (<i>Cc</i>)	C _s (m)	TlGaSe ₂	1.674	0	Type-III	<i>d</i> -wave
362	mp-680731	9 (<i>Cc</i>)	C _s (m)	Tl ₂ Te ₃	0.648	0	Type-III	<i>d</i> -wave
363	mp-683902	9 (<i>Cc</i>)	C _s (m)	Rb ₃ Nb ₂ AsSe ₁₁	1.173	0	Type-III	<i>d</i> -wave
364	mp-683903	9 (<i>Cc</i>)	C _s (m)	Cs ₃ Nb ₂ AsSe ₁₁	0.959	0	Type-III	<i>d</i> -wave
365	mp-683905	9 (<i>Cc</i>)	C _s (m)	K ₃ Ta ₂ AsSe ₁₁	1.188	0	Type-III	<i>d</i> -wave
366	mp-685991	9 (<i>Cc</i>)	C _s (m)	Li ₅ SiP ₃	1.316	0	Type-III	<i>d</i> -wave
367	mp-696347	9 (<i>Cc</i>)	C _s (m)	NaH ₃ SO ₅	5.359	1	Type-III	<i>d</i> -wave
368	mp-696853	9 (<i>Cc</i>)	C _s (m)	CaZnSiH ₂ O ₅	3.64	0	Type-III	<i>d</i> -wave
369	mp-752401	9 (<i>Cc</i>)	C _s (m)	Rb ₂ ZrO ₃	3.128	0	Type-III	<i>d</i> -wave
370	mp-752561	9 (<i>Cc</i>)	C _s (m)	SbO ₂ F	1.333	0	Type-III	<i>d</i> -wave
371	mp-754604	9 (<i>Cc</i>)	C _s (m)	BaBePO ₄ F	6.052	0	Type-III	<i>d</i> -wave
372	mp-774736	9 (<i>Cc</i>)	C _s (m)	LiCuS	1.698	0	Type-III	<i>d</i> -wave
373	mp-778194	9 (<i>Cc</i>)	C _s (m)	Ge ₂ N ₂ O	2.43	0	Type-III	<i>d</i> -wave
374	mp-863374	9 (<i>Cc</i>)	C _s (m)	BiTeO ₄	2.202	0	Type-III	<i>d</i> -wave
375	mp-866660	9 (<i>Cc</i>)	C _s (m)	K ₃ P ₂ AuSe ₈	1.196	0	Type-III	<i>d</i> -wave
376	mp-950995	9 (<i>Cc</i>)	C _s (m)	Li ₆ PS ₅ I	2.274	0	Type-III	<i>d</i> -wave
377	mp-560381	17 (<i>P2221</i>)	D ₂ (222)	RbIn ₃ F ₁₀	3.445	0	Type-II	<i>s</i> -wave
378	mp-27322	18 (<i>P2₁2₁2</i>)	D ₂ (222)	Nb ₂ Te ₃ O ₁₁	2.567	1	Type-II	<i>s</i> -wave
379	mp-29085	18 (<i>P2₁2₁2</i>)	D ₂ (222)	Sr ₅ Zr ₃ F ₂₂	5.367	0	Type-II	<i>s</i> -wave
380	mp-29499	18 (<i>P2₁2₁2</i>)	D ₂ (222)	Re ₃ Te ₈ Cl ₃	0.94	0	Type-II	<i>s</i> -wave
381	mp-540877	18 (<i>P2₁2₁2</i>)	D ₂ (222)	La ₃ InS ₆	1.359	0	Type-II	<i>s</i> -wave
382	mp-554554	18 (<i>P2₁2₁2</i>)	D ₂ (222)	K ₉ Bi(PS ₄) ₄	2.1	0	Type-II	<i>s</i> -wave
383	mp-556258	18 (<i>P2₁2₁2</i>)	D ₂ (222)	Na ₃ BeAl(SiO ₄) ₂	4.328	0	Type-II	<i>s</i> -wave
384	mp-556296	18 (<i>P2₁2₁2</i>)	D ₂ (222)	BaS ₃	1.047	0	Type-II	<i>s</i> -wave
385	mp-567129	18 (<i>P2₁2₁2</i>)	D ₂ (222)	KLaSi(CN ₂) ₄	3.678	0	Type-II	<i>s</i> -wave
386	mp-568525	18 (<i>P2₁2₁2</i>)	D ₂ (222)	Sr ₂ SnSe ₅	1.244	0	Type-II	<i>s</i> -wave
387	mp-630376	18 (<i>P2₁2₁2</i>)	D ₂ (222)	Sb ₆ Pb ₆ S ₁₇	0.781	1	Type-II	<i>s</i> -wave
388	mp-648932	18 (<i>P2₁2₁2</i>)	D ₂ (222)	Nb ₂ PS ₁₀	1.519	0	Type-II	<i>s</i> -wave
389	mp-773843	18 (<i>P2₁2₁2</i>)	D ₂ (222)	LiTi ₂ (PO ₄) ₃	2.34	0	Type-II	<i>s</i> -wave
390	mp-10070	19 (<i>P2₁2₁2₁</i>)	D ₂ (222)	BaAg(PO ₃) ₃	3.244	1	Type-II	<i>s</i> -wave
391	mp-10802	19 (<i>P2₁2₁2₁</i>)	D ₂ (222)	RbAs	0.588	0	Type-II	<i>s</i> -wave
392	mp-12843	19 (<i>P2₁2₁2₁</i>)	D ₂ (222)	YCuS ₂	1.791	0	Type-II	<i>s</i> -wave
393	mp-12955	19 (<i>P2₁2₁2₁</i>)	D ₂ (222)	HoAgSe ₂	1.271	0	Type-II	<i>s</i> -wave
394	mp-13755	19 (<i>P2₁2₁2₁</i>)	D ₂ (222)	BaNa(PO ₃) ₃	5.609	1	Type-II	<i>s</i> -wave
395	mp-13791	19 (<i>P2₁2₁2₁</i>)	D ₂ (222)	BaNaNd(SiO ₃) ₃	4.822	0	Type-II	<i>s</i> -wave
396	mp-13863	19 (<i>P2₁2₁2₁</i>)	D ₂ (222)	BaGeO ₃	3.552	0	Type-II	<i>s</i> -wave
397	mp-13956	19 (<i>P2₁2₁2₁</i>)	D ₂ (222)	Ag ₂ PSe ₃	1.187	0	Type-II	<i>s</i> -wave

398	mp-14353	19 ($P_{2_1}2_12_1$)	D ₂ (222)	BaNaNd(GeO ₃) ₃	3.787	0	Type-II	s-wave
399	mp-14367	19 ($P_{2_1}2_12_1$)	D ₂ (222)	AsPO ₅	2.02	0	Type-II	s-wave
400	mp-14368	19 ($P_{2_1}2_12_1$)	D ₂ (222)	SbAsO ₅	1.758	0	Type-II	s-wave
401	mp-14484	19 ($P_{2_1}2_12_1$)	D ₂ (222)	KNaLi ₂ (SO ₄) ₂	5.413	1	Type-II	s-wave
402	mp-16061	19 ($P_{2_1}2_12_1$)	D ₂ (222)	Sr ₆ Sb ₆ S ₁₇	1.848	1	Type-II	s-wave
403	mp-16911	19 ($P_{2_1}2_12_1$)	D ₂ (222)	Rb ₂ S ₅	1.954	0	Type-II	s-wave
404	mp-16934	19 ($P_{2_1}2_12_1$)	D ₂ (222)	BaLaAlO ₄	4.436	0	Type-II	s-wave
405	mp-16972	19 ($P_{2_1}2_12_1$)	D ₂ (222)	CsErSiS ₄	2.957	0	Type-II	s-wave
406	mp-17066	19 ($P_{2_1}2_12_1$)	D ₂ (222)	Y ₂ TeO ₆	3.072	0	Type-II	s-wave
407	mp-17095	19 ($P_{2_1}2_12_1$)	D ₂ (222)	CsCuSe ₄	1.105	0	Type-II	s-wave
408	mp-17350	19 ($P_{2_1}2_12_1$)	D ₂ (222)	La ₂ TeO ₆	2.962	0	Type-II	s-wave
409	mp-17691	19 ($P_{2_1}2_12_1$)	D ₂ (222)	Cu ₃ SbS ₃	0.998	0	Type-II	s-wave
410	mp-18003	19 ($P_{2_1}2_12_1$)	D ₂ (222)	CsCuS ₄	1.776	0	Type-II	s-wave
411	mp-18105	19 ($P_{2_1}2_12_1$)	D ₂ (222)	CsAgSe ₄	1.267	0	Type-II	s-wave
412	mp-18365	19 ($P_{2_1}2_12_1$)	D ₂ (222)	RbCuSe ₄	1.01	0	Type-II	s-wave
413	mp-18585	19 ($P_{2_1}2_12_1$)	D ₂ (222)	RbAgSe ₄	1.161	0	Type-II	s-wave
414	mp-23363	19 ($P_{2_1}2_12_1$)	D ₂ (222)	NaAlCl ₄	5.156	0	Type-II	s-wave
415	mp-23380	19 ($P_{2_1}2_12_1$)	D ₂ (222)	Tl ₃ PbI ₅	2.662	0	Type-II	s-wave
416	mp-23963	19 ($P_{2_1}2_12_1$)	D ₂ (222)	HIO ₃	3.102	0	Type-II	s-wave
417	mp-24018	19 ($P_{2_1}2_12_1$)	D ₂ (222)	CaZnAsHO ₅	2.637	0	Type-II	s-wave
418	mp-24402	19 ($P_{2_1}2_12_1$)	D ₂ (222)	CaAlSiHO ₅	5.245	0	Type-II	s-wave
419	mp-27365	19 ($P_{2_1}2_12_1$)	D ₂ (222)	BaBiSe ₃	0.994	0	Type-II	s-wave
420	mp-27451	19 ($P_{2_1}2_12_1$)	D ₂ (222)	Tl ₃ PbBr ₅	3.115	0	Type-II	s-wave
421	mp-27579	19 ($P_{2_1}2_12_1$)	D ₂ (222)	Na ₄ P ₂ O ₇	4.63	1	Type-II	s-wave
422	mp-27640	19 ($P_{2_1}2_12_1$)	D ₂ (222)	Cd(IO ₃) ₂	3.274	0	Type-II	s-wave
423	mp-27931	19 ($P_{2_1}2_12_1$)	D ₂ (222)	Rb ₂ SnO ₂	2.225	0	Type-II	s-wave
424	mp-27996	19 ($P_{2_1}2_12_1$)	D ₂ (222)	H ₂ SeO ₃	4.486	0	Type-II	s-wave
425	mp-28108	19 ($P_{2_1}2_12_1$)	D ₂ (222)	Na ₄ SnTe ₄	1.02	0	Type-II	s-wave
426	mp-28195	19 ($P_{2_1}2_12_1$)	D ₂ (222)	SiAg ₂ O ₃	0.637	0	Type-II	s-wave
427	mp-28476	19 ($P_{2_1}2_12_1$)	D ₂ (222)	SrBiSe ₃	0.798	0	Type-II	s-wave
428	mp-28569	19 ($P_{2_1}2_12_1$)	D ₂ (222)	NaInBr ₄	2.815	0	Type-II	s-wave
429	mp-29060	19 ($P_{2_1}2_12_1$)	D ₂ (222)	Ba ₅ (SiN ₃) ₂	1.516	0	Type-II	s-wave
430	mp-29155	19 ($P_{2_1}2_12_1$)	D ₂ (222)	TlB ₃ O ₅	4.223	0	Type-II	s-wave
431	mp-29381	19 ($P_{2_1}2_12_1$)	D ₂ (222)	Na ₂ Te ₂ As	1.152	0	Type-II	s-wave
432	mp-29705	19 ($P_{2_1}2_12_1$)	D ₂ (222)	Rb ₆ Sn ₂ S ₇	2.352	0	Type-II	s-wave
433	mp-29756	19 ($P_{2_1}2_12_1$)	D ₂ (222)	RbB ₃ O ₅	5.212	1	Type-II	s-wave
434	mp-29820	19 ($P_{2_1}2_12_1$)	D ₂ (222)	Ca ₃ (AlN ₂) ₂	2.195	0	Type-II	s-wave
435	mp-29946	19 ($P_{2_1}2_12_1$)	D ₂ (222)	IO ₂ F	2.895	0	Type-II	s-wave
436	mp-30905	19 ($P_{2_1}2_12_1$)	D ₂ (222)	Ba ₃ (BN ₂) ₂	2.586	0	Type-II	s-wave
437	mp-31307	19 ($P_{2_1}2_12_1$)	D ₂ (222)	Ba ₂ SnSe ₅	1.087	0	Type-II	s-wave
438	mp-31318	19 ($P_{2_1}2_12_1$)	D ₂ (222)	Nd ₂ TeO ₆	2.985	0	Type-II	s-wave
439	mp-32684	19 ($P_{2_1}2_12_1$)	D ₂ (222)	HBr	4.486	0	Type-II	s-wave
440	mp-4044	19 ($P_{2_1}2_12_1$)	D ₂ (222)	ErAgSe ₂	1.28	0	Type-II	s-wave
441	mp-4376	19 ($P_{2_1}2_12_1$)	D ₂ (222)	BaAlF ₅	7.289	0	Type-II	s-wave
442	mp-510279	19 ($P_{2_1}2_12_1$)	D ₂ (222)	ZnAsHPbO ₅	3.24	0	Type-II	s-wave
443	mp-541055	19 ($P_{2_1}2_12_1$)	D ₂ (222)	Cs ₂ Se ₅	0.962	0	Type-II	s-wave
444	mp-541280	19 ($P_{2_1}2_12_1$)	D ₂ (222)	BaLaGaO ₄	3.948	0	Type-II	s-wave
445	mp-541281	19 ($P_{2_1}2_12_1$)	D ₂ (222)	BaNdGaO ₄	3.736	0	Type-II	s-wave
446	mp-541629	19 ($P_{2_1}2_12_1$)	D ₂ (222)	BaGaF ₅	5.757	0	Type-II	s-wave
447	mp-553907	19 ($P_{2_1}2_12_1$)	D ₂ (222)	Rb ₃ AgO ₂	1.516	0	Type-II	s-wave
448	mp-554120	19 ($P_{2_1}2_12_1$)	D ₂ (222)	DyCuS ₂	1.632	0	Type-II	s-wave
449	mp-554359	19 ($P_{2_1}2_12_1$)	D ₂ (222)	Cs ₂ Si ₃ SnO ₉	3.923	0	Type-II	s-wave
450	mp-554390	19 ($P_{2_1}2_12_1$)	D ₂ (222)	SrAl ₂ SiN ₂ O ₃	3.724	0	Type-II	s-wave
451	mp-556463	19 ($P_{2_1}2_12_1$)	D ₂ (222)	KGe ₂ BO ₆	3.498	0	Type-II	s-wave
452	mp-556771	19 ($P_{2_1}2_12_1$)	D ₂ (222)	Nd ₂ Si ₂ O ₇	5.235	0	Type-II	s-wave
453	mp-556979	19 ($P_{2_1}2_12_1$)	D ₂ (222)	CsSmGeS ₄	2.463	0	Type-II	s-wave
454	mp-557614	19 ($P_{2_1}2_12_1$)	D ₂ (222)	Cd(PO ₃) ₂	3.717	0	Type-II	s-wave
455	mp-557974	19 ($P_{2_1}2_12_1$)	D ₂ (222)	BaZn ₂ (BO ₃) ₂	3.229	1	Type-II	s-wave
456	mp-558226	19 ($P_{2_1}2_12_1$)	D ₂ (222)	H ₂ O	5.776	1	Type-II	s-wave

457	mp-558521	19 ($P_{2_1}2_12_1$)	D ₂ (222)	B ₂ Se ₂ O ₇	3.942	0	Type-II	<i>s</i> -wave
458	mp-558958	19 ($P_{2_1}2_12_1$)	D ₂ (222)	H ₂ O	5.668	1	Type-II	<i>s</i> -wave
459	mp-559224	19 ($P_{2_1}2_12_1$)	D ₂ (222)	Sr ₃ Al ₂ Cl ₂ O ₅	4.421	0	Type-II	<i>s</i> -wave
460	mp-559530	19 ($P_{2_1}2_12_1$)	D ₂ (222)	Ti ₅ (PO ₅) ₄	2.931	1	Type-II	<i>s</i> -wave
461	mp-559645	19 ($P_{2_1}2_12_1$)	D ₂ (222)	KThP ₃ O ₁₀	5.012	1	Type-II	<i>s</i> -wave
462	mp-559826	19 ($P_{2_1}2_12_1$)	D ₂ (222)	ErCuS ₂	1.745	0	Type-II	<i>s</i> -wave
463	mp-559984	19 ($P_{2_1}2_12_1$)	D ₂ (222)	Rb ₈ AlAu ₃ O ₄	1.402	0	Type-II	<i>s</i> -wave
464	mp-560394	19 ($P_{2_1}2_12_1$)	D ₂ (222)	AsPbClO ₂	3.335	0	Type-II	<i>s</i> -wave
465	mp-560611	19 ($P_{2_1}2_12_1$)	D ₂ (222)	HoCuS ₂	1.66	0	Type-II	<i>s</i> -wave
466	mp-560668	19 ($P_{2_1}2_12_1$)	D ₂ (222)	K ₂ Zn ₃ (P ₂ O ₇) ₂	4.208	0	Type-II	<i>s</i> -wave
467	mp-560721	19 ($P_{2_1}2_12_1$)	D ₂ (222)	NaCaBeSi ₂ O ₆ F	5.511	0	Type-II	<i>s</i> -wave
468	mp-561224	19 ($P_{2_1}2_12_1$)	D ₂ (222)	TeO ₂	2.978	0	Type-II	<i>s</i> -wave
469	mp-561259	19 ($P_{2_1}2_12_1$)	D ₂ (222)	Na ₃ NbOF ₆	5.101	1	Type-II	<i>s</i> -wave
470	mp-561635	19 ($P_{2_1}2_12_1$)	D ₂ (222)	CsSmSiS ₄	2.841	0	Type-II	<i>s</i> -wave
471	mp-567855	19 ($P_{2_1}2_12_1$)	D ₂ (222)	RbGeI ₃	2.199	0	Type-II	<i>s</i> -wave
472	mp-567873	19 ($P_{2_1}2_12_1$)	D ₂ (222)	RbSmGeSe ₄	1.601	0	Type-II	<i>s</i> -wave
473	mp-568450	19 ($P_{2_1}2_12_1$)	D ₂ (222)	SrAlH ₅	3.527	0	Type-II	<i>s</i> -wave
474	mp-570622	19 ($P_{2_1}2_12_1$)	D ₂ (222)	NaGa ₃ Se ₅	1.861	0	Type-II	<i>s</i> -wave
475	mp-571057	19 ($P_{2_1}2_12_1$)	D ₂ (222)	KY(PSe ₃) ₂	1.939	0	Type-II	<i>s</i> -wave
476	mp-572510	19 ($P_{2_1}2_12_1$)	D ₂ (222)	K ₃ AgO ₂	1.751	0	Type-II	<i>s</i> -wave
477	mp-583071	19 ($P_{2_1}2_12_1$)	D ₂ (222)	CaAlH ₅	3.488	0	Type-II	<i>s</i> -wave
478	mp-620372	19 ($P_{2_1}2_12_1$)	D ₂ (222)	Rb ₂ Se ₅	0.836	0	Type-II	<i>s</i> -wave
479	mp-625830	19 ($P_{2_1}2_12_1$)	D ₂ (222)	Zn(HO) ₂	2.97	0	Type-II	<i>s</i> -wave
480	mp-625837	19 ($P_{2_1}2_12_1$)	D ₂ (222)	Be(HO) ₂	5.457	0	Type-II	<i>s</i> -wave
481	mp-6699	19 ($P_{2_1}2_12_1$)	D ₂ (222)	NaMgPO ₄	5.106	0	Type-II	<i>s</i> -wave
482	mp-677703	19 ($P_{2_1}2_12_1$)	D ₂ (222)	Nd ₄ Si ₄ N ₇ ClO ₃	3.186	0	Type-II	<i>s</i> -wave
483	mp-697136	19 ($P_{2_1}2_12_1$)	D ₂ (222)	Be(HO) ₂	5.404	0	Type-II	<i>s</i> -wave
484	mp-697139	19 ($P_{2_1}2_12_1$)	D ₂ (222)	PHN ₂	4.737	0	Type-II	<i>s</i> -wave
485	mp-697146	19 ($P_{2_1}2_12_1$)	D ₂ (222)	Zn(HO) ₂	2.883	0	Type-II	<i>s</i> -wave
486	mp-699219	19 ($P_{2_1}2_12_1$)	D ₂ (222)	NaZnSiHO ₄	3.427	0	Type-II	<i>s</i> -wave
487	mp-699390	19 ($P_{2_1}2_12_1$)	D ₂ (222)	Pr ₄ Si ₄ N ₇ ClO ₃	3.112	0	Type-II	<i>s</i> -wave
488	mp-713	19 ($P_{2_1}2_12_1$)	D ₂ (222)	KAs	0.669	0	Type-II	<i>s</i> -wave
489	mp-7339	19 ($P_{2_1}2_12_1$)	D ₂ (222)	BaSiO ₃	4.534	0	Type-II	<i>s</i> -wave
490	mp-7440	19 ($P_{2_1}2_12_1$)	D ₂ (222)	NaP	0.868	0	Type-II	<i>s</i> -wave
491	mp-7441	19 ($P_{2_1}2_12_1$)	D ₂ (222)	KP	1.035	0	Type-II	<i>s</i> -wave
492	mp-7444	19 ($P_{2_1}2_12_1$)	D ₂ (222)	RbSb	0.542	0	Type-II	<i>s</i> -wave
493	mp-7456	19 ($P_{2_1}2_12_1$)	D ₂ (222)	SnF ₂	3.263	0	Type-II	<i>s</i> -wave
494	mp-752526	19 ($P_{2_1}2_12_1$)	D ₂ (222)	Lu ₂ TeO ₆	3.277	0	Type-II	<i>s</i> -wave
495	mp-758597	19 ($P_{2_1}2_12_1$)	D ₂ (222)	K ₂ TiSi ₃ (HO ₅) ₂	3.125	0	Type-II	<i>s</i> -wave
496	mp-7595	19 ($P_{2_1}2_12_1$)	D ₂ (222)	GeF ₂	4.06	0	Type-II	<i>s</i> -wave
497	mp-768313	19 ($P_{2_1}2_12_1$)	D ₂ (222)	Dy ₂ TeO ₆	3.007	0	Type-II	<i>s</i> -wave
498	mp-768762	19 ($P_{2_1}2_12_1$)	D ₂ (222)	Ho ₂ TeO ₆	3.013	0	Type-II	<i>s</i> -wave
499	mp-770718	19 ($P_{2_1}2_12_1$)	D ₂ (222)	Mg(IO ₃) ₂	3.106	1	Type-II	<i>s</i> -wave
500	mp-772900	19 ($P_{2_1}2_12_1$)	D ₂ (222)	Sm ₂ TeO ₆	3.184	0	Type-II	<i>s</i> -wave
501	mp-774557	19 ($P_{2_1}2_12_1$)	D ₂ (222)	Er ₂ TeO ₆	3.181	0	Type-II	<i>s</i> -wave
502	mp-780172	19 ($P_{2_1}2_12_1$)	D ₂ (222)	Tm ₂ TeO ₆	3.115	0	Type-II	<i>s</i> -wave
503	mp-781712	19 ($P_{2_1}2_12_1$)	D ₂ (222)	Na ₂ SnO ₂	2.412	0	Type-II	<i>s</i> -wave
504	mp-8377	19 ($P_{2_1}2_12_1$)	D ₂ (222)	TeO ₂	3.06	0	Type-II	<i>s</i> -wave
505	mp-9512	19 ($P_{2_1}2_12_1$)	D ₂ (222)	SrAl ₂ P ₂ (O ₄ F) ₂	5.489	0	Type-II	<i>s</i> -wave
506	mp-983589	19 ($P_{2_1}2_12_1$)	D ₂ (222)	Ag ₂ GeO ₃	0.212	0	Type-II	<i>s</i> -wave
507	mp-985293	19 ($P_{2_1}2_12_1$)	D ₂ (222)	Al(HO) ₃	5.811	0	Type-II	<i>s</i> -wave
508	mp-11321	20 (C_{222_1})	D ₂ (222)	Y ₃ TaO ₇	3.5	1	Type-II	<i>s</i> -wave
509	mp-27167	20 (C_{222_1})	D ₂ (222)	Sn ₂ IF ₃	2.436	0	Type-II	<i>s</i> -wave
510	mp-29368	20 (C_{222_1})	D ₂ (222)	Th ₂ Ta ₂ O ₉	3.506	1	Type-II	<i>s</i> -wave
511	mp-30321	20 (C_{222_1})	D ₂ (222)	Y ₂ P ₄ O ₁₃	5.641	1	Type-II	<i>s</i> -wave
512	mp-30957	20 (C_{222_1})	D ₂ (222)	Pr(PO ₃) ₃	5.485	0	Type-II	<i>s</i> -wave
513	mp-31416	20 (C_{222_1})	D ₂ (222)	Ho ₃ TaO ₇	3.451	1	Type-II	<i>s</i> -wave
514	mp-4051	20 (C_{222_1})	D ₂ (222)	AlPO ₄	5.475	0	Type-II	<i>s</i> -wave
515	mp-553932	20 (C_{222_1})	D ₂ (222)	GaPO ₄	4.44	0	Type-II	<i>s</i> -wave

516	mp-554159	20 (C_{2221})	D ₂ (222)	Li ₂ BeSiO ₄	5.599	0	Type-II	<i>s</i> -wave
517	mp-554615	20 (C_{2221})	D ₂ (222)	KEr(PO ₃) ₄	5.567	1	Type-II	<i>s</i> -wave
518	mp-555050	20 (C_{2221})	D ₂ (222)	BaNb ₂ O ₆	2.904	1	Type-II	<i>s</i> -wave
519	mp-555203	20 (C_{2221})	D ₂ (222)	Sr ₅ B ₃ ClO ₉	3.964	0	Type-II	<i>s</i> -wave
520	mp-555318	20 (C_{2221})	D ₂ (222)	K ₂ Zn(SiO ₃) ₂	3.924	0	Type-II	<i>s</i> -wave
521	mp-555621	20 (C_{2221})	D ₂ (222)	RbAl ₃ (P ₃ O ₁₀) ₂	5.439	0	Type-II	<i>s</i> -wave
522	mp-557432	20 (C_{2221})	D ₂ (222)	GeClO ₂ F ₅	1.728	1	Type-II	<i>s</i> -wave
523	mp-557743	20 (C_{2221})	D ₂ (222)	KCaAl ₂ F ₉	7.289	1	Type-II	<i>s</i> -wave
524	mp-558125	20 (C_{2221})	D ₂ (222)	BaTiO ₃	2.081	0	Type-II	<i>s</i> -wave
525	mp-558568	20 (C_{2221})	D ₂ (222)	Rb ₂ CdSiO ₄	2.488	0	Type-II	<i>s</i> -wave
526	mp-560233	20 (C_{2221})	D ₂ (222)	Sr ₅ B ₃ BrO ₉	3.899	0	Type-II	<i>s</i> -wave
527	mp-560326	20 (C_{2221})	D ₂ (222)	Ba ₅ B ₃ CNO ₉	3.335	0	Type-II	<i>s</i> -wave
528	mp-560398	20 (C_{2221})	D ₂ (222)	K ₂ Zn(GeO ₃) ₂	2.872	0	Type-II	<i>s</i> -wave
529	mp-560761	20 (C_{2221})	D ₂ (222)	RbGa ₃ (P ₃ O ₁₀) ₂	4.591	0	Type-II	<i>s</i> -wave
530	mp-568328	20 (C_{2221})	D ₂ (222)	FeP ₄	0.829	0	Type-II	<i>s</i> -wave
531	mp-600049	20 (C_{2221})	D ₂ (222)	SiO ₂	5.828	1	Type-II	<i>s</i> -wave
532	mp-7264	20 (C_{2221})	D ₂ (222)	Nd(PO ₃) ₃	5.487	0	Type-II	<i>s</i> -wave
533	mp-752686	20 (C_{2221})	D ₂ (222)	Sm ₃ TaO ₇	3.426	1	Type-II	<i>s</i> -wave
534	mp-754415	20 (C_{2221})	D ₂ (222)	Tb ₃ NbO ₇	2.723	0	Type-II	<i>s</i> -wave
535	mp-755277	20 (C_{2221})	D ₂ (222)	Tb ₃ SbO ₇	3.012	0	Type-II	<i>s</i> -wave
536	mp-755652	20 (C_{2221})	D ₂ (222)	Dy ₃ TaO ₇	3.408	1	Type-II	<i>s</i> -wave
537	mp-755660	20 (C_{2221})	D ₂ (222)	Lu ₃ TaO ₇	3.418	1	Type-II	<i>s</i> -wave
538	mp-755898	20 (C_{2221})	D ₂ (222)	Er ₃ TaO ₇	3.562	1	Type-II	<i>s</i> -wave
539	mp-756591	20 (C_{2221})	D ₂ (222)	Sm ₃ NbO ₇	2.729	0	Type-II	<i>s</i> -wave
540	mp-758103	20 (C_{2221})	D ₂ (222)	YH ₂ (CO ₃) ₂	3.478	1	Type-II	<i>s</i> -wave
541	mp-769931	20 (C_{2221})	D ₂ (222)	Tm ₃ TaO ₇	3.504	1	Type-II	<i>s</i> -wave
542	mp-9646	20 (C_{2221})	D ₂ (222)	La(PO ₃) ₃	4.629	1	Type-II	<i>s</i> -wave
543	mp-974267	20 (C_{2221})	D ₂ (222)	KH ₈ N ₃	2.54	1	Type-II	<i>s</i> -wave
544	mp-532768	21 (C_{222})	D ₂ (222)	YZr ₅ Si ₅ PO ₂₄	3.942	1	Type-II	<i>s</i> -wave
545	mp-768257	22 (F_{222})	D ₂ (222)	Na ₄ Bi ₂ C ₄ SO ₁₆	0.349	1	Type-II	<i>s</i> -wave
546	mp-35220	24 ($I_{21}2_12_1$)	D ₂ (222)	PHN ₂	4.654	1	Type-II	<i>s</i> -wave
547	mp-639506	24 ($I_{21}2_12_1$)	D ₂ (222)	SiO ₂	5.704	0	Type-II	<i>s</i> -wave
548	mp-753671	24 ($I_{21}2_12_1$)	D ₂ (222)	PNO	5.118	0	Type-II	<i>s</i> -wave
549	mp-762307	24 ($I_{21}2_12_1$)	D ₂ (222)	Y ₇ HoO ₁₂	4.208	0	Type-II	<i>s</i> -wave
550	mp-766267	24 ($I_{21}2_12_1$)	D ₂ (222)	Y ₇ TmO ₁₂	4.221	0	Type-II	<i>s</i> -wave
551	mp-766292	24 ($I_{21}2_12_1$)	D ₂ (222)	DyY ₇ O ₁₂	4.189	0	Type-II	<i>s</i> -wave
552	mp-867607	24 ($I_{21}2_12_1$)	D ₂ (222)	Sm ₃ Y ₅ O ₁₂	3.946	0	Type-II	<i>s</i> -wave
553	icsd-108237	25 ($Pmm2$)	C _{2v} (mm2)	CdTe	0	1	Type-III	<i>d</i> -wave
554	mp-676038	25 ($Pmm2$)	C _{2v} (mm2)	Ga ₅ (PS) ₃	1.343	0	Type-III	<i>d</i> -wave
555	mp-677080	25 ($Pmm2$)	C _{2v} (mm2)	K ₆ Ba ₃ Ta ₁₂ (Si ₂ O ₁₃) ₄	2.94	1	Type-III	<i>d</i> -wave
556	mp-695214	25 ($Pmm2$)	C _{2v} (mm2)	Ba ₉ La ₃ Mg ₅ Nb ₇ O ₃₆	2.379	1	Type-III	<i>d</i> -wave
557	mp-20940	26 ($Pmc2_1$)	C _{2v} (mm2)	TiCdO ₃	2.464	1	Type-III	<i>d</i> -wave
558	mp-23904	26 ($Pmc2_1$)	C _{2v} (mm2)	BaH ₄ O ₃	4.259	0	Type-III	<i>d</i> -wave
559	mp-27411	26 ($Pmc2_1$)	C _{2v} (mm2)	TlP ₅	1.185	0	Type-III	<i>d</i> -wave
560	mp-28007	26 ($Pmc2_1$)	C _{2v} (mm2)	BaHgS ₂	1.157	0	Type-III	<i>d</i> -wave
561	mp-28420	26 ($Pmc2_1$)	C _{2v} (mm2)	SrH ₄ O ₃	4.337	0	Type-III	<i>d</i> -wave
562	mp-4681	26 ($Pmc2_1$)	C _{2v} (mm2)	NaNbO ₃	2.368	1	Type-III	<i>d</i> -wave
563	mp-542302	26 ($Pmc2_1$)	C _{2v} (mm2)	CuBi ₃ PbS ₆	0.625	0	Type-III	<i>d</i> -wave
564	mp-554929	26 ($Pmc2_1$)	C _{2v} (mm2)	CsNdNb ₂ O ₇	2.392	0	Type-III	<i>d</i> -wave
565	mp-555463	26 ($Pmc2_1$)	C _{2v} (mm2)	RbTh ₃ F ₁₃	6.449	0	Type-III	<i>d</i> -wave
566	mp-555976	26 ($Pmc2_1$)	C _{2v} (mm2)	Na ₂ TiSiO ₅	3.208	0	Type-III	<i>d</i> -wave
567	mp-556340	26 ($Pmc2_1$)	C _{2v} (mm2)	CaTaNO ₂	1.612	1	Type-III	<i>d</i> -wave
568	mp-557711	26 ($Pmc2_1$)	C _{2v} (mm2)	K ₃ Nb ₃ (BO ₆) ₂	2.381	1	Type-III	<i>d</i> -wave
569	mp-559287	26 ($Pmc2_1$)	C _{2v} (mm2)	Ho ₂ Sn ₃ (PbS ₄) ₃	0.623	0	Type-III	<i>d</i> -wave
570	mp-559653	26 ($Pmc2_1$)	C _{2v} (mm2)	SrCa(CO ₃) ₂	4.786	0	Type-III	<i>d</i> -wave
571	mp-559868	26 ($Pmc2_1$)	C _{2v} (mm2)	NaLa(CO ₃) ₂	3.858	0	Type-III	<i>d</i> -wave
572	mp-562854	26 ($Pmc2_1$)	C _{2v} (mm2)	CsNb ₂ BiO ₇	2.482	0	Type-III	<i>d</i> -wave
573	mp-604315	26 ($Pmc2_1$)	C _{2v} (mm2)	Zn(BH ₄) ₂	4.252	0	Type-III	<i>d</i> -wave
574	mp-644419	26 ($Pmc2_1$)	C _{2v} (mm2)	LiHS	3.525	1	Type-III	<i>d</i> -wave

575	mp-757224	26 (<i>Pmc</i> 2 ₁)	C _{2v} (mm2)	Th ₄ P ₆ O ₂₃	4.191	1	Type-III	<i>d</i> -wave
576	mp-757442	26 (<i>Pmc</i> 2 ₁)	C _{2v} (mm2)	Ca ₃ In ₂ O ₆	1.962	0	Type-III	<i>d</i> -wave
577	mp-983327	26 (<i>Pmc</i> 2 ₁)	C _{2v} (mm2)	KH ₄ O ₂ F	5.197	0	Type-III	<i>d</i> -wave
578	mp-989407	26 (<i>Pmc</i> 2 ₁)	C _{2v} (mm2)	YWN ₃	1.515	0	Type-III	<i>d</i> -wave
579	mp-29510	28 (<i>Pma</i> 2)	C _{2v} (mm2)	Hg ₂ TeO ₃	2.214	1	Type-III	<i>d</i> -wave
580	mp-15148	29 (<i>Pca</i> 2 ₁)	C _{2v} (mm2)	K ₄ Nb ₂ S ₁₁	1.394	0	Type-III	<i>d</i> -wave
581	mp-17945	29 (<i>Pca</i> 2 ₁)	C _{2v} (mm2)	RbPSe ₆	1.861	0	Type-III	<i>d</i> -wave
582	mp-18625	29 (<i>Pca</i> 2 ₁)	C _{2v} (mm2)	KPSe ₆	1.883	0	Type-III	<i>d</i> -wave
583	mp-20817	29 (<i>Pca</i> 2 ₁)	C _{2v} (mm2)	GePtSe	0.66	0	Type-III	<i>d</i> -wave
584	mp-23087	29 (<i>Pca</i> 2 ₁)	C _{2v} (mm2)	Mg ₃ B ₇ ClO ₁₃	5.705	0	Type-III	<i>d</i> -wave
585	mp-27198	29 (<i>Pca</i> 2 ₁)	C _{2v} (mm2)	Cd(NO ₃) ₂	3.458	1	Type-III	<i>d</i> -wave
586	mp-27367	29 (<i>Pca</i> 2 ₁)	C _{2v} (mm2)	SeOF ₂	4.083	0	Type-III	<i>d</i> -wave
587	mp-28134	29 (<i>Pca</i> 2 ₁)	C _{2v} (mm2)	Ba ₂ As ₂ S ₅	1.373	0	Type-III	<i>d</i> -wave
588	mp-4627	29 (<i>Pca</i> 2 ₁)	C _{2v} (mm2)	CoAsS	0.941	0	Type-III	<i>d</i> -wave
589	mp-554718	29 (<i>Pca</i> 2 ₁)	C _{2v} (mm2)	Bi(BO ₂) ₃	3.859	1	Type-III	<i>d</i> -wave
590	mp-554856	29 (<i>Pca</i> 2 ₁)	C _{2v} (mm2)	Na ₂ Si ₂ O ₅	4.426	0	Type-III	<i>d</i> -wave
591	mp-556578	29 (<i>Pca</i> 2 ₁)	C _{2v} (mm2)	Cd(IO ₃) ₂	3.335	0	Type-III	<i>d</i> -wave
592	mp-556605	29 (<i>Pca</i> 2 ₁)	C _{2v} (mm2)	ZrO ₂	3.691	0	Type-III	<i>d</i> -wave
593	mp-557955	29 (<i>Pca</i> 2 ₁)	C _{2v} (mm2)	Ca ₃ Al ₄ ZnO ₁₀	3.545	0	Type-III	<i>d</i> -wave
594	mp-558861	29 (<i>Pca</i> 2 ₁)	C _{2v} (mm2)	KI(OF) ₂	4.16	0	Type-III	<i>d</i> -wave
595	mp-558920	29 (<i>Pca</i> 2 ₁)	C _{2v} (mm2)	NaNbO ₃	2.41	1	Type-III	<i>d</i> -wave
596	mp-559138	29 (<i>Pca</i> 2 ₁)	C _{2v} (mm2)	Ba ₂ Zn(BO ₃) ₂	3.333	0	Type-III	<i>d</i> -wave
597	mp-559594	29 (<i>Pca</i> 2 ₁)	C _{2v} (mm2)	LaGaSe ₂ O	1.598	0	Type-III	<i>d</i> -wave
598	mp-560334	29 (<i>Pca</i> 2 ₁)	C _{2v} (mm2)	NaAlSiO ₄	4.599	0	Type-III	<i>d</i> -wave
599	mp-6236	29 (<i>Pca</i> 2 ₁)	C _{2v} (mm2)	Na ₂ BeSiO ₄	4.77	0	Type-III	<i>d</i> -wave
600	mp-6663	29 (<i>Pca</i> 2 ₁)	C _{2v} (mm2)	NaLiGe ₄ O ₉	2.659	0	Type-III	<i>d</i> -wave
601	mp-684022	29 (<i>Pca</i> 2 ₁)	C _{2v} (mm2)	LaTiGeSe ₄	1.462	0	Type-III	<i>d</i> -wave
602	mp-685097	29 (<i>Pca</i> 2 ₁)	C _{2v} (mm2)	HfO ₂	4.415	0	Type-III	<i>d</i> -wave
603	mp-6955	29 (<i>Pca</i> 2 ₁)	C _{2v} (mm2)	KGeNO	2.682	0	Type-III	<i>d</i> -wave
604	mp-721312	29 (<i>Pca</i> 2 ₁)	C _{2v} (mm2)	Na ₂ H ₂ CO ₄	4.169	0	Type-III	<i>d</i> -wave
605	mp-722369	29 (<i>Pca</i> 2 ₁)	C _{2v} (mm2)	Na ₃ B ₅ (HO ₅) ₂	4.658	1	Type-III	<i>d</i> -wave
606	mp-733853	29 (<i>Pca</i> 2 ₁)	C _{2v} (mm2)	K ₂ H ₂ ClO ₆	3.051	0	Type-III	<i>d</i> -wave
607	mp-768887	29 (<i>Pca</i> 2 ₁)	C _{2v} (mm2)	Y(BO ₂) ₃	5.245	1	Type-III	<i>d</i> -wave
608	mp-773017	29 (<i>Pca</i> 2 ₁)	C _{2v} (mm2)	LiTi ₂ (PO ₄) ₃	2.439	1	Type-III	<i>d</i> -wave
609	mp-9270	29 (<i>Pca</i> 2 ₁)	C _{2v} (mm2)	SbIrS	1.07	0	Type-III	<i>d</i> -wave
610	mp-555438	30 (<i>Pnc</i> 2)	C _{2v} (mm2)	Ba ₃ AlF ₉	6.654	1	Type-III	<i>d</i> -wave
611	mp-753378	30 (<i>Pnc</i> 2)	C _{2v} (mm2)	TaGaO ₄	3.282	0	Type-III	<i>d</i> -wave
612	mp-10796	31 (<i>Pmn</i> 2 ₁)	C _{2v} (mm2)	HgSeO ₄	0.844	0	Type-III	<i>d</i> -wave
613	mp-11000	31 (<i>Pmn</i> 2 ₁)	C _{2v} (mm2)	CaB ₄ O ₇	6.318	0	Type-III	<i>d</i> -wave
614	mp-12023	31 (<i>Pmn</i> 2 ₁)	C _{2v} (mm2)	MnCu ₂ SiS ₄	0	0	Type-III	<i>d</i> -wave
615	mp-12797	31 (<i>Pmn</i> 2 ₁)	C _{2v} (mm2)	BaBe ₂ Si ₂ O ₇	5.569	0	Type-III	<i>d</i> -wave
616	mp-13252	31 (<i>Pmn</i> 2 ₁)	C _{2v} (mm2)	SnB ₄ O ₇	3.572	0	Type-III	<i>d</i> -wave
617	mp-13725	31 (<i>Pmn</i> 2 ₁)	C _{2v} (mm2)	Li ₃ PO ₄	5.818	0	Type-III	<i>d</i> -wave
618	mp-13872	31 (<i>Pmn</i> 2 ₁)	C _{2v} (mm2)	Cu ₈ SiS ₆	0.83	0	Type-III	<i>d</i> -wave
619	mp-18073	31 (<i>Pmn</i> 2 ₁)	C _{2v} (mm2)	K ₇ TaAs ₄	1.041	0	Type-III	<i>d</i> -wave
620	mp-18361	31 (<i>Pmn</i> 2 ₁)	C _{2v} (mm2)	K ₇ NbAs ₄	1.129	0	Type-III	<i>d</i> -wave
621	mp-18440	31 (<i>Pmn</i> 2 ₁)	C _{2v} (mm2)	Rb ₇ NbAs ₄	0.768	0	Type-III	<i>d</i> -wave
622	mp-23803	31 (<i>Pmn</i> 2 ₁)	C _{2v} (mm2)	GaHO ₂	3.002	0	Type-III	<i>d</i> -wave
623	mp-23807	31 (<i>Pmn</i> 2 ₁)	C _{2v} (mm2)	AlHO ₂	5.657	0	Type-III	<i>d</i> -wave
624	mp-28295	31 (<i>Pmn</i> 2 ₁)	C _{2v} (mm2)	CsIO ₃	3.091	0	Type-III	<i>d</i> -wave
625	mp-3228	31 (<i>Pmn</i> 2 ₁)	C _{2v} (mm2)	HgSO ₄	1.353	0	Type-III	<i>d</i> -wave
626	mp-3934	31 (<i>Pmn</i> 2 ₁)	C _{2v} (mm2)	Cu ₃ PS ₄	1.02	0	Type-III	<i>d</i> -wave
627	mp-4309	31 (<i>Pmn</i> 2 ₁)	C _{2v} (mm2)	BaGa ₄ S ₇	2.58	0	Type-III	<i>d</i> -wave
628	mp-504535	31 (<i>Pmn</i> 2 ₁)	C _{2v} (mm2)	InHO ₂	1.776	0	Type-III	<i>d</i> -wave
629	mp-510346	31 (<i>Pmn</i> 2 ₁)	C _{2v} (mm2)	In ₅ Se ₅ Br	0.744	0	Type-III	<i>d</i> -wave
630	mp-5540	31 (<i>Pmn</i> 2 ₁)	C _{2v} (mm2)	SrB ₄ O ₇	7.119	0	Type-III	<i>d</i> -wave
631	mp-554105	31 (<i>Pmn</i> 2 ₁)	C _{2v} (mm2)	CdAg ₂ GeS ₄	0.579	0	Type-III	<i>d</i> -wave
632	mp-555150	31 (<i>Pmn</i> 2 ₁)	C _{2v} (mm2)	KTa(BO ₃) ₂	3.614	0	Type-III	<i>d</i> -wave
633	mp-555363	31 (<i>Pmn</i> 2 ₁)	C _{2v} (mm2)	Na ₂ Cd(SiO ₃) ₂	2.87	1	Type-III	<i>d</i> -wave

634	mp-556009	31 (<i>Pmn2</i> ₁)	C _{2v} (mm2)	MgTlAs(H ₆ O ₅) ₂	4.381	1	Type-III	<i>d</i> -wave
635	mp-557940	31 (<i>Pmn2</i> ₁)	C _{2v} (mm2)	KNd(CO ₃) ₂	4.36	0	Type-III	<i>d</i> -wave
636	mp-567269	31 (<i>Pmn2</i> ₁)	C _{2v} (mm2)	TeI ₄	1.829	0	Type-III	<i>d</i> -wave
637	mp-5679	31 (<i>Pmn2</i> ₁)	C _{2v} (mm2)	CdSO ₄	3.05	0	Type-III	<i>d</i> -wave
638	mp-568970	31 (<i>Pmn2</i> ₁)	C _{2v} (mm2)	K ₃ SnIrCl ₈	1.594	0	Type-III	<i>d</i> -wave
639	mp-604725	31 (<i>Pmn2</i> ₁)	C _{2v} (mm2)	RbMgP(H ₆ O ₅) ₂	4.795	1	Type-III	<i>d</i> -wave
640	mp-615850	31 (<i>Pmn2</i> ₁)	C _{2v} (mm2)	Pb ₂ Se(NO ₄) ₂	2.482	0	Type-III	<i>d</i> -wave
641	mp-6257	31 (<i>Pmn2</i> ₁)	C _{2v} (mm2)	CsNb(BO ₃) ₂	3.299	0	Type-III	<i>d</i> -wave
642	mp-628643	31 (<i>Pmn2</i> ₁)	C _{2v} (mm2)	CuAsPbS ₃	0.79	0	Type-III	<i>d</i> -wave
643	mp-6356	31 (<i>Pmn2</i> ₁)	C _{2v} (mm2)	Cd ₂ GaAgS ₄	1.044	0	Type-III	<i>d</i> -wave
644	mp-6449	31 (<i>Pmn2</i> ₁)	C _{2v} (mm2)	CdCu ₂ SiS ₄	0.98	0	Type-III	<i>d</i> -wave
645	mp-649774	31 (<i>Pmn2</i> ₁)	C _{2v} (mm2)	CuSbPbS ₃	0.77	0	Type-III	<i>d</i> -wave
646	mp-720570	31 (<i>Pmn2</i> ₁)	C _{2v} (mm2)	Na ₂ PH ₁₁ O ₈	5.262	1	Type-III	<i>d</i> -wave
647	mp-752484	31 (<i>Pmn2</i> ₁)	C _{2v} (mm2)	YbB ₄ O ₇	6.997	0	Type-III	<i>d</i> -wave
648	mp-753277	31 (<i>Pmn2</i> ₁)	C _{2v} (mm2)	LiAgF ₂	1.207	1	Type-III	<i>d</i> -wave
649	mp-753947	31 (<i>Pmn2</i> ₁)	C _{2v} (mm2)	LuHO ₂	4.856	0	Type-III	<i>d</i> -wave
650	mp-754117	31 (<i>Pmn2</i> ₁)	C _{2v} (mm2)	YHO ₂	4.838	0	Type-III	<i>d</i> -wave
651	mp-754202	31 (<i>Pmn2</i> ₁)	C _{2v} (mm2)	CsClO ₃	5.371	0	Type-III	<i>d</i> -wave
652	mp-755543	31 (<i>Pmn2</i> ₁)	C _{2v} (mm2)	HoHO ₂	4.757	0	Type-III	<i>d</i> -wave
653	mp-755642	31 (<i>Pmn2</i> ₁)	C _{2v} (mm2)	Li ₃ VS ₄	1.617	0	Type-III	<i>d</i> -wave
654	mp-756044	31 (<i>Pmn2</i> ₁)	C _{2v} (mm2)	Na ₃ AsO ₄	3.228	0	Type-III	<i>d</i> -wave
655	mp-756316	31 (<i>Pmn2</i> ₁)	C _{2v} (mm2)	Li ₃ SbS ₄	2.145	0	Type-III	<i>d</i> -wave
656	mp-7688	31 (<i>Pmn2</i> ₁)	C _{2v} (mm2)	Li ₂ CdGeO ₄	2.455	0	Type-III	<i>d</i> -wave
657	mp-769365	31 (<i>Pmn2</i> ₁)	C _{2v} (mm2)	ZnSeO ₄	2.065	0	Type-III	<i>d</i> -wave
658	mp-772052	31 (<i>Pmn2</i> ₁)	C _{2v} (mm2)	CdSeO ₄	1.847	0	Type-III	<i>d</i> -wave
659	mp-777422	31 (<i>Pmn2</i> ₁)	C _{2v} (mm2)	DyHO ₂	4.728	0	Type-III	<i>d</i> -wave
660	mp-8258	31 (<i>Pmn2</i> ₁)	C _{2v} (mm2)	BaAl ₄ S ₇	3.157	0	Type-III	<i>d</i> -wave
661	mp-9066	31 (<i>Pmn2</i> ₁)	C _{2v} (mm2)	NaLi ₂ AsO ₄	3.889	0	Type-III	<i>d</i> -wave
662	mp-9197	31 (<i>Pmn2</i> ₁)	C _{2v} (mm2)	Li ₃ AsO ₄	4.127	0	Type-III	<i>d</i> -wave
663	mp-9710	31 (<i>Pmn2</i> ₁)	C _{2v} (mm2)	Sr ₂ Si ₅ N ₈	3.197	0	Type-III	<i>d</i> -wave
664	mp-9711	31 (<i>Pmn2</i> ₁)	C _{2v} (mm2)	Ba ₂ Si ₅ N ₈	2.882	0	Type-III	<i>d</i> -wave
665	mp-9747	31 (<i>Pmn2</i> ₁)	C _{2v} (mm2)	B ₄ PbO ₇	4.208	0	Type-III	<i>d</i> -wave
666	mp-977414	31 (<i>Pmn2</i> ₁)	C _{2v} (mm2)	ZnCu ₂ SiS ₄	1.282	0	Type-III	<i>d</i> -wave
667	mp-28095	32 (<i>Pba</i> ₂)	C _{2v} (mm2)	Au ₂ Se ₂ O ₇	1.15	0	Type-III	<i>d</i> -wave
668	mp-555880	32 (<i>Pba</i> ₂)	C _{2v} (mm2)	ZnBi ₂ B ₂ O ₇	2.52	0	Type-III	<i>d</i> -wave
669	mp-647557	32 (<i>Pba</i> ₂)	C _{2v} (mm2)	ZrPbO ₃	3.209	1	Type-III	<i>d</i> -wave
670	mp-669414	32 (<i>Pba</i> ₂)	C _{2v} (mm2)	HfPbO ₃	2.779	1	Type-III	<i>d</i> -wave
671	mp-698033	32 (<i>Pba</i> ₂)	C _{2v} (mm2)	KAl ₂ P ₂ H ₈ O ₁₂ F	4.979	1	Type-III	<i>d</i> -wave
672	mp-776024	32 (<i>Pba</i> ₂)	C _{2v} (mm2)	CaZrO ₃	3.471	1	Type-III	<i>d</i> -wave
673	mp-11582	33 (<i>Pna</i> ₂ ₁)	C _{2v} (mm2)	LiGaSe ₂	2.066	0	Type-III	<i>d</i> -wave
674	mp-12192	33 (<i>Pna</i> ₂ ₁)	C _{2v} (mm2)	La ₂ Ti ₂ O ₇	2.928	1	Type-III	<i>d</i> -wave
675	mp-12295	33 (<i>Pna</i> ₂ ₁)	C _{2v} (mm2)	Sr ₃ La ₂ (BO ₃) ₄	4.156	1	Type-III	<i>d</i> -wave
676	mp-13774	33 (<i>Pna</i> ₂ ₁)	C _{2v} (mm2)	NaNdSiO ₄	4.477	1	Type-III	<i>d</i> -wave
677	mp-13960	33 (<i>Pna</i> ₂ ₁)	C _{2v} (mm2)	Sr ₃ Er ₂ (BO ₃) ₄	4.477	1	Type-III	<i>d</i> -wave
678	mp-14280	33 (<i>Pna</i> ₂ ₁)	C _{2v} (mm2)	Ga ₂ Sn ₂ S ₅	1.697	0	Type-III	<i>d</i> -wave
679	mp-14383	33 (<i>Pna</i> ₂ ₁)	C _{2v} (mm2)	KGePO ₅	3.229	0	Type-III	<i>d</i> -wave
680	mp-14401	33 (<i>Pna</i> ₂ ₁)	C _{2v} (mm2)	NaCaPO ₄	4.914	1	Type-III	<i>d</i> -wave
681	mp-14722	33 (<i>Pna</i> ₂ ₁)	C _{2v} (mm2)	NaSrAlF ₆	6.977	0	Type-III	<i>d</i> -wave
682	mp-15108	33 (<i>Pna</i> ₂ ₁)	C _{2v} (mm2)	RbSnAsO ₅	2.072	0	Type-III	<i>d</i> -wave
683	mp-15515	33 (<i>Pna</i> ₂ ₁)	C _{2v} (mm2)	BaNaAlF ₆	6.981	0	Type-III	<i>d</i> -wave
684	mp-15590	33 (<i>Pna</i> ₂ ₁)	C _{2v} (mm2)	Sr ₂ Nb ₂ O ₇	2.752	1	Type-III	<i>d</i> -wave
685	mp-15865	33 (<i>Pna</i> ₂ ₁)	C _{2v} (mm2)	RbScAsO ₄ F	4.048	0	Type-III	<i>d</i> -wave
686	mp-16996	33 (<i>Pna</i> ₂ ₁)	C _{2v} (mm2)	Li ₃ GaSiO ₅	3.643	0	Type-III	<i>d</i> -wave
687	mp-17685	33 (<i>Pna</i> ₂ ₁)	C _{2v} (mm2)	Li ₃ GaGeO ₅	3.266	0	Type-III	<i>d</i> -wave
688	mp-17709	33 (<i>Pna</i> ₂ ₁)	C _{2v} (mm2)	Na ₂ ZnSiO ₄	3.136	0	Type-III	<i>d</i> -wave
689	mp-17885	33 (<i>Pna</i> ₂ ₁)	C _{2v} (mm2)	Ba ₂ Ge ₂ Te ₅	0.624	0	Type-III	<i>d</i> -wave
690	mp-17964	33 (<i>Pna</i> ₂ ₁)	C _{2v} (mm2)	Na ₂ Ge ₂ Se ₅	1.402	0	Type-III	<i>d</i> -wave
691	mp-20205	33 (<i>Pna</i> ₂ ₁)	C _{2v} (mm2)	Yb ₂ Cu ₂ O ₅	0.922	0	Type-III	<i>d</i> -wave
692	mp-20310	33 (<i>Pna</i> ₂ ₁)	C _{2v} (mm2)	LiInSe ₂	1.623	0	Type-III	<i>d</i> -wave

693	mp-21459	33 (<i>Pna</i> 2 ₁)	C _{2v} (mm2)	InAgS ₂	0.508	0	Type-III	<i>d</i> -wave
694	mp-21724	33 (<i>Pna</i> 2 ₁)	C _{2v} (mm2)	ZnSiPbO ₄	3.101	1	Type-III	<i>d</i> -wave
695	mp-2254	33 (<i>Pna</i> 2 ₁)	C _{2v} (mm2)	Al ₂ O ₃	4.827	1	Type-III	<i>d</i> -wave
696	mp-22694	33 (<i>Pna</i> 2 ₁)	C _{2v} (mm2)	LiPPbO ₄	3.525	1	Type-III	<i>d</i> -wave
697	mp-22889	33 (<i>Pna</i> 2 ₁)	C _{2v} (mm2)	ZnCl ₂	4.04	0	Type-III	<i>d</i> -wave
698	mp-22994	33 (<i>Pna</i> 2 ₁)	C _{2v} (mm2)	LiIO ₃	3.655	0	Type-III	<i>d</i> -wave
699	mp-230	33 (<i>Pna</i> 2 ₁)	C _{2v} (mm2)	SbO ₂	1.89	0	Type-III	<i>d</i> -wave
700	mp-2412	33 (<i>Pna</i> 2 ₁)	C _{2v} (mm2)	LiP ₅	1.257	0	Type-III	<i>d</i> -wave
701	mp-2447	33 (<i>Pna</i> 2 ₁)	C _{2v} (mm2)	P ₄ Se ₅	1.824	0	Type-III	<i>d</i> -wave
702	mp-24473	33 (<i>Pna</i> 2 ₁)	C _{2v} (mm2)	BePH ₄ NO ₄	5.083	0	Type-III	<i>d</i> -wave
703	mp-24603	33 (<i>Pna</i> 2 ₁)	C _{2v} (mm2)	CaAl ₂ Si ₂ (H ₂ O ₅) ₂	5.062	0	Type-III	<i>d</i> -wave
704	mp-24610	33 (<i>Pna</i> 2 ₁)	C _{2v} (mm2)	LiP(HO ₂) ₂	5.578	1	Type-III	<i>d</i> -wave
705	mp-27017	33 (<i>Pna</i> 2 ₁)	C _{2v} (mm2)	LiSnPO ₄	3.407	1	Type-III	<i>d</i> -wave
706	mp-28027	33 (<i>Pna</i> 2 ₁)	C _{2v} (mm2)	AsF ₃	5.36	0	Type-III	<i>d</i> -wave
707	mp-28460	33 (<i>Pna</i> 2 ₁)	C _{2v} (mm2)	Br ₂ O	1.394	0	Type-III	<i>d</i> -wave
708	mp-28471	33 (<i>Pna</i> 2 ₁)	C _{2v} (mm2)	Li ₃ AsS ₃	2.285	0	Type-III	<i>d</i> -wave
709	mp-28558	33 (<i>Pna</i> 2 ₁)	C _{2v} (mm2)	RbGeBr ₃	1.985	0	Type-III	<i>d</i> -wave
710	mp-29295	33 (<i>Pna</i> 2 ₁)	C _{2v} (mm2)	Sr ₃ Sb ₄ S ₉	1.041	0	Type-III	<i>d</i> -wave
711	mp-2979	33 (<i>Pna</i> 2 ₁)	C _{2v} (mm2)	ZnGeN ₂	1.696	0	Type-III	<i>d</i> -wave
712	mp-3338	33 (<i>Pna</i> 2 ₁)	C _{2v} (mm2)	NaGaO ₂	2.858	0	Type-III	<i>d</i> -wave
713	mp-3491	33 (<i>Pna</i> 2 ₁)	C _{2v} (mm2)	NbSbO ₄	2.431	0	Type-III	<i>d</i> -wave
714	mp-3647	33 (<i>Pna</i> 2 ₁)	C _{2v} (mm2)	LiGaS ₂	2.961	0	Type-III	<i>d</i> -wave
715	mp-3660	33 (<i>Pna</i> 2 ₁)	C _{2v} (mm2)	LiB ₃ O ₅	6.353	0	Type-III	<i>d</i> -wave
716	mp-3677	33 (<i>Pna</i> 2 ₁)	C _{2v} (mm2)	MgSiN ₂	3.966	0	Type-III	<i>d</i> -wave
717	mp-402	33 (<i>Pna</i> 2 ₁)	C _{2v} (mm2)	CdP ₂	1.49	0	Type-III	<i>d</i> -wave
718	mp-5052	33 (<i>Pna</i> 2 ₁)	C _{2v} (mm2)	TiCdO ₃	2.416	0	Type-III	<i>d</i> -wave
719	mp-505321	33 (<i>Pna</i> 2 ₁)	C _{2v} (mm2)	CsNb(CuTe ₂) ₂	1.025	1	Type-III	<i>d</i> -wave
720	mp-505322	33 (<i>Pna</i> 2 ₁)	C _{2v} (mm2)	CsTa(CuTe ₂) ₂	1.244	0	Type-III	<i>d</i> -wave
721	mp-530262	33 (<i>Pna</i> 2 ₁)	C _{2v} (mm2)	Li ₁₅ Cr ₂ N ₉	1.336	0	Type-III	<i>d</i> -wave
722	mp-5363	33 (<i>Pna</i> 2 ₁)	C _{2v} (mm2)	Hg ₂ TeO ₅	0.535	0	Type-III	<i>d</i> -wave
723	mp-540689	33 (<i>Pna</i> 2 ₁)	C _{2v} (mm2)	Ba ₂ SnS ₄	2.31	0	Type-III	<i>d</i> -wave
724	mp-541459	33 (<i>Pna</i> 2 ₁)	C _{2v} (mm2)	KSnPO ₅	3.023	0	Type-III	<i>d</i> -wave
725	mp-541956	33 (<i>Pna</i> 2 ₁)	C _{2v} (mm2)	CsTiAsO ₅	3.005	0	Type-III	<i>d</i> -wave
726	mp-554006	33 (<i>Pna</i> 2 ₁)	C _{2v} (mm2)	SrCaSiO ₄	4.48	1	Type-III	<i>d</i> -wave
727	mp-554089	33 (<i>Pna</i> 2 ₁)	C _{2v} (mm2)	SiO ₂	5.66	0	Type-III	<i>d</i> -wave
728	mp-554288	33 (<i>Pna</i> 2 ₁)	C _{2v} (mm2)	NaPH ₄ O ₅	5.229	1	Type-III	<i>d</i> -wave
729	mp-554383	33 (<i>Pna</i> 2 ₁)	C _{2v} (mm2)	Na ₂ Si ₂ O ₅	4.457	0	Type-III	<i>d</i> -wave
730	mp-554529	33 (<i>Pna</i> 2 ₁)	C _{2v} (mm2)	Ba ₂ TiO ₄	4.263	1	Type-III	<i>d</i> -wave
731	mp-555076	33 (<i>Pna</i> 2 ₁)	C _{2v} (mm2)	KNaSnF ₆	5.171	0	Type-III	<i>d</i> -wave
732	mp-555816	33 (<i>Pna</i> 2 ₁)	C _{2v} (mm2)	KDy(SeO ₄) ₂	3.591	1	Type-III	<i>d</i> -wave
733	mp-555825	33 (<i>Pna</i> 2 ₁)	C _{2v} (mm2)	Na ₄ Sc ₂ Si ₄ O ₁₃	4.818	1	Type-III	<i>d</i> -wave
734	mp-556020	33 (<i>Pna</i> 2 ₁)	C _{2v} (mm2)	Li ₃ AlF ₆	7.915	0	Type-III	<i>d</i> -wave
735	mp-556206	33 (<i>Pna</i> 2 ₁)	C _{2v} (mm2)	Rb ₃ Y ₂ (BO ₃) ₃	4.168	0	Type-III	<i>d</i> -wave
736	mp-556623	33 (<i>Pna</i> 2 ₁)	C _{2v} (mm2)	K ₂ TiOF ₄	3.032	1	Type-III	<i>d</i> -wave
737	mp-556826	33 (<i>Pna</i> 2 ₁)	C _{2v} (mm2)	Ca(BO ₂) ₂	5.457	1	Type-III	<i>d</i> -wave
738	mp-556892	33 (<i>Pna</i> 2 ₁)	C _{2v} (mm2)	InBiO ₃	2.735	0	Type-III	<i>d</i> -wave
739	mp-557237	33 (<i>Pna</i> 2 ₁)	C _{2v} (mm2)	K ₅ In ₃ (SiO ₃) ₇	3.668	0	Type-III	<i>d</i> -wave
740	mp-557311	33 (<i>Pna</i> 2 ₁)	C _{2v} (mm2)	Sr ₂ GeO ₄	3.566	0	Type-III	<i>d</i> -wave
741	mp-557803	33 (<i>Pna</i> 2 ₁)	C _{2v} (mm2)	MgSiO ₃	4.675	0	Type-III	<i>d</i> -wave
742	mp-558085	33 (<i>Pna</i> 2 ₁)	C _{2v} (mm2)	KNaGeO ₃	3.04	0	Type-III	<i>d</i> -wave
743	mp-558105	33 (<i>Pna</i> 2 ₁)	C _{2v} (mm2)	LiB ₆ O ₉ F	6.456	1	Type-III	<i>d</i> -wave
744	mp-558174	33 (<i>Pna</i> 2 ₁)	C _{2v} (mm2)	TlSb ₃ (AsS ₄) ₂	1.534	1	Type-III	<i>d</i> -wave
745	mp-558807	33 (<i>Pna</i> 2 ₁)	C _{2v} (mm2)	ZnAgPS ₄	2.193	0	Type-III	<i>d</i> -wave
746	mp-559053	33 (<i>Pna</i> 2 ₁)	C _{2v} (mm2)	NaY(SeO ₃) ₂	4.226	1	Type-III	<i>d</i> -wave
747	mp-559689	33 (<i>Pna</i> 2 ₁)	C _{2v} (mm2)	LiAlSiO ₄	5.053	0	Type-III	<i>d</i> -wave
748	mp-559849	33 (<i>Pna</i> 2 ₁)	C _{2v} (mm2)	Ca(GaO ₂) ₂	2.986	0	Type-III	<i>d</i> -wave
749	mp-559934	33 (<i>Pna</i> 2 ₁)	C _{2v} (mm2)	LiZnPO ₄	4.13	0	Type-III	<i>d</i> -wave
750	mp-560040	33 (<i>Pna</i> 2 ₁)	C _{2v} (mm2)	Ca ₂ Nb ₂ O ₇	3.065	1	Type-III	<i>d</i> -wave
751	mp-560821	33 (<i>Pna</i> 2 ₁)	C _{2v} (mm2)	Ca ₂ SiO ₄	4.62	1	Type-III	<i>d</i> -wave

752	mp-561057	33 (<i>Pna</i> 2 ₁)	C _{2v} (mm2)	SbP ₂ O ₇	1.944	1	Type-III	<i>d</i> -wave
753	mp-561157	33 (<i>Pna</i> 2 ₁)	C _{2v} (mm2)	Sr ₃ Y ₂ (BO ₃) ₄	4.483	1	Type-III	<i>d</i> -wave
754	mp-568759	33 (<i>Pna</i> 2 ₁)	C _{2v} (mm2)	NaNd ₄ I ₇ N ₂	2.721	0	Type-III	<i>d</i> -wave
755	mp-569580	33 (<i>Pna</i> 2 ₁)	C _{2v} (mm2)	NaLa ₄ I ₇ N ₂	2.847	0	Type-III	<i>d</i> -wave
756	mp-570548	33 (<i>Pna</i> 2 ₁)	C _{2v} (mm2)	NaPr ₄ I ₇ N ₂	2.708	0	Type-III	<i>d</i> -wave
757	mp-570577	33 (<i>Pna</i> 2 ₁)	C _{2v} (mm2)	SrAlSi ₄ N ₇	3.691	1	Type-III	<i>d</i> -wave
758	mp-5854	33 (<i>Pna</i> 2 ₁)	C _{2v} (mm2)	LiGaO ₂	3.198	0	Type-III	<i>d</i> -wave
759	mp-604229	33 (<i>Pna</i> 2 ₁)	C _{2v} (mm2)	ZnH ₃ CNO ₃	3.683	0	Type-III	<i>d</i> -wave
760	mp-6057	33 (<i>Pna</i> 2 ₁)	C _{2v} (mm2)	TlSnPS ₄	1.827	0	Type-III	<i>d</i> -wave
761	mp-616185	33 (<i>Pna</i> 2 ₁)	C _{2v} (mm2)	Rb ₂ ZnCl ₄	4.475	0	Type-III	<i>d</i> -wave
762	mp-618177	33 (<i>Pna</i> 2 ₁)	C _{2v} (mm2)	K ₂ ZnCl ₄	4.408	0	Type-III	<i>d</i> -wave
763	mp-619032	33 (<i>Pna</i> 2 ₁)	C _{2v} (mm2)	PbCN ₂	1.73	0	Type-III	<i>d</i> -wave
764	mp-6249	33 (<i>Pna</i> 2 ₁)	C _{2v} (mm2)	Sr ₃ Nd ₂ (BO ₃) ₄	4.57	1	Type-III	<i>d</i> -wave
765	mp-625630	33 (<i>Pna</i> 2 ₁)	C _{2v} (mm2)	TeHO ₃	2.123	1	Type-III	<i>d</i> -wave
766	mp-625654	33 (<i>Pna</i> 2 ₁)	C _{2v} (mm2)	TeHO ₃	2.152	1	Type-III	<i>d</i> -wave
767	mp-6268	33 (<i>Pna</i> 2 ₁)	C _{2v} (mm2)	KTiPO ₅	3.044	0	Type-III	<i>d</i> -wave
768	mp-6394	33 (<i>Pna</i> 2 ₁)	C _{2v} (mm2)	RbTiAsO ₅	3.056	0	Type-III	<i>d</i> -wave
769	mp-6426	33 (<i>Pna</i> 2 ₁)	C _{2v} (mm2)	Na ₂ MgSiO ₄	3.769	0	Type-III	<i>d</i> -wave
770	mp-6434	33 (<i>Pna</i> 2 ₁)	C _{2v} (mm2)	RbAlSiO ₄	4.381	0	Type-III	<i>d</i> -wave
771	mp-644097	33 (<i>Pna</i> 2 ₁)	C _{2v} (mm2)	BaAlH ₅	2.754	0	Type-III	<i>d</i> -wave
772	mp-647575	33 (<i>Pna</i> 2 ₁)	C _{2v} (mm2)	K ₂ ZnCl ₄	4.784	0	Type-III	<i>d</i> -wave
773	mp-6639	33 (<i>Pna</i> 2 ₁)	C _{2v} (mm2)	RbGeSbO ₅	2.178	0	Type-III	<i>d</i> -wave
774	mp-6765	33 (<i>Pna</i> 2 ₁)	C _{2v} (mm2)	Li ₃ AlGeO ₅	3.969	0	Type-III	<i>d</i> -wave
775	mp-6803	33 (<i>Pna</i> 2 ₁)	C _{2v} (mm2)	Sr ₃ Pr ₂ (BO ₃) ₄	4.576	0	Type-III	<i>d</i> -wave
776	mp-7117	33 (<i>Pna</i> 2 ₁)	C _{2v} (mm2)	LiAlSe ₂	3.023	0	Type-III	<i>d</i> -wave
777	mp-7324	33 (<i>Pna</i> 2 ₁)	C _{2v} (mm2)	KBePO ₄	5.263	0	Type-III	<i>d</i> -wave
778	mp-752882	33 (<i>Pna</i> 2 ₁)	C _{2v} (mm2)	LiAgF ₂	1.527	0	Type-III	<i>d</i> -wave
779	mp-753520	33 (<i>Pna</i> 2 ₁)	C _{2v} (mm2)	Li ₃ BiS ₃	2.253	0	Type-III	<i>d</i> -wave
780	mp-756272	33 (<i>Pna</i> 2 ₁)	C _{2v} (mm2)	LaDyO ₃	4.363	0	Type-III	<i>d</i> -wave
781	mp-757874	33 (<i>Pna</i> 2 ₁)	C _{2v} (mm2)	LiSiBiO ₄	3.029	1	Type-III	<i>d</i> -wave
782	mp-770219	33 (<i>Pna</i> 2 ₁)	C _{2v} (mm2)	NbAsO ₄	2.635	0	Type-III	<i>d</i> -wave
783	mp-771248	33 (<i>Pna</i> 2 ₁)	C _{2v} (mm2)	Na ₂ Ge ₂ O ₅	2.99	0	Type-III	<i>d</i> -wave
784	mp-772187	33 (<i>Pna</i> 2 ₁)	C _{2v} (mm2)	AlGaO ₃	3.112	0	Type-III	<i>d</i> -wave
785	mp-772788	33 (<i>Pna</i> 2 ₁)	C _{2v} (mm2)	Ba ₂ Cu ₂ O ₅	0.77	0	Type-III	<i>d</i> -wave
786	mp-772813	33 (<i>Pna</i> 2 ₁)	C _{2v} (mm2)	Ca ₂ Cu ₂ O ₅	1.006	0	Type-III	<i>d</i> -wave
787	mp-772898	33 (<i>Pna</i> 2 ₁)	C _{2v} (mm2)	AlGaO ₃	3.213	0	Type-III	<i>d</i> -wave
788	mp-773906	33 (<i>Pna</i> 2 ₁)	C _{2v} (mm2)	KNaZrSi ₃ H ₄ O ₁₁	4.92	1	Type-III	<i>d</i> -wave
789	mp-779729	33 (<i>Pna</i> 2 ₁)	C _{2v} (mm2)	Na ₂ Ti ₂ O ₅	3.808	0	Type-III	<i>d</i> -wave
790	mp-7798	33 (<i>Pna</i> 2 ₁)	C _{2v} (mm2)	MgGeN ₂	2.636	0	Type-III	<i>d</i> -wave
791	mp-780263	33 (<i>Pna</i> 2 ₁)	C _{2v} (mm2)	Ba ₂ GeO ₄	3.798	1	Type-III	<i>d</i> -wave
792	mp-780395	33 (<i>Pna</i> 2 ₁)	C _{2v} (mm2)	Cd(BO ₂) ₂	2.908	1	Type-III	<i>d</i> -wave
793	mp-7913	33 (<i>Pna</i> 2 ₁)	C _{2v} (mm2)	BeSiN ₂	5.146	0	Type-III	<i>d</i> -wave
794	mp-8341	33 (<i>Pna</i> 2 ₁)	C _{2v} (mm2)	NaGeSbO ₅	2.324	0	Type-III	<i>d</i> -wave
795	mp-862754	33 (<i>Pna</i> 2 ₁)	C _{2v} (mm2)	PrBS ₃	2.444	0	Type-III	<i>d</i> -wave
796	mp-867286	33 (<i>Pna</i> 2 ₁)	C _{2v} (mm2)	TbBS ₃	2.342	0	Type-III	<i>d</i> -wave
797	mp-9212	33 (<i>Pna</i> 2 ₁)	C _{2v} (mm2)	NaAlO ₂	3.797	0	Type-III	<i>d</i> -wave
798	mp-9332	33 (<i>Pna</i> 2 ₁)	C _{2v} (mm2)	KGaPO ₄ F	4.108	0	Type-III	<i>d</i> -wave
799	mp-972448	33 (<i>Pna</i> 2 ₁)	C _{2v} (mm2)	SmBS ₃	2.43	0	Type-III	<i>d</i> -wave
800	mp-9770	33 (<i>Pna</i> 2 ₁)	C _{2v} (mm2)	Ag ₈ GeS ₆	0.61	0	Type-III	<i>d</i> -wave
801	mp-41109	34 (<i>Pnn</i> 2)	C _{2v} (mm2)	Ca ₃ Er ₃ Ge ₂ BO ₁₃	3.635	0	Type-III	<i>d</i> -wave
802	mp-555742	34 (<i>Pnn</i> 2)	C _{2v} (mm2)	Ba ₂ B ₅ ClO ₉	5.242	0	Type-III	<i>d</i> -wave
803	mp-557027	34 (<i>Pnn</i> 2)	C _{2v} (mm2)	Rb ₂ Be ₂ Si ₂ O ₇	4.394	0	Type-III	<i>d</i> -wave
804	mp-557387	34 (<i>Pnn</i> 2)	C _{2v} (mm2)	Sr ₂ TmNbO ₆	2.857	1	Type-III	<i>d</i> -wave
805	mp-756117	34 (<i>Pnn</i> 2)	C _{2v} (mm2)	Li ₂ TiTeO ₆	2.323	0	Type-III	<i>d</i> -wave
806	mp-8673	34 (<i>Pnn</i> 2)	C _{2v} (mm2)	Li ₂ SnTeO ₆	2.044	0	Type-III	<i>d</i> -wave
807	mp-29226	35 (<i>Cmm</i> 2)	C _{2v} (mm2)	Ca ₃ Ga ₄ O ₉	2.639	1	Type-III	<i>d</i> -wave
808	mp-757375	35 (<i>Cmm</i> 2)	C _{2v} (mm2)	Ti ₂ Sn ₃ O ₁₀	1.727	0	Type-III	<i>d</i> -wave
809	mp-759737	35 (<i>Cmm</i> 2)	C _{2v} (mm2)	Ti ₃ (SnO ₅) ₂	1.619	1	Type-III	<i>d</i> -wave
810	icsd-424850	36 (<i>Cmc</i> 2 ₁)	C _{2v} (mm2)	BrCl	1.8827	0	Type-III	<i>d</i> -wave

811	mp-10223	36 (<i>Cmc2</i> ₁)	C _{2v} (mm2)	Na ₂ PdS ₂	0.945	0	Type-III	<i>d</i> -wave
812	mp-10246	36 (<i>Cmc2</i> ₁)	C _{2v} (mm2)	Na ₂ PtS ₂	1.143	0	Type-III	<i>d</i> -wave
813	mp-10409	36 (<i>Cmc2</i> ₁)	C _{2v} (mm2)	Ba ₄ Nd ₂ Cd ₃ Se ₁₀	1.519	0	Type-III	<i>d</i> -wave
814	mp-10410	36 (<i>Cmc2</i> ₁)	C _{2v} (mm2)	Ba ₄ Sm ₂ Cd ₃ S ₁₀	1.893	0	Type-III	<i>d</i> -wave
815	mp-11773	36 (<i>Cmc2</i> ₁)	C _{2v} (mm2)	Nd ₃ GaO ₆	3.651	0	Type-III	<i>d</i> -wave
816	mp-13664	36 (<i>Cmc2</i> ₁)	C _{2v} (mm2)	Sr ₂ Ta ₂ O ₇	2.928	1	Type-III	<i>d</i> -wave
817	mp-13703	36 (<i>Cmc2</i> ₁)	C _{2v} (mm2)	Al ₄ CO ₄	3.823	0	Type-III	<i>d</i> -wave
818	mp-14363	36 (<i>Cmc2</i> ₁)	C _{2v} (mm2)	Rb ₂ LiAsO ₄	3.553	0	Type-III	<i>d</i> -wave
819	mp-14364	36 (<i>Cmc2</i> ₁)	C _{2v} (mm2)	Cs ₂ LiAsO ₄	3.73	0	Type-III	<i>d</i> -wave
820	mp-14433	36 (<i>Cmc2</i> ₁)	C _{2v} (mm2)	NaGe ₂ N ₃	2.34	0	Type-III	<i>d</i> -wave
821	mp-14568	36 (<i>Cmc2</i> ₁)	C _{2v} (mm2)	BaMgF ₄	6.8	0	Type-III	<i>d</i> -wave
822	mp-14588	36 (<i>Cmc2</i> ₁)	C _{2v} (mm2)	Na ₂ PtSe ₂	0.869	0	Type-III	<i>d</i> -wave
823	mp-15349	36 (<i>Cmc2</i> ₁)	C _{2v} (mm2)	Li ₂ GeO ₃	3.568	0	Type-III	<i>d</i> -wave
824	mp-16964	36 (<i>Cmc2</i> ₁)	C _{2v} (mm2)	SiO ₂	5.678	0	Type-III	<i>d</i> -wave
825	mp-17513	36 (<i>Cmc2</i> ₁)	C _{2v} (mm2)	Ba ₄ Tb ₂ Cd ₃ S ₁₀	1.918	0	Type-III	<i>d</i> -wave
826	mp-17694	36 (<i>Cmc2</i> ₁)	C _{2v} (mm2)	Ca ₅ Al ₆ O ₁₄	4.226	0	Type-III	<i>d</i> -wave
827	mp-19885	36 (<i>Cmc2</i> ₁)	C _{2v} (mm2)	InGaS ₃	1.676	0	Type-III	<i>d</i> -wave
828	mp-21489	36 (<i>Cmc2</i> ₁)	C _{2v} (mm2)	Rb ₂ PbO ₃	1.203	0	Type-III	<i>d</i> -wave
829	mp-21521	36 (<i>Cmc2</i> ₁)	C _{2v} (mm2)	Cs ₂ PbO ₃	1.391	0	Type-III	<i>d</i> -wave
830	mp-22756	36 (<i>Cmc2</i> ₁)	C _{2v} (mm2)	K ₂ PbO ₃	1.21	0	Type-III	<i>d</i> -wave
831	mp-23089	36 (<i>Cmc2</i> ₁)	C _{2v} (mm2)	SrTa ₂ Bi ₂ O ₉	2.514	1	Type-III	<i>d</i> -wave
832	mp-23297	36 (<i>Cmc2</i> ₁)	C _{2v} (mm2)	BrF ₃	2.211	0	Type-III	<i>d</i> -wave
833	mp-23446	36 (<i>Cmc2</i> ₁)	C _{2v} (mm2)	GeBi ₂ O ₅	2.322	0	Type-III	<i>d</i> -wave
834	mp-23614	36 (<i>Cmc2</i> ₁)	C _{2v} (mm2)	SrNb ₂ Bi ₂ O ₉	2.581	1	Type-III	<i>d</i> -wave
835	mp-27220	36 (<i>Cmc2</i> ₁)	C _{2v} (mm2)	Tl ₅ SbO ₅	1.47	0	Type-III	<i>d</i> -wave
836	mp-27390	36 (<i>Cmc2</i> ₁)	C _{2v} (mm2)	K ₅ ThF ₉	5.969	0	Type-III	<i>d</i> -wave
837	mp-2798	36 (<i>Cmc2</i> ₁)	C _{2v} (mm2)	SiP	1.74	0	Type-III	<i>d</i> -wave
838	mp-28035	36 (<i>Cmc2</i> ₁)	C _{2v} (mm2)	BaP ₁₀	1.296	0	Type-III	<i>d</i> -wave
839	mp-28144	36 (<i>Cmc2</i> ₁)	C _{2v} (mm2)	SiBi ₂ O ₅	2.708	0	Type-III	<i>d</i> -wave
840	mp-28264	36 (<i>Cmc2</i> ₁)	C _{2v} (mm2)	RbH ₃ O ₂	4.252	0	Type-III	<i>d</i> -wave
841	mp-28369	36 (<i>Cmc2</i> ₁)	C _{2v} (mm2)	GeH ₃ Cl	4.749	0	Type-III	<i>d</i> -wave
842	mp-28473	36 (<i>Cmc2</i> ₁)	C _{2v} (mm2)	CClF ₃	6.616	1	Type-III	<i>d</i> -wave
843	mp-28499	36 (<i>Cmc2</i> ₁)	C _{2v} (mm2)	Al ₁₀ Ge ₂ O ₁₉	2.12	1	Type-III	<i>d</i> -wave
844	mp-29186	36 (<i>Cmc2</i> ₁)	C _{2v} (mm2)	La(SiP ₃) ₂	0.898	0	Type-III	<i>d</i> -wave
845	mp-3080	36 (<i>Cmc2</i> ₁)	C _{2v} (mm2)	Ca ₅ (Ga ₃ O ₇) ₂	3.072	0	Type-III	<i>d</i> -wave
846	mp-31110	36 (<i>Cmc2</i> ₁)	C _{2v} (mm2)	Sm ₃ GaO ₆	3.68	0	Type-III	<i>d</i> -wave
847	mp-31112	36 (<i>Cmc2</i> ₁)	C _{2v} (mm2)	Tb ₃ GaO ₆	3.605	0	Type-III	<i>d</i> -wave
848	mp-31113	36 (<i>Cmc2</i> ₁)	C _{2v} (mm2)	Dy ₃ GaO ₆	3.591	0	Type-III	<i>d</i> -wave
849	mp-31114	36 (<i>Cmc2</i> ₁)	C _{2v} (mm2)	Ho ₃ GaO ₆	3.564	0	Type-III	<i>d</i> -wave
850	mp-31115	36 (<i>Cmc2</i> ₁)	C _{2v} (mm2)	Er ₃ GaO ₆	3.539	0	Type-III	<i>d</i> -wave
851	mp-32669	36 (<i>Cmc2</i> ₁)	C _{2v} (mm2)	Ag ₂ S	1.3	0	Type-III	<i>d</i> -wave
852	mp-3281	36 (<i>Cmc2</i> ₁)	C _{2v} (mm2)	Al ₅ BO ₉	4.938	0	Type-III	<i>d</i> -wave
853	mp-3870	36 (<i>Cmc2</i> ₁)	C _{2v} (mm2)	Sr ₂ Nb ₂ O ₇	2.684	1	Type-III	<i>d</i> -wave
854	mp-3881	36 (<i>Cmc2</i> ₁)	C _{2v} (mm2)	BaZnF ₄	4.549	0	Type-III	<i>d</i> -wave
855	mp-3933	36 (<i>Cmc2</i> ₁)	C _{2v} (mm2)	Mg ₂ PN ₃	3.537	0	Type-III	<i>d</i> -wave
856	mp-3998	36 (<i>Cmc2</i> ₁)	C _{2v} (mm2)	LaTaO ₄	3.389	1	Type-III	<i>d</i> -wave
857	mp-4004	36 (<i>Cmc2</i> ₁)	C _{2v} (mm2)	Ag ₅ SbS ₄	0.595	0	Type-III	<i>d</i> -wave
858	mp-4163	36 (<i>Cmc2</i> ₁)	C _{2v} (mm2)	Ca ₃ Ti ₂ O ₇	2.53	1	Type-III	<i>d</i> -wave
859	mp-4187	36 (<i>Cmc2</i> ₁)	C _{2v} (mm2)	Ge ₂ N ₂ O	2.616	0	Type-III	<i>d</i> -wave
860	mp-4497	36 (<i>Cmc2</i> ₁)	C _{2v} (mm2)	Si ₂ N ₂ O	4.925	0	Type-III	<i>d</i> -wave
861	mp-4533	36 (<i>Cmc2</i> ₁)	C _{2v} (mm2)	Na ₂ SiO ₃	3.866	0	Type-III	<i>d</i> -wave
862	mp-5012	36 (<i>Cmc2</i> ₁)	C _{2v} (mm2)	Li ₂ SiO ₃	5.077	0	Type-III	<i>d</i> -wave
863	mp-505045	36 (<i>Cmc2</i> ₁)	C _{2v} (mm2)	Na ₅ (InTe ₃) ₂	0.865	0	Type-III	<i>d</i> -wave
864	mp-510293	36 (<i>Cmc2</i> ₁)	C _{2v} (mm2)	Pb ₃ SeO ₅	2.463	0	Type-III	<i>d</i> -wave
865	mp-554722	36 (<i>Cmc2</i> ₁)	C _{2v} (mm2)	Y ₃ GaO ₆	3.685	0	Type-III	<i>d</i> -wave
866	mp-555867	36 (<i>Cmc2</i> ₁)	C _{2v} (mm2)	BaNb ₂ Bi ₂ O ₉	2.215	1	Type-III	<i>d</i> -wave
867	mp-555918	36 (<i>Cmc2</i> ₁)	C _{2v} (mm2)	Hg ₂ SeO ₃	2.311	1	Type-III	<i>d</i> -wave
868	mp-556697	36 (<i>Cmc2</i> ₁)	C _{2v} (mm2)	CaTa ₂ Bi ₂ O ₉	2.926	1	Type-III	<i>d</i> -wave
869	mp-556866	36 (<i>Cmc2</i> ₁)	C _{2v} (mm2)	Ag ₂ HgSI ₂	1.221	0	Type-III	<i>d</i> -wave

870	mp-557070	36 (<i>Cmc2</i> ₁)	<i>C</i> ₂ <i>v</i> (mm2)	Ca ₂ BiAsO ₆	3.239	0	Type-III	<i>d</i> -wave
871	mp-558907	36 (<i>Cmc2</i> ₁)	<i>C</i> ₂ <i>v</i> (mm2)	CsCu(BiS ₂) ₂	0.605	0	Type-III	<i>d</i> -wave
872	mp-559330	36 (<i>Cmc2</i> ₁)	<i>C</i> ₂ <i>v</i> (mm2)	Sr ₄ B ₁₄ O ₂₅	5.206	0	Type-III	<i>d</i> -wave
873	mp-560008	36 (<i>Cmc2</i> ₁)	<i>C</i> ₂ <i>v</i> (mm2)	PNF ₂	5.617	0	Type-III	<i>d</i> -wave
874	mp-570044	36 (<i>Cmc2</i> ₁)	<i>C</i> ₂ <i>v</i> (mm2)	NbI ₄	0.478	0	Type-III	<i>d</i> -wave
875	mp-570172	36 (<i>Cmc2</i> ₁)	<i>C</i> ₂ <i>v</i> (mm2)	HgIBr	2.362	0	Type-III	<i>d</i> -wave
876	mp-571636	36 (<i>Cmc2</i> ₁)	<i>C</i> ₂ <i>v</i> (mm2)	InCl	1.402	0	Type-III	<i>d</i> -wave
877	mp-5784	36 (<i>Cmc2</i> ₁)	<i>C</i> ₂ <i>v</i> (mm2)	Na ₂ GeO ₃	2.987	0	Type-III	<i>d</i> -wave
878	mp-583454	36 (<i>Cmc2</i> ₁)	<i>C</i> ₂ <i>v</i> (mm2)	Nb ₂ Bi ₂ PbO ₉	2.298	1	Type-III	<i>d</i> -wave
879	mp-5853	36 (<i>Cmc2</i> ₁)	<i>C</i> ₂ <i>v</i> (mm2)	LiSi ₂ N ₃	5.014	0	Type-III	<i>d</i> -wave
880	mp-625054	36 (<i>Cmc2</i> ₁)	<i>C</i> ₂ <i>v</i> (mm2)	AlHO ₂	5.14	0	Type-III	<i>d</i> -wave
881	mp-625136	36 (<i>Cmc2</i> ₁)	<i>C</i> ₂ <i>v</i> (mm2)	CsHO	3.433	0	Type-III	<i>d</i> -wave
882	mp-625150	36 (<i>Cmc2</i> ₁)	<i>C</i> ₂ <i>v</i> (mm2)	ScHO ₂	4.412	0	Type-III	<i>d</i> -wave
883	mp-626620	36 (<i>Cmc2</i> ₁)	<i>C</i> ₂ <i>v</i> (mm2)	RbHO	3.334	0	Type-III	<i>d</i> -wave
884	mp-626785	36 (<i>Cmc2</i> ₁)	<i>C</i> ₂ <i>v</i> (mm2)	KHO	3.678	0	Type-III	<i>d</i> -wave
885	mp-632229	36 (<i>Cmc2</i> ₁)	<i>C</i> ₂ <i>v</i> (mm2)	HBr	4.681	0	Type-III	<i>d</i> -wave
886	mp-643009	36 (<i>Cmc2</i> ₁)	<i>C</i> ₂ <i>v</i> (mm2)	SrMgH ₄	2.709	0	Type-III	<i>d</i> -wave
887	mp-707304	36 (<i>Cmc2</i> ₁)	<i>C</i> ₂ <i>v</i> (mm2)	Be ₄ Si ₂ H ₂ O ₉	5.739	0	Type-III	<i>d</i> -wave
888	mp-717	36 (<i>Cmc2</i> ₁)	<i>C</i> ₂ <i>v</i> (mm2)	B ₂ O ₃	8.375	0	Type-III	<i>d</i> -wave
889	mp-7290	36 (<i>Cmc2</i> ₁)	<i>C</i> ₂ <i>v</i> (mm2)	Er ₃ GaS ₆	2.106	0	Type-III	<i>d</i> -wave
890	mp-7446	36 (<i>Cmc2</i> ₁)	<i>C</i> ₂ <i>v</i> (mm2)	Rb ₂ S ₃	1.343	0	Type-III	<i>d</i> -wave
891	mp-7447	36 (<i>Cmc2</i> ₁)	<i>C</i> ₂ <i>v</i> (mm2)	Rb ₂ Se ₃	0.681	0	Type-III	<i>d</i> -wave
892	mp-7449	36 (<i>Cmc2</i> ₁)	<i>C</i> ₂ <i>v</i> (mm2)	Cs ₂ Se ₃	0.74	0	Type-III	<i>d</i> -wave
893	mp-752676	36 (<i>Cmc2</i> ₁)	<i>C</i> ₂ <i>v</i> (mm2)	TiBi ₂ O ₅	2.58	0	Type-III	<i>d</i> -wave
894	mp-753401	36 (<i>Cmc2</i> ₁)	<i>C</i> ₂ <i>v</i> (mm2)	Sc ₂ TiO ₅	3.132	0	Type-III	<i>d</i> -wave
895	mp-753798	36 (<i>Cmc2</i> ₁)	<i>C</i> ₂ <i>v</i> (mm2)	Rb ₂ SnO ₃	2.121	0	Type-III	<i>d</i> -wave
896	mp-753821	36 (<i>Cmc2</i> ₁)	<i>C</i> ₂ <i>v</i> (mm2)	Pr ₃ GaO ₆	3.629	0	Type-III	<i>d</i> -wave
897	mp-754150	36 (<i>Cmc2</i> ₁)	<i>C</i> ₂ <i>v</i> (mm2)	La ₃ GaO ₆	3.835	0	Type-III	<i>d</i> -wave
898	mp-754401	36 (<i>Cmc2</i> ₁)	<i>C</i> ₂ <i>v</i> (mm2)	Al ₂ O ₃	4.235	0	Type-III	<i>d</i> -wave
899	mp-754979	36 (<i>Cmc2</i> ₁)	<i>C</i> ₂ <i>v</i> (mm2)	Y ₃ AlO ₆	4.374	0	Type-III	<i>d</i> -wave
900	mp-755663	36 (<i>Cmc2</i> ₁)	<i>C</i> ₂ <i>v</i> (mm2)	Ta ₂ Pb ₂ O ₇	2.815	1	Type-III	<i>d</i> -wave
901	mp-756156	36 (<i>Cmc2</i> ₁)	<i>C</i> ₂ <i>v</i> (mm2)	Rb ₂ ZrO ₃	3.544	0	Type-III	<i>d</i> -wave
902	mp-758845	36 (<i>Cmc2</i> ₁)	<i>C</i> ₂ <i>v</i> (mm2)	Ba ₅ Nb ₂ O ₁₀	2.37	1	Type-III	<i>d</i> -wave
903	mp-766108	36 (<i>Cmc2</i> ₁)	<i>C</i> ₂ <i>v</i> (mm2)	Ba ₃ LiTi ₅ (SbO ₇) ₃	2.397	0	Type-III	<i>d</i> -wave
904	mp-766208	36 (<i>Cmc2</i> ₁)	<i>C</i> ₂ <i>v</i> (mm2)	Ba ₃ LiTi ₅ Nb ₃ O ₂₁	2.042	1	Type-III	<i>d</i> -wave
905	mp-7667	36 (<i>Cmc2</i> ₁)	<i>C</i> ₂ <i>v</i> (mm2)	K ₂ S ₃	1.286	0	Type-III	<i>d</i> -wave
906	mp-7670	36 (<i>Cmc2</i> ₁)	<i>C</i> ₂ <i>v</i> (mm2)	K ₂ Se ₃	0.644	0	Type-III	<i>d</i> -wave
907	mp-768573	36 (<i>Cmc2</i> ₁)	<i>C</i> ₂ <i>v</i> (mm2)	Lu ₃ AlO ₆	4.214	0	Type-III	<i>d</i> -wave
908	mp-771208	36 (<i>Cmc2</i> ₁)	<i>C</i> ₂ <i>v</i> (mm2)	Ba ₅ (Ga ₃ O ₇) ₂	2.722	0	Type-III	<i>d</i> -wave
909	mp-864638	36 (<i>Cmc2</i> ₁)	<i>C</i> ₂ <i>v</i> (mm2)	Ba ₂ InBiS ₅	1.453	0	Type-III	<i>d</i> -wave
910	mp-865143	36 (<i>Cmc2</i> ₁)	<i>C</i> ₂ <i>v</i> (mm2)	BaYbCdSb ₂	0.152	0	Type-III	<i>d</i> -wave
911	mp-865492	36 (<i>Cmc2</i> ₁)	<i>C</i> ₂ <i>v</i> (mm2)	LuCuPbSe ₃	1.087	0	Type-III	<i>d</i> -wave
912	mp-867203	36 (<i>Cmc2</i> ₁)	<i>C</i> ₂ <i>v</i> (mm2)	Sr ₂ CdAs ₂	1.066	0	Type-III	<i>d</i> -wave
913	mp-8973	36 (<i>Cmc2</i> ₁)	<i>C</i> ₂ <i>v</i> (mm2)	NaSi ₂ N ₃	4.184	0	Type-III	<i>d</i> -wave
914	mp-9248	36 (<i>Cmc2</i> ₁)	<i>C</i> ₂ <i>v</i> (mm2)	Cu ₂ SiS ₃	1.197	0	Type-III	<i>d</i> -wave
915	mp-9781	36 (<i>Cmc2</i> ₁)	<i>C</i> ₂ <i>v</i> (mm2)	K ₃ SbS ₄	2.185	0	Type-III	<i>d</i> -wave
916	mp-9900	36 (<i>Cmc2</i> ₁)	<i>C</i> ₂ <i>v</i> (mm2)	Ag ₂ GeS ₃	0.465	0	Type-III	<i>d</i> -wave
917	mp-27229	37 (<i>Ccc2</i>)	<i>C</i> ₂ <i>v</i> (mm2)	Sb ₆ S ₂ O ₁₅	3.247	1	Type-III	<i>d</i> -wave
918	mp-4117	37 (<i>Ccc2</i>)	<i>C</i> ₂ <i>v</i> (mm2)	Li ₂ Si ₂ O ₅	5.154	0	Type-III	<i>d</i> -wave
919	mp-557855	37 (<i>Ccc2</i>)	<i>C</i> ₂ <i>v</i> (mm2)	CaGaBO ₄	3.961	1	Type-III	<i>d</i> -wave
920	mp-559759	37 (<i>Ccc2</i>)	<i>C</i> ₂ <i>v</i> (mm2)	CaAlBO ₄	4.696	1	Type-III	<i>d</i> -wave
921	mp-756294	37 (<i>Ccc2</i>)	<i>C</i> ₂ <i>v</i> (mm2)	Li ₂ Ti ₂ O ₅	3.743	0	Type-III	<i>d</i> -wave
922	mp-7998	37 (<i>Ccc2</i>)	<i>C</i> ₂ <i>v</i> (mm2)	Li ₂ Ge ₂ O ₅	3.3	0	Type-III	<i>d</i> -wave
923	mp-14482	38 (<i>Amm2</i>)	<i>C</i> ₂ <i>v</i> (mm2)	SrNb ₆ O ₁₆	1.632	1	Type-III	<i>d</i> -wave
924	mp-20337	38 (<i>Amm2</i>)	<i>C</i> ₂ <i>v</i> (mm2)	ZrPbO ₃	2.673	1	Type-III	<i>d</i> -wave
925	mp-27376	38 (<i>Amm2</i>)	<i>C</i> ₂ <i>v</i> (mm2)	Rb ₆ Si ₁₀ O ₂₃	4.312	1	Type-III	<i>d</i> -wave
926	mp-30192	38 (<i>Amm2</i>)	<i>C</i> ₂ <i>v</i> (mm2)	Pr ₄ Se ₃ O ₄	1.315	0	Type-III	<i>d</i> -wave
927	mp-4412	38 (<i>Amm2</i>)	<i>C</i> ₂ <i>v</i> (mm2)	La ₄ Se ₃ O ₄	1.326	0	Type-III	<i>d</i> -wave
928	mp-5246	38 (<i>Amm2</i>)	<i>C</i> ₂ <i>v</i> (mm2)	KNbO ₃	2.058	0	Type-III	<i>d</i> -wave

929	mp-550117	38 (<i>Amm2</i>)	C _{2v} (mm2)	Sm ₄ Se ₃ O ₄	1.289	0	Type-III	<i>d-wave</i>
930	mp-553278	38 (<i>Amm2</i>)	C _{2v} (mm2)	Nd ₄ Se ₃ O ₄	1.323	0	Type-III	<i>d-wave</i>
931	mp-560129	38 (<i>Amm2</i>)	C _{2v} (mm2)	Na ₃ La ₂ (BO ₃) ₃	3.79	1	Type-III	<i>d-wave</i>
932	mp-569450	38 (<i>Amm2</i>)	C _{2v} (mm2)	LiB ₆ C	1.392	0	Type-III	<i>d-wave</i>
933	mp-5777	38 (<i>Amm2</i>)	C _{2v} (mm2)	BaTiO ₃	2.293	1	Type-III	<i>d-wave</i>
934	mp-626417	38 (<i>Amm2</i>)	C _{2v} (mm2)	CsH ₃ O ₂	4.095	1	Type-III	<i>d-wave</i>
935	mp-673798	38 (<i>Amm2</i>)	C _{2v} (mm2)	K ₃ ClO	1.026	0	Type-III	<i>d-wave</i>
936	mp-677011	38 (<i>Amm2</i>)	C _{2v} (mm2)	K ₄ BaTa ₆ (Si ₂ O ₁₃) ₂	2.847	1	Type-III	<i>d-wave</i>
937	mp-769349	38 (<i>Amm2</i>)	C _{2v} (mm2)	BaTa ₆ O ₁₆	2.182	1	Type-III	<i>d-wave</i>
938	mp-989613	38 (<i>Amm2</i>)	C _{2v} (mm2)	TiPN ₃	0.528	0	Type-III	<i>d-wave</i>
939	mp-23334	39 (<i>Aem2</i>)	C _{2v} (mm2)	Bi ₂ TeO ₅	2.428	1	Type-III	<i>d-wave</i>
940	mp-29839	39 (<i>Aem2</i>)	C _{2v} (mm2)	Bi ₂ SeO ₅	2.842	1	Type-III	<i>d-wave</i>
941	mp-532443	39 (<i>Aem2</i>)	C _{2v} (mm2)	Li ₅ V ₅ Cl ₁₆	0	0	Type-III	<i>d-wave</i>
942	mp-558134	39 (<i>Aem2</i>)	C _{2v} (mm2)	TlF	3.143	0	Type-III	<i>d-wave</i>
943	mp-625998	39 (<i>Aem2</i>)	C _{2v} (mm2)	LiHO	4.269	0	Type-III	<i>d-wave</i>
944	mp-643759	39 (<i>Aem2</i>)	C _{2v} (mm2)	GaH ₃ NF ₃	5.309	1	Type-III	<i>d-wave</i>
945	mp-686102	39 (<i>Aem2</i>)	C _{2v} (mm2)	Tl ₃ In ₂ Se ₅	0.721	1	Type-III	<i>d-wave</i>
946	mp-11925	40 (<i>Ama2</i>)	C _{2v} (mm2)	RbTa(CuSe ₂) ₂	1.733	0	Type-III	<i>d-wave</i>
947	mp-12364	40 (<i>Ama2</i>)	C _{2v} (mm2)	BaCu ₂ SnSe ₄	0.453	0	Type-III	<i>d-wave</i>
948	mp-16179	40 (<i>Ama2</i>)	C _{2v} (mm2)	SrCu ₂ GeSe ₄	0.6	0	Type-III	<i>d-wave</i>
949	mp-1880	40 (<i>Ama2</i>)	C _{2v} (mm2)	SbF ₃	4.44	0	Type-III	<i>d-wave</i>
950	mp-20496	40 (<i>Ama2</i>)	C _{2v} (mm2)	Ga ₂ PbO ₄	3.446	0	Type-III	<i>d-wave</i>
951	mp-21892	40 (<i>Ama2</i>)	C _{2v} (mm2)	Al ₂ PbO ₄	3.942	0	Type-III	<i>d-wave</i>
952	mp-30293	40 (<i>Ama2</i>)	C _{2v} (mm2)	Sr ₂ GeSe ₄	1.728	0	Type-III	<i>d-wave</i>
953	mp-30294	40 (<i>Ama2</i>)	C _{2v} (mm2)	Sr ₂ SnS ₄	2.478	0	Type-III	<i>d-wave</i>
954	mp-554240	40 (<i>Ama2</i>)	C _{2v} (mm2)	NaCa ₄ (BO ₃) ₃	4.087	0	Type-III	<i>d-wave</i>
955	mp-554346	40 (<i>Ama2</i>)	C _{2v} (mm2)	KSr ₄ (BO ₃) ₃	4.173	0	Type-III	<i>d-wave</i>
956	mp-554573	40 (<i>Ama2</i>)	C _{2v} (mm2)	SiO ₂	5.615	0	Type-III	<i>d-wave</i>
957	mp-555023	40 (<i>Ama2</i>)	C _{2v} (mm2)	KCa ₄ (BO ₃) ₃	4.589	0	Type-III	<i>d-wave</i>
958	mp-555954	40 (<i>Ama2</i>)	C _{2v} (mm2)	BaSnHgS ₄	1.859	0	Type-III	<i>d-wave</i>
959	mp-556062	40 (<i>Ama2</i>)	C _{2v} (mm2)	NaNb ₄ Tl ₃ P ₂ O ₁₇	2.492	1	Type-III	<i>d-wave</i>
960	mp-558347	40 (<i>Ama2</i>)	C _{2v} (mm2)	K ₄ Ba(SiO ₃) ₃	4.229	0	Type-III	<i>d-wave</i>
961	mp-559502	40 (<i>Ama2</i>)	C _{2v} (mm2)	Ba ₃ NaNd ₃ (Si ₃ O ₁₀) ₂	4.579	1	Type-III	<i>d-wave</i>
962	mp-560535	40 (<i>Ama2</i>)	C _{2v} (mm2)	K ₄ Sr(SiO ₃) ₃	4.161	0	Type-III	<i>d-wave</i>
963	mp-567702	40 (<i>Ama2</i>)	C _{2v} (mm2)	CsReCl ₄	1.134	0	Type-III	<i>d-wave</i>
964	mp-568854	40 (<i>Ama2</i>)	C _{2v} (mm2)	CsReBrCl ₃	1.178	0	Type-III	<i>d-wave</i>
965	mp-6013	40 (<i>Ama2</i>)	C _{2v} (mm2)	KTa(CuSe ₂) ₂	1.665	0	Type-III	<i>d-wave</i>
966	mp-6181	40 (<i>Ama2</i>)	C _{2v} (mm2)	NaNb(CuS ₂) ₂	1.72	0	Type-III	<i>d-wave</i>
967	mp-6376	40 (<i>Ama2</i>)	C _{2v} (mm2)	KV(CuS ₂) ₂	1.076	0	Type-III	<i>d-wave</i>
968	mp-644271	40 (<i>Ama2</i>)	C _{2v} (mm2)	LiHS	3.498	0	Type-III	<i>d-wave</i>
969	mp-6507	40 (<i>Ama2</i>)	C _{2v} (mm2)	Na ₂ Zn ₂ Si ₂ O ₇	3.323	0	Type-III	<i>d-wave</i>
970	mp-6599	40 (<i>Ama2</i>)	C _{2v} (mm2)	KNb(CuSe ₂) ₂	1.423	0	Type-III	<i>d-wave</i>
971	mp-753153	40 (<i>Ama2</i>)	C _{2v} (mm2)	Dy ₂ CO ₅	4.437	0	Type-III	<i>d-wave</i>
972	mp-757115	40 (<i>Ama2</i>)	C _{2v} (mm2)	KSb ₅ O ₁₃	1.048	0	Type-III	<i>d-wave</i>
973	mp-758571	40 (<i>Ama2</i>)	C _{2v} (mm2)	Al ₁₁ TlO ₁₇	4.59	1	Type-III	<i>d-wave</i>
974	mp-760405	40 (<i>Ama2</i>)	C _{2v} (mm2)	ErBO ₃	4.563	1	Type-III	<i>d-wave</i>
975	mp-760484	40 (<i>Ama2</i>)	C _{2v} (mm2)	TmBO ₃	4.506	1	Type-III	<i>d-wave</i>
976	mp-766341	40 (<i>Ama2</i>)	C _{2v} (mm2)	NaSb ₅ O ₁₃	1.063	1	Type-III	<i>d-wave</i>
977	mp-861942	40 (<i>Ama2</i>)	C _{2v} (mm2)	Ag ₂ GePbS ₄	1.37	0	Type-III	<i>d-wave</i>
978	mp-865532	40 (<i>Ama2</i>)	C _{2v} (mm2)	BaMgTe ₂ O ₇	1.849	1	Type-III	<i>d-wave</i>
979	mp-9815	40 (<i>Ama2</i>)	C _{2v} (mm2)	TaTl(CuS ₂) ₂	1.797	0	Type-III	<i>d-wave</i>
980	mp-989603	40 (<i>Ama2</i>)	C _{2v} (mm2)	LaMoN ₃	0.805	0	Type-III	<i>d-wave</i>
981	mp-989617	40 (<i>Ama2</i>)	C _{2v} (mm2)	YWN ₃	1.413	0	Type-III	<i>d-wave</i>
982	mp-1175	41 (<i>Aea2</i>)	C _{2v} (mm2)	SrS ₃	1.093	0	Type-III	<i>d-wave</i>
983	mp-17307	41 (<i>Aea2</i>)	C _{2v} (mm2)	K ₂ Hg ₃ (GeSe ₄) ₂	1.035	0	Type-III	<i>d-wave</i>
984	mp-17792	41 (<i>Aea2</i>)	C _{2v} (mm2)	K ₂ Hg ₃ (GeS ₄) ₂	1.552	0	Type-III	<i>d-wave</i>
985	mp-18115	41 (<i>Aea2</i>)	C _{2v} (mm2)	K ₂ Sn ₂ Hg ₃ S ₈	1.418	0	Type-III	<i>d-wave</i>
986	mp-23427	41 (<i>Aea2</i>)	C _{2v} (mm2)	Ti ₃ (BiO ₃) ₄	2.438	1	Type-III	<i>d-wave</i>
987	mp-27726	41 (<i>Aea2</i>)	C _{2v} (mm2)	SO ₂	2.837	1	Type-III	<i>d-wave</i>

988	mp-30161	41 (<i>Aea2</i>)	C_{2v} (mm2)	Si_2CN_4	4.374	0	Type-III	<i>d-wave</i>
989	mp-553948	41 (<i>Aea2</i>)	C_{2v} (mm2)	$\text{Tl}_4\text{Hg}_3\text{Sb}_2(\text{As}_2\text{S}_5)_4$	1.663	0	Type-III	<i>d-wave</i>
990	mp-558602	41 (<i>Aea2</i>)	C_{2v} (mm2)	$\text{CsAl}_3(\text{P}_3\text{O}_{10})_2$	5.432	0	Type-III	<i>d-wave</i>
991	mp-559951	41 (<i>Aea2</i>)	C_{2v} (mm2)	$\text{SrTa}_2\text{Bi}_2\text{O}_9$	2.271	1	Type-III	<i>d-wave</i>
992	mp-560456	41 (<i>Aea2</i>)	C_{2v} (mm2)	$\text{Hg}_2\text{Te}_2\text{O}_7$	1.434	1	Type-III	<i>d-wave</i>
993	mp-570589	41 (<i>Aea2</i>)	C_{2v} (mm2)	SeBr	1.524	0	Type-III	<i>d-wave</i>
994	mp-685150	41 (<i>Aea2</i>)	C_{2v} (mm2)	PbF_2	4.371	0	Type-III	<i>d-wave</i>
995	mp-686748	41 (<i>Aea2</i>)	C_{2v} (mm2)	$\text{Ca}_2\text{Al}_2\text{Si}(\text{HO}_4)_2$	4.465	0	Type-III	<i>d-wave</i>
996	mp-706621	41 (<i>Aea2</i>)	C_{2v} (mm2)	$\text{KB}_5(\text{H}_2\text{O}_3)_4$	5.635	0	Type-III	<i>d-wave</i>
997	mp-41191	42 (<i>Fmm2</i>)	C_{2v} (mm2)	$\text{Na}_3\text{Ti}_2\text{P}_2\text{O}_{10}\text{F}$	3.232	0	Type-III	<i>d-wave</i>
998	mp-558728	42 (<i>Fmm2</i>)	C_{2v} (mm2)	$\text{Cs}_3\text{Li}_2\text{F}_5$	5.727	0	Type-III	<i>d-wave</i>
999	mp-675286	42 (<i>Fmm2</i>)	C_{2v} (mm2)	Ca_3UN_4	1.369	0	Type-III	<i>d-wave</i>
1000	mp-676598	42 (<i>Fmm2</i>)	C_{2v} (mm2)	TlPbCl_3	2.602	0	Type-III	<i>d-wave</i>
1001	mp-677078	42 (<i>Fmm2</i>)	C_{2v} (mm2)	$\text{Ca}_{11}\text{AlSi}_3\text{ClO}_{18}$	3.585	1	Type-III	<i>d-wave</i>
1002	mp-760411	42 (<i>Fmm2</i>)	C_{2v} (mm2)	Bi_2CO_5	2.04	1	Type-III	<i>d-wave</i>
1003	mp-766262	42 (<i>Fmm2</i>)	C_{2v} (mm2)	$\text{H}_{20}\text{C}_3(\text{N}_2\text{O}_5)_2$	4.713	1	Type-III	<i>d-wave</i>
1004	mp-770118	42 (<i>Fmm2</i>)	C_{2v} (mm2)	$\text{Ba}_3\text{Ti}_2\text{O}_7$	2.271	0	Type-III	<i>d-wave</i>
1005	mp-771189	42 (<i>Fmm2</i>)	C_{2v} (mm2)	$\text{Ba}_4\text{Ti}_3\text{O}_{10}$	2.213	1	Type-III	<i>d-wave</i>
1006	mp-13666	43 (<i>Fdd2</i>)	C_{2v} (mm2)	$\text{Ti}(\text{PS}_3)_2$	1.45	0	Type-III	<i>d-wave</i>
1007	mp-13868	43 (<i>Fdd2</i>)	C_{2v} (mm2)	PdF_4	0.618	0	Type-III	<i>d-wave</i>
1008	mp-14288	43 (<i>Fdd2</i>)	C_{2v} (mm2)	Sr_3P_4	0.89	0	Type-III	<i>d-wave</i>
1009	mp-14289	43 (<i>Fdd2</i>)	C_{2v} (mm2)	Ba_3P_4	0.484	0	Type-III	<i>d-wave</i>
1010	mp-14444	43 (<i>Fdd2</i>)	C_{2v} (mm2)	$\text{Hf}(\text{PS}_3)_2$	2.318	0	Type-III	<i>d-wave</i>
1011	mp-15339	43 (<i>Fdd2</i>)	C_{2v} (mm2)	Sr_3As_4	0.617	0	Type-III	<i>d-wave</i>
1012	mp-22966	43 (<i>Fdd2</i>)	C_{2v} (mm2)	$\text{C}(\text{ClF})_2$	5.711	0	Type-III	<i>d-wave</i>
1013	mp-23667	43 (<i>Fdd2</i>)	C_{2v} (mm2)	$\text{RbP}(\text{HO}_2)_2$	5.237	1	Type-III	<i>d-wave</i>
1014	mp-23959	43 (<i>Fdd2</i>)	C_{2v} (mm2)	$\text{KP}(\text{HO}_2)_2$	5.433	1	Type-III	<i>d-wave</i>
1015	mp-2452	43 (<i>Fdd2</i>)	C_{2v} (mm2)	P_2O_5	5.202	0	Type-III	<i>d-wave</i>
1016	mp-27253	43 (<i>Fdd2</i>)	C_{2v} (mm2)	Au_2O_3	0.869	0	Type-III	<i>d-wave</i>
1017	mp-28477	43 (<i>Fdd2</i>)	C_{2v} (mm2)	$\text{Sr}(\text{ClO}_3)_2$	5.239	0	Type-III	<i>d-wave</i>
1018	mp-28512	43 (<i>Fdd2</i>)	C_{2v} (mm2)	$\text{Ba}(\text{ClO}_3)_2$	5.283	0	Type-III	<i>d-wave</i>
1019	mp-28513	43 (<i>Fdd2</i>)	C_{2v} (mm2)	$\text{Pb}(\text{ClO}_3)_2$	4.334	1	Type-III	<i>d-wave</i>
1020	mp-28514	43 (<i>Fdd2</i>)	C_{2v} (mm2)	$\text{Ba}(\text{BrO}_3)_2$	4.346	0	Type-III	<i>d-wave</i>
1021	mp-29576	43 (<i>Fdd2</i>)	C_{2v} (mm2)	Cd_7P_{10}	1.08	0	Type-III	<i>d-wave</i>
1022	mp-542613	43 (<i>Fdd2</i>)	C_{2v} (mm2)	GeS_2	2.254	0	Type-III	<i>d-wave</i>
1023	mp-553926	43 (<i>Fdd2</i>)	C_{2v} (mm2)	NaLiB_4O_7	5.797	1	Type-III	<i>d-wave</i>
1024	mp-554782	43 (<i>Fdd2</i>)	C_{2v} (mm2)	$\text{Li}_2\text{Ga}_2\text{GeS}_6$	2.134	0	Type-III	<i>d-wave</i>
1025	mp-556013	43 (<i>Fdd2</i>)	C_{2v} (mm2)	$\text{Na}_2\text{Be}(\text{SiO}_3)_2$	4.789	1	Type-III	<i>d-wave</i>
1026	mp-556778	43 (<i>Fdd2</i>)	C_{2v} (mm2)	BaTeF_6	4.852	1	Type-III	<i>d-wave</i>
1027	mp-570544	43 (<i>Fdd2</i>)	C_{2v} (mm2)	$\text{Zr}(\text{SeCl}_6)_2$	2.811	0	Type-III	<i>d-wave</i>
1028	mp-571313	43 (<i>Fdd2</i>)	C_{2v} (mm2)	$\text{Hf}(\text{SeCl}_6)_2$	2.792	0	Type-III	<i>d-wave</i>
1029	mp-626218	43 (<i>Fdd2</i>)	C_{2v} (mm2)	SbHO_3	1.414	0	Type-III	<i>d-wave</i>
1030	mp-675531	43 (<i>Fdd2</i>)	C_{2v} (mm2)	NaBiS_2	1.232	0	Type-III	<i>d-wave</i>
1031	mp-697027	43 (<i>Fdd2</i>)	C_{2v} (mm2)	$\text{NaSi}_2(\text{HO}_2)_3$	5.19	0	Type-III	<i>d-wave</i>
1032	mp-753813	43 (<i>Fdd2</i>)	C_{2v} (mm2)	$\text{Ca}(\text{ClO}_3)_2$	5.04	1	Type-III	<i>d-wave</i>
1033	mp-758253	43 (<i>Fdd2</i>)	C_{2v} (mm2)	$\text{CaH}_{12}(\text{IO}_6)_2$	4.099	1	Type-III	<i>d-wave</i>
1034	mp-780656	43 (<i>Fdd2</i>)	C_{2v} (mm2)	Na_2BiO_3	1.197	0	Type-III	<i>d-wave</i>
1035	mp-8943	43 (<i>Fdd2</i>)	C_{2v} (mm2)	PtF_4	1.295	0	Type-III	<i>d-wave</i>
1036	mp-2964	44 (<i>Imm2</i>)	C_{2v} (mm2)	NaNO_2	2.449	0	Type-III	<i>d-wave</i>
1037	mp-29761	44 (<i>Imm2</i>)	C_{2v} (mm2)	UCO_5	2.286	0	Type-III	<i>d-wave</i>
1038	mp-34381	44 (<i>Imm2</i>)	C_{2v} (mm2)	H_4IN	3.762	1	Type-III	<i>d-wave</i>
1039	mp-554206	44 (<i>Imm2</i>)	C_{2v} (mm2)	$\text{Cs}_2\text{Al}_2\text{As}_2\text{O}_7$	3.662	0	Type-III	<i>d-wave</i>
1040	mp-561446	44 (<i>Imm2</i>)	C_{2v} (mm2)	$\text{BaCa}(\text{GaO}_2)_4$	3.068	0	Type-III	<i>d-wave</i>
1041	mp-567278	44 (<i>Imm2</i>)	C_{2v} (mm2)	$\text{Sr}(\text{Si}_3\text{N}_4)_2$	3.208	0	Type-III	<i>d-wave</i>
1042	mp-567771	44 (<i>Imm2</i>)	C_{2v} (mm2)	$\text{Ba}(\text{Si}_3\text{N}_4)_2$	3.26	0	Type-III	<i>d-wave</i>
1043	mp-5770	44 (<i>Imm2</i>)	C_{2v} (mm2)	AgNO_2	1.773	0	Type-III	<i>d-wave</i>
1044	mp-581403	44 (<i>Imm2</i>)	C_{2v} (mm2)	$\text{K}_3\text{Na}_4\text{Si}_3\text{BF}_{22}$	6.979	0	Type-III	<i>d-wave</i>
1045	mp-638070	44 (<i>Imm2</i>)	C_{2v} (mm2)	$\text{LiB}_{13}\text{C}_2$	2.711	0	Type-III	<i>d-wave</i>
1046	mp-643814	44 (<i>Imm2</i>)	C_{2v} (mm2)	$\text{Zn}_2\text{SiH}_2\text{O}_5$	3.143	1	Type-III	<i>d-wave</i>

1047	mp-655489	44 (<i>Imm</i> 2)	C _{2v} (mm2)	Pb ₄ SeBr ₆	1.967	1	Type-III	<i>d</i> -wave
1048	mp-29722	45 (<i>Iba</i> 2)	C _{2v} (mm2)	Ca ₁₁ InSb ₉	0.838	0	Type-III	<i>d</i> -wave
1049	mp-556356	45 (<i>Iba</i> 2)	C _{2v} (mm2)	Na ₂ SrAl ₄ (SiO ₄) ₄	4.704	0	Type-III	<i>d</i> -wave
1050	mp-569811	45 (<i>Iba</i> 2)	C _{2v} (mm2)	Yb ₁₁ GaSb ₉	0.638	0	Type-III	<i>d</i> -wave
1051	mp-570504	45 (<i>Iba</i> 2)	C _{2v} (mm2)	Yb ₁₁ InSb ₉	0.657	0	Type-III	<i>d</i> -wave
1052	mp-578752	45 (<i>Iba</i> 2)	C _{2v} (mm2)	Sr ₁₁ InSb ₉	0.861	0	Type-III	<i>d</i> -wave
1053	mp-622930	45 (<i>Iba</i> 2)	C _{2v} (mm2)	Ba ₄ In ₆ O ₁₃	0.442	0	Type-III	<i>d</i> -wave
1054	mp-6875	45 (<i>Iba</i> 2)	C _{2v} (mm2)	BaNa ₂ Al ₄ (SiO ₄) ₄	4.735	0	Type-III	<i>d</i> -wave
1055	mp-10444	46 (<i>Ima</i> 2)	C _{2v} (mm2)	Ca ₂ Al ₂ O ₅	3.566	0	Type-III	<i>d</i> -wave
1056	mp-16433	46 (<i>Ima</i> 2)	C _{2v} (mm2)	Ca ₂ Ga ₂ O ₅	2.171	0	Type-III	<i>d</i> -wave
1057	mp-20546	46 (<i>Ima</i> 2)	C _{2v} (mm2)	Ba ₂ In ₂ O ₅	0.919	0	Type-III	<i>d</i> -wave
1058	mp-22512	46 (<i>Ima</i> 2)	C _{2v} (mm2)	Sr ₂ In ₂ O ₅	0.997	0	Type-III	<i>d</i> -wave
1059	mp-560530	46 (<i>Ima</i> 2)	C _{2v} (mm2)	Nb ₂ Cd ₂ O ₇	1.935	1	Type-III	<i>d</i> -wave
1060	mp-561352	46 (<i>Ima</i> 2)	C _{2v} (mm2)	BaNa ₂ Ti ₂ (Si ₂ O ₇) ₂	3.367	1	Type-III	<i>d</i> -wave
1061	mp-585516	46 (<i>Ima</i> 2)	C _{2v} (mm2)	Ca ₃ Si ₂ O ₇	4.62	1	Type-III	<i>d</i> -wave
1062	mp-633099	46 (<i>Ima</i> 2)	C _{2v} (mm2)	Sb ₂ Pb ₂ O ₇	1.649	1	Type-III	<i>d</i> -wave
1063	mp-676410	46 (<i>Ima</i> 2)	C _{2v} (mm2)	LuAgS ₂	0.731	1	Type-III	<i>d</i> -wave
1064	mp-677103	46 (<i>Ima</i> 2)	C _{2v} (mm2)	RbHF ₂	6.671	0	Type-III	<i>d</i> -wave
1065	mp-699136	46 (<i>Ima</i> 2)	C _{2v} (mm2)	NaAlH ₂ CO ₅	5.044	0	Type-III	<i>d</i> -wave
1066	mp-752573	46 (<i>Ima</i> 2)	C _{2v} (mm2)	Ba(NaSi ₂) ₂	1.012	0	Type-III	<i>d</i> -wave
1067	mp-28244	76 (<i>P</i> 4 ₁)	C ₄ (4)	TlBO ₂	2.866	0	Type-II	<i>s</i> -wave
1068	mp-30519	76 (<i>P</i> 4 ₁)	C ₄ (4)	Tl ₃ PbCl ₅	3.427	0	Type-II	<i>s</i> -wave
1069	mp-541113	76 (<i>P</i> 4 ₁)	C ₄ (4)	Cs ₃ P ₇	2.428	0	Type-II	<i>s</i> -wave
1070	mp-555021	76 (<i>P</i> 4 ₁)	C ₄ (4)	TePbO ₃	2.675	0	Type-II	<i>s</i> -wave
1071	mp-570753	76 (<i>P</i> 4 ₁)	C ₄ (4)	Tl ₃ PbBr ₅	3.022	0	Type-II	<i>s</i> -wave
1072	mp-984766	77 (<i>P</i> 4 ₂)	C ₄ (4)	Ca(BH ₄) ₂	5.095	0	Type-II	<i>s</i> -wave
1073	mp-29033	79 (<i>I</i> 4)	C ₄ (4)	P ₃ BrCl ₁₄	1.568	0	Type-II	<i>s</i> -wave
1074	mp-34292	79 (<i>I</i> 4)	C ₄ (4)	Tl ₉ SbTe ₆	0.73	0	Type-II	<i>s</i> -wave
1075	mp-540653	79 (<i>I</i> 4)	C ₄ (4)	SrAlF ₅	6.952	1	Type-II	<i>s</i> -wave
1076	mp-556364	79 (<i>I</i> 4)	C ₄ (4)	Ca ₂ SiCl ₂ O ₃	5.105	0	Type-II	<i>s</i> -wave
1077	mp-568100	79 (<i>I</i> 4)	C ₄ (4)	ReNCl ₄	1.078	0	Type-II	<i>s</i> -wave
1078	mp-505145	80 (<i>I</i> 4 ₁)	C ₄ (4)	Ag ₃ BiO ₃	1.547	0	Type-II	<i>s</i> -wave
1079	mp-43030	81 (<i>P</i> 4)	S ₄ (4)	Na ₂ Li ₂ Al ₃ Si ₃ ClO ₁₂	4.63	0	Type-III	<i>d</i> -wave
1080	mp-559065	81 (<i>P</i> 4)	S ₄ (4)	NaI ₃ O ₈	3.142	1	Type-III	<i>d</i> -wave
1081	icsd-90956	82 (<i>I</i> 4)	S ₄ (4)	GeSe ₂	1.0011	0	Type-III	<i>d</i> -wave
1082	mp-11175	82 (<i>I</i> 4)	S ₄ (4)	LiZnPS ₄	2.731	0	Type-III	<i>d</i> -wave
1083	mp-13949	82 (<i>I</i> 4)	S ₄ (4)	Cd(GaTe ₂) ₂	1.036	0	Type-III	<i>d</i> -wave
1084	mp-15777	82 (<i>I</i> 4)	S ₄ (4)	Zn(GaTe ₂) ₂	1.018	0	Type-III	<i>d</i> -wave
1085	mp-16337	82 (<i>I</i> 4)	S ₄ (4)	Ga ₂ HgTe ₄	0.661	0	Type-III	<i>d</i> -wave
1086	mp-16577	82 (<i>I</i> 4)	S ₄ (4)	Li ₂ CaHfF ₈	6.995	0	Type-III	<i>d</i> -wave
1087	mp-17677	82 (<i>I</i> 4)	S ₄ (4)	Nb ₉ PO ₂₅	2.109	1	Type-III	<i>d</i> -wave
1088	mp-19765	82 (<i>I</i> 4)	S ₄ (4)	In ₂ HgTe ₄	0.53	0	Type-III	<i>d</i> -wave
1089	mp-20025	82 (<i>I</i> 4)	S ₄ (4)	Mn(GaS ₂) ₂	1.179	1	Type-III	<i>d</i> -wave
1090	mp-20261	82 (<i>I</i> 4)	S ₄ (4)	Mn(GaSe ₂) ₂	0.857	1	Type-III	<i>d</i> -wave
1091	mp-20731	82 (<i>I</i> 4)	S ₄ (4)	In ₂ HgSe ₄	0.634	0	Type-III	<i>d</i> -wave
1092	mp-20790	82 (<i>I</i> 4)	S ₄ (4)	InPS ₄	2.319	0	Type-III	<i>d</i> -wave
1093	mp-20832	82 (<i>I</i> 4)	S ₄ (4)	Zn(InTe ₂) ₂	0.829	0	Type-III	<i>d</i> -wave
1094	mp-21374	82 (<i>I</i> 4)	S ₄ (4)	Cd(InTe ₂) ₂	0.848	0	Type-III	<i>d</i> -wave
1095	mp-22304	82 (<i>I</i> 4)	S ₄ (4)	Cd(InSe ₂) ₂	0.956	0	Type-III	<i>d</i> -wave
1096	mp-22607	82 (<i>I</i> 4)	S ₄ (4)	Zn(InSe ₂) ₂	0.993	0	Type-III	<i>d</i> -wave
1097	mp-23151	82 (<i>I</i> 4)	S ₄ (4)	Na ₄ BeAlSi ₄ ClO ₁₂	4.634	0	Type-III	<i>d</i> -wave
1098	mp-23485	82 (<i>I</i> 4)	S ₄ (4)	Ag ₂ HgI ₄	1.222	0	Type-III	<i>d</i> -wave
1099	mp-23702	82 (<i>I</i> 4)	S ₄ (4)	LiH ₂ N	3.136	0	Type-III	<i>d</i> -wave
1100	mp-27211	82 (<i>I</i> 4)	S ₄ (4)	KSb ₄ F ₁₃	4.661	1	Type-III	<i>d</i> -wave
1101	mp-28719	82 (<i>I</i> 4)	S ₄ (4)	Ba(AuF ₄) ₂	2.488	0	Type-III	<i>d</i> -wave
1102	mp-29201	82 (<i>I</i> 4)	S ₄ (4)	TbCd ₂ F ₈	0	1	Type-III	<i>d</i> -wave
1103	mp-29403	82 (<i>I</i> 4)	S ₄ (4)	GaCuI ₄	1.697	0	Type-III	<i>d</i> -wave
1104	mp-3038	82 (<i>I</i> 4)	S ₄ (4)	Al ₂ HgSe ₄	1.425	0	Type-III	<i>d</i> -wave
1105	mp-30927	82 (<i>I</i> 4)	S ₄ (4)	CsAs ₄ F ₁₃	5.266	1	Type-III	<i>d</i> -wave

1106	mp-3159	82 (<i>I</i> 4)	S ₄ (4)	Al ₂ CdSe ₄	2.005	0	Type-III	<i>d</i> -wave
1107	mp-3167	82 (<i>I</i> 4)	S ₄ (4)	Hg ₂ GeSe ₄	0.434	0	Type-III	<i>d</i> -wave
1108	mp-3277	82 (<i>I</i> 4)	S ₄ (4)	BAsO ₄	4.261	0	Type-III	<i>d</i> -wave
1109	mp-33449	82 (<i>I</i> 4)	S ₄ (4)	Tb ₅ AgS ₈	1.705	0	Type-III	<i>d</i> -wave
1110	mp-33775	82 (<i>I</i> 4)	S ₄ (4)	La ₅ AgSe ₈	1.423	0	Type-III	<i>d</i> -wave
1111	mp-34034	82 (<i>I</i> 4)	S ₄ (4)	Ba ₈ P ₅ Br	1.164	0	Type-III	<i>d</i> -wave
1112	mp-34486	82 (<i>I</i> 4)	S ₄ (4)	Pr ₅ AgS ₈	1.577	0	Type-III	<i>d</i> -wave
1113	mp-35264	82 (<i>I</i> 4)	S ₄ (4)	Pr ₅ AgSe ₈	1.454	0	Type-III	<i>d</i> -wave
1114	mp-35512	82 (<i>I</i> 4)	S ₄ (4)	Dy ₅ AgS ₈	1.732	0	Type-III	<i>d</i> -wave
1115	mp-35714	82 (<i>I</i> 4)	S ₄ (4)	La ₅ TlS ₈	1.395	0	Type-III	<i>d</i> -wave
1116	mp-3589	82 (<i>I</i> 4)	S ₄ (4)	BPO ₄	7.256	0	Type-III	<i>d</i> -wave
1117	mp-35907	82 (<i>I</i> 4)	S ₄ (4)	La ₅ TlTe ₈	1.081	0	Type-III	<i>d</i> -wave
1118	mp-36592	82 (<i>I</i> 4)	S ₄ (4)	Nd ₅ AgSe ₈	1.488	0	Type-III	<i>d</i> -wave
1119	mp-37449	82 (<i>I</i> 4)	S ₄ (4)	Nd ₅ AgS ₈	1.612	0	Type-III	<i>d</i> -wave
1120	mp-37478	82 (<i>I</i> 4)	S ₄ (4)	La ₅ AgS ₈	1.595	0	Type-III	<i>d</i> -wave
1121	mp-3772	82 (<i>I</i> 4)	S ₄ (4)	Cd(GaSe ₂) ₂	1.349	0	Type-III	<i>d</i> -wave
1122	mp-37829	82 (<i>I</i> 4)	S ₄ (4)	La ₅ TlSe ₈	1.3	0	Type-III	<i>d</i> -wave
1123	mp-37923	82 (<i>I</i> 4)	S ₄ (4)	Sm ₅ AgS ₈	1.638	0	Type-III	<i>d</i> -wave
1124	mp-38442	82 (<i>I</i> 4)	S ₄ (4)	CsNd ₅ Se ₈	1.622	0	Type-III	<i>d</i> -wave
1125	mp-38805	82 (<i>I</i> 4)	S ₄ (4)	Sm ₅ AgSe ₈	1.472	0	Type-III	<i>d</i> -wave
1126	mp-4452	82 (<i>I</i> 4)	S ₄ (4)	Cd(GaS ₂) ₂	2.12	0	Type-III	<i>d</i> -wave
1127	mp-4730	82 (<i>I</i> 4)	S ₄ (4)	Ga ₂ HgSe ₄	0.917	0	Type-III	<i>d</i> -wave
1128	mp-4809	82 (<i>I</i> 4)	S ₄ (4)	Ga ₂ HgS ₄	1.571	0	Type-III	<i>d</i> -wave
1129	mp-5046	82 (<i>I</i> 4)	S ₄ (4)	BeSO ₄	6.95	0	Type-III	<i>d</i> -wave
1130	mp-530149	82 (<i>I</i> 4)	S ₄ (4)	Ca ₁₂ Al ₁₄ O ₃₃	2.04	0	Type-III	<i>d</i> -wave
1131	mp-554151	82 (<i>I</i> 4)	S ₄ (4)	SiO ₂	5.725	0	Type-III	<i>d</i> -wave
1132	mp-556228	82 (<i>I</i> 4)	S ₄ (4)	Na ₅ Ca ₄ P ₄ O ₁₆ F	4.716	0	Type-III	<i>d</i> -wave
1133	mp-557696	82 (<i>I</i> 4)	S ₄ (4)	Na ₅ Y ₄ Si ₄ O ₁₆ F	4.77	0	Type-III	<i>d</i> -wave
1134	mp-558990	82 (<i>I</i> 4)	S ₄ (4)	K ₂ Sr(PO ₃) ₄	5.609	1	Type-III	<i>d</i> -wave
1135	mp-561350	82 (<i>I</i> 4)	S ₄ (4)	AlBiSCl ₄	2.83	0	Type-III	<i>d</i> -wave
1136	mp-568228	82 (<i>I</i> 4)	S ₄ (4)	RbLaSi(CN ₂) ₄	3.856	0	Type-III	<i>d</i> -wave
1137	mp-5928	82 (<i>I</i> 4)	S ₄ (4)	Al ₂ CdS ₄	2.726	0	Type-III	<i>d</i> -wave
1138	mp-628665	82 (<i>I</i> 4)	S ₄ (4)	AlBiTeCl ₄	2.104	0	Type-III	<i>d</i> -wave
1139	mp-637206	82 (<i>I</i> 4)	S ₄ (4)	AlBiSeCl ₄	2.542	0	Type-III	<i>d</i> -wave
1140	mp-677335	82 (<i>I</i> 4)	S ₄ (4)	GaPO ₄	4.698	0	Type-III	<i>d</i> -wave
1141	mp-758196	82 (<i>I</i> 4)	S ₄ (4)	Mg ₃ (AsO ₄) ₂	3.032	1	Type-III	<i>d</i> -wave
1142	mp-760729	82 (<i>I</i> 4)	S ₄ (4)	Ca ₂ Ga ₂ Si(HO ₄) ₂	3.538	0	Type-III	<i>d</i> -wave
1143	mp-770481	82 (<i>I</i> 4)	S ₄ (4)	Ta ₉ PO ₂₅	2.703	0	Type-III	<i>d</i> -wave
1144	mp-7906	82 (<i>I</i> 4)	S ₄ (4)	Al ₂ HgS ₄	2.024	0	Type-III	<i>d</i> -wave
1145	mp-7907	82 (<i>I</i> 4)	S ₄ (4)	Al ₂ ZnSe ₄	2.153	0	Type-III	<i>d</i> -wave
1146	mp-7908	82 (<i>I</i> 4)	S ₄ (4)	Al ₂ ZnTe ₄	1.625	0	Type-III	<i>d</i> -wave
1147	mp-7909	82 (<i>I</i> 4)	S ₄ (4)	Al ₂ CdTe ₄	1.625	0	Type-III	<i>d</i> -wave
1148	mp-7910	82 (<i>I</i> 4)	S ₄ (4)	Al ₂ HgTe ₄	1.111	0	Type-III	<i>d</i> -wave
1149	mp-866662	82 (<i>I</i> 4)	S ₄ (4)	K ₅ La ₄ Si ₄ O ₁₆ F	4.659	0	Type-III	<i>d</i> -wave
1150	mp-8873	82 (<i>I</i> 4)	S ₄ (4)	LiGeBO ₄	4.526	0	Type-III	<i>d</i> -wave
1151	mp-8874	82 (<i>I</i> 4)	S ₄ (4)	LiSiBO ₄	6.431	0	Type-III	<i>d</i> -wave
1152	mp-13843	91 (<i>P</i> 4 ₁ 22)	D ₄ (422)	Li ₂ TeO ₄	2.42	0	Type-II	<i>s</i> -wave
1153	mp-27794	91 (<i>P</i> 4 ₁ 22)	D ₄ (422)	Ba ₈ O ₁₃	5.781	1	Type-II	<i>s</i> -wave
1154	mp-39419	91 (<i>P</i> 4 ₁ 22)	D ₄ (422)	NdTlCdSbO ₇	2.649	1	Type-II	<i>s</i> -wave
1155	mp-42897	91 (<i>P</i> 4 ₁ 22)	D ₄ (422)	NaPrTiNbO ₆ F	2.958	1	Type-II	<i>s</i> -wave
1156	mp-43134	91 (<i>P</i> 4 ₁ 22)	D ₄ (422)	NaNdTiNbO ₆ F	2.933	1	Type-II	<i>s</i> -wave
1157	mp-542737	91 (<i>P</i> 4 ₁ 22)	D ₄ (422)	TiZn ₂ O ₄	2.31	0	Type-II	<i>s</i> -wave
1158	mp-6146	91 (<i>P</i> 4 ₁ 22)	D ₄ (422)	LiNbZnO ₄	2.778	0	Type-II	<i>s</i> -wave
1159	mp-757031	91 (<i>P</i> 4 ₁ 22)	D ₄ (422)	Mg ₂ TiO ₄	3.404	0	Type-II	<i>s</i> -wave
1160	mp-12112	92 (<i>P</i> 4 ₁ 2 ₁ 2)	D ₄ (422)	CdP ₂	1.456	0	Type-II	<i>s</i> -wave
1161	mp-12807	92 (<i>P</i> 4 ₁ 2 ₁ 2)	D ₄ (422)	KAlO ₂	4.562	1	Type-II	<i>s</i> -wave
1162	mp-13643	92 (<i>P</i> 4 ₁ 2 ₁ 2)	D ₄ (422)	Er ₂ Ge ₂ O ₇	3.737	1	Type-II	<i>s</i> -wave
1163	mp-14649	92 (<i>P</i> 4 ₁ 2 ₁ 2)	D ₄ (422)	Tb ₂ Ge ₂ O ₇	3.758	1	Type-II	<i>s</i> -wave
1164	mp-14708	92 (<i>P</i> 4 ₁ 2 ₁ 2)	D ₄ (422)	Tm ₂ Ge ₂ O ₇	3.725	1	Type-II	<i>s</i> -wave

1165	mp-18385	92 ($P_{4_1}2_12$)	D ₄ (422)	Lu ₂ Si ₂ O ₇	5.199	0	Type-II	<i>s</i> -wave
1166	mp-2782	92 ($P_{4_1}2_12$)	D ₄ (422)	ZnP ₂	1.462	0	Type-II	<i>s</i> -wave
1167	mp-28320	92 ($P_{4_1}2_12$)	D ₄ (422)	Pt ₃ I ₈	0.8	0	Type-II	<i>s</i> -wave
1168	mp-29289	92 ($P_{4_1}2_12$)	D ₄ (422)	BaPt ₂ S ₃	0.979	0	Type-II	<i>s</i> -wave
1169	mp-3427	92 ($P_{4_1}2_12$)	D ₄ (422)	LiAlO ₂	4.59	0	Type-II	<i>s</i> -wave
1170	mp-555434	92 ($P_{4_1}2_12$)	D ₄ (422)	As ₂ O ₅	1.628	0	Type-II	<i>s</i> -wave
1171	mp-557	92 ($P_{4_1}2_12$)	D ₄ (422)	TeO ₂	2.804	0	Type-II	<i>s</i> -wave
1172	mp-558588	92 ($P_{4_1}2_12$)	D ₄ (422)	BaPt ₂ S ₃	1.365	0	Type-II	<i>s</i> -wave
1173	mp-559613	92 ($P_{4_1}2_12$)	D ₄ (422)	K ₆ Se ₂ O ₉	1.632	0	Type-II	<i>s</i> -wave
1174	mp-560082	92 ($P_{4_1}2_12$)	D ₄ (422)	Ho ₂ Ge ₂ O ₇	3.748	1	Type-II	<i>s</i> -wave
1175	mp-561066	92 ($P_{4_1}2_12$)	D ₄ (422)	TlS	1.039	1	Type-II	<i>s</i> -wave
1176	mp-662553	92 ($P_{4_1}2_12$)	D ₄ (422)	B ₂ Pb ₂ S ₅	1.736	0	Type-II	<i>s</i> -wave
1177	mp-6945	92 ($P_{4_1}2_12$)	D ₄ (422)	SiO ₂	5.504	0	Type-II	<i>s</i> -wave
1178	mp-703316	92 ($P_{4_1}2_12$)	D ₄ (422)	LaMg ₂ H ₇	2.645	0	Type-II	<i>s</i> -wave
1179	mp-707105	92 ($P_{4_1}2_12$)	D ₄ (422)	Li ₃ B ₅ (HO ₅) ₂	5.885	0	Type-II	<i>s</i> -wave
1180	mp-7457	92 ($P_{4_1}2_12$)	D ₄ (422)	SnF ₂	3.249	0	Type-II	<i>s</i> -wave
1181	mp-7623	92 ($P_{4_1}2_12$)	D ₄ (422)	MgAs ₄	0.814	0	Type-II	<i>s</i> -wave
1182	mp-769953	92 ($P_{4_1}2_12$)	D ₄ (422)	Tb ₂ Ti ₂ O ₇	3.904	1	Type-II	<i>s</i> -wave
1183	mp-772793	92 ($P_{4_1}2_12$)	D ₄ (422)	Dy ₂ Ge ₂ O ₇	3.741	1	Type-II	<i>s</i> -wave
1184	mp-772840	92 ($P_{4_1}2_12$)	D ₄ (422)	Sm ₂ Ge ₂ O ₇	3.672	1	Type-II	<i>s</i> -wave
1185	mp-779502	92 ($P_{4_1}2_12$)	D ₄ (422)	Na ₃ CuO ₂	1.605	1	Type-II	<i>s</i> -wave
1186	mp-7812	92 ($P_{4_1}2_12$)	D ₄ (422)	GeO ₂	3.278	0	Type-II	<i>s</i> -wave
1187	mp-8346	92 ($P_{4_1}2_12$)	D ₄ (422)	Lu ₂ Ge ₂ O ₇	3.707	1	Type-II	<i>s</i> -wave
1188	mp-18037	95 ($P_{4_3}2_2$)	D ₄ (422)	LiNbZnO ₄	2.9	0	Type-II	<i>s</i> -wave
1189	mp-11025	96 ($P_{4_3}2_12$)	D ₄ (422)	ZnP ₂	1.462	0	Type-II	<i>s</i> -wave
1190	mp-13546	96 ($P_{4_3}2_12$)	D ₄ (422)	Y ₂ Ge ₂ O ₇	3.78	1	Type-II	<i>s</i> -wave
1191	mp-2739	96 ($P_{4_3}2_12$)	D ₄ (422)	TeO ₂	2.804	0	Type-II	<i>s</i> -wave
1192	mp-29313	96 ($P_{4_3}2_12$)	D ₄ (422)	Ta ₄ P ₄ S ₂₉	1.167	0	Type-II	<i>s</i> -wave
1193	mp-29816	96 ($P_{4_3}2_12$)	D ₄ (422)	Ag ₂ HgO ₂	0.41	0	Type-II	<i>s</i> -wave
1194	mp-554845	96 ($P_{4_3}2_12$)	D ₄ (422)	Na ₂ Zn ₂ O ₃	1.249	0	Type-II	<i>s</i> -wave
1195	mp-7029	96 ($P_{4_3}2_12$)	D ₄ (422)	SiO ₂	5.508	0	Type-II	<i>s</i> -wave
1196	mp-733729	96 ($P_{4_3}2_12$)	D ₄ (422)	RbInPHO ₅	3.648	0	Type-II	<i>s</i> -wave
1197	mp-769025	96 ($P_{4_3}2_12$)	D ₄ (422)	K ₂ Mg ₂ O ₃	3.252	0	Type-II	<i>s</i> -wave
1198	mp-771976	96 ($P_{4_3}2_12$)	D ₄ (422)	Rb ₂ Be ₂ O ₃	3.913	0	Type-II	<i>s</i> -wave
1199	mp-913	96 ($P_{4_3}2_12$)	D ₄ (422)	CdP ₂	1.456	0	Type-II	<i>s</i> -wave
1200	mp-33985	97 ($I422$)	D ₄ (422)	Ba(InTe ₂) ₂	0.864	0	Type-II	<i>s</i> -wave
1201	mp-37091	97 ($I422$)	D ₄ (422)	Sr(AlTe ₂) ₂	1.445	0	Type-II	<i>s</i> -wave
1202	mp-38117	97 ($I422$)	D ₄ (422)	Ba(GaTe ₂) ₂	0.529	0	Type-II	<i>s</i> -wave
1203	mp-38394	97 ($I422$)	D ₄ (422)	Ba(AlTe ₂) ₂	1.505	0	Type-II	<i>s</i> -wave
1204	mp-555528	97 ($I422$)	D ₄ (422)	Ca ₂ Th(Si ₂ O ₅) ₄	4.987	0	Type-II	<i>s</i> -wave
1205	icsd-16037	98 ($I4_122$)	D ₄ (422)	CdAs ₂	0.3297	0	Type-II	<i>s</i> -wave
1206	mp-13108	99 ($P4mm$)	C _{4v} (4mm)	SrHfO ₃	3.73	1	Type-III	<i>g</i> -wave
1207	mp-20459	99 ($P4mm$)	C _{4v} (4mm)	TiPbO ₃	1.813	0	Type-III	<i>g</i> -wave
1208	mp-4342	99 ($P4mm$)	C _{4v} (4mm)	KNbO ₃	1.476	1	Type-III	<i>g</i> -wave
1209	mp-5986	99 ($P4mm$)	C _{4v} (4mm)	BaTiO ₃	1.728	1	Type-III	<i>g</i> -wave
1210	mp-15983	100 ($P4bm$)	C _{4v} (4mm)	Ba ₂ NaNb ₅ O ₁₅	2.465	1	Type-III	<i>g</i> -wave
1211	mp-16929	100 ($P4bm$)	C _{4v} (4mm)	Pr ₃ Si ₆ N ₁₁	2.99	0	Type-III	<i>g</i> -wave
1212	mp-16995	100 ($P4bm$)	C _{4v} (4mm)	Sm ₃ Si ₆ N ₁₁	3.011	0	Type-III	<i>g</i> -wave
1213	mp-557072	100 ($P4bm$)	C _{4v} (4mm)	Ba ₃ TiNb ₄ O ₁₅	2.415	1	Type-III	<i>g</i> -wave
1214	mp-560407	100 ($P4bm$)	C _{4v} (4mm)	KNbSi ₂ O ₇	3.431	1	Type-III	<i>g</i> -wave
1215	mp-6081	100 ($P4bm$)	C _{4v} (4mm)	Ba ₂ Ti(SiO ₄) ₂	3.727	0	Type-III	<i>g</i> -wave
1216	mp-6289	100 ($P4bm$)	C _{4v} (4mm)	Ba ₂ Ti(GeO ₄) ₂	3.713	1	Type-III	<i>g</i> -wave
1217	mp-766938	100 ($P4bm$)	C _{4v} (4mm)	K ₃ Li ₂ Nb ₅ O ₁₅	2.558	1	Type-III	<i>g</i> -wave
1218	mp-17905	102 ($P4_2nm$)	C _{4v} (4mm)	Cs ₂ Hg ₆ S ₇	0.623	0	Type-III	<i>g</i> -wave
1219	mp-559112	102 ($P4_2nm$)	C _{4v} (4mm)	K ₂ Zn ₆ O ₇	0.792	1	Type-III	<i>g</i> -wave
1220	mp-27809	105 ($P4_2mc$)	C _{4v} (4mm)	Ba(GeP) ₂	0.513	0	Type-III	<i>g</i> -wave
1221	mp-29136	105 ($P4_2mc$)	C _{4v} (4mm)	Sr ₆ Cu ₃ N ₅	0.477	0	Type-III	<i>g</i> -wave
1222	mp-696127	105 ($P4_2mc$)	C _{4v} (4mm)	Li ₁₀ Ge(PSe ₆) ₂	1.049	1	Type-III	<i>g</i> -wave
1223	mp-696128	105 ($P4_2mc$)	C _{4v} (4mm)	Li ₁₀ Ge(PS ₆) ₂	2.055	1	Type-III	<i>g</i> -wave

1224	mp-696129	105 (<i>P4₂mc</i>)	C _{4v} (4mm)	Li ₁₀ Si(PS ₆) ₂	2.383	1	Type-III	<i>g</i> -wave
1225	mp-706277	105 (<i>P4₂mc</i>)	C _{4v} (4mm)	Li ₁₀ Si(PSe ₆) ₂	1.328	1	Type-III	<i>g</i> -wave
1226	mp-24461	107 (<i>I4mm</i>)	C _{4v} (4mm)	H ₁₂ OsN ₅ Cl ₃ O	2.402	1	Type-III	<i>g</i> -wave
1227	mp-34932	107 (<i>I4mm</i>)	C _{4v} (4mm)	CaHN	2.193	1	Type-III	<i>g</i> -wave
1228	mp-35152	107 (<i>I4mm</i>)	C _{4v} (4mm)	Sr ₂ H ₅ Rh	0.58	0	Type-III	<i>g</i> -wave
1229	mp-39542	107 (<i>I4mm</i>)	C _{4v} (4mm)	KRb ₂ ZrOF ₅	4.584	1	Type-III	<i>g</i> -wave
1230	mp-40143	107 (<i>I4mm</i>)	C _{4v} (4mm)	Cs ₂ KZrOF ₅	4.877	1	Type-III	<i>g</i> -wave
1231	mp-42022	107 (<i>I4mm</i>)	C _{4v} (4mm)	Cs ₂ RbZrOF ₅	4.71	1	Type-III	<i>g</i> -wave
1232	mp-42190	107 (<i>I4mm</i>)	C _{4v} (4mm)	K ₂ NaTiOF ₅	3.964	0	Type-III	<i>g</i> -wave
1233	mp-545359	107 (<i>I4mm</i>)	C _{4v} (4mm)	KNa ₂ CuO ₂	1.514	0	Type-III	<i>g</i> -wave
1234	mp-563025	107 (<i>I4mm</i>)	C _{4v} (4mm)	Na ₆ PbO ₅	1.056	0	Type-III	<i>g</i> -wave
1235	mp-696597	107 (<i>I4mm</i>)	C _{4v} (4mm)	B ₅ H ₉	5.709	1	Type-III	<i>g</i> -wave
1236	mp-540995	108 (<i>I4cm</i>)	C _{4v} (4mm)	Rb ₅ Nb ₃ OF ₁₈	3.985	1	Type-III	<i>g</i> -wave
1237	mp-541732	108 (<i>I4cm</i>)	C _{4v} (4mm)	Al ₃ Pb ₅ F ₁₉	5.138	1	Type-III	<i>g</i> -wave
1238	mp-556117	108 (<i>I4cm</i>)	C _{4v} (4mm)	Ga ₃ Pb ₅ F ₁₉	4.715	1	Type-III	<i>g</i> -wave
1239	mp-556500	108 (<i>I4cm</i>)	C _{4v} (4mm)	NCIOF ₄	1.621	1	Type-III	<i>g</i> -wave
1240	mp-758272	108 (<i>I4cm</i>)	C _{4v} (4mm)	Zr ₄ N ₂ O ₅	2.277	0	Type-III	<i>g</i> -wave
1241	mp-771411	108 (<i>I4cm</i>)	C _{4v} (4mm)	Sr ₃ GeO ₅	2.565	1	Type-III	<i>g</i> -wave
1242	icsd-81493	109 (<i>I4₁md</i>)	C _{4v} (4mm)	NbP	0	0	Type-III	<i>g</i> -wave
1243	mp-27255	109 (<i>I4₁md</i>)	C _{4v} (4mm)	Ga ₂ TeS ₂	2.02	0	Type-III	<i>g</i> -wave
1244	mp-28423	109 (<i>I4₁md</i>)	C _{4v} (4mm)	Ga ₂ TeSe ₂	1.614	0	Type-III	<i>g</i> -wave
1245	mp-703559	109 (<i>I4₁md</i>)	C _{4v} (4mm)	KSrAs(H ₄ O ₃) ₄	4.302	1	Type-III	<i>g</i> -wave
1246	mp-756638	109 (<i>I4₁md</i>)	C _{4v} (4mm)	NbRhO ₄	0.873	0	Type-III	<i>g</i> -wave
1247	mp-760402	109 (<i>I4₁md</i>)	C _{4v} (4mm)	TaRhO ₄	0.971	0	Type-III	<i>g</i> -wave
1248	mp-973793	109 (<i>I4₁md</i>)	C _{4v} (4mm)	Li ₈ SeN ₂	1.752	0	Type-III	<i>g</i> -wave
1249	mp-4779	110 (<i>I4₁cd</i>)	C _{4v} (4mm)	Li ₂ B ₄ O ₇	5.668	1	Type-III	<i>g</i> -wave
1250	mp-554935	110 (<i>I4₁cd</i>)	C _{4v} (4mm)	Pr ₈ Sb ₂ S ₁₅	1.814	0	Type-III	<i>g</i> -wave
1251	mp-707540	110 (<i>I4₁cd</i>)	C _{4v} (4mm)	ZrP ₂ (HO ₄) ₂	4.375	1	Type-III	<i>g</i> -wave
1252	mp-568032	111 (<i>P42m</i>)	D _{2d} (42m)	Cd(InSe ₂) ₂	0.871	0	Type-III	<i>d</i> -wave
1253	mp-570256	111 (<i>P42m</i>)	D _{2d} (42m)	Ag ₂ HgI ₄	1.1	0	Type-III	<i>d</i> -wave
1254	mp-694876	111 (<i>P42m</i>)	D _{2d} (42m)	NaSr ₂ LaTi ₄ O ₁₂	1.885	1	Type-III	<i>d</i> -wave
1255	mp-695514	111 (<i>P42m</i>)	D _{2d} (42m)	NaSr ₂ NdTi ₄ O ₁₂	1.857	1	Type-III	<i>d</i> -wave
1256	mp-8976	111 (<i>P42m</i>)	D _{2d} (42m)	Cu ₂ WS ₄	1.444	0	Type-III	<i>d</i> -wave
1257	mp-28020	112 (<i>P42c</i>)	D _{2d} (42m)	AlCuCl ₄	2.511	0	Type-III	<i>d</i> -wave
1258	mp-29362	112 (<i>P42c</i>)	D _{2d} (42m)	GaCuCl ₄	1.817	0	Type-III	<i>d</i> -wave
1259	mp-12240	113 (<i>P42₁m</i>)	D _{2d} (42m)	Na ₂ LiBe ₂ F ₇	6.948	0	Type-III	<i>d</i> -wave
1260	mp-12902	113 (<i>P42₁m</i>)	D _{2d} (42m)	ErAgTe ₂	0.894	0	Type-III	<i>d</i> -wave
1261	mp-12903	113 (<i>P42₁m</i>)	D _{2d} (42m)	YAgTe ₂	0.898	0	Type-III	<i>d</i> -wave
1262	mp-12904	113 (<i>P42₁m</i>)	D _{2d} (42m)	HoAgTe ₂	0.9	0	Type-III	<i>d</i> -wave
1263	mp-14415	113 (<i>P42₁m</i>)	D _{2d} (42m)	Pr ₂ Be ₂ GeO ₇	4.274	0	Type-III	<i>d</i> -wave
1264	mp-14416	113 (<i>P42₁m</i>)	D _{2d} (42m)	Sm ₂ Be ₂ GeO ₇	4.42	0	Type-III	<i>d</i> -wave
1265	mp-14420	113 (<i>P42₁m</i>)	D _{2d} (42m)	Er ₂ Be ₂ GeO ₇	4.431	0	Type-III	<i>d</i> -wave
1266	mp-17244	113 (<i>P42₁m</i>)	D _{2d} (42m)	Ba ₂ ZnGe ₂ S ₆ O	2.108	0	Type-III	<i>d</i> -wave
1267	mp-17392	113 (<i>P42₁m</i>)	D _{2d} (42m)	Sr ₂ ZnGe ₂ O ₇	3.116	0	Type-III	<i>d</i> -wave
1268	mp-18129	113 (<i>P42₁m</i>)	D _{2d} (42m)	La ₂ ZnGa ₂ S ₆ O	2.585	0	Type-III	<i>d</i> -wave
1269	mp-18596	113 (<i>P42₁m</i>)	D _{2d} (42m)	Ca ₂ ZnGe ₂ O ₇	3.049	1	Type-III	<i>d</i> -wave
1270	mp-19926	113 (<i>P42₁m</i>)	D _{2d} (42m)	La ₂ Be ₂ GeO ₇	4.131	0	Type-III	<i>d</i> -wave
1271	mp-20778	113 (<i>P42₁m</i>)	D _{2d} (42m)	Dy ₂ Be ₂ GeO ₇	4.469	0	Type-III	<i>d</i> -wave
1272	mp-23778	113 (<i>P42₁m</i>)	D _{2d} (42m)	H ₄ CN ₂ O	5.071	0	Type-III	<i>d</i> -wave
1273	mp-239	113 (<i>P42₁m</i>)	D _{2d} (42m)	BaS ₃	1.391	0	Type-III	<i>d</i> -wave
1274	mp-27767	113 (<i>P42₁m</i>)	D _{2d} (42m)	Li ₆ Si ₂ O ₇	4.795	0	Type-III	<i>d</i> -wave
1275	mp-27824	113 (<i>P42₁m</i>)	D _{2d} (42m)	PICl ₆	1.791	0	Type-III	<i>d</i> -wave
1276	mp-3551	113 (<i>P42₁m</i>)	D _{2d} (42m)	TbAgTe ₂	0.899	0	Type-III	<i>d</i> -wave
1277	mp-4024	113 (<i>P42₁m</i>)	D _{2d} (42m)	DyAgTe ₂	0.896	0	Type-III	<i>d</i> -wave
1278	mp-4674	113 (<i>P42₁m</i>)	D _{2d} (42m)	BNF ₈	2.998	0	Type-III	<i>d</i> -wave
1279	mp-541040	113 (<i>P42₁m</i>)	D _{2d} (42m)	Y ₂ Be ₂ GeO ₇	4.548	0	Type-III	<i>d</i> -wave
1280	mp-556422	113 (<i>P42₁m</i>)	D _{2d} (42m)	NbCl ₃ O	2.808	0	Type-III	<i>d</i> -wave
1281	mp-559691	113 (<i>P42₁m</i>)	D _{2d} (42m)	Ca ₂ Al ₂ SiO ₇	4.285	0	Type-III	<i>d</i> -wave
1282	mp-606393	113 (<i>P42₁m</i>)	D _{2d} (42m)	NbBr ₃ O	1.966	0	Type-III	<i>d</i> -wave

1283	mp-6094	113 (<i>P42</i> ₁ <i>m</i>)	D _{2d} (42m)	Ca ₂ MgSi ₂ O ₇	4.468	1	Type-III	<i>d</i> -wave
1284	mp-6208	113 (<i>P42</i> ₁ <i>m</i>)	D _{2d} (42m)	Ca ₂ BeSi ₂ O ₇	4.987	0	Type-III	<i>d</i> -wave
1285	mp-6227	113 (<i>P42</i> ₁ <i>m</i>)	D _{2d} (42m)	Ca ₂ ZnSi ₂ O ₇	4.055	1	Type-III	<i>d</i> -wave
1286	mp-6564	113 (<i>P42</i> ₁ <i>m</i>)	D _{2d} (42m)	Sr ₂ MgSi ₂ O ₇	4.496	0	Type-III	<i>d</i> -wave
1287	mp-6655	113 (<i>P42</i> ₁ <i>m</i>)	D _{2d} (42m)	Y ₂ Be ₂ SiO ₇	5.155	0	Type-III	<i>d</i> -wave
1288	mp-6941	113 (<i>P42</i> ₁ <i>m</i>)	D _{2d} (42m)	Y ₂ Si ₃ N ₄ O ₃	2.794	0	Type-III	<i>d</i> -wave
1289	mp-695470	113 (<i>P42</i> ₁ <i>m</i>)	D _{2d} (42m)	NaSr ₈ NdTi ₁₀ O ₃₀	1.784	1	Type-III	<i>d</i> -wave
1290	mp-7013	113 (<i>P42</i> ₁ <i>m</i>)	D _{2d} (42m)	Ho ₂ Be ₂ SiO ₇	5.086	0	Type-III	<i>d</i> -wave
1291	mp-752851	113 (<i>P42</i> ₁ <i>m</i>)	D _{2d} (42m)	Ca ₂ Si ₂ O ₇	5.681	0	Type-III	<i>d</i> -wave
1292	mp-7548	113 (<i>P42</i> ₁ <i>m</i>)	D _{2d} (42m)	BaSe ₃	0.926	0	Type-III	<i>d</i> -wave
1293	mp-758096	113 (<i>P42</i> ₁ <i>m</i>)	D _{2d} (42m)	SbOF ₃	1.923	1	Type-III	<i>d</i> -wave
1294	mp-758693	113 (<i>P42</i> ₁ <i>m</i>)	D _{2d} (42m)	Na ₄ Al ₄ H ₁₀ O ₁₃	4.317	0	Type-III	<i>d</i> -wave
1295	mp-8234	113 (<i>P42</i> ₁ <i>m</i>)	D _{2d} (42m)	BaTe ₃	0.82	0	Type-III	<i>d</i> -wave
1296	mp-9077	113 (<i>P42</i> ₁ <i>m</i>)	D _{2d} (42m)	Nd ₂ Be ₂ SiO ₇	5.023	0	Type-III	<i>d</i> -wave
1297	mp-9338	113 (<i>P42</i> ₁ <i>m</i>)	D _{2d} (42m)	Ba ₂ MgSi ₂ O ₇	4.453	0	Type-III	<i>d</i> -wave
1298	mp-972387	113 (<i>P42</i> ₁ <i>m</i>)	D _{2d} (42m)	Sr ₂ MgGe ₂ O ₇	3.604	0	Type-III	<i>d</i> -wave
1299	mp-23195	114 (<i>P42</i> ₁ <i>c</i>)	D _{2d} (42m)	Bi ₂ O ₃	1.658	0	Type-III	<i>d</i> -wave
1300	mp-24144	114 (<i>P42</i> ₁ <i>c</i>)	D _{2d} (42m)	Na ₅ ScH ₄ (C ₂ O ₇) ₂	4.837	0	Type-III	<i>d</i> -wave
1301	mp-27144	114 (<i>P42</i> ₁ <i>c</i>)	D _{2d} (42m)	TlPO ₃	3.459	1	Type-III	<i>d</i> -wave
1302	mp-28090	114 (<i>P42</i> ₁ <i>c</i>)	D _{2d} (42m)	Si ₂ H ₂ S ₃	3.366	0	Type-III	<i>d</i> -wave
1303	mp-28475	114 (<i>P42</i> ₁ <i>c</i>)	D _{2d} (42m)	H ₂ Pb ₃ O ₄	2.839	0	Type-III	<i>d</i> -wave
1304	mp-28676	114 (<i>P42</i> ₁ <i>c</i>)	D _{2d} (42m)	S ₂ O ₅ F ₂	5.588	1	Type-III	<i>d</i> -wave
1305	mp-28768	114 (<i>P42</i> ₁ <i>c</i>)	D _{2d} (42m)	Na ₄ SnSe ₄	1.465	0	Type-III	<i>d</i> -wave
1306	mp-28782	114 (<i>P42</i> ₁ <i>c</i>)	D _{2d} (42m)	Na ₃ PS ₄	2.292	0	Type-III	<i>d</i> -wave
1307	mp-29143	114 (<i>P42</i> ₁ <i>c</i>)	D _{2d} (42m)	Na ₃ VS ₄	1.47	0	Type-III	<i>d</i> -wave
1308	mp-29628	114 (<i>P42</i> ₁ <i>c</i>)	D _{2d} (42m)	Na ₄ SnS ₄	2.078	0	Type-III	<i>d</i> -wave
1309	mp-4223	114 (<i>P42</i> ₁ <i>c</i>)	D _{2d} (42m)	Na ₃ PO ₄	4.173	0	Type-III	<i>d</i> -wave
1310	mp-625541	114 (<i>P42</i> ₁ <i>c</i>)	D _{2d} (42m)	Sr ₃ (HO) ₂	2.304	0	Type-III	<i>d</i> -wave
1311	mp-723002	114 (<i>P42</i> ₁ <i>c</i>)	D _{2d} (42m)	Ag ₂ H ₁₂ S(NO) ₄	2.941	0	Type-III	<i>d</i> -wave
1312	mp-14873	115 (<i>P4</i> ₂ <i>m</i> ₂)	D _{2d} (42m)	K ₄ Nb ₈ Si(P ₂ O ₁₇) ₂	1.886	1	Type-III	<i>d</i> -wave
1313	mp-28153	115 (<i>P4</i> ₂ <i>m</i> ₂)	D _{2d} (42m)	Ca(AuF ₆) ₂	1.53	0	Type-III	<i>d</i> -wave
1314	mp-569055	115 (<i>P4</i> ₂ <i>m</i> ₂)	D _{2d} (42m)	CsLi ₂ I ₃	4.42	0	Type-III	<i>d</i> -wave
1315	mp-600001	115 (<i>P4</i> ₂ <i>m</i> ₂)	D _{2d} (42m)	SiO ₂	5.491	0	Type-III	<i>d</i> -wave
1316	mp-675564	115 (<i>P4</i> ₂ <i>m</i> ₂)	D _{2d} (42m)	La ₂ Th ₈ O ₁₉	3.09	0	Type-III	<i>d</i> -wave
1317	mp-676552	115 (<i>P4</i> ₂ <i>m</i> ₂)	D _{2d} (42m)	Nd ₂ Th ₈ O ₁₉	2.954	0	Type-III	<i>d</i> -wave
1318	mp-676629	115 (<i>P4</i> ₂ <i>m</i> ₂)	D _{2d} (42m)	Sm ₂ Th ₈ O ₁₉	2.778	0	Type-III	<i>d</i> -wave
1319	mp-971712	115 (<i>P4</i> ₂ <i>m</i> ₂)	D _{2d} (42m)	ZnCdS ₂	1.369	0	Type-III	<i>d</i> -wave
1320	mp-16609	116 (<i>P4</i> ₂ <i>c</i>)	D _{2d} (42m)	Si ₃ Os ₂	0.719	1	Type-III	<i>d</i> -wave
1321	mp-510032	116 (<i>P4</i> ₂ <i>c</i>)	D _{2d} (42m)	Ge ₃ Os ₂	0.846	0	Type-III	<i>d</i> -wave
1322	mp-680339	116 (<i>P4</i> ₂ <i>c</i>)	D _{2d} (42m)	Mn ₄ Si ₇	0.756	0	Type-III	<i>d</i> -wave
1323	mp-29213	117 (<i>P4</i> ₂ <i>b</i>)	D _{2d} (42m)	Cd ₂ Ge ₇ O ₁₆	2.1	0	Type-III	<i>d</i> -wave
1324	mp-29273	117 (<i>P4</i> ₂ <i>b</i>)	D _{2d} (42m)	Ca ₂ Ge ₇ O ₁₆	2.948	1	Type-III	<i>d</i> -wave
1325	mp-31292	117 (<i>P4</i> ₂ <i>b</i>)	D _{2d} (42m)	Rb ₂ PdSe ₁₆	0.851	0	Type-III	<i>d</i> -wave
1326	mp-766351	117 (<i>P4</i> ₂ <i>b</i>)	D _{2d} (42m)	Ba ₂ CaI ₆	3.551	1	Type-III	<i>d</i> -wave
1327	mp-772861	117 (<i>P4</i> ₂ <i>b</i>)	D _{2d} (42m)	BaSrI ₆	3.277	0	Type-III	<i>d</i> -wave
1328	mp-772875	117 (<i>P4</i> ₂ <i>b</i>)	D _{2d} (42m)	Ba ₂ SrI ₆	3.432	0	Type-III	<i>d</i> -wave
1329	mp-28130	118 (<i>P4</i> _n <i>2</i>)	D _{2d} (42m)	Nb(PS ₄) ₂	1.438	0	Type-III	<i>d</i> -wave
1330	mp-30311	118 (<i>P4</i> _n <i>2</i>)	D _{2d} (42m)	Zn ₃ (PS ₄) ₂	2.431	0	Type-III	<i>d</i> -wave
1331	mp-568556	118 (<i>P4</i> _n <i>2</i>)	D _{2d} (42m)	Mg ₂ B ₂₄ C	2.491	0	Type-III	<i>d</i> -wave
1332	mp-569901	118 (<i>P4</i> _n <i>2</i>)	D _{2d} (42m)	Ge ₂₃ Mo ₁₃	0	0	Type-III	<i>d</i> -wave
1333	mp-32880	119 (<i>I4</i> ₂ <i>m</i> ₂)	D _{2d} (42m)	CuBr	0.445	0	Type-III	<i>d</i> -wave
1334	mp-555508	119 (<i>I4</i> ₂ <i>m</i> ₂)	D _{2d} (42m)	Ca ₁₁ Si ₄ SO ₁₈	3.525	1	Type-III	<i>d</i> -wave
1335	mp-639682	119 (<i>I4</i> ₂ <i>m</i> ₂)	D _{2d} (42m)	SiO ₂	5.645	0	Type-III	<i>d</i> -wave
1336	mp-641018	119 (<i>I4</i> ₂ <i>m</i> ₂)	D _{2d} (42m)	CsK ₅ Zn ₄ Sn ₅ S ₁₇	1.641	0	Type-III	<i>d</i> -wave
1337	mp-673677	119 (<i>I4</i> ₂ <i>m</i> ₂)	D _{2d} (42m)	La ₂ Th ₃ O ₉	2.548	0	Type-III	<i>d</i> -wave
1338	mp-684580	119 (<i>I4</i> ₂ <i>m</i> ₂)	D _{2d} (42m)	AgI	1.314	0	Type-III	<i>d</i> -wave
1339	mp-753719	119 (<i>I4</i> ₂ <i>m</i> ₂)	D _{2d} (42m)	SrLiNb ₂ O ₆ F	1.77	1	Type-III	<i>d</i> -wave
1340	mp-774907	119 (<i>I4</i> ₂ <i>m</i> ₂)	D _{2d} (42m)	KLiZnS ₂	2.436	0	Type-III	<i>d</i> -wave
1341	mp-23996	120 (<i>I4</i> ₂ <i>c</i>)	D _{2d} (42m)	BeH ₈ SO ₈	5.201	1	Type-III	<i>d</i> -wave

1342	mp-6044	120 (<i>I4c2</i>)	D _{2d} (42m)	Sr ₆ B(PO ₄) ₅	4.812	1	Type-III	<i>d</i> -wave
1343	mp-12532	121 (<i>I42m</i>)	D _{2d} (42m)	KAg ₂ PS ₄	1.244	0	Type-III	<i>d</i> -wave
1344	mp-14175	121 (<i>I42m</i>)	D _{2d} (42m)	K ₃ NbO ₈	2.611	0	Type-III	<i>d</i> -wave
1345	mp-15472	121 (<i>I42m</i>)	D _{2d} (42m)	Ba ₄ LiCu(CO ₅) ₂	0.926	0	Type-III	<i>d</i> -wave
1346	mp-19896	121 (<i>I42m</i>)	D _{2d} (42m)	Li ₂ GePbS ₄	2.265	0	Type-III	<i>d</i> -wave
1347	mp-22993	121 (<i>I42m</i>)	D _{2d} (42m)	AgClO ₄	2.676	0	Type-III	<i>d</i> -wave
1348	mp-23576	121 (<i>I42m</i>)	D _{2d} (42m)	CsSbClF ₃	3.66	0	Type-III	<i>d</i> -wave
1349	mp-27888	121 (<i>I42m</i>)	D _{2d} (42m)	Zr ₃ GeO ₈	3.902	0	Type-III	<i>d</i> -wave
1350	mp-29091	121 (<i>I42m</i>)	D _{2d} (42m)	Ti(CuS) ₄	1.426	0	Type-III	<i>d</i> -wave
1351	mp-3269	121 (<i>I42m</i>)	D _{2d} (42m)	NaTh ₂ F ₉	6.253	0	Type-III	<i>d</i> -wave
1352	mp-35539	121 (<i>I42m</i>)	D _{2d} (42m)	Zn ₂ GeSe ₄	1.387	0	Type-III	<i>d</i> -wave
1353	mp-38103	121 (<i>I42m</i>)	D _{2d} (42m)	NaClO ₄	5.304	0	Type-III	<i>d</i> -wave
1354	mp-40830	121 (<i>I42m</i>)	D _{2d} (42m)	NaSr ₃ LaTi ₅ O ₁₅	1.864	1	Type-III	<i>d</i> -wave
1355	mp-4690	121 (<i>I42m</i>)	D _{2d} (42m)	K ₃ TaO ₈	3.04	0	Type-III	<i>d</i> -wave
1356	mp-557373	121 (<i>I42m</i>)	D _{2d} (42m)	Cu ₂ WS ₄	1.562	0	Type-III	<i>d</i> -wave
1357	mp-557930	121 (<i>I42m</i>)	D _{2d} (42m)	SiO ₂	5.64	0	Type-III	<i>d</i> -wave
1358	mp-561942	121 (<i>I42m</i>)	D _{2d} (42m)	Cs ₃ TaO ₈	3.071	0	Type-III	<i>d</i> -wave
1359	mp-568661	121 (<i>I42m</i>)	D _{2d} (42m)	Cd(InSe ₂) ₂	0.774	0	Type-III	<i>d</i> -wave
1360	mp-568968	121 (<i>I42m</i>)	D _{2d} (42m)	K ₂ SnHgSe ₄	1.479	0	Type-III	<i>d</i> -wave
1361	mp-675748	121 (<i>I42m</i>)	D _{2d} (42m)	Zn ₂ GeS ₄	2.327	0	Type-III	<i>d</i> -wave
1362	mp-6841	121 (<i>I42m</i>)	D _{2d} (42m)	Ba ₄ NaCu(CO ₅) ₂	1.029	0	Type-III	<i>d</i> -wave
1363	mp-703275	121 (<i>I42m</i>)	D _{2d} (42m)	NaSr ₃ NdTi ₅ O ₁₅	1.914	1	Type-III	<i>d</i> -wave
1364	mp-7394	121 (<i>I42m</i>)	D _{2d} (42m)	BaAg ₂ GeS ₄	0.596	0	Type-III	<i>d</i> -wave
1365	mp-753353	121 (<i>I42m</i>)	D _{2d} (42m)	Sr ₄ LiCu(CO ₅) ₂	1.026	0	Type-III	<i>d</i> -wave
1366	mp-760415	121 (<i>I42m</i>)	D _{2d} (42m)	Li ₃ SbS ₄	2.098	0	Type-III	<i>d</i> -wave
1367	mp-867699	121 (<i>I42m</i>)	D _{2d} (42m)	Li ₄ TiS ₄	2.474	0	Type-III	<i>d</i> -wave
1368	icsd-188890	122 (<i>I42d</i>)	D _{2d} (42m)	CO ₂	6.9529	0	Type-III	<i>d</i> -wave
1369	mp-10074	122 (<i>I42d</i>)	D _{2d} (42m)	GeSe ₂	1.519	0	Type-III	<i>d</i> -wave
1370	mp-10572	122 (<i>I42d</i>)	D _{2d} (42m)	NaPN ₂	4.681	0	Type-III	<i>d</i> -wave
1371	mp-12180	122 (<i>I42d</i>)	D _{2d} (42m)	NaS ₂	2.018	0	Type-III	<i>d</i> -wave
1372	mp-12954	122 (<i>I42d</i>)	D _{2d} (42m)	CuBS ₂	1.742	0	Type-III	<i>d</i> -wave
1373	mp-14091	122 (<i>I42d</i>)	D _{2d} (42m)	AlAgSe ₂	1.135	0	Type-III	<i>d</i> -wave
1374	mp-14092	122 (<i>I42d</i>)	D _{2d} (42m)	AlAgTe ₂	1.047	0	Type-III	<i>d</i> -wave
1375	mp-14232	122 (<i>I42d</i>)	D _{2d} (42m)	LiBO ₂	7.281	0	Type-III	<i>d</i> -wave
1376	mp-15514	122 (<i>I42d</i>)	D _{2d} (42m)	NaSe ₂	1.182	0	Type-III	<i>d</i> -wave
1377	mp-15701	122 (<i>I42d</i>)	D _{2d} (42m)	MgSiN ₂	3.471	0	Type-III	<i>d</i> -wave
1378	mp-15703	122 (<i>I42d</i>)	D _{2d} (42m)	BeCN ₂	3.851	0	Type-III	<i>d</i> -wave
1379	mp-15704	122 (<i>I42d</i>)	D _{2d} (42m)	BeSiN ₂	3.562	0	Type-III	<i>d</i> -wave
1380	mp-17771	122 (<i>I42d</i>)	D _{2d} (42m)	NaMg ₄ (AsO ₄) ₃	3.192	1	Type-III	<i>d</i> -wave
1381	mp-20187	122 (<i>I42d</i>)	D _{2d} (42m)	LiInSe ₂	1.573	0	Type-III	<i>d</i> -wave
1382	mp-20782	122 (<i>I42d</i>)	D _{2d} (42m)	LiInTe ₂	1.385	0	Type-III	<i>d</i> -wave
1383	mp-22909	122 (<i>I42d</i>)	D _{2d} (42m)	ZnCl ₂	4.053	0	Type-III	<i>d</i> -wave
1384	mp-23672	122 (<i>I42d</i>)	D _{2d} (42m)	PH ₆ NO ₄	5.506	1	Type-III	<i>d</i> -wave
1385	mp-23884	122 (<i>I42d</i>)	D _{2d} (42m)	SrGe(HO ₂) ₂	4.128	1	Type-III	<i>d</i> -wave
1386	mp-2961	122 (<i>I42d</i>)	D _{2d} (42m)	MgSiP ₂	1.373	0	Type-III	<i>d</i> -wave
1387	mp-29826	122 (<i>I42d</i>)	D _{2d} (42m)	ZnCN ₂	3.451	0	Type-III	<i>d</i> -wave
1388	mp-3078	122 (<i>I42d</i>)	D _{2d} (42m)	CdSiAs ₂	0.4	0	Type-III	<i>d</i> -wave
1389	mp-32581	122 (<i>I42d</i>)	D _{2d} (42m)	Pr ₂ Te ₃	0.883	0	Type-III	<i>d</i> -wave
1390	mp-32586	122 (<i>I42d</i>)	D _{2d} (42m)	Nd ₂ S ₃	1.787	0	Type-III	<i>d</i> -wave
1391	mp-32594	122 (<i>I42d</i>)	D _{2d} (42m)	Sm ₂ Se ₃	1.454	0	Type-III	<i>d</i> -wave
1392	mp-32645	122 (<i>I42d</i>)	D _{2d} (42m)	Sm ₂ S ₃	1.808	0	Type-III	<i>d</i> -wave
1393	mp-32688	122 (<i>I42d</i>)	D _{2d} (42m)	Nd ₂ Se ₃	1.428	0	Type-III	<i>d</i> -wave
1394	mp-32689	122 (<i>I42d</i>)	D _{2d} (42m)	Pr ₂ Se ₃	1.426	0	Type-III	<i>d</i> -wave
1395	mp-32692	122 (<i>I42d</i>)	D _{2d} (42m)	Pr ₂ S ₃	1.948	0	Type-III	<i>d</i> -wave
1396	mp-32755	122 (<i>I42d</i>)	D _{2d} (42m)	La ₂ Te ₃	0.999	0	Type-III	<i>d</i> -wave
1397	mp-32787	122 (<i>I42d</i>)	D _{2d} (42m)	Ho ₂ S ₃	1.934	0	Type-III	<i>d</i> -wave
1398	mp-32798	122 (<i>I42d</i>)	D _{2d} (42m)	La ₂ Se ₃	1.539	0	Type-III	<i>d</i> -wave
1399	mp-32826	122 (<i>I42d</i>)	D _{2d} (42m)	Dy ₂ S ₃	1.909	0	Type-III	<i>d</i> -wave
1400	mp-32850	122 (<i>I42d</i>)	D _{2d} (42m)	Tm ₂ Se ₃	1.656	0	Type-III	<i>d</i> -wave

1401	mp-32891	122 (<i>I42d</i>)	D _{2d} (42m)	Y ₂ S ₃	1.902	0	Type-III	<i>d</i> -wave
1402	mp-32906	122 (<i>I42d</i>)	D _{2d} (42m)	La ₂ S ₃	1.92	0	Type-III	<i>d</i> -wave
1403	mp-33406	122 (<i>I42d</i>)	D _{2d} (42m)	La ₂ PbSe ₄	1.828	0	Type-III	<i>d</i> -wave
1404	mp-33569	122 (<i>I42d</i>)	D _{2d} (42m)	Sr(LaSe ₂) ₂	1.883	0	Type-III	<i>d</i> -wave
1405	mp-33606	122 (<i>I42d</i>)	D _{2d} (42m)	Ba(PrSe ₂) ₂	1.619	0	Type-III	<i>d</i> -wave
1406	mp-33615	122 (<i>I42d</i>)	D _{2d} (42m)	Ba(LaS ₂) ₂	2.068	0	Type-III	<i>d</i> -wave
1407	mp-34011	122 (<i>I42d</i>)	D _{2d} (42m)	Ca(HoS ₂) ₂	2.191	0	Type-III	<i>d</i> -wave
1408	mp-34141	122 (<i>I42d</i>)	D _{2d} (42m)	Sr(LaS ₂) ₂	2.236	0	Type-III	<i>d</i> -wave
1409	mp-34185	122 (<i>I42d</i>)	D _{2d} (42m)	Ca(PrS ₂) ₂	2.057	0	Type-III	<i>d</i> -wave
1410	mp-34293	122 (<i>I42d</i>)	D _{2d} (42m)	CsTaN ₂	2.145	0	Type-III	<i>d</i> -wave
1411	mp-34508	122 (<i>I42d</i>)	D _{2d} (42m)	Sr(SmS ₂) ₂	2.128	0	Type-III	<i>d</i> -wave
1412	mp-34903	122 (<i>I42d</i>)	D _{2d} (42m)	MgGeP ₂	1.496	0	Type-III	<i>d</i> -wave
1413	mp-3524	122 (<i>I42d</i>)	D _{2d} (42m)	LiPN ₂	3.802	0	Type-III	<i>d</i> -wave
1414	mp-35269	122 (<i>I42d</i>)	D _{2d} (42m)	Ca ₄ Sb ₂ S	1.082	0	Type-III	<i>d</i> -wave
1415	mp-35421	122 (<i>I42d</i>)	D _{2d} (42m)	Ca(LaS ₂) ₂	2.146	0	Type-III	<i>d</i> -wave
1416	mp-35787	122 (<i>I42d</i>)	D _{2d} (42m)	Ca(DyS ₂) ₂	2.166	0	Type-III	<i>d</i> -wave
1417	mp-35876	122 (<i>I42d</i>)	D _{2d} (42m)	Ca(NdS ₂) ₂	2.061	0	Type-III	<i>d</i> -wave
1418	mp-3595	122 (<i>I42d</i>)	D _{2d} (42m)	ZnSiAs ₂	0.887	0	Type-III	<i>d</i> -wave
1419	mp-36007	122 (<i>I42d</i>)	D _{2d} (42m)	Ba(NdSe ₂) ₂	1.6	0	Type-III	<i>d</i> -wave
1420	mp-36031	122 (<i>I42d</i>)	D _{2d} (42m)	Ca(LaTe ₂) ₂	1.261	0	Type-III	<i>d</i> -wave
1421	mp-36100	122 (<i>I42d</i>)	D _{2d} (42m)	Ca(SmS ₂) ₂	2.083	0	Type-III	<i>d</i> -wave
1422	mp-36223	122 (<i>I42d</i>)	D _{2d} (42m)	Ba(PrS ₂) ₂	1.935	0	Type-III	<i>d</i> -wave
1423	mp-36538	122 (<i>I42d</i>)	D _{2d} (42m)	La ₂ PbS ₄	2.155	0	Type-III	<i>d</i> -wave
1424	mp-3668	122 (<i>I42d</i>)	D _{2d} (42m)	CdGeP ₂	0.646	0	Type-III	<i>d</i> -wave
1425	mp-37108	122 (<i>I42d</i>)	D _{2d} (42m)	Sr(NdS ₂) ₂	2.103	0	Type-III	<i>d</i> -wave
1426	mp-37263	122 (<i>I42d</i>)	D _{2d} (42m)	Ca(NdT _e) ₂	1.1	0	Type-III	<i>d</i> -wave
1427	mp-37520	122 (<i>I42d</i>)	D _{2d} (42m)	Ca(PrTe ₂) ₂	1.103	0	Type-III	<i>d</i> -wave
1428	mp-37741	122 (<i>I42d</i>)	D _{2d} (42m)	Ba(LaSe ₂) ₂	1.76	0	Type-III	<i>d</i> -wave
1429	mp-37859	122 (<i>I42d</i>)	D _{2d} (42m)	Sr(PrSe ₂) ₂	1.75	0	Type-III	<i>d</i> -wave
1430	mp-38099	122 (<i>I42d</i>)	D _{2d} (42m)	Rb ₄ Cl ₂ O	1.516	1	Type-III	<i>d</i> -wave
1431	mp-38152	122 (<i>I42d</i>)	D _{2d} (42m)	Sr(SmSe ₂) ₂	1.778	0	Type-III	<i>d</i> -wave
1432	mp-38240	122 (<i>I42d</i>)	D _{2d} (42m)	Sr(PrS ₂) ₂	2.095	0	Type-III	<i>d</i> -wave
1433	mp-38327	122 (<i>I42d</i>)	D _{2d} (42m)	Ca(TbS ₂) ₂	2.143	0	Type-III	<i>d</i> -wave
1434	mp-39033	122 (<i>I42d</i>)	D _{2d} (42m)	Sr(NdSe ₂) ₂	1.752	0	Type-III	<i>d</i> -wave
1435	mp-4175	122 (<i>I42d</i>)	D _{2d} (42m)	ZnSnP ₂	0.704	0	Type-III	<i>d</i> -wave
1436	mp-4524	122 (<i>I42d</i>)	D _{2d} (42m)	ZnGeP ₂	1.178	0	Type-III	<i>d</i> -wave
1437	mp-4586	122 (<i>I42d</i>)	D _{2d} (42m)	LiAlTe ₂	2.441	0	Type-III	<i>d</i> -wave
1438	mp-4666	122 (<i>I42d</i>)	D _{2d} (42m)	CdSiP ₂	1.426	0	Type-III	<i>d</i> -wave
1439	mp-4763	122 (<i>I42d</i>)	D _{2d} (42m)	ZnSiP ₂	1.364	0	Type-III	<i>d</i> -wave
1440	mp-4979	122 (<i>I42d</i>)	D _{2d} (42m)	AlCuS ₂	1.676	0	Type-III	<i>d</i> -wave
1441	mp-5048	122 (<i>I42d</i>)	D _{2d} (42m)	LiGaTe ₂	1.589	0	Type-III	<i>d</i> -wave
1442	mp-505138	122 (<i>I42d</i>)	D _{2d} (42m)	K ₂ PdSe ₁₀	1.074	0	Type-III	<i>d</i> -wave
1443	mp-5238	122 (<i>I42d</i>)	D _{2d} (42m)	GaCuS ₂	0.706	0	Type-III	<i>d</i> -wave
1444	mp-531296	122 (<i>I42d</i>)	D _{2d} (42m)	Ge(PbS ₂) ₂	1.979	0	Type-III	<i>d</i> -wave
1445	mp-532680	122 (<i>I42d</i>)	D _{2d} (42m)	Ba ₆ CdAg ₂ (SnS ₄) ₄	1.703	0	Type-III	<i>d</i> -wave
1446	mp-5342	122 (<i>I42d</i>)	D _{2d} (42m)	GaAgS ₂	0.962	0	Type-III	<i>d</i> -wave
1447	mp-540900	122 (<i>I42d</i>)	D _{2d} (42m)	B ₂ PdO ₄	0.779	0	Type-III	<i>d</i> -wave
1448	mp-550433	122 (<i>I42d</i>)	D _{2d} (42m)	BeZnO ₂	2.658	0	Type-III	<i>d</i> -wave
1449	mp-556163	122 (<i>I42d</i>)	D _{2d} (42m)	Zn ₂ SiO ₄	2.686	0	Type-III	<i>d</i> -wave
1450	mp-574580	122 (<i>I42d</i>)	D _{2d} (42m)	Tl ₄ Pd ₃ Cl ₁₀	1.137	0	Type-III	<i>d</i> -wave
1451	mp-5782	122 (<i>I42d</i>)	D _{2d} (42m)	AlAgS ₂	1.899	0	Type-III	<i>d</i> -wave
1452	mp-5990	122 (<i>I42d</i>)	D _{2d} (42m)	CsLi(B ₃ O ₅) ₂	5.078	0	Type-III	<i>d</i> -wave
1453	mp-642831	122 (<i>I42d</i>)	D _{2d} (42m)	RbP(HO ₂) ₂	5.408	1	Type-III	<i>d</i> -wave
1454	mp-673644	122 (<i>I42d</i>)	D _{2d} (42m)	Tb ₂ S ₃	1.872	0	Type-III	<i>d</i> -wave
1455	mp-673650	122 (<i>I42d</i>)	D _{2d} (42m)	Lu ₂ Se ₃	1.75	0	Type-III	<i>d</i> -wave
1456	mp-673656	122 (<i>I42d</i>)	D _{2d} (42m)	Y ₂ Se ₃	1.555	0	Type-III	<i>d</i> -wave
1457	mp-673682	122 (<i>I42d</i>)	D _{2d} (42m)	Tb ₂ YbS ₄	2.116	0	Type-III	<i>d</i> -wave
1458	mp-674804	122 (<i>I42d</i>)	D _{2d} (42m)	Sm ₂ PbSe ₄	1.641	0	Type-III	<i>d</i> -wave
1459	mp-675100	122 (<i>I42d</i>)	D _{2d} (42m)	Nd ₂ PbSe ₄	1.66	0	Type-III	<i>d</i> -wave

1460	mp-675146	122 (<i>I42d</i>)	D _{2d} (42m)	Pr ₂ PbSe ₄	1.659	0	Type-III	<i>d</i> -wave
1461	mp-675244	122 (<i>I42d</i>)	D _{2d} (42m)	Yb(NdS ₂) ₂	2.039	0	Type-III	<i>d</i> -wave
1462	mp-675293	122 (<i>I42d</i>)	D _{2d} (42m)	Yb(YS ₂) ₂	2.128	0	Type-III	<i>d</i> -wave
1463	mp-675406	122 (<i>I42d</i>)	D _{2d} (42m)	Yb(HoS ₂) ₂	2.172	0	Type-III	<i>d</i> -wave
1464	mp-675458	122 (<i>I42d</i>)	D _{2d} (42m)	La ₂ Te ₄ Pb	1.249	0	Type-III	<i>d</i> -wave
1465	mp-675511	122 (<i>I42d</i>)	D _{2d} (42m)	Sm ₂ PbS ₄	2.026	0	Type-III	<i>d</i> -wave
1466	mp-675620	122 (<i>I42d</i>)	D _{2d} (42m)	Nd ₂ PbS ₄	2.029	0	Type-III	<i>d</i> -wave
1467	mp-675638	122 (<i>I42d</i>)	D _{2d} (42m)	Pr ₂ PbS ₄	2.03	0	Type-III	<i>d</i> -wave
1468	mp-675668	122 (<i>I42d</i>)	D _{2d} (42m)	Yb(PrS ₂) ₂	2.015	0	Type-III	<i>d</i> -wave
1469	mp-675677	122 (<i>I42d</i>)	D _{2d} (42m)	Yb(SmS ₂) ₂	2.058	0	Type-III	<i>d</i> -wave
1470	mp-675767	122 (<i>I42d</i>)	D _{2d} (42m)	La ₂ YbS ₄	2.13	0	Type-III	<i>d</i> -wave
1471	mp-676154	122 (<i>I42d</i>)	D _{2d} (42m)	Yb(DyS ₂) ₂	2.148	0	Type-III	<i>d</i> -wave
1472	mp-684708	122 (<i>I42d</i>)	D _{2d} (42m)	Er ₂ S ₃	1.972	0	Type-III	<i>d</i> -wave
1473	mp-684911	122 (<i>I42d</i>)	D _{2d} (42m)	Sm ₂ Te ₃	0.917	0	Type-III	<i>d</i> -wave
1474	mp-685003	122 (<i>I42d</i>)	D _{2d} (42m)	Tb ₂ Se ₃	1.531	0	Type-III	<i>d</i> -wave
1475	mp-696752	122 (<i>I42d</i>)	D _{2d} (42m)	KP(HO ₂) ₂	5.605	1	Type-III	<i>d</i> -wave
1476	mp-703470	122 (<i>I42d</i>)	D _{2d} (42m)	AsH ₆ NO ₄	4.151	1	Type-III	<i>d</i> -wave
1477	mp-7582	122 (<i>I42d</i>)	D _{2d} (42m)	GeS ₂	2.597	0	Type-III	<i>d</i> -wave
1478	mp-758604	122 (<i>I42d</i>)	D _{2d} (42m)	LiAgF ₂	1.384	0	Type-III	<i>d</i> -wave
1479	mp-7801	122 (<i>I42d</i>)	D _{2d} (42m)	CaGeN ₂	2.662	1	Type-III	<i>d</i> -wave
1480	mp-8016	122 (<i>I42d</i>)	D _{2d} (42m)	AlCuSe ₂	0.892	0	Type-III	<i>d</i> -wave
1481	mp-8017	122 (<i>I42d</i>)	D _{2d} (42m)	AlCuTe ₂	1.019	0	Type-III	<i>d</i> -wave
1482	mp-971837	122 (<i>I42d</i>)	D _{2d} (42m)	ZnCdTe ₂	0.772	0	Type-III	<i>d</i> -wave
1483	mp-983565	122 (<i>I42d</i>)	D _{2d} (42m)	CuBSe ₂	1.487	0	Type-III	<i>d</i> -wave
1484	mp-554885	143 (<i>P3</i>)	C ₃ (3)	Ba ₃ Si ₆ N ₄ O ₉	4.372	0	Type-II	<i>s</i> -wave
1485	mp-557340	143 (<i>P3</i>)	C ₃ (3)	Ge ₃ Pb ₅ O ₁₁	2.501	0	Type-II	<i>s</i> -wave
1486	mp-767393	143 (<i>P3</i>)	C ₃ (3)	Li ₁₅ Ti ₁₁ Nb ₅ O ₄₂	2.273	1	Type-II	<i>s</i> -wave
1487	mp-767498	143 (<i>P3</i>)	C ₃ (3)	Li ₁₀ Ti ₁₁ Nb ₆ O ₄₂	2.189	1	Type-II	<i>s</i> -wave
1488	mp-10080	144 (<i>P3₁</i>)	C ₃ (3)	PrGeBO ₅	4.015	0	Type-II	<i>s</i> -wave
1489	mp-19957	144 (<i>P3₁</i>)	C ₃ (3)	LaGeBO ₅	4.031	0	Type-II	<i>s</i> -wave
1490	mp-22430	144 (<i>P3₁</i>)	C ₃ (3)	BAsPbO ₅	3.385	0	Type-II	<i>s</i> -wave
1491	mp-27209	144 (<i>P3₁</i>)	C ₃ (3)	KTlF ₄	2.323	0	Type-II	<i>s</i> -wave
1492	mp-28726	144 (<i>P3₁</i>)	C ₃ (3)	KYF ₄	6.971	0	Type-II	<i>s</i> -wave
1493	mp-559590	144 (<i>P3₁</i>)	C ₃ (3)	PrGeBO ₅	4	0	Type-II	<i>s</i> -wave
1494	mp-560832	144 (<i>P3₁</i>)	C ₃ (3)	CaH ₂ CO ₄	5.218	0	Type-II	<i>s</i> -wave
1495	mp-756639	144 (<i>P3₁</i>)	C ₃ (3)	Li ₂ NbOF ₅	3.689	0	Type-II	<i>s</i> -wave
1496	mp-38975	145 (<i>P3₂</i>)	C ₃ (3)	PNO	5.132	0	Type-II	<i>s</i> -wave
1497	mp-531687	145 (<i>P3₂</i>)	C ₃ (3)	Nd ₆ F ₁₇	0.697	1	Type-II	<i>s</i> -wave
1498	mp-558753	145 (<i>P3₂</i>)	C ₃ (3)	BiB ₂ O ₄ F	4.192	0	Type-II	<i>s</i> -wave
1499	mp-757917	145 (<i>P3₂</i>)	C ₃ (3)	Be(GaO ₂) ₂	2.89	1	Type-II	<i>s</i> -wave
1500	mp-11016	146 (<i>R3</i>)	C ₃ (3)	RbCd(NO ₂) ₃	2.352	0	Type-II	<i>s</i> -wave
1501	mp-11018	146 (<i>R3</i>)	C ₃ (3)	TlCd(NO ₂) ₃	2.14	0	Type-II	<i>s</i> -wave
1502	mp-14322	146 (<i>R3</i>)	C ₃ (3)	Ba ₃ Tm ₄ O ₉	3.277	1	Type-II	<i>s</i> -wave
1503	mp-14323	146 (<i>R3</i>)	C ₃ (3)	Ba ₃ Ho ₄ O ₉	3.256	1	Type-II	<i>s</i> -wave
1504	mp-14853	146 (<i>R3</i>)	C ₃ (3)	Ba ₃ Er ₄ O ₉	3.275	1	Type-II	<i>s</i> -wave
1505	mp-15751	146 (<i>R3</i>)	C ₃ (3)	Ba ₃ Y ₄ O ₉	3.32	1	Type-II	<i>s</i> -wave
1506	mp-17056	146 (<i>R3</i>)	C ₃ (3)	LiZnPO ₄	4.285	0	Type-II	<i>s</i> -wave
1507	mp-18048	146 (<i>R3</i>)	C ₃ (3)	LiZnAsO ₄	3.112	0	Type-II	<i>s</i> -wave
1508	mp-18147	146 (<i>R3</i>)	C ₃ (3)	LiGaSiO ₄	4.229	0	Type-II	<i>s</i> -wave
1509	mp-18220	146 (<i>R3</i>)	C ₃ (3)	LiAlSiO ₄	5.249	0	Type-II	<i>s</i> -wave
1510	mp-23887	146 (<i>R3</i>)	C ₃ (3)	MgH ₁₂ SO ₉	4.964	0	Type-II	<i>s</i> -wave
1511	mp-23888	146 (<i>R3</i>)	C ₃ (3)	MgTe(H ₄ O ₃) ₃	4.419	0	Type-II	<i>s</i> -wave
1512	mp-27453	146 (<i>R3</i>)	C ₃ (3)	Li ₇ SbO ₆	3.497	1	Type-II	<i>s</i> -wave
1513	mp-28891	146 (<i>R3</i>)	C ₃ (3)	Li ₇ TaO ₆	4.373	0	Type-II	<i>s</i> -wave
1514	mp-31408	146 (<i>R3</i>)	C ₃ (3)	Al ₄ (B ₂ O ₅) ₃	5.817	0	Type-II	<i>s</i> -wave
1515	mp-33872	146 (<i>R3</i>)	C ₃ (3)	Na ₇ Zr ₆ F ₃₁	5.262	1	Type-II	<i>s</i> -wave
1516	mp-36381	146 (<i>R3</i>)	C ₃ (3)	Sn(PS ₃) ₂	1.194	0	Type-II	<i>s</i> -wave
1517	mp-37399	146 (<i>R3</i>)	C ₃ (3)	Li ₇ NbO ₆	3.538	1	Type-II	<i>s</i> -wave
1518	mp-39681	146 (<i>R3</i>)	C ₃ (3)	NaTi ₂ BiO ₆	2.738	0	Type-II	<i>s</i> -wave

1519	mp-39823	146 (R3)	C ₃ (3)	Na ₈ Al ₆ Si ₆ CO ₂₇	3.366	0	Type-II	s-wave
1520	mp-504894	146 (R3)	C ₃ (3)	MgH ₁₂ SeO ₉	5.069	0	Type-II	s-wave
1521	mp-531213	146 (R3)	C ₃ (3)	Ca ₁₃ Y ₆ F ₄₃	0.577	1	Type-II	s-wave
1522	mp-542832	146 (R3)	C ₃ (3)	Ba ₃ Lu ₄ O ₉	3.168	1	Type-II	s-wave
1523	mp-546757	146 (R3)	C ₃ (3)	Sn ₃ PO ₄ F ₃	3.784	1	Type-II	s-wave
1524	mp-556516	146 (R3)	C ₃ (3)	Tl ₂ S	0.767	0	Type-II	s-wave
1525	mp-556797	146 (R3)	C ₃ (3)	K ₂ Si ₃ SnO ₉	4.013	1	Type-II	s-wave
1526	mp-633158	146 (R3)	C ₃ (3)	NaTeH ₆ O ₆ F	3.581	1	Type-II	s-wave
1527	mp-6628	146 (R3)	C ₃ (3)	CsCd(NO ₂) ₃	2.437	0	Type-II	s-wave
1528	mp-667	146 (R3)	C ₃ (3)	Tl ₂ S	0.891	0	Type-II	s-wave
1529	mp-675672	146 (R3)	C ₃ (3)	Zr ₅ Sc ₂ O ₁₃	3.647	0	Type-II	s-wave
1530	mp-676801	146 (R3)	C ₃ (3)	K ₇ Th ₆ F ₃₁	5.853	1	Type-II	s-wave
1531	mp-677164	146 (R3)	C ₃ (3)	CuAs ₂ Pb ₆ Cl ₇ O ₆	2.312	0	Type-II	s-wave
1532	mp-6782	146 (R3)	C ₃ (3)	Li ₂ ZrTeO ₆	2.779	0	Type-II	s-wave
1533	mp-680170	146 (R3)	C ₃ (3)	Cs ₂ Ti ₂ S ₉	0.811	0	Type-II	s-wave
1534	mp-754060	146 (R3)	C ₃ (3)	Li ₇ BiO ₆	1.915	0	Type-II	s-wave
1535	mp-755478	146 (R3)	C ₃ (3)	CdBiO ₃	0.767	0	Type-II	s-wave
1536	mp-757785	146 (R3)	C ₃ (3)	Bi ₁₂ PbO ₁₉	2.232	1	Type-II	s-wave
1537	mp-757826	146 (R3)	C ₃ (3)	CsCa(NO ₂) ₃	2.618	0	Type-II	s-wave
1538	mp-760311	146 (R3)	C ₃ (3)	Na ₇ SbO ₆	1.752	1	Type-II	s-wave
1539	mp-766103	146 (R3)	C ₃ (3)	Li ₇ Zr ₃ Nb(TeO ₆) ₄	2.369	1	Type-II	s-wave
1540	mp-767146	146 (R3)	C ₃ (3)	Li ₇ Ti ₁₂ NbO ₃₀	2.62	1	Type-II	s-wave
1541	mp-768907	146 (R3)	C ₃ (3)	Sr ₃ TeO ₆	3.059	0	Type-II	s-wave
1542	mp-769380	146 (R3)	C ₃ (3)	Li ₂ TiSn ₃ (PO ₄) ₆	2.749	1	Type-II	s-wave
1543	mp-772416	146 (R3)	C ₃ (3)	Li ₂ Ti ₃ Sn(PO ₄) ₆	2.505	1	Type-II	s-wave
1544	mp-776125	146 (R3)	C ₃ (3)	Ti ₃ Cu ₂ Sn(PO ₄) ₆	0.565	1	Type-II	s-wave
1545	mp-863678	146 (R3)	C ₃ (3)	KZn ₄ (SbO ₄) ₃	1.651	0	Type-II	s-wave
1546	mp-8974	146 (R3)	C ₃ (3)	Ba ₃ Dy ₄ O ₉	3.231	1	Type-II	s-wave
1547	mp-549697	149 (P312)	D ₃ (32)	RbGeIO ₆	2.429	0	Type-II	s-wave
1548	mp-12881	150 (P321)	D ₃ (32)	Ba ₃ NbGa ₃ (SiO ₇) ₂	3.296	0	Type-II	s-wave
1549	mp-16136	150 (P321)	D ₃ (32)	Sr ₃ TaGa ₃ (SiO ₇) ₂	3.854	0	Type-II	s-wave
1550	mp-17297	150 (P321)	D ₃ (32)	Na ₂ GeF ₆	5.787	0	Type-II	s-wave
1551	mp-17944	150 (P321)	D ₃ (32)	NaCaAlF ₆	7.114	0	Type-II	s-wave
1552	mp-23885	150 (P321)	D ₃ (32)	SrH ₁₂ (ClO ₃) ₂	5.051	0	Type-II	s-wave
1553	mp-23914	150 (P321)	D ₃ (32)	CaH ₁₂ (ClO ₃) ₂	4.987	0	Type-II	s-wave
1554	mp-24044	150 (P321)	D ₃ (32)	CaH ₁₂ (BrO ₃) ₂	4.137	0	Type-II	s-wave
1555	mp-28200	150 (P321)	D ₃ (32)	LaNb ₇ O ₁₉	2.087	1	Type-II	s-wave
1556	mp-29787	150 (P321)	D ₃ (32)	Ba ₅ Pt ₂ O ₉	1.63	0	Type-II	s-wave
1557	mp-3404	150 (P321)	D ₃ (32)	RbSO ₃	5.021	0	Type-II	s-wave
1558	mp-3775	150 (P321)	D ₃ (32)	Na ₂ SiF ₆	6.995	0	Type-II	s-wave
1559	mp-3848	150 (P321)	D ₃ (32)	BaGe ₄ O ₉	3.055	0	Type-II	s-wave
1560	mp-4829	150 (P321)	D ₃ (32)	Na ₂ ThF ₆	6.474	0	Type-II	s-wave
1561	mp-504908	150 (P321)	D ₃ (32)	In ₂ TeO ₆	1.017	0	Type-II	s-wave
1562	mp-5368	150 (P321)	D ₃ (32)	Li ₂ GeF ₆	6.049	0	Type-II	s-wave
1563	mp-541156	150 (P321)	D ₃ (32)	Ge ₄ PbO ₉	3.191	1	Type-II	s-wave
1564	mp-554139	150 (P321)	D ₃ (32)	Ba ₃ Ga ₂ (Ge ₂ O ₇) ₂	2.259	0	Type-II	s-wave
1565	mp-556024	150 (P321)	D ₃ (32)	Na ₂ TiF ₆	4.181	0	Type-II	s-wave
1566	mp-556458	150 (P321)	D ₃ (32)	BaCa(CO ₃) ₂	4.126	0	Type-II	s-wave
1567	mp-556936	150 (P321)	D ₃ (32)	CsBa(BO ₂) ₃	4.042	0	Type-II	s-wave
1568	mp-557773	150 (P321)	D ₃ (32)	Sc ₂ TeO ₆	2.897	0	Type-II	s-wave
1569	mp-558298	150 (P321)	D ₃ (32)	Zn ₃ TeAs ₂ Pb ₃ O ₁₄	2.959	0	Type-II	s-wave
1570	mp-560217	150 (P321)	D ₃ (32)	K ₂ Al ₂ B ₂ O ₇	4.595	0	Type-II	s-wave
1571	mp-561525	150 (P321)	D ₃ (32)	K ₂ Ga ₂ B ₂ O ₇	3.8	0	Type-II	s-wave
1572	mp-567196	150 (P321)	D ₃ (32)	Cs ₃ Sb ₂ Cl ₉	2.47	0	Type-II	s-wave
1573	mp-636461	150 (P321)	D ₃ (32)	Ga ₂ Ge ₄ Pb ₃ O ₁₄	2.169	1	Type-II	s-wave
1574	mp-669367	150 (P321)	D ₃ (32)	KAl(SO ₄) ₂	5.5	1	Type-II	s-wave
1575	mp-6788	150 (P321)	D ₃ (32)	La ₃ Ga ₅ SnO ₁₄	3.311	0	Type-II	s-wave
1576	mp-6853	150 (P321)	D ₃ (32)	Ca ₃ TaGa ₃ (SiO ₇) ₂	3.912	0	Type-II	s-wave
1577	mp-752439	150 (P321)	D ₃ (32)	BaSr ₂ I ₆	3.831	0	Type-II	s-wave

1578	mp-752671	150 (<i>P</i> 321)	D ₃ (32)	Ba ₂ SrI ₆	4.057	0	Type-II	<i>s</i> -wave
1579	mp-752695	150 (<i>P</i> 321)	D ₃ (32)	SrCa ₂ I ₆	3.675	0	Type-II	<i>s</i> -wave
1580	mp-754341	150 (<i>P</i> 321)	D ₃ (32)	Ho ₂ TeO ₆	3.103	1	Type-II	<i>s</i> -wave
1581	mp-755317	150 (<i>P</i> 321)	D ₃ (32)	Y ₂ TeO ₆	3.084	1	Type-II	<i>s</i> -wave
1582	mp-755376	150 (<i>P</i> 321)	D ₃ (32)	Er ₂ TeO ₆	3.033	0	Type-II	<i>s</i> -wave
1583	mp-755515	150 (<i>P</i> 321)	D ₃ (32)	Lu ₂ TeO ₆	2.982	0	Type-II	<i>s</i> -wave
1584	mp-756238	150 (<i>P</i> 321)	D ₃ (32)	Sr ₂ CaI ₆	3.963	0	Type-II	<i>s</i> -wave
1585	mp-769039	150 (<i>P</i> 321)	D ₃ (32)	Dy ₂ TeO ₆	3.039	1	Type-II	<i>s</i> -wave
1586	mp-772191	150 (<i>P</i> 321)	D ₃ (32)	Tm ₂ TeO ₆	3.053	0	Type-II	<i>s</i> -wave
1587	mp-778052	150 (<i>P</i> 321)	D ₃ (32)	Sm ₂ TeO ₆	3.028	1	Type-II	<i>s</i> -wave
1588	mp-867953	150 (<i>P</i> 321)	D ₃ (32)	Ba ₂ CaI ₆	3.987	0	Type-II	<i>s</i> -wave
1589	mp-9380	150 (<i>P</i> 321)	D ₃ (32)	SrGe ₄ O ₉	3.069	1	Type-II	<i>s</i> -wave
1590	mp-28714	151 (<i>P</i> 312)	D ₃ (32)	Dy(AlCl ₄) ₃	3.956	0	Type-II	<i>s</i> -wave
1591	mp-554540	151 (<i>P</i> 312)	D ₃ (32)	Li ₅ ReO ₆	2.206	0	Type-II	<i>s</i> -wave
1592	mp-570857	151 (<i>P</i> 312)	D ₃ (32)	Y(AlCl ₄) ₃	3.698	0	Type-II	<i>s</i> -wave
1593	mp-707138	151 (<i>P</i> 312)	D ₃ (32)	Ag ₂ PHO ₄	1.327	1	Type-II	<i>s</i> -wave
1594	icsd-222251	152 (<i>P</i> 3 ₁ 21)	D ₃ (32)	Se	0.9858	0	Type-II	<i>s</i> -wave
1595	icsd-23059	152 (<i>P</i> 3 ₁ 21)	D ₃ (32)	Te	0	0	Type-II	<i>s</i> -wave
1596	icsd-23060	152 (<i>P</i> 3 ₁ 21)	D ₃ (32)	Te	0	0	Type-II	<i>s</i> -wave
1597	icsd-23062	152 (<i>P</i> 3 ₁ 21)	D ₃ (32)	Te	0	0	Type-II	<i>s</i> -wave
1598	icsd-23064	152 (<i>P</i> 3 ₁ 21)	D ₃ (32)	Te	0	0	Type-II	<i>s</i> -wave
1599	icsd-23065	152 (<i>P</i> 3 ₁ 21)	D ₃ (32)	Te	0	0	Type-II	<i>s</i> -wave
1600	icsd-23066	152 (<i>P</i> 3 ₁ 21)	D ₃ (32)	Te	0	0	Type-II	<i>s</i> -wave
1601	icsd-23067	152 (<i>P</i> 3 ₁ 21)	D ₃ (32)	Te	0	0	Type-II	<i>s</i> -wave
1602	icsd-23068	152 (<i>P</i> 3 ₁ 21)	D ₃ (32)	Se	0.4294	0	Type-II	<i>s</i> -wave
1603	icsd-23069	152 (<i>P</i> 3 ₁ 21)	D ₃ (32)	Se	0.2705	0	Type-II	<i>s</i> -wave
1604	icsd-23070	152 (<i>P</i> 3 ₁ 21)	D ₃ (32)	Se	0.1729	0	Type-II	<i>s</i> -wave
1605	icsd-23071	152 (<i>P</i> 3 ₁ 21)	D ₃ (32)	Se	0.0297	0	Type-II	<i>s</i> -wave
1606	icsd-23072	152 (<i>P</i> 3 ₁ 21)	D ₃ (32)	Se	0	0	Type-II	<i>s</i> -wave
1607	icsd-23073	152 (<i>P</i> 3 ₁ 21)	D ₃ (32)	Se	0	0	Type-II	<i>s</i> -wave
1608	icsd-31129	152 (<i>P</i> 3 ₁ 21)	D ₃ (32)	HgS	0	1	Type-II	<i>s</i> -wave
1609	icsd-40008	152 (<i>P</i> 3 ₁ 21)	D ₃ (32)	Te	0	0	Type-II	<i>s</i> -wave
1610	icsd-40018	152 (<i>P</i> 3 ₁ 21)	D ₃ (32)	Se	0.9813	0	Type-II	<i>s</i> -wave
1611	icsd-40041	152 (<i>P</i> 3 ₁ 21)	D ₃ (32)	Te	0	0	Type-II	<i>s</i> -wave
1612	icsd-53801	152 (<i>P</i> 3 ₁ 21)	D ₃ (32)	Se	0.9101	0	Type-II	<i>s</i> -wave
1613	icsd-76150	152 (<i>P</i> 3 ₁ 21)	D ₃ (32)	Te	0	0	Type-II	<i>s</i> -wave
1614	icsd-79634	152 (<i>P</i> 3 ₁ 21)	D ₃ (32)	SiO ₂	5.9854	0	Type-II	<i>s</i> -wave
1615	icsd-96502	152 (<i>P</i> 3 ₁ 21)	D ₃ (32)	Te	0	0	Type-II	<i>s</i> -wave
1616	icsd-161690	152 (<i>P</i> 3 ₁ 21)	D ₃ (32)	Te	0	0	Type-II	<i>s</i> -wave
1617	icsd-164261	152 (<i>P</i> 3 ₁ 21)	D ₃ (32)	Se	0.9846	0	Type-II	<i>s</i> -wave
1618	icsd-164262	152 (<i>P</i> 3 ₁ 21)	D ₃ (32)	Se	0.9857	0	Type-II	<i>s</i> -wave
1619	icsd-164263	152 (<i>P</i> 3 ₁ 21)	D ₃ (32)	Se	0.6025	0	Type-II	<i>s</i> -wave
1620	icsd-164264	152 (<i>P</i> 3 ₁ 21)	D ₃ (32)	Se	0.5578	0	Type-II	<i>s</i> -wave
1621	icsd-164265	152 (<i>P</i> 3 ₁ 21)	D ₃ (32)	Se	0.39	0	Type-II	<i>s</i> -wave
1622	icsd-164266	152 (<i>P</i> 3 ₁ 21)	D ₃ (32)	Se	0.3079	0	Type-II	<i>s</i> -wave
1623	icsd-164267	152 (<i>P</i> 3 ₁ 21)	D ₃ (32)	Se	0.1765	0	Type-II	<i>s</i> -wave
1624	icsd-164269	152 (<i>P</i> 3 ₁ 21)	D ₃ (32)	Se	0.0185	0	Type-II	<i>s</i> -wave
1625	icsd-164270	152 (<i>P</i> 3 ₁ 21)	D ₃ (32)	Se	0.9857	0	Type-II	<i>s</i> -wave
1626	icsd-164271	152 (<i>P</i> 3 ₁ 21)	D ₃ (32)	Se	0.9856	0	Type-II	<i>s</i> -wave
1627	icsd-200685	152 (<i>P</i> 3 ₁ 21)	D ₃ (32)	Se	0.4294	0	Type-II	<i>s</i> -wave
1628	icsd-200722	152 (<i>P</i> 3 ₁ 21)	D ₃ (32)	SiO ₂	6.0699	0	Type-II	<i>s</i> -wave
1629	icsd-651846	152 (<i>P</i> 3 ₁ 21)	D ₃ (32)	Se	0.9205	0	Type-II	<i>s</i> -wave
1630	icsd-651850	152 (<i>P</i> 3 ₁ 21)	D ₃ (32)	Se	0.9343	0	Type-II	<i>s</i> -wave
1631	icsd-651852	152 (<i>P</i> 3 ₁ 21)	D ₃ (32)	Se	0.9399	0	Type-II	<i>s</i> -wave
1632	icsd-653045	152 (<i>P</i> 3 ₁ 21)	D ₃ (32)	Te	0	0	Type-II	<i>s</i> -wave
1633	icsd-653047	152 (<i>P</i> 3 ₁ 21)	D ₃ (32)	Te	0	0	Type-II	<i>s</i> -wave
1634	mp-11653	152 (<i>P</i> 3 ₁ 21)	D ₃ (32)	BPO ₄	6.998	0	Type-II	<i>s</i> -wave
1635	mp-11654	152 (<i>P</i> 3 ₁ 21)	D ₃ (32)	BAsO ₄	3.876	0	Type-II	<i>s</i> -wave
1636	mp-12403	152 (<i>P</i> 3 ₁ 21)	D ₃ (32)	LiBF ₄	8.246	0	Type-II	<i>s</i> -wave

1637	mp-15840	152 (P_3 121)	D ₃ (32)	BaBPO ₅	5.496	0	Type-II	s-wave
1638	mp-15951	152 (P_3 121)	D ₃ (32)	BeF ₂	8.32	0	Type-II	s-wave
1639	mp-17947	152 (P_3 121)	D ₃ (32)	BaCu ₂ GeS ₄	0.974	0	Type-II	s-wave
1640	mp-21266	152 (P_3 121)	D ₃ (32)	BPPbO ₅	4.259	1	Type-II	s-wave
1641	mp-28205	152 (P_3 121)	D ₃ (32)	Na ₃ ReO ₅	2.431	0	Type-II	s-wave
1642	mp-306	152 (P_3 121)	D ₃ (32)	B ₂ O ₃	6.302	0	Type-II	s-wave
1643	mp-3288	152 (P_3 121)	D ₃ (32)	CsNO ₂	2.363	0	Type-II	s-wave
1644	mp-3996	152 (P_3 121)	D ₃ (32)	GaAsO ₄	3.069	0	Type-II	s-wave
1645	mp-4122	152 (P_3 121)	D ₃ (32)	GaPO ₄	4.439	0	Type-II	s-wave
1646	mp-4236	152 (P_3 121)	D ₃ (32)	BaZnO ₂	2.272	0	Type-II	s-wave
1647	mp-5189	152 (P_3 121)	D ₃ (32)	AlAsO ₄	3.865	0	Type-II	s-wave
1648	mp-5331	152 (P_3 121)	D ₃ (32)	AlPO ₄	5.613	0	Type-II	s-wave
1649	mp-557508	152 (P_3 121)	D ₃ (32)	NaLaH ₂ S ₂ O ₉	4.496	1	Type-II	s-wave
1650	mp-560316	152 (P_3 121)	D ₃ (32)	Hg ₃ SO ₆	0.56	1	Type-II	s-wave
1651	mp-560799	152 (P_3 121)	D ₃ (32)	NaNdH ₂ S ₂ O ₉	5.748	1	Type-II	s-wave
1652	mp-561011	152 (P_3 121)	D ₃ (32)	Li ₂ Ta ₂ (OF ₂) ₃	3.841	1	Type-II	s-wave
1653	mp-561243	152 (P_3 121)	D ₃ (32)	Sr ₂ CuClO ₂	2.384	0	Type-II	s-wave
1654	mp-571464	152 (P_3 121)	D ₃ (32)	RbPSe ₃	1.123	0	Type-II	s-wave
1655	mp-6267	152 (P_3 121)	D ₃ (32)	LaSiBO ₅	4.143	1	Type-II	s-wave
1656	mp-634	152 (P_3 121)	D ₃ (32)	HgS	1.708	0	Type-II	s-wave
1657	mp-6486	152 (P_3 121)	D ₃ (32)	SrBPO ₅	5.387	1	Type-II	s-wave
1658	mp-6667	152 (P_3 121)	D ₃ (32)	CaBPO ₅	5.323	1	Type-II	s-wave
1659	mp-7000	152 (P_3 121)	D ₃ (32)	SiO ₂	5.719	0	Type-II	s-wave
1660	mp-733	152 (P_3 121)	D ₃ (32)	GeO ₂	3.25	0	Type-II	s-wave
1661	mp-752580	152 (P_3 121)	D ₃ (32)	RbNO ₂	2.079	0	Type-II	s-wave
1662	mp-754629	152 (P_3 121)	D ₃ (32)	WN ₂	1.003	1	Type-II	s-wave
1663	mp-756018	152 (P_3 121)	D ₃ (32)	BaMgO ₂	3.16	0	Type-II	s-wave
1664	mp-769138	152 (P_3 121)	D ₃ (32)	Dy ₂ Sb ₂ O ₇	1.899	1	Type-II	s-wave
1665	mp-772137	152 (P_3 121)	D ₃ (32)	Er ₂ Sb ₂ O ₇	1.751	1	Type-II	s-wave
1666	mp-772486	152 (P_3 121)	D ₃ (32)	Lu ₂ Sb ₂ O ₇	2.098	1	Type-II	s-wave
1667	mp-777990	152 (P_3 121)	D ₃ (32)	Tm ₂ Sb ₂ O ₇	2.131	1	Type-II	s-wave
1668	mp-780448	152 (P_3 121)	D ₃ (32)	Ho ₂ Sb ₂ O ₇	1.831	1	Type-II	s-wave
1669	mp-7826	152 (P_3 121)	D ₃ (32)	HgO	1.31	0	Type-II	s-wave
1670	mp-9784	152 (P_3 121)	D ₃ (32)	BaBAsO ₅	3.544	1	Type-II	s-wave
1671	icsd-18172	154 (P_3 221)	D ₃ (32)	SiO ₂	5.9962	0	Type-II	s-wave
1672	icsd-26429	154 (P_3 221)	D ₃ (32)	SiO ₂	6.0016	0	Type-II	s-wave
1673	icsd-27826	154 (P_3 221)	D ₃ (32)	SiO ₂	5.9687	0	Type-II	s-wave
1674	icsd-31228	154 (P_3 221)	D ₃ (32)	SiO ₂	6.0053	0	Type-II	s-wave
1675	icsd-166602	154 (P_3 221)	D ₃ (32)	SiO ₂	0	0	Type-II	s-wave
1676	icsd-653048	154 (P_3 221)	D ₃ (32)	Te	0	0	Type-II	s-wave
1677	mp-11168	154 (P_3 221)	D ₃ (32)	Ca(PIr) ₂	0.494	0	Type-II	s-wave
1678	mp-15074	154 (P_3 221)	D ₃ (32)	Sr(PIr) ₂	0.442	0	Type-II	s-wave
1679	mp-17756	154 (P_3 221)	D ₃ (32)	RbAg ₂ SbS ₄	0.618	0	Type-II	s-wave
1680	mp-18685	154 (P_3 221)	D ₃ (32)	SrCu ₂ GeS ₄	1.046	0	Type-II	s-wave
1681	mp-223	154 (P_3 221)	D ₃ (32)	GeO ₂	3.249	0	Type-II	s-wave
1682	mp-3955	154 (P_3 221)	D ₃ (32)	AlPO ₄	5.618	0	Type-II	s-wave
1683	mp-555818	154 (P_3 221)	D ₃ (32)	Cu ₂ SiPbS ₄	1.343	0	Type-II	s-wave
1684	mp-558022	154 (P_3 221)	D ₃ (32)	SrBPO ₅	5.388	1	Type-II	s-wave
1685	mp-569030	154 (P_3 221)	D ₃ (32)	BeCl ₂	6.375	0	Type-II	s-wave
1686	mp-6040	154 (P_3 221)	D ₃ (32)	BaBPO ₅	5.495	0	Type-II	s-wave
1687	mp-9252	154 (P_3 221)	D ₃ (32)	HgS	1.686	0	Type-II	s-wave
1688	mp-10348	155 (R 32)	D ₃ (32)	LaSc ₃ (BO ₃) ₄	4.086	0	Type-II	s-wave
1689	mp-12885	155 (R 32)	D ₃ (32)	BaAl ₂ Sb ₂ O ₇	3.411	0	Type-II	s-wave
1690	mp-13516	155 (R 32)	D ₃ (32)	TmAl ₃ (BO ₃) ₄	5.672	0	Type-II	s-wave
1691	mp-14506	155 (R 32)	D ₃ (32)	Al ₇ Te ₁₀	1.08	0	Type-II	s-wave
1692	mp-15939	155 (R 32)	D ₃ (32)	SrAl ₂ B ₂ O ₇	4.652	0	Type-II	s-wave
1693	mp-18388	155 (R 32)	D ₃ (32)	Ga ₇ Te ₁₀	0.575	0	Type-II	s-wave
1694	mp-29462	155 (R 32)	D ₃ (32)	NaGa ₃ Te ₅	1.208	0	Type-II	s-wave
1695	mp-546546	155 (R 32)	D ₃ (32)	SiO ₂	5.56	0	Type-II	s-wave

1696	mp-553342	155 (<i>R</i> 32)	D ₃ (32)	CsBe ₂ BO ₃ F ₂	5.883	0	Type-II	<i>s</i> -wave
1697	mp-555808	155 (<i>R</i> 32)	D ₃ (32)	Zn ₈ B ₃ H ₃ O ₁₄	2.651	1	Type-II	<i>s</i> -wave
1698	mp-556120	155 (<i>R</i> 32)	D ₃ (32)	RbTl(SO ₄) ₂	1.989	1	Type-II	<i>s</i> -wave
1699	mp-559773	155 (<i>R</i> 32)	D ₃ (32)	Na ₄ Sr(SiO ₃) ₃	4.247	1	Type-II	<i>s</i> -wave
1700	mp-561187	155 (<i>R</i> 32)	D ₃ (32)	NdGa ₃ (BO ₃) ₄	4.339	0	Type-II	<i>s</i> -wave
1701	mp-568116	155 (<i>R</i> 32)	D ₃ (32)	Lu ₂ (CN ₂) ₃	3.712	0	Type-II	<i>s</i> -wave
1702	mp-6062	155 (<i>R</i> 32)	D ₃ (32)	YAl ₃ (BO ₃) ₄	5.359	0	Type-II	<i>s</i> -wave
1703	mp-6524	155 (<i>R</i> 32)	D ₃ (32)	CaMg ₃ (CO ₃) ₄	4.815	0	Type-II	<i>s</i> -wave
1704	mp-669311	155 (<i>R</i> 32)	D ₃ (32)	In ₇ Te ₁₀	0.822	0	Type-II	<i>s</i> -wave
1705	mp-675022	155 (<i>R</i> 32)	D ₃ (32)	CsPbCl ₃	2.31	1	Type-II	<i>s</i> -wave
1706	mp-676851	155 (<i>R</i> 32)	D ₃ (32)	KNO ₃	3.015	1	Type-II	<i>s</i> -wave
1707	mp-686583	155 (<i>R</i> 32)	D ₃ (32)	Na ₅ Zr ₄ Si ₃ (PO ₈) ₃	4.173	1	Type-II	<i>s</i> -wave
1708	mp-6870	155 (<i>R</i> 32)	D ₃ (32)	KBe ₂ BO ₃ F ₂	6.052	0	Type-II	<i>s</i> -wave
1709	mp-7323	155 (<i>R</i> 32)	D ₃ (32)	RbBe ₂ BO ₃ F ₂	5.964	0	Type-II	<i>s</i> -wave
1710	mp-7337	155 (<i>R</i> 32)	D ₃ (32)	NdAl ₃ (BO ₃) ₄	5.308	0	Type-II	<i>s</i> -wave
1711	mp-752446	155 (<i>R</i> 32)	D ₃ (32)	RbNO ₃	2.981	1	Type-II	<i>s</i> -wave
1712	mp-22965	156 (<i>P</i> 3m1)	C _{3v} (3m)	BiTeI	1.232	0	Type-III	<i>g</i> -wave
1713	mp-29057	156 (<i>P</i> 3m1)	C _{3v} (3m)	Nb ₃ SBr ₇	0.744	0	Type-III	<i>g</i> -wave
1714	mp-33335	156 (<i>P</i> 3m1)	C _{3v} (3m)	MgAl ₂ O ₄	4.252	1	Type-III	<i>g</i> -wave
1715	mp-34144	156 (<i>P</i> 3m1)	C _{3v} (3m)	MgAl ₂ O ₄	4.59	1	Type-III	<i>g</i> -wave
1716	mp-530146	156 (<i>P</i> 3m1)	C _{3v} (3m)	MgAl ₂ O ₄	4.123	1	Type-III	<i>g</i> -wave
1717	mp-531238	156 (<i>P</i> 3m1)	C _{3v} (3m)	Cd(GaO ₂) ₂	0.623	1	Type-III	<i>g</i> -wave
1718	mp-532294	156 (<i>P</i> 3m1)	C _{3v} (3m)	Er ₂ CdSe ₄	0.585	0	Type-III	<i>g</i> -wave
1719	mp-553880	156 (<i>P</i> 3m1)	C _{3v} (3m)	ZnS	2.031	0	Type-III	<i>g</i> -wave
1720	mp-553916	156 (<i>P</i> 3m1)	C _{3v} (3m)	ZnS	2.026	0	Type-III	<i>g</i> -wave
1721	mp-554004	156 (<i>P</i> 3m1)	C _{3v} (3m)	ZnS	2.028	0	Type-III	<i>g</i> -wave
1722	mp-554115	156 (<i>P</i> 3m1)	C _{3v} (3m)	ZnS	2.018	0	Type-III	<i>g</i> -wave
1723	mp-554253	156 (<i>P</i> 3m1)	C _{3v} (3m)	ZnS	1.977	0	Type-III	<i>g</i> -wave
1724	mp-554503	156 (<i>P</i> 3m1)	C _{3v} (3m)	ZnS	2.019	0	Type-III	<i>g</i> -wave
1725	mp-554608	156 (<i>P</i> 3m1)	C _{3v} (3m)	ZnS	2.015	0	Type-III	<i>g</i> -wave
1726	mp-554630	156 (<i>P</i> 3m1)	C _{3v} (3m)	ZnS	1.982	0	Type-III	<i>g</i> -wave
1727	mp-554681	156 (<i>P</i> 3m1)	C _{3v} (3m)	ZnS	2.016	0	Type-III	<i>g</i> -wave
1728	mp-554713	156 (<i>P</i> 3m1)	C _{3v} (3m)	ZnS	2.034	0	Type-III	<i>g</i> -wave
1729	mp-554820	156 (<i>P</i> 3m1)	C _{3v} (3m)	ZnS	2.019	0	Type-III	<i>g</i> -wave
1730	mp-554829	156 (<i>P</i> 3m1)	C _{3v} (3m)	ZnS	2.022	0	Type-III	<i>g</i> -wave
1731	mp-554889	156 (<i>P</i> 3m1)	C _{3v} (3m)	ZnS	2.038	0	Type-III	<i>g</i> -wave
1732	mp-554918	156 (<i>P</i> 3m1)	C _{3v} (3m)	BaY ₆ Si ₃ B ₆ (O ₁₂ F) ₂	5.232	0	Type-III	<i>g</i> -wave
1733	mp-554961	156 (<i>P</i> 3m1)	C _{3v} (3m)	ZnS	2.018	0	Type-III	<i>g</i> -wave
1734	mp-555079	156 (<i>P</i> 3m1)	C _{3v} (3m)	ZnS	2.019	0	Type-III	<i>g</i> -wave
1735	mp-555151	156 (<i>P</i> 3m1)	C _{3v} (3m)	ZnS	2.023	0	Type-III	<i>g</i> -wave
1736	mp-555311	156 (<i>P</i> 3m1)	C _{3v} (3m)	ZnS	2.032	0	Type-III	<i>g</i> -wave
1737	mp-555628	156 (<i>P</i> 3m1)	C _{3v} (3m)	ZnS	2.036	0	Type-III	<i>g</i> -wave
1738	mp-555666	156 (<i>P</i> 3m1)	C _{3v} (3m)	ZnS	1.858	0	Type-III	<i>g</i> -wave
1739	mp-555773	156 (<i>P</i> 3m1)	C _{3v} (3m)	ZnS	2.028	0	Type-III	<i>g</i> -wave
1740	mp-555779	156 (<i>P</i> 3m1)	C _{3v} (3m)	ZnS	2.019	0	Type-III	<i>g</i> -wave
1741	mp-556000	156 (<i>P</i> 3m1)	C _{3v} (3m)	ZnS	2.025	0	Type-III	<i>g</i> -wave
1742	mp-556005	156 (<i>P</i> 3m1)	C _{3v} (3m)	ZnS	2.039	0	Type-III	<i>g</i> -wave
1743	mp-556152	156 (<i>P</i> 3m1)	C _{3v} (3m)	ZnS	2.026	0	Type-III	<i>g</i> -wave
1744	mp-556155	156 (<i>P</i> 3m1)	C _{3v} (3m)	ZnS	2.022	0	Type-III	<i>g</i> -wave
1745	mp-556207	156 (<i>P</i> 3m1)	C _{3v} (3m)	ZnS	2.028	0	Type-III	<i>g</i> -wave
1746	mp-556280	156 (<i>P</i> 3m1)	C _{3v} (3m)	ZnS	2.024	0	Type-III	<i>g</i> -wave
1747	mp-556363	156 (<i>P</i> 3m1)	C _{3v} (3m)	ZnS	2.028	0	Type-III	<i>g</i> -wave
1748	mp-556392	156 (<i>P</i> 3m1)	C _{3v} (3m)	ZnS	2.037	0	Type-III	<i>g</i> -wave
1749	mp-556395	156 (<i>P</i> 3m1)	C _{3v} (3m)	ZnS	1.956	0	Type-III	<i>g</i> -wave
1750	mp-556543	156 (<i>P</i> 3m1)	C _{3v} (3m)	ZnS	2.016	0	Type-III	<i>g</i> -wave
1751	mp-556716	156 (<i>P</i> 3m1)	C _{3v} (3m)	ZnS	1.213	0	Type-III	<i>g</i> -wave
1752	mp-556784	156 (<i>P</i> 3m1)	C _{3v} (3m)	ZnS	1.992	0	Type-III	<i>g</i> -wave
1753	mp-556815	156 (<i>P</i> 3m1)	C _{3v} (3m)	ZnS	2.042	0	Type-III	<i>g</i> -wave
1754	mp-556989	156 (<i>P</i> 3m1)	C _{3v} (3m)	ZnS	2.03	0	Type-III	<i>g</i> -wave

1755	mp-557009	156 ($P3m1$)	C_{3v} (3m)	ZnS	2.031	0	Type-III	g -wave
1756	mp-557026	156 ($P3m1$)	C_{3v} (3m)	ZnS	2.023	0	Type-III	g -wave
1757	mp-557175	156 ($P3m1$)	C_{3v} (3m)	ZnS	2.028	0	Type-III	g -wave
1758	mp-557308	156 ($P3m1$)	C_{3v} (3m)	ZnS	2.025	0	Type-III	g -wave
1759	mp-557346	156 ($P3m1$)	C_{3v} (3m)	ZnS	2.027	0	Type-III	g -wave
1760	mp-558632	156 ($P3m1$)	C_{3v} (3m)	KNaSO ₄	4.972	1	Type-III	g -wave
1761	mp-567178	156 ($P3m1$)	C_{3v} (3m)	PbI ₂	2.387	0	Type-III	g -wave
1762	mp-567199	156 ($P3m1$)	C_{3v} (3m)	PbI ₂	2.354	0	Type-III	g -wave
1763	mp-567246	156 ($P3m1$)	C_{3v} (3m)	PbI ₂	2.402	0	Type-III	g -wave
1764	mp-567713	156 ($P3m1$)	C_{3v} (3m)	Nb ₃ TeI ₇	0.48	0	Type-III	g -wave
1765	mp-568619	156 ($P3m1$)	C_{3v} (3m)	SiC	1.751	0	Type-III	g -wave
1766	mp-568656	156 ($P3m1$)	C_{3v} (3m)	SiC	2.005	0	Type-III	g -wave
1767	mp-568696	156 ($P3m1$)	C_{3v} (3m)	SiC	1.814	0	Type-III	g -wave
1768	mp-569510	156 ($P3m1$)	C_{3v} (3m)	CdI ₂	2.355	0	Type-III	g -wave
1769	mp-569611	156 ($P3m1$)	C_{3v} (3m)	CdI ₂	2.363	0	Type-III	g -wave
1770	mp-569666	156 ($P3m1$)	C_{3v} (3m)	CdI ₂	2.389	0	Type-III	g -wave
1771	mp-569722	156 ($P3m1$)	C_{3v} (3m)	CdI ₂	2.391	0	Type-III	g -wave
1772	mp-569964	156 ($P3m1$)	C_{3v} (3m)	CdI ₂	2.377	0	Type-III	g -wave
1773	mp-570019	156 ($P3m1$)	C_{3v} (3m)	CdI ₂	2.355	0	Type-III	g -wave
1774	mp-570082	156 ($P3m1$)	C_{3v} (3m)	CdI ₂	2.363	0	Type-III	g -wave
1775	mp-570127	156 ($P3m1$)	C_{3v} (3m)	CdI ₂	2.339	0	Type-III	g -wave
1776	mp-570136	156 ($P3m1$)	C_{3v} (3m)	CuI	1.462	0	Type-III	g -wave
1777	mp-570165	156 ($P3m1$)	C_{3v} (3m)	CdI ₂	2.373	0	Type-III	g -wave
1778	mp-570314	156 ($P3m1$)	C_{3v} (3m)	CdI ₂	2.361	0	Type-III	g -wave
1779	mp-570410	156 ($P3m1$)	C_{3v} (3m)	CdI ₂	2.363	0	Type-III	g -wave
1780	mp-570437	156 ($P3m1$)	C_{3v} (3m)	CdI ₂	2.338	0	Type-III	g -wave
1781	mp-570448	156 ($P3m1$)	C_{3v} (3m)	CdI ₂	2.395	0	Type-III	g -wave
1782	mp-570472	156 ($P3m1$)	C_{3v} (3m)	CdI ₂	2.233	0	Type-III	g -wave
1783	mp-570485	156 ($P3m1$)	C_{3v} (3m)	SrAlSiH	0.626	0	Type-III	g -wave
1784	mp-570492	156 ($P3m1$)	C_{3v} (3m)	CdI ₂	2.408	0	Type-III	g -wave
1785	mp-570511	156 ($P3m1$)	C_{3v} (3m)	CdI ₂	2.371	0	Type-III	g -wave
1786	mp-570552	156 ($P3m1$)	C_{3v} (3m)	CdI ₂	2.406	0	Type-III	g -wave
1787	mp-570559	156 ($P3m1$)	C_{3v} (3m)	CdI ₂	2.373	0	Type-III	g -wave
1788	mp-570610	156 ($P3m1$)	C_{3v} (3m)	CdI ₂	2.411	0	Type-III	g -wave
1789	mp-570613	156 ($P3m1$)	C_{3v} (3m)	CdI ₂	1.911	0	Type-III	g -wave
1790	mp-570671	156 ($P3m1$)	C_{3v} (3m)	CdI ₂	2.382	0	Type-III	g -wave
1791	mp-570695	156 ($P3m1$)	C_{3v} (3m)	CdI ₂	2.352	0	Type-III	g -wave
1792	mp-570781	156 ($P3m1$)	C_{3v} (3m)	CdI ₂	2.393	0	Type-III	g -wave
1793	mp-570791	156 ($P3m1$)	C_{3v} (3m)	SiC	1.97	0	Type-III	g -wave
1794	mp-570882	156 ($P3m1$)	C_{3v} (3m)	CdI ₂	2.37	0	Type-III	g -wave
1795	mp-570939	156 ($P3m1$)	C_{3v} (3m)	CdI ₂	2.4	0	Type-III	g -wave
1796	mp-570985	156 ($P3m1$)	C_{3v} (3m)	SiC	1.942	0	Type-III	g -wave
1797	mp-571037	156 ($P3m1$)	C_{3v} (3m)	CdI ₂	2.351	0	Type-III	g -wave
1798	mp-571091	156 ($P3m1$)	C_{3v} (3m)	CdI ₂	2.365	0	Type-III	g -wave
1799	mp-571093	156 ($P3m1$)	C_{3v} (3m)	BaAlSiH	0.709	0	Type-III	g -wave
1800	mp-571136	156 ($P3m1$)	C_{3v} (3m)	CdI ₂	2.364	0	Type-III	g -wave
1801	mp-571197	156 ($P3m1$)	C_{3v} (3m)	CdI ₂	2.379	0	Type-III	g -wave
1802	mp-571225	156 ($P3m1$)	C_{3v} (3m)	CdI ₂	2.402	0	Type-III	g -wave
1803	mp-571286	156 ($P3m1$)	C_{3v} (3m)	SiC	1.8	0	Type-III	g -wave
1804	mp-571298	156 ($P3m1$)	C_{3v} (3m)	SiC	1.636	0	Type-III	g -wave
1805	mp-571414	156 ($P3m1$)	C_{3v} (3m)	KNa(BH ₄) ₂	6.187	0	Type-III	g -wave
1806	mp-571514	156 ($P3m1$)	C_{3v} (3m)	CdI ₂	2.36	0	Type-III	g -wave
1807	mp-571516	156 ($P3m1$)	C_{3v} (3m)	CdI ₂	2.464	0	Type-III	g -wave
1808	mp-571519	156 ($P3m1$)	C_{3v} (3m)	CdI ₂	2.37	0	Type-III	g -wave
1809	mp-571535	156 ($P3m1$)	C_{3v} (3m)	CdI ₂	2.361	0	Type-III	g -wave
1810	mp-571538	156 ($P3m1$)	C_{3v} (3m)	CdI ₂	2.35	0	Type-III	g -wave
1811	mp-571539	156 ($P3m1$)	C_{3v} (3m)	CdI ₂	2.361	0	Type-III	g -wave
1812	mp-571559	156 ($P3m1$)	C_{3v} (3m)	CdI ₂	2.354	0	Type-III	g -wave
1813	mp-571568	156 ($P3m1$)	C_{3v} (3m)	CdI ₂	2.354	0	Type-III	g -wave

1814	mp-571569	156 (<i>P3m1</i>)	C_{3v} (3m)	CdI ₂	2.36	0	Type-III	<i>g-wave</i>
1815	mp-571578	156 (<i>P3m1</i>)	C_{3v} (3m)	CdI ₂	2.356	0	Type-III	<i>g-wave</i>
1816	mp-571579	156 (<i>P3m1</i>)	C_{3v} (3m)	CdI ₂	2.424	0	Type-III	<i>g-wave</i>
1817	mp-571583	156 (<i>P3m1</i>)	C_{3v} (3m)	CdI ₂	2.362	0	Type-III	<i>g-wave</i>
1818	mp-571592	156 (<i>P3m1</i>)	C_{3v} (3m)	CdI ₂	2.386	0	Type-III	<i>g-wave</i>
1819	mp-571595	156 (<i>P3m1</i>)	C_{3v} (3m)	CdI ₂	2.401	0	Type-III	<i>g-wave</i>
1820	mp-571603	156 (<i>P3m1</i>)	C_{3v} (3m)	CdI ₂	2.376	0	Type-III	<i>g-wave</i>
1821	mp-571605	156 (<i>P3m1</i>)	C_{3v} (3m)	CdI ₂	2.373	0	Type-III	<i>g-wave</i>
1822	mp-571607	156 (<i>P3m1</i>)	C_{3v} (3m)	CdI ₂	2.355	0	Type-III	<i>g-wave</i>
1823	mp-571613	156 (<i>P3m1</i>)	C_{3v} (3m)	CdI ₂	2.373	0	Type-III	<i>g-wave</i>
1824	mp-571615	156 (<i>P3m1</i>)	C_{3v} (3m)	CdI ₂	2.374	0	Type-III	<i>g-wave</i>
1825	mp-571646	156 (<i>P3m1</i>)	C_{3v} (3m)	CdI ₂	2.355	0	Type-III	<i>g-wave</i>
1826	mp-571654	156 (<i>P3m1</i>)	C_{3v} (3m)	CdI ₂	2.372	0	Type-III	<i>g-wave</i>
1827	mp-571667	156 (<i>P3m1</i>)	C_{3v} (3m)	CdI ₂	2.405	0	Type-III	<i>g-wave</i>
1828	mp-571668	156 (<i>P3m1</i>)	C_{3v} (3m)	CdI ₂	2.38	0	Type-III	<i>g-wave</i>
1829	mp-580202	156 (<i>P3m1</i>)	C_{3v} (3m)	PbI ₂	2.394	0	Type-III	<i>g-wave</i>
1830	mp-581425	156 (<i>P3m1</i>)	C_{3v} (3m)	ZnS	2.019	0	Type-III	<i>g-wave</i>
1831	mp-582034	156 (<i>P3m1</i>)	C_{3v} (3m)	SiC	1.689	0	Type-III	<i>g-wave</i>
1832	mp-582042	156 (<i>P3m1</i>)	C_{3v} (3m)	CdI ₂	2.407	0	Type-III	<i>g-wave</i>
1833	mp-582084	156 (<i>P3m1</i>)	C_{3v} (3m)	CdI ₂	2.374	0	Type-III	<i>g-wave</i>
1834	mp-582680	156 (<i>P3m1</i>)	C_{3v} (3m)	ZnS	1.985	0	Type-III	<i>g-wave</i>
1835	mp-624399	156 (<i>P3m1</i>)	C_{3v} (3m)	CdI ₂	2.341	0	Type-III	<i>g-wave</i>
1836	mp-624400	156 (<i>P3m1</i>)	C_{3v} (3m)	CdI ₂	2.332	0	Type-III	<i>g-wave</i>
1837	mp-624406	156 (<i>P3m1</i>)	C_{3v} (3m)	CdI ₂	2.334	0	Type-III	<i>g-wave</i>
1838	mp-624417	156 (<i>P3m1</i>)	C_{3v} (3m)	CdI ₂	2.337	0	Type-III	<i>g-wave</i>
1839	mp-624418	156 (<i>P3m1</i>)	C_{3v} (3m)	CdI ₂	2.33	0	Type-III	<i>g-wave</i>
1840	mp-627557	156 (<i>P3m1</i>)	C_{3v} (3m)	CdI ₂	2.355	0	Type-III	<i>g-wave</i>
1841	mp-647075	156 (<i>P3m1</i>)	C_{3v} (3m)	ZnS	1.999	0	Type-III	<i>g-wave</i>
1842	mp-647489	156 (<i>P3m1</i>)	C_{3v} (3m)	CdI ₂	2.355	0	Type-III	<i>g-wave</i>
1843	mp-669326	156 (<i>P3m1</i>)	C_{3v} (3m)	CdI ₂	2.366	0	Type-III	<i>g-wave</i>
1844	mp-669334	156 (<i>P3m1</i>)	C_{3v} (3m)	CdI ₂	2.341	0	Type-III	<i>g-wave</i>
1845	mp-669340	156 (<i>P3m1</i>)	C_{3v} (3m)	CdI ₂	2.329	0	Type-III	<i>g-wave</i>
1846	mp-669357	156 (<i>P3m1</i>)	C_{3v} (3m)	CdI ₂	2.339	0	Type-III	<i>g-wave</i>
1847	mp-669358	156 (<i>P3m1</i>)	C_{3v} (3m)	CdI ₂	2.361	0	Type-III	<i>g-wave</i>
1848	mp-669360	156 (<i>P3m1</i>)	C_{3v} (3m)	CdI ₂	2.339	0	Type-III	<i>g-wave</i>
1849	mp-680046	156 (<i>P3m1</i>)	C_{3v} (3m)	CdI ₂	2.337	0	Type-III	<i>g-wave</i>
1850	mp-680047	156 (<i>P3m1</i>)	C_{3v} (3m)	CdI ₂	2.338	0	Type-III	<i>g-wave</i>
1851	mp-680055	156 (<i>P3m1</i>)	C_{3v} (3m)	CdI ₂	2.35	0	Type-III	<i>g-wave</i>
1852	mp-680085	156 (<i>P3m1</i>)	C_{3v} (3m)	ZnS	2.015	0	Type-III	<i>g-wave</i>
1853	mp-680087	156 (<i>P3m1</i>)	C_{3v} (3m)	ZnS	2.02	0	Type-III	<i>g-wave</i>
1854	mp-680092	156 (<i>P3m1</i>)	C_{3v} (3m)	CdI ₂	2.331	0	Type-III	<i>g-wave</i>
1855	mp-680093	156 (<i>P3m1</i>)	C_{3v} (3m)	CdI ₂	2.335	0	Type-III	<i>g-wave</i>
1856	mp-680094	156 (<i>P3m1</i>)	C_{3v} (3m)	CdI ₂	2.335	0	Type-III	<i>g-wave</i>
1857	mp-680095	156 (<i>P3m1</i>)	C_{3v} (3m)	CdI ₂	2.325	0	Type-III	<i>g-wave</i>
1858	mp-680111	156 (<i>P3m1</i>)	C_{3v} (3m)	CdI ₂	2.367	0	Type-III	<i>g-wave</i>
1859	mp-680112	156 (<i>P3m1</i>)	C_{3v} (3m)	CdI ₂	2.332	0	Type-III	<i>g-wave</i>
1860	mp-680113	156 (<i>P3m1</i>)	C_{3v} (3m)	CdI ₂	2.328	0	Type-III	<i>g-wave</i>
1861	mp-680114	156 (<i>P3m1</i>)	C_{3v} (3m)	CdI ₂	2.341	0	Type-III	<i>g-wave</i>
1862	mp-680115	156 (<i>P3m1</i>)	C_{3v} (3m)	CdI ₂	2.344	0	Type-III	<i>g-wave</i>
1863	mp-680116	156 (<i>P3m1</i>)	C_{3v} (3m)	CdI ₂	2.335	0	Type-III	<i>g-wave</i>
1864	mp-680118	156 (<i>P3m1</i>)	C_{3v} (3m)	CdI ₂	2.332	0	Type-III	<i>g-wave</i>
1865	mp-680119	156 (<i>P3m1</i>)	C_{3v} (3m)	CdI ₂	2.337	0	Type-III	<i>g-wave</i>
1866	mp-680120	156 (<i>P3m1</i>)	C_{3v} (3m)	CdI ₂	2.34	0	Type-III	<i>g-wave</i>
1867	mp-680133	156 (<i>P3m1</i>)	C_{3v} (3m)	CdI ₂	2.34	0	Type-III	<i>g-wave</i>
1868	mp-680144	156 (<i>P3m1</i>)	C_{3v} (3m)	CdI ₂	2.325	0	Type-III	<i>g-wave</i>
1869	mp-680145	156 (<i>P3m1</i>)	C_{3v} (3m)	CdI ₂	2.319	0	Type-III	<i>g-wave</i>
1870	mp-680146	156 (<i>P3m1</i>)	C_{3v} (3m)	CdI ₂	2.335	0	Type-III	<i>g-wave</i>
1871	mp-680148	156 (<i>P3m1</i>)	C_{3v} (3m)	CdI ₂	2.321	0	Type-III	<i>g-wave</i>
1872	mp-680152	156 (<i>P3m1</i>)	C_{3v} (3m)	CdI ₂	2.357	0	Type-III	<i>g-wave</i>

1873	mp-680153	156 (<i>P3m1</i>)	C _{3v} (3m)	CdI ₂	2.345	0	Type-III	<i>g-wave</i>
1874	mp-680163	156 (<i>P3m1</i>)	C _{3v} (3m)	CdI ₂	2.36	0	Type-III	<i>g-wave</i>
1875	mp-680172	156 (<i>P3m1</i>)	C _{3v} (3m)	CdI ₂	2.34	0	Type-III	<i>g-wave</i>
1876	mp-680196	156 (<i>P3m1</i>)	C _{3v} (3m)	CdI ₂	2.357	0	Type-III	<i>g-wave</i>
1877	mp-680205	156 (<i>P3m1</i>)	C _{3v} (3m)	PbI ₂	2.354	0	Type-III	<i>g-wave</i>
1878	mp-684029	156 (<i>P3m1</i>)	C _{3v} (3m)	CdI ₂	2.347	0	Type-III	<i>g-wave</i>
1879	mp-6980	156 (<i>P3m1</i>)	C _{3v} (3m)	ScCuS ₂	0.871	0	Type-III	<i>g-wave</i>
1880	mp-978852	156 (<i>P3m1</i>)	C _{3v} (3m)	SrGaSnH	0.415	0	Type-III	<i>g-wave</i>
1881	mp-979137	156 (<i>P3m1</i>)	C _{3v} (3m)	SrGaSiH	0.417	0	Type-III	<i>g-wave</i>
1882	mp-980057	156 (<i>P3m1</i>)	C _{3v} (3m)	SrAlGeH	0.723	0	Type-III	<i>g-wave</i>
1883	mp-23764	157 (<i>P31m</i>)	C _{3v} (3m)	Mg ₃ Si ₂ H ₄ O ₉	4.245	0	Type-III	<i>g-wave</i>
1884	mp-30300	157 (<i>P31m</i>)	C _{3v} (3m)	Cs ₃ As ₅ O ₉	3.143	0	Type-III	<i>g-wave</i>
1885	mp-554285	157 (<i>P31m</i>)	C _{3v} (3m)	Na ₁₅ S ₅ Cl(O ₅ F) ₄	4.947	1	Type-III	<i>g-wave</i>
1886	mp-558828	157 (<i>P31m</i>)	C _{3v} (3m)	K ₃ Nb ₃ (BO ₆) ₂	2.338	0	Type-III	<i>g-wave</i>
1887	mp-680169	157 (<i>P31m</i>)	C _{3v} (3m)	Na ₂₁ S ₇ Cl(O ₁₄ F ₃) ₂	4.905	0	Type-III	<i>g-wave</i>
1888	mp-768770	157 (<i>P31m</i>)	C _{3v} (3m)	Mg(ReO ₄) ₂	3.874	0	Type-III	<i>g-wave</i>
1889	icsd-22093	158 (<i>P3c1</i>)	C _{3v} (3m)	RuCl ₃	0	0	Type-III	<i>g-wave</i>
1890	mp-558769	158 (<i>P3c1</i>)	C _{3v} (3m)	Na ₃ Li ₄ Th ₆ F ₃₁	6.309	1	Type-III	<i>g-wave</i>
1891	mp-16000	159 (<i>P31c</i>)	C _{3v} (3m)	Cs ₅ Ti ₆ AgSe ₂₇	0.59	0	Type-III	<i>g-wave</i>
1892	mp-16001	159 (<i>P31c</i>)	C _{3v} (3m)	Rb ₅ Ti ₆ AgSe ₂₇	0.562	0	Type-III	<i>g-wave</i>
1893	mp-16804	159 (<i>P31c</i>)	C _{3v} (3m)	LiCaPO ₄	5.18	1	Type-III	<i>g-wave</i>
1894	mp-2245	159 (<i>P31c</i>)	C _{3v} (3m)	Si ₃ N ₄	4.655	0	Type-III	<i>g-wave</i>
1895	mp-26725	159 (<i>P31c</i>)	C _{3v} (3m)	LiSnPO ₄	2.557	1	Type-III	<i>g-wave</i>
1896	mp-560944	159 (<i>P31c</i>)	C _{3v} (3m)	Cs ₄ Ba(PO ₃) ₆	5.106	0	Type-III	<i>g-wave</i>
1897	mp-569806	159 (<i>P31c</i>)	C _{3v} (3m)	K ₅ Na(Ti ₂ Se ₉) ₃	0.823	0	Type-III	<i>g-wave</i>
1898	mp-570021	159 (<i>P31c</i>)	C _{3v} (3m)	Ti ₆ Tl ₅ AgSe ₂₇	0.665	0	Type-III	<i>g-wave</i>
1899	mp-581922	159 (<i>P31c</i>)	C _{3v} (3m)	CsMo ₃ Br ₃ Cl ₄	2.586	0	Type-III	<i>g-wave</i>
1900	mp-672289	159 (<i>P31c</i>)	C _{3v} (3m)	Ge ₃ N ₄	2.064	0	Type-III	<i>g-wave</i>
1901	mp-6783	159 (<i>P31c</i>)	C _{3v} (3m)	NaLiSO ₄	5.538	1	Type-III	<i>g-wave</i>
1902	mp-6800	159 (<i>P31c</i>)	C _{3v} (3m)	KLiSO ₄	5.325	0	Type-III	<i>g-wave</i>
1903	mp-680015	159 (<i>P31c</i>)	C _{3v} (3m)	Re ₃ (SeBr) ₇	1.315	0	Type-III	<i>g-wave</i>
1904	mp-707874	159 (<i>P31c</i>)	C _{3v} (3m)	Ba ₇ Cu ₃ H ₁₇	1.459	0	Type-III	<i>g-wave</i>
1905	mp-9480	159 (<i>P31c</i>)	C _{3v} (3m)	KAlSiO ₄	4.501	0	Type-III	<i>g-wave</i>
1906	icsd-24315	160 (<i>R3m</i>)	C _{3v} (3m)	TaSe ₂	0	0	Type-III	<i>g-wave</i>
1907	icsd-38401	160 (<i>R3m</i>)	C _{3v} (3m)	MoS ₂	1.21	0	Type-III	<i>g-wave</i>
1908	icsd-151599	160 (<i>R3m</i>)	C _{3v} (3m)	NiS	0	1	Type-III	<i>g-wave</i>
1909	icsd-651952	160 (<i>R3m</i>)	C _{3v} (3m)	TaSe ₂	0	0	Type-III	<i>g-wave</i>
1910	mp-11342	160 (<i>R3m</i>)	C _{3v} (3m)	GaSe	1.223	0	Type-III	<i>g-wave</i>
1911	mp-11713	160 (<i>R3m</i>)	C _{3v} (3m)	SiC	1.954	1	Type-III	<i>g-wave</i>
1912	mp-1434	160 (<i>R3m</i>)	C _{3v} (3m)	MoS ₂	1.204	0	Type-III	<i>g-wave</i>
1913	mp-18377	160 (<i>R3m</i>)	C _{3v} (3m)	ZnS	2.046	0	Type-III	<i>g-wave</i>
1914	mp-22691	160 (<i>R3m</i>)	C _{3v} (3m)	InSe	1.786	0	Type-III	<i>g-wave</i>
1915	mp-22958	160 (<i>R3m</i>)	C _{3v} (3m)	KBrO ₃	3.857	0	Type-III	<i>g-wave</i>
1916	mp-22981	160 (<i>R3m</i>)	C _{3v} (3m)	TlIO ₃	2.763	0	Type-III	<i>g-wave</i>
1917	mp-22988	160 (<i>R3m</i>)	C _{3v} (3m)	CsGeCl ₃	2.153	0	Type-III	<i>g-wave</i>
1918	mp-23011	160 (<i>R3m</i>)	C _{3v} (3m)	RbClO ₃	5.329	0	Type-III	<i>g-wave</i>
1919	mp-23162	160 (<i>R3m</i>)	C _{3v} (3m)	ZrCl ₂	0.848	0	Type-III	<i>g-wave</i>
1920	mp-23612	160 (<i>R3m</i>)	C _{3v} (3m)	K ₃ B ₆ BrO ₁₀	5.212	0	Type-III	<i>g-wave</i>
1921	mp-23837	160 (<i>R3m</i>)	C _{3v} (3m)	NdH ₃ (CO ₂) ₃	4.182	1	Type-III	<i>g-wave</i>
1922	mp-27193	160 (<i>R3m</i>)	C _{3v} (3m)	RbIO ₃	2.837	0	Type-III	<i>g-wave</i>
1923	mp-27594	160 (<i>R3m</i>)	C _{3v} (3m)	As ₄ (Pb ₃ S ₅) ₃	1.576	0	Type-III	<i>g-wave</i>
1924	mp-28377	160 (<i>R3m</i>)	C _{3v} (3m)	CsGeI ₃	0.991	0	Type-III	<i>g-wave</i>
1925	mp-28781	160 (<i>R3m</i>)	C _{3v} (3m)	PrZr ₃ F ₁₅	5.763	0	Type-III	<i>g-wave</i>
1926	mp-28872	160 (<i>R3m</i>)	C _{3v} (3m)	RbBrO ₃	3.995	0	Type-III	<i>g-wave</i>
1927	mp-28873	160 (<i>R3m</i>)	C _{3v} (3m)	CsBrO ₃	4.168	0	Type-III	<i>g-wave</i>
1928	mp-29738	160 (<i>R3m</i>)	C _{3v} (3m)	TlClO ₃	4.348	0	Type-III	<i>g-wave</i>
1929	mp-29798	160 (<i>R3m</i>)	C _{3v} (3m)	TlBrO ₃	3.51	0	Type-III	<i>g-wave</i>
1930	mp-30925	160 (<i>R3m</i>)	C _{3v} (3m)	La(NO ₂) ₃	2.205	0	Type-III	<i>g-wave</i>
1931	mp-3107	160 (<i>R3m</i>)	C _{3v} (3m)	Ga ₃ PO ₇	3.131	0	Type-III	<i>g-wave</i>

1932	mp-32750	160 (<i>R3m</i>)	C _{3v} (3m)	CuI	1.164	0	Type-III	<i>g-wave</i>
1933	mp-33302	160 (<i>R3m</i>)	C _{3v} (3m)	MgAl ₂ O ₄	4.266	1	Type-III	<i>g-wave</i>
1934	mp-34078	160 (<i>R3m</i>)	C _{3v} (3m)	H ₃ ClO	5.386	0	Type-III	<i>g-wave</i>
1935	mp-34330	160 (<i>R3m</i>)	C _{3v} (3m)	MgAl ₂ O ₄	4.357	1	Type-III	<i>g-wave</i>
1936	mp-36582	160 (<i>R3m</i>)	C _{3v} (3m)	NaHS	3.147	0	Type-III	<i>g-wave</i>
1937	mp-38011	160 (<i>R3m</i>)	C _{3v} (3m)	KHS	3.225	0	Type-III	<i>g-wave</i>
1938	mp-39215	160 (<i>R3m</i>)	C _{3v} (3m)	Zn ₃ GaB ₆ PO ₁₂	4.071	0	Type-III	<i>g-wave</i>
1939	mp-4182	160 (<i>R3m</i>)	C _{3v} (3m)	CrAgS ₂	0.729	1	Type-III	<i>g-wave</i>
1940	mp-42458	160 (<i>R3m</i>)	C _{3v} (3m)	SrAl ₃ P ₂ (HO ₂) ₇	4.988	1	Type-III	<i>g-wave</i>
1941	mp-4559	160 (<i>R3m</i>)	C _{3v} (3m)	BaCO ₃	4.364	0	Type-III	<i>g-wave</i>
1942	mp-5020	160 (<i>R3m</i>)	C _{3v} (3m)	BaTiO ₃	2.509	0	Type-III	<i>g-wave</i>
1943	mp-530164	160 (<i>R3m</i>)	C _{3v} (3m)	MgAl ₂ O ₄	4.555	1	Type-III	<i>g-wave</i>
1944	mp-531530	160 (<i>R3m</i>)	C _{3v} (3m)	MgAl ₂ O ₄	4.203	1	Type-III	<i>g-wave</i>
1945	mp-531793	160 (<i>R3m</i>)	C _{3v} (3m)	MgAl ₂ O ₄	4.021	1	Type-III	<i>g-wave</i>
1946	mp-543011	160 (<i>R3m</i>)	C _{3v} (3m)	ZnS	2.04	0	Type-III	<i>g-wave</i>
1947	mp-546500	160 (<i>R3m</i>)	C _{3v} (3m)	NaCNO	4.432	0	Type-III	<i>g-wave</i>
1948	mp-550506	160 (<i>R3m</i>)	C _{3v} (3m)	KClO ₃	5.073	0	Type-III	<i>g-wave</i>
1949	mp-552729	160 (<i>R3m</i>)	C _{3v} (3m)	KIO ₃	2.568	1	Type-III	<i>g-wave</i>
1950	mp-554405	160 (<i>R3m</i>)	C _{3v} (3m)	ZnS	2.072	0	Type-III	<i>g-wave</i>
1951	mp-555410	160 (<i>R3m</i>)	C _{3v} (3m)	ZnS	2.064	1	Type-III	<i>g-wave</i>
1952	mp-555763	160 (<i>R3m</i>)	C _{3v} (3m)	ZnS	2.064	0	Type-III	<i>g-wave</i>
1953	mp-555858	160 (<i>R3m</i>)	C _{3v} (3m)	ZnS	2.019	0	Type-III	<i>g-wave</i>
1954	mp-556105	160 (<i>R3m</i>)	C _{3v} (3m)	ZnS	2.011	0	Type-III	<i>g-wave</i>
1955	mp-556468	160 (<i>R3m</i>)	C _{3v} (3m)	ZnS	2.033	0	Type-III	<i>g-wave</i>
1956	mp-556576	160 (<i>R3m</i>)	C _{3v} (3m)	ZnS	2.089	0	Type-III	<i>g-wave</i>
1957	mp-557151	160 (<i>R3m</i>)	C _{3v} (3m)	ZnS	2.057	0	Type-III	<i>g-wave</i>
1958	mp-558273	160 (<i>R3m</i>)	C _{3v} (3m)	Ca ₃ SiO ₅	3.278	0	Type-III	<i>g-wave</i>
1959	mp-558608	160 (<i>R3m</i>)	C _{3v} (3m)	Nb ₂ PbO ₆	2.461	1	Type-III	<i>g-wave</i>
1960	mp-560831	160 (<i>R3m</i>)	C _{3v} (3m)	Na ₆ P ₄ Pb ₃ S ₁₆	2.326	0	Type-III	<i>g-wave</i>
1961	mp-569978	160 (<i>R3m</i>)	C _{3v} (3m)	Na ₂ Ti ₃ Cl ₈	0.434	0	Type-III	<i>g-wave</i>
1962	mp-570641	160 (<i>R3m</i>)	C _{3v} (3m)	SiC	1.7	0	Type-III	<i>g-wave</i>
1963	mp-570690	160 (<i>R3m</i>)	C _{3v} (3m)	SiC	1.664	0	Type-III	<i>g-wave</i>
1964	mp-570804	160 (<i>R3m</i>)	C _{3v} (3m)	SiC	1.843	0	Type-III	<i>g-wave</i>
1965	mp-574663	160 (<i>R3m</i>)	C _{3v} (3m)	CdI ₂	2.43	0	Type-III	<i>g-wave</i>
1966	mp-581258	160 (<i>R3m</i>)	C _{3v} (3m)	ZnS	2.038	0	Type-III	<i>g-wave</i>
1967	mp-581476	160 (<i>R3m</i>)	C _{3v} (3m)	ZnS	2.024	0	Type-III	<i>g-wave</i>
1968	mp-581601	160 (<i>R3m</i>)	C _{3v} (3m)	ZnS	2.026	0	Type-III	<i>g-wave</i>
1969	mp-625051	160 (<i>R3m</i>)	C _{3v} (3m)	NaHO	3.355	1	Type-III	<i>g-wave</i>
1970	mp-625509	160 (<i>R3m</i>)	C _{3v} (3m)	H ₃ BrO	4.418	0	Type-III	<i>g-wave</i>
1971	mp-627401	160 (<i>R3m</i>)	C _{3v} (3m)	CdI ₂	2.357	0	Type-III	<i>g-wave</i>
1972	mp-6296	160 (<i>R3m</i>)	C _{3v} (3m)	K ₆ Cd ₄ Sn ₃ Se ₁₃	1.406	0	Type-III	<i>g-wave</i>
1973	mp-703273	160 (<i>R3m</i>)	C _{3v} (3m)	KBaLiZnF ₆	4.994	1	Type-III	<i>g-wave</i>
1974	mp-7375	160 (<i>R3m</i>)	C _{3v} (3m)	KNbO ₃	2.293	0	Type-III	<i>g-wave</i>
1975	mp-753846	160 (<i>R3m</i>)	C _{3v} (3m)	Mg(GaO ₂) ₂	2.358	1	Type-III	<i>g-wave</i>
1976	mp-756142	160 (<i>R3m</i>)	C _{3v} (3m)	La ₂ Th ₅ O ₁₃	2.425	0	Type-III	<i>g-wave</i>
1977	mp-756637	160 (<i>R3m</i>)	C _{3v} (3m)	Ba ₃ GeO ₅	2.596	1	Type-III	<i>g-wave</i>
1978	mp-757911	160 (<i>R3m</i>)	C _{3v} (3m)	MgAl ₁₀ O ₁₆	4.407	1	Type-III	<i>g-wave</i>
1979	mp-7581	160 (<i>R3m</i>)	C _{3v} (3m)	MoSe ₂	1.362	0	Type-III	<i>g-wave</i>
1980	mp-759230	160 (<i>R3m</i>)	C _{3v} (3m)	NaAl ₁₁ O ₁₇	4.402	1	Type-III	<i>g-wave</i>
1981	mp-760386	160 (<i>R3m</i>)	C _{3v} (3m)	CsClO ₃	5.466	0	Type-III	<i>g-wave</i>
1982	mp-760755	160 (<i>R3m</i>)	C _{3v} (3m)	KAl ₁₁ O ₁₇	4.616	1	Type-III	<i>g-wave</i>
1983	mp-760795	160 (<i>R3m</i>)	C _{3v} (3m)	Al ₁₀ ZnO ₁₆	4.241	1	Type-III	<i>g-wave</i>
1984	mp-7684	160 (<i>R3m</i>)	C _{3v} (3m)	Tl ₃ AsSe ₃	0.881	0	Type-III	<i>g-wave</i>
1985	mp-770959	160 (<i>R3m</i>)	C _{3v} (3m)	Ba ₃ GeO ₅	2.69	0	Type-III	<i>g-wave</i>
1986	mp-8196	160 (<i>R3m</i>)	C _{3v} (3m)	AgNO ₃	1.72	1	Type-III	<i>g-wave</i>
1987	mp-8393	160 (<i>R3m</i>)	C _{3v} (3m)	Tl ₃ SbS ₃	1.592	0	Type-III	<i>g-wave</i>
1988	mp-8612	160 (<i>R3m</i>)	C _{3v} (3m)	Sb ₂ TeSe ₂	0.486	0	Type-III	<i>g-wave</i>
1989	mp-938	160 (<i>R3m</i>)	C _{3v} (3m)	GeTe	0.556	0	Type-III	<i>g-wave</i>
1990	mp-9813	160 (<i>R3m</i>)	C _{3v} (3m)	WS ₂	1.841	0	Type-III	<i>g-wave</i>

1991	mp-989601	160 (<i>R3m</i>)	C _{3v} (3m)	LaWN ₃	0.706	1	Type-III	<i>g-wave</i>
1992	mp-9947	160 (<i>R3m</i>)	C _{3v} (3m)	SiC	1.849	0	Type-III	<i>g-wave</i>
1993	mp-13334	161 (<i>R3c</i>)	C _{3v} (3m)	ZnSnO ₃	1.081	0	Type-III	<i>g-wave</i>
1994	mp-17864	161 (<i>R3c</i>)	C _{3v} (3m)	BaNa(B ₃ O ₅) ₃	5.501	1	Type-III	<i>g-wave</i>
1995	mp-18495	161 (<i>R3c</i>)	C _{3v} (3m)	SrLi(B ₃ O ₅) ₃	5.648	1	Type-III	<i>g-wave</i>
1996	mp-20282	161 (<i>R3c</i>)	C _{3v} (3m)	CsPbF ₃	3.337	0	Type-III	<i>g-wave</i>
1997	mp-23609	161 (<i>R3c</i>)	C _{3v} (3m)	Zn ₃ B ₇ ClO ₁₃	4.485	0	Type-III	<i>g-wave</i>
1998	mp-23736	161 (<i>R3c</i>)	C _{3v} (3m)	LiMgH ₃	4.049	0	Type-III	<i>g-wave</i>
1999	mp-28680	161 (<i>R3c</i>)	C _{3v} (3m)	KGaBr ₄	3.577	0	Type-III	<i>g-wave</i>
2000	mp-31135	161 (<i>R3c</i>)	C _{3v} (3m)	Si ₁₉ Te ₈	0.887	0	Type-III	<i>g-wave</i>
2001	mp-3666	161 (<i>R3c</i>)	C _{3v} (3m)	LiTaO ₃	3.7	0	Type-III	<i>g-wave</i>
2002	mp-3731	161 (<i>R3c</i>)	C _{3v} (3m)	LiNbO ₃	3.336	0	Type-III	<i>g-wave</i>
2003	mp-39140	161 (<i>R3c</i>)	C _{3v} (3m)	Na ₄ Al ₃ Si ₃ HO ₁₃	4.056	0	Type-III	<i>g-wave</i>
2004	mp-4360	161 (<i>R3c</i>)	C _{3v} (3m)	NaCdF ₃	3.482	0	Type-III	<i>g-wave</i>
2005	mp-4431	161 (<i>R3c</i>)	C _{3v} (3m)	Ag ₃ AsS ₃	1.177	0	Type-III	<i>g-wave</i>
2006	mp-4514	161 (<i>R3c</i>)	C _{3v} (3m)	NaNbO ₃	2.787	0	Type-III	<i>g-wave</i>
2007	mp-4515	161 (<i>R3c</i>)	C _{3v} (3m)	Ag ₃ SbS ₃	0.952	0	Type-III	<i>g-wave</i>
2008	mp-542269	161 (<i>R3c</i>)	C _{3v} (3m)	Pr ₄ (GeS ₄) ₃	1.996	0	Type-III	<i>g-wave</i>
2009	mp-542464	161 (<i>R3c</i>)	C _{3v} (3m)	Ga ₂ H ₆ (SeO ₄) ₃	3.965	1	Type-III	<i>g-wave</i>
2010	mp-543040	161 (<i>R3c</i>)	C _{3v} (3m)	Ga ₂ Te ₃ (HO ₂) ₆	3.763	1	Type-III	<i>g-wave</i>
2011	mp-555472	161 (<i>R3c</i>)	C _{3v} (3m)	Na ₄ Zr ₂ (SiO ₄) ₃	4.389	1	Type-III	<i>g-wave</i>
2012	mp-555843	161 (<i>R3c</i>)	C _{3v} (3m)	Ag ₃ AsS ₃	1.699	0	Type-III	<i>g-wave</i>
2013	mp-558862	161 (<i>R3c</i>)	C _{3v} (3m)	NaGe ₄ (PO ₄) ₃	4.384	1	Type-III	<i>g-wave</i>
2014	mp-560086	161 (<i>R3c</i>)	C _{3v} (3m)	Nd ₄ (GeS ₄) ₃	1.995	0	Type-III	<i>g-wave</i>
2015	mp-569854	161 (<i>R3c</i>)	C _{3v} (3m)	Ga ₃ Bi ₅ Cl ₁₂	1.813	0	Type-III	<i>g-wave</i>
2016	mp-5730	161 (<i>R3c</i>)	C _{3v} (3m)	Ba(BO ₂) ₂	4.785	0	Type-III	<i>g-wave</i>
2017	mp-6226	161 (<i>R3c</i>)	C _{3v} (3m)	NaSn ₄ (PO ₄) ₃	3.741	1	Type-III	<i>g-wave</i>
2018	mp-650031	161 (<i>R3c</i>)	C _{3v} (3m)	La ₄ (GeS ₄) ₃	1.936	0	Type-III	<i>g-wave</i>
2019	mp-730190	161 (<i>R3c</i>)	C _{3v} (3m)	H ₄ NF	6.18	0	Type-III	<i>g-wave</i>
2020	mp-753677	161 (<i>R3c</i>)	C _{3v} (3m)	Li ₃ BiS ₃	2.558	0	Type-III	<i>g-wave</i>
2021	mp-754009	161 (<i>R3c</i>)	C _{3v} (3m)	ScBiO ₃	3.083	0	Type-III	<i>g-wave</i>
2022	mp-754323	161 (<i>R3c</i>)	C _{3v} (3m)	TmBiO ₃	3.113	0	Type-III	<i>g-wave</i>
2023	mp-754943	161 (<i>R3c</i>)	C _{3v} (3m)	ErBiO ₃	3.114	0	Type-III	<i>g-wave</i>
2024	mp-768221	161 (<i>R3c</i>)	C _{3v} (3m)	YBiO ₃	3.075	0	Type-III	<i>g-wave</i>
2025	mp-768310	161 (<i>R3c</i>)	C _{3v} (3m)	LaBiO ₃	3.07	0	Type-III	<i>g-wave</i>
2026	mp-780362	161 (<i>R3c</i>)	C _{3v} (3m)	La(ClO ₄) ₃	4.49	1	Type-III	<i>g-wave</i>
2027	mp-8704	161 (<i>R3c</i>)	C _{3v} (3m)	K ₃ SbSe ₄	1.432	0	Type-III	<i>g-wave</i>
2028	mp-9467	161 (<i>R3c</i>)	C _{3v} (3m)	NaCa ₉ Mg(PO ₄) ₇	5.172	0	Type-III	<i>g-wave</i>
2029	mp-984755	161 (<i>R3c</i>)	C _{3v} (3m)	Nb ₄ Ag ₂ O ₁₁	2.372	1	Type-III	<i>g-wave</i>
2030	mp-989524	161 (<i>R3c</i>)	C _{3v} (3m)	LaWN ₃	1.21	0	Type-III	<i>g-wave</i>
2031	mp-989552	161 (<i>R3c</i>)	C _{3v} (3m)	LaMoN ₃	1.151	0	Type-III	<i>g-wave</i>
2032	mp-2654	169 (<i>P6</i> ₁)	C ₆ (6)	Al ₂ S ₃	2.817	0	Type-II	<i>s-wave</i>
2033	mp-504482	169 (<i>P6</i> ₁)	C ₆ (6)	AlInS ₃	2.081	0	Type-II	<i>s-wave</i>
2034	mp-504951	169 (<i>P6</i> ₁)	C ₆ (6)	InGaS ₃	2.094	0	Type-II	<i>s-wave</i>
2035	mp-504952	169 (<i>P6</i> ₁)	C ₆ (6)	InGaSe ₃	1.317	0	Type-II	<i>s-wave</i>
2036	mp-612740	169 (<i>P6</i> ₁)	C ₆ (6)	In ₂ Se ₃	0.99	0	Type-II	<i>s-wave</i>
2037	mp-862787	169 (<i>P6</i> ₁)	C ₆ (6)	AllnSe ₃	1.633	0	Type-II	<i>s-wave</i>
2038	mp-676934	172 (<i>P6</i> ₄)	C ₆ (6)	KCaNd(PO ₄) ₂	4.743	1	Type-II	<i>s-wave</i>
2039	mp-12485	173 (<i>P6</i> ₃)	C ₆ (6)	NaSm ₃ SiS ₇	2.017	0	Type-II	<i>s-wave</i>
2040	mp-13335	173 (<i>P6</i> ₃)	C ₆ (6)	Cd(BO ₂) ₂	3.343	0	Type-II	<i>s-wave</i>
2041	mp-15573	173 (<i>P6</i> ₃)	C ₆ (6)	Tl ₃ AsO ₄	2.584	0	Type-II	<i>s-wave</i>
2042	mp-17155	173 (<i>P6</i> ₃)	C ₆ (6)	La ₃ AgSnSe ₇	1.3	0	Type-II	<i>s-wave</i>
2043	mp-17243	173 (<i>P6</i> ₃)	C ₆ (6)	Pr ₃ CuSnSe ₇	1.217	0	Type-II	<i>s-wave</i>
2044	mp-17389	173 (<i>P6</i> ₃)	C ₆ (6)	Pr ₃ SiAgSe ₇	1.442	0	Type-II	<i>s-wave</i>
2045	mp-17486	173 (<i>P6</i> ₃)	C ₆ (6)	Ho ₃ CuSiS ₇	1.822	0	Type-II	<i>s-wave</i>
2046	mp-17719	173 (<i>P6</i> ₃)	C ₆ (6)	La ₃ SiAgS ₇	1.966	0	Type-II	<i>s-wave</i>
2047	mp-17747	173 (<i>P6</i> ₃)	C ₆ (6)	Y ₃ CuSnS ₇	1.489	0	Type-II	<i>s-wave</i>
2048	mp-17827	173 (<i>P6</i> ₃)	C ₆ (6)	Nd ₃ SiAgSe ₇	1.446	0	Type-II	<i>s-wave</i>
2049	mp-17916	173 (<i>P6</i> ₃)	C ₆ (6)	Y ₃ CuGeSe ₇	1.118	0	Type-II	<i>s-wave</i>

2050	mp-18126	173 (P_{6_3})	C ₆ (6)	Tb ₃ CuSnSe ₇	1.018	0	Type-II	s-wave
2051	mp-18303	173 (P_{6_3})	C ₆ (6)	Nd ₃ CuSnSe ₇	1.193	0	Type-II	s-wave
2052	mp-22955	173 (P_{6_3})	C ₆ (6)	LiIO ₃	3.686	0	Type-II	s-wave
2053	mp-23400	173 (P_{6_3})	C ₆ (6)	In(VO ₃) ₃	3.411	0	Type-II	s-wave
2054	mp-27573	173 (P_{6_3})	C ₆ (6)	NaSb ₃ F ₁₀	4.968	1	Type-II	s-wave
2055	mp-4202	173 (P_{6_3})	C ₆ (6)	BaAl ₂ O ₄	4.103	0	Type-II	s-wave
2056	mp-504891	173 (P_{6_3})	C ₆ (6)	La ₃ MnGaS ₇	0.45	0	Type-II	s-wave
2057	mp-505558	173 (P_{6_3})	C ₆ (6)	Dy ₃ CuGeSe ₇	1.128	0	Type-II	s-wave
2058	mp-510566	173 (P_{6_3})	C ₆ (6)	La ₃ CuSnS ₇	1.869	0	Type-II	s-wave
2059	mp-542888	173 (P_{6_3})	C ₆ (6)	La ₃ AgSnS ₇	1.952	0	Type-II	s-wave
2060	mp-5492	173 (P_{6_3})	C ₆ (6)	SrAl ₂ O ₄	4.056	1	Type-II	s-wave
2061	mp-554097	173 (P_{6_3})	C ₆ (6)	Sm ₃ CuSiS ₇	1.656	0	Type-II	s-wave
2062	mp-554150	173 (P_{6_3})	C ₆ (6)	Nd ₃ CuGeS ₇	1.676	0	Type-II	s-wave
2063	mp-554781	173 (P_{6_3})	C ₆ (6)	Tb ₃ CuSnS ₇	1.555	0	Type-II	s-wave
2064	mp-554947	173 (P_{6_3})	C ₆ (6)	NaSiBO ₄	5.414	0	Type-II	s-wave
2065	mp-555081	173 (P_{6_3})	C ₆ (6)	Er ₃ CuGeS ₇	1.747	0	Type-II	s-wave
2066	mp-555421	173 (P_{6_3})	C ₆ (6)	Na ₃ TmSi ₂ O ₇	3.96	0	Type-II	s-wave
2067	mp-555893	173 (P_{6_3})	C ₆ (6)	Pr ₃ CuSiS ₇	1.298	0	Type-II	s-wave
2068	mp-555903	173 (P_{6_3})	C ₆ (6)	Al(VO ₃) ₃	3.347	0	Type-II	s-wave
2069	mp-555978	173 (P_{6_3})	C ₆ (6)	Sm ₃ CuGeS ₇	1.774	0	Type-II	s-wave
2070	mp-556740	173 (P_{6_3})	C ₆ (6)	NaSiBO ₄	5.503	0	Type-II	s-wave
2071	mp-556781	173 (P_{6_3})	C ₆ (6)	Y ₃ CuGeS ₇	1.788	0	Type-II	s-wave
2072	mp-556962	173 (P_{6_3})	C ₆ (6)	Pr ₃ CuGeS ₇	1.66	0	Type-II	s-wave
2073	mp-556975	173 (P_{6_3})	C ₆ (6)	Nd ₃ CuSiS ₇	1.636	0	Type-II	s-wave
2074	mp-557517	173 (P_{6_3})	C ₆ (6)	Tb ₃ CuGeS ₇	1.807	0	Type-II	s-wave
2075	mp-557998	173 (P_{6_3})	C ₆ (6)	Dy ₃ CuSiS ₇	1.801	0	Type-II	s-wave
2076	mp-558042	173 (P_{6_3})	C ₆ (6)	Sm ₃ CuSnS ₇	1.704	0	Type-II	s-wave
2077	mp-558980	173 (P_{6_3})	C ₆ (6)	Er ₃ CuSiS ₇	1.876	0	Type-II	s-wave
2078	mp-559390	173 (P_{6_3})	C ₆ (6)	CaAl ₂ O ₄	4.191	0	Type-II	s-wave
2079	mp-559901	173 (P_{6_3})	C ₆ (6)	KNa ₃ Al ₄ (SiO ₄) ₄	4.506	1	Type-II	s-wave
2080	mp-560014	173 (P_{6_3})	C ₆ (6)	Pr ₃ CuSnS ₇	1.778	0	Type-II	s-wave
2081	mp-560186	173 (P_{6_3})	C ₆ (6)	BaMgSiO ₄	4.114	1	Type-II	s-wave
2082	mp-560300	173 (P_{6_3})	C ₆ (6)	Nd ₃ CuSnS ₇	1.759	0	Type-II	s-wave
2083	mp-560501	173 (P_{6_3})	C ₆ (6)	Tb ₃ CuSiS ₇	1.733	0	Type-II	s-wave
2084	mp-560632	173 (P_{6_3})	C ₆ (6)	NaGaSiO ₄	3.822	0	Type-II	s-wave
2085	mp-561104	173 (P_{6_3})	C ₆ (6)	Ga(VO ₃) ₃	3.319	0	Type-II	s-wave
2086	mp-561173	173 (P_{6_3})	C ₆ (6)	Y ₃ CuSiS ₇	1.737	0	Type-II	s-wave
2087	mp-561305	173 (P_{6_3})	C ₆ (6)	BaZnSiO ₄	3.586	1	Type-II	s-wave
2088	mp-561499	173 (P_{6_3})	C ₆ (6)	Dy ₃ CuSnS ₇	1.491	0	Type-II	s-wave
2089	mp-567428	173 (P_{6_3})	C ₆ (6)	Tb ₃ CuGeSe ₇	1.126	0	Type-II	s-wave
2090	mp-567753	173 (P_{6_3})	C ₆ (6)	La ₃ CuSnSe ₇	1.209	0	Type-II	s-wave
2091	mp-568638	173 (P_{6_3})	C ₆ (6)	Y ₃ CuSiSe ₇	1.51	0	Type-II	s-wave
2092	mp-568779	173 (P_{6_3})	C ₆ (6)	Tb ₃ CuSiSe ₇	1.488	0	Type-II	s-wave
2093	mp-568801	173 (P_{6_3})	C ₆ (6)	Pr ₃ CuSiSe ₇	1.363	0	Type-II	s-wave
2094	mp-568954	173 (P_{6_3})	C ₆ (6)	Nd ₃ CuGeSe ₇	1.223	0	Type-II	s-wave
2095	mp-569557	173 (P_{6_3})	C ₆ (6)	Dy ₃ CuSiSe ₇	1.52	0	Type-II	s-wave
2096	mp-570045	173 (P_{6_3})	C ₆ (6)	Sm ₃ CuSiSe ₇	1.437	0	Type-II	s-wave
2097	mp-570226	173 (P_{6_3})	C ₆ (6)	Sm ₃ CuGeSe ₇	1.161	0	Type-II	s-wave
2098	mp-570594	173 (P_{6_3})	C ₆ (6)	Sm ₃ CuSnSe ₇	1.157	0	Type-II	s-wave
2099	mp-570709	173 (P_{6_3})	C ₆ (6)	Tl ₃ PO ₄	2.641	0	Type-II	s-wave
2100	mp-571347	173 (P_{6_3})	C ₆ (6)	Pr ₃ CuGeSe ₇	1.219	0	Type-II	s-wave
2101	mp-571468	173 (P_{6_3})	C ₆ (6)	Ho ₃ CuSiSe ₇	1.349	0	Type-II	s-wave
2102	mp-582767	173 (P_{6_3})	C ₆ (6)	La ₃ CuGeS ₇	1.796	0	Type-II	s-wave
2103	mp-601241	173 (P_{6_3})	C ₆ (6)	Na ₃ YH ₁₂ (CO ₅) ₃	4.597	1	Type-II	s-wave
2104	mp-617632	173 (P_{6_3})	C ₆ (6)	La ₃ AgGeS ₇	1.976	0	Type-II	s-wave
2105	mp-6179	173 (P_{6_3})	C ₆ (6)	KLiSO ₄	5.322	0	Type-II	s-wave
2106	mp-6253	173 (P_{6_3})	C ₆ (6)	KLiBeF ₄	6.853	0	Type-II	s-wave
2107	mp-625677	173 (P_{6_3})	C ₆ (6)	Y(HO) ₃	3.909	1	Type-II	s-wave
2108	mp-625733	173 (P_{6_3})	C ₆ (6)	La(HO) ₃	4.02	0	Type-II	s-wave

2109	mp-632684	173 (P_{6_3})	C ₆ (6)	NaPH ₃ NO ₃	5.109	0	Type-II	<i>s</i> -wave
2110	mp-641534	173 (P_{6_3})	C ₆ (6)	Nd ₃ CuSiSe ₇	1.341	0	Type-II	<i>s</i> -wave
2111	mp-645364	173 (P_{6_3})	C ₆ (6)	Sr(PN ₂) ₂	4.271	0	Type-II	<i>s</i> -wave
2112	mp-6485	173 (P_{6_3})	C ₆ (6)	La ₃ SiAgSe ₇	1.653	0	Type-II	<i>s</i> -wave
2113	mp-6566	173 (P_{6_3})	C ₆ (6)	NaZnAsO ₄	2.79	0	Type-II	<i>s</i> -wave
2114	mp-673101	173 (P_{6_3})	C ₆ (6)	LiSn ₄ (PO ₄) ₃	3.262	1	Type-II	<i>s</i> -wave
2115	mp-680374	173 (P_{6_3})	C ₆ (6)	KAlSiO ₄	4.7	0	Type-II	<i>s</i> -wave
2116	mp-757722	173 (P_{6_3})	C ₆ (6)	BaZnGeO ₄	2.896	1	Type-II	<i>s</i> -wave
2117	mp-757777	173 (P_{6_3})	C ₆ (6)	LiSiBi ₃ O ₇	2.976	1	Type-II	<i>s</i> -wave
2118	mp-759031	173 (P_{6_3})	C ₆ (6)	Bi ₁₉ (O ₉ F) ₃	2.01	0	Type-II	<i>s</i> -wave
2119	mp-8355	173 (P_{6_3})	C ₆ (6)	KAlSiO ₄	4.502	0	Type-II	<i>s</i> -wave
2120	mp-862792	173 (P_{6_3})	C ₆ (6)	Pr ₃ AgGeS ₇	1.829	0	Type-II	<i>s</i> -wave
2121	mp-864666	173 (P_{6_3})	C ₆ (6)	Nd ₃ SiAgS ₇	1.771	0	Type-II	<i>s</i> -wave
2122	mp-866696	173 (P_{6_3})	C ₆ (6)	La ₃ ScBeS ₇	0.934	0	Type-II	<i>s</i> -wave
2123	mp-867322	173 (P_{6_3})	C ₆ (6)	Pr ₃ SiAgS ₇	1.83	0	Type-II	<i>s</i> -wave
2124	mp-867929	173 (P_{6_3})	C ₆ (6)	Sm ₃ SiAgS ₇	1.879	0	Type-II	<i>s</i> -wave
2125	mp-23547	174 (P_6)	C _{3h} (6)	Ba ₇ (ClF ₆) ₂	6.048	0	Type-III	<i>g</i> -wave
2126	mp-23827	174 (P_6)	C _{3h} (6)	Sr ₇ (H ₆ Cl) ₂	3.862	0	Type-III	<i>g</i> -wave
2127	mp-23828	174 (P_6)	C _{3h} (6)	Sr ₇ (H ₆ Br) ₂	3.703	0	Type-III	<i>g</i> -wave
2128	mp-29760	174 (P_6)	C _{3h} (6)	Ca ₁₀ P ₆ O ₂₅	3.148	1	Type-III	<i>g</i> -wave
2129	mp-29927	174 (P_6)	C _{3h} (6)	Pb ₇ (BrF ₆) ₂	4.063	1	Type-III	<i>g</i> -wave
2130	mp-556063	174 (P_6)	C _{3h} (6)	PrP ₃ (HO ₂) ₆	5.193	1	Type-III	<i>g</i> -wave
2131	mp-557375	174 (P_6)	C _{3h} (6)	NaLiCO ₃	4.458	0	Type-III	<i>g</i> -wave
2132	mp-557667	174 (P_6)	C _{3h} (6)	Ge ₃ Pb ₃ O ₁₁	2.411	0	Type-III	<i>g</i> -wave
2133	mp-559533	174 (P_6)	C _{3h} (6)	NaLiCO ₃	4.463	0	Type-III	<i>g</i> -wave
2134	mp-6126	174 (P_6)	C _{3h} (6)	LiCdBO ₃	2.116	0	Type-III	<i>g</i> -wave
2135	mp-754929	174 (P_6)	C _{3h} (6)	Ga ₃ NO ₃	1.005	1	Type-III	<i>g</i> -wave
2136	mp-984055	174 (P_6)	C _{3h} (6)	Ca ₇ (H ₆ Cl) ₂	3.695	0	Type-III	<i>g</i> -wave
2137	mp-23032	178 (P_{6_122})	D ₆ (622)	CsCuCl ₃	0.549	0	Type-II	<i>s</i> -wave
2138	mp-559569	178 (P_{6_122})	D ₆ (622)	YSiNO ₂	4.216	1	Type-II	<i>s</i> -wave
2139	mp-942	178 (P_{6_122})	D ₆ (622)	AuF ₃	1.554	0	Type-II	<i>s</i> -wave
2140	mp-554243	179 (P_{6_522})	D ₆ (622)	SiO ₂	5.627	1	Type-II	<i>s</i> -wave
2141	icsd-638946	180 (P_{6_222})	D ₆ (622)	HfSn ₂	0	0	Type-II	<i>s</i> -wave
2142	mp-14190	180 (P_{6_222})	D ₆ (622)	NdPO ₄	5.309	0	Type-II	<i>s</i> -wave
2143	mp-14399	180 (P_{6_222})	D ₆ (622)	LiAlSiO ₄	4.849	0	Type-II	<i>s</i> -wave
2144	mp-23110	180 (P_{6_222})	D ₆ (622)	NaHg ₂ IO ₂	1.388	0	Type-II	<i>s</i> -wave
2145	mp-3082	180 (P_{6_222})	D ₆ (622)	CaSO ₄	5.684	0	Type-II	<i>s</i> -wave
2146	mp-554515	180 (P_{6_222})	D ₆ (622)	KScH ₄ (C ₂ O ₅) ₂	3.274	0	Type-II	<i>s</i> -wave
2147	mp-557319	180 (P_{6_222})	D ₆ (622)	InH ₈ C ₄ NO ₁₀	3.567	0	Type-II	<i>s</i> -wave
2148	mp-558118	180 (P_{6_222})	D ₆ (622)	BeF ₂	8.087	1	Type-II	<i>s</i> -wave
2149	mp-558713	180 (P_{6_222})	D ₆ (622)	LiAlSiO ₄	4.694	0	Type-II	<i>s</i> -wave
2150	mp-642740	180 (P_{6_222})	D ₆ (622)	CsLi(H ₂ N) ₂	1.997	1	Type-II	<i>s</i> -wave
2151	mp-6922	180 (P_{6_222})	D ₆ (622)	SiO ₂	5.531	1	Type-II	<i>s</i> -wave
2152	mp-8133	180 (P_{6_222})	D ₆ (622)	LaPO ₄	4.897	0	Type-II	<i>s</i> -wave
2153	mp-10851	181 (P_{6_422})	D ₆ (622)	SiO ₂	5.532	1	Type-II	<i>s</i> -wave
2154	mp-556372	181 (P_{6_422})	D ₆ (622)	CaSO ₄	5.694	0	Type-II	<i>s</i> -wave
2155	mp-560151	181 (P_{6_422})	D ₆ (622)	AlPO ₄	5.485	1	Type-II	<i>s</i> -wave
2156	mp-6326	181 (P_{6_422})	D ₆ (622)	LiAlSiO ₄	4.848	0	Type-II	<i>s</i> -wave
2157	mp-6327	181 (P_{6_422})	D ₆ (622)	LiAlSiO ₄	4.799	0	Type-II	<i>s</i> -wave
2158	mp-941221	181 (P_{6_422})	D ₆ (622)	Li(BH) ₅	4.995	0	Type-II	<i>s</i> -wave
2159	mp-3079	182 (P_{6_322})	D ₆ (622)	CaTa ₄ O ₁₁	3.544	0	Type-II	<i>s</i> -wave
2160	mp-3828	182 (P_{6_322})	D ₆ (622)	BaAl ₂ O ₄	3.945	1	Type-II	<i>s</i> -wave
2161	mp-541462	182 (P_{6_322})	D ₆ (622)	SrTa ₄ O ₁₁	3.523	0	Type-II	<i>s</i> -wave
2162	mp-554199	182 (P_{6_322})	D ₆ (622)	RbSnIO ₆	2.166	0	Type-II	<i>s</i> -wave
2163	mp-559091	182 (P_{6_322})	D ₆ (622)	SiO ₂	5.438	1	Type-II	<i>s</i> -wave
2164	mp-616564	182 (P_{6_322})	D ₆ (622)	RbPbIO ₆	1.375	0	Type-II	<i>s</i> -wave
2165	mp-769399	182 (P_{6_322})	D ₆ (622)	BaTa ₄ O ₁₁	3.484	1	Type-II	<i>s</i> -wave
2166	mp-867839	182 (P_{6_322})	D ₆ (622)	Ta ₇ BiO ₁₉	3.033	1	Type-II	<i>s</i> -wave
2167	mp-14384	185 (P_{6_3cm})	C _{6v} (6mm)	Ba ₃ Ho(BO ₃) ₃	3.822	0	Type-III	<i>i</i> -wave

2168	mp-14385	185 ($P6_3cm$)	C_{6v} (6mm)	$\text{Ba}_3\text{Tm}(\text{BO}_3)_3$	3.844	0	Type-III	<i>i-wave</i>
2169	mp-14386	185 ($P6_3cm$)	C_{6v} (6mm)	$\text{Ba}_3\text{Lu}(\text{BO}_3)_3$	3.858	0	Type-III	<i>i-wave</i>
2170	mp-14972	185 ($P6_3cm$)	C_{6v} (6mm)	$\text{Ba}_3\text{Sc}(\text{BO}_3)_3$	3.474	0	Type-III	<i>i-wave</i>
2171	mp-17853	185 ($P6_3cm$)	C_{6v} (6mm)	YGaO_3	2.904	0	Type-III	<i>i-wave</i>
2172	mp-18511	185 ($P6_3cm$)	C_{6v} (6mm)	NdF_3	7.803	1	Type-III	<i>i-wave</i>
2173	mp-24097	185 ($P6_3cm$)	C_{6v} (6mm)	$\text{Mg}_3\text{Si}_2\text{H}_4\text{O}_9$	4.248	0	Type-III	<i>i-wave</i>
2174	mp-27366	185 ($P6_3cm$)	C_{6v} (6mm)	KNiCl_3	0.702	0	Type-III	<i>i-wave</i>
2175	mp-28548	185 ($P6_3cm$)	C_{6v} (6mm)	Li_8GeO_6	3.488	0	Type-III	<i>i-wave</i>
2176	mp-28549	185 ($P6_3cm$)	C_{6v} (6mm)	Li_8SiO_6	4.45	0	Type-III	<i>i-wave</i>
2177	mp-29314	185 ($P6_3cm$)	C_{6v} (6mm)	RbVBr_3	0.605	1	Type-III	<i>i-wave</i>
2178	mp-334	185 ($P6_3cm$)	C_{6v} (6mm)	LaF_3	6.045	0	Type-III	<i>i-wave</i>
2179	mp-504607	185 ($P6_3cm$)	C_{6v} (6mm)	YInO_3	2.052	0	Type-III	<i>i-wave</i>
2180	mp-556103	185 ($P6_3cm$)	C_{6v} (6mm)	$\text{Cs}_3\text{Ga}_2\text{F}_9$	5.746	0	Type-III	<i>i-wave</i>
2181	mp-556647	185 ($P6_3cm$)	C_{6v} (6mm)	$\text{Ba}_5\text{Re}_3\text{ClO}_{15}$	2.531	0	Type-III	<i>i-wave</i>
2182	mp-556721	185 ($P6_3cm$)	C_{6v} (6mm)	$\text{Ba}_5\text{Re}_3\text{BrO}_{15}$	2.54	0	Type-III	<i>i-wave</i>
2183	mp-558310	185 ($P6_3cm$)	C_{6v} (6mm)	$\text{BaLi}_2\text{SiO}_4$	4.39	0	Type-III	<i>i-wave</i>
2184	mp-570311	185 ($P6_3cm$)	C_{6v} (6mm)	$\text{K}_4\text{Sr}_2\text{SnAs}_4$	0.538	0	Type-III	<i>i-wave</i>
2185	mp-6310	185 ($P6_3cm$)	C_{6v} (6mm)	$\text{Ba}_3\text{Y}(\text{BO}_3)_3$	3.815	0	Type-III	<i>i-wave</i>
2186	mp-703459	185 ($P6_3cm$)	C_{6v} (6mm)	H_2O	5.529	1	Type-III	<i>i-wave</i>
2187	mp-753546	185 ($P6_3cm$)	C_{6v} (6mm)	Li_8TiS_6	2.289	0	Type-III	<i>i-wave</i>
2188	mp-761931	185 ($P6_3cm$)	C_{6v} (6mm)	Na_8SnO_6	1.055	0	Type-III	<i>i-wave</i>
2189	mp-768149	185 ($P6_3cm$)	C_{6v} (6mm)	DyInO_3	1.987	0	Type-III	<i>i-wave</i>
2190	mp-768267	185 ($P6_3cm$)	C_{6v} (6mm)	HoInO_3	1.968	0	Type-III	<i>i-wave</i>
2191	mp-768469	185 ($P6_3cm$)	C_{6v} (6mm)	TmGaO_3	2.922	0	Type-III	<i>i-wave</i>
2192	mp-768505	185 ($P6_3cm$)	C_{6v} (6mm)	LuGaO_3	2.883	0	Type-III	<i>i-wave</i>
2193	mp-769007	185 ($P6_3cm$)	C_{6v} (6mm)	YScO_3	3.141	0	Type-III	<i>i-wave</i>
2194	mp-769015	185 ($P6_3cm$)	C_{6v} (6mm)	DyGaO_3	2.866	0	Type-III	<i>i-wave</i>
2195	mp-769045	185 ($P6_3cm$)	C_{6v} (6mm)	HoGaO_3	2.872	0	Type-III	<i>i-wave</i>
2196	mp-769079	185 ($P6_3cm$)	C_{6v} (6mm)	ScGaO_3	3.171	0	Type-III	<i>i-wave</i>
2197	mp-769294	185 ($P6_3cm$)	C_{6v} (6mm)	Rb_8SnO_6	1.071	0	Type-III	<i>i-wave</i>
2198	mp-772180	185 ($P6_3cm$)	C_{6v} (6mm)	LuScO_3	3.086	0	Type-III	<i>i-wave</i>
2199	mp-772217	185 ($P6_3cm$)	C_{6v} (6mm)	ErInO_3	1.956	0	Type-III	<i>i-wave</i>
2200	mp-772521	185 ($P6_3cm$)	C_{6v} (6mm)	Li_8TiO_6	3.992	0	Type-III	<i>i-wave</i>
2201	icsd-24923	186 ($P6_3mc$)	C_{6v} (6mm)	PtO_2	1.3984	0	Type-III	<i>i-wave</i>
2202	icsd-41482	186 ($P6_3mc$)	C_{6v} (6mm)	AlN	4.2156	0	Type-III	<i>i-wave</i>
2203	icsd-43595	186 ($P6_3mc$)	C_{6v} (6mm)	ZnSe	1.2037	0	Type-III	<i>i-wave</i>
2204	icsd-56553	186 ($P6_3mc$)	C_{6v} (6mm)	AgI	1.2912	0	Type-III	<i>i-wave</i>
2205	icsd-62727	186 ($P6_3mc$)	C_{6v} (6mm)	BeO	7.6003	0	Type-III	<i>i-wave</i>
2206	icsd-154187	186 ($P6_3mc$)	C_{6v} (6mm)	CdS	1.2923	0	Type-III	<i>i-wave</i>
2207	icsd-620415	186 ($P6_3mc$)	C_{6v} (6mm)	CdSe	0.5929	0	Type-III	<i>i-wave</i>
2208	mp-10096	186 ($P6_3mc$)	C_{6v} (6mm)	$\text{Na}_3\text{Sr}_3\text{GaP}_4$	0.747	0	Type-III	<i>i-wave</i>
2209	mp-10097	186 ($P6_3mc$)	C_{6v} (6mm)	$\text{Na}_3\text{Sr}_3\text{GaAs}_4$	0.438	0	Type-III	<i>i-wave</i>
2210	mp-10281	186 ($P6_3mc$)	C_{6v} (6mm)	ZnS	2.047	0	Type-III	<i>i-wave</i>
2211	mp-1039	186 ($P6_3mc$)	C_{6v} (6mm)	MgTe	2.361	0	Type-III	<i>i-wave</i>
2212	mp-1070	186 ($P6_3mc$)	C_{6v} (6mm)	CdSe	0.572	0	Type-III	<i>i-wave</i>
2213	mp-11670	186 ($P6_3mc$)	C_{6v} (6mm)	BaYSi_4N_7	2.733	0	Type-III	<i>i-wave</i>
2214	mp-11714	186 ($P6_3mc$)	C_{6v} (6mm)	SiC	2.223	0	Type-III	<i>i-wave</i>
2215	mp-12171	186 ($P6_3mc$)	C_{6v} (6mm)	K_6MgO_4	1.678	0	Type-III	<i>i-wave</i>
2216	mp-12779	186 ($P6_3mc$)	C_{6v} (6mm)	CdTe	0.619	0	Type-III	<i>i-wave</i>
2217	mp-13002	186 ($P6_3mc$)	C_{6v} (6mm)	K_2SiF_6	7.189	0	Type-III	<i>i-wave</i>
2218	mp-13954	186 ($P6_3mc$)	C_{6v} (6mm)	Rb_2GeF_6	5.884	0	Type-III	<i>i-wave</i>
2219	mp-14168	186 ($P6_3mc$)	C_{6v} (6mm)	K_2GeF_6	5.9	0	Type-III	<i>i-wave</i>
2220	mp-14780	186 ($P6_3mc$)	C_{6v} (6mm)	Na_6MnSe_4	1.133	0	Type-III	<i>i-wave</i>
2221	mp-14782	186 ($P6_3mc$)	C_{6v} (6mm)	Na_6MnTe_4	0	0	Type-III	<i>i-wave</i>
2222	mp-15572	186 ($P6_3mc$)	C_{6v} (6mm)	$\text{Na}_3\text{Ca}_3\text{AlAs}_4$	0.943	0	Type-III	<i>i-wave</i>
2223	mp-16792	186 ($P6_3mc$)	C_{6v} (6mm)	$\text{Ba}_4\text{LiTa}_3\text{O}_{12}$	3.113	0	Type-III	<i>i-wave</i>
2224	mp-17161	186 ($P6_3mc$)	C_{6v} (6mm)	K_6CdO_4	1.582	0	Type-III	<i>i-wave</i>
2225	mp-17313	186 ($P6_3mc$)	C_{6v} (6mm)	$\text{Mg}_3\text{BeAl}_8\text{O}_{16}$	5.175	1	Type-III	<i>i-wave</i>
2226	mp-17698	186 ($P6_3mc$)	C_{6v} (6mm)	K_6CdTe_4	1.661	0	Type-III	<i>i-wave</i>

2227	mp-18246	186 ($P6_3mc$)	C_{6v} (6mm)	K_6MnTe_4	1.423	0	Type-III	<i>i-wave</i>
2228	mp-18274	186 ($P6_3mc$)	C_{6v} (6mm)	$Ba_4LiNb_3O_{12}$	2.58	1	Type-III	<i>i-wave</i>
2229	mp-18481	186 ($P6_3mc$)	C_{6v} (6mm)	K_6MnSe_4	1.232	0	Type-III	<i>i-wave</i>
2230	mp-2133	186 ($P6_3mc$)	C_{6v} (6mm)	ZnO	0.723	0	Type-III	<i>i-wave</i>
2231	mp-22894	186 ($P6_3mc$)	C_{6v} (6mm)	AgI	1.388	0	Type-III	<i>i-wave</i>
2232	mp-23063	186 ($P6_3mc$)	C_{6v} (6mm)	Ba_4Cl_6O	4.365	0	Type-III	<i>i-wave</i>
2233	mp-23321	186 ($P6_3mc$)	C_{6v} (6mm)	Sr_4Cl_6O	4.559	0	Type-III	<i>i-wave</i>
2234	mp-23326	186 ($P6_3mc$)	C_{6v} (6mm)	Ca_4Cl_6O	5.224	0	Type-III	<i>i-wave</i>
2235	mp-23794	186 ($P6_3mc$)	C_{6v} (6mm)	H_4NF	5.959	0	Type-III	<i>i-wave</i>
2236	mp-23797	186 ($P6_3mc$)	C_{6v} (6mm)	LiH_6ClO_7	5.294	1	Type-III	<i>i-wave</i>
2237	mp-23985	186 ($P6_3mc$)	C_{6v} (6mm)	LiH_6BrO_7	3.123	0	Type-III	<i>i-wave</i>
2238	mp-24066	186 ($P6_3mc$)	C_{6v} (6mm)	$SrHClO$	4.98	0	Type-III	<i>i-wave</i>
2239	mp-2542	186 ($P6_3mc$)	C_{6v} (6mm)	BeO	7.464	0	Type-III	<i>i-wave</i>
2240	mp-27934	186 ($P6_3mc$)	C_{6v} (6mm)	$CdBr_2$	2.938	0	Type-III	<i>i-wave</i>
2241	mp-28248	186 ($P6_3mc$)	C_{6v} (6mm)	CdI_2	2.366	0	Type-III	<i>i-wave</i>
2242	mp-28944	186 ($P6_3mc$)	C_{6v} (6mm)	BiTeCl	1.514	0	Type-III	<i>i-wave</i>
2243	mp-28987	186 ($P6_3mc$)	C_{6v} (6mm)	$NaPt_2Se_3$	0.99	0	Type-III	<i>i-wave</i>
2244	mp-29116	186 ($P6_3mc$)	C_{6v} (6mm)	Ta_3SeI_7	0.573	0	Type-III	<i>i-wave</i>
2245	mp-29117	186 ($P6_3mc$)	C_{6v} (6mm)	Ta_3TeI_7	0.55	0	Type-III	<i>i-wave</i>
2246	mp-29529	186 ($P6_3mc$)	C_{6v} (6mm)	$NaSnP$	0.583	0	Type-III	<i>i-wave</i>
2247	mp-29689	186 ($P6_3mc$)	C_{6v} (6mm)	Nb_3TeI_7	0.514	0	Type-III	<i>i-wave</i>
2248	mp-29909	186 ($P6_3mc$)	C_{6v} (6mm)	Ba_4I_6O	3.979	0	Type-III	<i>i-wave</i>
2249	mp-29910	186 ($P6_3mc$)	C_{6v} (6mm)	Sr_4I_6O	3.586	0	Type-III	<i>i-wave</i>
2250	mp-37657	186 ($P6_3mc$)	C_{6v} (6mm)	Ca_3SiO_5	2.915	0	Type-III	<i>i-wave</i>
2251	mp-380	186 ($P6_3mc$)	C_{6v} (6mm)	ZnSe	1.2	0	Type-III	<i>i-wave</i>
2252	mp-5055	186 ($P6_3mc$)	C_{6v} (6mm)	Na_6MnS_4	1.4	0	Type-III	<i>i-wave</i>
2253	mp-5114	186 ($P6_3mc$)	C_{6v} (6mm)	K_6HgS_4	1.716	0	Type-III	<i>i-wave</i>
2254	mp-545974	186 ($P6_3mc$)	C_{6v} (6mm)	$AlPO_4$	5.323	1	Type-III	<i>i-wave</i>
2255	mp-554018	186 ($P6_3mc$)	C_{6v} (6mm)	$Mg_3BeAl_8O_{16}$	5.24	1	Type-III	<i>i-wave</i>
2256	mp-554294	186 ($P6_3mc$)	C_{6v} (6mm)	$Na_7SnS_3(O_4F)_3$	4.991	1	Type-III	<i>i-wave</i>
2257	mp-554364	186 ($P6_3mc$)	C_{6v} (6mm)	$MgBeAl_4O_8$	5.528	1	Type-III	<i>i-wave</i>
2258	mp-554479	186 ($P6_3mc$)	C_{6v} (6mm)	$Ba_3BP_2O_7$	3.337	1	Type-III	<i>i-wave</i>
2259	mp-554831	186 ($P6_3mc$)	C_{6v} (6mm)	Yb_4Cl_6O	5.176	0	Type-III	<i>i-wave</i>
2260	mp-555217	186 ($P6_3mc$)	C_{6v} (6mm)	$Dy_3Se_4O_{12}F$	3.741	0	Type-III	<i>i-wave</i>
2261	mp-555218	186 ($P6_3mc$)	C_{6v} (6mm)	Ba_4Br_6O	4.165	0	Type-III	<i>i-wave</i>
2262	mp-555932	186 ($P6_3mc$)	C_{6v} (6mm)	$RbEr_3F_{10}$	7.282	0	Type-III	<i>i-wave</i>
2263	mp-556049	186 ($P6_3mc$)	C_{6v} (6mm)	Sr_4Br_6O	4.216	0	Type-III	<i>i-wave</i>
2264	mp-556100	186 ($P6_3mc$)	C_{6v} (6mm)	$Si(Sn_3O_4)_2$	1.9	1	Type-III	<i>i-wave</i>
2265	mp-556562	186 ($P6_3mc$)	C_{6v} (6mm)	$LiAsH_6(OF_2)_3$	3.784	1	Type-III	<i>i-wave</i>
2266	mp-560588	186 ($P6_3mc$)	C_{6v} (6mm)	ZnS	2.07	0	Type-III	<i>i-wave</i>
2267	mp-560725	186 ($P6_3mc$)	C_{6v} (6mm)	ZnS	2.022	0	Type-III	<i>i-wave</i>
2268	mp-561118	186 ($P6_3mc$)	C_{6v} (6mm)	ZnS	2.034	0	Type-III	<i>i-wave</i>
2269	mp-561124	186 ($P6_3mc$)	C_{6v} (6mm)	$Ho_3Se_4O_{12}F$	3.709	0	Type-III	<i>i-wave</i>
2270	mp-561196	186 ($P6_3mc$)	C_{6v} (6mm)	ZnS	2.027	0	Type-III	<i>i-wave</i>
2271	mp-561286	186 ($P6_3mc$)	C_{6v} (6mm)	ZnS	2.022	0	Type-III	<i>i-wave</i>
2272	mp-561681	186 ($P6_3mc$)	C_{6v} (6mm)	$CsSO_3$	5.111	0	Type-III	<i>i-wave</i>
2273	mp-567290	186 ($P6_3mc$)	C_{6v} (6mm)	LaN	1.117	0	Type-III	<i>i-wave</i>
2274	mp-567503	186 ($P6_3mc$)	C_{6v} (6mm)	PbI_2	2.446	0	Type-III	<i>i-wave</i>
2275	mp-567505	186 ($P6_3mc$)	C_{6v} (6mm)	SiC	1.777	0	Type-III	<i>i-wave</i>
2276	mp-567542	186 ($P6_3mc$)	C_{6v} (6mm)	PbI_2	2.383	0	Type-III	<i>i-wave</i>
2277	mp-567551	186 ($P6_3mc$)	C_{6v} (6mm)	SiC	1.971	0	Type-III	<i>i-wave</i>
2278	mp-567949	186 ($P6_3mc$)	C_{6v} (6mm)	Hg_3AsSe_4Br	1.303	0	Type-III	<i>i-wave</i>
2279	mp-568263	186 ($P6_3mc$)	C_{6v} (6mm)	GaSe	1.212	0	Type-III	<i>i-wave</i>
2280	mp-568916	186 ($P6_3mc$)	C_{6v} (6mm)	K_6InTe_4Cl	1.95	0	Type-III	<i>i-wave</i>
2281	mp-569346	186 ($P6_3mc$)	C_{6v} (6mm)	CuI	1.212	0	Type-III	<i>i-wave</i>
2282	mp-569994	186 ($P6_3mc$)	C_{6v} (6mm)	CdI_2	2.362	0	Type-III	<i>i-wave</i>
2283	mp-570054	186 ($P6_3mc$)	C_{6v} (6mm)	CdI_2	2.354	0	Type-III	<i>i-wave</i>
2284	mp-570079	186 ($P6_3mc$)	C_{6v} (6mm)	Al_5C_3N	0.837	0	Type-III	<i>i-wave</i>
2285	mp-570084	186 ($P6_3mc$)	C_{6v} (6mm)	Hg_3AsSe_4I	1.221	0	Type-III	<i>i-wave</i>

2286	mp-570089	186 ($P_{63}mc$)	C_{6v} (6mm)	CdI ₂	2.395	0	Type-III	<i>i</i> -wave
2287	mp-570935	186 ($P_{63}mc$)	C_{6v} (6mm)	LiI	4.382	0	Type-III	<i>i</i> -wave
2288	mp-580941	186 ($P_{63}mc$)	C_{6v} (6mm)	AgI	1.376	0	Type-III	<i>i</i> -wave
2289	mp-626161	186 ($P_{63}mc$)	C_{6v} (6mm)	Al ₅ HO ₈	4.766	0	Type-III	<i>i</i> -wave
2290	mp-642725	186 ($P_{63}mc$)	C_{6v} (6mm)	CaHClO	5.329	0	Type-III	<i>i</i> -wave
2291	mp-644222	186 ($P_{63}mc$)	C_{6v} (6mm)	CdHClO	2.466	0	Type-III	<i>i</i> -wave
2292	mp-644223	186 ($P_{63}mc$)	C_{6v} (6mm)	LiBH ₄	6.685	1	Type-III	<i>i</i> -wave
2293	mp-6606	186 ($P_{63}mc$)	C_{6v} (6mm)	SrYSi ₄ N ₇	2.752	1	Type-III	<i>i</i> -wave
2294	mp-661	186 ($P_{63}mc$)	C_{6v} (6mm)	AlN	4.047	0	Type-III	<i>i</i> -wave
2295	mp-6709	186 ($P_{63}mc$)	C_{6v} (6mm)	Ca ₃ La ₃ (BO ₃) ₅	4.137	0	Type-III	<i>i</i> -wave
2296	mp-672	186 ($P_{63}mc$)	C_{6v} (6mm)	CdS	1.125	0	Type-III	<i>i</i> -wave
2297	mp-7140	186 ($P_{63}mc$)	C_{6v} (6mm)	SiC	2.303	0	Type-III	<i>i</i> -wave
2298	mp-740711	186 ($P_{63}mc$)	C_{6v} (6mm)	Cs ₃ B ₆ H ₁₂ Se ₄ Br	4.493	0	Type-III	<i>i</i> -wave
2299	mp-753816	186 ($P_{63}mc$)	C_{6v} (6mm)	Na ₆ MgO ₄	2.099	0	Type-III	<i>i</i> -wave
2300	mp-755546	186 ($P_{63}mc$)	C_{6v} (6mm)	Na ₆ BeO ₄	1.985	0	Type-III	<i>i</i> -wave
2301	mp-757333	186 ($P_{63}mc$)	C_{6v} (6mm)	Al ₁₂ PbO ₁₉	4.519	1	Type-III	<i>i</i> -wave
2302	mp-7631	186 ($P_{63}mc$)	C_{6v} (6mm)	SiC	2.023	0	Type-III	<i>i</i> -wave
2303	mp-7664	186 ($P_{63}mc$)	C_{6v} (6mm)	Na ₆ ZnO ₄	1.534	0	Type-III	<i>i</i> -wave
2304	mp-7868	186 ($P_{63}mc$)	C_{6v} (6mm)	PtO ₂	1.536	0	Type-III	<i>i</i> -wave
2305	mp-804	186 ($P_{63}mc$)	C_{6v} (6mm)	GaN	1.726	0	Type-III	<i>i</i> -wave
2306	mp-8075	186 ($P_{63}mc$)	C_{6v} (6mm)	NaBe ₄ SbO ₇	3.386	0	Type-III	<i>i</i> -wave
2307	mp-8389	186 ($P_{63}mc$)	C_{6v} (6mm)	Na ₆ ZnS ₄	2.158	0	Type-III	<i>i</i> -wave
2308	mp-850213	186 ($P_{63}mc$)	C_{6v} (6mm)	Yb ₄ Br ₆ O	4.252	0	Type-III	<i>i</i> -wave
2309	mp-850536	186 ($P_{63}mc$)	C_{6v} (6mm)	BaGa ₁₂ O ₁₉	1.927	1	Type-III	<i>i</i> -wave
2310	mp-863423	186 ($P_{63}mc$)	C_{6v} (6mm)	SrGa ₁₂ O ₁₉	1.858	1	Type-III	<i>i</i> -wave
2311	mp-8880	186 ($P_{63}mc$)	C_{6v} (6mm)	AlP	1.953	0	Type-III	<i>i</i> -wave
2312	mp-8881	186 ($P_{63}mc$)	C_{6v} (6mm)	AlAs	1.687	0	Type-III	<i>i</i> -wave
2313	mp-8882	186 ($P_{63}mc$)	C_{6v} (6mm)	GaP	1.3	0	Type-III	<i>i</i> -wave
2314	mp-8884	186 ($P_{63}mc$)	C_{6v} (6mm)	ZnTe	1.1	0	Type-III	<i>i</i> -wave
2315	mp-9007	186 ($P_{63}mc$)	C_{6v} (6mm)	Na ₆ P ₄ W	1.263	0	Type-III	<i>i</i> -wave
2316	mp-9575	186 ($P_{63}mc$)	C_{6v} (6mm)	LiBeSb	0.873	0	Type-III	<i>i</i> -wave
2317	mp-966800	186 ($P_{63}mc$)	C_{6v} (6mm)	InP	0.528	0	Type-III	<i>i</i> -wave
2318	mp-9737	186 ($P_{63}mc$)	C_{6v} (6mm)	Ba ₄ Sm ₄ Zn ₃ PtO ₁₅	2.489	0	Type-III	<i>i</i> -wave
2319	mp-976280	186 ($P_{63}mc$)	C_{6v} (6mm)	LiBr	4.935	0	Type-III	<i>i</i> -wave
2320	mp-978534	186 ($P_{63}mc$)	C_{6v} (6mm)	SiGe	0.409	0	Type-III	<i>i</i> -wave
2321	mp-9919	186 ($P_{63}mc$)	C_{6v} (6mm)	LiZnSb	0.406	0	Type-III	<i>i</i> -wave
2322	mp-9946	186 ($P_{63}mc$)	C_{6v} (6mm)	ZnS	2.037	0	Type-III	<i>i</i> -wave
2323	icsd-76005	187 ($P_{6m}2$)	D_{3h} (6m2)	WN	0	1	Type-III	<i>g</i> -wave
2324	icsd-644084	187 ($P_{6m}2$)	D_{3h} (6m2)	MoP	0	0	Type-III	<i>g</i> -wave
2325	icsd-645320	187 ($P_{6m}2$)	D_{3h} (6m2)	NbS	0	1	Type-III	<i>g</i> -wave
2326	icsd-653209	187 ($P_{6m}2$)	D_{3h} (6m2)	ZrTe	0	0	Type-III	<i>g</i> -wave
2327	mp-10615	187 ($P_{6m}2$)	D_{3h} (6m2)	BaLiP	0.698	0	Type-III	<i>g</i> -wave
2328	mp-10616	187 ($P_{6m}2$)	D_{3h} (6m2)	BaLiAs	0.593	0	Type-III	<i>g</i> -wave
2329	mp-1572	187 ($P_{6m}2$)	D_{3h} (6m2)	GaSe	1.241	0	Type-III	<i>g</i> -wave
2330	mp-24012	187 ($P_{6m}2$)	D_{3h} (6m2)	HoHSe	1.498	0	Type-III	<i>g</i> -wave
2331	mp-28797	187 ($P_{6m}2$)	D_{3h} (6m2)	YHSe	1.507	0	Type-III	<i>g</i> -wave
2332	mp-28989	187 ($P_{6m}2$)	D_{3h} (6m2)	Li ₁₀ BrN ₃	1.367	0	Type-III	<i>g</i> -wave
2333	mp-6867	187 ($P_{6m}2$)	D_{3h} (6m2)	KCaCO ₃ F	4.355	0	Type-III	<i>g</i> -wave
2334	mp-865427	187 ($P_{6m}2$)	D_{3h} (6m2)	KSrCO ₃ F	4.103	1	Type-III	<i>g</i> -wave
2335	mp-867261	187 ($P_{6m}2$)	D_{3h} (6m2)	RbSrCO ₃ F	4.133	0	Type-III	<i>g</i> -wave
2336	mp-11625	188 ($P_{6c}2$)	D_{3h} (6m2)	KCa(PO ₃) ₃	5.047	0	Type-III	<i>g</i> -wave
2337	mp-14058	188 ($P_{6c}2$)	D_{3h} (6m2)	KMg(PO ₃) ₃	4.947	0	Type-III	<i>g</i> -wave
2338	mp-14485	188 ($P_{6c}2$)	D_{3h} (6m2)	LaTa ₇ O ₁₉	3.117	1	Type-III	<i>g</i> -wave
2339	mp-14676	188 ($P_{6c}2$)	D_{3h} (6m2)	NdTa ₇ O ₁₉	3.166	1	Type-III	<i>g</i> -wave
2340	mp-15492	188 ($P_{6c}2$)	D_{3h} (6m2)	DyTa ₇ O ₁₉	3.222	1	Type-III	<i>g</i> -wave
2341	mp-17229	188 ($P_{6c}2$)	D_{3h} (6m2)	RbBe ₃ ZnF ₉	6.294	0	Type-III	<i>g</i> -wave
2342	mp-18502	188 ($P_{6c}2$)	D_{3h} (6m2)	BaSi ₃ SnO ₉	3.731	0	Type-III	<i>g</i> -wave
2343	mp-18509	188 ($P_{6c}2$)	D_{3h} (6m2)	KBe ₃ ZnF ₉	6.246	0	Type-III	<i>g</i> -wave
2344	mp-26897	188 ($P_{6c}2$)	D_{3h} (6m2)	LiSn(PO ₃) ₃	3.114	1	Type-III	<i>g</i> -wave

2345	mp-540631	188 ($P6c2$)	D_{3h} (6m2)	KTa(GeO ₃) ₃	3.518	0	Type-III	<i>g</i> -wave
2346	mp-540632	188 ($P6c2$)	D_{3h} (6m2)	RbTa(GeO ₃) ₃	3.485	0	Type-III	<i>g</i> -wave
2347	mp-540633	188 ($P6c2$)	D_{3h} (6m2)	RbNb(GeO ₃) ₃	3.173	0	Type-III	<i>g</i> -wave
2348	mp-540634	188 ($P6c2$)	D_{3h} (6m2)	TaTl(GeO ₃) ₃	3.658	0	Type-III	<i>g</i> -wave
2349	mp-540635	188 ($P6c2$)	D_{3h} (6m2)	BaSn(GeO ₃) ₃	2.787	0	Type-III	<i>g</i> -wave
2350	mp-556498	188 ($P6c2$)	D_{3h} (6m2)	Sr ₂ Be ₂ B ₂ O ₇	4.08	1	Type-III	<i>g</i> -wave
2351	mp-6661	188 ($P6c2$)	D_{3h} (6m2)	BaTi(SiO ₃) ₃	3.066	0	Type-III	<i>g</i> -wave
2352	mp-772036	188 ($P6c2$)	D_{3h} (6m2)	YTa ₇ O ₁₉	3.155	1	Type-III	<i>g</i> -wave
2353	mp-772869	188 ($P6c2$)	D_{3h} (6m2)	Ta ₇ InO ₁₉	2.034	1	Type-III	<i>g</i> -wave
2354	mp-773103	188 ($P6c2$)	D_{3h} (6m2)	ErTa ₇ O ₁₉	3.175	1	Type-III	<i>g</i> -wave
2355	mp-780049	188 ($P6c2$)	D_{3h} (6m2)	LuTa ₇ O ₁₉	3.193	1	Type-III	<i>g</i> -wave
2356	mp-850779	188 ($P6c2$)	D_{3h} (6m2)	HoTa ₇ O ₁₉	3.165	1	Type-III	<i>g</i> -wave
2357	mp-9478	188 ($P6c2$)	D_{3h} (6m2)	BaSi ₄ O ₉	4.345	0	Type-III	<i>g</i> -wave
2358	mp-11772	189 ($P62m$)	D_{3h} (6m2)	Ba ₃ Ti ₃ (BO ₆) ₂	2.131	1	Type-III	<i>g</i> -wave
2359	mp-13275	189 ($P62m$)	D_{3h} (6m2)	NaSrP	1.236	0	Type-III	<i>g</i> -wave
2360	mp-13978	189 ($P62m$)	D_{3h} (6m2)	Rb ₂ ThF ₆	6.273	0	Type-III	<i>g</i> -wave
2361	mp-14193	189 ($P62m$)	D_{3h} (6m2)	K ₂ ThF ₆	6.381	0	Type-III	<i>g</i> -wave
2362	mp-15248	189 ($P62m$)	D_{3h} (6m2)	K ₃ Nb ₃ (BO ₆) ₂	1.921	1	Type-III	<i>g</i> -wave
2363	mp-16855	189 ($P62m$)	D_{3h} (6m2)	K ₃ Ta ₄ Si ₂ O ₁₃	2.973	1	Type-III	<i>g</i> -wave
2364	mp-17059	189 ($P62m$)	D_{3h} (6m2)	K ₃ Nb ₃ Si ₂ O ₁₃	2.226	1	Type-III	<i>g</i> -wave
2365	mp-17103	189 ($P62m$)	D_{3h} (6m2)	Sr ₃ Ta ₆ (Si ₂ O ₁₃) ₂	3.085	1	Type-III	<i>g</i> -wave
2366	mp-2340	189 ($P62m$)	D_{3h} (6m2)	Na ₂ O ₂	1.736	0	Type-III	<i>g</i> -wave
2367	mp-27370	189 ($P62m$)	D_{3h} (6m2)	P ₁₀ AuI	0.531	0	Type-III	<i>g</i> -wave
2368	mp-28802	189 ($P62m$)	D_{3h} (6m2)	Sr ₄ Zn ₃ F ₁₄	4.784	1	Type-III	<i>g</i> -wave
2369	mp-29877	189 ($P62m$)	D_{3h} (6m2)	K ₂ ReH ₉	5.213	0	Type-III	<i>g</i> -wave
2370	mp-409	189 ($P62m$)	D_{3h} (6m2)	NaS	0.869	0	Type-III	<i>g</i> -wave
2371	mp-541626	189 ($P62m$)	D_{3h} (6m2)	K ₃ Nb ₃ Ge ₂ O ₁₃	2.324	1	Type-III	<i>g</i> -wave
2372	mp-554899	189 ($P62m$)	D_{3h} (6m2)	CsAlF ₄	6.977	0	Type-III	<i>g</i> -wave
2373	mp-560641	189 ($P62m$)	D_{3h} (6m2)	Ba ₁₂ Cl ₅ F ₁₉	5.98	0	Type-III	<i>g</i> -wave
2374	mp-561189	189 ($P62m$)	D_{3h} (6m2)	Rb ₆ Si ₁₀ O ₂₃	4.044	1	Type-III	<i>g</i> -wave
2375	mp-561310	189 ($P62m$)	D_{3h} (6m2)	NaLiCO ₃	4.313	1	Type-III	<i>g</i> -wave
2376	mp-567680	189 ($P62m$)	D_{3h} (6m2)	BaCl ₂	4.572	0	Type-III	<i>g</i> -wave
2377	mp-568536	189 ($P62m$)	D_{3h} (6m2)	BaI ₂	3.049	0	Type-III	<i>g</i> -wave
2378	mp-6169	189 ($P62m$)	D_{3h} (6m2)	Ba ₃ Ta ₆ (Si ₂ O ₁₃) ₂	3.029	1	Type-III	<i>g</i> -wave
2379	mp-638731	189 ($P62m$)	D_{3h} (6m2)	LaCO ₃ F	3.926	1	Type-III	<i>g</i> -wave
2380	mp-643070	189 ($P62m$)	D_{3h} (6m2)	Ca ₄ Mg ₃ H ₁₄	3.111	1	Type-III	<i>g</i> -wave
2381	mp-643108	189 ($P62m$)	D_{3h} (6m2)	Yb ₄ Mg ₃ H ₁₄	3.093	1	Type-III	<i>g</i> -wave
2382	mp-667379	189 ($P62m$)	D_{3h} (6m2)	Ba ₇ Al ₆₄ O ₁₀₃	4.254	1	Type-III	<i>g</i> -wave
2383	mp-6760	189 ($P62m$)	D_{3h} (6m2)	Na ₃ La ₉ B ₈ O ₂₇	4.01	0	Type-III	<i>g</i> -wave
2384	mp-760418	189 ($P62m$)	D_{3h} (6m2)	Ba ₂ SrI ₆	2.906	0	Type-III	<i>g</i> -wave
2385	mp-7931	189 ($P62m$)	D_{3h} (6m2)	SrP	0.459	0	Type-III	<i>g</i> -wave
2386	mp-862701	189 ($P62m$)	D_{3h} (6m2)	CsCaCO ₃ F	4.526	0	Type-III	<i>g</i> -wave
2387	mp-867757	189 ($P62m$)	D_{3h} (6m2)	RbCaCO ₃ F	4.312	0	Type-III	<i>g</i> -wave
2388	mp-9062	189 ($P62m$)	D_{3h} (6m2)	RbS	1.578	0	Type-III	<i>g</i> -wave
2389	mp-9064	189 ($P62m$)	D_{3h} (6m2)	RbTe	0.437	0	Type-III	<i>g</i> -wave
2390	mp-9732	189 ($P62m$)	D_{3h} (6m2)	BaNaP	0.856	0	Type-III	<i>g</i> -wave
2391	mp-9775	189 ($P62m$)	D_{3h} (6m2)	NaSrAs	0.807	0	Type-III	<i>g</i> -wave
2392	mp-9870	189 ($P62m$)	D_{3h} (6m2)	K ₃ Ta ₃ (BO ₆) ₂	2.67	0	Type-III	<i>g</i> -wave
2393	mp-27791	190 ($P62c$)	D_{3h} (6m2)	SrBe ₃ O ₄	4.13	0	Type-III	<i>g</i> -wave
2394	mp-28043	190 ($P62c$)	D_{3h} (6m2)	Tl ₃ AgI ₅	1.051	0	Type-III	<i>g</i> -wave
2395	mp-28468	190 ($P62c$)	D_{3h} (6m2)	KAg ₅ S ₃	0.697	0	Type-III	<i>g</i> -wave
2396	mp-28485	190 ($P62c$)	D_{3h} (6m2)	Sb ₅ IO ₇	2.452	1	Type-III	<i>g</i> -wave
2397	mp-28703	190 ($P62c$)	D_{3h} (6m2)	RbAg ₅ S ₃	0.767	0	Type-III	<i>g</i> -wave
2398	mp-29090	190 ($P62c$)	D_{3h} (6m2)	Rb ₄ Au ₆ S ₅	1.698	0	Type-III	<i>g</i> -wave
2399	mp-29341	190 ($P62c$)	D_{3h} (6m2)	K ₄ Au ₆ S ₅	1.584	0	Type-III	<i>g</i> -wave
2400	mp-30295	190 ($P62c$)	D_{3h} (6m2)	W ₆ CCl ₁₈	1.155	0	Type-III	<i>g</i> -wave
2401	mp-541995	190 ($P62c$)	D_{3h} (6m2)	LaSiO ₃ F	4.541	0	Type-III	<i>g</i> -wave
2402	mp-557407	190 ($P62c$)	D_{3h} (6m2)	K ₃ NaUC ₃ O ₁₁	2.142	1	Type-III	<i>g</i> -wave
2403	mp-557810	190 ($P62c$)	D_{3h} (6m2)	BaH ₆ F ₈	7.567	0	Type-III	<i>g</i> -wave

2404	mp-558491	190 (<i>P</i> 62 <i>c</i>)	D _{3h} (6m2)	BaAlBO ₃ F ₂	6.064	0	Type-III	<i>g</i> -wave
2405	mp-559346	190 (<i>P</i> 62 <i>c</i>)	D _{3h} (6m2)	K ₃ Nb ₃ Si ₂ O ₁₃	2.145	1	Type-III	<i>g</i> -wave
2406	mp-707424	190 (<i>P</i> 62 <i>c</i>)	D _{3h} (6m2)	Al ₂ H ₁₂ (SeO ₅) ₃	4.745	1	Type-III	<i>g</i> -wave
2407	mp-762063	190 (<i>P</i> 62 <i>c</i>)	D _{3h} (6m2)	Na ₄ Cu ₆ O ₅	0.829	1	Type-III	<i>g</i> -wave
2408	mp-41734	195 (<i>P</i> 23)	T (23)	Na ₈ Al ₆ Si ₆ SO ₂₈	4.036	1	Type-II	<i>s</i> -wave
2409	mp-23122	196 (<i>F</i> 23)	T (23)	Li ₁₀ B ₁₄ Cl ₂ O ₂₅	6.402	0	Type-II	<i>s</i> -wave
2410	mp-23352	197 (<i>I</i> 23)	T (23)	Ge(Bi ₃ O ₅) ₄	2.376	0	Type-II	<i>s</i> -wave
2411	mp-23492	197 (<i>I</i> 23)	T (23)	Si(Bi ₃ O ₅) ₄	2.348	0	Type-II	<i>s</i> -wave
2412	mp-23494	197 (<i>I</i> 23)	T (23)	Ti(Bi ₃ O ₅) ₄	2.313	0	Type-II	<i>s</i> -wave
2413	mp-28632	197 (<i>I</i> 23)	T (23)	Ga(Bi ₃ O ₅) ₄	0	0	Type-II	<i>s</i> -wave
2414	mp-32597	197 (<i>I</i> 23)	T (23)	Bi ₁₃ O ₂₀	0.355	1	Type-II	<i>s</i> -wave
2415	mp-667342	197 (<i>I</i> 23)	T (23)	Bi ₁₂ PbO ₂₀	1.692	0	Type-II	<i>s</i> -wave
2416	icsd-15819	198 (<i>P</i> 213)	T (23)	N ₂	7.3395	0	Type-II	<i>s</i> -wave
2417	icsd-27249	198 (<i>P</i> 213)	T (23)	N ₂	7.8407	0	Type-II	<i>s</i> -wave
2418	icsd-53890	198 (<i>P</i> 213)	T (23)	GeRh	0	1	Type-II	<i>s</i> -wave
2419	icsd-633543	198 (<i>P</i> 213)	T (23)	FeSi	0.1096	0	Type-II	<i>s</i> -wave
2420	mp-13613	198 (<i>P</i> 213)	T (23)	K ₂ Mg ₂ Be ₃ F ₁₂	7.133	1	Type-II	<i>s</i> -wave
2421	mp-13614	198 (<i>P</i> 213)	T (23)	Rb ₂ Be ₃ Cd ₂ F ₁₂	5.333	0	Type-II	<i>s</i> -wave
2422	mp-14889	198 (<i>P</i> 213)	T (23)	K ₉ Fe ₂ S ₇	0.749	0	Type-II	<i>s</i> -wave
2423	mp-14890	198 (<i>P</i> 213)	T (23)	Rb ₉ Fe ₂ S ₇	0.452	0	Type-II	<i>s</i> -wave
2424	mp-15077	198 (<i>P</i> 213)	T (23)	Ag ₇ AsS ₆	0.73	0	Type-II	<i>s</i> -wave
2425	mp-154	198 (<i>P</i> 213)	T (23)	N ₂	7.341	0	Type-II	<i>s</i> -wave
2426	mp-15599	198 (<i>P</i> 213)	T (23)	K ₂ Ca ₂ (SO ₄) ₃	5.428	1	Type-II	<i>s</i> -wave
2427	mp-16363	198 (<i>P</i> 213)	T (23)	CoAsS	0.851	0	Type-II	<i>s</i> -wave
2428	mp-17250	198 (<i>P</i> 213)	T (23)	K ₃ SbO ₃	3.235	0	Type-II	<i>s</i> -wave
2429	mp-17538	198 (<i>P</i> 213)	T (23)	K ₃ SbSe ₃	2.308	0	Type-II	<i>s</i> -wave
2430	mp-17912	198 (<i>P</i> 213)	T (23)	Rb ₃ SbSe ₃	2	0	Type-II	<i>s</i> -wave
2431	mp-18594	198 (<i>P</i> 213)	T (23)	K ₃ AsSe ₃	2.125	0	Type-II	<i>s</i> -wave
2432	mp-23276	198 (<i>P</i> 213)	T (23)	InCl	2.205	0	Type-II	<i>s</i> -wave
2433	mp-23330	198 (<i>P</i> 213)	T (23)	NaClO ₃	5.633	1	Type-II	<i>s</i> -wave
2434	mp-23333	198 (<i>P</i> 213)	T (23)	Hg ₃ Cl ₄ O	1.462	0	Type-II	<i>s</i> -wave
2435	mp-23339	198 (<i>P</i> 213)	T (23)	NaBrO ₃	4.481	0	Type-II	<i>s</i> -wave
2436	mp-23644	198 (<i>P</i> 213)	T (23)	Hg ₃ AsClO ₄	2.041	0	Type-II	<i>s</i> -wave
2437	mp-24052	198 (<i>P</i> 213)	T (23)	CaMgNiH ₄	1.873	0	Type-II	<i>s</i> -wave
2438	mp-24507	198 (<i>P</i> 213)	T (23)	Na ₆ Zn ₃ P ₄ H ₆ O ₁₉	3.985	0	Type-II	<i>s</i> -wave
2439	mp-2488	198 (<i>P</i> 213)	T (23)	SiOs	0.512	0	Type-II	<i>s</i> -wave
2440	mp-28140	198 (<i>P</i> 213)	T (23)	P ₂ Pb ₃ S ₈	2.313	0	Type-II	<i>s</i> -wave
2441	mp-28980	198 (<i>P</i> 213)	T (23)	K ₃ BiSe ₃	2.076	0	Type-II	<i>s</i> -wave
2442	mp-29145	198 (<i>P</i> 213)	T (23)	H ₃ N	4.341	0	Type-II	<i>s</i> -wave
2443	mp-29168	198 (<i>P</i> 213)	T (23)	Rb ₃ BiSe ₃	1.777	0	Type-II	<i>s</i> -wave
2444	mp-29252	198 (<i>P</i> 213)	T (23)	Sn ₂ ClF ₃	3.557	0	Type-II	<i>s</i> -wave
2445	mp-29379	198 (<i>P</i> 213)	T (23)	K ₃ BiTe ₃	1.228	0	Type-II	<i>s</i> -wave
2446	mp-29513	198 (<i>P</i> 213)	T (23)	CsXeF ₇	3.268	1	Type-II	<i>s</i> -wave
2447	mp-29525	198 (<i>P</i> 213)	T (23)	Rb ₃ BiO ₃	3.102	0	Type-II	<i>s</i> -wave
2448	mp-4876	198 (<i>P</i> 213)	T (23)	Tl ₃ SbSe ₃	1.015	0	Type-II	<i>s</i> -wave
2449	mp-532727	198 (<i>P</i> 213)	T (23)	K ₂ YZr(PO ₄) ₃	4.576	0	Type-II	<i>s</i> -wave
2450	mp-556867	198 (<i>P</i> 213)	T (23)	K ₂ PrZr(PO ₄) ₃	4.428	1	Type-II	<i>s</i> -wave
2451	mp-558752	198 (<i>P</i> 213)	T (23)	Rb ₂ Ca ₂ (SO ₄) ₃	5.514	1	Type-II	<i>s</i> -wave
2452	mp-558945	198 (<i>P</i> 213)	T (23)	Hg ₃ AsBrO ₄	1.844	0	Type-II	<i>s</i> -wave
2453	mp-561202	198 (<i>P</i> 213)	T (23)	K ₆ NbAs ₃ O	1.097	0	Type-II	<i>s</i> -wave
2454	mp-562057	198 (<i>P</i> 213)	T (23)	Cs ₂ Ca ₂ Be ₃ F ₁₂	7.216	0	Type-II	<i>s</i> -wave
2455	mp-562072	198 (<i>P</i> 213)	T (23)	Cs ₃ SbO ₃	3.084	0	Type-II	<i>s</i> -wave
2456	mp-5626	198 (<i>P</i> 213)	T (23)	K ₃ SbTe ₃	1.717	0	Type-II	<i>s</i> -wave
2457	mp-567185	198 (<i>P</i> 213)	T (23)	SnHg ₆ (As ₂ Br ₃) ₂	1.371	0	Type-II	<i>s</i> -wave
2458	mp-568612	198 (<i>P</i> 213)	T (23)	SnHg ₆ (P ₂ Cl ₃) ₂	2.132	0	Type-II	<i>s</i> -wave
2459	mp-570135	198 (<i>P</i> 213)	T (23)	SnHg ₇ (P ₂ Br ₃) ₂	1.65	0	Type-II	<i>s</i> -wave
2460	mp-571478	198 (<i>P</i> 213)	T (23)	SnHg ₇ (As ₂ I ₃) ₂	0.95	0	Type-II	<i>s</i> -wave
2461	mp-581738	198 (<i>P</i> 213)	T (23)	Cs ₃ BiSe ₃	2.035	0	Type-II	<i>s</i> -wave
2462	mp-5830	198 (<i>P</i> 213)	T (23)	Na ₃ AsS ₃	2.522	0	Type-II	<i>s</i> -wave

2463	mp-6115	198 ($P_{21}3$)	T (23)	$K_2Zn_2(SO_4)_3$	4.494	1	Type-II	<i>s</i> -wave
2464	mp-621964	198 ($P_{21}3$)	T (23)	$K_2RbBiSe_3$	2.131	0	Type-II	<i>s</i> -wave
2465	mp-6276	198 ($P_{21}3$)	T (23)	$K_2Cd_2(SO_4)_3$	3.803	1	Type-II	<i>s</i> -wave
2466	mp-6299	198 ($P_{21}3$)	T (23)	$K_2Mg_2(SO_4)_3$	5.684	0	Type-II	<i>s</i> -wave
2467	mp-6372	198 ($P_{21}3$)	T (23)	$K_2Be_3Zn_2F_{12}$	5.787	1	Type-II	<i>s</i> -wave
2468	mp-643246	198 ($P_{21}3$)	T (23)	$YbMgNiH_4$	1.992	0	Type-II	<i>s</i> -wave
2469	mp-643293	198 ($P_{21}3$)	T (23)	$SrMgNiH_4$	1.812	0	Type-II	<i>s</i> -wave
2470	mp-675142	198 ($P_{21}3$)	T (23)	Yb_3DySb_3	0.532	0	Type-II	<i>s</i> -wave
2471	mp-677014	198 ($P_{21}3$)	T (23)	$K_2ErTi(PO_4)_3$	2.565	0	Type-II	<i>s</i> -wave
2472	mp-677179	198 ($P_{21}3$)	T (23)	$BaNaIn_2(PO_4)_3$	3.479	1	Type-II	<i>s</i> -wave
2473	mp-677250	198 ($P_{21}3$)	T (23)	$K_2LuZr(PO_4)_3$	4.323	0	Type-II	<i>s</i> -wave
2474	mp-677733	198 ($P_{21}3$)	T (23)	$K_2TiAl(PO_4)_3$	2.912	0	Type-II	<i>s</i> -wave
2475	mp-6860	198 ($P_{21}3$)	T (23)	$Na_3AlP_3NO_9$	5.152	0	Type-II	<i>s</i> -wave
2476	mp-756361	198 ($P_{21}3$)	T (23)	$ZrSeO$	1.957	0	Type-II	<i>s</i> -wave
2477	mp-758925	198 ($P_{21}3$)	T (23)	$Na_6Zn_3As_4H_6O_{19}$	3.005	0	Type-II	<i>s</i> -wave
2478	mp-768232	198 ($P_{21}3$)	T (23)	Rb_3SbO_3	3.2	0	Type-II	<i>s</i> -wave
2479	mp-774752	198 ($P_{21}3$)	T (23)	$Li_2MgTi_3O_8$	3.321	0	Type-II	<i>s</i> -wave
2480	mp-774797	198 ($P_{21}3$)	T (23)	$Li_2Ti_3ZnO_8$	3.175	1	Type-II	<i>s</i> -wave
2481	mp-775761	198 ($P_{21}3$)	T (23)	$AgClO_3$	3.1	1	Type-II	<i>s</i> -wave
2482	mp-7787	198 ($P_{21}3$)	T (23)	$HfSO$	2.869	0	Type-II	<i>s</i> -wave
2483	mp-779689	198 ($P_{21}3$)	T (23)	H_3N	3.734	0	Type-II	<i>s</i> -wave
2484	mp-8059	198 ($P_{21}3$)	T (23)	SiO_2	5.589	0	Type-II	<i>s</i> -wave
2485	mp-8351	198 ($P_{21}3$)	T (23)	$NaAlSiO_4$	4.484	1	Type-II	<i>s</i> -wave
2486	mp-8594	198 ($P_{21}3$)	T (23)	Ag_7PSe_6	0.784	0	Type-II	<i>s</i> -wave
2487	mp-8630	198 ($P_{21}3$)	T (23)	$SbIrS$	1.396	0	Type-II	<i>s</i> -wave
2488	mp-8686	198 ($P_{21}3$)	T (23)	Na_3AsSe_3	2.008	0	Type-II	<i>s</i> -wave
2489	mp-9191	198 ($P_{21}3$)	T (23)	Na_3SbTe_3	1.467	0	Type-II	<i>s</i> -wave
2490	mp-20694	199 ($I_{21}3$)	T (23)	$K_2Pb_2O_3$	1.691	0	Type-II	<i>s</i> -wave
2491	mp-27851	199 ($I_{21}3$)	T (23)	$Hg_3(SeCl)_2$	1.77	0	Type-II	<i>s</i> -wave
2492	mp-27852	199 ($I_{21}3$)	T (23)	$Hg_3(TeCl)_2$	1.913	0	Type-II	<i>s</i> -wave
2493	mp-27853	199 ($I_{21}3$)	T (23)	$Hg_3(TeBr)_2$	1.704	0	Type-II	<i>s</i> -wave
2494	mp-555730	199 ($I_{21}3$)	T (23)	$Na_2Ca_3Al_2F_{14}$	7.143	0	Type-II	<i>s</i> -wave
2495	mp-558539	199 ($I_{21}3$)	T (23)	$Cs_2Ba_2(CO_3)_3$	4.338	0	Type-II	<i>s</i> -wave
2496	mp-560036	199 ($I_{21}3$)	T (23)	$Li_2Ca_3Be_3Si_3(O_6F)_2$	5.843	0	Type-II	<i>s</i> -wave
2497	mp-643579	199 ($I_{21}3$)	T (23)	SbH_3OF_6	4.655	1	Type-II	<i>s</i> -wave
2498	mp-757715	199 ($I_{21}3$)	T (23)	$Tb(BiO_2)_3$	2.664	0	Type-II	<i>s</i> -wave
2499	mp-8624	199 ($I_{21}3$)	T (23)	$K_2Sn_2O_3$	1.302	1	Type-II	<i>s</i> -wave
2500	mp-866617	199 ($I_{21}3$)	T (23)	$Cs_2Sr_2(CO_3)_3$	4.623	0	Type-II	<i>s</i> -wave
2501	mp-866635	199 ($I_{21}3$)	T (23)	CuH_3NCl	2.126	0	Type-II	<i>s</i> -wave
2502	mp-984332	199 ($I_{21}3$)	T (23)	$Rb_2Sr_2(CO_3)_3$	4.623	0	Type-II	<i>s</i> -wave
2503	mp-27843	212 ($P_{43}32$)	O (432)	$Zn_2Ge_3O_8$	2.339	0	Type-II	<i>s</i> -wave
2504	mp-28146	212 ($P_{43}32$)	O (432)	$LiGa_5O_8$	2.877	0	Type-II	<i>s</i> -wave
2505	mp-29104	212 ($P_{43}32$)	O (432)	$Ti_3Zn_2O_8$	2.585	1	Type-II	<i>s</i> -wave
2506	mp-530399	212 ($P_{43}32$)	O (432)	$LiAl_5O_8$	5.517	0	Type-II	<i>s</i> -wave
2507	mp-554801	212 ($P_{43}32$)	O (432)	$Ca_3Nb_4(O_6F)_2$	3.005	1	Type-II	<i>s</i> -wave
2508	mp-560378	212 ($P_{43}32$)	O (432)	$Ca_3Ta_4(O_6F)_2$	3.898	1	Type-II	<i>s</i> -wave
2509	mp-571066	212 ($P_{43}32$)	O (432)	K_6Sn_{25}	0.02	1	Type-II	<i>s</i> -wave
2510	mp-14389	213 ($P_{41}32$)	O (432)	$Na_3AlP_8O_{23}$	5.266	0	Type-II	<i>s</i> -wave
2511	mp-14390	213 ($P_{41}32$)	O (432)	$Na_3GaP_8O_{23}$	5	0	Type-II	<i>s</i> -wave
2512	mp-14565	213 ($P_{41}32$)	O (432)	$K_3P_6N_{11}$	4.13	0	Type-II	<i>s</i> -wave
2513	mp-16107	213 ($P_{41}32$)	O (432)	$Rb_3P_6N_{11}$	4.058	0	Type-II	<i>s</i> -wave
2514	mp-16108	213 ($P_{41}32$)	O (432)	$Cs_3P_6N_{11}$	4.218	0	Type-II	<i>s</i> -wave
2515	mp-27192	213 ($P_{41}32$)	O (432)	$CsBe_2F_5$	7.181	0	Type-II	<i>s</i> -wave
2516	mp-530571	213 ($P_{41}32$)	O (432)	$Na_4Sn_3O_8$	2.598	0	Type-II	<i>s</i> -wave
2517	mp-27272	214 ($I_{41}32$)	O (432)	Ca_3PI_3	2.217	0	Type-II	<i>s</i> -wave
2518	mp-568923	214 ($I_{41}32$)	O (432)	Ba_2BN_2Cl	2.753	0	Type-II	<i>s</i> -wave
2519	mp-10748	215 ($P_{43}m$)	T _d (43m)	$TaCu_3S_4$	1.923	0	Type-III	<i>i</i> -wave
2520	mp-21855	215 ($P_{43}m$)	T _d (43m)	VCu_3Se_4	0.816	0	Type-III	<i>i</i> -wave
2521	mp-28040	215 ($P_{43}m$)	T _d (43m)	$Hf(BH_4)_4$	5.72	1	Type-III	<i>i</i> -wave

2522	mp-34337	215 (<i>P43m</i>)	T _d (43m)	H ₄ NCl	4.936	0	Type-III	<i>i</i> -wave
2523	mp-36248	215 (<i>P43m</i>)	T _d (43m)	H ₄ BrN	4.036	0	Type-III	<i>i</i> -wave
2524	mp-3762	215 (<i>P43m</i>)	T _d (43m)	VCu ₃ S ₄	1.036	0	Type-III	<i>i</i> -wave
2525	mp-4043	215 (<i>P43m</i>)	T _d (43m)	NbCu ₃ Se ₄	1.36	0	Type-III	<i>i</i> -wave
2526	mp-4081	215 (<i>P43m</i>)	T _d (43m)	TaCu ₃ Se ₄	1.598	0	Type-III	<i>i</i> -wave
2527	mp-555606	215 (<i>P43m</i>)	T _d (43m)	Na ₁₀ Be ₄ Si ₄ O ₁₇	3.943	1	Type-III	<i>i</i> -wave
2528	mp-5621	215 (<i>P43m</i>)	T _d (43m)	NbCu ₃ S ₄	1.657	0	Type-III	<i>i</i> -wave
2529	mp-643071	215 (<i>P43m</i>)	T _d (43m)	Yb ₄ Mg ₄ Fe ₃ H ₂₂	1.472	0	Type-III	<i>i</i> -wave
2530	mp-644264	215 (<i>P43m</i>)	T _d (43m)	Ca ₄ Mg ₄ Fe ₃ H ₂₂	1.446	0	Type-III	<i>i</i> -wave
2531	mp-755309	215 (<i>P43m</i>)	T _d (43m)	Li ₃ NbS ₄	2.76	0	Type-III	<i>i</i> -wave
2532	mp-760375	215 (<i>P43m</i>)	T _d (43m)	Li ₃ VS ₄	1.883	0	Type-III	<i>i</i> -wave
2533	mp-866640	215 (<i>P43m</i>)	T _d (43m)	LiMgH ₆ Ir	3.376	1	Type-III	<i>i</i> -wave
2534	mp-9295	215 (<i>P43m</i>)	T _d (43m)	TaCu ₃ Te ₄	1.141	0	Type-III	<i>i</i> -wave
2535	mp-981379	215 (<i>P43m</i>)	T _d (43m)	Zn ₃ CdS ₄	1.68	0	Type-III	<i>i</i> -wave
2536	mp-991652	215 (<i>P43m</i>)	T _d (43m)	VCu ₃ Te ₄	0.574	0	Type-III	<i>i</i> -wave
2537	mp-991676	215 (<i>P43m</i>)	T _d (43m)	NbCu ₃ Te ₄	0.917	0	Type-III	<i>i</i> -wave
2538	icsd-43714	216 (<i>F43m</i>)	T _d (43m)	HgTe	0	0	Type-III	<i>i</i> -wave
2539	icsd-54985	216 (<i>F43m</i>)	T _d (43m)	ZrNi ₅	0	0	Type-III	<i>i</i> -wave
2540	icsd-60378	216 (<i>F43m</i>)	T _d (43m)	ZnS	2.0832	0	Type-III	<i>i</i> -wave
2541	icsd-103795	216 (<i>F43m</i>)	T _d (43m)	GaP	1.5845	0	Type-III	<i>i</i> -wave
2542	icsd-162196	216 (<i>F43m</i>)	T _d (43m)	InSb	0	1	Type-III	<i>i</i> -wave
2543	icsd-603115	216 (<i>F43m</i>)	T _d (43m)	CdTe	0.5257	0	Type-III	<i>i</i> -wave
2544	icsd-603798	216 (<i>F43m</i>)	T _d (43m)	SiC	1.3523	0	Type-III	<i>i</i> -wave
2545	icsd-610533	216 (<i>F43m</i>)	T _d (43m)	GaAs	0.4951	0	Type-III	<i>i</i> -wave
2546	icsd-610537	216 (<i>F43m</i>)	T _d (43m)	GaAs	0.5088	0	Type-III	<i>i</i> -wave
2547	icsd-614868	216 (<i>F43m</i>)	T _d (43m)	BN	4.4522	0	Type-III	<i>i</i> -wave
2548	icsd-618779	216 (<i>F43m</i>)	T _d (43m)	SiC	1.3536	0	Type-III	<i>i</i> -wave
2549	icsd-620514	216 (<i>F43m</i>)	T _d (43m)	CdTe	0.5098	0	Type-III	<i>i</i> -wave
2550	icsd-639237	216 (<i>F43m</i>)	T _d (43m)	HgTe	0	0	Type-III	<i>i</i> -wave
2551	icsd-652222	216 (<i>F43m</i>)	T _d (43m)	ZnSe	1.1982	0	Type-III	<i>i</i> -wave
2552	mp-10182	216 (<i>F43m</i>)	T _d (43m)	LiZnP	1.339	0	Type-III	<i>i</i> -wave
2553	mp-10623	216 (<i>F43m</i>)	T _d (43m)	ThSbRh	0.744	0	Type-III	<i>i</i> -wave
2554	mp-10695	216 (<i>F43m</i>)	T _d (43m)	ZnS	2.019	0	Type-III	<i>i</i> -wave
2555	mp-1190	216 (<i>F43m</i>)	T _d (43m)	ZnSe	1.166	0	Type-III	<i>i</i> -wave
2556	mp-12558	216 (<i>F43m</i>)	T _d (43m)	LiMgAs	1.372	0	Type-III	<i>i</i> -wave
2557	mp-13031	216 (<i>F43m</i>)	T _d (43m)	MgSe	2.548	0	Type-III	<i>i</i> -wave
2558	mp-13032	216 (<i>F43m</i>)	T _d (43m)	MgS	3.369	0	Type-III	<i>i</i> -wave
2559	mp-13033	216 (<i>F43m</i>)	T _d (43m)	MgTe	2.319	0	Type-III	<i>i</i> -wave
2560	mp-1479	216 (<i>F43m</i>)	T _d (43m)	BP	1.243	0	Type-III	<i>i</i> -wave
2561	mp-1541	216 (<i>F43m</i>)	T _d (43m)	BeSe	2.664	0	Type-III	<i>i</i> -wave
2562	mp-1550	216 (<i>F43m</i>)	T _d (43m)	AlP	1.629	0	Type-III	<i>i</i> -wave
2563	mp-15988	216 (<i>F43m</i>)	T _d (43m)	Li ₂ CuSb	0.454	0	Type-III	<i>i</i> -wave
2564	mp-16327	216 (<i>F43m</i>)	T _d (43m)	DySbPt	0.049	0	Type-III	<i>i</i> -wave
2565	mp-16329	216 (<i>F43m</i>)	T _d (43m)	ErSbPt	0	0	Type-III	<i>i</i> -wave
2566	mp-16376	216 (<i>F43m</i>)	T _d (43m)	HoSbPt	0	0	Type-III	<i>i</i> -wave
2567	mp-1700	216 (<i>F43m</i>)	T _d (43m)	AlN	3.306	0	Type-III	<i>i</i> -wave
2568	mp-1986	216 (<i>F43m</i>)	T _d (43m)	ZnO	0.631	0	Type-III	<i>i</i> -wave
2569	mp-19886	216 (<i>F43m</i>)	T _d (43m)	ThSnPt	0.674	0	Type-III	<i>i</i> -wave
2570	mp-20351	216 (<i>F43m</i>)	T _d (43m)	InP	0.455	0	Type-III	<i>i</i> -wave
2571	mp-2172	216 (<i>F43m</i>)	T _d (43m)	AlAs	1.504	0	Type-III	<i>i</i> -wave
2572	mp-2176	216 (<i>F43m</i>)	T _d (43m)	ZnTe	1.073	0	Type-III	<i>i</i> -wave
2573	mp-22913	216 (<i>F43m</i>)	T _d (43m)	CuBr	0.487	0	Type-III	<i>i</i> -wave
2574	mp-22914	216 (<i>F43m</i>)	T _d (43m)	CuCl	0.565	0	Type-III	<i>i</i> -wave
2575	mp-22925	216 (<i>F43m</i>)	T _d (43m)	AgI	1.367	0	Type-III	<i>i</i> -wave
2576	mp-2469	216 (<i>F43m</i>)	T _d (43m)	CdS	1.049	0	Type-III	<i>i</i> -wave
2577	mp-2490	216 (<i>F43m</i>)	T _d (43m)	GaP	1.604	0	Type-III	<i>i</i> -wave
2578	mp-252	216 (<i>F43m</i>)	T _d (43m)	BeTe	2.017	0	Type-III	<i>i</i> -wave
2579	mp-2624	216 (<i>F43m</i>)	T _d (43m)	AlSb	1.226	0	Type-III	<i>i</i> -wave
2580	mp-2691	216 (<i>F43m</i>)	T _d (43m)	CdSe	0.51	0	Type-III	<i>i</i> -wave

2581	mp-27407	216 (<i>F</i> 43 <i>m</i>)	T _d (43m)	Ca ₁₂ Be ₁₇ O ₂₉	3.67	0	Type-III	<i>i</i> -wave
2582	mp-27608	216 (<i>F</i> 43 <i>m</i>)	T _d (43m)	Be ₄ TeO ₇	1.281	0	Type-III	<i>i</i> -wave
2583	mp-30530	216 (<i>F</i> 43 <i>m</i>)	T _d (43m)	TlClO ₄	4.571	1	Type-III	<i>i</i> -wave
2584	mp-30847	216 (<i>F</i> 43 <i>m</i>)	T _d (43m)	TiSnPt	0.791	0	Type-III	<i>i</i> -wave
2585	mp-31451	216 (<i>F</i> 43 <i>m</i>)	T _d (43m)	ZrCoBi	0.977	0	Type-III	<i>i</i> -wave
2586	mp-31454	216 (<i>F</i> 43 <i>m</i>)	T _d (43m)	TaSbRu	0.665	0	Type-III	<i>i</i> -wave
2587	mp-35267	216 (<i>F</i> 43 <i>m</i>)	T _d (43m)	Al ₅ CuS ₈	1.422	0	Type-III	<i>i</i> -wave
2588	mp-36111	216 (<i>F</i> 43 <i>m</i>)	T _d (43m)	LiMgP	1.539	0	Type-III	<i>i</i> -wave
2589	mp-37405	216 (<i>F</i> 43 <i>m</i>)	T _d (43m)	Al ₅ CuSe ₈	0.505	0	Type-III	<i>i</i> -wave
2590	mp-37906	216 (<i>F</i> 43 <i>m</i>)	T _d (43m)	LiMgN	2.271	0	Type-III	<i>i</i> -wave
2591	mp-37990	216 (<i>F</i> 43 <i>m</i>)	T _d (43m)	AlPO ₄	5.459	1	Type-III	<i>i</i> -wave
2592	mp-40189	216 (<i>F</i> 43 <i>m</i>)	T _d (43m)	BaLiLaTeO ₆	2.951	1	Type-III	<i>i</i> -wave
2593	mp-406	216 (<i>F</i> 43 <i>m</i>)	T _d (43m)	CdTe	0.585	0	Type-III	<i>i</i> -wave
2594	mp-41219	216 (<i>F</i> 43 <i>m</i>)	T _d (43m)	BaLiPrTeO ₆	3.14	1	Type-III	<i>i</i> -wave
2595	mp-422	216 (<i>F</i> 43 <i>m</i>)	T _d (43m)	BeS	3.145	0	Type-III	<i>i</i> -wave
2596	mp-546633	216 (<i>F</i> 43 <i>m</i>)	T _d (43m)	KClO ₄	5.144	1	Type-III	<i>i</i> -wave
2597	mp-546711	216 (<i>F</i> 43 <i>m</i>)	T _d (43m)	CsClO ₄	5.323	0	Type-III	<i>i</i> -wave
2598	mp-550759	216 (<i>F</i> 43 <i>m</i>)	T _d (43m)	RbClO ₄	5.214	1	Type-III	<i>i</i> -wave
2599	mp-554066	216 (<i>F</i> 43 <i>m</i>)	T _d (43m)	Ba ₃ Lu ₂ Zn ₅ O ₁₁	2.289	0	Type-III	<i>i</i> -wave
2600	mp-558992	216 (<i>F</i> 43 <i>m</i>)	T _d (43m)	In ₇ GeIrO ₈	0.41	0	Type-III	<i>i</i> -wave
2601	mp-560544	216 (<i>F</i> 43 <i>m</i>)	T _d (43m)	Ba ₃ Zn ₅ In ₂ O ₁₁	1.619	0	Type-III	<i>i</i> -wave
2602	mp-567636	216 (<i>F</i> 43 <i>m</i>)	T _d (43m)	VFeSb	0.349	0	Type-III	<i>i</i> -wave
2603	mp-5967	216 (<i>F</i> 43 <i>m</i>)	T _d (43m)	TiCoSb	1.043	0	Type-III	<i>i</i> -wave
2604	mp-706657	216 (<i>F</i> 43 <i>m</i>)	T _d (43m)	Al ₁₃ Si ₅ H ₁₈ ClO ₃₈	4.269	1	Type-III	<i>i</i> -wave
2605	mp-7173	216 (<i>F</i> 43 <i>m</i>)	T _d (43m)	ScSbPt	0.644	0	Type-III	<i>i</i> -wave
2606	mp-7575	216 (<i>F</i> 43 <i>m</i>)	T _d (43m)	LiZnN	0.519	0	Type-III	<i>i</i> -wave
2607	mp-761178	216 (<i>F</i> 43 <i>m</i>)	T _d (43m)	CsMgP(H ₆ O ₅) ₂	4.825	1	Type-III	<i>i</i> -wave
2608	mp-8062	216 (<i>F</i> 43 <i>m</i>)	T _d (43m)	SiC	1.367	0	Type-III	<i>i</i> -wave
2609	mp-830	216 (<i>F</i> 43 <i>m</i>)	T _d (43m)	GaN	1.57	0	Type-III	<i>i</i> -wave
2610	mp-866291	216 (<i>F</i> 43 <i>m</i>)	T _d (43m)	AgBr	1.171	0	Type-III	<i>i</i> -wave
2611	mp-9124	216 (<i>F</i> 43 <i>m</i>)	T _d (43m)	LiZnAs	0.552	0	Type-III	<i>i</i> -wave
2612	mp-924129	216 (<i>F</i> 43 <i>m</i>)	T _d (43m)	ZrNiSn	0.495	0	Type-III	<i>i</i> -wave
2613	mp-924130	216 (<i>F</i> 43 <i>m</i>)	T _d (43m)	TiNiSn	0.453	0	Type-III	<i>i</i> -wave
2614	mp-9437	216 (<i>F</i> 43 <i>m</i>)	T _d (43m)	NbFeSb	0.514	0	Type-III	<i>i</i> -wave
2615	mp-961682	216 (<i>F</i> 43 <i>m</i>)	T _d (43m)	TiSnPd	0.204	0	Type-III	<i>i</i> -wave
2616	mp-961684	216 (<i>F</i> 43 <i>m</i>)	T _d (43m)	LiCaAs	1.877	0	Type-III	<i>i</i> -wave
2617	mp-961685	216 (<i>F</i> 43 <i>m</i>)	T _d (43m)	NaCaAs	1.582	0	Type-III	<i>i</i> -wave
2618	mp-961687	216 (<i>F</i> 43 <i>m</i>)	T _d (43m)	ZrSnPd	0.125	0	Type-III	<i>i</i> -wave
2619	mp-961693	216 (<i>F</i> 43 <i>m</i>)	T _d (43m)	ZrInAu	0.441	0	Type-III	<i>i</i> -wave
2620	mp-961706	216 (<i>F</i> 43 <i>m</i>)	T _d (43m)	TiSiPt	0.901	0	Type-III	<i>i</i> -wave
2621	mp-961711	216 (<i>F</i> 43 <i>m</i>)	T _d (43m)	ZrSiPt	1.33	0	Type-III	<i>i</i> -wave
2622	mp-961713	216 (<i>F</i> 43 <i>m</i>)	T _d (43m)	ZrSnPt	0.963	0	Type-III	<i>i</i> -wave
2623	mp-976181	216 (<i>F</i> 43 <i>m</i>)	T _d (43m)	NaBH ₄	6.587	0	Type-III	<i>i</i> -wave
2624	mp-985582	216 (<i>F</i> 43 <i>m</i>)	T _d (43m)	Li ₆ PS ₅ I	2.021	1	Type-III	<i>i</i> -wave
2625	mp-10167	217 (<i>I</i> 43 <i>m</i>)	T _d (43m)	Na ₃ SbS ₄	0	0	Type-III	<i>i</i> -wave
2626	mp-10644	217 (<i>I</i> 43 <i>m</i>)	T _d (43m)	TaTl ₃ Se ₄	2.253	0	Type-III	<i>i</i> -wave
2627	mp-14150	217 (<i>I</i> 43 <i>m</i>)	T _d (43m)	Ca ₄ Al ₆ SO ₁₆	4.668	1	Type-III	<i>i</i> -wave
2628	mp-14161	217 (<i>I</i> 43 <i>m</i>)	T _d (43m)	Sr ₄ Al ₆ SO ₁₆	4.397	1	Type-III	<i>i</i> -wave
2629	mp-14921	217 (<i>I</i> 43 <i>m</i>)	T _d (43m)	Zn ₄ B ₆ SeO ₁₂	1.857	0	Type-III	<i>i</i> -wave
2630	mp-15312	217 (<i>I</i> 43 <i>m</i>)	T _d (43m)	Ca ₄ Al ₆ TeO ₁₂	3.146	0	Type-III	<i>i</i> -wave
2631	mp-15833	217 (<i>I</i> 43 <i>m</i>)	T _d (43m)	Zn ₄ P ₆ Sn ₁₂	4.093	0	Type-III	<i>i</i> -wave
2632	mp-17862	217 (<i>I</i> 43 <i>m</i>)	T _d (43m)	Ag ₃ Ge ₅ P ₆	0.539	0	Type-III	<i>i</i> -wave
2633	mp-18062	217 (<i>I</i> 43 <i>m</i>)	T _d (43m)	Na ₁₀ YbSn ₁₂	0.681	0	Type-III	<i>i</i> -wave
2634	mp-1818	217 (<i>I</i> 43 <i>m</i>)	T _d (43m)	SiF ₄	7.717	0	Type-III	<i>i</i> -wave
2635	mp-27914	217 (<i>I</i> 43 <i>m</i>)	T _d (43m)	Na ₃ BiO ₃	2.843	0	Type-III	<i>i</i> -wave
2636	mp-28617	217 (<i>I</i> 43 <i>m</i>)	T _d (43m)	In ₃ Sb ₅ O ₁₂	2.328	1	Type-III	<i>i</i> -wave
2637	mp-2973	217 (<i>I</i> 43 <i>m</i>)	T _d (43m)	Pr ₃ Sb ₅ O ₁₂	3.168	0	Type-III	<i>i</i> -wave
2638	mp-30252	217 (<i>I</i> 43 <i>m</i>)	T _d (43m)	Na ₁₀ CaSn ₁₂	0.665	0	Type-III	<i>i</i> -wave
2639	mp-30253	217 (<i>I</i> 43 <i>m</i>)	T _d (43m)	Na ₁₀ SrSn ₁₂	0.67	0	Type-III	<i>i</i> -wave

2640	mp-31488	217 (<i>I43m</i>)	T _d (43m)	Li ₃ NbO ₄	3.776	1	Type-III	<i>i-wave</i>
2641	mp-3154	217 (<i>I43m</i>)	T _d (43m)	Sm ₃ Sb ₅ O ₁₂	3.133	0	Type-III	<i>i-wave</i>
2642	mp-3782	217 (<i>I43m</i>)	T _d (43m)	Nd ₃ Sb ₅ O ₁₂	3.155	0	Type-III	<i>i-wave</i>
2643	mp-4812	217 (<i>I43m</i>)	T _d (43m)	Zn ₄ B ₆ O ₁₃	3.413	0	Type-III	<i>i-wave</i>
2644	mp-5513	217 (<i>I43m</i>)	T _d (43m)	Tl ₃ VS ₄	1.955	0	Type-III	<i>i-wave</i>
2645	mp-555863	217 (<i>I43m</i>)	T _d (43m)	P ₄ PtF ₁₂	4.931	0	Type-III	<i>i-wave</i>
2646	mp-557537	217 (<i>I43m</i>)	T _d (43m)	Zn ₄ P ₆ N ₁₂ O	2.972	0	Type-III	<i>i-wave</i>
2647	mp-561543	217 (<i>I43m</i>)	T _d (43m)	BeF ₂	8.037	0	Type-III	<i>i-wave</i>
2648	mp-569571	217 (<i>I43m</i>)	T _d (43m)	Nb ₃ Sb ₂ Te ₅	0.845	0	Type-III	<i>i-wave</i>
2649	mp-570227	217 (<i>I43m</i>)	T _d (43m)	BeCl ₂	6.636	0	Type-III	<i>i-wave</i>
2650	mp-6137	217 (<i>I43m</i>)	T _d (43m)	Mg ₄ P ₆ SN ₁₂	4.831	0	Type-III	<i>i-wave</i>
2651	mp-7531	217 (<i>I43m</i>)	T _d (43m)	Ca ₄ Al ₆ O ₁₃	3.942	0	Type-III	<i>i-wave</i>
2652	mp-755260	217 (<i>I43m</i>)	T _d (43m)	Cd ₄ B ₆ O ₁₃	2.431	0	Type-III	<i>i-wave</i>
2653	mp-7562	217 (<i>I43m</i>)	T _d (43m)	TaTl ₃ S ₄	2.533	0	Type-III	<i>i-wave</i>
2654	mp-756935	217 (<i>I43m</i>)	T _d (43m)	Li ₃ SbO ₃	2.894	1	Type-III	<i>i-wave</i>
2655	mp-768450	217 (<i>I43m</i>)	T _d (43m)	Tm ₃ Sb ₅ O ₁₂	3.109	0	Type-III	<i>i-wave</i>
2656	mp-768483	217 (<i>I43m</i>)	T _d (43m)	Lu ₃ Sb ₅ O ₁₂	3.106	0	Type-III	<i>i-wave</i>
2657	mp-768638	217 (<i>I43m</i>)	T _d (43m)	Dy ₃ Sb ₅ O ₁₂	3.158	0	Type-III	<i>i-wave</i>
2658	mp-769004	217 (<i>I43m</i>)	T _d (43m)	Li ₃ BiO ₄	0.95	0	Type-III	<i>i-wave</i>
2659	mp-769032	217 (<i>I43m</i>)	T _d (43m)	Li ₃ NbS ₄	1.408	1	Type-III	<i>i-wave</i>
2660	mp-771762	217 (<i>I43m</i>)	T _d (43m)	Ho ₃ Sb ₅ O ₁₂	3.129	0	Type-III	<i>i-wave</i>
2661	mp-772087	217 (<i>I43m</i>)	T _d (43m)	Er ₃ Sb ₅ O ₁₂	3.117	0	Type-III	<i>i-wave</i>
2662	mp-779453	217 (<i>I43m</i>)	T _d (43m)	BaNa ₆ O ₄	1.648	0	Type-III	<i>i-wave</i>
2663	mp-8076	217 (<i>I43m</i>)	T _d (43m)	Na ₃ SbO ₃	3.087	0	Type-III	<i>i-wave</i>
2664	mp-866667	217 (<i>I43m</i>)	T _d (43m)	Li ₃ AsH ₃₆ (SeN ₃) ₄	1.862	1	Type-III	<i>i-wave</i>
2665	mp-8703	217 (<i>I43m</i>)	T _d (43m)	Na ₃ SbSe ₄	0.987	0	Type-III	<i>i-wave</i>
2666	mp-8876	217 (<i>I43m</i>)	T _d (43m)	Ca ₄ Al ₆ SO ₁₂	3.725	0	Type-III	<i>i-wave</i>
2667	mp-8877	217 (<i>I43m</i>)	T _d (43m)	Sr ₄ Al ₆ SO ₁₂	3.343	1	Type-III	<i>i-wave</i>
2668	mp-8921	217 (<i>I43m</i>)	T _d (43m)	Cd ₄ P ₆ SN ₁₂	2.99	0	Type-III	<i>i-wave</i>
2669	mp-9203	217 (<i>I43m</i>)	T _d (43m)	Al ₆ Cd ₄ SO ₁₂	2.713	0	Type-III	<i>i-wave</i>
2670	mp-9392	217 (<i>I43m</i>)	T _d (43m)	Sr ₄ Al ₆ TeO ₁₂	2.838	1	Type-III	<i>i-wave</i>
2671	mp-9535	217 (<i>I43m</i>)	T _d (43m)	Al ₆ Cd ₄ TeO ₁₂	2.565	0	Type-III	<i>i-wave</i>
2672	mp-9816	217 (<i>I43m</i>)	T _d (43m)	GeF ₄	5.501	0	Type-III	<i>i-wave</i>
2673	mp-985584	217 (<i>I43m</i>)	T _d (43m)	Na ₃ PS ₄	2.288	1	Type-III	<i>i-wave</i>
2674	mp-9911	217 (<i>I43m</i>)	T _d (43m)	K ₃ SbS ₄	2.134	0	Type-III	<i>i-wave</i>
2675	mp-1074	218 (<i>P43n</i>)	T _d (43m)	RbSi	1.349	0	Type-III	<i>i-wave</i>
2676	mp-1217	218 (<i>P43n</i>)	T _d (43m)	KSi	1.262	0	Type-III	<i>i-wave</i>
2677	mp-14001	218 (<i>P43n</i>)	T _d (43m)	Ba ₄ SiAs ₄	0.986	0	Type-III	<i>i-wave</i>
2678	mp-14002	218 (<i>P43n</i>)	T _d (43m)	Ba ₄ GeAs ₄	0.823	0	Type-III	<i>i-wave</i>
2679	mp-14213	218 (<i>P43n</i>)	T _d (43m)	Sr ₄ GeP ₄	1.053	0	Type-III	<i>i-wave</i>
2680	mp-14214	218 (<i>P43n</i>)	T _d (43m)	Ba ₄ SiP ₄	1.09	0	Type-III	<i>i-wave</i>
2681	mp-14215	218 (<i>P43n</i>)	T _d (43m)	Ba ₄ GeP ₄	1.014	0	Type-III	<i>i-wave</i>
2682	mp-14712	218 (<i>P43n</i>)	T _d (43m)	Li ₇ PN ₄	3.474	0	Type-III	<i>i-wave</i>
2683	mp-15500	218 (<i>P43n</i>)	T _d (43m)	Sr ₄ TiP ₄	1.432	0	Type-III	<i>i-wave</i>
2684	mp-15501	218 (<i>P43n</i>)	T _d (43m)	Sr ₄ TiAs ₄	1.35	0	Type-III	<i>i-wave</i>
2685	mp-15502	218 (<i>P43n</i>)	T _d (43m)	Ba ₄ TiP ₄	1.068	0	Type-III	<i>i-wave</i>
2686	mp-15503	218 (<i>P43n</i>)	T _d (43m)	Ba ₄ TiAs ₄	1.05	0	Type-III	<i>i-wave</i>
2687	mp-16793	218 (<i>P43n</i>)	T _d (43m)	Be ₃ Cd ₄ Si ₃ SeO ₁₂	2.499	0	Type-III	<i>i-wave</i>
2688	mp-17167	218 (<i>P43n</i>)	T _d (43m)	Be ₃ Cd ₄ Si ₃ TeO ₁₂	3.125	0	Type-III	<i>i-wave</i>
2689	mp-17493	218 (<i>P43n</i>)	T _d (43m)	Be ₃ Cd ₄ Si ₃ SO ₁₂	0.998	0	Type-III	<i>i-wave</i>
2690	mp-1888	218 (<i>P43n</i>)	T _d (43m)	RbGe	1.015	0	Type-III	<i>i-wave</i>
2691	mp-2146	218 (<i>P43n</i>)	T _d (43m)	KGe	0.911	0	Type-III	<i>i-wave</i>
2692	mp-23145	218 (<i>P43n</i>)	T _d (43m)	Na ₄ Al ₃ Si ₃ ClO ₁₂	4.698	0	Type-III	<i>i-wave</i>
2693	mp-23147	218 (<i>P43n</i>)	T _d (43m)	Na ₄ Al ₃ Si ₃ BrO ₁₂	4.61	0	Type-III	<i>i-wave</i>
2694	mp-23149	218 (<i>P43n</i>)	T _d (43m)	K ₄ Al ₃ Si ₃ ClO ₁₂	4.582	0	Type-III	<i>i-wave</i>
2695	mp-23420	218 (<i>P43n</i>)	T _d (43m)	Ge ₁₉ (PI) ₄	1.077	0	Type-III	<i>i-wave</i>
2696	mp-23648	218 (<i>P43n</i>)	T _d (43m)	Li ₄ Al ₃ Si ₃ ClO ₁₂	5.261	0	Type-III	<i>i-wave</i>
2697	mp-23651	218 (<i>P43n</i>)	T _d (43m)	Na ₄ Al ₃ Ge ₃ IO ₁₂	3.401	0	Type-III	<i>i-wave</i>
2698	mp-23655	218 (<i>P43n</i>)	T _d (43m)	Na ₄ Al ₃ Si ₃ IO ₁₂	4.151	0	Type-III	<i>i-wave</i>

2699	mp-23656	218 (<i>P43n</i>)	T _d (43m)	Na ₄ Ga ₃ Si ₃ ClO ₁₂	4.107	0	Type-III	<i>i</i> -wave
2700	mp-23659	218 (<i>P43n</i>)	T _d (43m)	Na ₄ Ga ₃ Si ₃ BrO ₁₂	4.051	0	Type-III	<i>i</i> -wave
2701	mp-27625	218 (<i>P43n</i>)	T _d (43m)	Ge ₁₉ (PBr) ₄	1.405	0	Type-III	<i>i</i> -wave
2702	mp-27626	218 (<i>P43n</i>)	T _d (43m)	Ge ₁₉ (AsI) ₄	1.013	0	Type-III	<i>i</i> -wave
2703	mp-29834	218 (<i>P43n</i>)	T _d (43m)	Cs ₄ SiSe ₄	2.215	0	Type-III	<i>i</i> -wave
2704	mp-30230	218 (<i>P43n</i>)	T _d (43m)	Rb ₄ SnS ₄	2.408	0	Type-III	<i>i</i> -wave
2705	mp-40226	218 (<i>P43n</i>)	T _d (43m)	Na ₄ Ga ₃ Si ₃ IO ₁₂	3.61	0	Type-III	<i>i</i> -wave
2706	mp-4825	218 (<i>P43n</i>)	T _d (43m)	Li ₇ VN ₄	2.84	0	Type-III	<i>i</i> -wave
2707	mp-534870	218 (<i>P43n</i>)	T _d (43m)	Na ₄ Ga ₃ Si ₃ B(HO ₃) ₄	4.252	0	Type-III	<i>i</i> -wave
2708	mp-554203	218 (<i>P43n</i>)	T _d (43m)	Li ₄ Ga ₃ Si ₃ ClO ₁₂	4.412	0	Type-III	<i>i</i> -wave
2709	mp-554560	218 (<i>P43n</i>)	T _d (43m)	Li ₄ Be ₃ P ₃ BrO ₁₂	6.064	0	Type-III	<i>i</i> -wave
2710	mp-554733	218 (<i>P43n</i>)	T _d (43m)	Li ₄ Al ₃ Ge ₃ BrO ₁₂	3.634	0	Type-III	<i>i</i> -wave
2711	mp-556627	218 (<i>P43n</i>)	T _d (43m)	K ₄ GeS ₄	2.713	0	Type-III	<i>i</i> -wave
2712	mp-556649	218 (<i>P43n</i>)	T _d (43m)	Li ₄ Ga ₃ Si ₃ BrO ₁₂	3.951	0	Type-III	<i>i</i> -wave
2713	mp-556886	218 (<i>P43n</i>)	T _d (43m)	Li ₄ Al ₃ Ge ₃ ClO ₁₂	4.117	0	Type-III	<i>i</i> -wave
2714	mp-557112	218 (<i>P43n</i>)	T _d (43m)	Li ₄ Ga ₃ Si ₃ IO ₁₂	3.44	0	Type-III	<i>i</i> -wave
2715	mp-557456	218 (<i>P43n</i>)	T _d (43m)	Li ₄ Al ₃ Ge ₃ IO ₁₂	3.121	0	Type-III	<i>i</i> -wave
2716	mp-559084	218 (<i>P43n</i>)	T _d (43m)	Na ₄ Al ₃ Ge ₃ BrO ₁₂	3.881	0	Type-III	<i>i</i> -wave
2717	mp-559286	218 (<i>P43n</i>)	T _d (43m)	Na ₄ Al ₃ Ge ₃ ClO ₁₂	4.083	0	Type-III	<i>i</i> -wave
2718	mp-560072	218 (<i>P43n</i>)	T _d (43m)	Li ₄ Be ₃ As ₂ ClO ₁₂	4.449	0	Type-III	<i>i</i> -wave
2719	mp-560894	218 (<i>P43n</i>)	T _d (43m)	Li ₄ Be ₃ P ₃ ClO ₁₂	6.415	0	Type-III	<i>i</i> -wave
2720	mp-568847	218 (<i>P43n</i>)	T _d (43m)	K ₄ GeSe ₄	2	0	Type-III	<i>i</i> -wave
2721	mp-571056	218 (<i>P43n</i>)	T _d (43m)	CsSn	1.137	0	Type-III	<i>i</i> -wave
2722	mp-574224	218 (<i>P43n</i>)	T _d (43m)	Cs ₄ SiTe ₄	1.837	0	Type-III	<i>i</i> -wave
2723	mp-6856	218 (<i>P43n</i>)	T _d (43m)	Be ₃ Zn ₄ Si ₃ SO ₁₂	4.203	0	Type-III	<i>i</i> -wave
2724	mp-694981	218 (<i>P43n</i>)	T _d (43m)	Na ₄ Al ₃ Si ₃ B(HO ₃) ₄	4.947	0	Type-III	<i>i</i> -wave
2725	mp-721851	218 (<i>P43n</i>)	T _d (43m)	BHO ₂	7.074	0	Type-III	<i>i</i> -wave
2726	mp-23617	219 (<i>F43c</i>)	T _d (43m)	Mg ₃ B ₇ ClO ₁₃	5.931	1	Type-III	<i>i</i> -wave
2727	mp-27189	219 (<i>F43c</i>)	T _d (43m)	Si ₃ Cl ₈	4.752	0	Type-III	<i>i</i> -wave
2728	icsd-12173	220 (<i>I43d</i>)	T _d (43m)	Ga	0	1	Type-III	<i>i</i> -wave
2729	mp-11661	220 (<i>I43d</i>)	T _d (43m)	Zr ₃ N ₄	0.686	0	Type-III	<i>i</i> -wave
2730	mp-13654	220 (<i>I43d</i>)	T _d (43m)	Y ₃ Sb ₄ Au ₃	0.575	0	Type-III	<i>i</i> -wave
2731	mp-14011	220 (<i>I43d</i>)	T _d (43m)	Al(PO ₃) ₃	5.628	0	Type-III	<i>i</i> -wave
2732	mp-17926	220 (<i>I43d</i>)	T _d (43m)	Zr ₃ Ni ₃ Sb ₄	0.434	0	Type-III	<i>i</i> -wave
2733	mp-23331	220 (<i>I43d</i>)	T _d (43m)	Si ₃ (BiO ₃) ₄	3.898	0	Type-III	<i>i</i> -wave
2734	mp-23560	220 (<i>I43d</i>)	T _d (43m)	Ge ₃ (BiO ₃) ₄	3.494	0	Type-III	<i>i</i> -wave
2735	mp-28708	220 (<i>I43d</i>)	T _d (43m)	In ₃ (PO ₄) ₂	3.069	0	Type-III	<i>i</i> -wave
2736	mp-560174	220 (<i>I43d</i>)	T _d (43m)	NaZn(PO ₃) ₃	4.82	0	Type-III	<i>i</i> -wave
2737	mp-861503	220 (<i>I43d</i>)	T _d (43m)	Pr ₃ Sb ₄ Au ₃	0.506	0	Type-III	<i>i</i> -wave
2738	mp-984350	220 (<i>I43d</i>)	T _d (43m)	Dy ₃ Sb ₄ Au ₃	0.567	0	Type-III	<i>i</i> -wave

Appendix F: Ideal chiral phonon materials

In Table S6, we present the list of ideal chiral phonon materials, which have remarkable chiral phonon bands, stable crystal structures and simple chemical formulas. These materials are the most promising candidates for future experimental studies.

In Figs. S4-S173, for each material in Table S6 we provide the phonon dispersion along the high-symmetry momentum path in the Brillouin zone. It contains projections of phonon angular momentum and phonon helicity. For the ones with three- or four-fold (screw) rotational symmetry, the pseudo angular momentum (l) along specific q -paths are also provided.

Notation about the pseudo angular momentum (l) in Figs. S4-S173: for symmorphic groups, l is an integer: $l = 0, 1, 2$ for a three-fold rotation and $l = 0, 1, 2, 3$ for a four-fold rotation. For non-symmorphic (screw) groups, l can be fractional, with $0 \leq l < 3$ for three-fold and $0 \leq l < 4$ for four-fold screw rotations. Values of l in $[0, 1]$, $(1, 2]$, $(2, 3]$ and $(3, 4)$ are shown in orange, blue, red and green, respectively, with dot sizes indicating the amplitude relative to the lower bound of each interval.

TABLE S6: The ideal chiral phonon materials on CPMDB. For each material entry, the table lists its identification number (ID) — which links to its CPMDB page - along with the space group (SG), associated point group (PG), chemical formula, and electronic band gap. If the phonon spectrum exhibits a negative (imaginary) frequency (NF) issue, NF is marked as 1; otherwise, it is 0. The final four columns specify the point group type (Type), the anisotropy characteristics of the phonon helicity pattern in the presence of time-reversal symmetry (TRS), a link to a figure of the chiral phonon spectrum for each material, and the momentum paths that possess three-fold or four-fold rotation symmetry (C_3 or C_4 , with the corresponding rotation axis given in square brackets).

#	ID	SG	PG	Material	Gap (eV)	NF	Type	Helicity	Figure	PAM
1	mp-21097	4 ($P2_1$)	C_2 (2)	KLaGeSe ₄	1.622	0	Type-II	s-wave	Fig. S4	-
2	mp-7595	19 ($P2_12_12_1$)	D_2 (222)	GeF ₂	4.060	0	Type-II	s-wave	Fig. S5	-
3	mp-542737	91 ($P4_12_2$)	D_4 (422)	TiZn ₂ O ₄	2.310	0	Type-II	s-wave	Fig. S6	$\Gamma-Z$ C_4 [0,0,1] $M-A$ C_4 [0,0,1]
4	mp-12112	92 ($P4_12_12$)	D_4 (422)	CdP ₂	1.456	0	Type-II	s-wave	Fig. S7	$\Gamma-Z$ C_4 [0,0,1] $M-A$ C_4 [0,0,1]
5	mp-2782	92 ($P4_12_12$)	D_4 (422)	ZnP ₂	1.462	0	Type-II	s-wave	Fig. S8	$\Gamma-Z$ C_4 [0,0,1] $M-A$ C_4 [0,0,1]
6	mp-3427	92 ($P4_12_12$)	D_4 (422)	LiAlO ₂	4.590	0	Type-II	s-wave	Fig. S9	$\Gamma-Z$ C_4 [0,0,1] $M-A$ C_4 [0,0,1]
7	mp-6945	92 ($P4_12_12$)	D_4 (422)	SiO ₂	5.504	0	Type-II	s-wave	Fig. S10	$\Gamma-Z$ C_4 [0,0,1] $M-A$ C_4 [0,0,1]
8	mp-7812	92 ($P4_12_12$)	D_4 (422)	GeO ₂	3.278	0	Type-II	s-wave	Fig. S11	$\Gamma-Z$ C_4 [0,0,1] $M-A$ C_4 [0,0,1]
9	mp-11025	96 ($P4_32_12$)	D_4 (422)	ZnP ₂	1.462	0	Type-II	s-wave	Fig. S12	$\Gamma-Z$ C_4 [0,0,1] $M-A$ C_4 [0,0,1]
10	mp-29816	96 ($P4_32_12$)	D_4 (422)	Ag ₂ HgO ₂	0.410	0	Type-II	s-wave	Fig. S13	$\Gamma-Z$ C_4 [0,0,1] $M-A$ C_4 [0,0,1]
11	mp-554845	96 ($P4_32_12$)	D_4 (422)	Na ₂ Zn ₂ O ₃	1.249	0	Type-II	s-wave	Fig. S14	$\Gamma-Z$ C_4 [0,0,1] $M-A$ C_4 [0,0,1]
12	mp-7029	96 ($P4_32_12$)	D_4 (422)	SiO ₂	5.508	0	Type-II	s-wave	Fig. S15	$\Gamma-Z$ C_4 [0,0,1] $M-A$ C_4 [0,0,1]
13	mp-913	96 ($P4_32_12$)	D_4 (422)	CdP ₂	1.456	0	Type-II	s-wave	Fig. S16	$\Gamma-Z$ C_4 [0,0,1] $M-A$ C_4 [0,0,1]
14	mp-33985	97 ($I42_2$)	D_4 (422)	Ba(InTe ₂) ₂	0.864	0	Type-II	s-wave	Fig. S17	$\Gamma-M_1$ C_4 [1,1,0]
15	mp-37091	97 ($I42_2$)	D_4 (422)	Sr(AlTe ₂) ₂	1.445	0	Type-II	s-wave	Fig. S18	$\Gamma-M_1$ C_4 [1,1,0]
16	mp-38117	97 ($I42_2$)	D_4 (422)	Ba(GaTe ₂) ₂	0.529	0	Type-II	s-wave	Fig. S19	$\Gamma-M_1$ C_4 [1,1,0]
17	mp-38394	97 ($I42_2$)	D_4 (422)	Ba(AlTe ₂) ₂	1.505	0	Type-II	s-wave	Fig. S20	$\Gamma-M_1$ C_4 [1,1,0]
18	icsd-16037	98 ($I4_12_2$)	D_4 (422)	CdAs ₂	0.3297	0	Type-II	s-wave	Fig. S21	$\Gamma-M_1$ C_4 [1,1,0]
19	mp-38975	145 ($P3_2$)	C_3 (3)	PNO	5.132	0	Type-II	s-wave	Fig. S22	$\Gamma-A$ C_3 [0,0,1]

										$K-H C_3 [0,0,1]$
20	mp-4829	150 ($P3_21$)	D ₃ (32)	Na ₂ ThF ₆	6.474	0	Type-II	s-wave	Fig. S23	$\Gamma-A C_3 [0,0,1]$ $K-H C_3 [0,0,1]$
21	mp-11653	152 ($P3_121$)	D ₃ (32)	BPO ₄	6.998	0	Type-II	s-wave	Fig. S24	$\Gamma-A C_3 [0,0,1]$ $K-H C_3 [0,0,1]$
22	mp-11654	152 ($P3_121$)	D ₃ (32)	BAsO ₄	3.876	0	Type-II	s-wave	Fig. S25	$\Gamma-A C_3 [0,0,1]$ $K-H C_3 [0,0,1]$
23	mp-15951	152 ($P3_121$)	D ₃ (32)	BeF ₂	8.320	0	Type-II	s-wave	Fig. S26	$\Gamma-A C_3 [0,0,1]$ $K-H C_3 [0,0,1]$
24	mp-17947	152 ($P3_121$)	D ₃ (32)	BaCu ₂ GeS ₄	0.974	0	Type-II	s-wave	Fig. S27	$\Gamma-A C_3 [0,0,1]$ $K-H C_3 [0,0,1]$
25	mp-306	152 ($P3_121$)	D ₃ (32)	B ₂ O ₃	6.302	0	Type-II	s-wave	Fig. S28	$\Gamma-A C_3 [0,0,1]$ $K-H C_3 [0,0,1]$
26	mp-3996	152 ($P3_121$)	D ₃ (32)	GaAsO ₄	3.069	0	Type-II	s-wave	Fig. S29	$\Gamma-A C_3 [0,0,1]$ $K-H C_3 [0,0,1]$
27	mp-4236	152 ($P3_121$)	D ₃ (32)	BaZnO ₂	2.272	0	Type-II	s-wave	Fig. S30	$\Gamma-A C_3 [0,0,1]$ $K-H C_3 [0,0,1]$
28	mp-5189	152 ($P3_121$)	D ₃ (32)	AlAsO ₄	3.865	0	Type-II	s-wave	Fig. S31	$\Gamma-A C_3 [0,0,1]$ $K-H C_3 [0,0,1]$
29	mp-634	152 ($P3_121$)	D ₃ (32)	HgS	1.708	0	Type-II	s-wave	Fig. S32	$\Gamma-A C_3 [0,0,1]$ $K-H C_3 [0,0,1]$
30	mp-7000	152 ($P3_121$)	D ₃ (32)	SiO ₂	5.719	0	Type-II	s-wave	Fig. S33	$\Gamma-A C_3 [0,0,1]$ $K-H C_3 [0,0,1]$
31	mp-733	152 ($P3_121$)	D ₃ (32)	GeO ₂	3.250	0	Type-II	s-wave	Fig. S34	$\Gamma-A C_3 [0,0,1]$ $K-H C_3 [0,0,1]$
32	mp-756018	152 ($P3_121$)	D ₃ (32)	BaMgO ₂	3.160	0	Type-II	s-wave	Fig. S35	$\Gamma-A C_3 [0,0,1]$ $K-H C_3 [0,0,1]$
33	mp-7826	152 ($P3_121$)	D ₃ (32)	HgO	1.310	0	Type-II	s-wave	Fig. S36	$\Gamma-A C_3 [0,0,1]$ $K-H C_3 [0,0,1]$
34	icsd-22251	152 ($P3_121$)	D ₃ (32)	Se	0.9858	0	Type-II	s-wave	Fig. S37	$\Gamma-A C_3 [0,0,1]$ $K-H C_3 [0,0,1]$
35	icsd-23059	152 ($P3_121$)	D ₃ (32)	Te	0	0	Type-II	s-wave	Fig. S38	$\Gamma-A C_3 [0,0,1]$ $K-H C_3 [0,0,1]$
36	mp-15074	154 ($P3_221$)	D ₃ (32)	Sr(PIr) ₂	0.442	0	Type-II	s-wave	Fig. S39	$\Gamma-A C_3 [0,0,1]$ $K-H C_3 [0,0,1]$
37	mp-17756	154 ($P3_221$)	D ₃ (32)	RbAg ₂ SbS ₄	0.618	0	Type-II	s-wave	Fig. S40	$\Gamma-A C_3 [0,0,1]$ $K-H C_3 [0,0,1]$
38	mp-223	154 ($P3_221$)	D ₃ (32)	GeO ₂	3.249	0	Type-II	s-wave	Fig. S41	$\Gamma-A C_3 [0,0,1]$ $K-H C_3 [0,0,1]$
39	mp-555818	154 ($P3_221$)	D ₃ (32)	Cu ₂ SiPbS ₄	1.343	0	Type-II	s-wave	Fig. S42	$\Gamma-A C_3 [0,0,1]$ $K-H C_3 [0,0,1]$
40	mp-9252	154 ($P3_221$)	D ₃ (32)	HgS	1.686	0	Type-II	s-wave	Fig. S43	$\Gamma-A C_3 [0,0,1]$ $K-H C_3 [0,0,1]$
41	icsd-18172	154 ($P3_221$)	D ₃ (32)	SiO ₂	5.9962	0	Type-II	s-wave	Fig. S44	$\Gamma-A C_3 [0,0,1]$ $K-H C_3 [0,0,1]$
42	mp-546546	155 ($R3_2$)	D ₃ (32)	SiO ₂	5.560	0	Type-II	s-wave	Fig. S45	$T-\Gamma C_3 [1,1,1]$
43	mp-2654	169 ($P6_1$)	C ₆ (6)	Al ₂ S ₃	2.817	0	Type-II	s-wave	Fig. S46	$\Gamma-A C_3 [0,0,1]$ $K-H C_3 [0,0,1]$
44	mp-504482	169 ($P6_1$)	C ₆ (6)	AlInS ₃	2.081	0	Type-II	s-wave	Fig. S47	$\Gamma-A C_3 [0,0,1]$ $K-H C_3 [0,0,1]$
45	mp-504951	169 ($P6_1$)	C ₆ (6)	InGaS ₃	2.094	0	Type-II	s-wave	Fig. S48	$\Gamma-A C_3 [0,0,1]$

										$K-H C_3 [0,0,1]$
46	mp-612740	169 ($P6_1$)	C ₆ (6)	In ₂ Se ₃	0.990	0	Type-II	s-wave	Fig. S49	$\Gamma-A C_3 [0,0,1]$ $K-H C_3 [0,0,1]$
47	mp-15573	173 ($P6_3$)	C ₆ (6)	Tl ₃ AsO ₄	2.584	0	Type-II	s-wave	Fig. S50	$\Gamma-A C_3 [0,0,1]$ $K-H C_3 [0,0,1]$
48	mp-942	178 ($P6_122$)	D ₆ (622)	AuF ₃	1.554	0	Type-II	s-wave	Fig. S51	$\Gamma-A C_3 [0,0,1]$ $K-H C_3 [0,0,1]$
49	mp-14190	180 ($P6_222$)	D ₆ (622)	NdPO ₄	5.309	0	Type-II	s-wave	Fig. S52	$\Gamma-A C_3 [0,0,1]$ $K-H C_3 [0,0,1]$
50	mp-558713	180 ($P6_222$)	D ₆ (622)	LiAlSiO ₄	4.694	0	Type-II	s-wave	Fig. S53	$\Gamma-A C_3 [0,0,1]$ $K-H C_3 [0,0,1]$
51	mp-6922	180 ($P6_222$)	D ₆ (622)	SiO ₂	5.531	1	Type-II	s-wave	Fig. S54	$\Gamma-A C_3 [0,0,1]$ $K-H C_3 [0,0,1]$
52	icsd-638946	180 ($P6_222$)	D ₆ (622)	HfSn ₂	0	0	Type-II	s-wave	Fig. S55	$\Gamma-A C_3 [0,0,1]$ $K-H C_3 [0,0,1]$
53	mp-2488	198 ($P2_{1}3$)	T (23)	SiOs	0.512	0	Type-II	s-wave	Fig. S56	$\Gamma-R C_3 [1,1,1]$
54	mp-756361	198 ($P2_{1}3$)	T (23)	ZrSeO	1.957	0	Type-II	s-wave	Fig. S57	$\Gamma-R C_3 [1,1,1]$
55	mp-7787	198 ($P2_{1}3$)	T (23)	HfSO	2.869	0	Type-II	s-wave	Fig. S58	$\Gamma-R C_3 [1,1,1]$
56	icsd-633543	198 ($P2_{1}3$)	T (23)	FeSi	0.1096	0	Type-II	s-wave	Fig. S59	$\Gamma-R C_3 [1,1,1]$
57	mp-675286	42 ($Fmm2$)	C _{2v} (mm2)	Ca ₃ UN ₄	1.369	0	Type-III	d-wave	Fig. S60	-
58	mp-22607	82 ($I\bar{4}$)	S ₄ ($\bar{4}$)	Zn(InSe ₂) ₂	0.993	0	Type-III	d-wave	Fig. S61	-
59	mp-33449	82 ($I\bar{4}$)	S ₄ ($\bar{4}$)	Tb ₅ AgS ₈	1.705	0	Type-III	d-wave	Fig. S62	-
60	mp-35512	82 ($I\bar{4}$)	S ₄ ($\bar{4}$)	Dy ₅ AgS ₈	1.732	0	Type-III	d-wave	Fig. S63	-
61	mp-37923	82 ($I\bar{4}$)	S ₄ ($\bar{4}$)	Sm ₅ AgS ₈	1.638	0	Type-III	d-wave	Fig. S64	-
62	mp-38442	82 ($I\bar{4}$)	S ₄ ($\bar{4}$)	CsNd ₅ Se ₈	1.622	0	Type-III	d-wave	Fig. S65	-
63	mp-4452	82 ($I\bar{4}$)	S ₄ ($\bar{4}$)	Cd(GaS ₂) ₂	2.120	0	Type-III	d-wave	Fig. S66	-
64	mp-4730	82 ($I\bar{4}$)	S ₄ ($\bar{4}$)	Ga ₂ HgSe ₄	0.917	0	Type-III	d-wave	Fig. S67	-
65	mp-4809	82 ($I\bar{4}$)	S ₄ ($\bar{4}$)	Ga ₂ HgS ₄	1.571	0	Type-III	d-wave	Fig. S68	-
66	mp-770481	82 ($I\bar{4}$)	S ₄ ($\bar{4}$)	Ta ₉ PO ₂₅	2.703	0	Type-III	d-wave	Fig. S69	-
67	mp-7907	82 ($I\bar{4}$)	S ₄ ($\bar{4}$)	Al ₂ ZnSe ₄	2.153	0	Type-III	d-wave	Fig. S70	-
68	mp-7908	82 ($I\bar{4}$)	S ₄ ($\bar{4}$)	Al ₂ ZnTe ₄	1.625	0	Type-III	d-wave	Fig. S71	-
69	mp-7909	82 ($I\bar{4}$)	S ₄ ($\bar{4}$)	Al ₂ CdTe ₄	1.625	0	Type-III	d-wave	Fig. S72	-
70	mp-8874	82 ($I\bar{4}$)	S ₄ ($\bar{4}$)	LiSiBO ₄	6.431	0	Type-III	d-wave	Fig. S73	-
71	mp-568032	111 ($P\bar{4}2m$)	D _{2d} ($\bar{4}2m$)	Cd(InSe ₂) ₂	0.871	0	Type-III	d-wave	Fig. S74	-
72	mp-22993	121 ($I\bar{4}2m$)	D _{2d} ($\bar{4}2m$)	AgClO ₄	2.676	0	Type-III	d-wave	Fig. S75	-
73	mp-38103	121 ($I\bar{4}2m$)	D _{2d} ($\bar{4}2m$)	NaClO ₄	5.304	0	Type-III	d-wave	Fig. S76	-
74	mp-867699	121 ($I\bar{4}2m$)	D _{2d} ($\bar{4}2m$)	Li ₄ TiS ₄	2.474	0	Type-III	d-wave	Fig. S77	-
75	mp-34011	122 ($I\bar{4}2d$)	D _{2d} ($\bar{4}2m$)	Ca(HoS ₂) ₂	2.191	0	Type-III	d-wave	Fig. S78	-
76	mp-35787	122 ($I\bar{4}2d$)	D _{2d} ($\bar{4}2m$)	Ca(DyS ₂) ₂	2.166	0	Type-III	d-wave	Fig. S79	-
77	mp-3668	122 ($I\bar{4}2d$)	D _{2d} ($\bar{4}2m$)	CdGeP ₂	0.646	0	Type-III	d-wave	Fig. S80	-
78	mp-38240	122 ($I\bar{4}2d$)	D _{2d} ($\bar{4}2m$)	Sr(PrS ₂) ₂	2.095	0	Type-III	d-wave	Fig. S81	-
79	mp-4175	122 ($I\bar{4}2d$)	D _{2d} ($\bar{4}2m$)	ZnSnP ₂	0.704	0	Type-III	d-wave	Fig. S82	-
80	mp-4524	122 ($I\bar{4}2d$)	D _{2d} ($\bar{4}2m$)	ZnGeP ₂	1.178	0	Type-III	d-wave	Fig. S83	-
81	mp-4666	122 ($I\bar{4}2d$)	D _{2d} ($\bar{4}2m$)	CdSiP ₂	1.426	0	Type-III	d-wave	Fig. S84	-
82	mp-4763	122 ($I\bar{4}2d$)	D _{2d} ($\bar{4}2m$)	ZnSiP ₂	1.364	0	Type-III	d-wave	Fig. S85	-
83	mp-675244	122 ($I\bar{4}2d$)	D _{2d} ($\bar{4}2m$)	Yb(NdS ₂) ₂	2.039	0	Type-III	d-wave	Fig. S86	-
84	mp-675293	122 ($I\bar{4}2d$)	D _{2d} ($\bar{4}2m$)	Yb(YS ₂) ₂	2.128	0	Type-III	d-wave	Fig. S87	-
85	mp-675406	122 ($I\bar{4}2d$)	D _{2d} ($\bar{4}2m$)	Yb(HoS ₂) ₂	2.172	0	Type-III	d-wave	Fig. S88	-
86	mp-675458	122 ($I\bar{4}2d$)	D _{2d} ($\bar{4}2m$)	La ₂ Te ₄ Pb	1.249	0	Type-III	d-wave	Fig. S89	-
87	mp-675511	122 ($I\bar{4}2d$)	D _{2d} ($\bar{4}2m$)	Sm ₂ PbS ₄	2.026	0	Type-III	d-wave	Fig. S90	-

88	mp-675677	122 ($I\bar{4}2d$)	D_{2d} ($\bar{4}2m$)	$Yb(SmS_2)_2$	2.058	0	Type-III	d -wave	Fig. S91	-
89	mp-6081	100 ($P4bm$)	C_{4v} (4mm)	$Ba_2Ti(SiO_4)_2$	3.727	0	Type-III	g -wave	Fig. S92	-
90	mp-545359	107 ($I4mm$)	C_{4v} (4mm)	KNa_2CuO_2	1.514	0	Type-III	g -wave	Fig. S93	-
91	mp-27255	109 ($I4_1md$)	C_{4v} (4mm)	Ga_2TeS_2	2.020	0	Type-III	g -wave	Fig. S94	-
92	mp-28423	109 ($I4_1md$)	C_{4v} (4mm)	Ga_2TeSe_2	1.614	0	Type-III	g -wave	Fig. S95	-
93	mp-760402	109 ($I4_1md$)	C_{4v} (4mm)	$TaRhO_4$	0.971	0	Type-III	g -wave	Fig. S96	-
94	icsd-81493	109 ($I4_1md$)	C_{4v} (4mm)	NbP	0	0	Type-III	g -wave	Fig. S97	-
95	mp-567713	156 ($P3m1$)	C_{3v} (3m)	Nb_3TeI_7	0.480	0	Type-III	g -wave	Fig. S98	$K-H$ C ₃ [0,0,1]
96	mp-2245	159 ($P31c$)	C_{3v} (3m)	Si_3N_4	4.655	0	Type-III	g -wave	Fig. S99	-
97	mp-11342	160 ($R3m$)	C_{3v} (3m)	GaSe	1.223	0	Type-III	g -wave	Fig. S100	-
98	mp-1434	160 ($R3m$)	C_{3v} (3m)	MoS_2	1.204	0	Type-III	g -wave	Fig. S101	-
99	mp-22691	160 ($R3m$)	C_{3v} (3m)	InSe	1.786	0	Type-III	g -wave	Fig. S102	-
100	mp-22981	160 ($R3m$)	C_{3v} (3m)	$TlIO_3$	2.763	0	Type-III	g -wave	Fig. S103	-
101	mp-23162	160 ($R3m$)	C_{3v} (3m)	$ZrCl_2$	0.848	0	Type-III	g -wave	Fig. S104	-
102	mp-36582	160 ($R3m$)	C_{3v} (3m)	NaHS	3.147	0	Type-III	g -wave	Fig. S105	-
103	mp-38011	160 ($R3m$)	C_{3v} (3m)	KHS	3.225	0	Type-III	g -wave	Fig. S106	-
104	mp-7581	160 ($R3m$)	C_{3v} (3m)	$MoSe_2$	1.362	0	Type-III	g -wave	Fig. S107	-
105	icsd-24315	160 ($R3m$)	C_{3v} (3m)	TaSe ₂	0	0	Type-III	g -wave	Fig. S108	-
106	icsd-38401	160 ($R3m$)	C_{3v} (3m)	MoS_2	1.21	0	Type-III	g -wave	Fig. S109	-
107	mp-754009	161 ($R3c$)	C_{3v} (3m)	$ScBiO_3$	3.083	0	Type-III	g -wave	Fig. S110	-
108	mp-754323	161 ($R3c$)	C_{3v} (3m)	$TmBiO_3$	3.113	0	Type-III	g -wave	Fig. S111	-
109	mp-754943	161 ($R3c$)	C_{3v} (3m)	$ErBiO_3$	3.114	0	Type-III	g -wave	Fig. S112	-
110	mp-768221	161 ($R3c$)	C_{3v} (3m)	$YBiO_3$	3.075	0	Type-III	g -wave	Fig. S113	-
111	mp-768310	161 ($R3c$)	C_{3v} (3m)	$LaBiO_3$	3.070	0	Type-III	g -wave	Fig. S114	-
112	mp-989552	161 ($R3c$)	C_{3v} (3m)	$LaMoN_3$	1.151	0	Type-III	g -wave	Fig. S115	-
113	mp-13978	189 ($P\bar{6}2m$)	D_{3h} ($\bar{6}m2$)	Rb_2ThF_6	6.273	0	Type-III	g -wave	Fig. S116	-
114	mp-14193	189 ($P\bar{6}2m$)	D_{3h} ($\bar{6}m2$)	K_2ThF_6	6.381	0	Type-III	g -wave	Fig. S117	-
115	mp-9732	189 ($P\bar{6}2m$)	D_{3h} ($\bar{6}m2$)	BaNaP	0.856	0	Type-III	g -wave	Fig. S118	-
116	mp-9775	189 ($P\bar{6}2m$)	D_{3h} ($\bar{6}m2$)	NaSrAs	0.807	0	Type-III	g -wave	Fig. S119	-
117	mp-1039	186 ($P6_3mc$)	C_{6v} (6mm)	MgTe	2.361	0	Type-III	i -wave	Fig. S120	-
118	mp-2133	186 ($P6_3mc$)	C_{6v} (6mm)	ZnO	0.723	0	Type-III	i -wave	Fig. S121	-
119	mp-23326	186 ($P6_3mc$)	C_{6v} (6mm)	Ca_4Cl_6O	5.224	0	Type-III	i -wave	Fig. S122	-
120	mp-2542	186 ($P6_3mc$)	C_{6v} (6mm)	BeO	7.464	0	Type-III	i -wave	Fig. S123	-
121	mp-380	186 ($P6_3mc$)	C_{6v} (6mm)	ZnSe	1.200	0	Type-III	i -wave	Fig. S124	-
122	mp-560588	186 ($P6_3mc$)	C_{6v} (6mm)	ZnS	2.070	0	Type-III	i -wave	Fig. S125	-
123	mp-567290	186 ($P6_3mc$)	C_{6v} (6mm)	LaN	1.117	0	Type-III	i -wave	Fig. S126	-
124	mp-570935	186 ($P6_3mc$)	C_{6v} (6mm)	LiI	4.382	0	Type-III	i -wave	Fig. S127	-
125	mp-661	186 ($P6_3mc$)	C_{6v} (6mm)	AlN	4.047	0	Type-III	i -wave	Fig. S128	-
126	mp-672	186 ($P6_3mc$)	C_{6v} (6mm)	CdS	1.125	0	Type-III	i -wave	Fig. S129	-
127	mp-7140	186 ($P6_3mc$)	C_{6v} (6mm)	SiC	2.303	0	Type-III	i -wave	Fig. S130	-
128	mp-804	186 ($P6_3mc$)	C_{6v} (6mm)	GaN	1.726	0	Type-III	i -wave	Fig. S131	-
129	mp-8075	186 ($P6_3mc$)	C_{6v} (6mm)	$NaBe_4SbO_7$	3.386	0	Type-III	i -wave	Fig. S132	-
130	mp-8389	186 ($P6_3mc$)	C_{6v} (6mm)	Na_6ZnS_4	2.158	0	Type-III	i -wave	Fig. S133	-
131	mp-8880	186 ($P6_3mc$)	C_{6v} (6mm)	AlP	1.953	0	Type-III	i -wave	Fig. S134	-
132	mp-8881	186 ($P6_3mc$)	C_{6v} (6mm)	AlAs	1.687	0	Type-III	i -wave	Fig. S135	-
133	mp-8882	186 ($P6_3mc$)	C_{6v} (6mm)	GaP	1.300	0	Type-III	i -wave	Fig. S136	-
134	mp-8884	186 ($P6_3mc$)	C_{6v} (6mm)	ZnTe	1.100	0	Type-III	i -wave	Fig. S137	-
135	mp-9575	186 ($P6_3mc$)	C_{6v} (6mm)	LiBeSb	0.873	0	Type-III	i -wave	Fig. S138	-
136	mp-976280	186 ($P6_3mc$)	C_{6v} (6mm)	LiBr	4.935	0	Type-III	i -wave	Fig. S139	-

137	icsd-154187	186 ($P6_3mc$)	C_{6v} (6mm)	CdS	1.2923	0	Type-III	<i>i</i> -wave	Fig. S140	-
138	icsd-41482	186 ($P6_3mc$)	C_{6v} (6mm)	AlN	4.2156	0	Type-III	<i>i</i> -wave	Fig. S141	-
139	icsd-43595	186 ($P6_3mc$)	C_{6v} (6mm)	ZnSe	1.2037	0	Type-III	<i>i</i> -wave	Fig. S142	-
140	icsd-56553	186 ($P6_3mc$)	C_{6v} (6mm)	AgI	1.2912	0	Type-III	<i>i</i> -wave	Fig. S143	-
141	icsd-62727	186 ($P6_3mc$)	C_{6v} (6mm)	BeO	7.6003	0	Type-III	<i>i</i> -wave	Fig. S144	-
142	icsd-620415	186 ($P6_3mc$)	C_{6v} (6mm)	CdSe	0.5929	0	Type-III	<i>i</i> -wave	Fig. S145	-
143	mp-9295	215 ($P\bar{4}3m$)	T_d ($\bar{4}3m$)	TaCu ₃ Te ₄	1.141	0	Type-III	<i>i</i> -wave	Fig. S146	-
144	mp-10623	216 ($F\bar{4}3m$)	T_d ($\bar{4}3m$)	ThSbRh	0.744	0	Type-III	<i>i</i> -wave	Fig. S147	-
145	mp-12558	216 ($F\bar{4}3m$)	T_d ($\bar{4}3m$)	LiMgAs	1.372	0	Type-III	<i>i</i> -wave	Fig. S148	-
146	mp-16327	216 ($F\bar{4}3m$)	T_d ($\bar{4}3m$)	DySbPt	0.049	0	Type-III	<i>i</i> -wave	Fig. S149	-
147	mp-16329	216 ($F\bar{4}3m$)	T_d ($\bar{4}3m$)	ErSbPt	0.000	0	Type-III	<i>i</i> -wave	Fig. S150	-
148	mp-16376	216 ($F\bar{4}3m$)	T_d ($\bar{4}3m$)	HoSbPt	0.000	0	Type-III	<i>i</i> -wave	Fig. S151	-
149	mp-19886	216 ($F\bar{4}3m$)	T_d ($\bar{4}3m$)	ThSnPt	0.674	0	Type-III	<i>i</i> -wave	Fig. S152	-
150	mp-22914	216 ($F\bar{4}3m$)	T_d ($\bar{4}3m$)	CuCl	0.565	0	Type-III	<i>i</i> -wave	Fig. S153	-
151	mp-27608	216 ($F\bar{4}3m$)	T_d ($\bar{4}3m$)	Be ₄ TeO ₇	1.281	0	Type-III	<i>i</i> -wave	Fig. S154	-
152	mp-30847	216 ($F\bar{4}3m$)	T_d ($\bar{4}3m$)	TiSnPt	0.791	0	Type-III	<i>i</i> -wave	Fig. S155	-
153	mp-31454	216 ($F\bar{4}3m$)	T_d ($\bar{4}3m$)	TaSbRu	0.665	0	Type-III	<i>i</i> -wave	Fig. S156	-
154	mp-36111	216 ($F\bar{4}3m$)	T_d ($\bar{4}3m$)	LiMgP	1.539	0	Type-III	<i>i</i> -wave	Fig. S157	-
155	mp-567636	216 ($F\bar{4}3m$)	T_d ($\bar{4}3m$)	VFeSb	0.349	0	Type-III	<i>i</i> -wave	Fig. S158	-
156	mp-7173	216 ($F\bar{4}3m$)	T_d ($\bar{4}3m$)	ScSbPt	0.644	0	Type-III	<i>i</i> -wave	Fig. S159	-
157	mp-866291	216 ($F\bar{4}3m$)	T_d ($\bar{4}3m$)	AgBr	1.171	0	Type-III	<i>i</i> -wave	Fig. S160	-
158	mp-924129	216 ($F\bar{4}3m$)	T_d ($\bar{4}3m$)	ZrNiSn	0.495	0	Type-III	<i>i</i> -wave	Fig. S161	-
159	mp-924130	216 ($F\bar{4}3m$)	T_d ($\bar{4}3m$)	TiNiSn	0.453	0	Type-III	<i>i</i> -wave	Fig. S162	-
160	mp-961684	216 ($F\bar{4}3m$)	T_d ($\bar{4}3m$)	LiCaAs	1.877	0	Type-III	<i>i</i> -wave	Fig. S163	-
161	mp-961685	216 ($F\bar{4}3m$)	T_d ($\bar{4}3m$)	NaCaAs	1.582	0	Type-III	<i>i</i> -wave	Fig. S164	-
162	mp-961693	216 ($F\bar{4}3m$)	T_d ($\bar{4}3m$)	ZrInAu	0.441	0	Type-III	<i>i</i> -wave	Fig. S165	-
163	mp-961713	216 ($F\bar{4}3m$)	T_d ($\bar{4}3m$)	ZrSnPt	0.963	0	Type-III	<i>i</i> -wave	Fig. S166	-
164	icsd-43714	216 ($F\bar{4}3m$)	T_d ($\bar{4}3m$)	HgTe	0	0	Type-III	<i>i</i> -wave	Fig. S167	-
165	icsd-60378	216 ($F\bar{4}3m$)	T_d ($\bar{4}3m$)	ZnS	2.0832	0	Type-III	<i>i</i> -wave	Fig. S168	-
166	mp-561543	217 ($I\bar{4}3m$)	T_d ($\bar{4}3m$)	BeF ₂	8.037	0	Type-III	<i>i</i> -wave	Fig. S169	-
167	mp-8703	217 ($I\bar{4}3m$)	T_d ($\bar{4}3m$)	Na ₃ SbSe ₄	0.987	0	Type-III	<i>i</i> -wave	Fig. S170	-
168	mp-9911	217 ($I\bar{4}3m$)	T_d ($\bar{4}3m$)	K ₃ SbS ₄	2.134	0	Type-III	<i>i</i> -wave	Fig. S171	-
169	mp-23420	218 ($P\bar{4}3n$)	T_d ($\bar{4}3m$)	Ge ₁₉ (PI) ₄	1.077	0	Type-III	<i>i</i> -wave	Fig. S172	-
170	mp-27625	218 ($P\bar{4}3n$)	T_d ($\bar{4}3m$)	Ge ₁₉ (PBr) ₄	1.405	0	Type-III	<i>i</i> -wave	Fig. S173	-

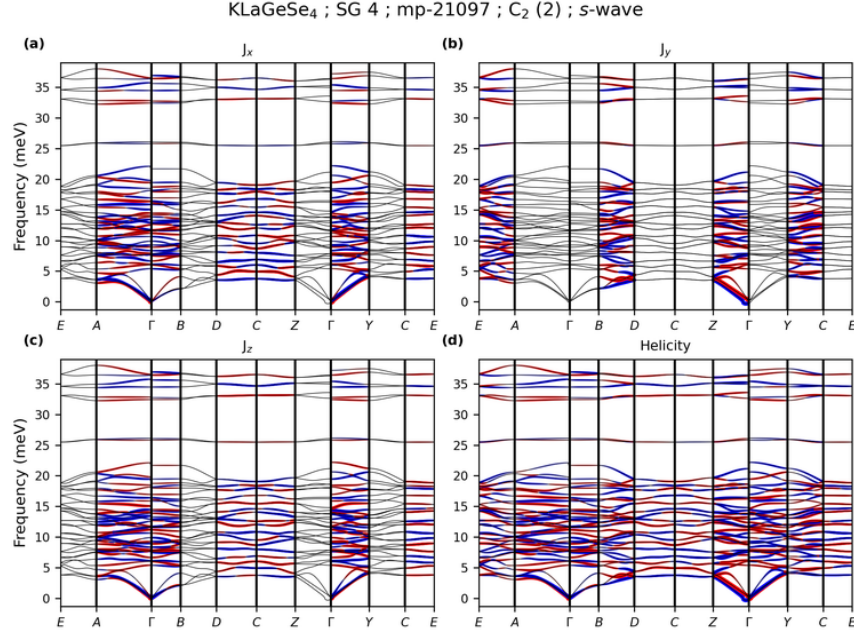


FIG. S4. Phonon dispersion of KLaGeSe₄ (mp-21097) along the specific momentum paths in the Brillouin zone of SG 4 (see Table S7). (a-c) Projections of the phonon angular momentum components J_x , J_y , and J_z onto the dispersion. (d) Projection of the phonon helicity onto the dispersion. In (a-d), red (blue) dots denote positive (negative) angular momentum or helicity, and their size is proportional to the magnitude.

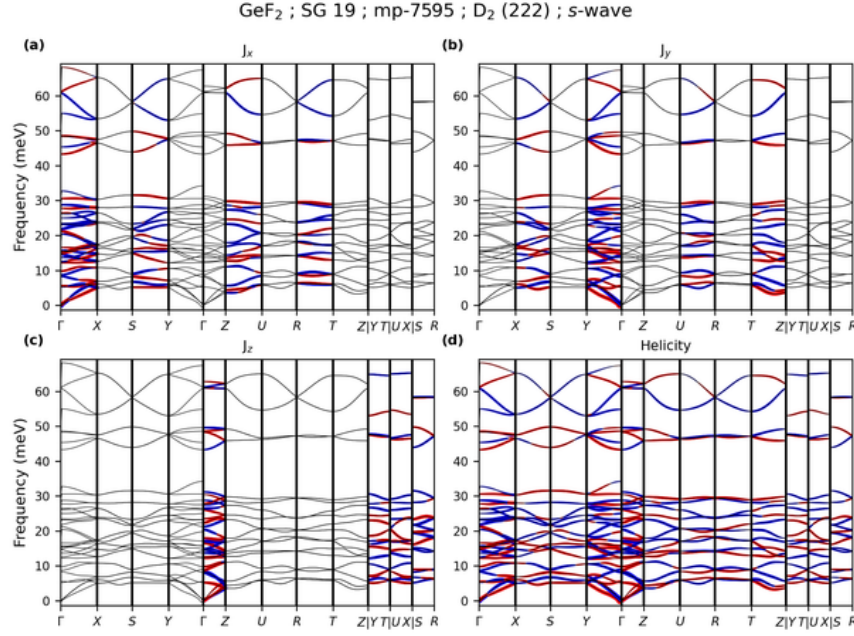


FIG. S5. Phonon dispersion of GeF₂ (mp-7595) along the specific momentum paths in the Brillouin zone of SG 19 (see Table S8). (a-c) Projections of the phonon angular momentum components J_x , J_y , and J_z onto the dispersion. (d) Projection of the phonon helicity onto the dispersion. In (a-d), red (blue) dots denote positive (negative) angular momentum or helicity, and their size is proportional to the magnitude.

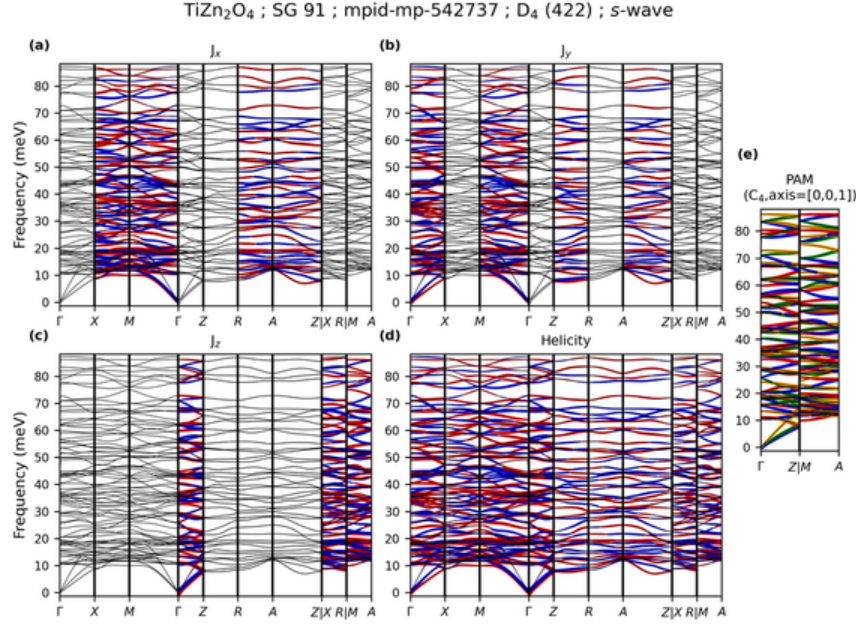


FIG. S6. Phonon dispersion of TiZn₂O₄ ([mp-542737](#)) along the specific momentum paths in the Brillouin zone of SG 91 (see Table S11). (a-c) Projections of the phonon angular momentum components J_x , J_y , and J_z onto the dispersion. (d) Projection of the phonon helicity onto the dispersion. In (a-d), red (blue) dots denote positive (negative) angular momentum or helicity, and their size is proportional to the magnitude. (e) Pseudo-angular momentum (PAM) calculated along high-symmetry paths exhibiting three- or four-fold (screw) rotational symmetry. See more descriptions about the PAM in (e).

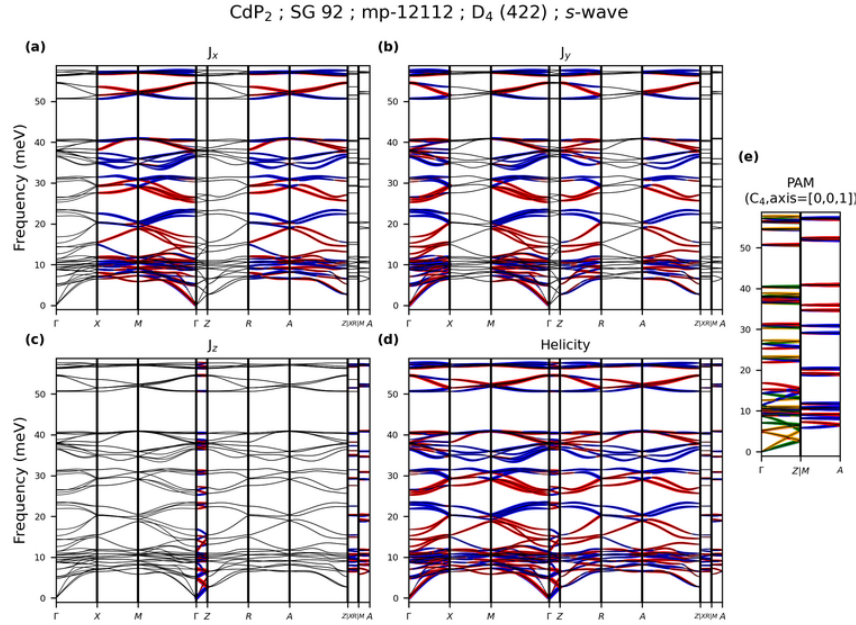


FIG. S7. Phonon dispersion of CdP₂ ([mp-12112](#)) along the specific momentum paths in the Brillouin zone of SG 92 (see Table S12). (a-c) Projections of the phonon angular momentum components J_x , J_y , and J_z onto the dispersion. (d) Projection of the phonon helicity onto the dispersion. In (a-d), red (blue) dots denote positive (negative) angular momentum or helicity, and their size is proportional to the magnitude. (e) Pseudo-angular momentum (PAM) calculated along high-symmetry paths exhibiting three- or four-fold (screw) rotational symmetry. See more descriptions about the PAM in (e).

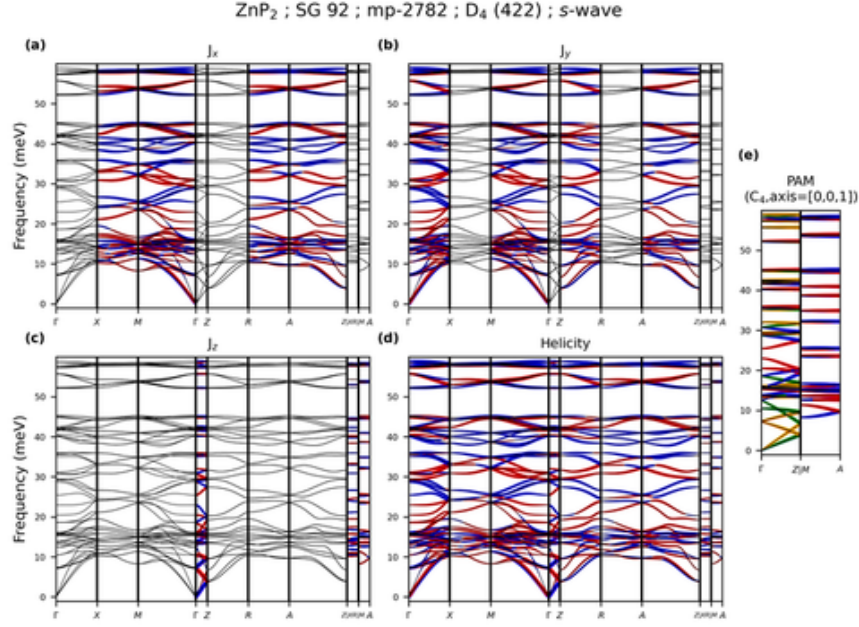


FIG. S8. Phonon dispersion of ZnP₂ (mp-2782) along the specific momentum paths in the Brillouin zone of SG 92 (see Table S12). (a-c) Projections of the phonon angular momentum components J_x , J_y , and J_z onto the dispersion. (d) Projection of the phonon helicity onto the dispersion. In (a-d), red (blue) dots denote positive (negative) angular momentum or helicity, and their size is proportional to the magnitude. (e) Pseudo-angular momentum (PAM) calculated along high-symmetry paths exhibiting three- or four-fold (screw) rotational symmetry. [See more descriptions about the PAM in \(e\).](#)

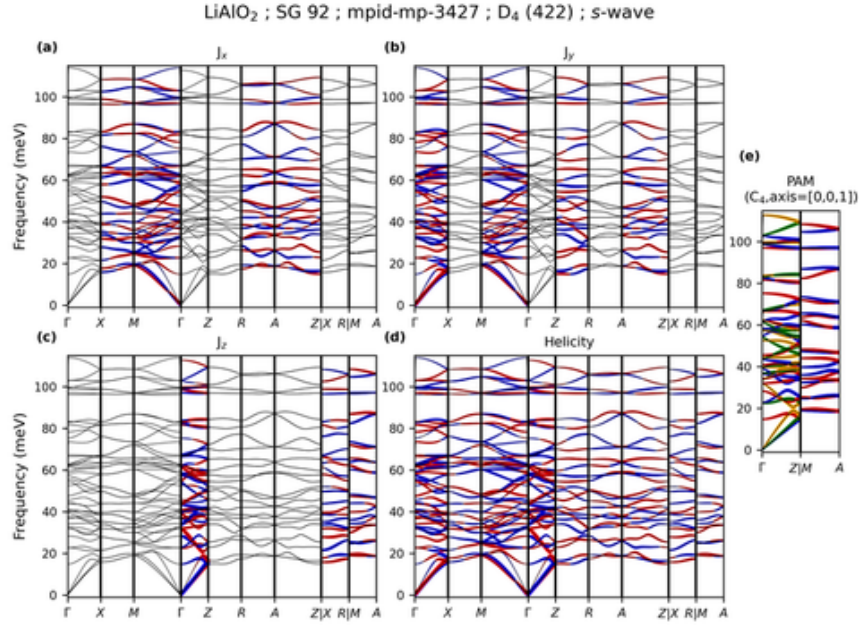


FIG. S9. Phonon dispersion of LiAlO₂ (mp-3427) along the specific momentum paths in the Brillouin zone of SG 92 (see Table S12). (a-c) Projections of the phonon angular momentum components J_x , J_y , and J_z onto the dispersion. (d) Projection of the phonon helicity onto the dispersion. In (a-d), red (blue) dots denote positive (negative) angular momentum or helicity, and their size is proportional to the magnitude. (e) Pseudo-angular momentum (PAM) calculated along high-symmetry paths exhibiting three- or four-fold (screw) rotational symmetry. [See more descriptions about the PAM in \(e\).](#)

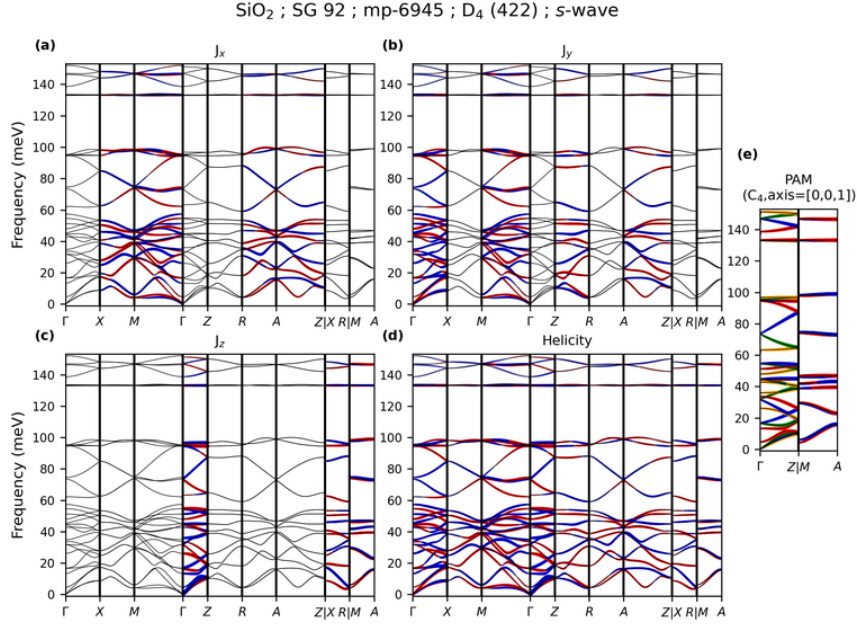


FIG. S10. Phonon dispersion of SiO_2 (mp-6945) along the specific momentum paths in the Brillouin zone of SG 92 (see Table S12). (a-c) Projections of the phonon angular momentum components J_x , J_y , and J_z onto the dispersion. (d) Projection of the phonon helicity onto the dispersion. In (a-d), red (blue) dots denote positive (negative) angular momentum or helicity, and their size is proportional to the magnitude. (e) Pseudo-angular momentum (PAM) calculated along high-symmetry paths exhibiting three- or four-fold (screw) rotational symmetry. [See more descriptions about the PAM in \(e\).](#)

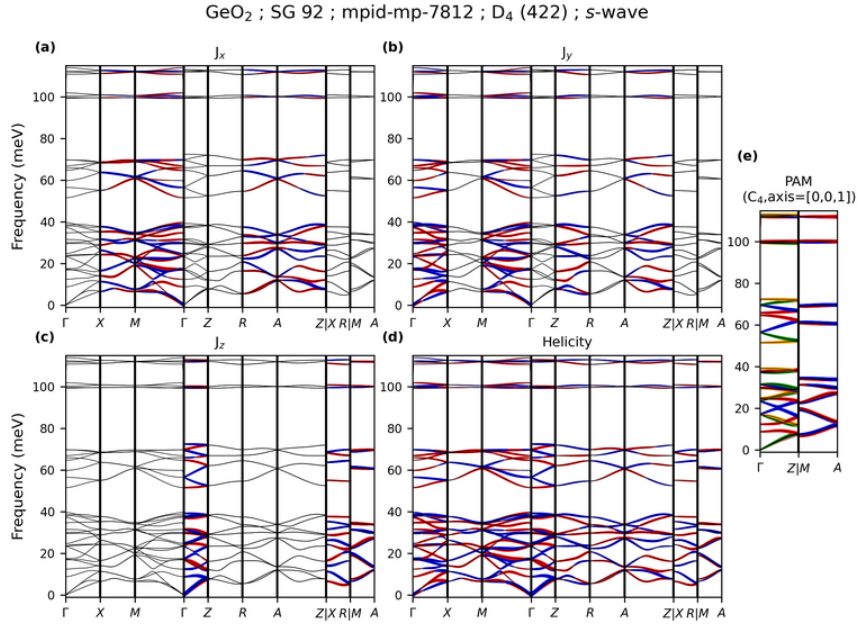


FIG. S11. Phonon dispersion of GeO_2 (mp-7812) along the specific momentum paths in the Brillouin zone of SG 92 (see Table S12). (a-c) Projections of the phonon angular momentum components J_x , J_y , and J_z onto the dispersion. (d) Projection of the phonon helicity onto the dispersion. In (a-d), red (blue) dots denote positive (negative) angular momentum or helicity, and their size is proportional to the magnitude. (e) Pseudo-angular momentum (PAM) calculated along high-symmetry paths exhibiting three- or four-fold (screw) rotational symmetry. [See more descriptions about the PAM in \(e\).](#)

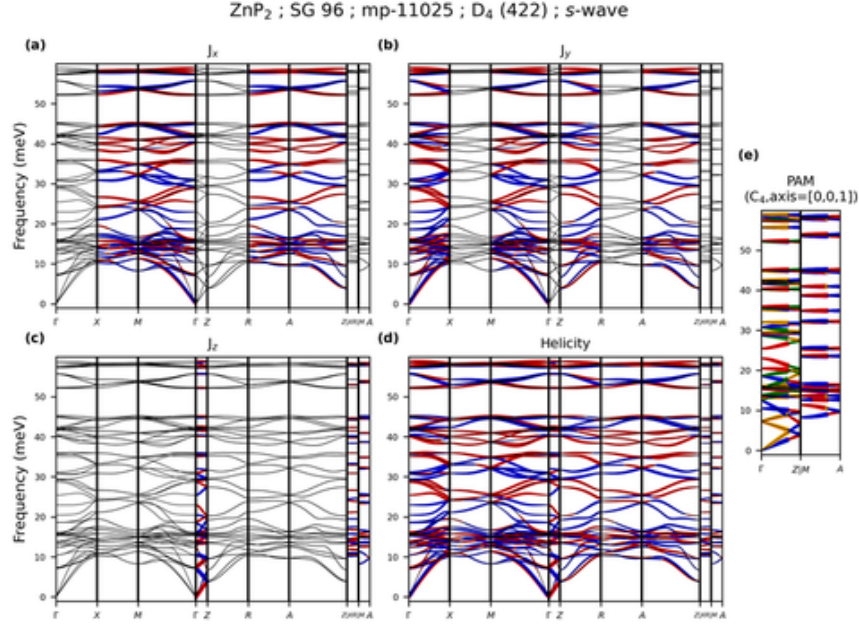


FIG. S12. Phonon dispersion of ZnP_2 (mp-11025) along the specific momentum paths in the Brillouin zone of SG 96 (see Table S13). (a-c) Projections of the phonon angular momentum components J_x , J_y , and J_z onto the dispersion. (d) Projection of the phonon helicity onto the dispersion. In (a-d), red (blue) dots denote positive (negative) angular momentum or helicity, and their size is proportional to the magnitude. (e) Pseudo-angular momentum (PAM) calculated along high-symmetry paths exhibiting three- or four-fold (screw) rotational symmetry. See more descriptions about the PAM in (e).

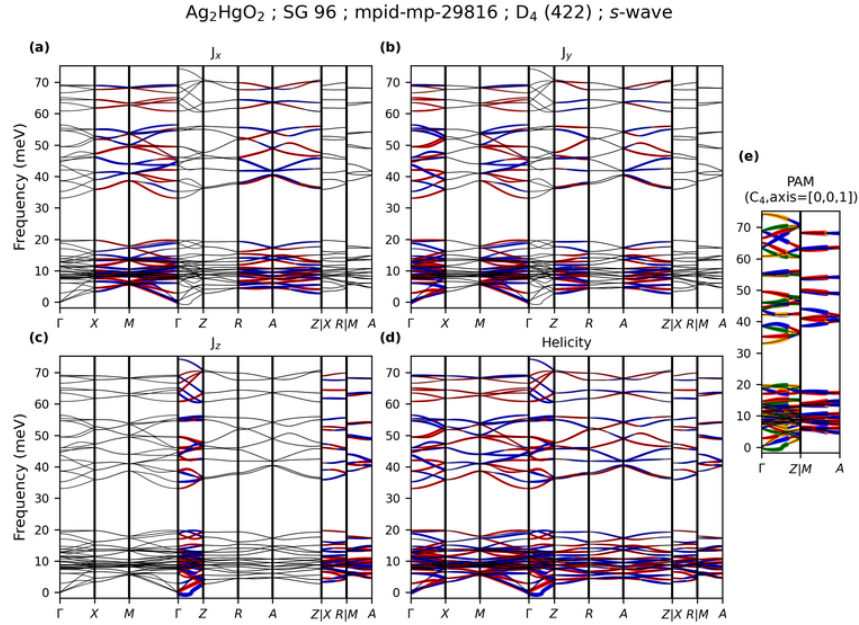


FIG. S13. Phonon dispersion of Ag_2HgO_2 (mp-29816) along the specific momentum paths in the Brillouin zone of SG 96 (see Table S13). (a-c) Projections of the phonon angular momentum components J_x , J_y , and J_z onto the dispersion. (d) Projection of the phonon helicity onto the dispersion. In (a-d), red (blue) dots denote positive (negative) angular momentum or helicity, and their size is proportional to the magnitude. (e) Pseudo-angular momentum (PAM) calculated along high-symmetry paths exhibiting three- or four-fold (screw) rotational symmetry. See more descriptions about the PAM in (e).

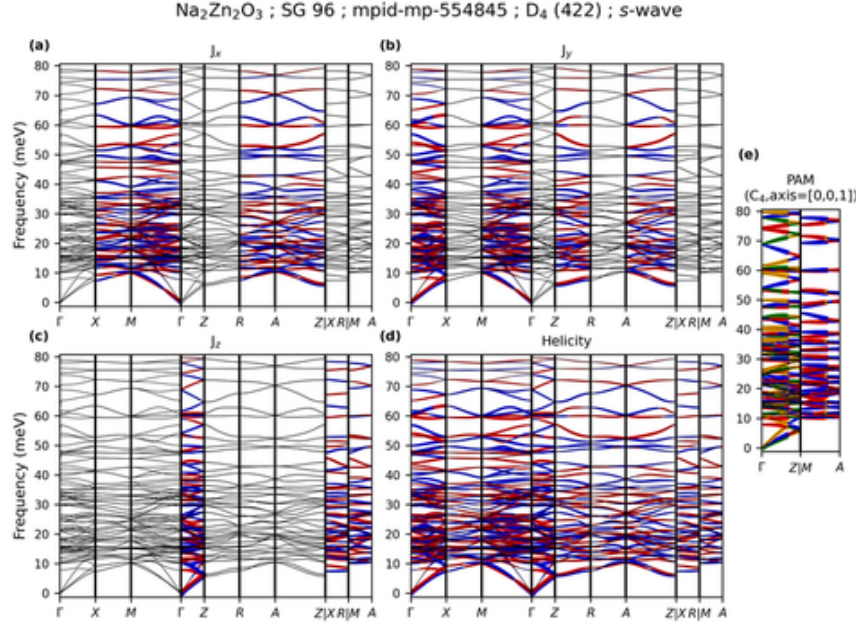


FIG. S14. Phonon dispersion of $\text{Na}_2\text{Zn}_2\text{O}_3$ (mp-554845) along the specific momentum paths in the Brillouin zone of SG 96 (see Table S13). (a-c) Projections of the phonon angular momentum components J_x , J_y , and J_z onto the dispersion. (d) Projection of the phonon helicity onto the dispersion. In (a-d), red (blue) dots denote positive (negative) angular momentum or helicity, and their size is proportional to the magnitude. (e) Pseudo-angular momentum (PAM) calculated along high-symmetry paths exhibiting three- or four-fold (screw) rotational symmetry. See more descriptions about the PAM in (e).

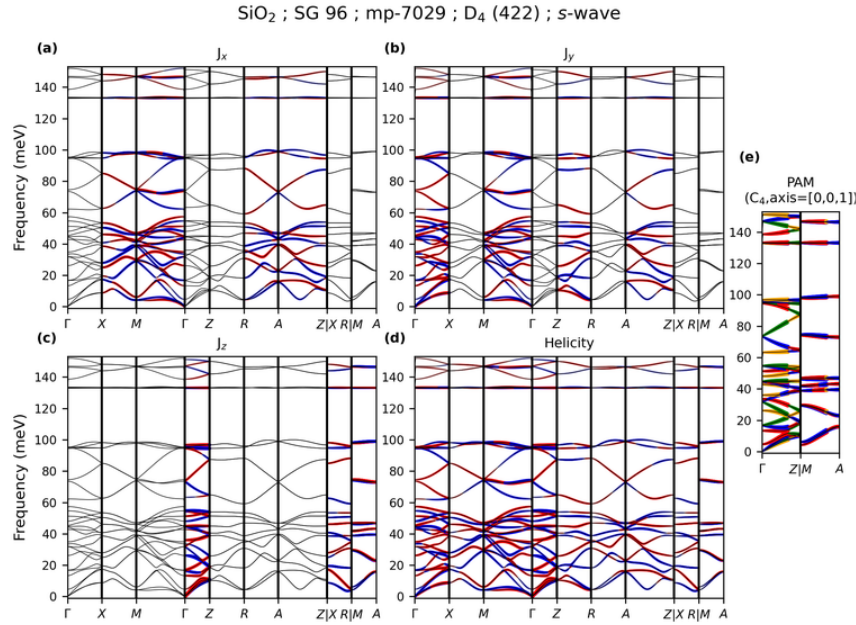


FIG. S15. Phonon dispersion of SiO_2 (mp-7029) along the specific momentum paths in the Brillouin zone of SG 96 (see Table S13). (a-d) Projections of the phonon angular momentum components J_x , J_y , and J_z onto the dispersion. (d) Projection of the phonon helicity onto the dispersion. In (a-d), red (blue) dots denote positive (negative) angular momentum or helicity, and their size is proportional to the magnitude. (e) Pseudo-angular momentum (PAM) calculated along high-symmetry paths exhibiting three- or four-fold (screw) rotational symmetry. See more descriptions about the PAM in (e).

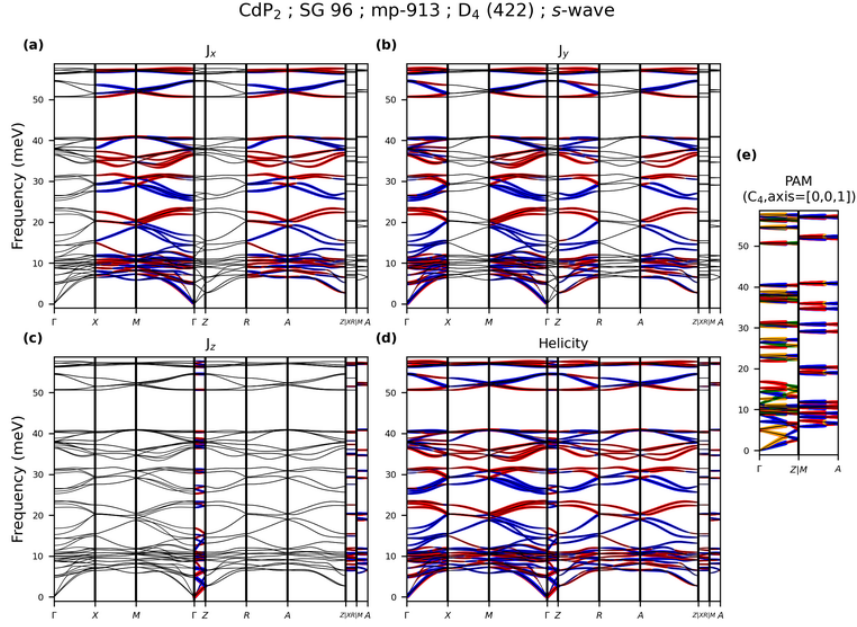


FIG. S16. Phonon dispersion of CdP₂ (mp-913) along the specific momentum paths in the Brillouin zone of SG 96 (see Table S13). (a-c) Projections of the phonon angular momentum components J_x , J_y , and J_z onto the dispersion. (d) Projection of the phonon helicity onto the dispersion. In (a-d), red (blue) dots denote positive (negative) angular momentum or helicity, and their size is proportional to the magnitude. (e) Pseudo-angular momentum (PAM) calculated along high-symmetry paths exhibiting three- or four-fold (screw) rotational symmetry. [See more descriptions about the PAM in \(e\).](#)

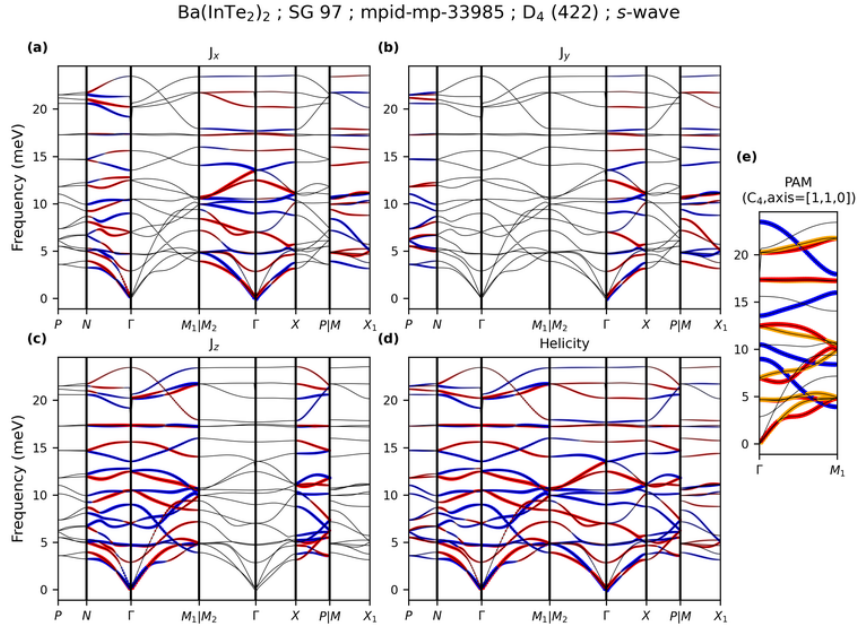


FIG. S17. Phonon dispersion of Ba(InTe₂)₂ (mp-33985) along the specific momentum paths in the Brillouin zone of SG 97 (see Table S14). (a-c) Projections of the phonon angular momentum components J_x , J_y , and J_z onto the dispersion. (d) Projection of the phonon helicity onto the dispersion. In (a-d), red (blue) dots denote positive (negative) angular momentum or helicity, and their size is proportional to the magnitude. (e) Pseudo-angular momentum (PAM) calculated along high-symmetry paths exhibiting three- or four-fold (screw) rotational symmetry. [See more descriptions about the PAM in \(e\).](#)

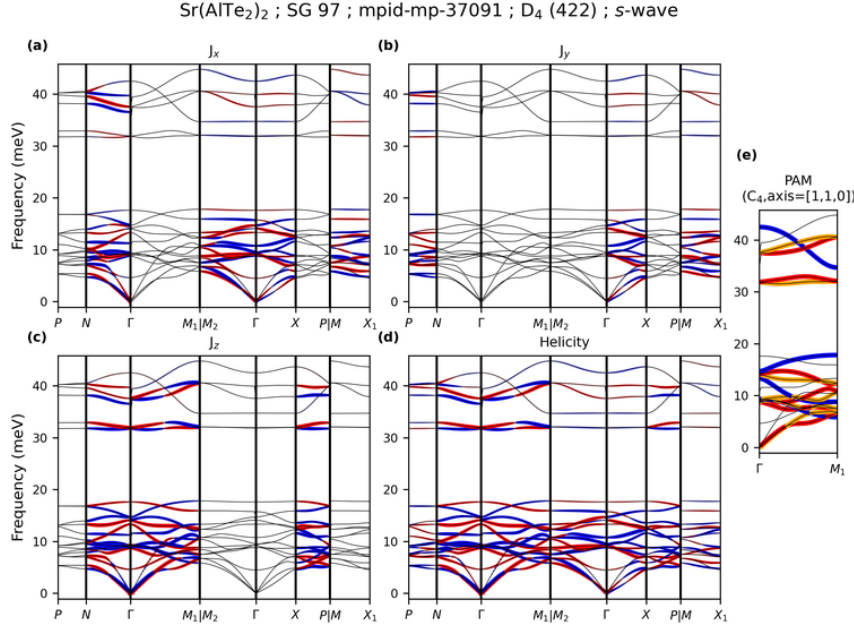


FIG. S18. Phonon dispersion of Sr(AlTe₂)₂ (mp-37091) along the specific momentum paths in the Brillouin zone of SG 97 (see Table S14). (a-c) Projections of the phonon angular momentum components J_x , J_y , and J_z onto the dispersion. (d) Projection of the phonon helicity onto the dispersion. In (a-d), red (blue) dots denote positive (negative) angular momentum or helicity, and their size is proportional to the magnitude. (e) Pseudo-angular momentum (PAM) calculated along high-symmetry paths exhibiting three- or four-fold (screw) rotational symmetry. See more descriptions about the PAM in (e).

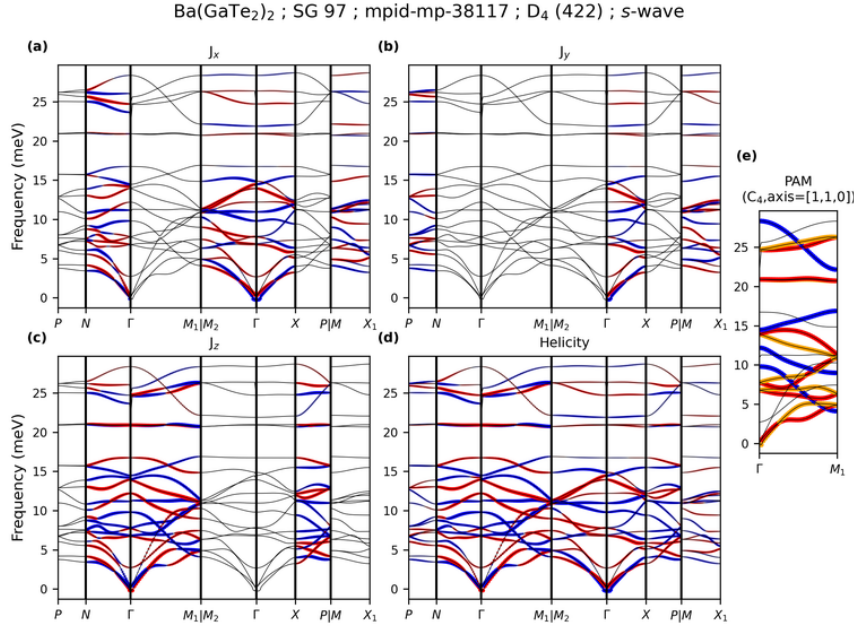


FIG. S19. Phonon dispersion of Ba(GaTe₂)₂ (mp-38117) along the specific momentum paths in the Brillouin zone of SG 97 (see Table S14). (a-c) Projections of the phonon angular momentum components J_x , J_y , and J_z onto the dispersion. (d) Projection of the phonon helicity onto the dispersion. In (a-d), red (blue) dots denote positive (negative) angular momentum or helicity, and their size is proportional to the magnitude. (e) Pseudo-angular momentum (PAM) calculated along high-symmetry paths exhibiting three- or four-fold (screw) rotational symmetry. See more descriptions about the PAM in (e).

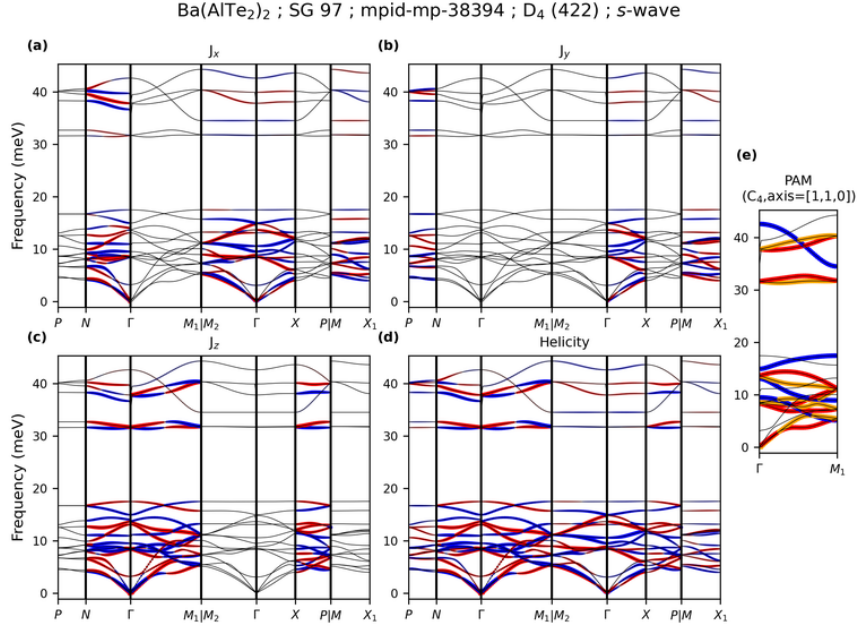


FIG. S20. Phonon dispersion of $\text{Ba(AlTe}_2)_2$ (mp-38394) along the specific momentum paths in the Brillouin zone of SG 97 (see Table S14). (a-c) Projections of the phonon angular momentum components J_x , J_y , and J_z onto the dispersion. (d) Projection of the phonon helicity onto the dispersion. In (a-d), red (blue) dots denote positive (negative) angular momentum or helicity, and their size is proportional to the magnitude. (e) Pseudo-angular momentum (PAM) calculated along high-symmetry paths exhibiting three- or four-fold (screw) rotational symmetry. See more descriptions about the PAM in (e).

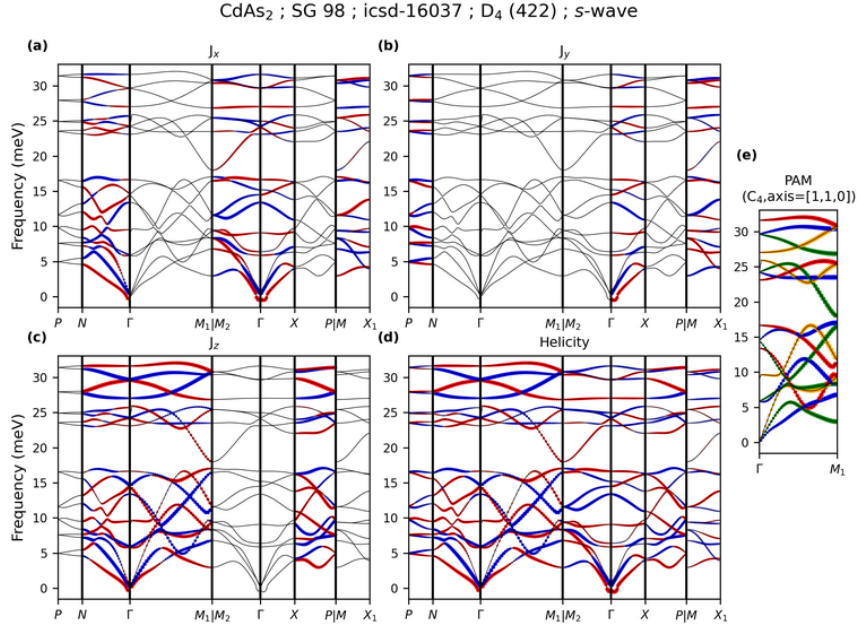


FIG. S21. Phonon dispersion of CdAs_2 (icsd-16037) along the specific momentum paths in the Brillouin zone of SG 98 (see Table S15). (a-c) Projections of the phonon angular momentum components J_x , J_y , and J_z onto the dispersion. (d) Projection of the phonon helicity onto the dispersion. In (a-d), red (blue) dots denote positive (negative) angular momentum or helicity, and their size is proportional to the magnitude. (e) Pseudo-angular momentum (PAM) calculated along high-symmetry paths exhibiting three- or four-fold (screw) rotational symmetry. See more descriptions about the PAM in (e).

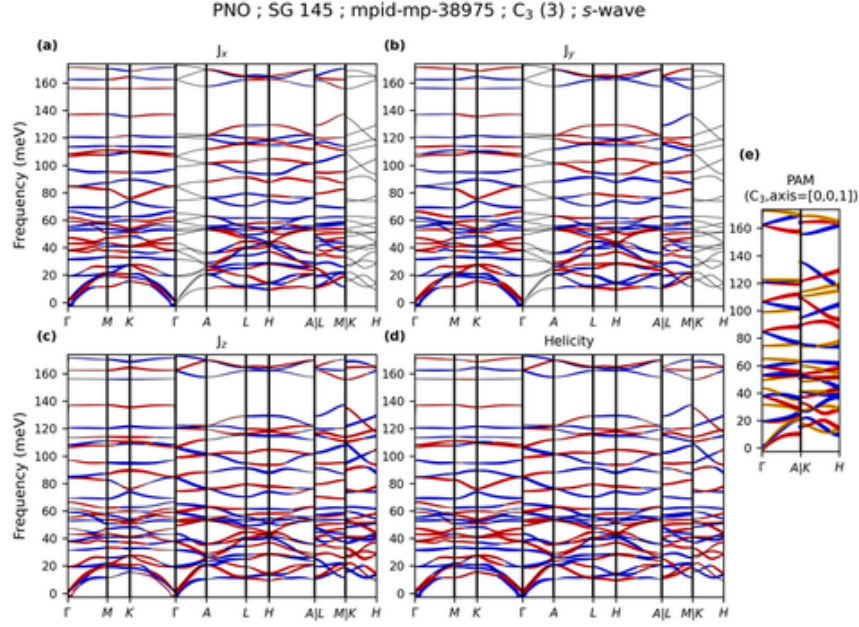


FIG. S22. Phonon dispersion of PNO (mp-38975) along the specific momentum paths in the Brillouin zone of SG 145 (see Table S22). (a-c) Projections of the phonon angular momentum components J_x , J_y , and J_z onto the dispersion. (d) Projection of the phonon helicity onto the dispersion. In (a-d), red (blue) dots denote positive (negative) angular momentum or helicity, and their size is proportional to the magnitude. (e) Pseudo-angular momentum (PAM) calculated along high-symmetry paths exhibiting three- or four-fold (screw) rotational symmetry. See more descriptions about the PAM in (e).

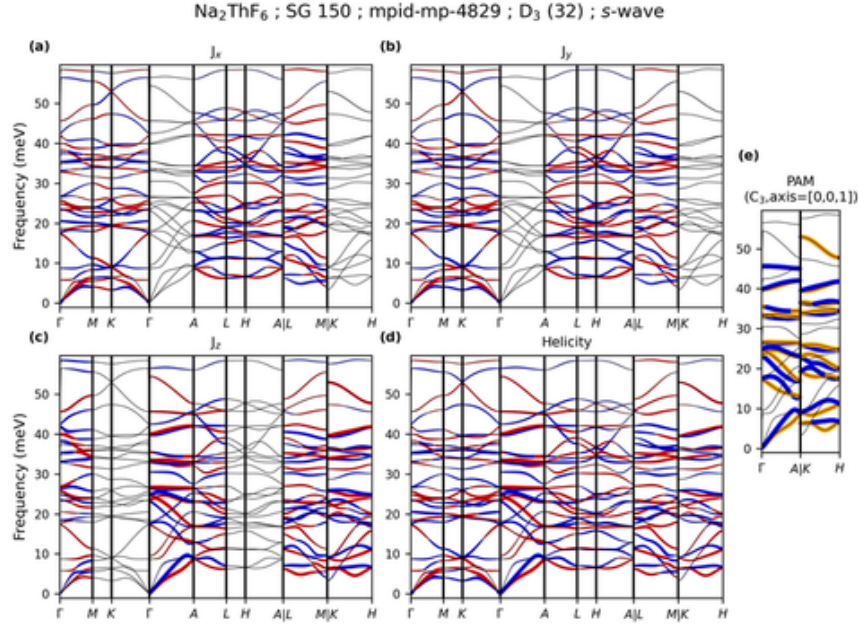


FIG. S23. Phonon dispersion of Na_2ThF_6 (mp-4829) along the specific momentum paths in the Brillouin zone of SG 150 (see Table S23). (a-c) Projections of the phonon angular momentum components J_x , J_y , and J_z onto the dispersion. (d) Projection of the phonon helicity onto the dispersion. In (a-d), red (blue) dots denote positive (negative) angular momentum or helicity, and their size is proportional to the magnitude. (e) Pseudo-angular momentum (PAM) calculated along high-symmetry paths exhibiting three- or four-fold (screw) rotational symmetry. See more descriptions about the PAM in (e).

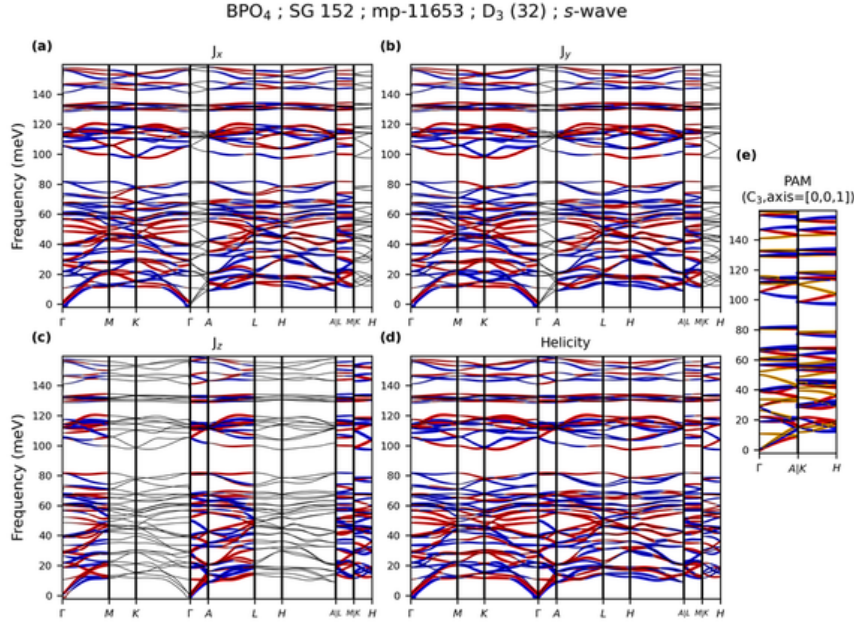


FIG. S24. Phonon dispersion of BPO₄ (mp-11653) along the specific momentum paths in the Brillouin zone of SG 152 (see Table S24). (a-c) Projections of the phonon angular momentum components J_x , J_y , and J_z onto the dispersion. (d) Projection of the phonon helicity onto the dispersion. In (a-d), red (blue) dots denote positive (negative) angular momentum or helicity, and their size is proportional to the magnitude. (e) Pseudo-angular momentum (PAM) calculated along high-symmetry paths exhibiting three- or four-fold (screw) rotational symmetry. See more descriptions about the PAM in (e).

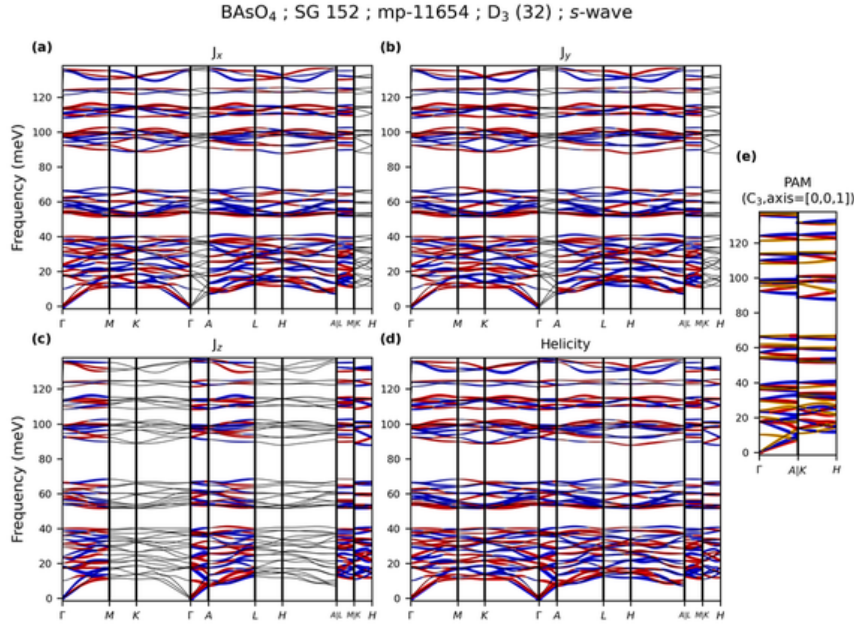


FIG. S25. Phonon dispersion of BAsO₄ (mp-11654) along the specific momentum paths in the Brillouin zone of SG 152 (see Table S24). (a-c) Projections of the phonon angular momentum components J_x , J_y , and J_z onto the dispersion. (d) Projection of the phonon helicity onto the dispersion. In (a-d), red (blue) dots denote positive (negative) angular momentum or helicity, and their size is proportional to the magnitude. (e) Pseudo-angular momentum (PAM) calculated along high-symmetry paths exhibiting three- or four-fold (screw) rotational symmetry. See more descriptions about the PAM in (e).

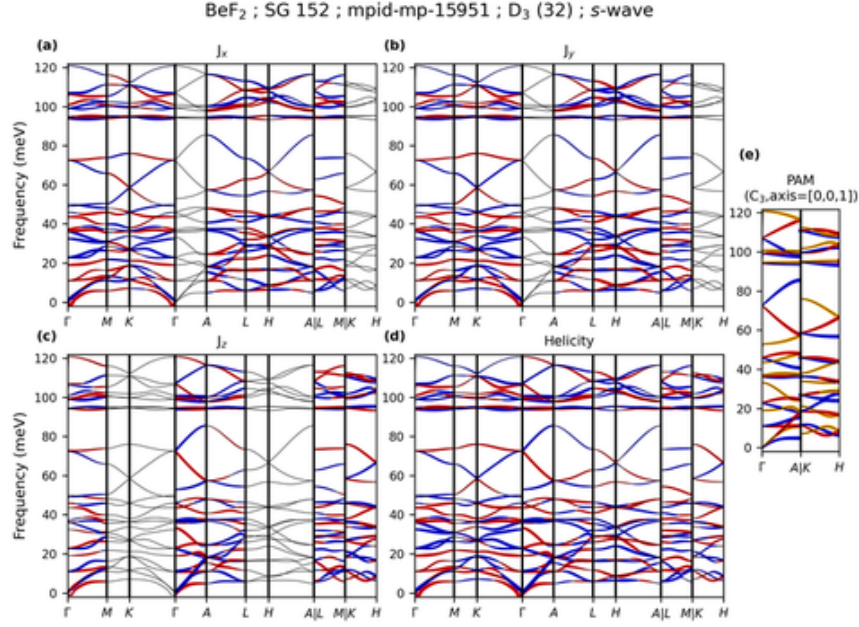


FIG. S26. Phonon dispersion of BeF₂ ([mp-15951](#)) along the specific momentum paths in the Brillouin zone of SG 152 (see Table [S24](#)). (a-c) Projections of the phonon angular momentum components J_x , J_y , and J_z onto the dispersion. (d) Projection of the phonon helicity onto the dispersion. In (a-d), red (blue) dots denote positive (negative) angular momentum or helicity, and their size is proportional to the magnitude. (e) Pseudo-angular momentum (PAM) calculated along high-symmetry paths exhibiting three- or four-fold (screw) rotational symmetry. See more descriptions about the PAM in (e).

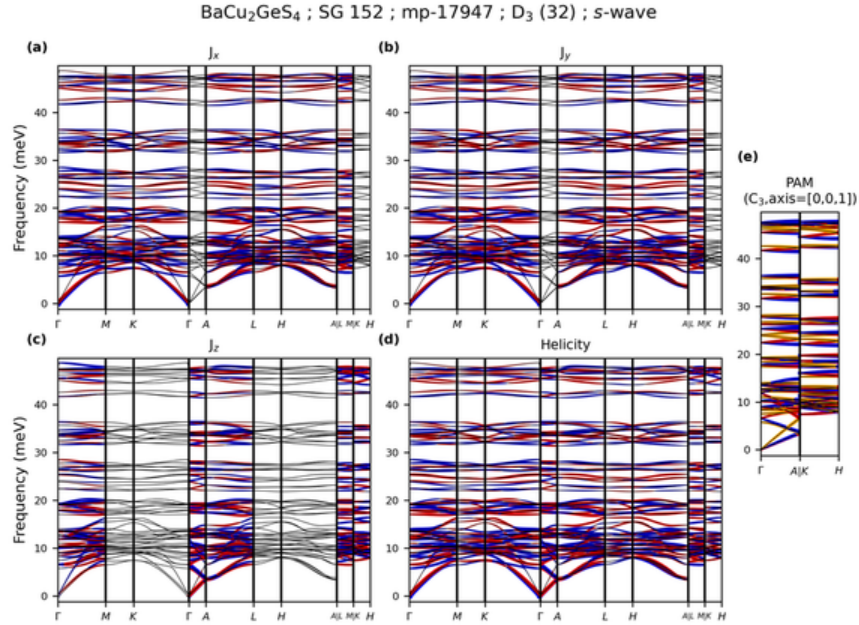


FIG. S27. Phonon dispersion of BaCu₂GeS₄ ([mp-17947](#)) along the specific momentum paths in the Brillouin zone of SG 152 (see Table [S24](#)). (a-c) Projections of the phonon angular momentum components J_x , J_y , and J_z onto the dispersion. (d) Projection of the phonon helicity onto the dispersion. In (a-d), red (blue) dots denote positive (negative) angular momentum or helicity, and their size is proportional to the magnitude. (e) Pseudo-angular momentum (PAM) calculated along high-symmetry paths exhibiting three- or four-fold (screw) rotational symmetry. See more descriptions about the PAM in (e).

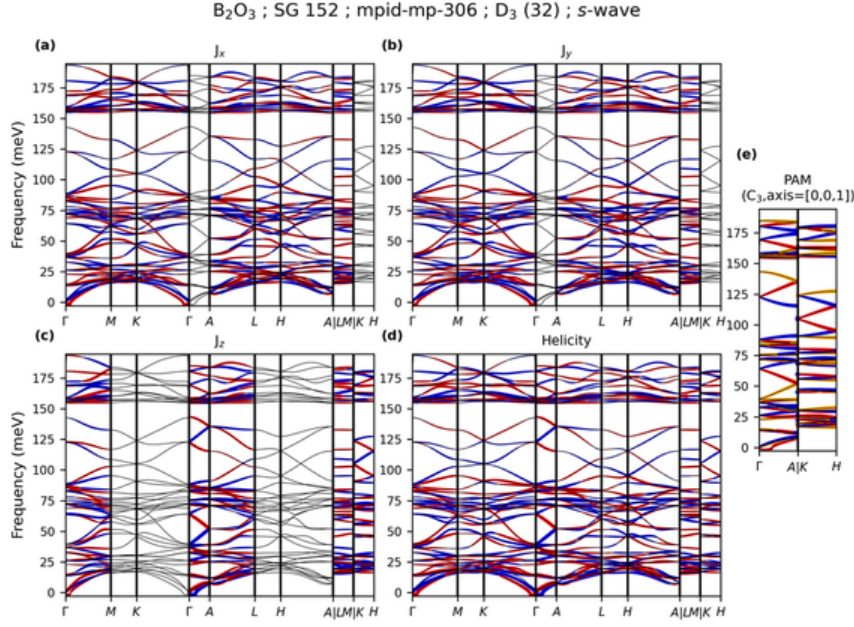


FIG. S28. Phonon dispersion of B_2O_3 (mp-306) along the specific momentum paths in the Brillouin zone of SG 152 (see Table S24). (a-c) Projections of the phonon angular momentum components J_x , J_y , and J_z onto the dispersion. (d) Projection of the phonon helicity onto the dispersion. In (a-d), red (blue) dots denote positive (negative) angular momentum or helicity, and their size is proportional to the magnitude. (e) Pseudo-angular momentum (PAM) calculated along high-symmetry paths exhibiting three- or four-fold (screw) rotational symmetry. See more descriptions about the PAM in (e).

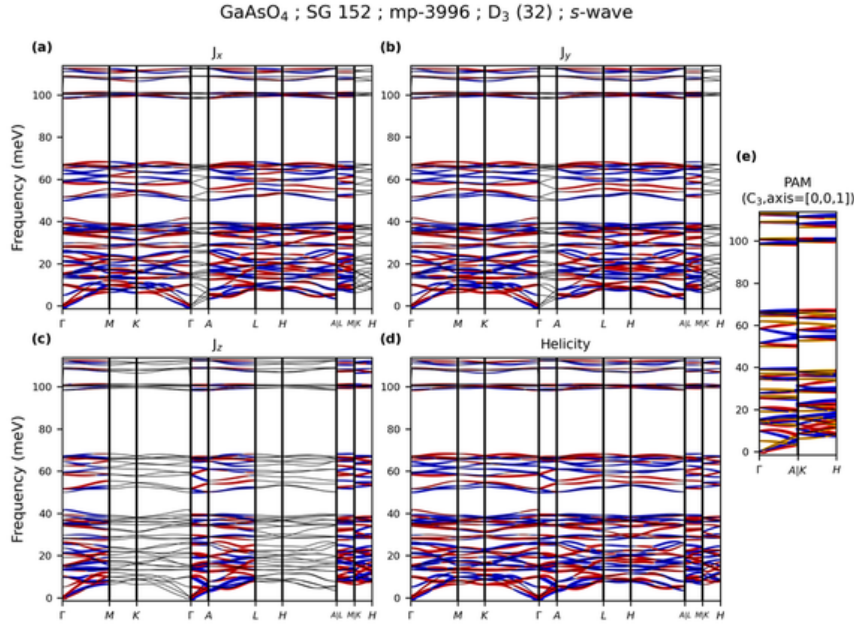


FIG. S29. Phonon dispersion of GaAsO_4 (mp-3996) along the specific momentum paths in the Brillouin zone of SG 152 (see Table S24). (a-c) Projections of the phonon angular momentum components J_x , J_y , and J_z onto the dispersion. (d) Projection of the phonon helicity onto the dispersion. In (a-d), red (blue) dots denote positive (negative) angular momentum or helicity, and their size is proportional to the magnitude. (e) Pseudo-angular momentum (PAM) calculated along high-symmetry paths exhibiting three- or four-fold (screw) rotational symmetry. See more descriptions about the PAM in (e).

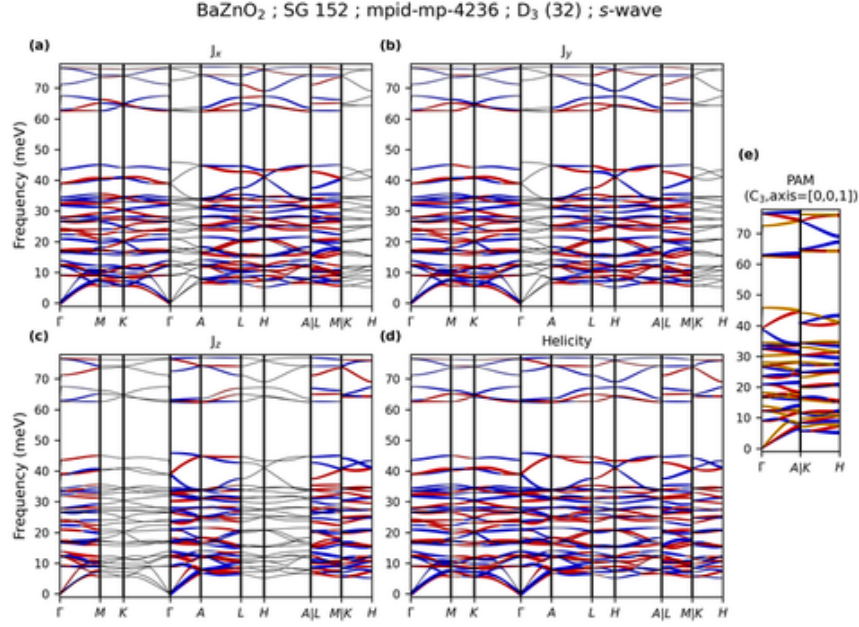


FIG. S30. Phonon dispersion of BaZnO_2 (mp-4236) along the specific momentum paths in the Brillouin zone of SG 152 (see Table S24). (a-c) Projections of the phonon angular momentum components J_x , J_y , and J_z onto the dispersion. (d) Projection of the phonon helicity onto the dispersion. In (a-d), red (blue) dots denote positive (negative) angular momentum or helicity, and their size is proportional to the magnitude. (e) Pseudo-angular momentum (PAM) calculated along high-symmetry paths exhibiting three- or four-fold (screw) rotational symmetry. See more descriptions about the PAM in (e).

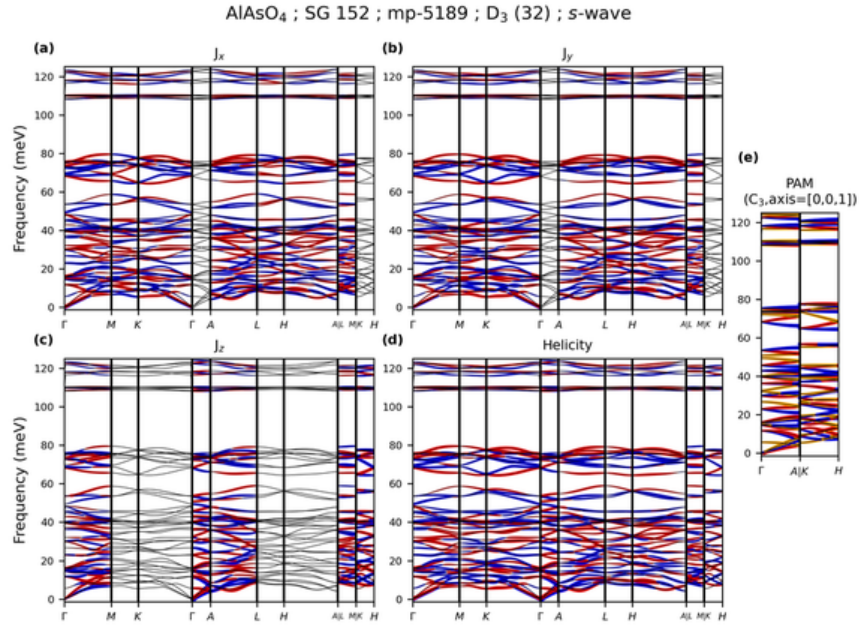


FIG. S31. Phonon dispersion of AlAsO_4 (mp-5189) along the specific momentum paths in the Brillouin zone of SG 152 (see Table S24). (a-c) Projections of the phonon angular momentum components J_x , J_y , and J_z onto the dispersion. (d) Projection of the phonon helicity onto the dispersion. In (a-d), red (blue) dots denote positive (negative) angular momentum or helicity, and their size is proportional to the magnitude. (e) Pseudo-angular momentum (PAM) calculated along high-symmetry paths exhibiting three- or four-fold (screw) rotational symmetry. See more descriptions about the PAM in (e).

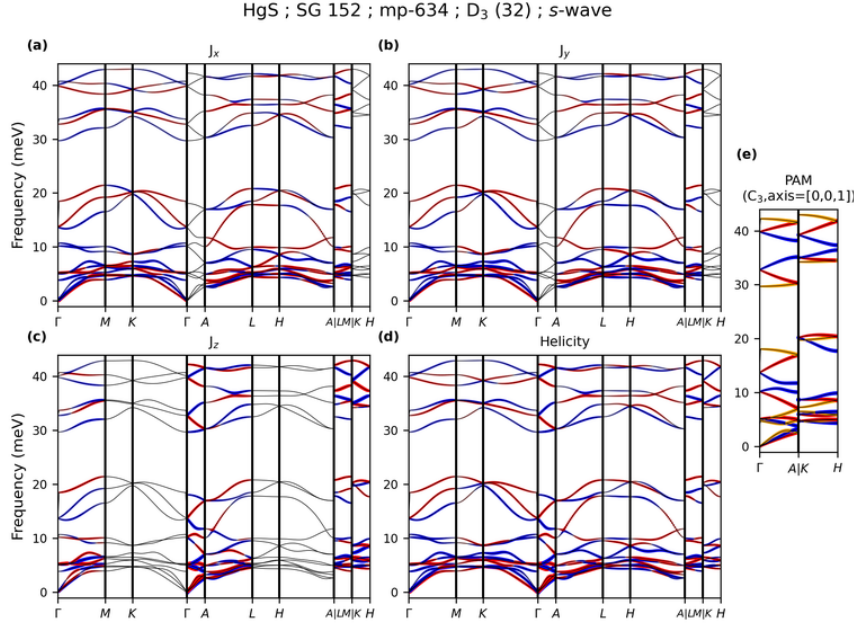


FIG. S32. Phonon dispersion of HgS (mp-634) along the specific momentum paths in the Brillouin zone of SG 152 (see Table S24). (a-c) Projections of the phonon angular momentum components J_x , J_y , and J_z onto the dispersion. (d) Projection of the phonon helicity onto the dispersion. In (a-d), red (blue) dots denote positive (negative) angular momentum or helicity, and their size is proportional to the magnitude. (e) Pseudo-angular momentum (PAM) calculated along high-symmetry paths exhibiting three- or four-fold (screw) rotational symmetry. See more descriptions about the PAM in (e).

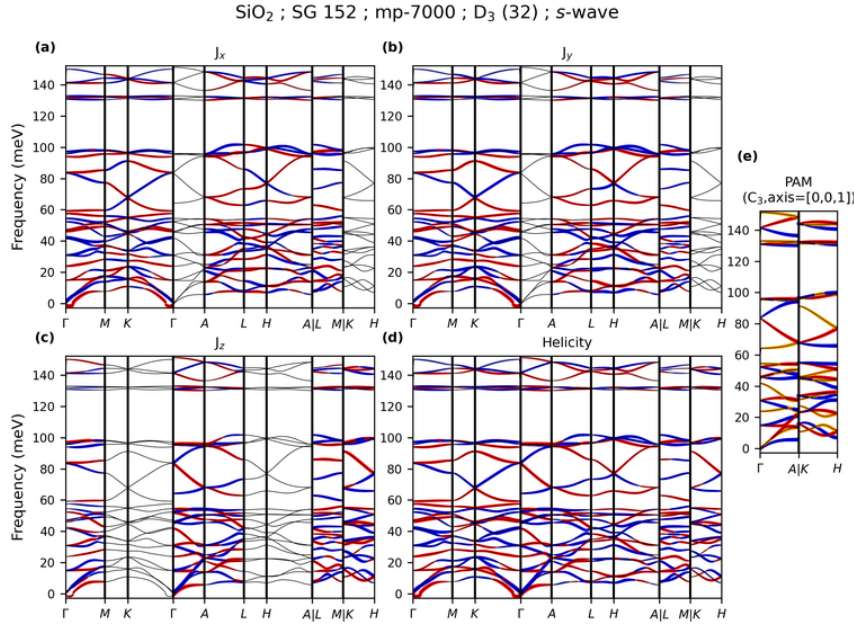


FIG. S33. Phonon dispersion of SiO₂ (mp-7000) along the specific momentum paths in the Brillouin zone of SG 152 (see Table S24). (a-c) Projections of the phonon angular momentum components J_x , J_y , and J_z onto the dispersion. (d) Projection of the phonon helicity onto the dispersion. In (a-d), red (blue) dots denote positive (negative) angular momentum or helicity, and their size is proportional to the magnitude. (e) Pseudo-angular momentum (PAM) calculated along high-symmetry paths exhibiting three- or four-fold (screw) rotational symmetry. See more descriptions about the PAM in (e).

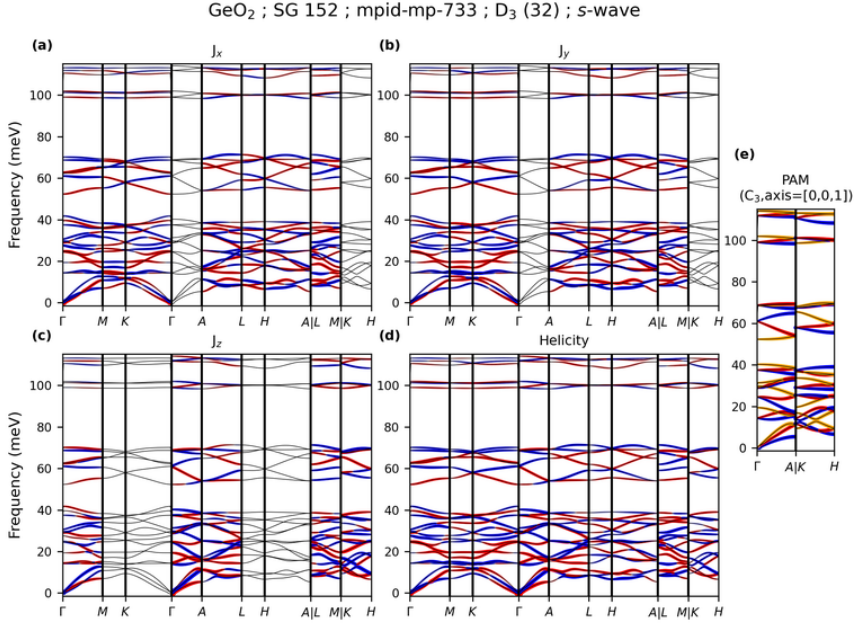


FIG. S34. Phonon dispersion of GeO₂ (mp-733) along the specific momentum paths in the Brillouin zone of SG 152 (see Table S24). (a-c) Projections of the phonon angular momentum components J_x , J_y , and J_z onto the dispersion. (d) Projection of the phonon helicity onto the dispersion. In (a-d), red (blue) dots denote positive (negative) angular momentum or helicity, and their size is proportional to the magnitude. (e) Pseudo-angular momentum (PAM) calculated along high-symmetry paths exhibiting three- or four-fold (screw) rotational symmetry. See more descriptions about the PAM in (e).

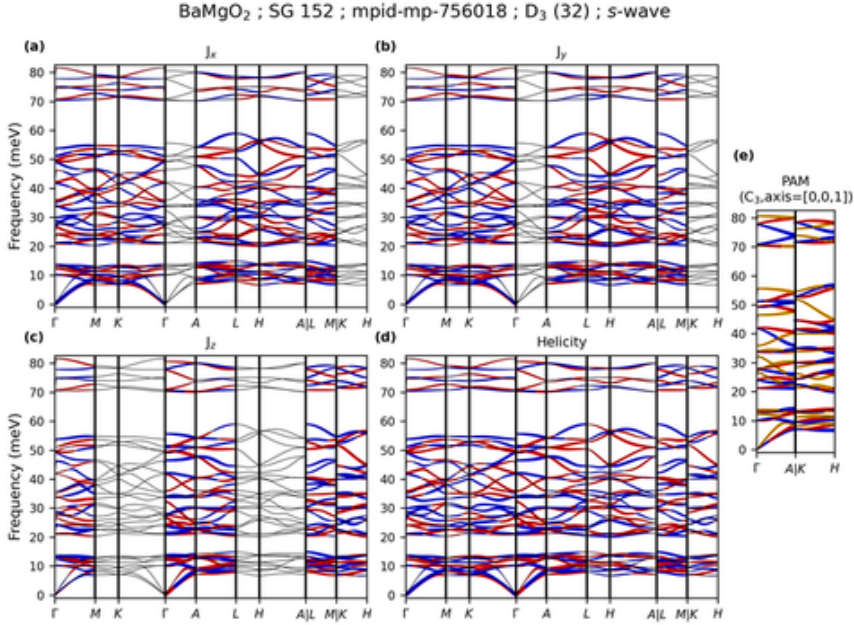


FIG. S35. Phonon dispersion of BaMgO₂ (mp-756018) along the specific momentum paths in the Brillouin zone of SG 152 (see Table S24). (a-c) Projections of the phonon angular momentum components J_x , J_y , and J_z onto the dispersion. (d) Projection of the phonon helicity onto the dispersion. In (a-d), red (blue) dots denote positive (negative) angular momentum or helicity, and their size is proportional to the magnitude. (e) Pseudo-angular momentum (PAM) calculated along high-symmetry paths exhibiting three- or four-fold (screw) rotational symmetry. See more descriptions about the PAM in (e).

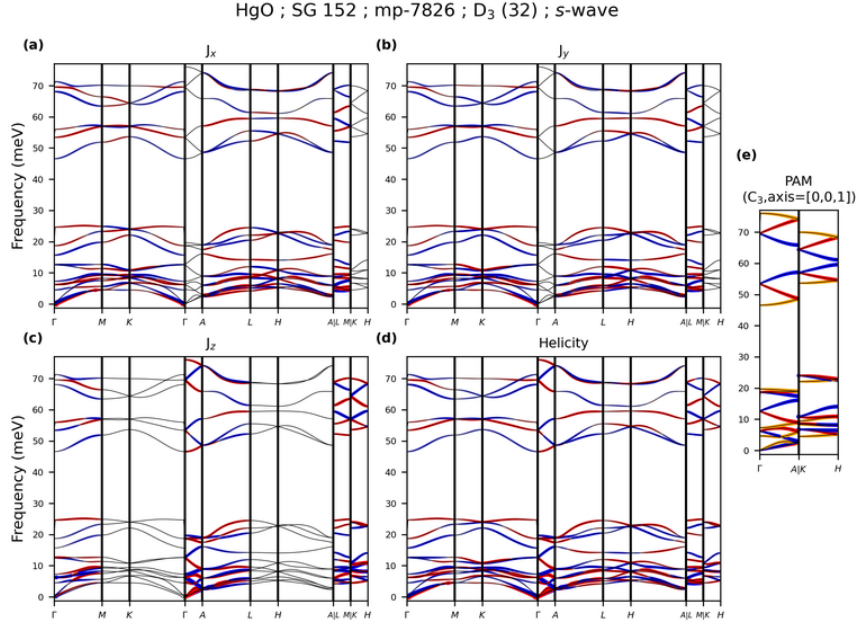


FIG. S36. Phonon dispersion of HgO ([mp-7826](#)) along the specific momentum paths in the Brillouin zone of SG 152 (see Table [S24](#)). (a-c) Projections of the phonon angular momentum components J_x , J_y , and J_z onto the dispersion. (d) Projection of the phonon helicity onto the dispersion. In (a-d), red (blue) dots denote positive (negative) angular momentum or helicity, and their size is proportional to the magnitude. (e) Pseudo-angular momentum (PAM) calculated along high-symmetry paths exhibiting three- or four-fold (screw) rotational symmetry. See more descriptions about the PAM in (e).

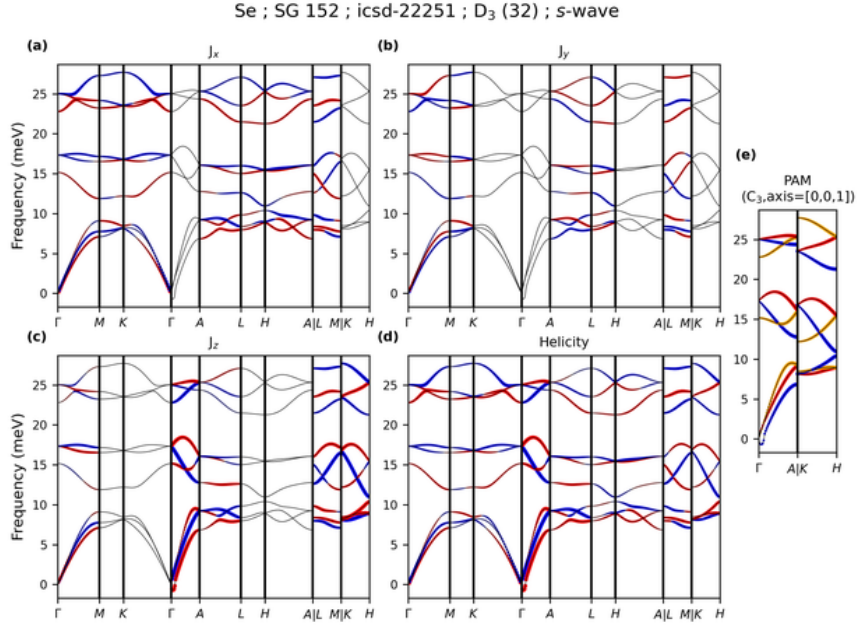


FIG. S37. Phonon dispersion of Se ([icsd-22251](#)) along the specific momentum paths in the Brillouin zone of SG 152 (see Table [S24](#)). (a-c) Projections of the phonon angular momentum components J_x , J_y , and J_z onto the dispersion. (d) Projection of the phonon helicity onto the dispersion. In (a-d), red (blue) dots denote positive (negative) angular momentum or helicity, and their size is proportional to the magnitude. (e) Pseudo-angular momentum (PAM) calculated along high-symmetry paths exhibiting three- or four-fold (screw) rotational symmetry. See more descriptions about the PAM in (e).

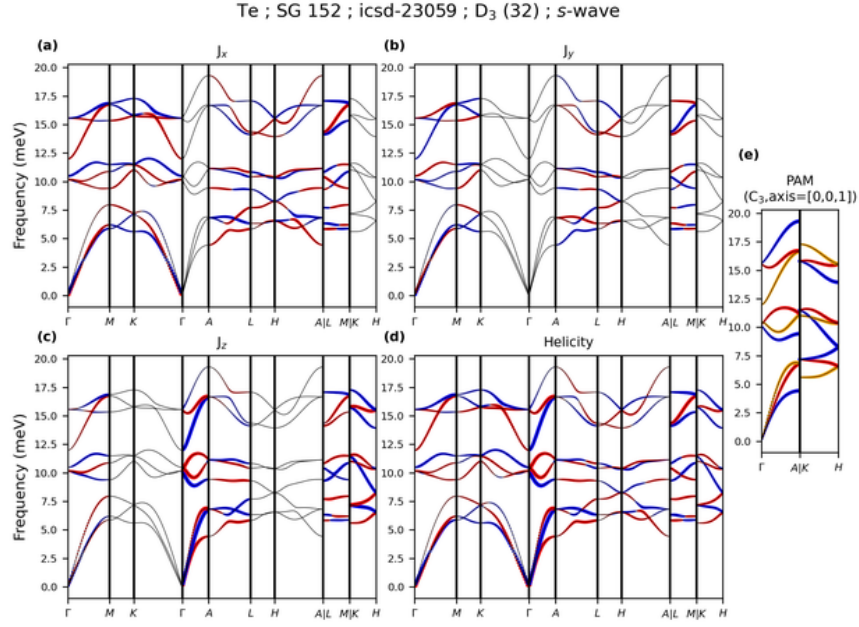


FIG. S38. Phonon dispersion of Te (icsd-23059) along the specific momentum paths in the Brillouin zone of SG 152 (see Table S24). (a-c) Projections of the phonon angular momentum components J_x , J_y , and J_z onto the dispersion. (d) Projection of the phonon helicity onto the dispersion. In (a-d), red (blue) dots denote positive (negative) angular momentum or helicity, and their size is proportional to the magnitude. (e) Pseudo-angular momentum (PAM) calculated along high-symmetry paths exhibiting three- or four-fold (screw) rotational symmetry. See more descriptions about the PAM in (e).

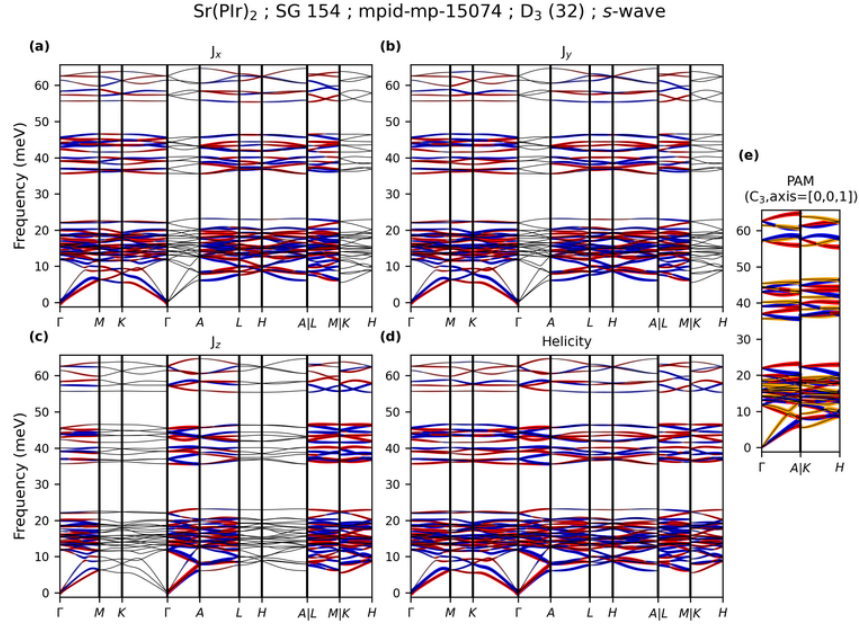


FIG. S39. Phonon dispersion of Sr(PIr)₂ (mp-15074) along the specific momentum paths in the Brillouin zone of SG 154 (see Table S25). (a-c) Projections of the phonon angular momentum components J_x , J_y , and J_z onto the dispersion. (d) Projection of the phonon helicity onto the dispersion. In (a-d), red (blue) dots denote positive (negative) angular momentum or helicity, and their size is proportional to the magnitude. (e) Pseudo-angular momentum (PAM) calculated along high-symmetry paths exhibiting three- or four-fold (screw) rotational symmetry. See more descriptions about the PAM in (e).

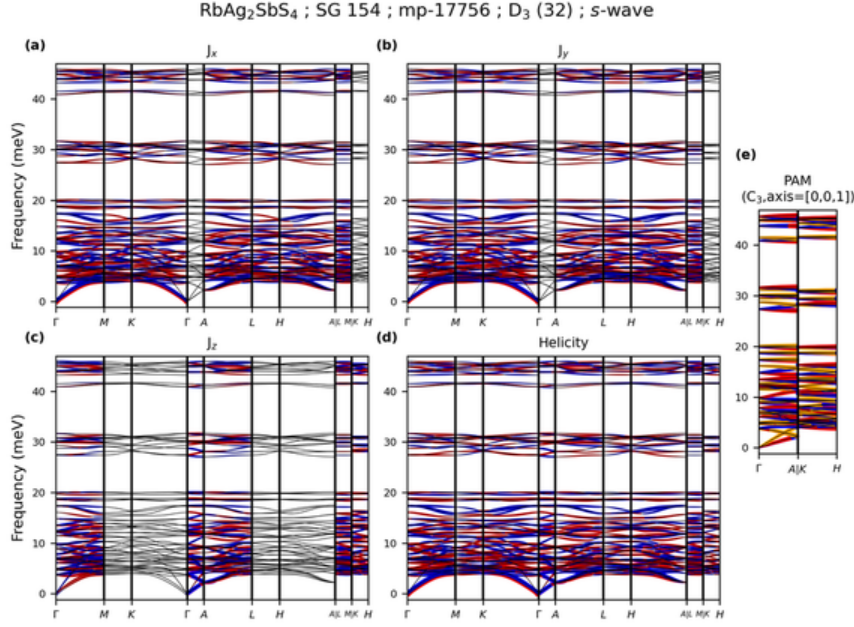


FIG. S40. Phonon dispersion of RbAg₂SbS₄ ([mp-17756](#)) along the specific momentum paths in the Brillouin zone of SG 154 (see Table [S25](#)). (a-c) Projections of the phonon angular momentum components J_x , J_y , and J_z onto the dispersion. (d) Projection of the phonon helicity onto the dispersion. In (a-d), red (blue) dots denote positive (negative) angular momentum or helicity, and their size is proportional to the magnitude. (e) Pseudo-angular momentum (PAM) calculated along high-symmetry paths exhibiting three- or four-fold (screw) rotational symmetry. See more descriptions about the PAM in (e).

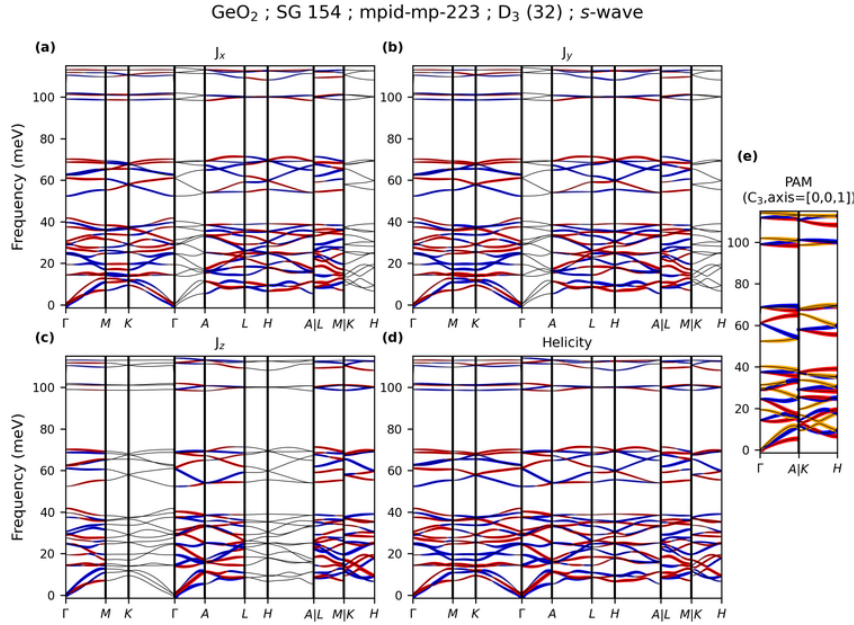


FIG. S41. Phonon dispersion of GeO₂ ([mp-223](#)) along the specific momentum paths in the Brillouin zone of SG 154 (see Table [S25](#)). (a-c) Projections of the phonon angular momentum components J_x , J_y , and J_z onto the dispersion. (d) Projection of the phonon helicity onto the dispersion. In (a-d), red (blue) dots denote positive (negative) angular momentum or helicity, and their size is proportional to the magnitude. (e) Pseudo-angular momentum (PAM) calculated along high-symmetry paths exhibiting three- or four-fold (screw) rotational symmetry. See more descriptions about the PAM in (e).

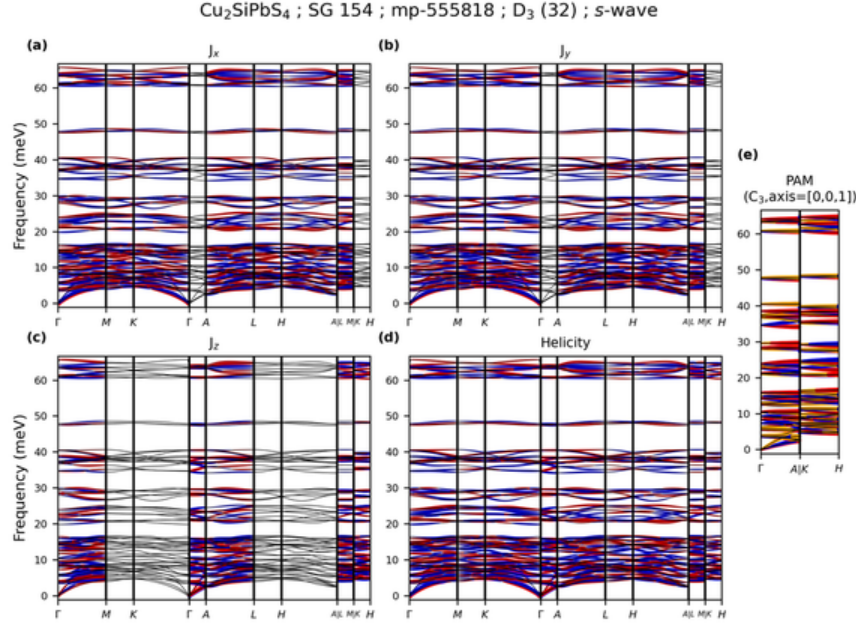


FIG. S42. Phonon dispersion of $\text{Cu}_2\text{SiPbS}_4$ (mp-555818) along the specific momentum paths in the Brillouin zone of SG 154 (see Table S25). (a-c) Projections of the phonon angular momentum components J_x , J_y , and J_z onto the dispersion. (d) Projection of the phonon helicity onto the dispersion. In (a-d), red (blue) dots denote positive (negative) angular momentum or helicity, and their size is proportional to the magnitude. (e) Pseudo-angular momentum (PAM) calculated along high-symmetry paths exhibiting three- or four-fold (screw) rotational symmetry. See more descriptions about the PAM in (e).

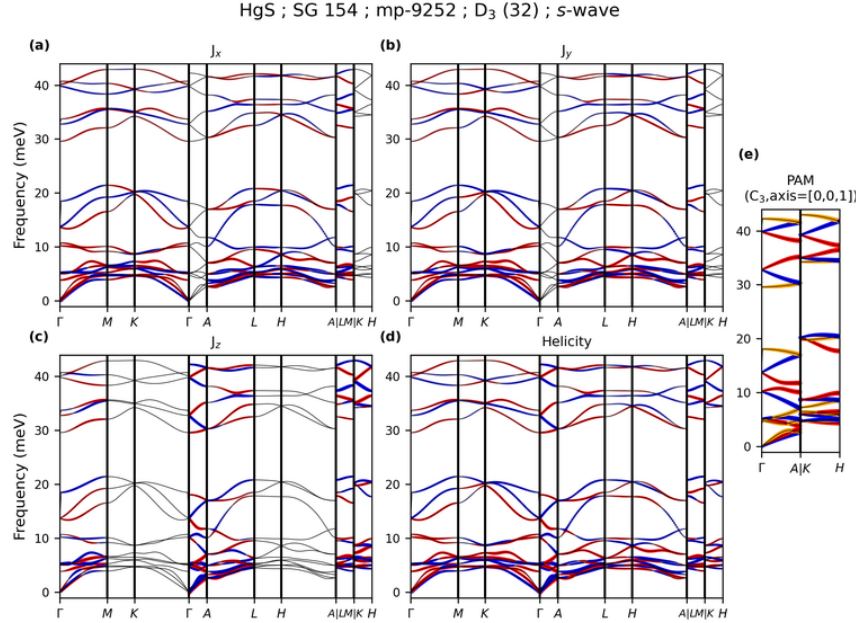


FIG. S43. Phonon dispersion of HgS (mp-9252) along the specific momentum paths in the Brillouin zone of SG 154 (see Table S25). (a-c) Projections of the phonon angular momentum components J_x , J_y , and J_z onto the dispersion. (d) Projection of the phonon helicity onto the dispersion. In (a-d), red (blue) dots denote positive (negative) angular momentum or helicity, and their size is proportional to the magnitude. (e) Pseudo-angular momentum (PAM) calculated along high-symmetry paths exhibiting three- or four-fold (screw) rotational symmetry. See more descriptions about the PAM in (e).

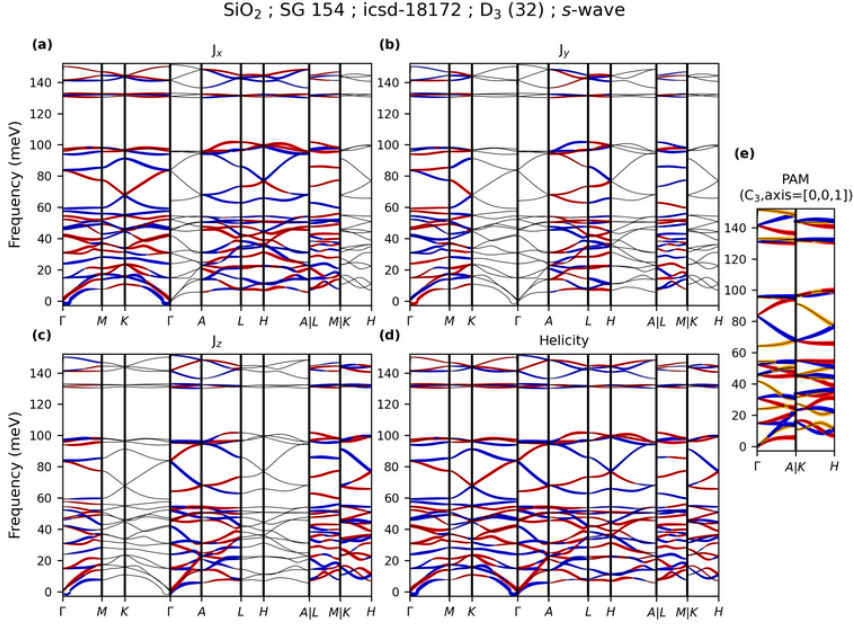


FIG. S44. Phonon dispersion of SiO₂ (icsd-18172) along the specific momentum paths in the Brillouin zone of SG 154 (see Table S25). (a-c) Projections of the phonon angular momentum components J_x , J_y , and J_z onto the dispersion. (d) Projection of the phonon helicity onto the dispersion. In (a-d), red (blue) dots denote positive (negative) angular momentum or helicity, and their size is proportional to the magnitude. (e) Pseudo-angular momentum (PAM) calculated along high-symmetry paths exhibiting three- or four-fold (screw) rotational symmetry. See more descriptions about the PAM in (e).

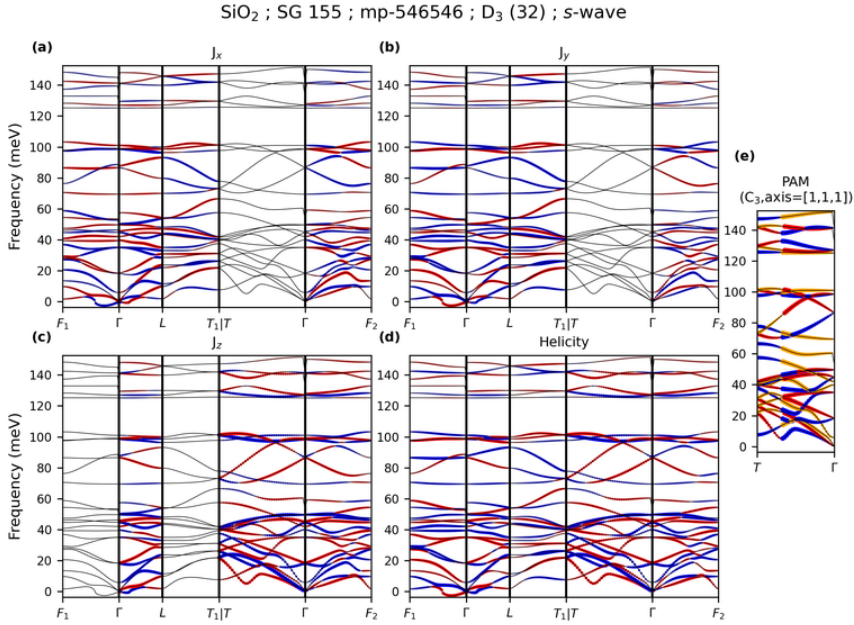


FIG. S45. Phonon dispersion of SiO₂ (mp-546546) along the specific momentum paths in the Brillouin zone of SG 155 (see Table S26). (a-c) Projections of the phonon angular momentum components J_x , J_y , and J_z onto the dispersion. (d) Projection of the phonon helicity onto the dispersion. In (a-d), red (blue) dots denote positive (negative) angular momentum or helicity, and their size is proportional to the magnitude. (e) Pseudo-angular momentum (PAM) calculated along high-symmetry paths exhibiting three- or four-fold (screw) rotational symmetry. See more descriptions about the PAM in (e).

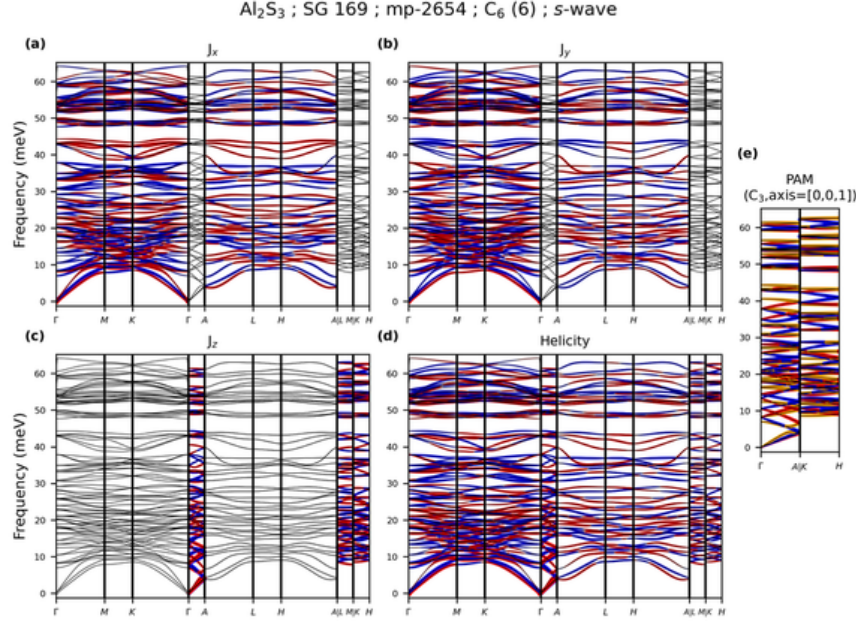


FIG. S46. Phonon dispersion of Al_2S_3 (mp-2654) along the specific momentum paths in the Brillouin zone of SG 169 (see Table S31). (a-c) Projections of the phonon angular momentum components J_x , J_y , and J_z onto the dispersion. (d) Projection of the phonon helicity onto the dispersion. In (a-d), red (blue) dots denote positive (negative) angular momentum or helicity, and their size is proportional to the magnitude. (e) Pseudo-angular momentum (PAM) calculated along high-symmetry paths exhibiting three- or four-fold (screw) rotational symmetry. See more descriptions about the PAM in (e).

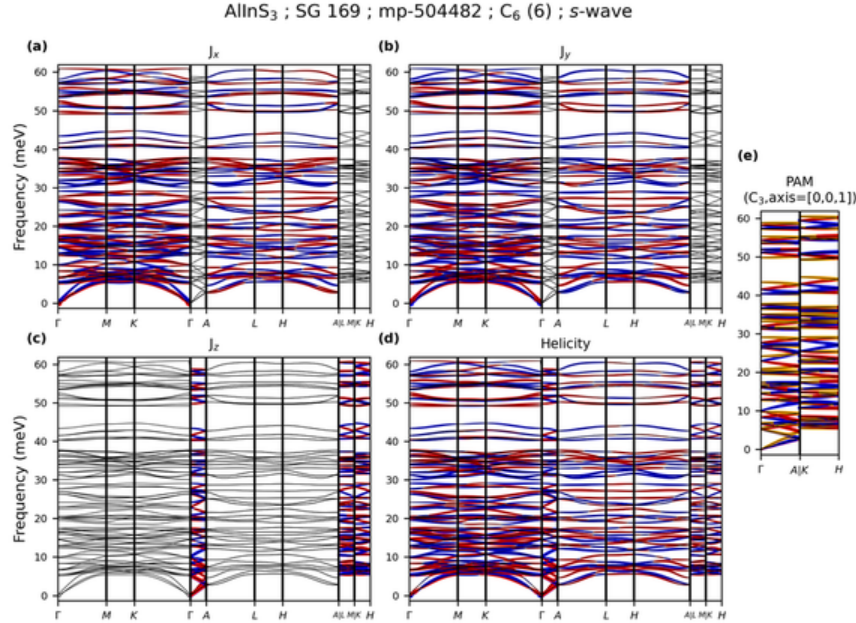


FIG. S47. Phonon dispersion of AlInS_3 (mp-504482) along the specific momentum paths in the Brillouin zone of SG 169 (see Table S31). (a-c) Projections of the phonon angular momentum components J_x , J_y , and J_z onto the dispersion. (d) Projection of the phonon helicity onto the dispersion. In (a-d), red (blue) dots denote positive (negative) angular momentum or helicity, and their size is proportional to the magnitude. (e) Pseudo-angular momentum (PAM) calculated along high-symmetry paths exhibiting three- or four-fold (screw) rotational symmetry. See more descriptions about the PAM in (e).

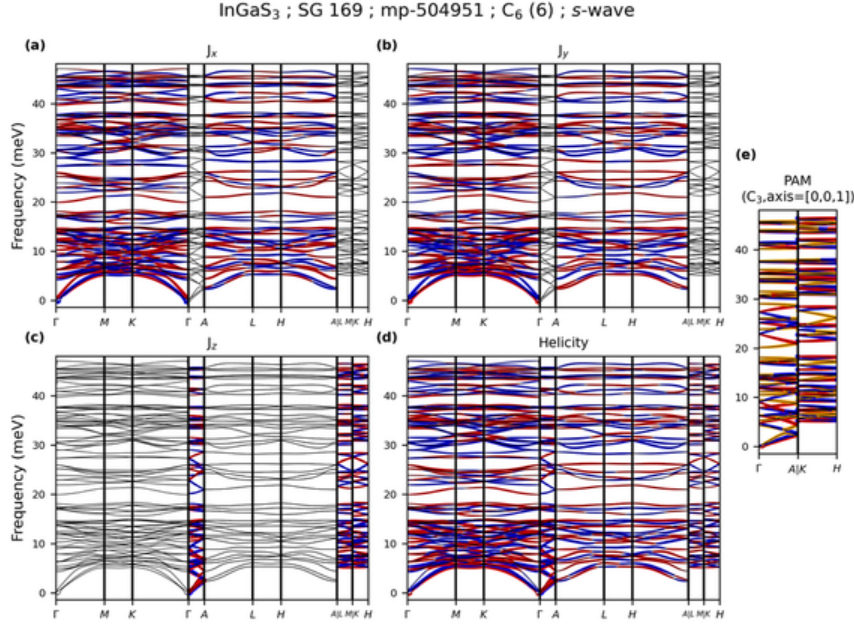


FIG. S48. Phonon dispersion of InGaS_3 (mp-504951) along the specific momentum paths in the Brillouin zone of SG 169 (see Table S31). (a-c) Projections of the phonon angular momentum components J_x , J_y , and J_z onto the dispersion. (d) Projection of the phonon helicity onto the dispersion. In (a-d), red (blue) dots denote positive (negative) angular momentum or helicity, and their size is proportional to the magnitude. (e) Pseudo-angular momentum (PAM) calculated along high-symmetry paths exhibiting three- or four-fold (screw) rotational symmetry. See more descriptions about the PAM in (e).

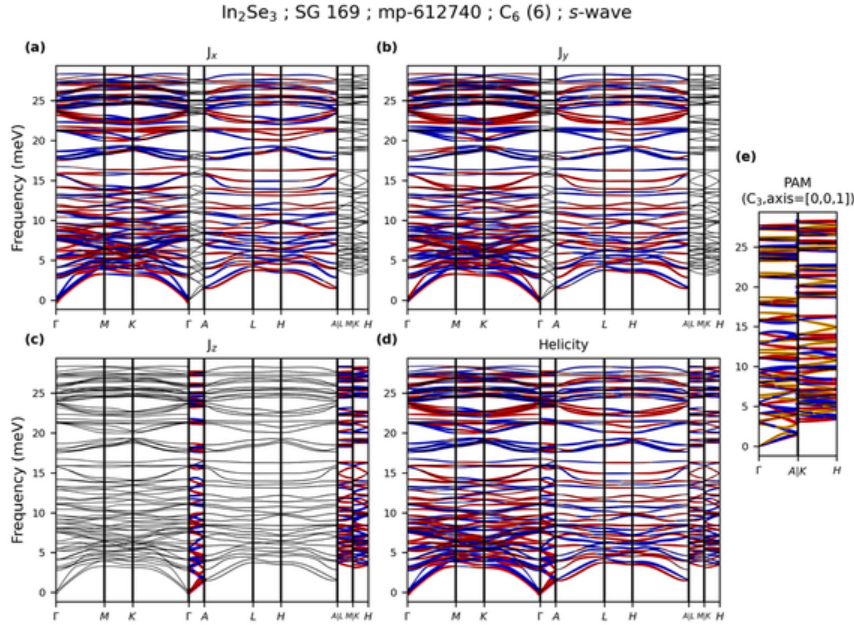


FIG. S49. Phonon dispersion of In_2Se_3 (mp-612740) along the specific momentum paths in the Brillouin zone of SG 169 (see Table S31). (a-c) Projections of the phonon angular momentum components J_x , J_y , and J_z onto the dispersion. (d) Projection of the phonon helicity onto the dispersion. In (a-d), red (blue) dots denote positive (negative) angular momentum or helicity, and their size is proportional to the magnitude. (e) Pseudo-angular momentum (PAM) calculated along high-symmetry paths exhibiting three- or four-fold (screw) rotational symmetry. See more descriptions about the PAM in (e).

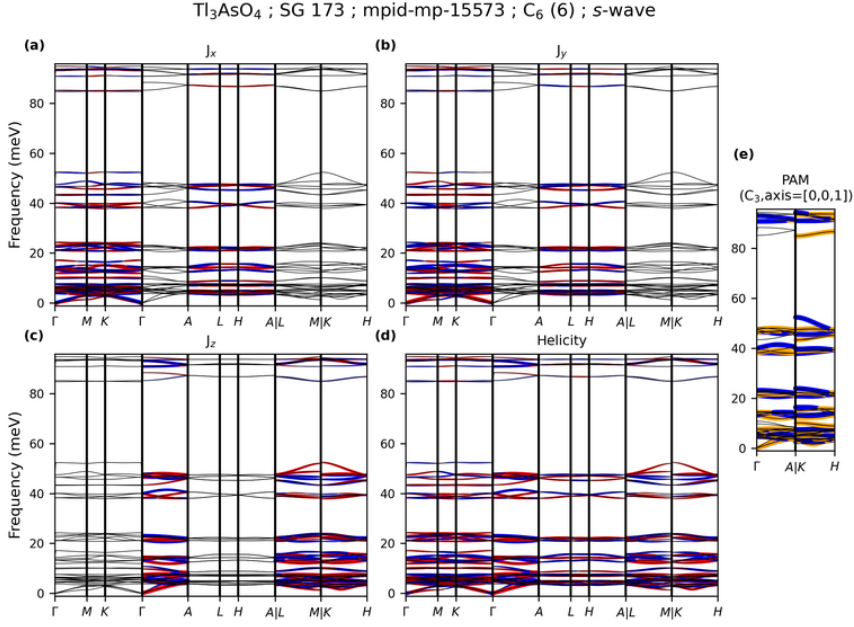


FIG. S50. Phonon dispersion of Ti_3AsO_4 (mp-15573) along the specific momentum paths in the Brillouin zone of SG 173 (see Table S32). (a-c) Projections of the phonon angular momentum components J_x , J_y , and J_z onto the dispersion. (d) Projection of the phonon helicity onto the dispersion. In (a-d), red (blue) dots denote positive (negative) angular momentum or helicity, and their size is proportional to the magnitude. (e) Pseudo-angular momentum (PAM) calculated along high-symmetry paths exhibiting three- or four-fold (screw) rotational symmetry. See more descriptions about the PAM in (e).

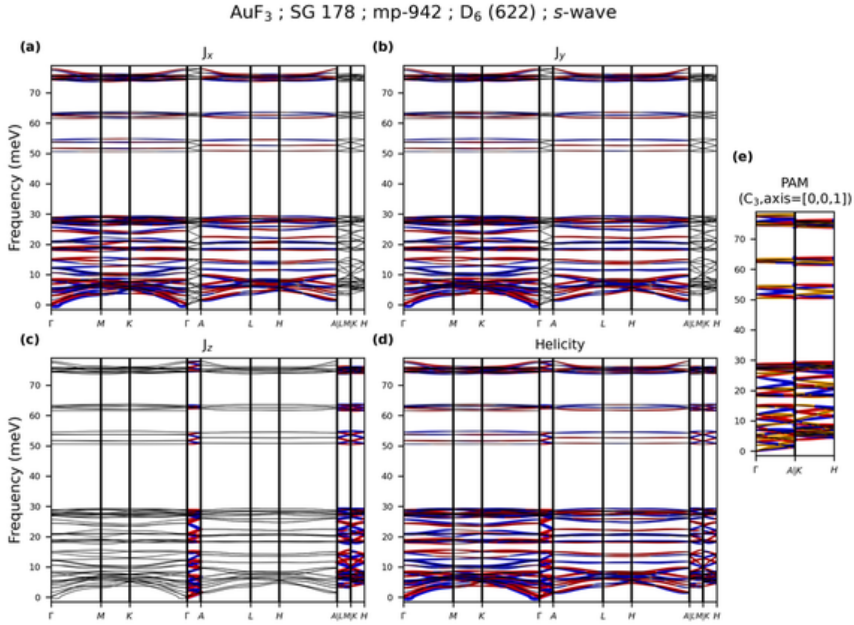


FIG. S51. Phonon dispersion of AuF_3 (mp-942) along the specific momentum paths in the Brillouin zone of SG 178 (see Table S33). (a-c) Projections of the phonon angular momentum components J_x , J_y , and J_z onto the dispersion. (d) Projection of the phonon helicity onto the dispersion. In (a-d), red (blue) dots denote positive (negative) angular momentum or helicity, and their size is proportional to the magnitude. (e) Pseudo-angular momentum (PAM) calculated along high-symmetry paths exhibiting three- or four-fold (screw) rotational symmetry. See more descriptions about the PAM in (e).

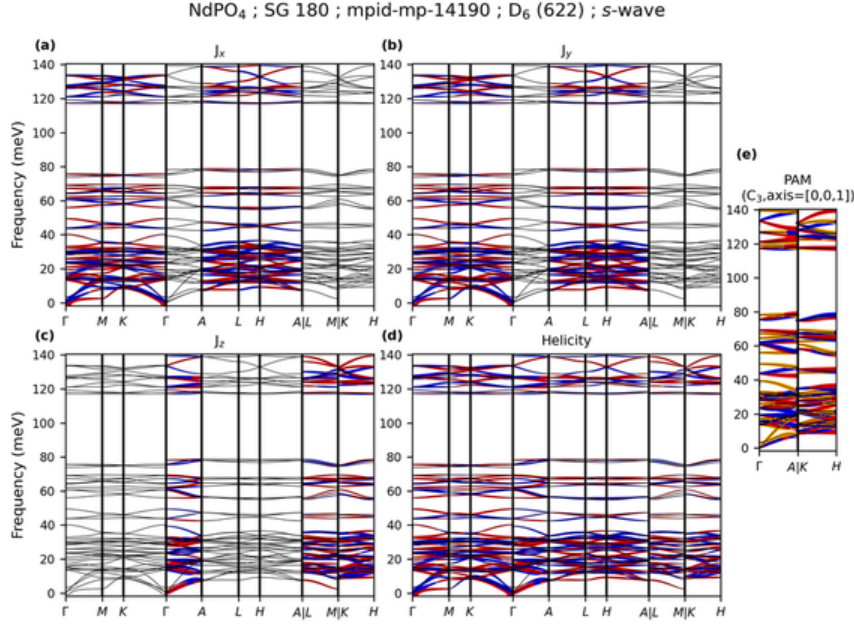


FIG. S52. Phonon dispersion of NdPO₄ ([mp-14190](#)) along the specific momentum paths in the Brillouin zone of SG 180 (see Table [S34](#)). (a-c) Projections of the phonon angular momentum components J_x , J_y , and J_z onto the dispersion. (d) Projection of the phonon helicity onto the dispersion. In (a-d), red (blue) dots denote positive (negative) angular momentum or helicity, and their size is proportional to the magnitude. (e) Pseudo-angular momentum (PAM) calculated along high-symmetry paths exhibiting three- or four-fold (screw) rotational symmetry. See more descriptions about the PAM in (e).

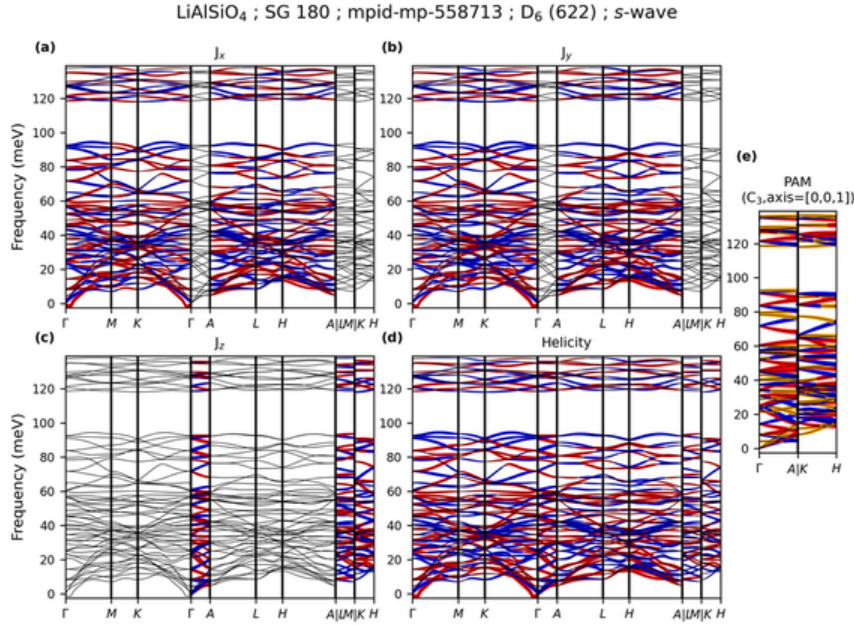


FIG. S53. Phonon dispersion of LiAlSiO₄ ([mp-558713](#)) along the specific momentum paths in the Brillouin zone of SG 180 (see Table [S34](#)). (a-c) Projections of the phonon angular momentum components J_x , J_y , and J_z onto the dispersion. (d) Projection of the phonon helicity onto the dispersion. In (a-d), red (blue) dots denote positive (negative) angular momentum or helicity, and their size is proportional to the magnitude. (e) Pseudo-angular momentum (PAM) calculated along high-symmetry paths exhibiting three- or four-fold (screw) rotational symmetry. See more descriptions about the PAM in (e).

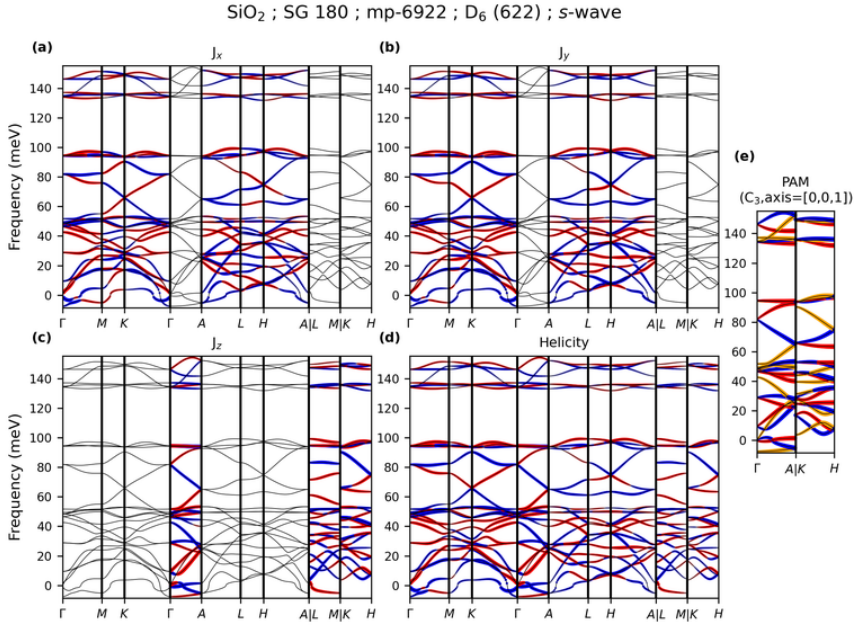


FIG. S54. Phonon dispersion of SiO₂ (mp-6922) along the specific momentum paths in the Brillouin zone of SG 180 (see Table S34). (a-c) Projections of the phonon angular momentum components J_x , J_y , and J_z onto the dispersion. (d) Projection of the phonon helicity onto the dispersion. In (a-d), red (blue) dots denote positive (negative) angular momentum or helicity, and their size is proportional to the magnitude. (e) Pseudo-angular momentum (PAM) calculated along high-symmetry paths exhibiting three- or four-fold (screw) rotational symmetry. See more descriptions about the PAM in (e).

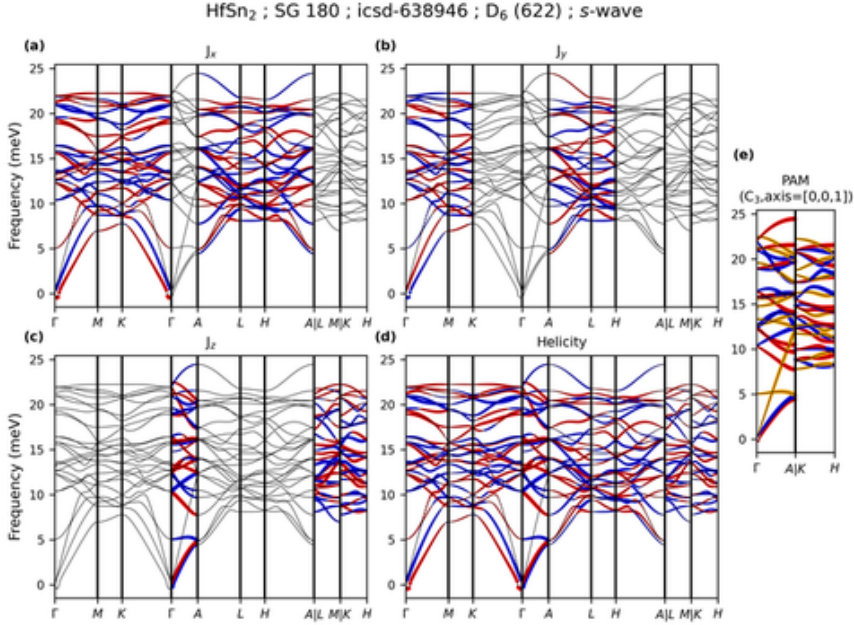


FIG. S55. Phonon dispersion of HfSn₂ (icsd-638946) along the specific momentum paths in the Brillouin zone of SG 180 (see Table S34). (a-c) Projections of the phonon angular momentum components J_x , J_y , and J_z onto the dispersion. (d) Projection of the phonon helicity onto the dispersion. In (a-d), red (blue) dots denote positive (negative) angular momentum or helicity, and their size is proportional to the magnitude. (e) Pseudo-angular momentum (PAM) calculated along high-symmetry paths exhibiting three- or four-fold (screw) rotational symmetry. See more descriptions about the PAM in (e).

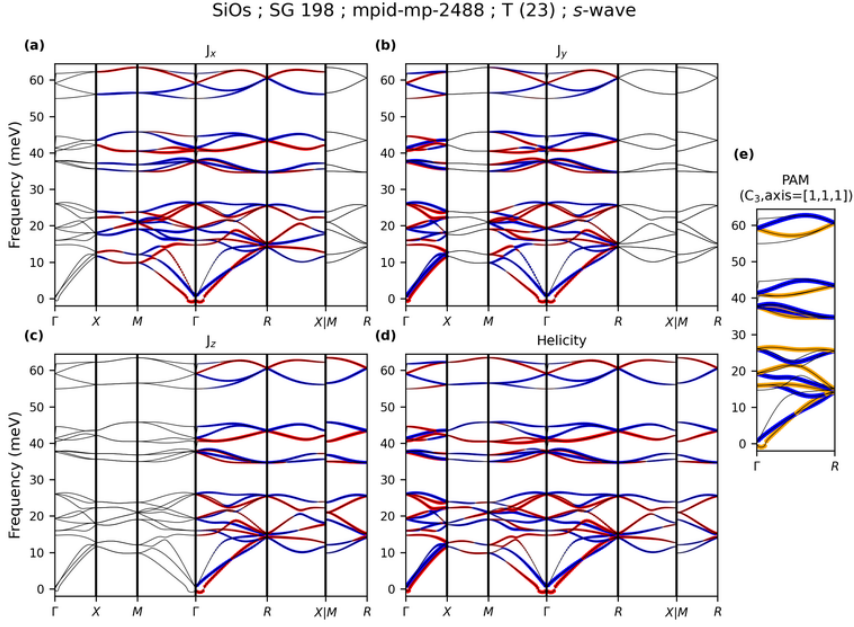


FIG. S56. Phonon dispersion of SiOs (mp-2488) along the specific momentum paths in the Brillouin zone of SG 198 (see Table S37). (a-c) Projections of the phonon angular momentum components J_x , J_y , and J_z onto the dispersion. (d) Projection of the phonon helicity onto the dispersion. In (a-d), red (blue) dots denote positive (negative) angular momentum or helicity, and their size is proportional to the magnitude. (e) Pseudo-angular momentum (PAM) calculated along high-symmetry paths exhibiting three- or four-fold (screw) rotational symmetry. See more descriptions about the PAM in (e).

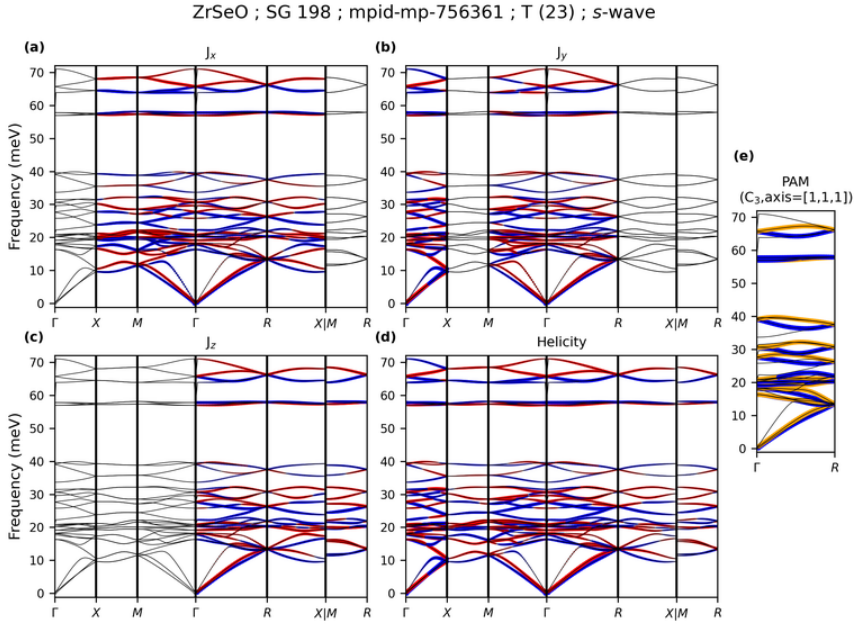


FIG. S57. Phonon dispersion of ZrSeO (mp-756361) along the specific momentum paths in the Brillouin zone of SG 198 (see Table S37). (a-c) Projections of the phonon angular momentum components J_x , J_y , and J_z onto the dispersion. (d) Projection of the phonon helicity onto the dispersion. In (a-d), red (blue) dots denote positive (negative) angular momentum or helicity, and their size is proportional to the magnitude. (e) Pseudo-angular momentum (PAM) calculated along high-symmetry paths exhibiting three- or four-fold (screw) rotational symmetry. See more descriptions about the PAM in (e).

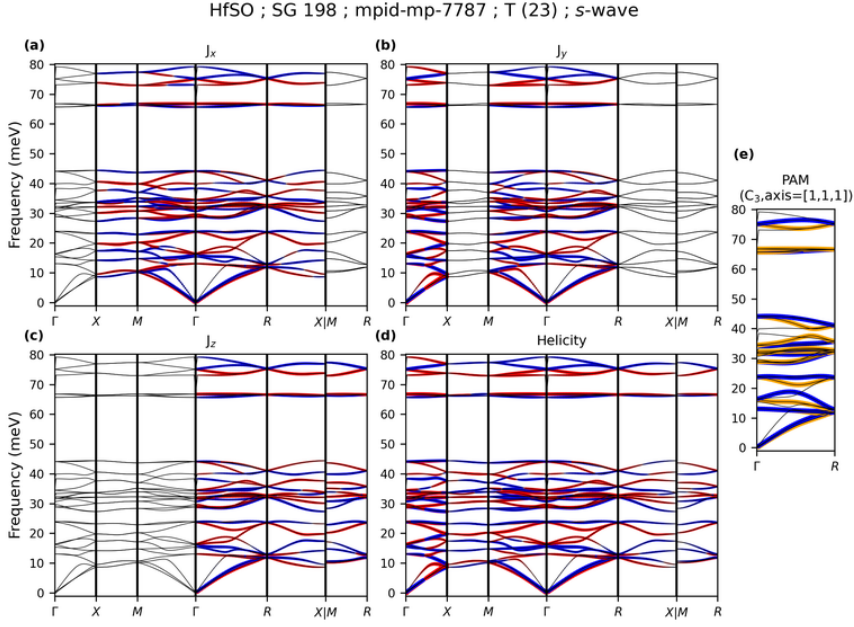


FIG. S58. Phonon dispersion of HfSO ([mp-7787](#)) along the specific momentum paths in the Brillouin zone of SG 198 (see Table S37). (a-c) Projections of the phonon angular momentum components J_x , J_y , and J_z onto the dispersion. (d) Projection of the phonon helicity onto the dispersion. In (a-d), red (blue) dots denote positive (negative) angular momentum or helicity, and their size is proportional to the magnitude. (e) Pseudo-angular momentum (PAM) calculated along high-symmetry paths exhibiting three- or four-fold (screw) rotational symmetry. See more descriptions about the PAM in (e).

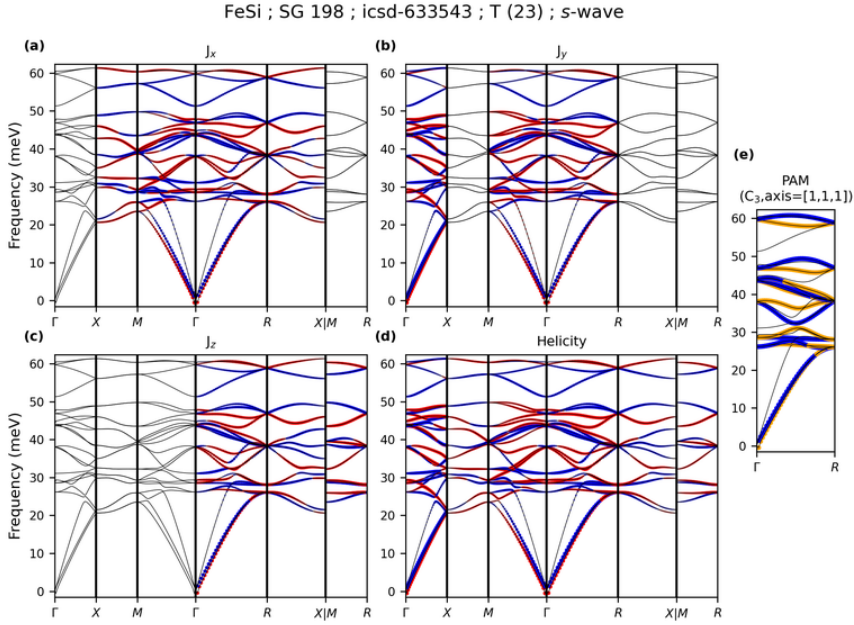


FIG. S59. Phonon dispersion of FeSi ([icsd-633543](#)) along the specific momentum paths in the Brillouin zone of SG 198 (see Table S37). (a-c) Projections of the phonon angular momentum components J_x , J_y , and J_z onto the dispersion. (d) Projection of the phonon helicity onto the dispersion. In (a-d), red (blue) dots denote positive (negative) angular momentum or helicity, and their size is proportional to the magnitude. (e) Pseudo-angular momentum (PAM) calculated along high-symmetry paths exhibiting three- or four-fold (screw) rotational symmetry. See more descriptions about the PAM in (e).

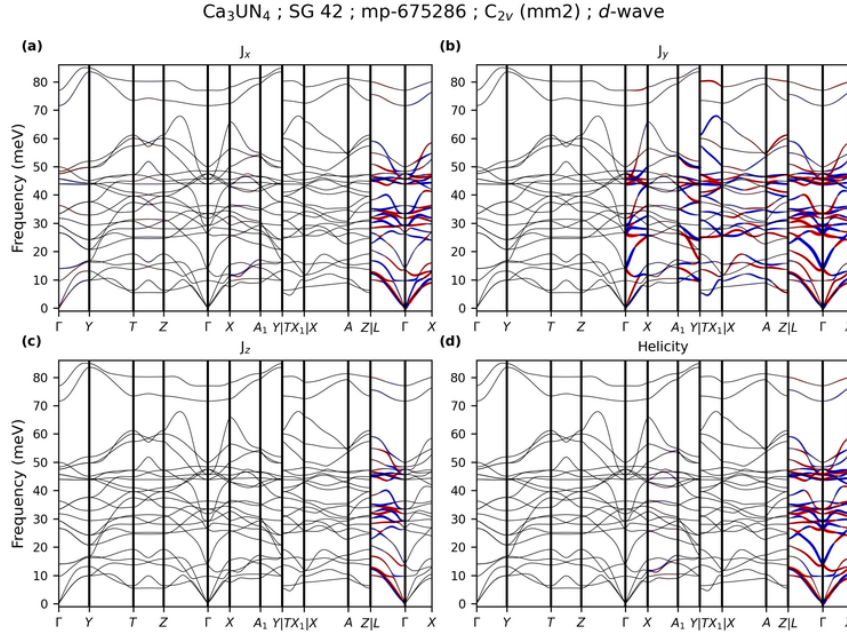


FIG. S60. Phonon dispersion of Ca_3UN_4 (mp-675286) along the specific momentum paths in the Brillouin zone of SG 42 (see Table S9). (a-c) Projections of the phonon angular momentum components J_x , J_y , and J_z onto the dispersion. (d) Projection of the phonon helicity onto the dispersion. In (a-d), red (blue) dots denote positive (negative) angular momentum or helicity, and their size is proportional to the magnitude.

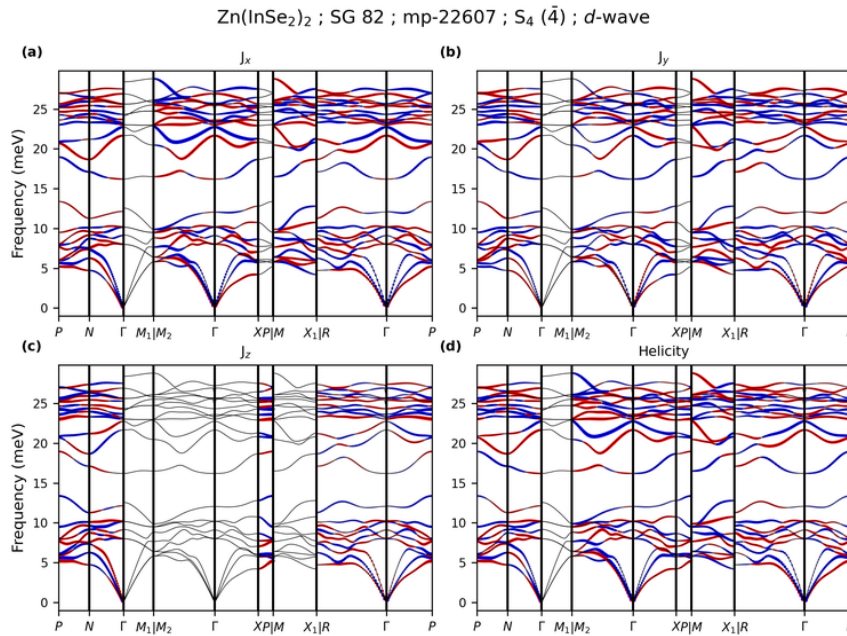


FIG. S61. Phonon dispersion of $\text{Zn}(\text{InSe}_2)_2$ (mp-22607) along the specific momentum paths in the Brillouin zone of SG 82 (see Table S10). (a-c) Projections of the phonon angular momentum components J_x , J_y , and J_z onto the dispersion. (d) Projection of the phonon helicity onto the dispersion. In (a-d), red (blue) dots denote positive (negative) angular momentum or helicity, and their size is proportional to the magnitude.

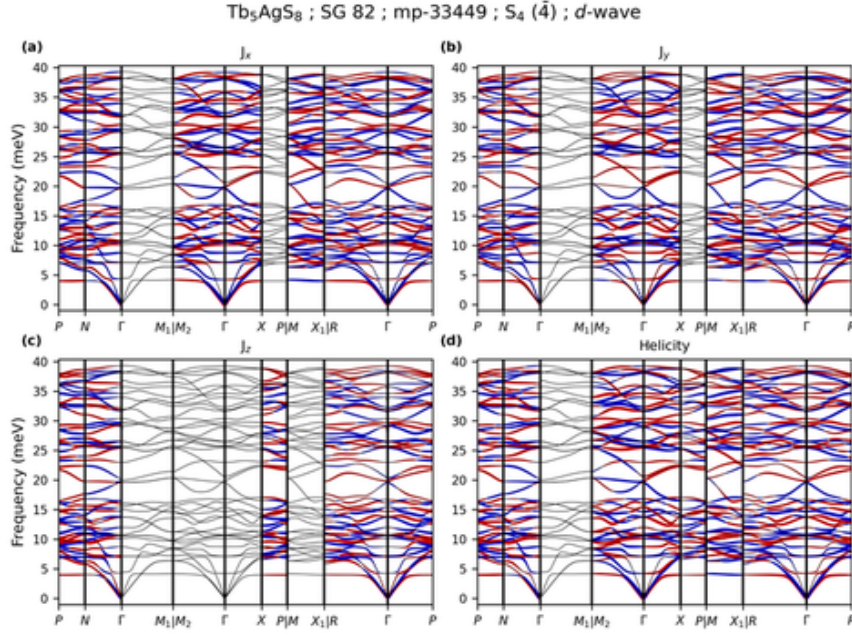


FIG. S62. Phonon dispersion of Tb₅AgS₈ (mp-33449) along the specific momentum paths in the Brillouin zone of SG 82 (see Table S10). (a-c) Projections of the phonon angular momentum components J_x , J_y , and J_z onto the dispersion. (d) Projection of the phonon helicity onto the dispersion. In (a-d), red (blue) dots denote positive (negative) angular momentum or helicity, and their size is proportional to the magnitude.

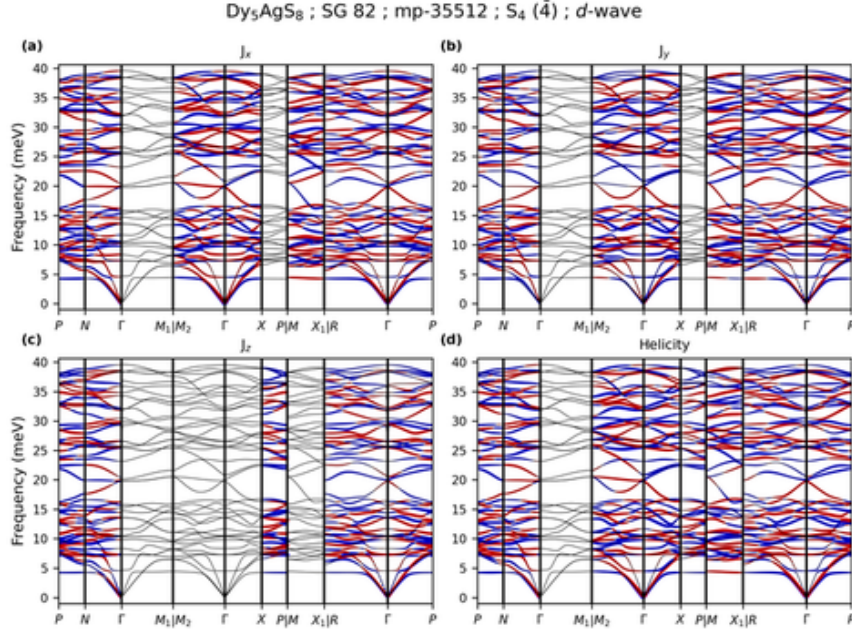


FIG. S63. Phonon dispersion of Dy₅AgS₈ (mp-35512) along the specific momentum paths in the Brillouin zone of SG 82 (see Table S10). (a-c) Projections of the phonon angular momentum components J_x , J_y , and J_z onto the dispersion. (d) Projection of the phonon helicity onto the dispersion. In (a-d), red (blue) dots denote positive (negative) angular momentum or helicity, and their size is proportional to the magnitude.

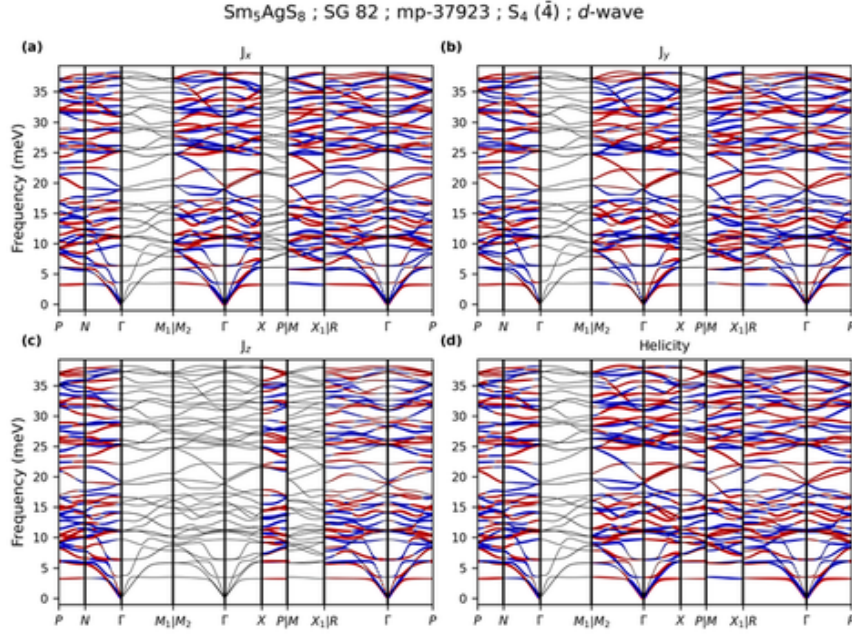


FIG. S64. Phonon dispersion of Sm_5AgS_8 (mp-37923) along the specific momentum paths in the Brillouin zone of SG 82 (see Table S10). (a-c) Projections of the phonon angular momentum components J_x , J_y , and J_z onto the dispersion. (d) Projection of the phonon helicity onto the dispersion. In (a-d), red (blue) dots denote positive (negative) angular momentum or helicity, and their size is proportional to the magnitude.

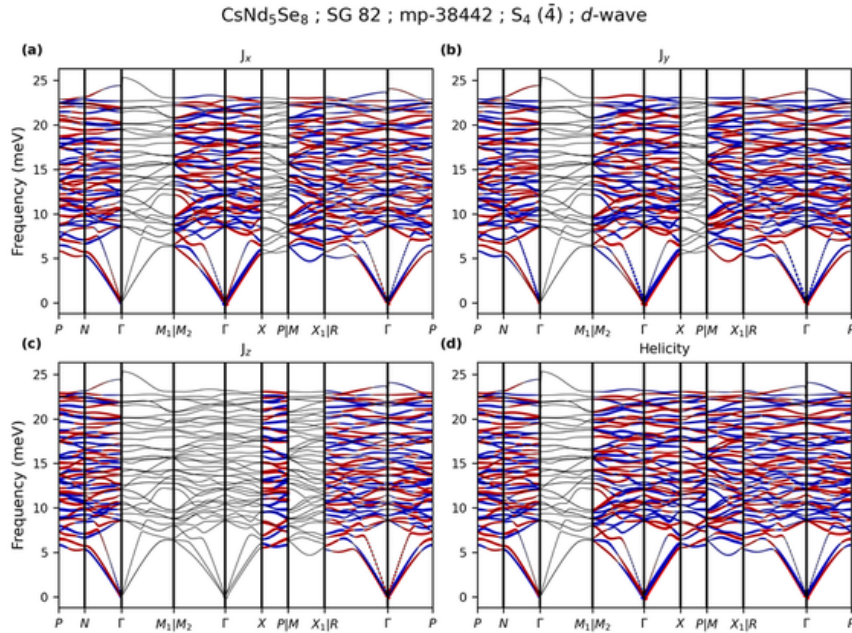


FIG. S65. Phonon dispersion of CsNd_5Se_8 (mp-38442) along the specific momentum paths in the Brillouin zone of SG 82 (see Table S10). (a-c) Projections of the phonon angular momentum components J_x , J_y , and J_z onto the dispersion. (d) Projection of the phonon helicity onto the dispersion. In (a-d), red (blue) dots denote positive (negative) angular momentum or helicity, and their size is proportional to the magnitude.

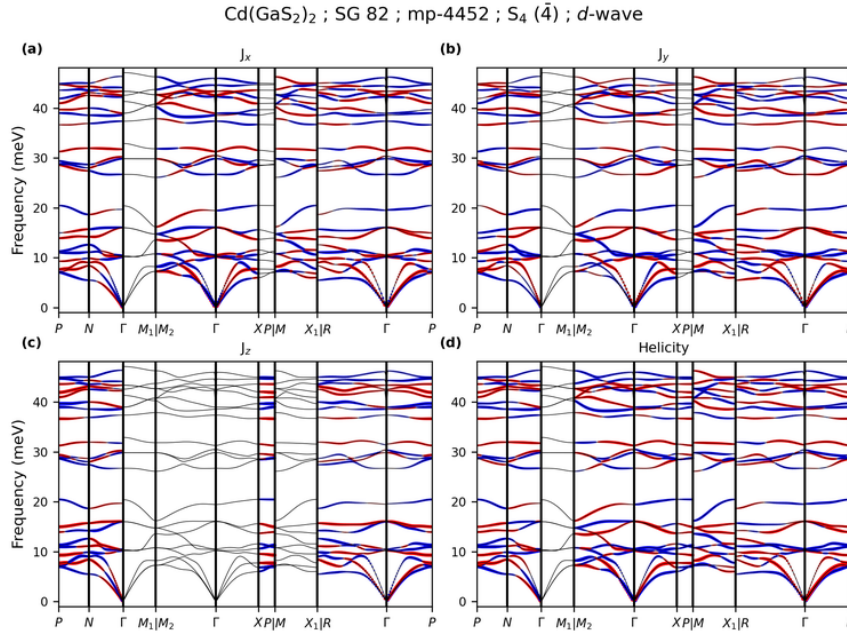


FIG. S66. Phonon dispersion of $\text{Cd}(\text{GaS}_2)_2$ (mp-4452) along the specific momentum paths in the Brillouin zone of SG 82 (see Table S10). (a-c) Projections of the phonon angular momentum components J_x , J_y , and J_z onto the dispersion. (d) Projection of the phonon helicity onto the dispersion. In (a-d), red (blue) dots denote positive (negative) angular momentum or helicity, and their size is proportional to the magnitude.

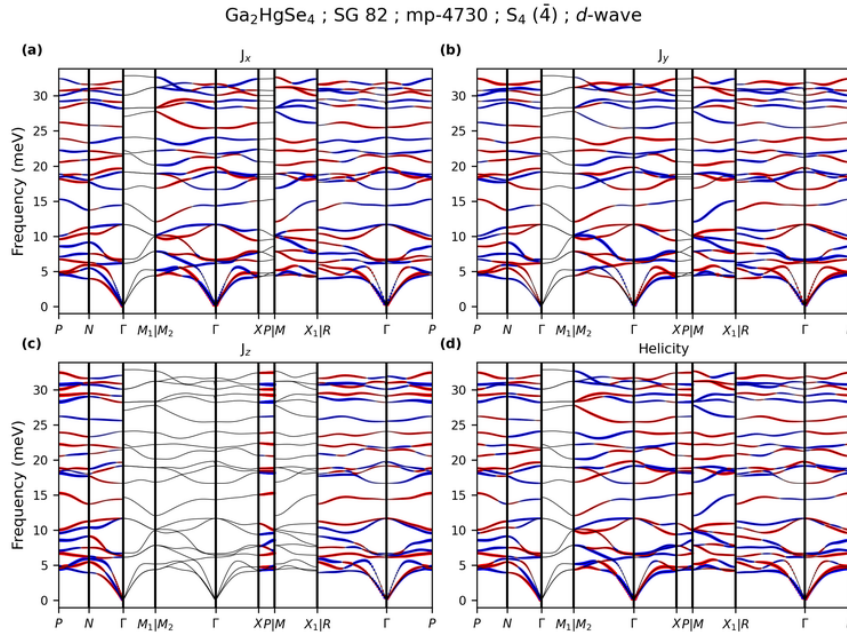


FIG. S67. Phonon dispersion of Ga_2HgSe_4 (mp-4730) along the specific momentum paths in the Brillouin zone of SG 82 (see Table S10). (a-c) Projections of the phonon angular momentum components J_x , J_y , and J_z onto the dispersion. (d) Projection of the phonon helicity onto the dispersion. In (a-d), red (blue) dots denote positive (negative) angular momentum or helicity, and their size is proportional to the magnitude.

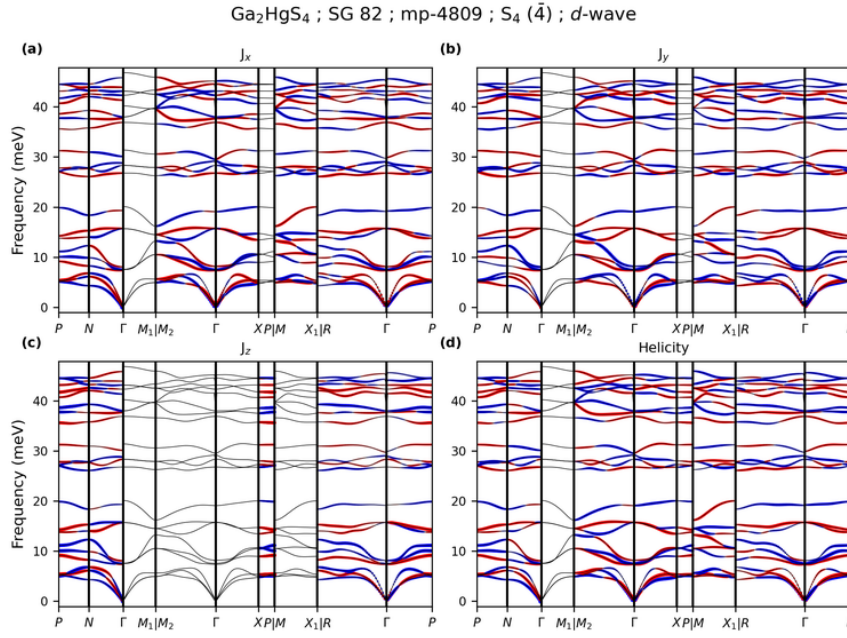


FIG. S68. Phonon dispersion of Ga_2HgS_4 (mp-4809) along the specific momentum paths in the Brillouin zone of SG 82 (see Table S10). (a-c) Projections of the phonon angular momentum components J_x , J_y , and J_z onto the dispersion. (d) Projection of the phonon helicity onto the dispersion. In (a-d), red (blue) dots denote positive (negative) angular momentum or helicity, and their size is proportional to the magnitude.

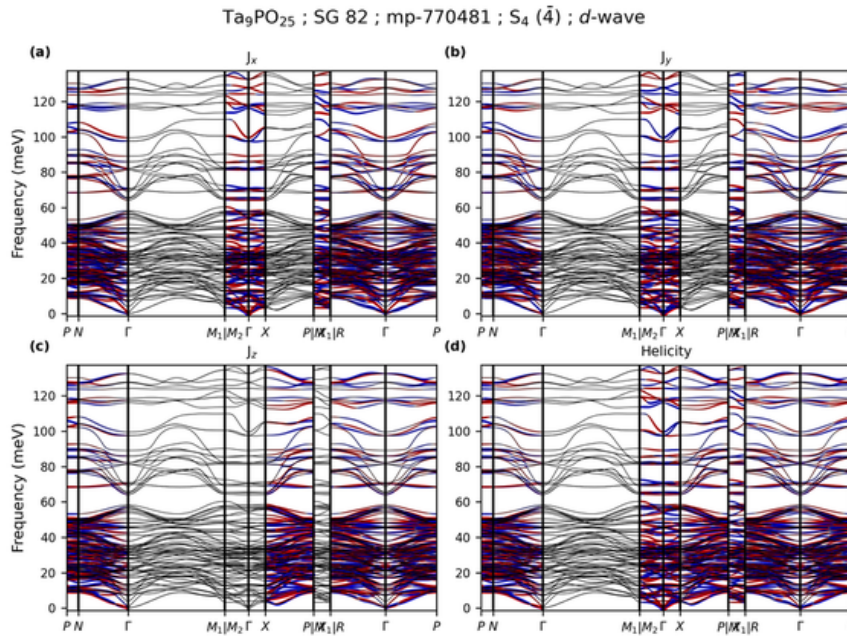


FIG. S69. Phonon dispersion of $\text{Ta}_9\text{PO}_{25}$ (mp-770481) along the specific momentum paths in the Brillouin zone of SG 82 (see Table S10). (a-c) Projections of the phonon angular momentum components J_x , J_y , and J_z onto the dispersion. (d) Projection of the phonon helicity onto the dispersion. In (a-d), red (blue) dots denote positive (negative) angular momentum or helicity, and their size is proportional to the magnitude.

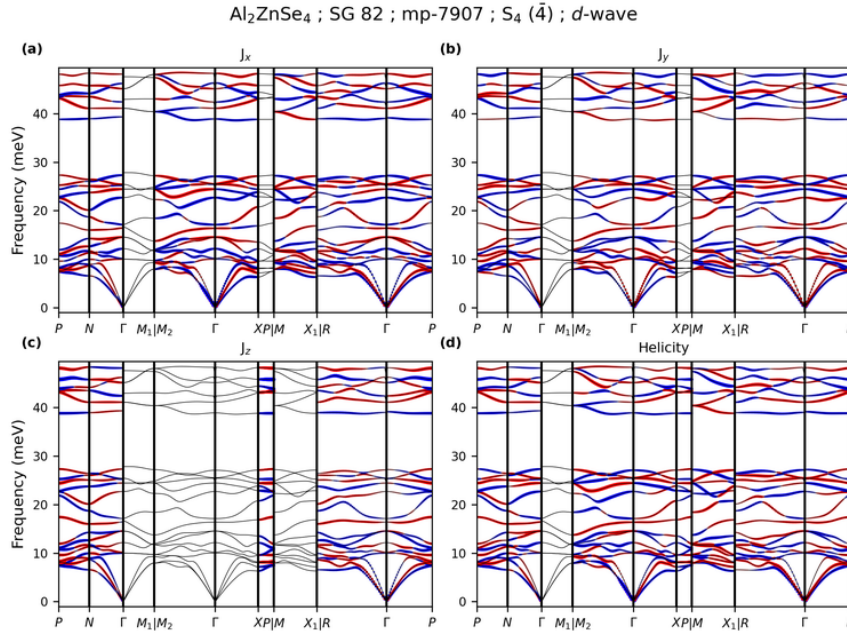


FIG. S70. Phonon dispersion of Al_2ZnSe_4 (mp-7907) along the specific momentum paths in the Brillouin zone of SG 82 (see Table S10). (a-c) Projections of the phonon angular momentum components J_x , J_y , and J_z onto the dispersion. (d) Projection of the phonon helicity onto the dispersion. In (a-d), red (blue) dots denote positive (negative) angular momentum or helicity, and their size is proportional to the magnitude.

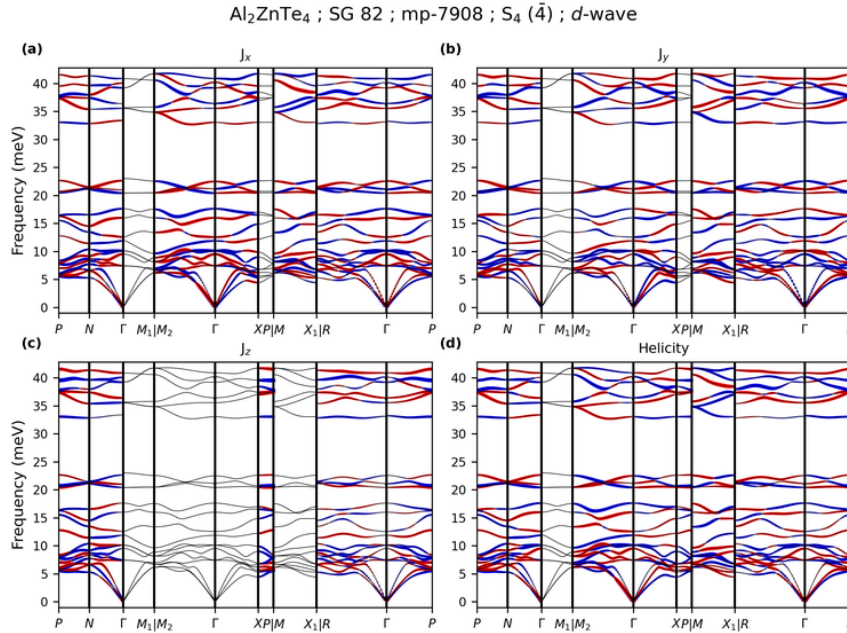


FIG. S71. Phonon dispersion of Al_2ZnTe_4 (mp-7908) along the specific momentum paths in the Brillouin zone of SG 82 (see Table S10). (a-c) Projections of the phonon angular momentum components J_x , J_y , and J_z onto the dispersion. (d) Projection of the phonon helicity onto the dispersion. In (a-d), red (blue) dots denote positive (negative) angular momentum or helicity, and their size is proportional to the magnitude.

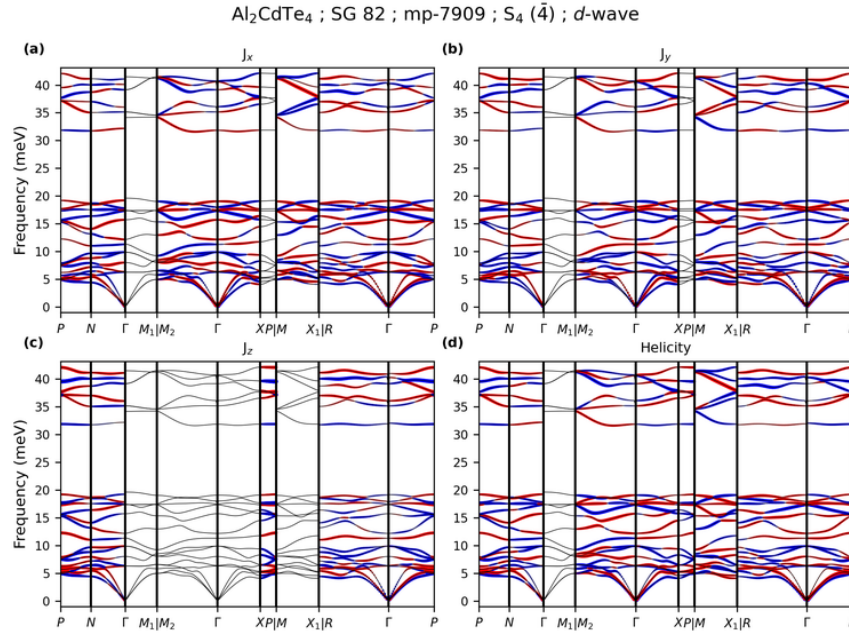


FIG. S72. Phonon dispersion of Al_2CdTe_4 (mp-7909) along the specific momentum paths in the Brillouin zone of SG 82 (see Table S10). (a-c) Projections of the phonon angular momentum components J_x , J_y , and J_z onto the dispersion. (d) Projection of the phonon helicity onto the dispersion. In (a-d), red (blue) dots denote positive (negative) angular momentum or helicity, and their size is proportional to the magnitude.

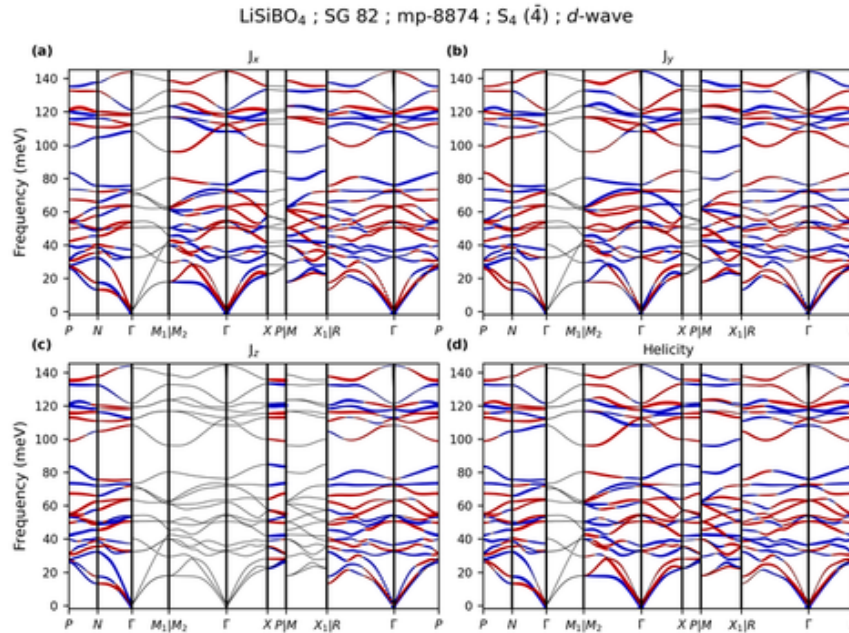


FIG. S73. Phonon dispersion of LiSiBO_4 (mp-8874) along the specific momentum paths in the Brillouin zone of SG 82 (see Table S10). (a-c) Projections of the phonon angular momentum components J_x , J_y , and J_z onto the dispersion. (d) Projection of the phonon helicity onto the dispersion. In (a-d), red (blue) dots denote positive (negative) angular momentum or helicity, and their size is proportional to the magnitude.

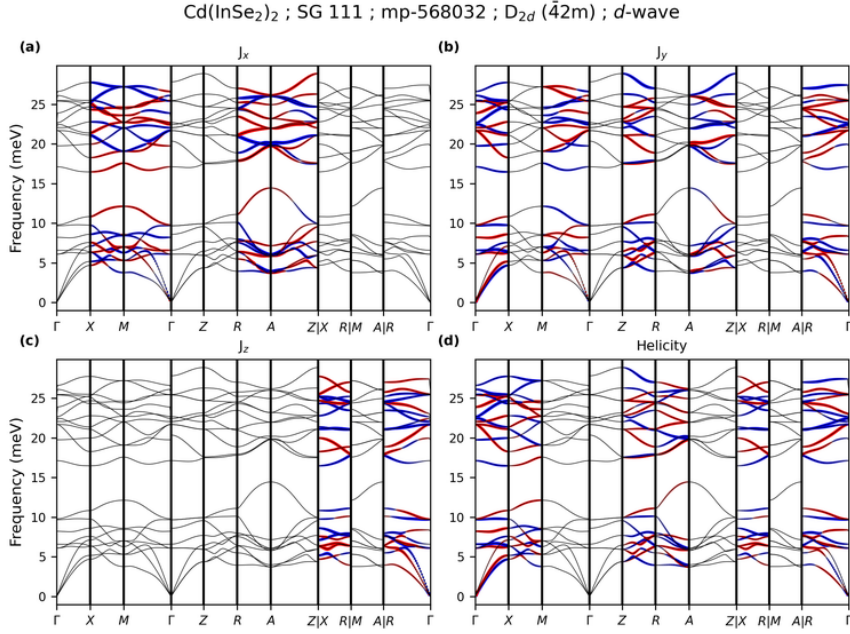


FIG. S74. Phonon dispersion of $\text{Cd}(\text{InSe}_2)_2$ (mp-568032) along the specific momentum paths in the Brillouin zone of SG 111 (see Table S19). (a-c) Projections of the phonon angular momentum components J_x , J_y , and J_z onto the dispersion. (d) Projection of the phonon helicity onto the dispersion. In (a-d), red (blue) dots denote positive (negative) angular momentum or helicity, and their size is proportional to the magnitude.

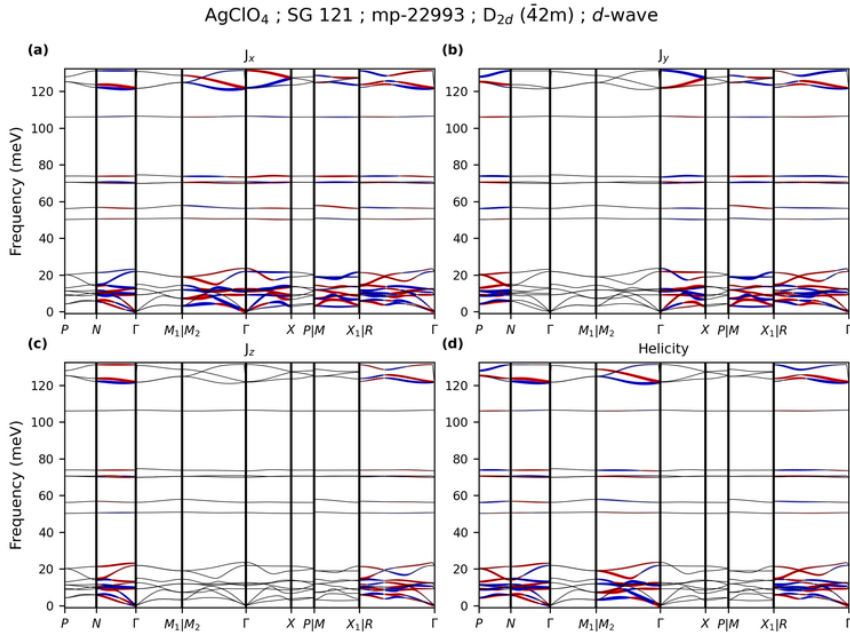


FIG. S75. Phonon dispersion of AgClO_4 (mp-22993) along the specific momentum paths in the Brillouin zone of SG 121 (see Table S20). (a-c) Projections of the phonon angular momentum components J_x , J_y , and J_z onto the dispersion. (d) Projection of the phonon helicity onto the dispersion. In (a-d), red (blue) dots denote positive (negative) angular momentum or helicity, and their size is proportional to the magnitude.

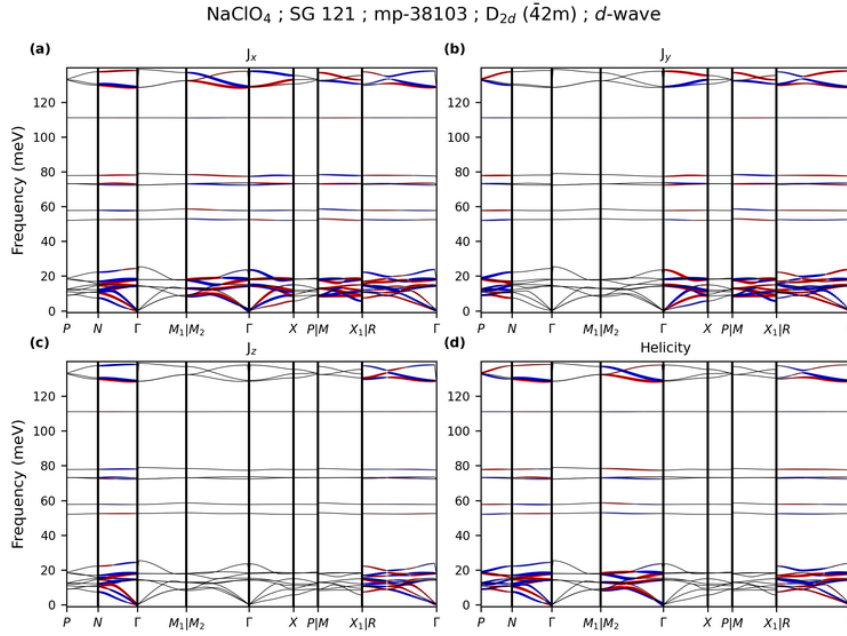


FIG. S76. Phonon dispersion of NaClO_4 (mp-38103) along the specific momentum paths in the Brillouin zone of SG 121 (see Table S20). (a-c) Projections of the phonon angular momentum components J_x , J_y , and J_z onto the dispersion. (d) Projection of the phonon helicity onto the dispersion. In (a-d), red (blue) dots denote positive (negative) angular momentum or helicity, and their size is proportional to the magnitude.

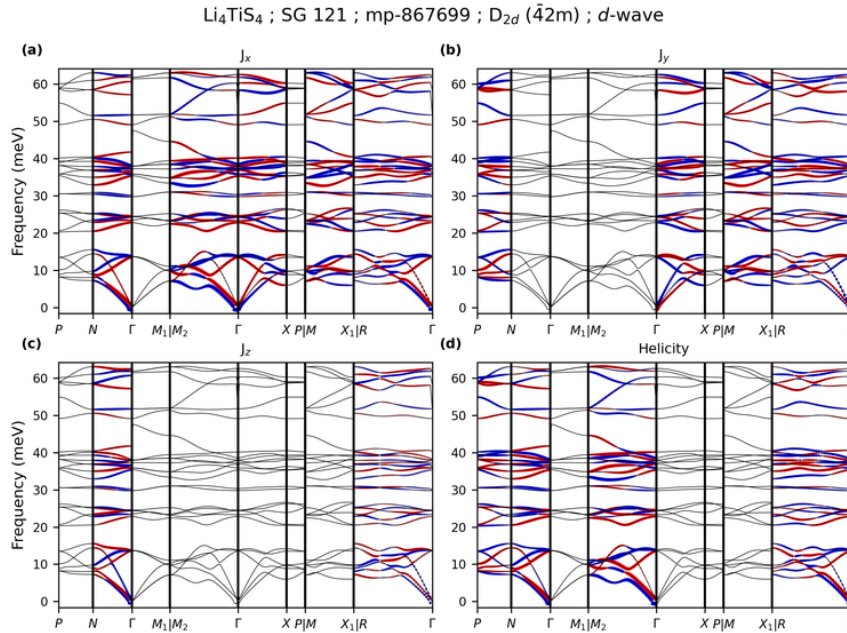


FIG. S77. Phonon dispersion of Li_4TiS_4 (mp-867699) along the specific momentum paths in the Brillouin zone of SG 121 (see Table S20). (a-c) Projections of the phonon angular momentum components J_x , J_y , and J_z onto the dispersion. (d) Projection of the phonon helicity onto the dispersion. In (a-d), red (blue) dots denote positive (negative) angular momentum or helicity, and their size is proportional to the magnitude.

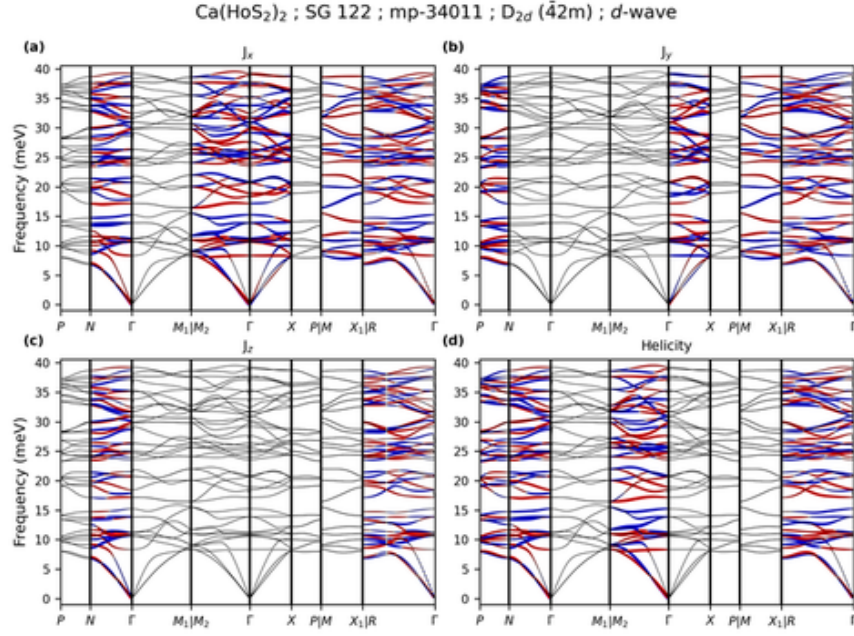


FIG. S78. Phonon dispersion of Ca(HoS₂)₂ (mp-34011) along the specific momentum paths in the Brillouin zone of SG 122 (see Table S21). (a-c) Projections of the phonon angular momentum components J_x , J_y , and J_z onto the dispersion. (d) Projection of the phonon helicity onto the dispersion. In (a-d), red (blue) dots denote positive (negative) angular momentum or helicity, and their size is proportional to the magnitude.

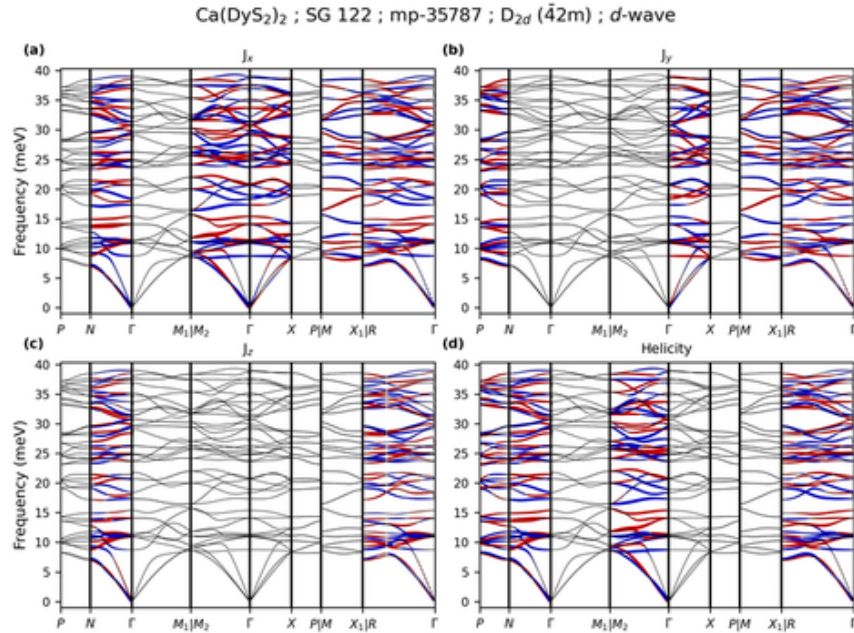


FIG. S79. Phonon dispersion of Ca(DyS₂)₂ (mp-35787) along the specific momentum paths in the Brillouin zone of SG 122 (see Table S21). (a-c) Projections of the phonon angular momentum components J_x , J_y , and J_z onto the dispersion. (d) Projection of the phonon helicity onto the dispersion. In (a-d), red (blue) dots denote positive (negative) angular momentum or helicity, and their size is proportional to the magnitude.

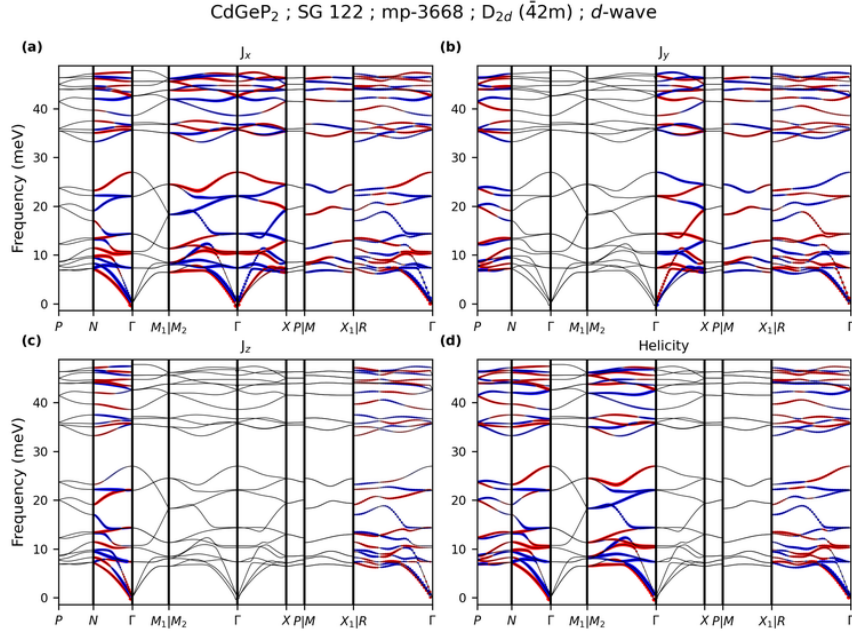


FIG. S80. Phonon dispersion of CdGeP₂ (mp-3668) along the specific momentum paths in the Brillouin zone of SG 122 (see Table S21). (a-c) Projections of the phonon angular momentum components J_x , J_y , and J_z onto the dispersion. (d) Projection of the phonon helicity onto the dispersion. In (a-d), red (blue) dots denote positive (negative) angular momentum or helicity, and their size is proportional to the magnitude.

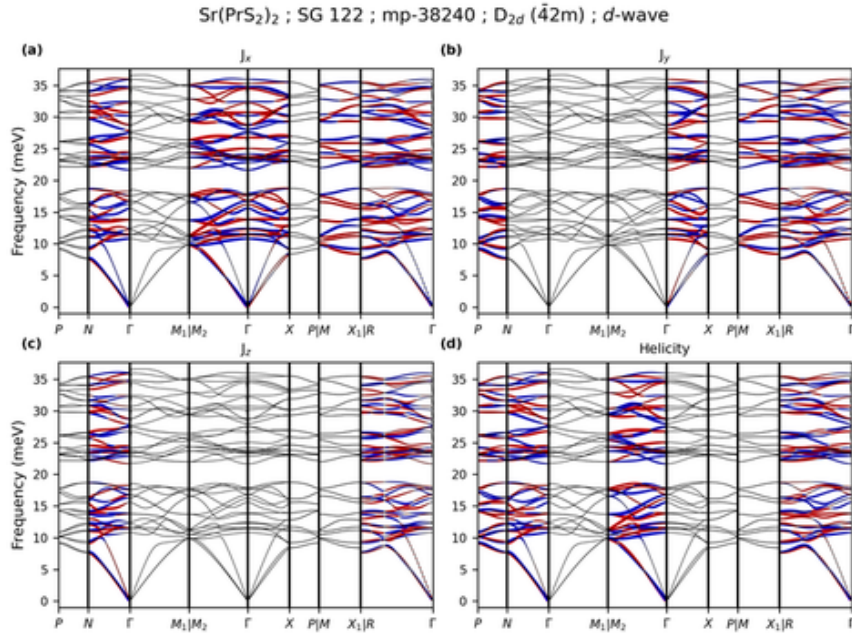


FIG. S81. Phonon dispersion of Sr(PrS₂)₂ (mp-38240) along the specific momentum paths in the Brillouin zone of SG 122 (see Table S21). (a-c) Projections of the phonon angular momentum components J_x , J_y , and J_z onto the dispersion. (d) Projection of the phonon helicity onto the dispersion. In (a-d), red (blue) dots denote positive (negative) angular momentum or helicity, and their size is proportional to the magnitude.

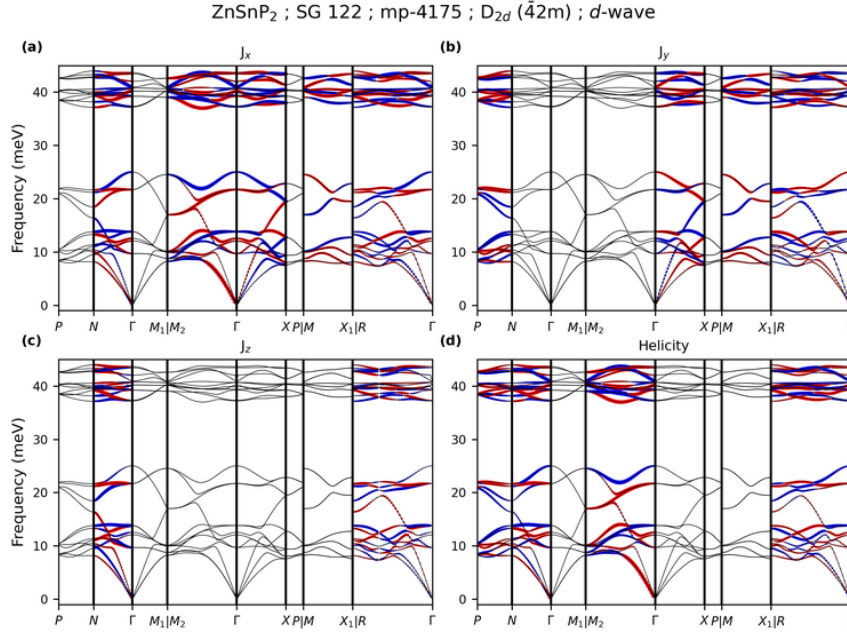


FIG. S82. Phonon dispersion of ZnSnP₂ (mp-4175) along the specific momentum paths in the Brillouin zone of SG 122 (see Table S21). (a-c) Projections of the phonon angular momentum components J_x , J_y , and J_z onto the dispersion. (d) Projection of the phonon helicity onto the dispersion. In (a-d), red (blue) dots denote positive (negative) angular momentum or helicity, and their size is proportional to the magnitude.

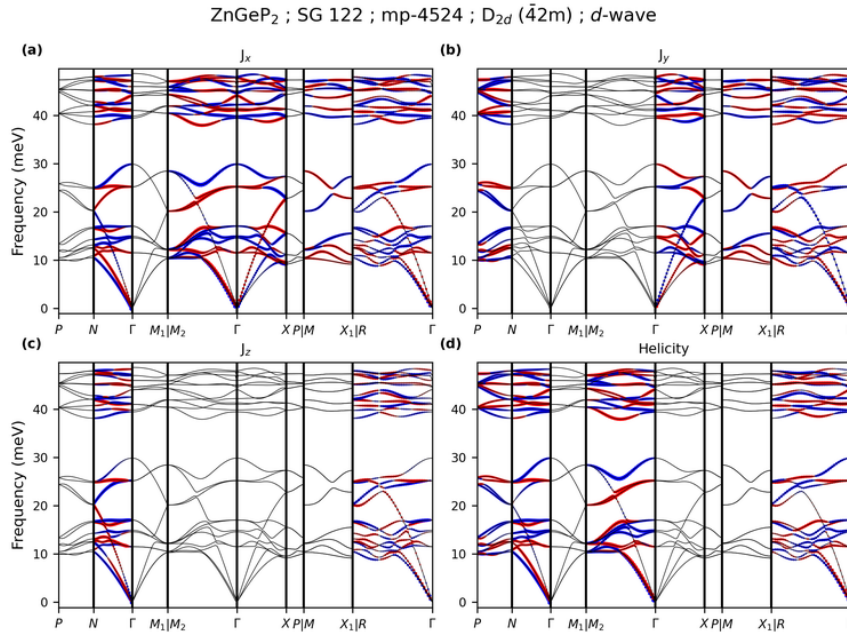


FIG. S83. Phonon dispersion of ZnGeP₂ (mp-4524) along the specific momentum paths in the Brillouin zone of SG 122 (see Table S21). (a-c) Projections of the phonon angular momentum components J_x , J_y , and J_z onto the dispersion. (d) Projection of the phonon helicity onto the dispersion. In (a-d), red (blue) dots denote positive (negative) angular momentum or helicity, and their size is proportional to the magnitude.

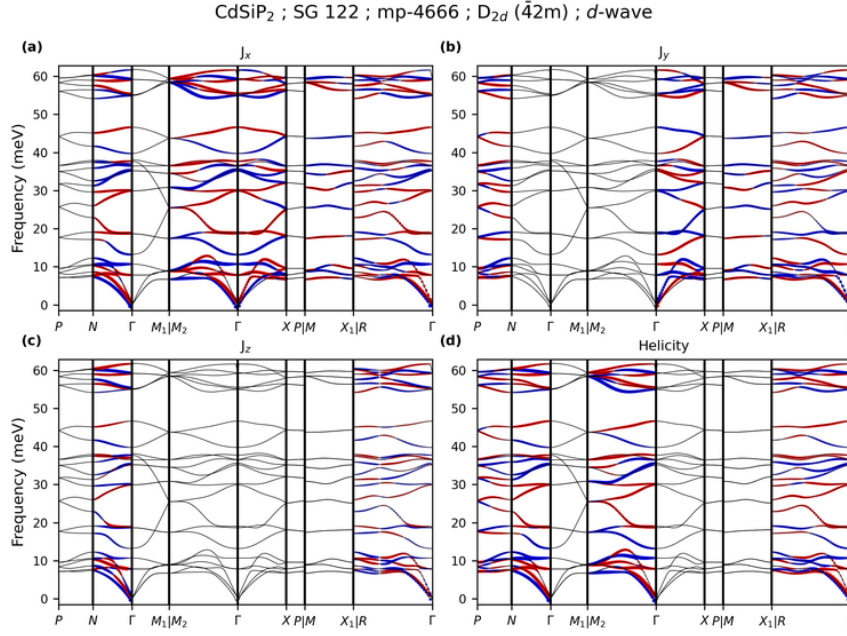


FIG. S84. Phonon dispersion of CdSiP₂ (mp-4666) along the specific momentum paths in the Brillouin zone of SG 122 (see Table S21). (a-c) Projections of the phonon angular momentum components J_x , J_y , and J_z onto the dispersion. (d) Projection of the phonon helicity onto the dispersion. In (a-d), red (blue) dots denote positive (negative) angular momentum or helicity, and their size is proportional to the magnitude.

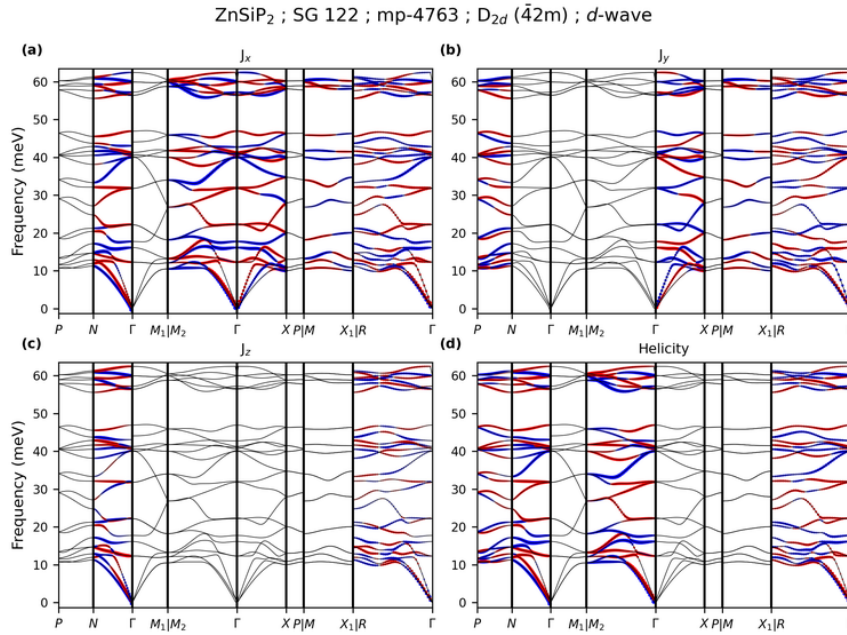


FIG. S85. Phonon dispersion of ZnSiP₂ (mp-4763) along the specific momentum paths in the Brillouin zone of SG 122 (see Table S21). (a-c) Projections of the phonon angular momentum components J_x , J_y , and J_z onto the dispersion. (d) Projection of the phonon helicity onto the dispersion. In (a-d), red (blue) dots denote positive (negative) angular momentum or helicity, and their size is proportional to the magnitude.

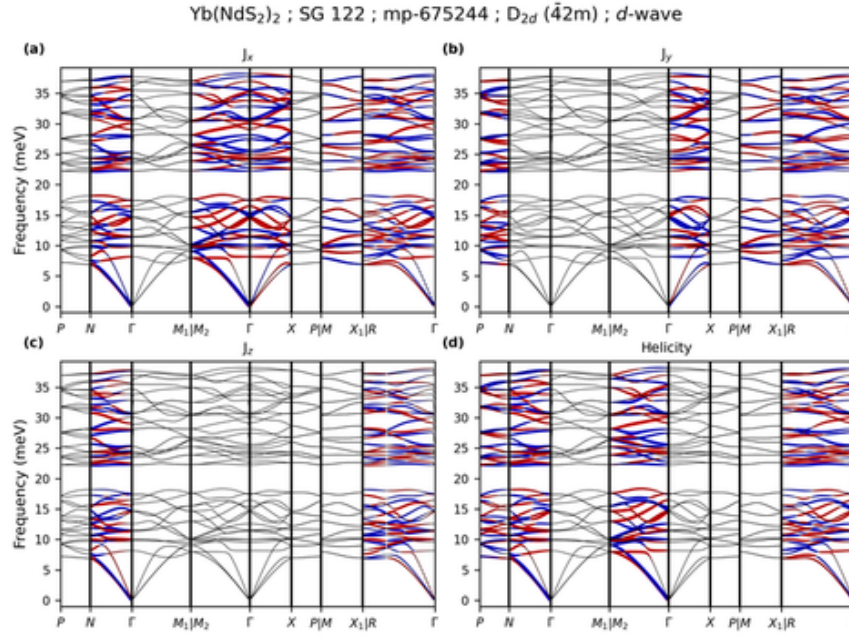


FIG. S86. Phonon dispersion of Yb(NdS₂)₂ (mp-675244) along the specific momentum paths in the Brillouin zone of SG 122 (see Table S21). (a-c) Projections of the phonon angular momentum components J_x , J_y , and J_z onto the dispersion. (d) Projection of the phonon helicity onto the dispersion. In (a-d), red (blue) dots denote positive (negative) angular momentum or helicity, and their size is proportional to the magnitude.

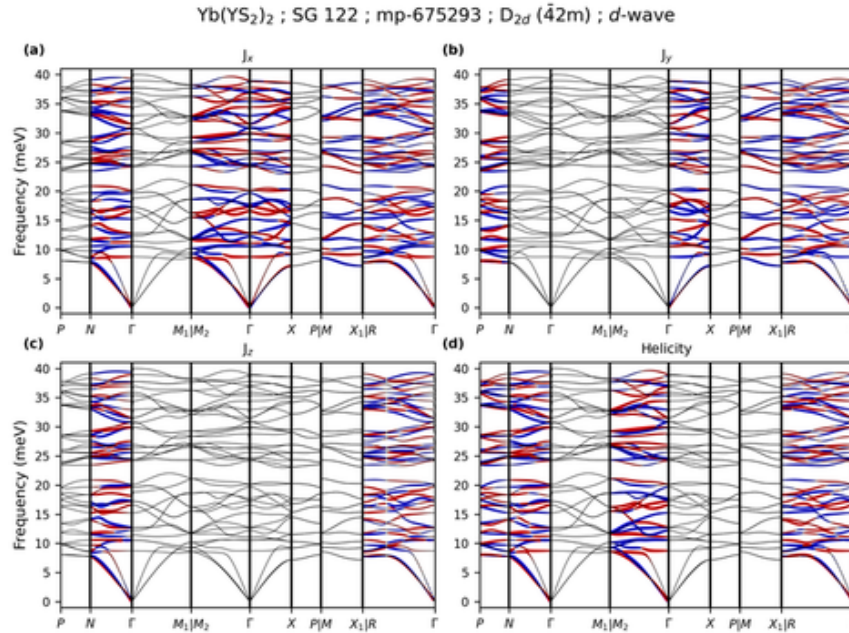


FIG. S87. Phonon dispersion of Yb(YS₂)₂ (mp-675293) along the specific momentum paths in the Brillouin zone of SG 122 (see Table S21). (a-c) Projections of the phonon angular momentum components J_x , J_y , and J_z onto the dispersion. (d) Projection of the phonon helicity onto the dispersion. In (a-d), red (blue) dots denote positive (negative) angular momentum or helicity, and their size is proportional to the magnitude.

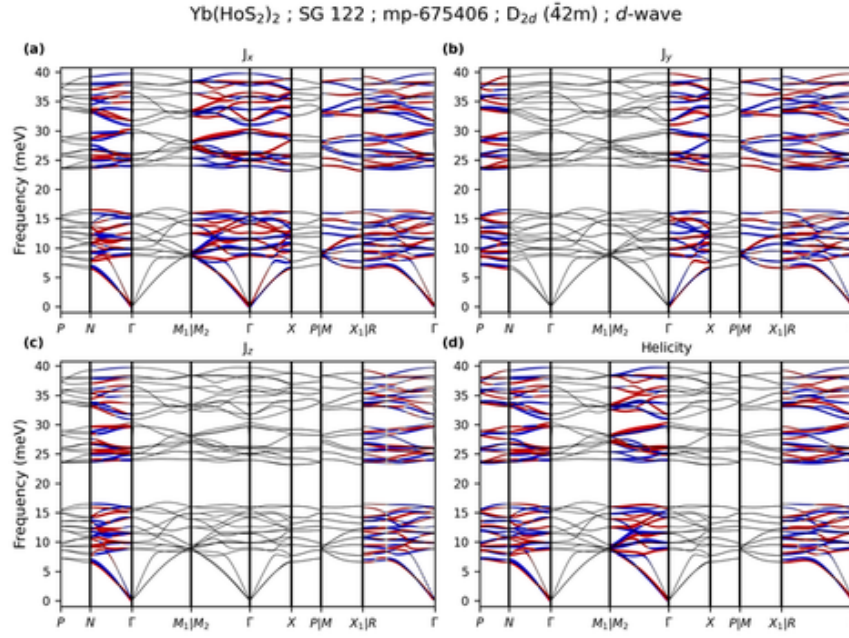


FIG. S88. Phonon dispersion of Yb(HoS₂)₂ (mp-675406) along the specific momentum paths in the Brillouin zone of SG 122 (see Table S21). (a-c) Projections of the phonon angular momentum components J_x , J_y , and J_z onto the dispersion. (d) Projection of the phonon helicity onto the dispersion. In (a-d), red (blue) dots denote positive (negative) angular momentum or helicity, and their size is proportional to the magnitude.

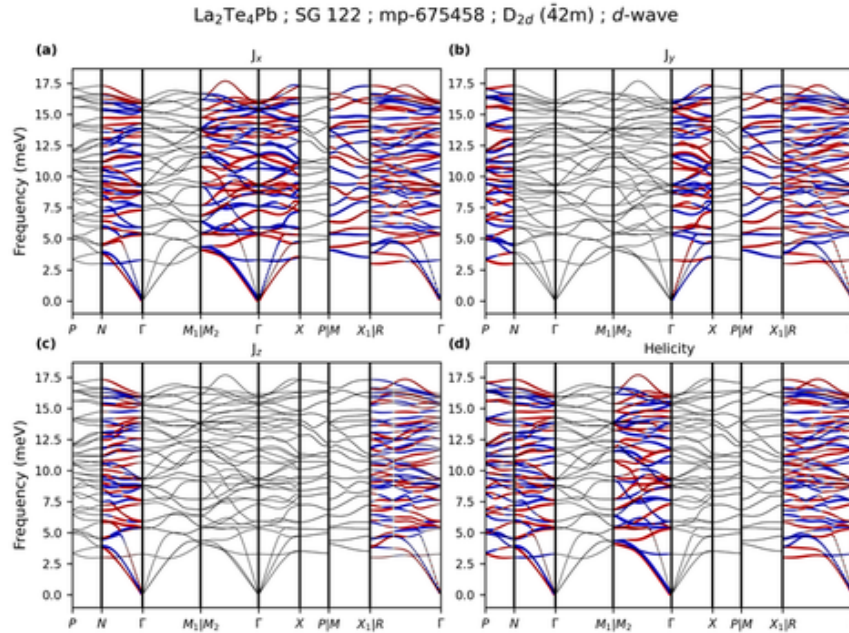


FIG. S89. Phonon dispersion of La₂Te₄Pb (mp-675458) along the specific momentum paths in the Brillouin zone of SG 122 (see Table S21). (a-c) Projections of the phonon angular momentum components J_x , J_y , and J_z onto the dispersion. (d) Projection of the phonon helicity onto the dispersion. In (a-d), red (blue) dots denote positive (negative) angular momentum or helicity, and their size is proportional to the magnitude.

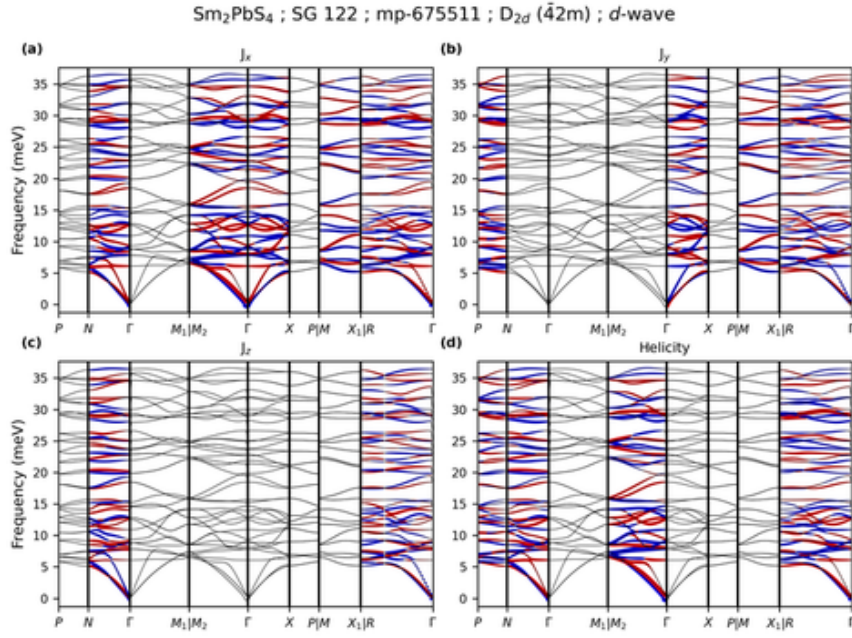


FIG. S90. Phonon dispersion of Sm_2PbS_4 (mp-675511) along the specific momentum paths in the Brillouin zone of SG 122 (see Table S21). (a-c) Projections of the phonon angular momentum components J_x , J_y , and J_z onto the dispersion. (d) Projection of the phonon helicity onto the dispersion. In (a-d), red (blue) dots denote positive (negative) angular momentum or helicity, and their size is proportional to the magnitude.

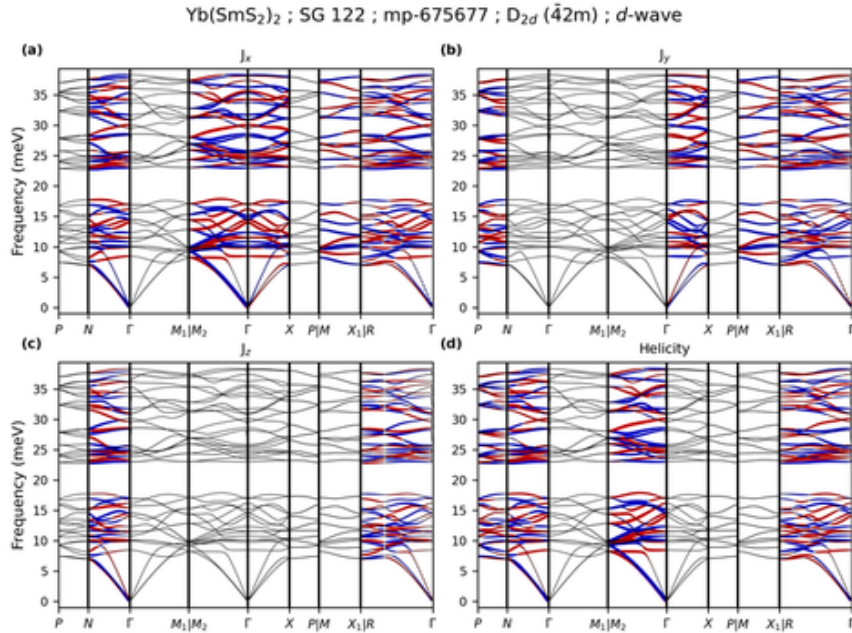


FIG. S91. Phonon dispersion of $\text{Yb}(\text{SmS}_2)_2$ (mp-675677) along the specific momentum paths in the Brillouin zone of SG 122 (see Table S21). (a-c) Projections of the phonon angular momentum components J_x , J_y , and J_z onto the dispersion. (d) Projection of the phonon helicity onto the dispersion. In (a-d), red (blue) dots denote positive (negative) angular momentum or helicity, and their size is proportional to the magnitude.

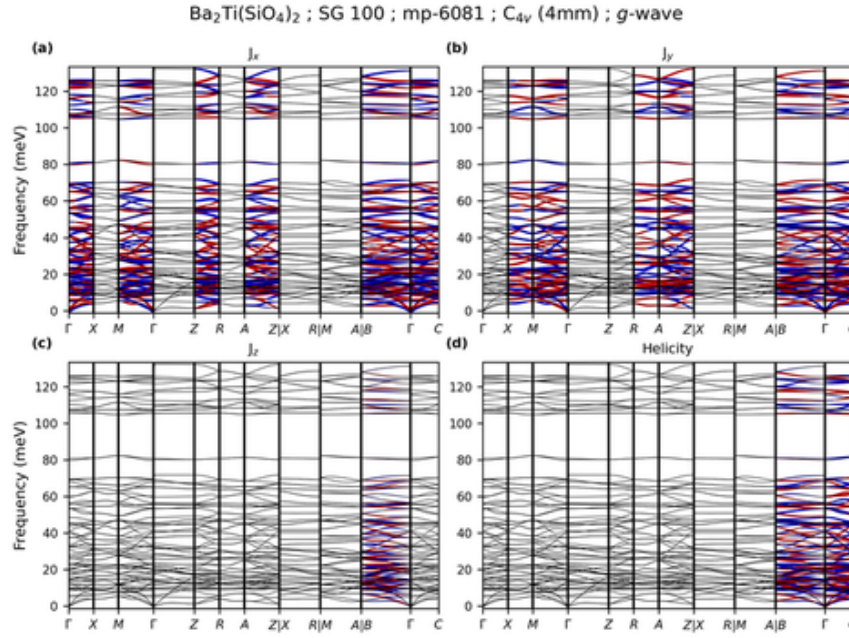


FIG. S92. Phonon dispersion of $\text{Ba}_2\text{Ti}(\text{SiO}_4)_2$ (mp-6081) along the specific momentum paths in the Brillouin zone of SG 100 (see Table S16). (a-c) Projections of the phonon angular momentum components J_x , J_y , and J_z onto the dispersion. (d) Projection of the phonon helicity onto the dispersion. In (a-d), red (blue) dots denote positive (negative) angular momentum or helicity, and their size is proportional to the magnitude.

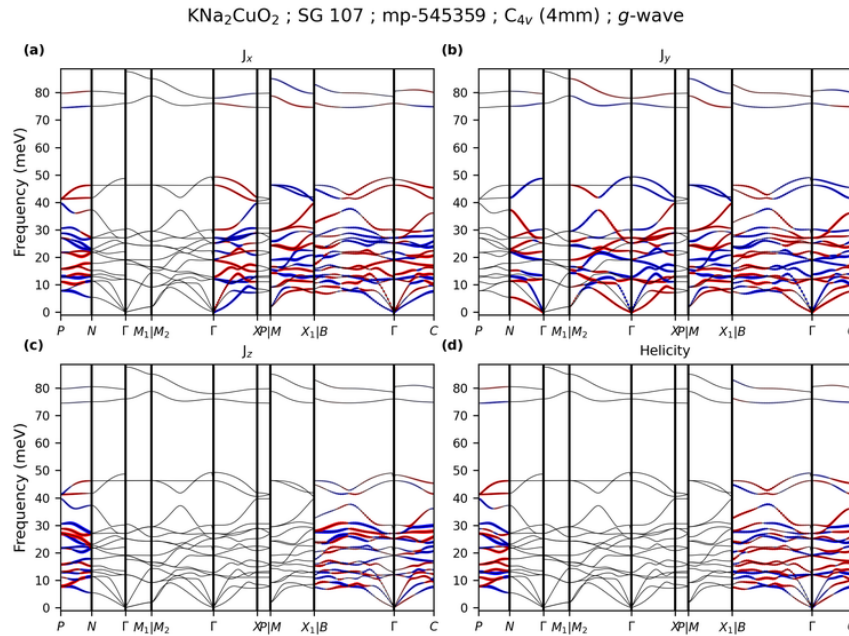


FIG. S93. Phonon dispersion of KNa_2CuO_2 (mp-545359) along the specific momentum paths in the Brillouin zone of SG 107 (see Table S17). (a-c) Projections of the phonon angular momentum components J_x , J_y , and J_z onto the dispersion. (d) Projection of the phonon helicity onto the dispersion. In (a-d), red (blue) dots denote positive (negative) angular momentum or helicity, and their size is proportional to the magnitude.

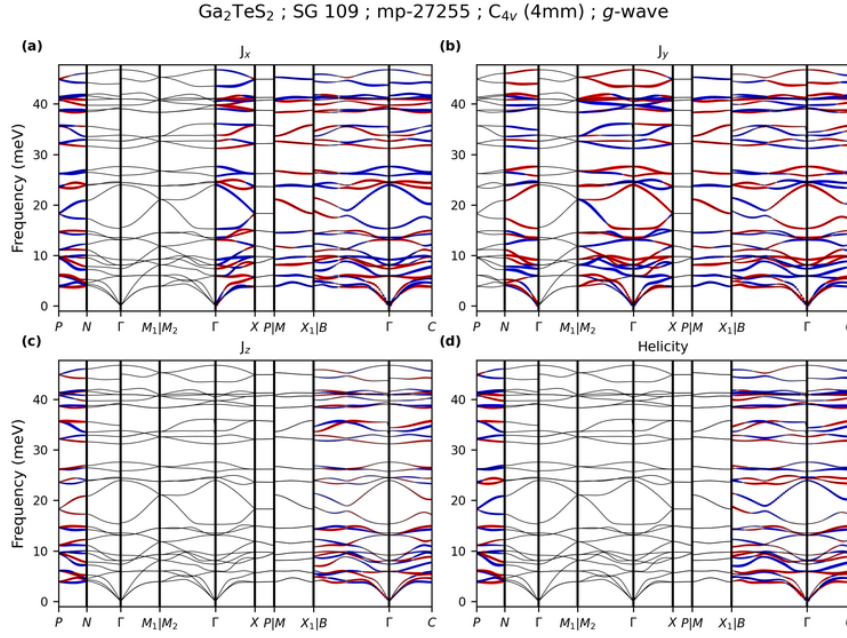


FIG. S94. Phonon dispersion of Ga_2TeS_2 (mp-27255) along the specific momentum paths in the Brillouin zone of SG 109 (see Table S18). (a-c) Projections of the phonon angular momentum components J_x , J_y , and J_z onto the dispersion. (d) Projection of the phonon helicity onto the dispersion. In (a-d), red (blue) dots denote positive (negative) angular momentum or helicity, and their size is proportional to the magnitude.

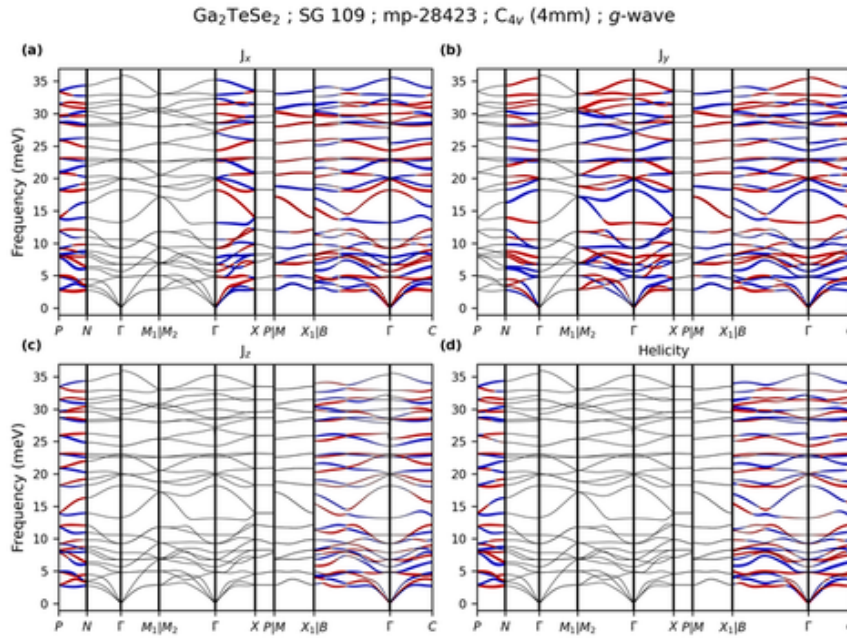


FIG. S95. Phonon dispersion of Ga_2TeSe_2 (mp-28423) along the specific momentum paths in the Brillouin zone of SG 109 (see Table S18). (a-c) Projections of the phonon angular momentum components J_x , J_y , and J_z onto the dispersion. (d) Projection of the phonon helicity onto the dispersion. In (a-d), red (blue) dots denote positive (negative) angular momentum or helicity, and their size is proportional to the magnitude.

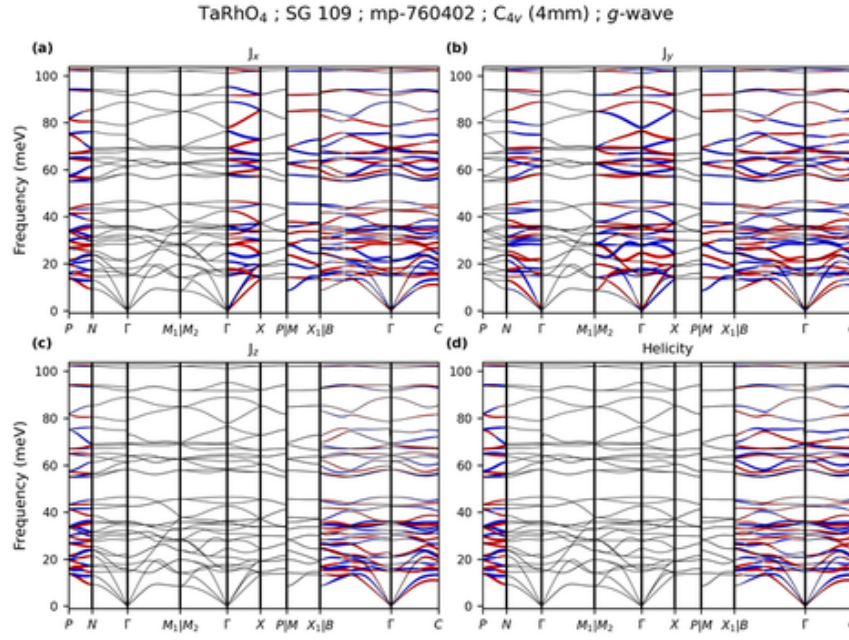


FIG. S96. Phonon dispersion of TaRhO₄ (mp-760402) along the specific momentum paths in the Brillouin zone of SG 109 (see Table S18). (a-c) Projections of the phonon angular momentum components J_x , J_y , and J_z onto the dispersion. (d) Projection of the phonon helicity onto the dispersion. In (a-d), red (blue) dots denote positive (negative) angular momentum or helicity, and their size is proportional to the magnitude.

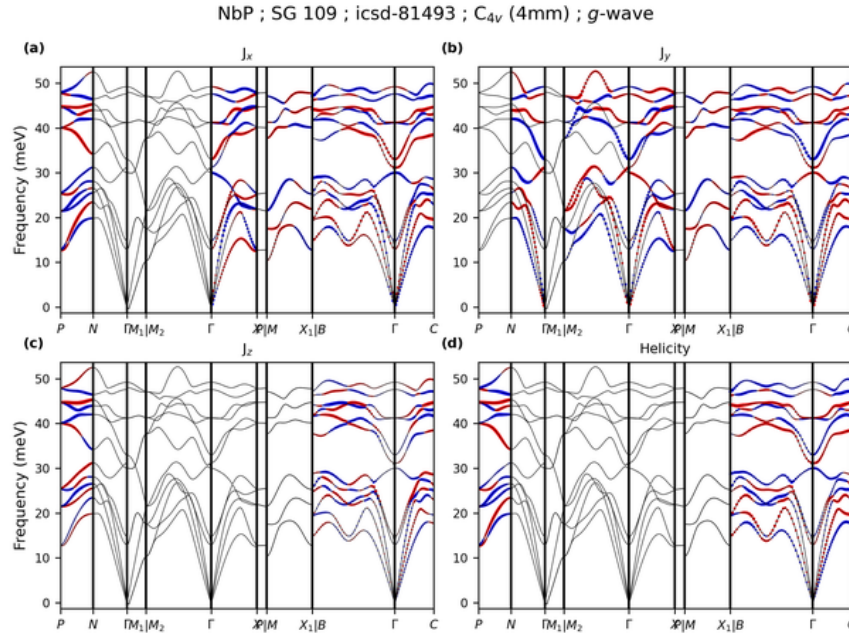


FIG. S97. Phonon dispersion of NbP (icse-81493) along the specific momentum paths in the Brillouin zone of SG 109 (see Table S18). (a-c) Projections of the phonon angular momentum components J_x , J_y , and J_z onto the dispersion. (d) Projection of the phonon helicity onto the dispersion. In (a-d), red (blue) dots denote positive (negative) angular momentum or helicity, and their size is proportional to the magnitude.

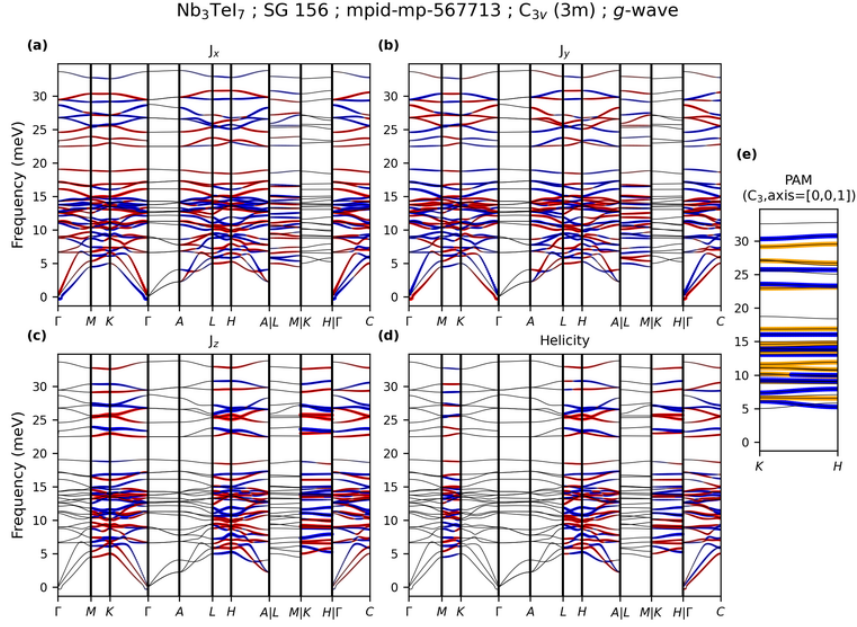


FIG. S98. Phonon dispersion of Nb_3TeI_7 (mp-567713) along the specific momentum paths in the Brillouin zone of SG 156 (see Table S27). (a-c) Projections of the phonon angular momentum components J_x , J_y , and J_z onto the dispersion. (d) Projection of the phonon helicity onto the dispersion. In (a-d), red (blue) dots denote positive (negative) angular momentum or helicity, and their size is proportional to the magnitude. (e) Pseudo-angular momentum (PAM) calculated along high-symmetry paths exhibiting three- or four-fold (screw) rotational symmetry. See more descriptions about the PAM in (e).

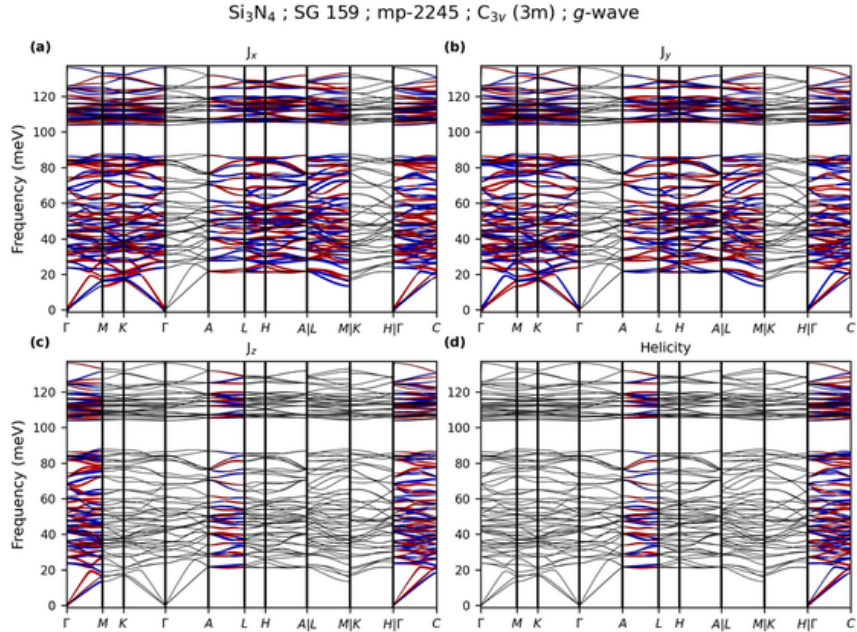


FIG. S99. Phonon dispersion of Si_3N_4 (mp-2245) along the specific momentum paths in the Brillouin zone of SG 159 (see Table S28). (a-c) Projections of the phonon angular momentum components J_x , J_y , and J_z onto the dispersion. (d) Projection of the phonon helicity onto the dispersion. In (a-d), red (blue) dots denote positive (negative) angular momentum or helicity, and their size is proportional to the magnitude.

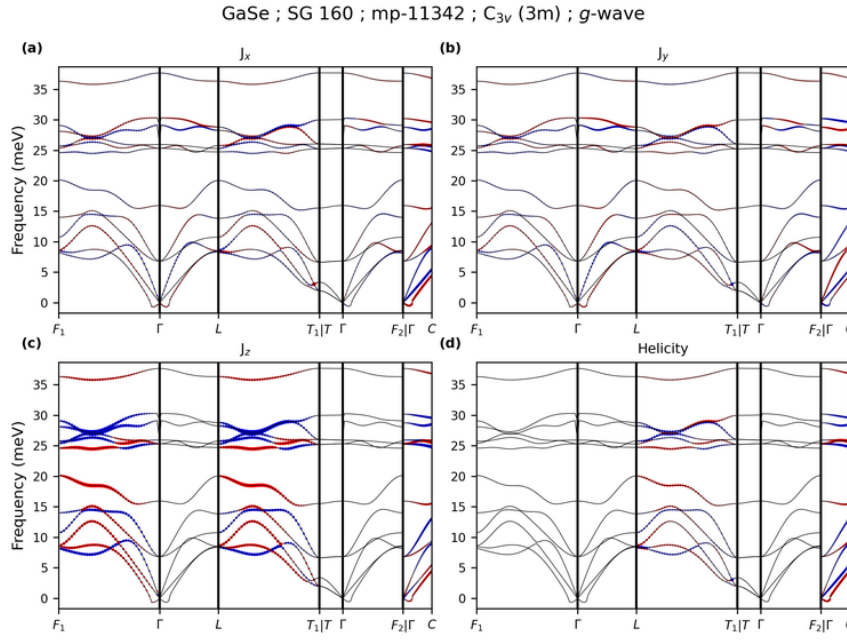


FIG. S100. Phonon dispersion of GaSe (mp-11342) along the specific momentum paths in the Brillouin zone of SG 160 (see Table S29). (a-c) Projections of the phonon angular momentum components J_x , J_y , and J_z onto the dispersion. (d) Projection of the phonon helicity onto the dispersion. In (a-d), red (blue) dots denote positive (negative) angular momentum or helicity, and their size is proportional to the magnitude.

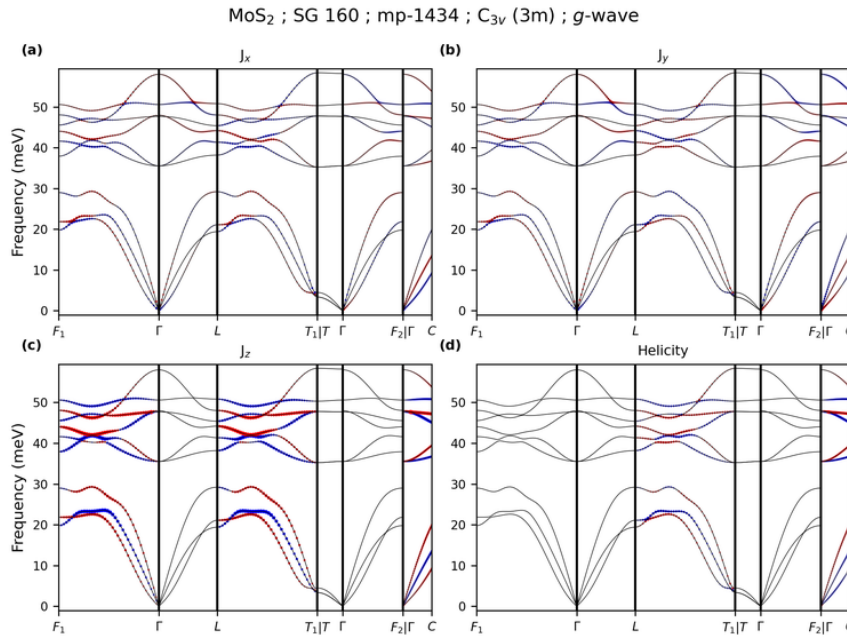


FIG. S101. Phonon dispersion of MoS₂ (mp-1434) along the specific momentum paths in the Brillouin zone of SG 160 (see Table S29). (a-c) Projections of the phonon angular momentum components J_x , J_y , and J_z onto the dispersion. (d) Projection of the phonon helicity onto the dispersion. In (a-d), red (blue) dots denote positive (negative) angular momentum or helicity, and their size is proportional to the magnitude.

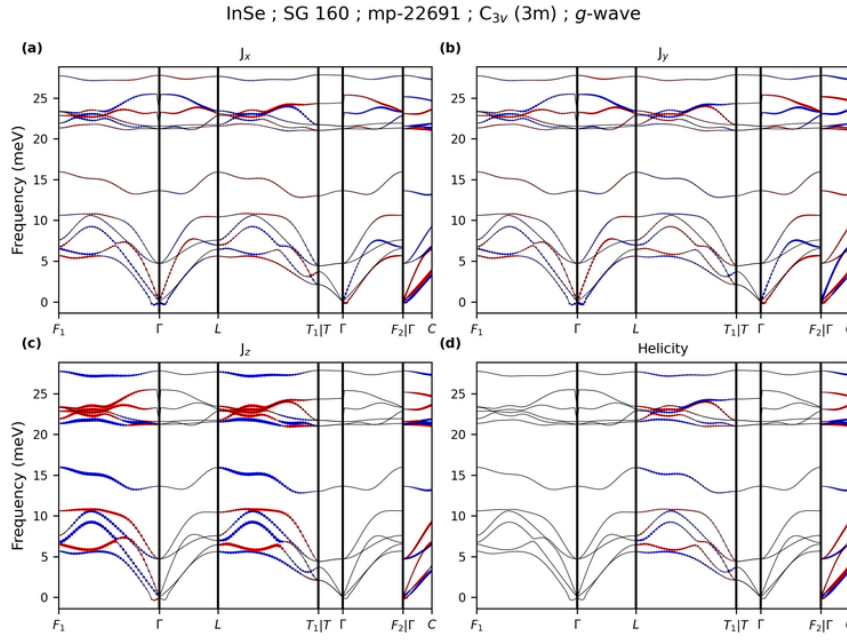


FIG. S102. Phonon dispersion of InSe (mp-22691) along the specific momentum paths in the Brillouin zone of SG 160 (see Table S29). (a-c) Projections of the phonon angular momentum components J_x , J_y , and J_z onto the dispersion. (d) Projection of the phonon helicity onto the dispersion. In (a-d), red (blue) dots denote positive (negative) angular momentum or helicity, and their size is proportional to the magnitude.

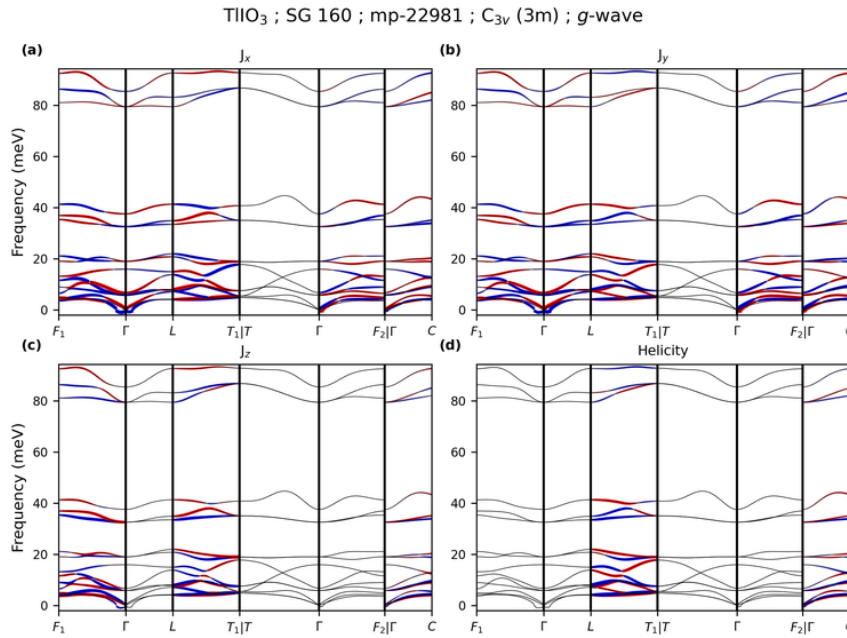


FIG. S103. Phonon dispersion of TiO₃ (mp-22981) along the specific momentum paths in the Brillouin zone of SG 160 (see Table S29). (a-c) Projections of the phonon angular momentum components J_x , J_y , and J_z onto the dispersion. (d) Projection of the phonon helicity onto the dispersion. In (a-d), red (blue) dots denote positive (negative) angular momentum or helicity, and their size is proportional to the magnitude.

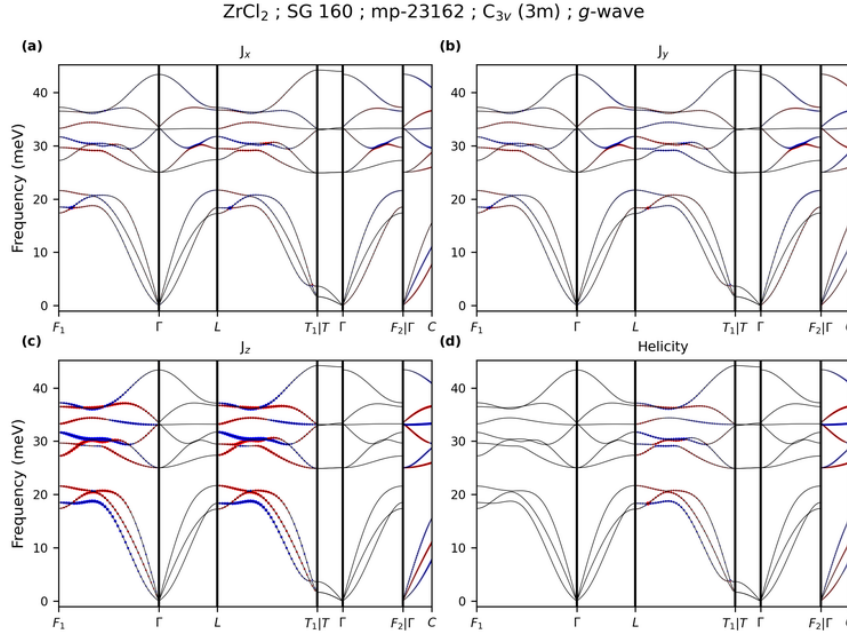


FIG. S104. Phonon dispersion of ZrCl_2 (mp-23162) along the specific momentum paths in the Brillouin zone of SG 160 (see Table S29). (a-c) Projections of the phonon angular momentum components J_x , J_y , and J_z onto the dispersion. (d) Projection of the phonon helicity onto the dispersion. In (a-d), red (blue) dots denote positive (negative) angular momentum or helicity, and their size is proportional to the magnitude.

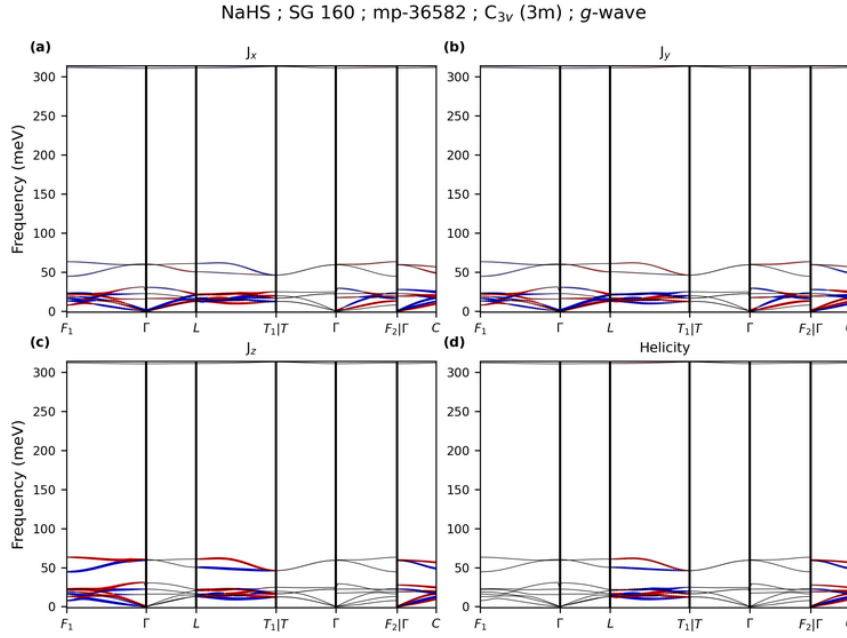


FIG. S105. Phonon dispersion of NaHS (mp-36582) along the specific momentum paths in the Brillouin zone of SG 160 (see Table S29). (a-c) Projections of the phonon angular momentum components J_x , J_y , and J_z onto the dispersion. (d) Projection of the phonon helicity onto the dispersion. In (a-d), red (blue) dots denote positive (negative) angular momentum or helicity, and their size is proportional to the magnitude.

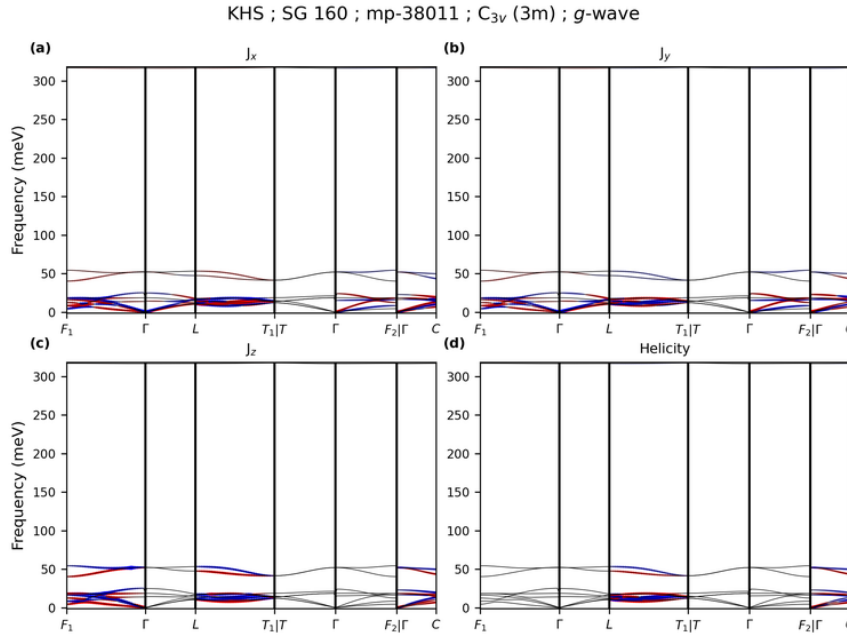


FIG. S106. Phonon dispersion of KHS (mp-38011) along the specific momentum paths in the Brillouin zone of SG 160 (see Table S29). (a-c) Projections of the phonon angular momentum components J_x , J_y , and J_z onto the dispersion. (d) Projection of the phonon helicity onto the dispersion. In (a-d), red (blue) dots denote positive (negative) angular momentum or helicity, and their size is proportional to the magnitude.

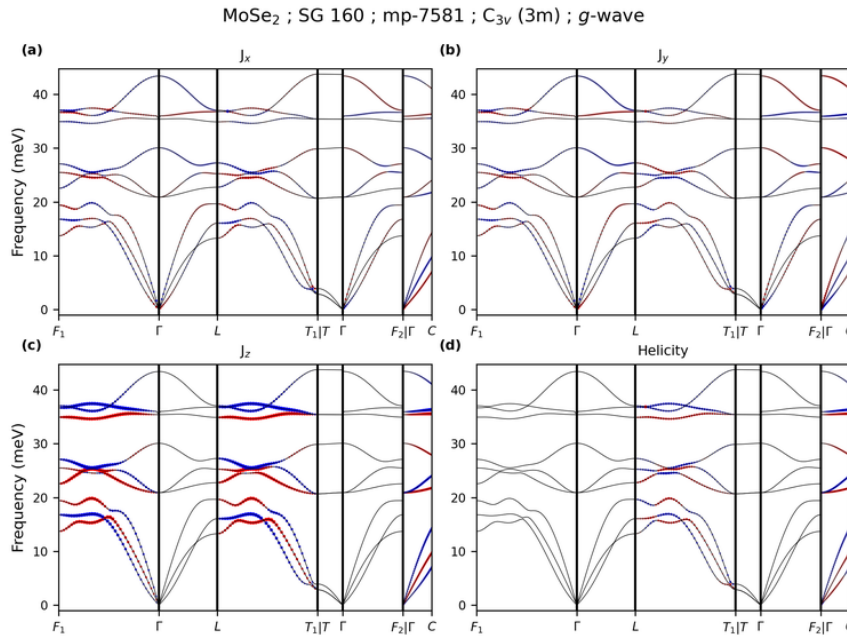


FIG. S107. Phonon dispersion of MoSe₂ (mp-7581) along the specific momentum paths in the Brillouin zone of SG 160 (see Table S29). (a-c) Projections of the phonon angular momentum components J_x , J_y , and J_z onto the dispersion. (d) Projection of the phonon helicity onto the dispersion. In (a-d), red (blue) dots denote positive (negative) angular momentum or helicity, and their size is proportional to the magnitude.

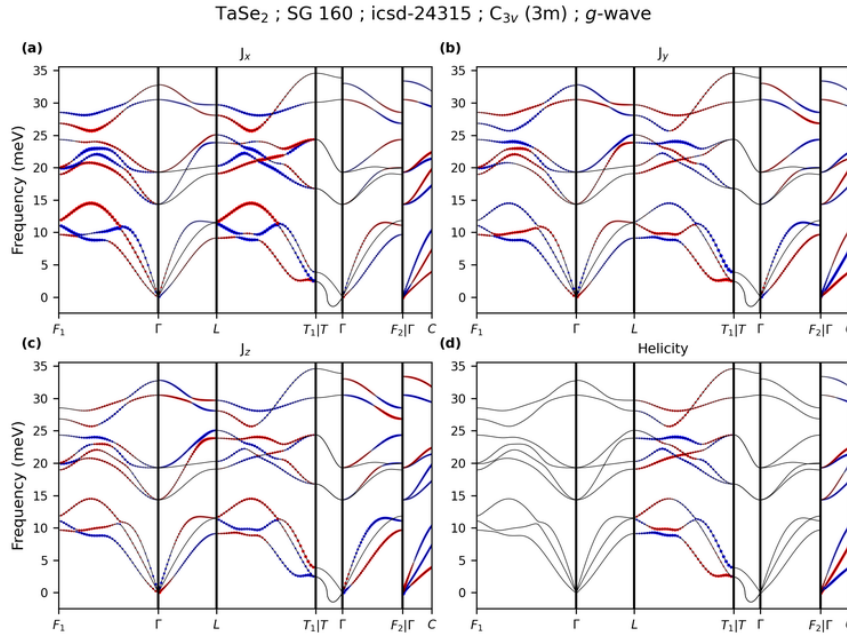


FIG. S108. Phonon dispersion of TaSe₂ (icsd-24315) along the specific momentum paths in the Brillouin zone of SG 160 (see Table S29). (a-c) Projections of the phonon angular momentum components J_x , J_y , and J_z onto the dispersion. (d) Projection of the phonon helicity onto the dispersion. In (a-d), red (blue) dots denote positive (negative) angular momentum or helicity, and their size is proportional to the magnitude.

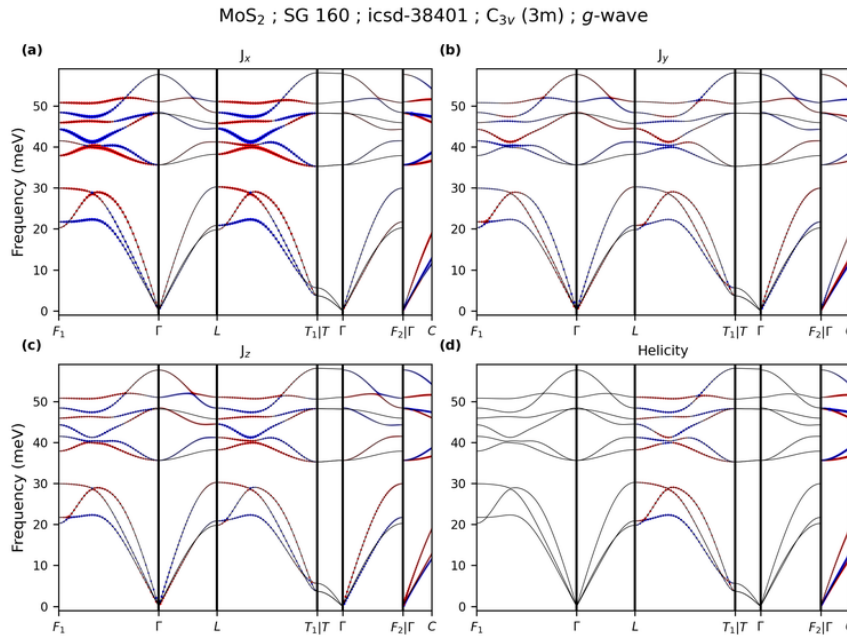


FIG. S109. Phonon dispersion of MoS₂ (icsd-38401) along the specific momentum paths in the Brillouin zone of SG 160 (see Table S29). (a-c) Projections of the phonon angular momentum components J_x , J_y , and J_z onto the dispersion. (d) Projection of the phonon helicity onto the dispersion. In (a-d), red (blue) dots denote positive (negative) angular momentum or helicity, and their size is proportional to the magnitude.

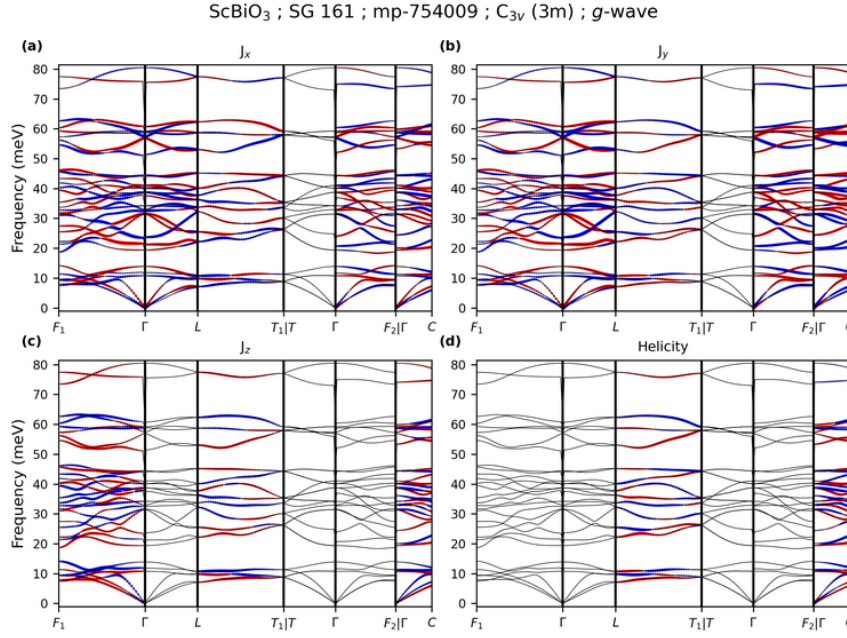


FIG. S110. Phonon dispersion of ScBiO₃ (mp-754009) along the specific momentum paths in the Brillouin zone of SG 161 (see Table S30). (a-c) Projections of the phonon angular momentum components J_x , J_y , and J_z onto the dispersion. (d) Projection of the phonon helicity onto the dispersion. In (a-d), red (blue) dots denote positive (negative) angular momentum or helicity, and their size is proportional to the magnitude.

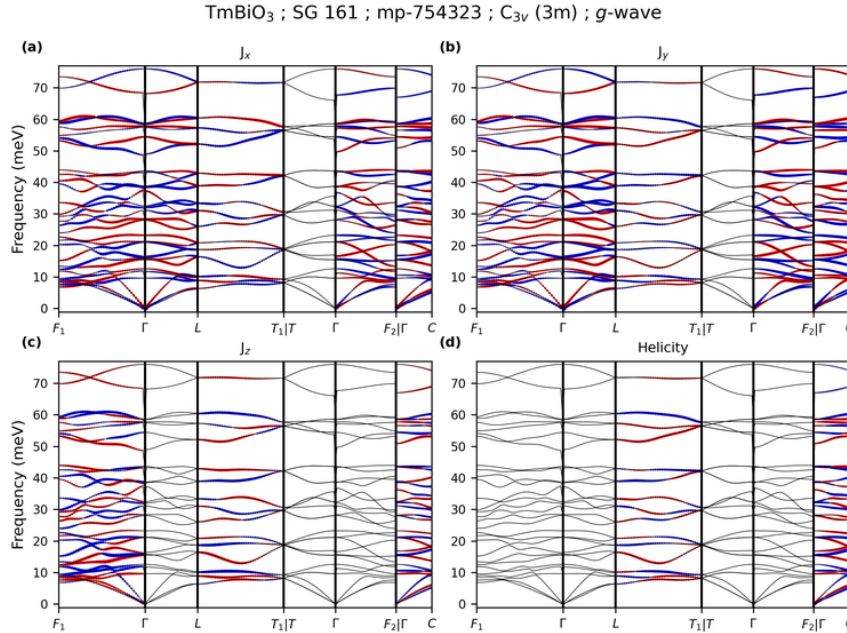


FIG. S111. Phonon dispersion of TmBiO₃ (mp-754323) along the specific momentum paths in the Brillouin zone of SG 161 (see Table S30). (a-c) Projections of the phonon angular momentum components J_x , J_y , and J_z onto the dispersion. (d) Projection of the phonon helicity onto the dispersion. In (a-d), red (blue) dots denote positive (negative) angular momentum or helicity, and their size is proportional to the magnitude.

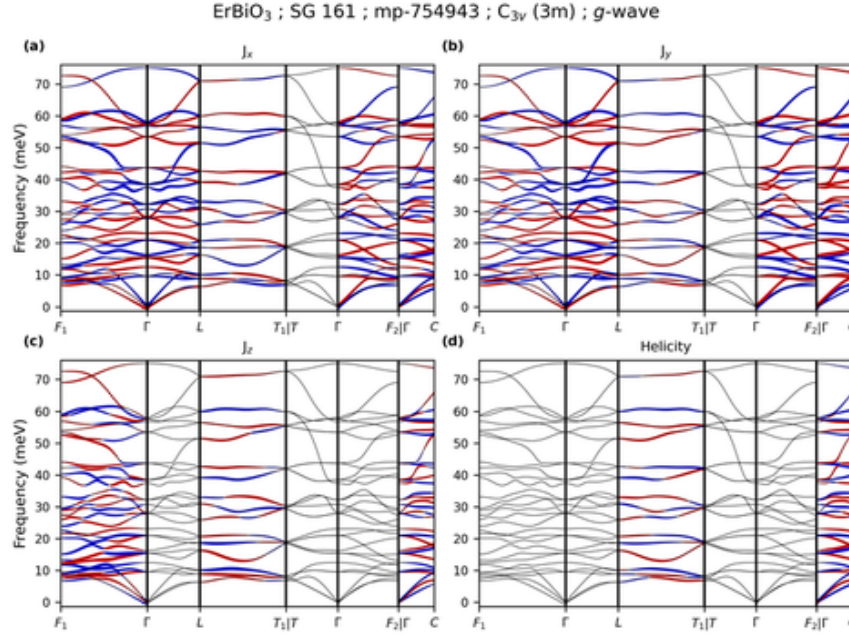


FIG. S112. Phonon dispersion of ErBiO₃ (mp-754943) along the specific momentum paths in the Brillouin zone of SG 161 (see Table S30). (a-c) Projections of the phonon angular momentum components J_x , J_y , and J_z onto the dispersion. (d) Projection of the phonon helicity onto the dispersion. In (a-d), red (blue) dots denote positive (negative) angular momentum or helicity, and their size is proportional to the magnitude.

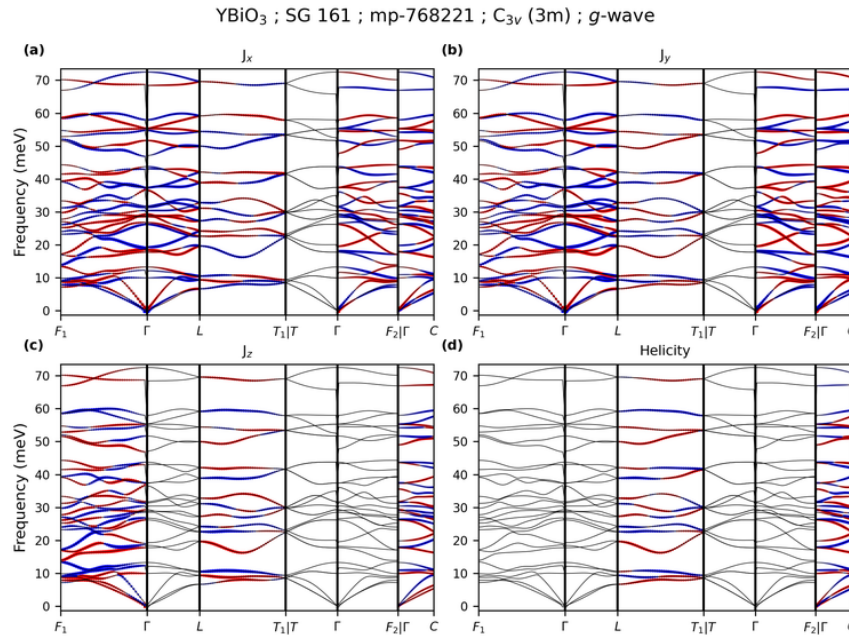


FIG. S113. Phonon dispersion of YBiO₃ (mp-768221) along the specific momentum paths in the Brillouin zone of SG 161 (see Table S30). (a-c) Projections of the phonon angular momentum components J_x , J_y , and J_z onto the dispersion. (d) Projection of the phonon helicity onto the dispersion. In (a-d), red (blue) dots denote positive (negative) angular momentum or helicity, and their size is proportional to the magnitude.

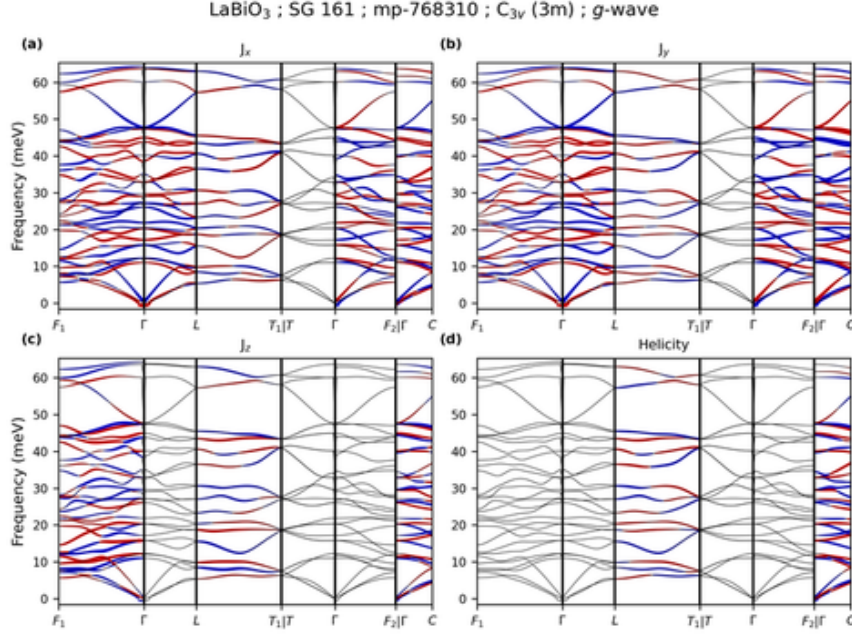


FIG. S114. Phonon dispersion of LaBiO₃ (mp-768310) along the specific momentum paths in the Brillouin zone of SG 161 (see Table S30). (a-c) Projections of the phonon angular momentum components J_x , J_y , and J_z onto the dispersion. (d) Projection of the phonon helicity onto the dispersion. In (a-d), red (blue) dots denote positive (negative) angular momentum or helicity, and their size is proportional to the magnitude.

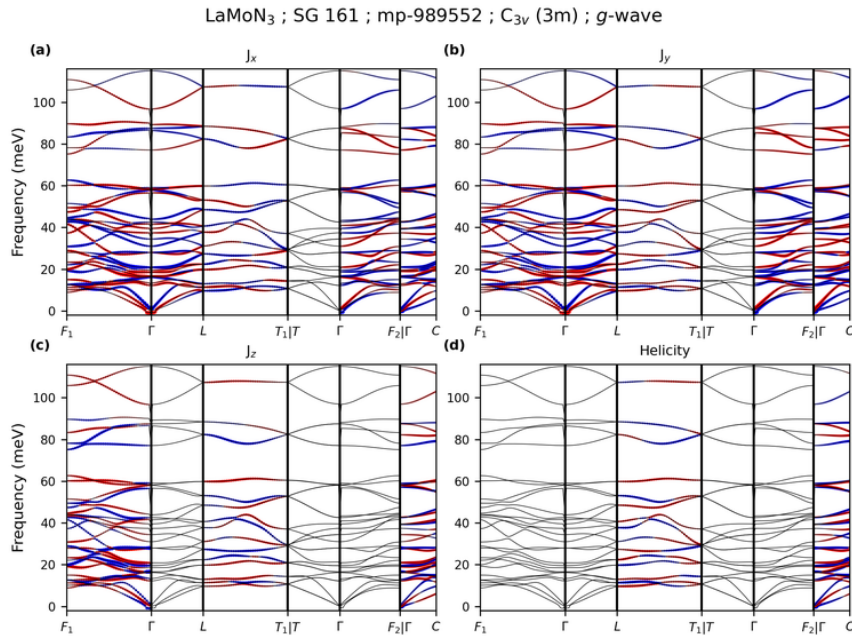


FIG. S115. Phonon dispersion of LaMoN₃ (mp-989552) along the specific momentum paths in the Brillouin zone of SG 161 (see Table S30). (a-c) Projections of the phonon angular momentum components J_x , J_y , and J_z onto the dispersion. (d) Projection of the phonon helicity onto the dispersion. In (a-d), red (blue) dots denote positive (negative) angular momentum or helicity, and their size is proportional to the magnitude.

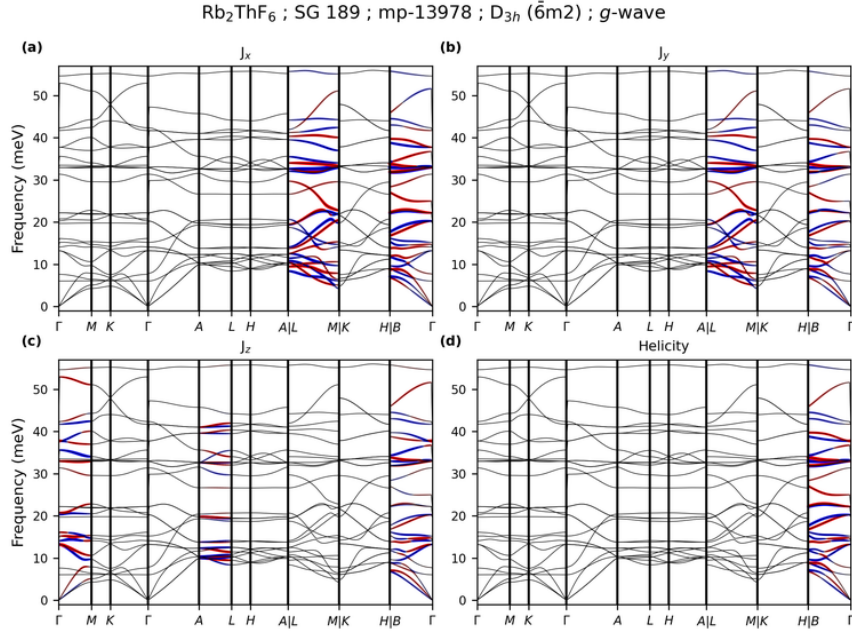


FIG. S116. Phonon dispersion of Rb_2ThF_6 (mp-13978) along the specific momentum paths in the Brillouin zone of SG 189 (see Table S36). (a-c) Projections of the phonon angular momentum components J_x , J_y , and J_z onto the dispersion. (d) Projection of the phonon helicity onto the dispersion. In (a-d), red (blue) dots denote positive (negative) angular momentum or helicity, and their size is proportional to the magnitude.

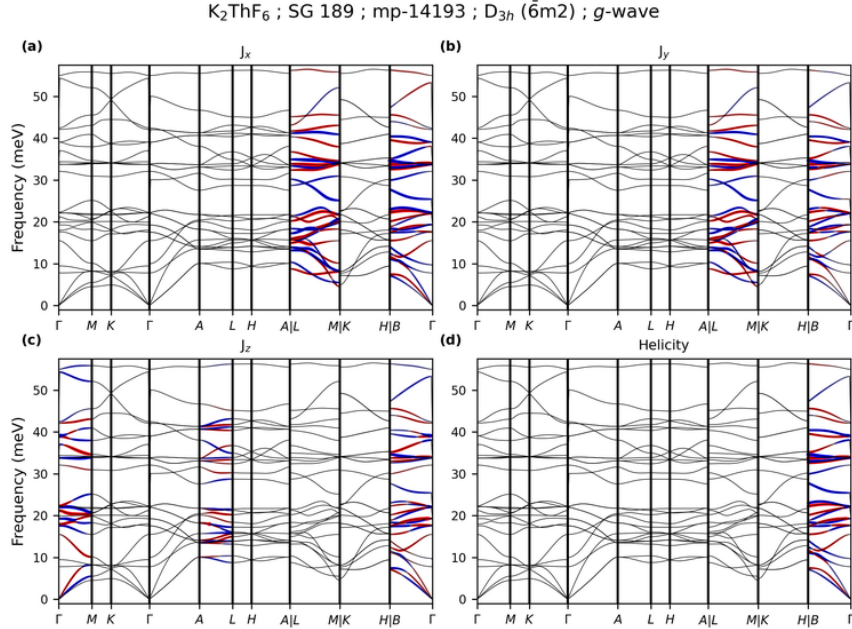


FIG. S117. Phonon dispersion of K_2ThF_6 (mp-14193) along the specific momentum paths in the Brillouin zone of SG 189 (see Table S36). (a-c) Projections of the phonon angular momentum components J_x , J_y , and J_z onto the dispersion. (d) Projection of the phonon helicity onto the dispersion. In (a-d), red (blue) dots denote positive (negative) angular momentum or helicity, and their size is proportional to the magnitude.

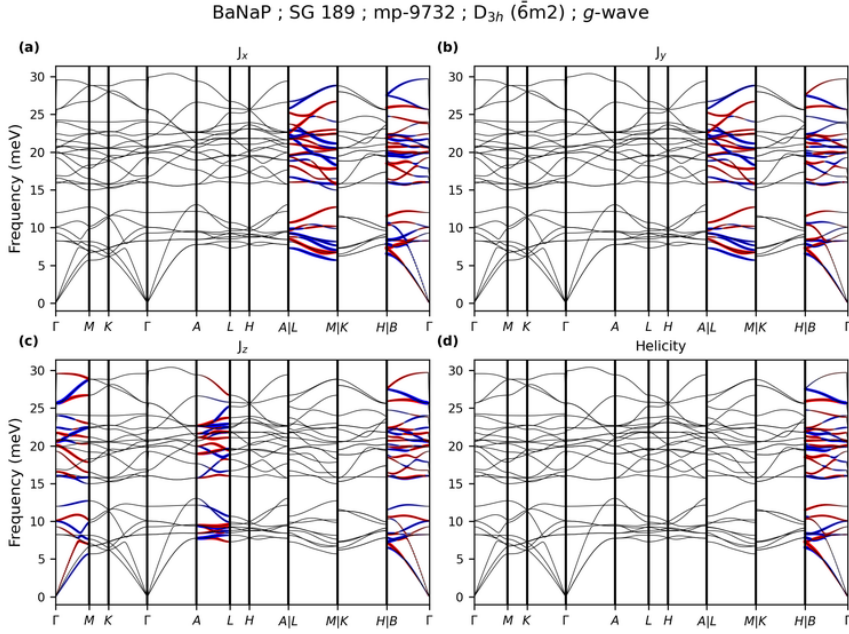


FIG. S118. Phonon dispersion of BaNaP (mp-9732) along the specific momentum paths in the Brillouin zone of SG 189 (see Table S36). (a-c) Projections of the phonon angular momentum components J_x , J_y , and J_z onto the dispersion. (d) Projection of the phonon helicity onto the dispersion. In (a-d), red (blue) dots denote positive (negative) angular momentum or helicity, and their size is proportional to the magnitude.

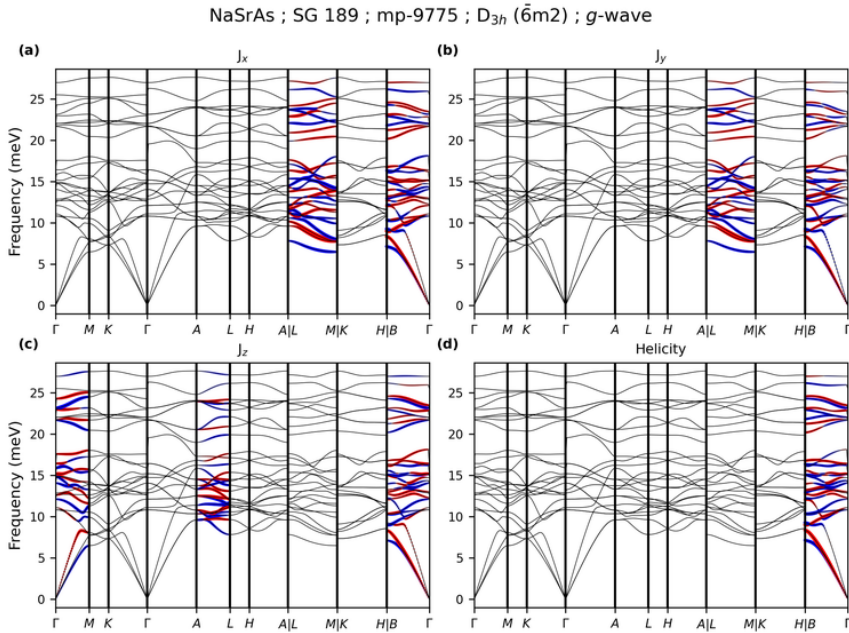


FIG. S119. Phonon dispersion of NaSrAs (mp-9775) along the specific momentum paths in the Brillouin zone of SG 189 (see Table S36). (a-c) Projections of the phonon angular momentum components J_x , J_y , and J_z onto the dispersion. (d) Projection of the phonon helicity onto the dispersion. In (a-d), red (blue) dots denote positive (negative) angular momentum or helicity, and their size is proportional to the magnitude.

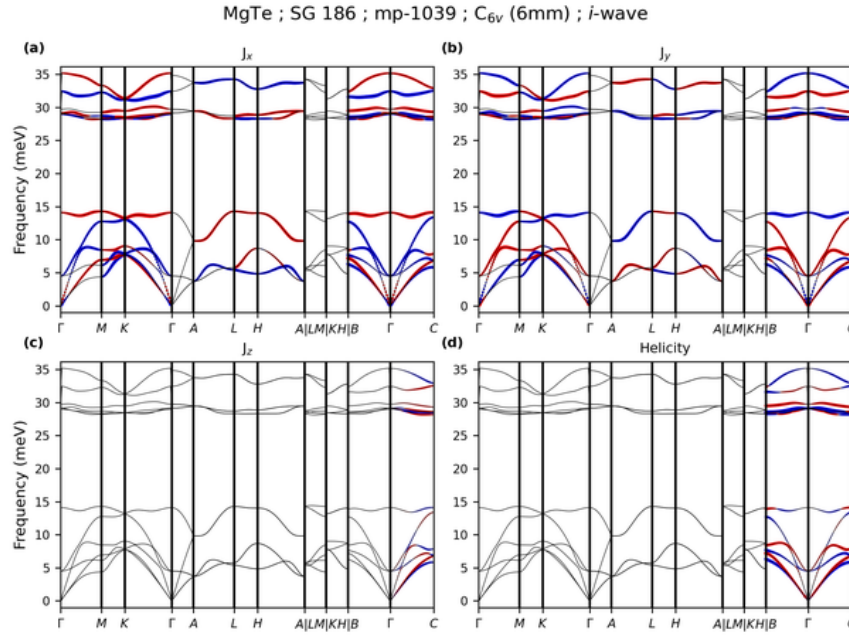


FIG. S120. Phonon dispersion of MgTe (mp-1039) along the specific momentum paths in the Brillouin zone of SG 186 (see Table S35). (a-c) Projections of the phonon angular momentum components J_x , J_y , and J_z onto the dispersion. (d) Projection of the phonon helicity onto the dispersion. In (a-d), red (blue) dots denote positive (negative) angular momentum or helicity, and their size is proportional to the magnitude.

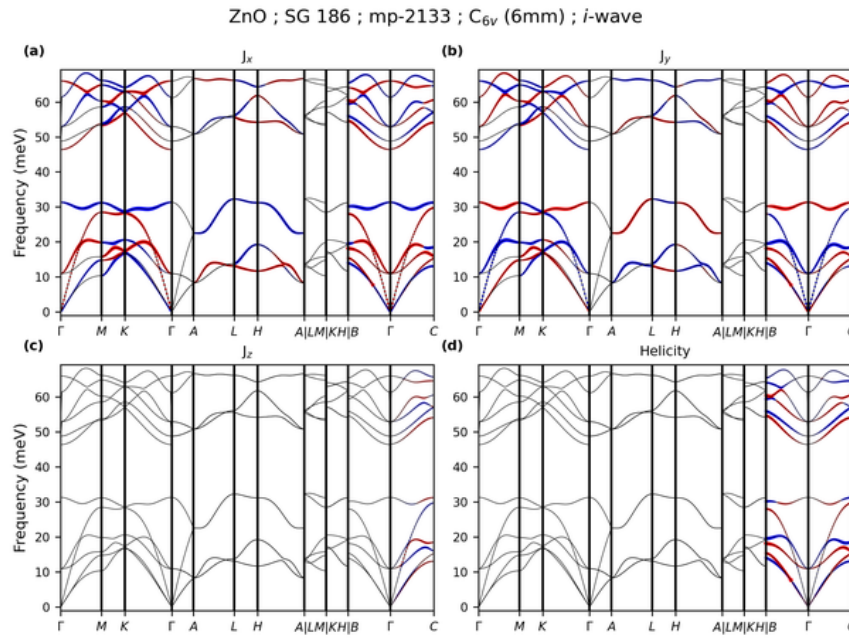


FIG. S121. Phonon dispersion of ZnO (mp-2133) along the specific momentum paths in the Brillouin zone of SG 186 (see Table S35). (a-c) Projections of the phonon angular momentum components J_x , J_y , and J_z onto the dispersion. (d) Projection of the phonon helicity onto the dispersion. In (a-d), red (blue) dots denote positive (negative) angular momentum or helicity, and their size is proportional to the magnitude.

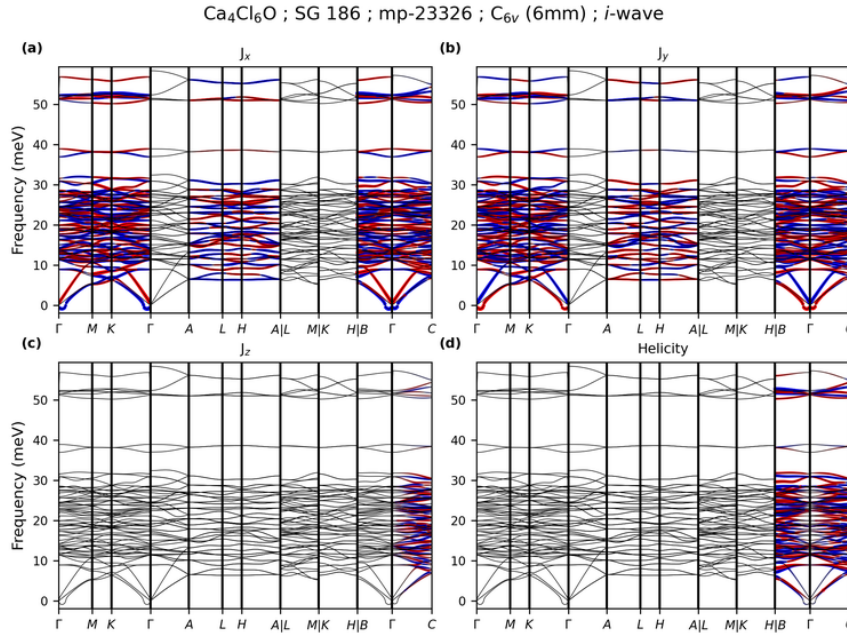


FIG. S122. Phonon dispersion of $\text{Ca}_4\text{Cl}_6\text{O}$ (mp-23326) along the specific momentum paths in the Brillouin zone of SG 186 (see Table S35). (a-c) Projections of the phonon angular momentum components J_x , J_y , and J_z onto the dispersion. (d) Projection of the phonon helicity onto the dispersion. In (a-d), red (blue) dots denote positive (negative) angular momentum or helicity, and their size is proportional to the magnitude.

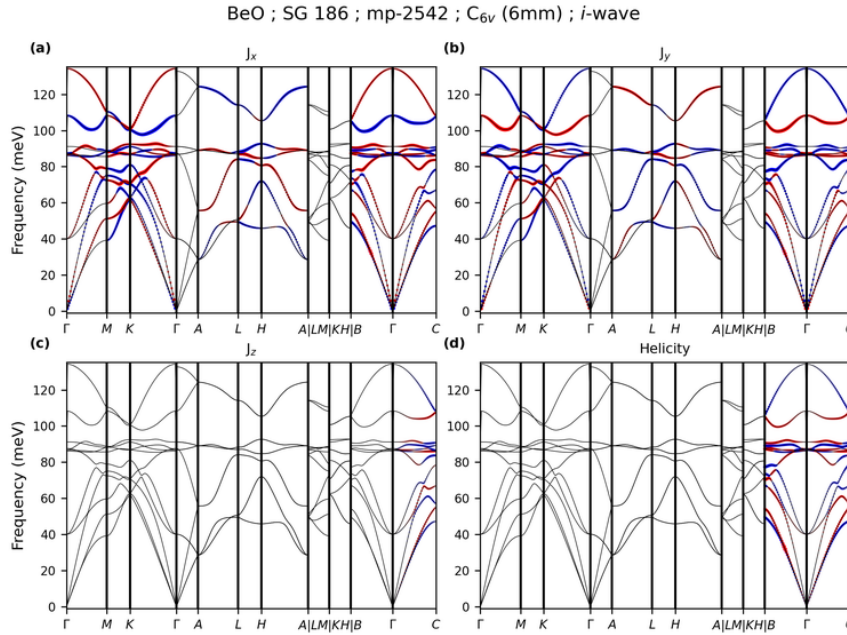


FIG. S123. Phonon dispersion of BeO (mp-2542) along the specific momentum paths in the Brillouin zone of SG 186 (see Table S35). (a-d) Projections of the phonon angular momentum components J_x , J_y , and J_z onto the dispersion. (d) Projection of the phonon helicity onto the dispersion. In (a-d), red (blue) dots denote positive (negative) angular momentum or helicity, and their size is proportional to the magnitude.

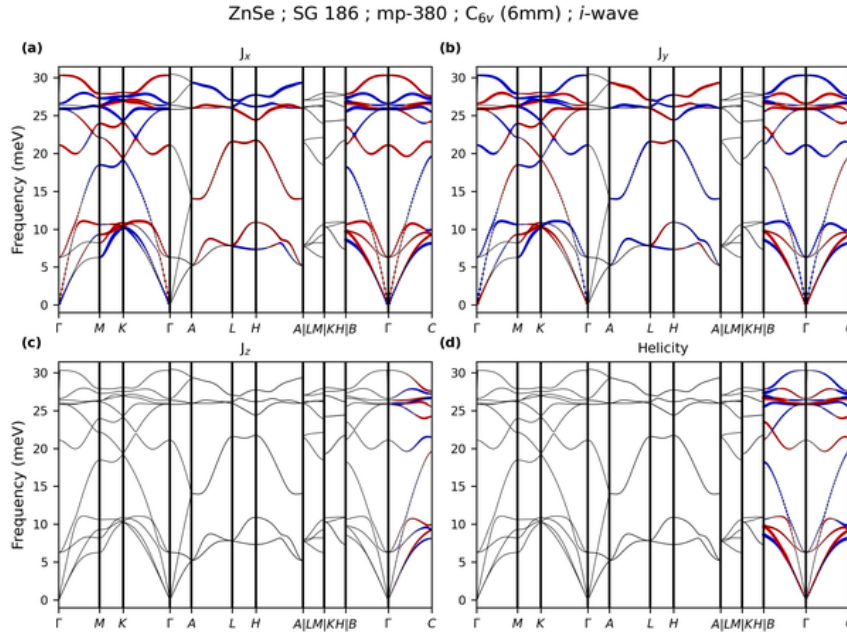


FIG. S124. Phonon dispersion of ZnSe (mp-380) along the specific momentum paths in the Brillouin zone of SG 186 (see Table S35). (a-c) Projections of the phonon angular momentum components J_x , J_y , and J_z onto the dispersion. (d) Projection of the phonon helicity onto the dispersion. In (a-d), red (blue) dots denote positive (negative) angular momentum or helicity, and their size is proportional to the magnitude.

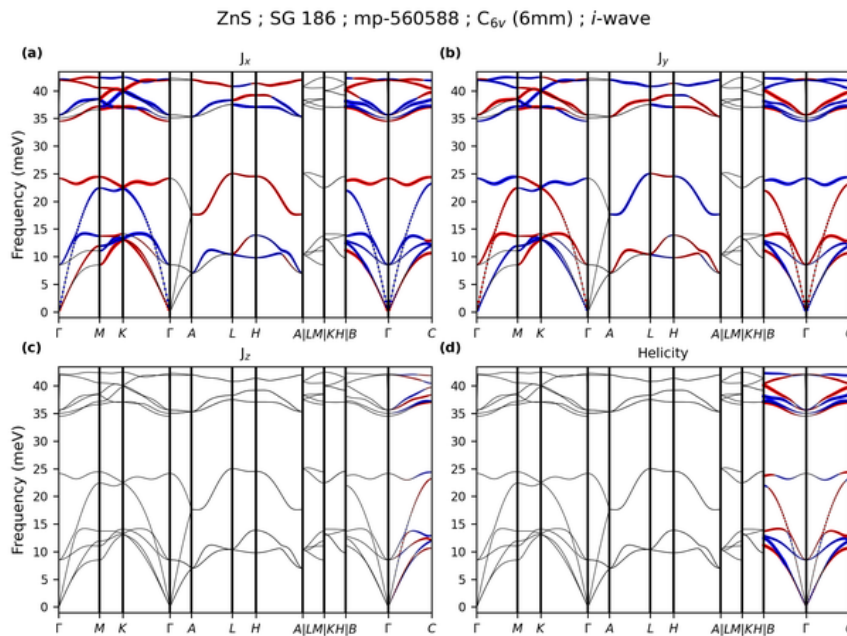


FIG. S125. Phonon dispersion of ZnS (mp-560588) along the specific momentum paths in the Brillouin zone of SG 186 (see Table S35). (a-c) Projections of the phonon angular momentum components J_x , J_y , and J_z onto the dispersion. (d) Projection of the phonon helicity onto the dispersion. In (a-d), red (blue) dots denote positive (negative) angular momentum or helicity, and their size is proportional to the magnitude.

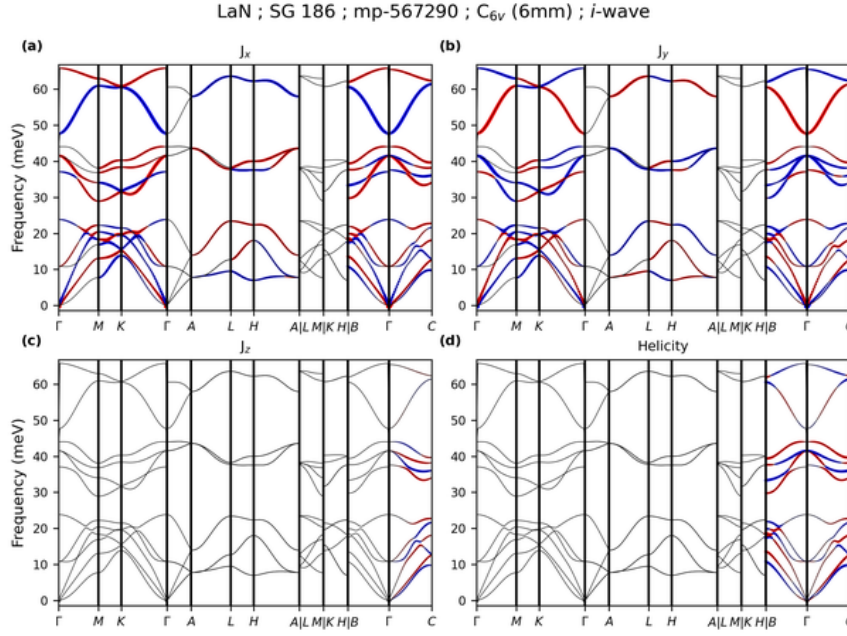


FIG. S126. Phonon dispersion of LaN (mp-567290) along the specific momentum paths in the Brillouin zone of SG 186 (see Table S35). (a-c) Projections of the phonon angular momentum components J_x , J_y , and J_z onto the dispersion. (d) Projection of the phonon helicity onto the dispersion. In (a-d), red (blue) dots denote positive (negative) angular momentum or helicity, and their size is proportional to the magnitude.

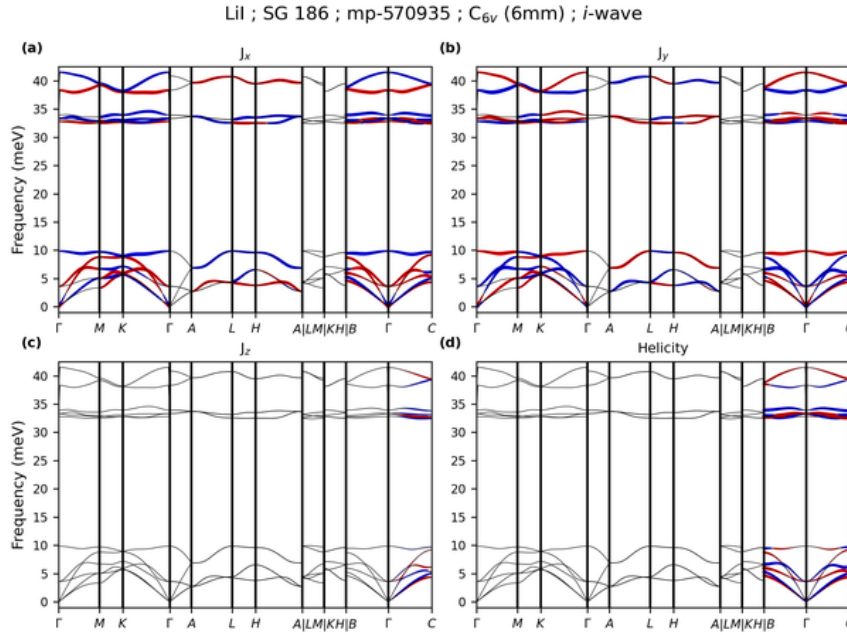


FIG. S127. Phonon dispersion of LiI (mp-570935) along the specific momentum paths in the Brillouin zone of SG 186 (see Table S35). (a-c) Projections of the phonon angular momentum components J_x , J_y , and J_z onto the dispersion. (d) Projection of the phonon helicity onto the dispersion. In (a-d), red (blue) dots denote positive (negative) angular momentum or helicity, and their size is proportional to the magnitude.

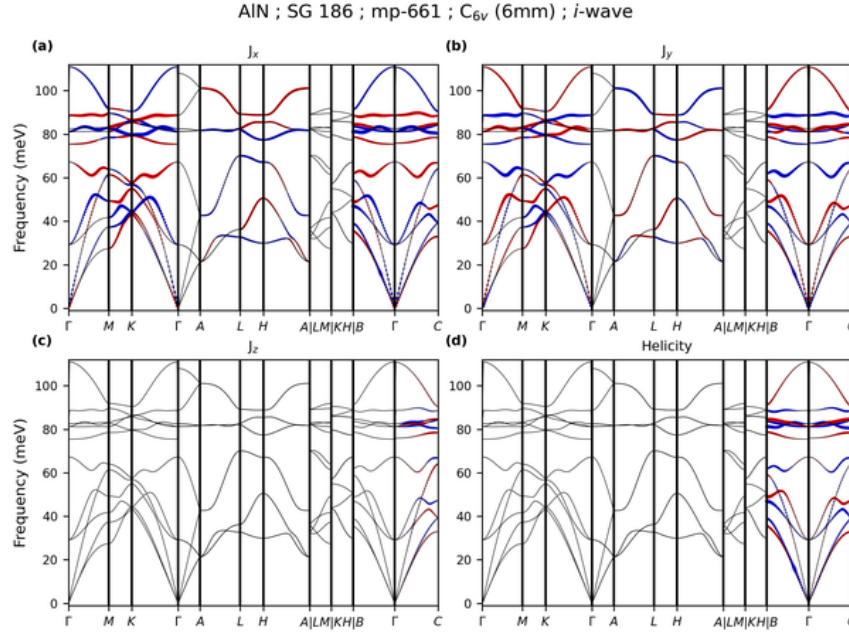


FIG. S128. Phonon dispersion of AlN (mp-661) along the specific momentum paths in the Brillouin zone of SG 186 (see Table S35). (a-c) Projections of the phonon angular momentum components J_x , J_y , and J_z onto the dispersion. (d) Projection of the phonon helicity onto the dispersion. In (a-d), red (blue) dots denote positive (negative) angular momentum or helicity, and their size is proportional to the magnitude.

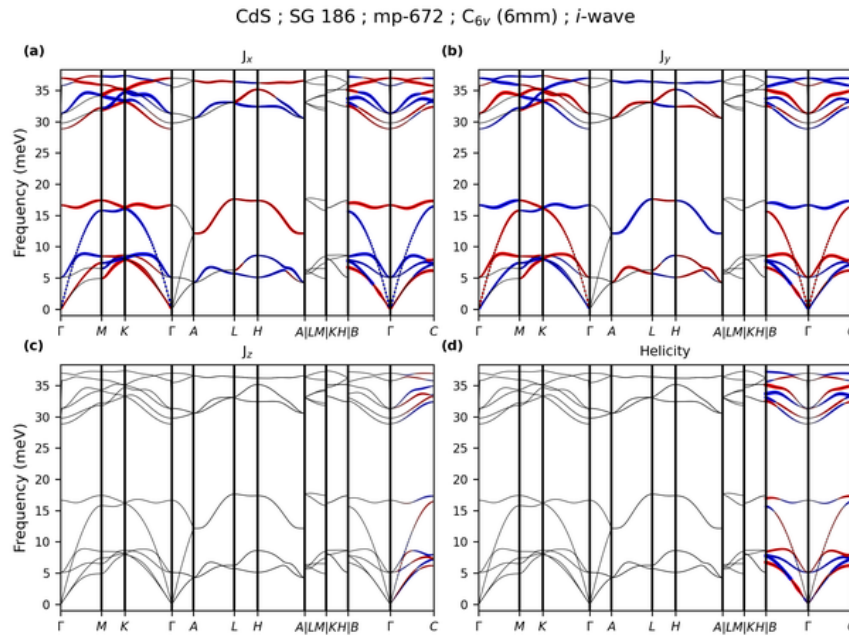


FIG. S129. Phonon dispersion of CdS (mp-672) along the specific momentum paths in the Brillouin zone of SG 186 (see Table S35). (a-c) Projections of the phonon angular momentum components J_x , J_y , and J_z onto the dispersion. (d) Projection of the phonon helicity onto the dispersion. In (a-d), red (blue) dots denote positive (negative) angular momentum or helicity, and their size is proportional to the magnitude.

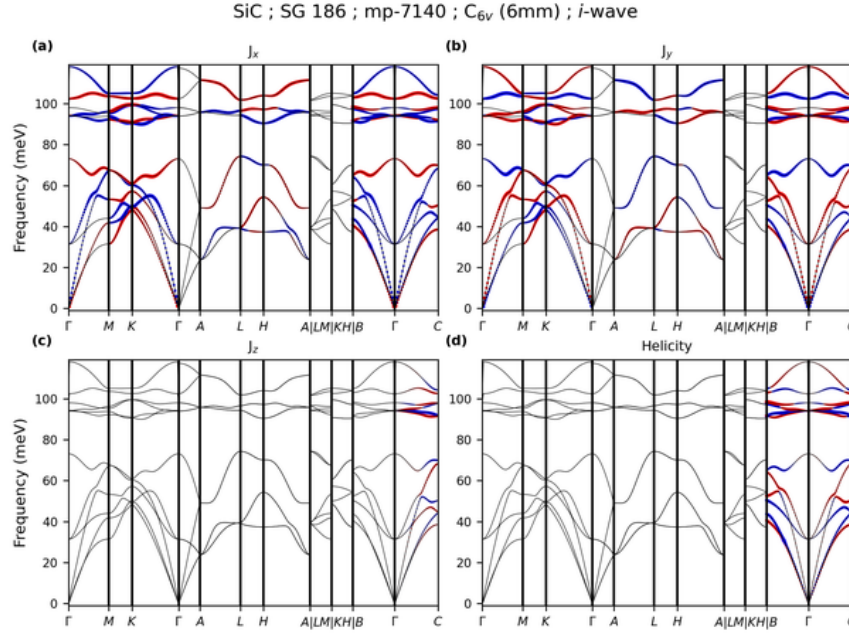


FIG. S130. Phonon dispersion of SiC (mp-7140) along the specific momentum paths in the Brillouin zone of SG 186 (see Table S35). (a-c) Projections of the phonon angular momentum components J_x , J_y , and J_z onto the dispersion. (d) Projection of the phonon helicity onto the dispersion. In (a-d), red (blue) dots denote positive (negative) angular momentum or helicity, and their size is proportional to the magnitude.

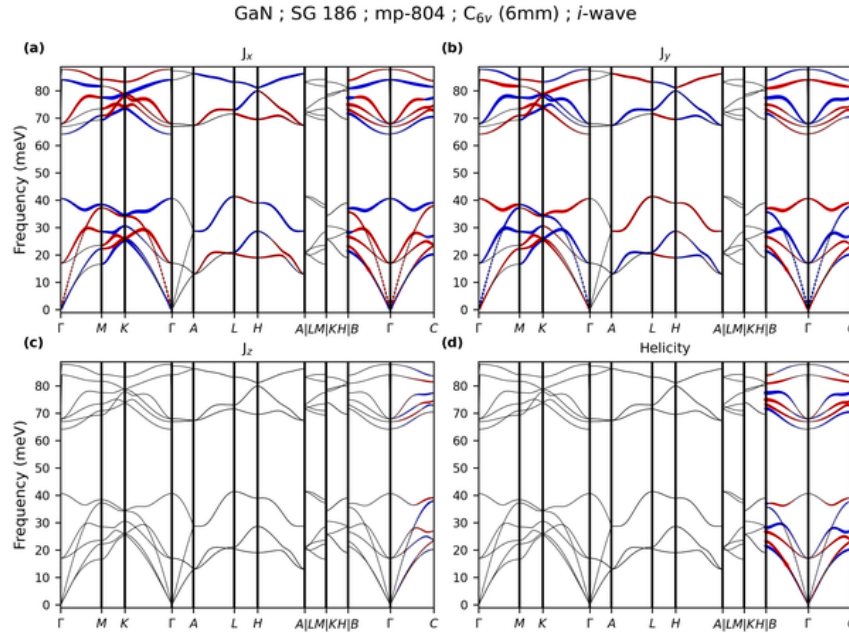


FIG. S131. Phonon dispersion of GaN (mp-804) along the specific momentum paths in the Brillouin zone of SG 186 (see Table S35). (a-c) Projections of the phonon angular momentum components J_x , J_y , and J_z onto the dispersion. (d) Projection of the phonon helicity onto the dispersion. In (a-d), red (blue) dots denote positive (negative) angular momentum or helicity, and their size is proportional to the magnitude.

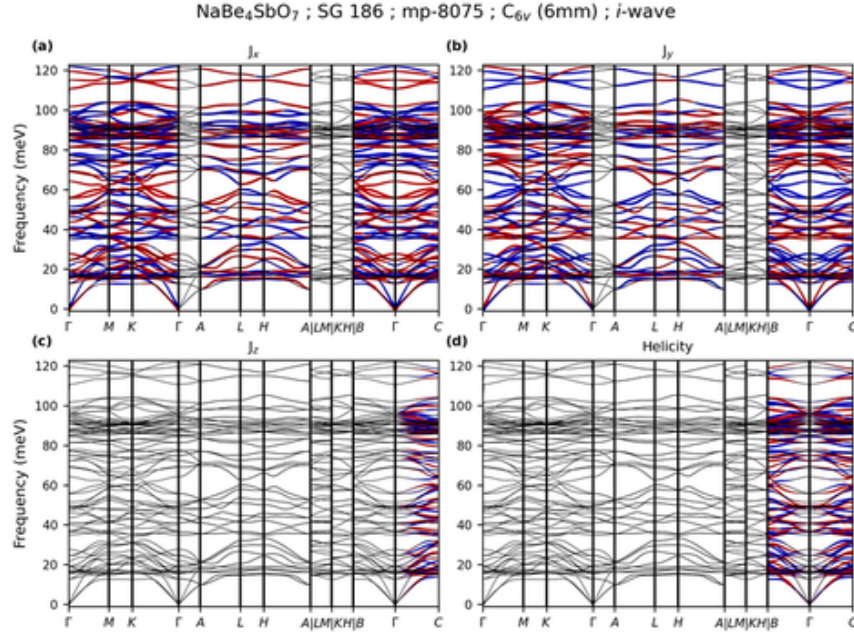


FIG. S132. Phonon dispersion of $\text{NaBe}_4\text{SbO}_7$ (mp-8075) along the specific momentum paths in the Brillouin zone of SG 186 (see Table S35). (a-c) Projections of the phonon angular momentum components J_x , J_y , and J_z onto the dispersion. (d) Projection of the phonon helicity onto the dispersion. In (a-d), red (blue) dots denote positive (negative) angular momentum or helicity, and their size is proportional to the magnitude.

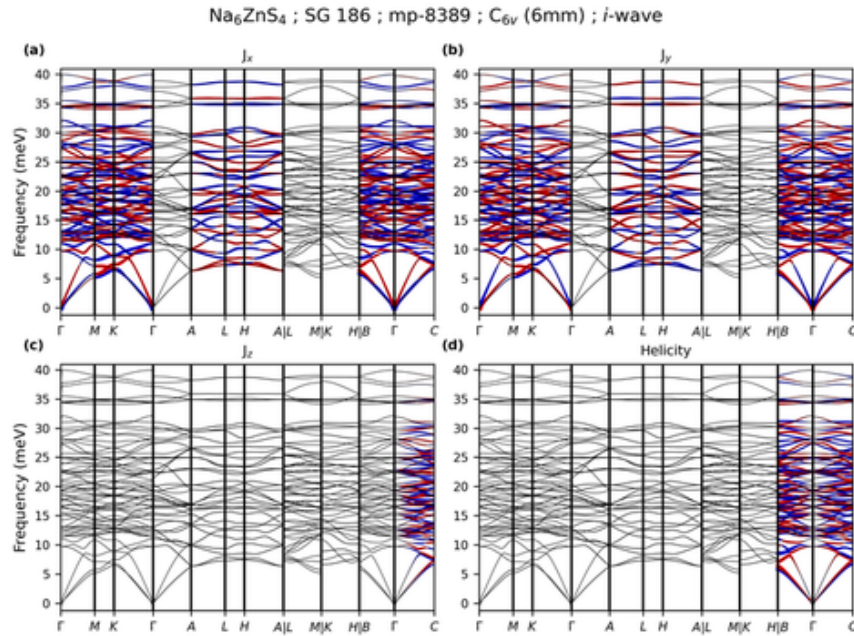


FIG. S133. Phonon dispersion of Na_6ZnS_4 (mp-8389) along the specific momentum paths in the Brillouin zone of SG 186 (see Table S35). (a-c) Projections of the phonon angular momentum components J_x , J_y , and J_z onto the dispersion. (d) Projection of the phonon helicity onto the dispersion. In (a-d), red (blue) dots denote positive (negative) angular momentum or helicity, and their size is proportional to the magnitude.

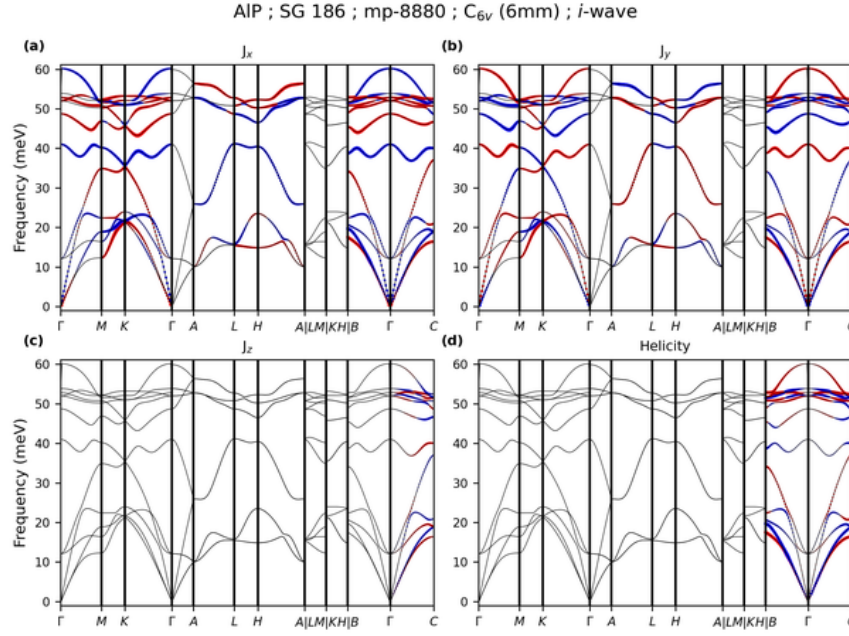


FIG. S134. Phonon dispersion of AlP (mp-8880) along the specific momentum paths in the Brillouin zone of SG 186 (see Table S35). (a-c) Projections of the phonon angular momentum components J_x , J_y , and J_z onto the dispersion. (d) Projection of the phonon helicity onto the dispersion. In (a-d), red (blue) dots denote positive (negative) angular momentum or helicity, and their size is proportional to the magnitude.

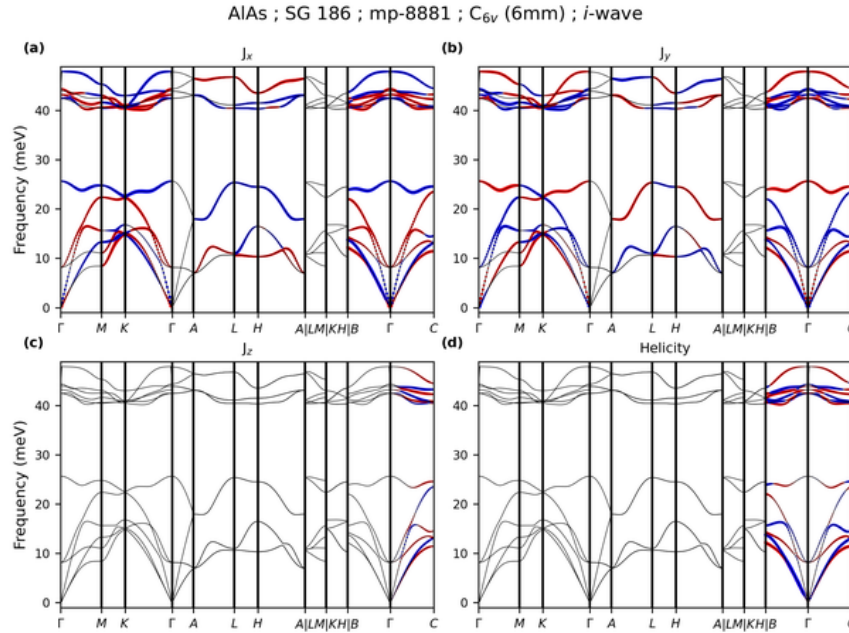


FIG. S135. Phonon dispersion of AlAs (mp-8881) along the specific momentum paths in the Brillouin zone of SG 186 (see Table S35). (a-c) Projections of the phonon angular momentum components J_x , J_y , and J_z onto the dispersion. (d) Projection of the phonon helicity onto the dispersion. In (a-d), red (blue) dots denote positive (negative) angular momentum or helicity, and their size is proportional to the magnitude.

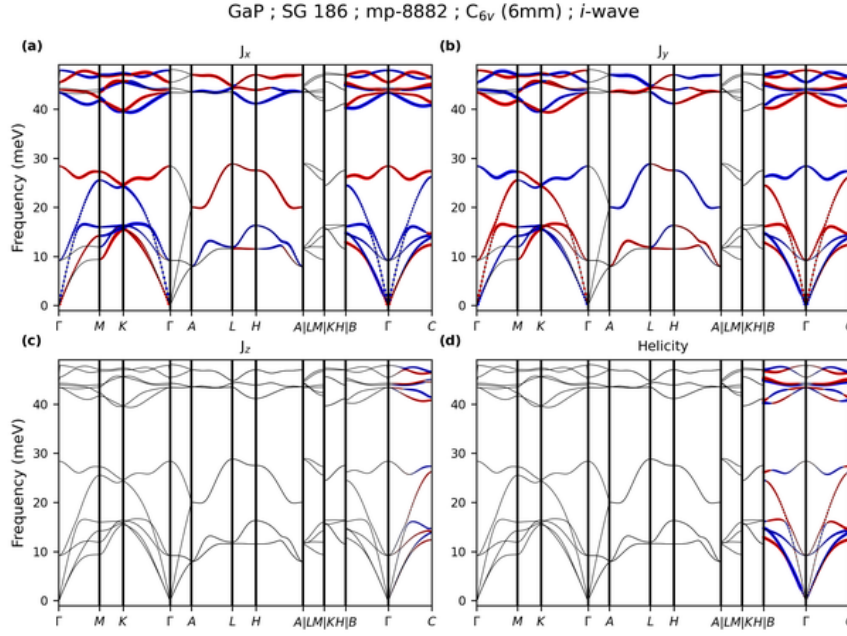


FIG. S136. Phonon dispersion of GaP (mp-8882) along the specific momentum paths in the Brillouin zone of SG 186 (see Table S35). (a-c) Projections of the phonon angular momentum components J_x , J_y , and J_z onto the dispersion. (d) Projection of the phonon helicity onto the dispersion. In (a-d), red (blue) dots denote positive (negative) angular momentum or helicity, and their size is proportional to the magnitude.

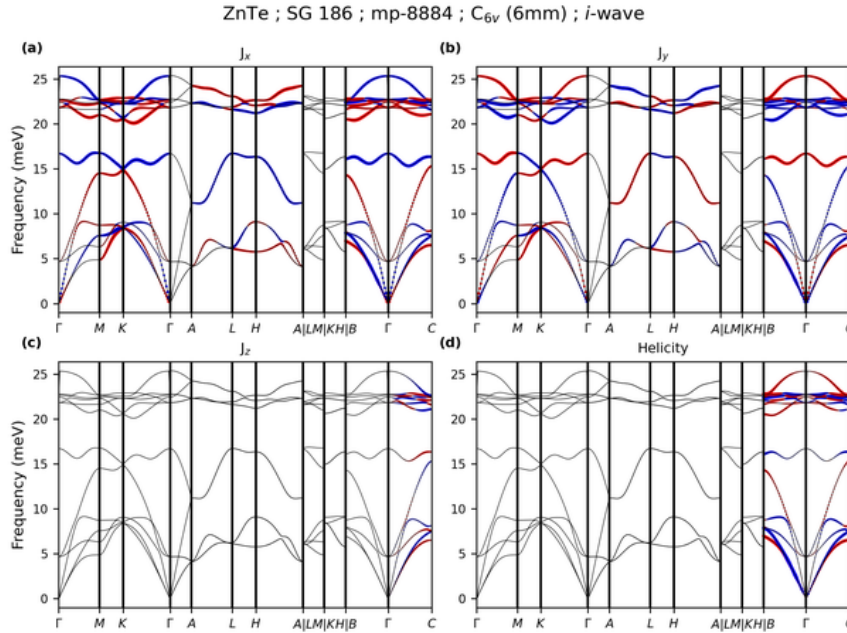


FIG. S137. Phonon dispersion of ZnTe (mp-8884) along the specific momentum paths in the Brillouin zone of SG 186 (see Table S35). (a-c) Projections of the phonon angular momentum components J_x , J_y , and J_z onto the dispersion. (d) Projection of the phonon helicity onto the dispersion. In (a-d), red (blue) dots denote positive (negative) angular momentum or helicity, and their size is proportional to the magnitude.

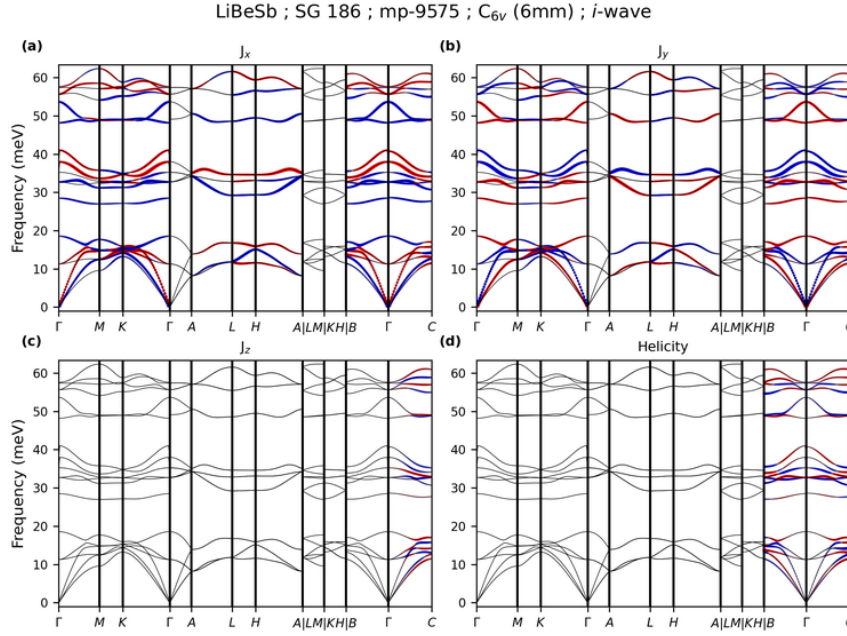


FIG. S138. Phonon dispersion of LiBeSb (mp-9575) along the specific momentum paths in the Brillouin zone of SG 186 (see Table S35). (a-c) Projections of the phonon angular momentum components J_x , J_y , and J_z onto the dispersion. (d) Projection of the phonon helicity onto the dispersion. In (a-d), red (blue) dots denote positive (negative) angular momentum or helicity, and their size is proportional to the magnitude.

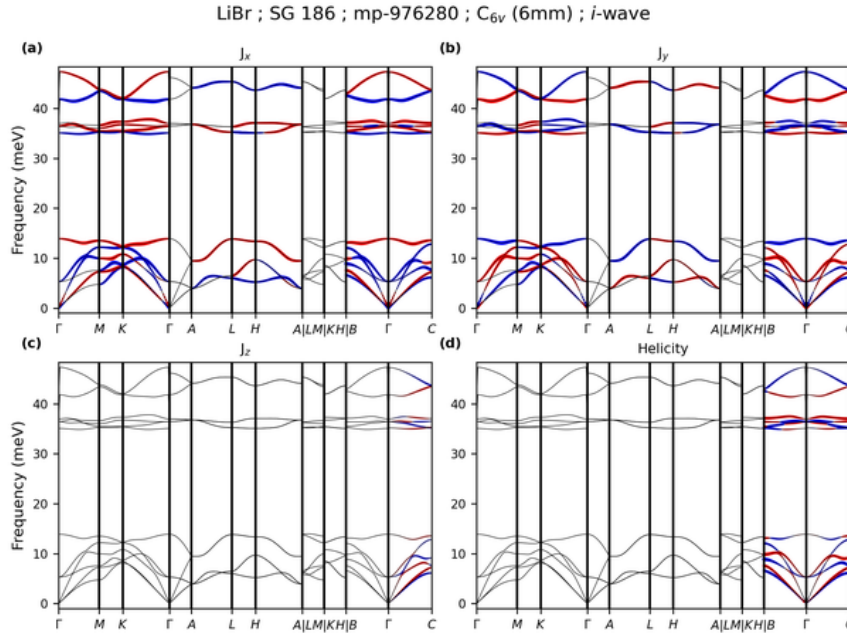


FIG. S139. Phonon dispersion of LiBr (mp-976280) along the specific momentum paths in the Brillouin zone of SG 186 (see Table S35). (a-c) Projections of the phonon angular momentum components J_x , J_y , and J_z onto the dispersion. (d) Projection of the phonon helicity onto the dispersion. In (a-d), red (blue) dots denote positive (negative) angular momentum or helicity, and their size is proportional to the magnitude.

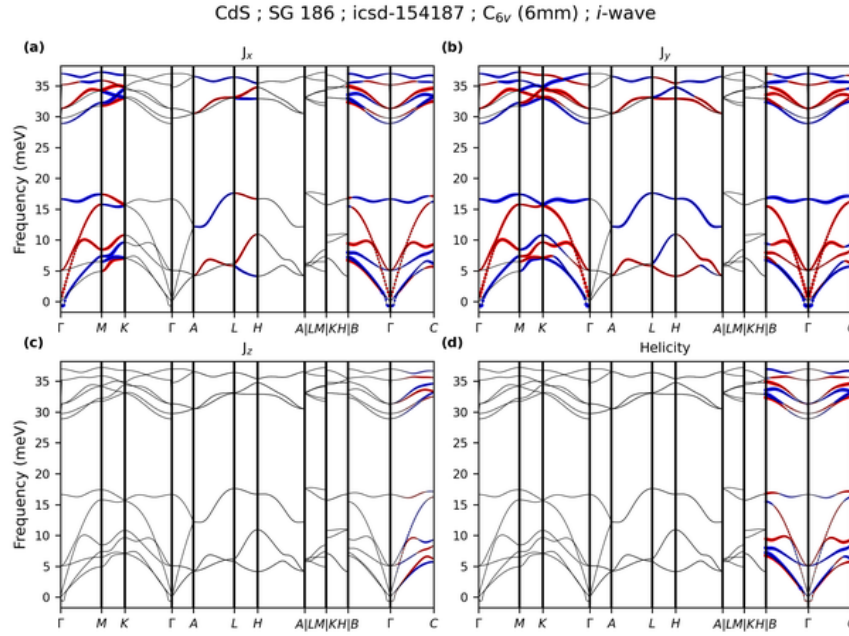


FIG. S140. Phonon dispersion of CdS (icsd-154187) along the specific momentum paths in the Brillouin zone of SG 186 (see Table S35). (a-c) Projections of the phonon angular momentum components J_x , J_y , and J_z onto the dispersion. (d) Projection of the phonon helicity onto the dispersion. In (a-d), red (blue) dots denote positive (negative) angular momentum or helicity, and their size is proportional to the magnitude.

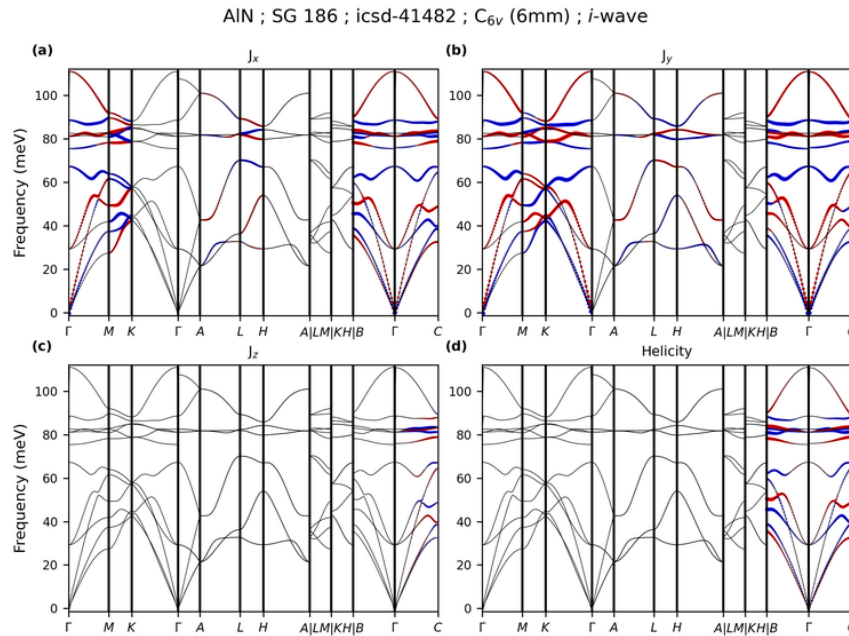


FIG. S141. Phonon dispersion of AlN (icsd-41482) along the specific momentum paths in the Brillouin zone of SG 186 (see Table S35). (a-c) Projections of the phonon angular momentum components J_x , J_y , and J_z onto the dispersion. (d) Projection of the phonon helicity onto the dispersion. In (a-d), red (blue) dots denote positive (negative) angular momentum or helicity, and their size is proportional to the magnitude.

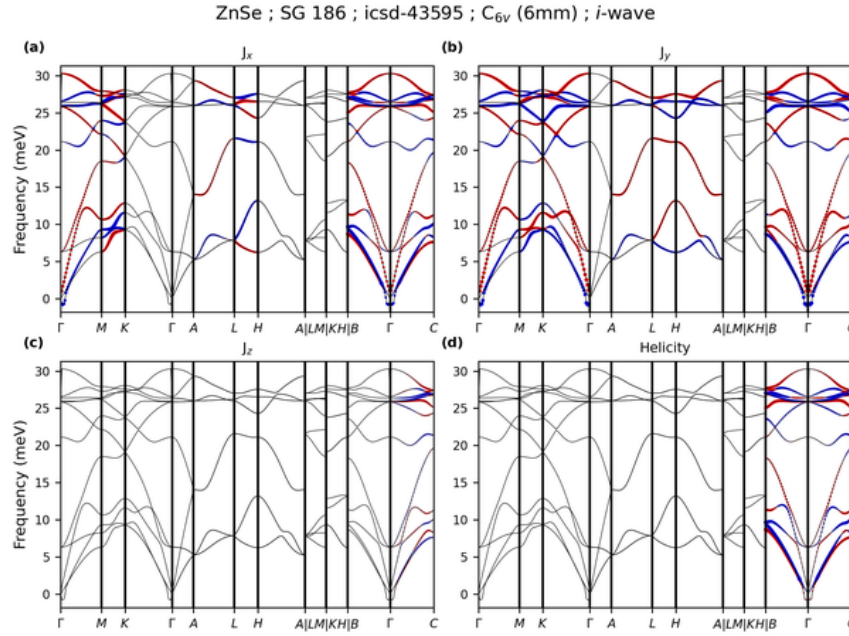


FIG. S142. Phonon dispersion of ZnSe (icsd-43595) along the specific momentum paths in the Brillouin zone of SG 186 (see Table S35). (a-c) Projections of the phonon angular momentum components J_x , J_y , and J_z onto the dispersion. (d) Projection of the phonon helicity onto the dispersion. In (a-d), red (blue) dots denote positive (negative) angular momentum or helicity, and their size is proportional to the magnitude.

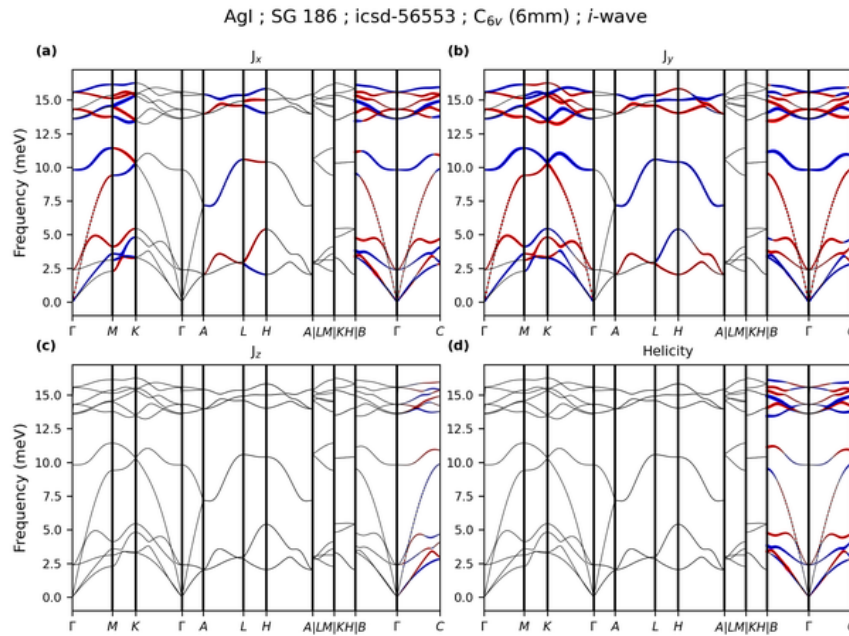


FIG. S143. Phonon dispersion of AgI (icsd-56553) along the specific momentum paths in the Brillouin zone of SG 186 (see Table S35). (a-c) Projections of the phonon angular momentum components J_x , J_y , and J_z onto the dispersion. (d) Projection of the phonon helicity onto the dispersion. In (a-d), red (blue) dots denote positive (negative) angular momentum or helicity, and their size is proportional to the magnitude.

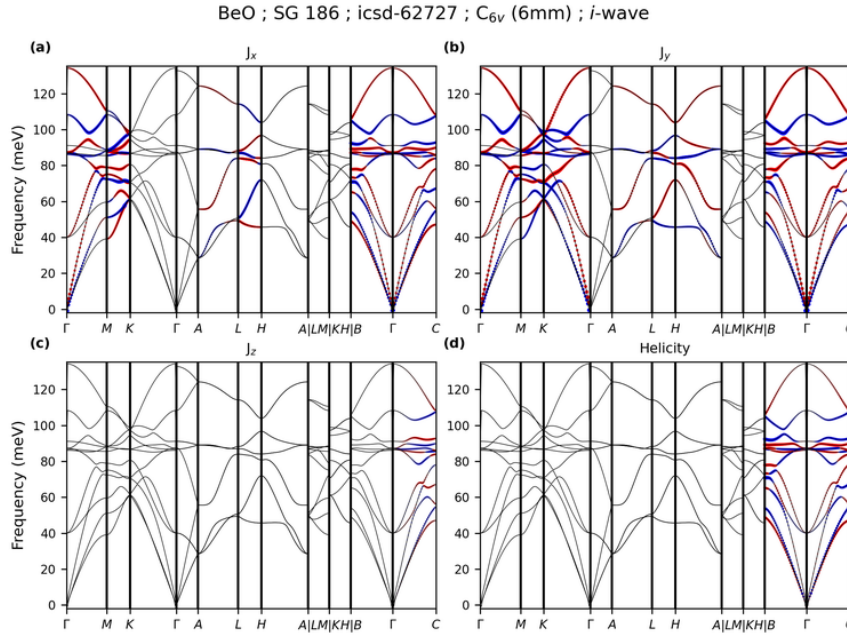


FIG. S144. Phonon dispersion of BeO (icsd-62727) along the specific momentum paths in the Brillouin zone of SG 186 (see Table S35). (a-c) Projections of the phonon angular momentum components J_x , J_y , and J_z onto the dispersion. (d) Projection of the phonon helicity onto the dispersion. In (a-d), red (blue) dots denote positive (negative) angular momentum or helicity, and their size is proportional to the magnitude.

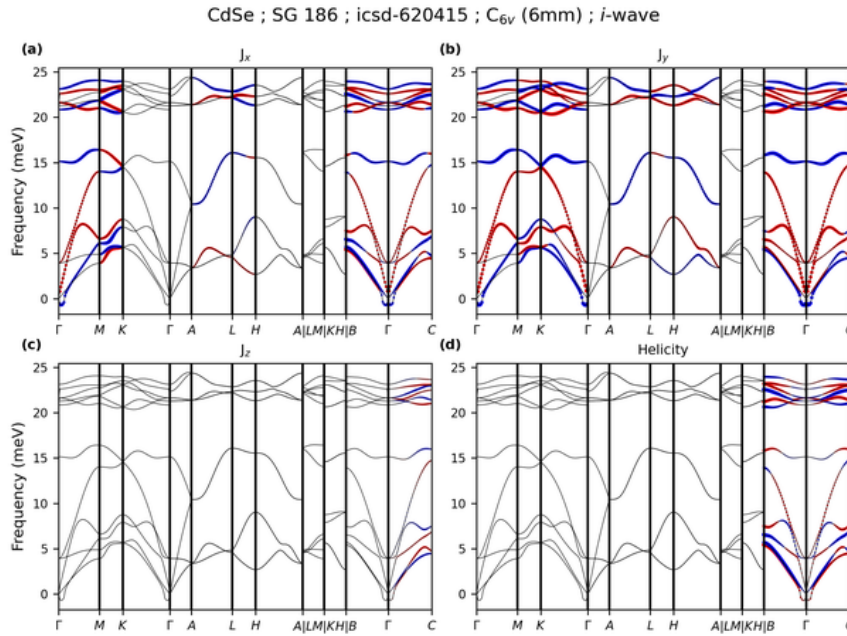


FIG. S145. Phonon dispersion of CdSe (icsd-620415) along the specific momentum paths in the Brillouin zone of SG 186 (see Table S35). (a-c) Projections of the phonon angular momentum components J_x , J_y , and J_z onto the dispersion. (d) Projection of the phonon helicity onto the dispersion. In (a-d), red (blue) dots denote positive (negative) angular momentum or helicity, and their size is proportional to the magnitude.

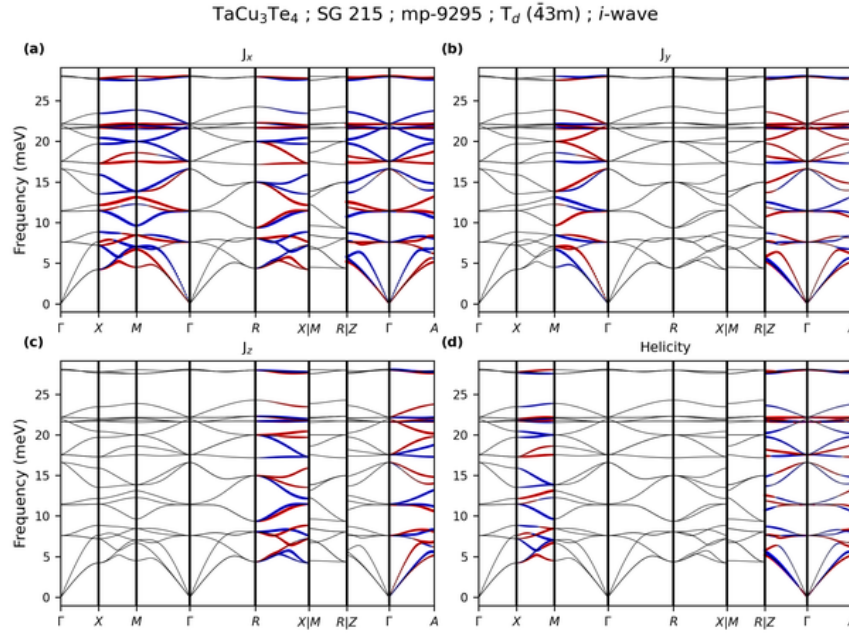


FIG. S146. Phonon dispersion of TaCu_3Te_4 (mp-9295) along the specific momentum paths in the Brillouin zone of SG 215 (see Table S38). (a-c) Projections of the phonon angular momentum components J_x , J_y , and J_z onto the dispersion. (d) Projection of the phonon helicity onto the dispersion. In (a-d), red (blue) dots denote positive (negative) angular momentum or helicity, and their size is proportional to the magnitude.

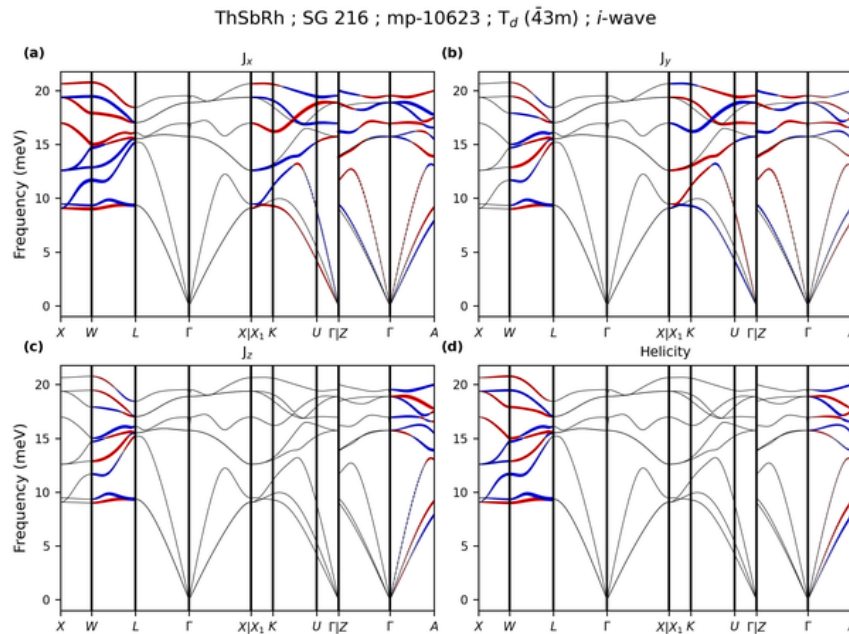


FIG. S147. Phonon dispersion of ThSbRh (mp-10623) along the specific momentum paths in the Brillouin zone of SG 216 (see Table S39). (a-c) Projections of the phonon angular momentum components J_x , J_y , and J_z onto the dispersion. (d) Projection of the phonon helicity onto the dispersion. In (a-d), red (blue) dots denote positive (negative) angular momentum or helicity, and their size is proportional to the magnitude.

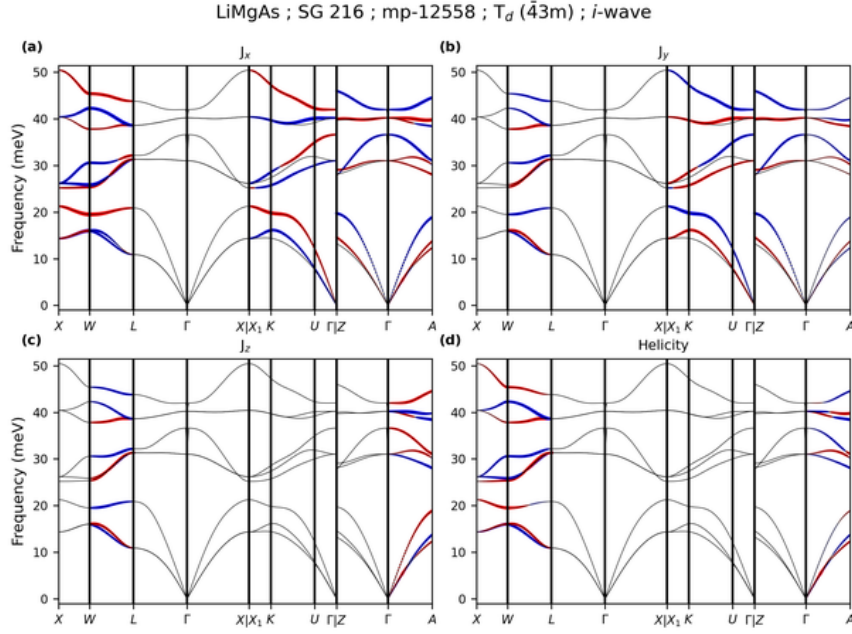


FIG. S148. Phonon dispersion of LiMgAs (mp-12558) along the specific momentum paths in the Brillouin zone of SG 216 (see Table S39). (a-c) Projections of the phonon angular momentum components J_x , J_y , and J_z onto the dispersion. (d) Projection of the phonon helicity onto the dispersion. In (a-d), red (blue) dots denote positive (negative) angular momentum or helicity, and their size is proportional to the magnitude.

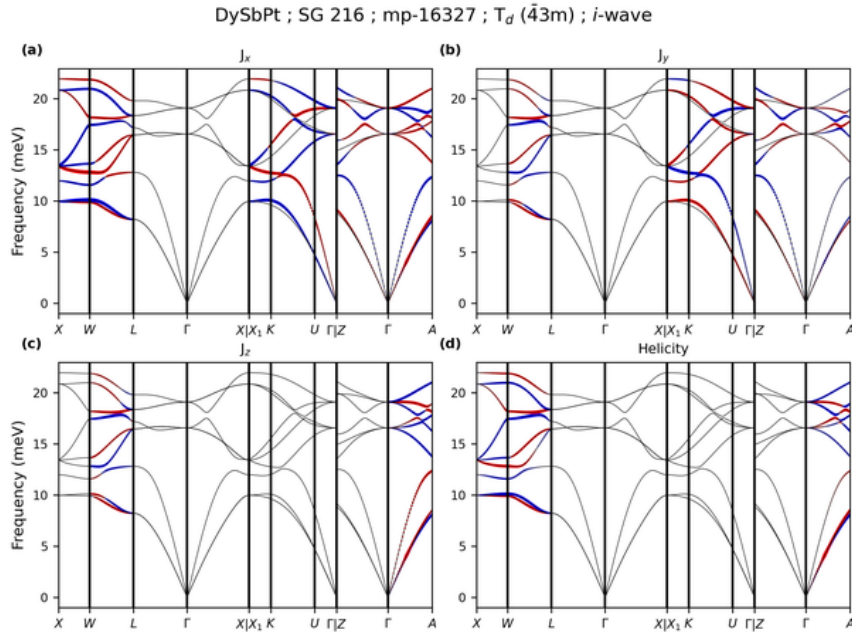


FIG. S149. Phonon dispersion of DySbPt (mp-16327) along the specific momentum paths in the Brillouin zone of SG 216 (see Table S39). (a-c) Projections of the phonon angular momentum components J_x , J_y , and J_z onto the dispersion. (d) Projection of the phonon helicity onto the dispersion. In (a-d), red (blue) dots denote positive (negative) angular momentum or helicity, and their size is proportional to the magnitude.

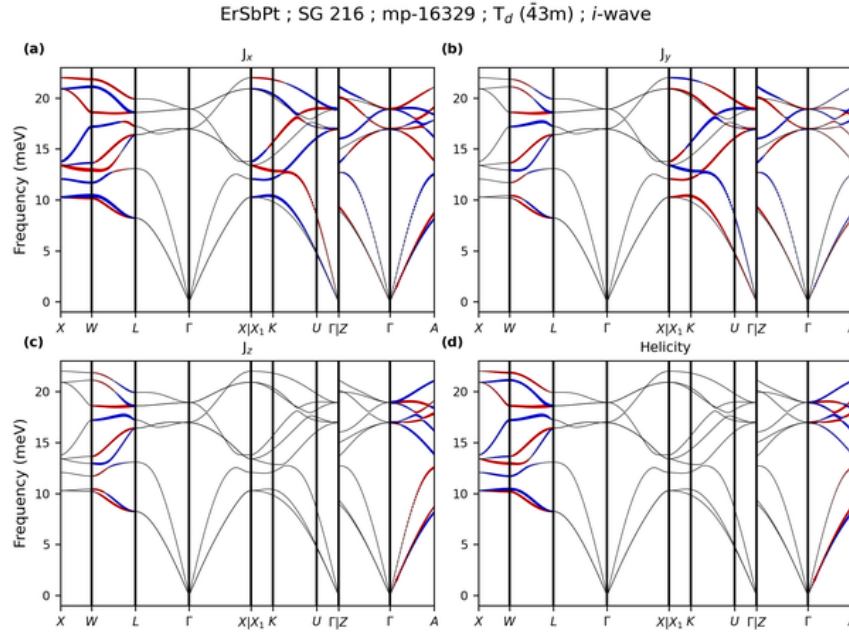


FIG. S150. Phonon dispersion of ErSbPt (mp-16329) along the specific momentum paths in the Brillouin zone of SG 216 (see Table S39). (a-c) Projections of the phonon angular momentum components J_x , J_y , and J_z onto the dispersion. (d) Projection of the phonon helicity onto the dispersion. In (a-d), red (blue) dots denote positive (negative) angular momentum or helicity, and their size is proportional to the magnitude.

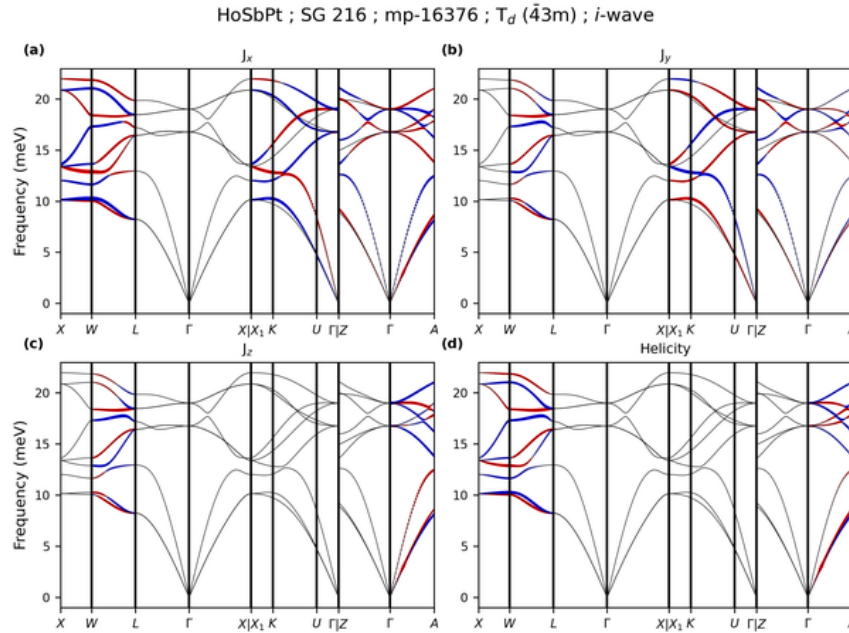


FIG. S151. Phonon dispersion of HoSbPt (mp-16376) along the specific momentum paths in the Brillouin zone of SG 216 (see Table S39). (a-c) Projections of the phonon angular momentum components J_x , J_y , and J_z onto the dispersion. (d) Projection of the phonon helicity onto the dispersion. In (a-d), red (blue) dots denote positive (negative) angular momentum or helicity, and their size is proportional to the magnitude.

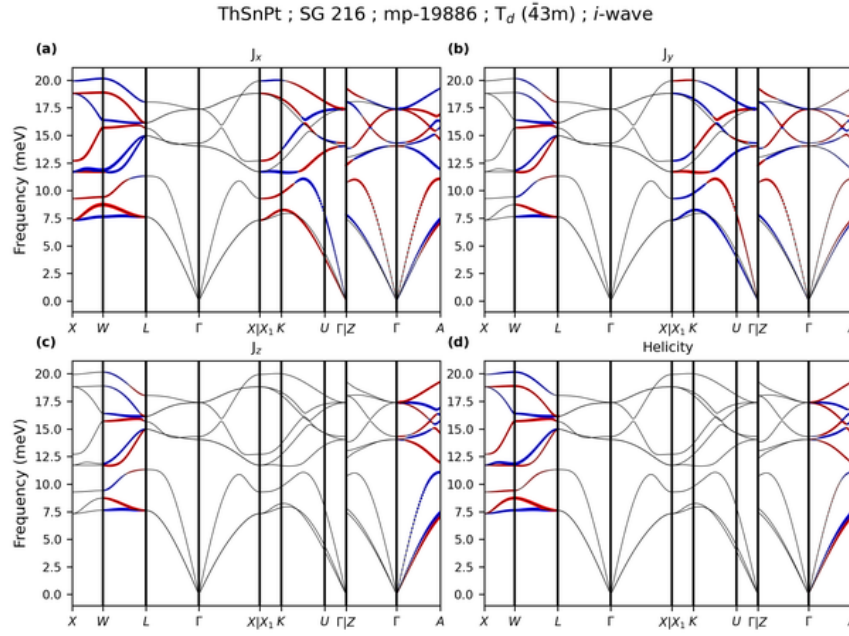


FIG. S152. Phonon dispersion of ThSnPt (mp-19886) along the specific momentum paths in the Brillouin zone of SG 216 (see Table S39). (a-c) Projections of the phonon angular momentum components J_x , J_y , and J_z onto the dispersion. (d) Projection of the phonon helicity onto the dispersion. In (a-d), red (blue) dots denote positive (negative) angular momentum or helicity, and their size is proportional to the magnitude.

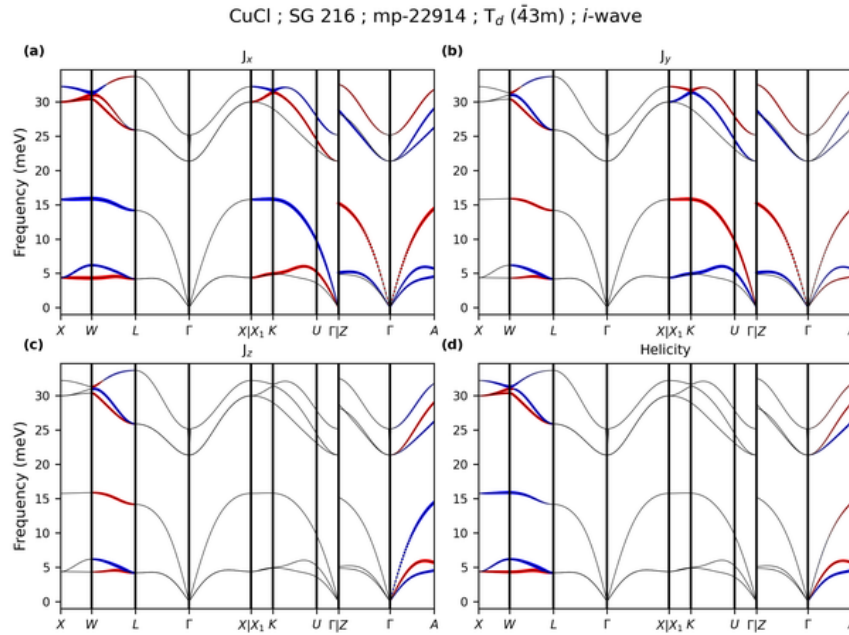


FIG. S153. Phonon dispersion of CuCl (mp-22914) along the specific momentum paths in the Brillouin zone of SG 216 (see Table S39). (a-c) Projections of the phonon angular momentum components J_x , J_y , and J_z onto the dispersion. (d) Projection of the phonon helicity onto the dispersion. In (a-d), red (blue) dots denote positive (negative) angular momentum or helicity, and their size is proportional to the magnitude.

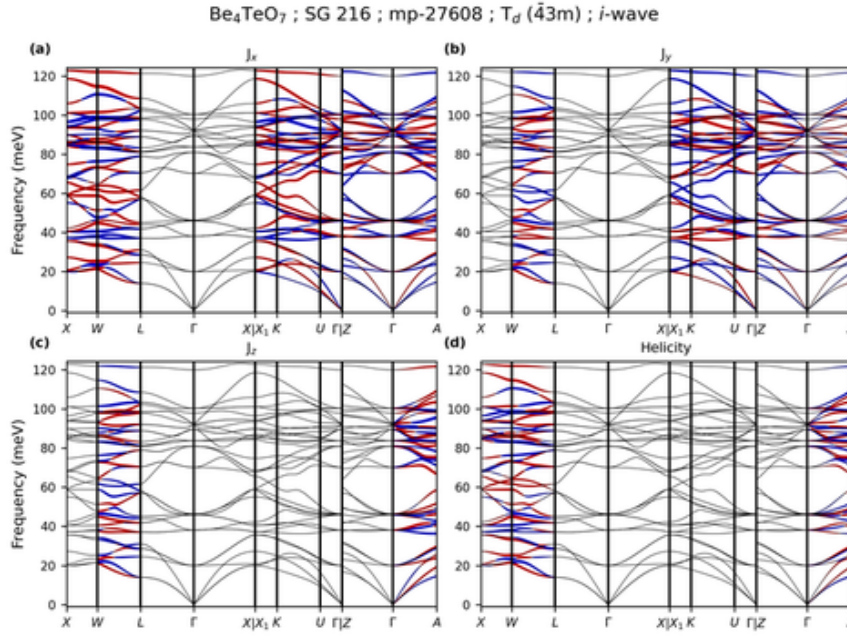


FIG. S154. Phonon dispersion of Be_4TeO_7 (mp-27608) along the specific momentum paths in the Brillouin zone of SG 216 (see Table S39). (a-c) Projections of the phonon angular momentum components J_x , J_y , and J_z onto the dispersion. (d) Projection of the phonon helicity onto the dispersion. In (a-d), red (blue) dots denote positive (negative) angular momentum or helicity, and their size is proportional to the magnitude.

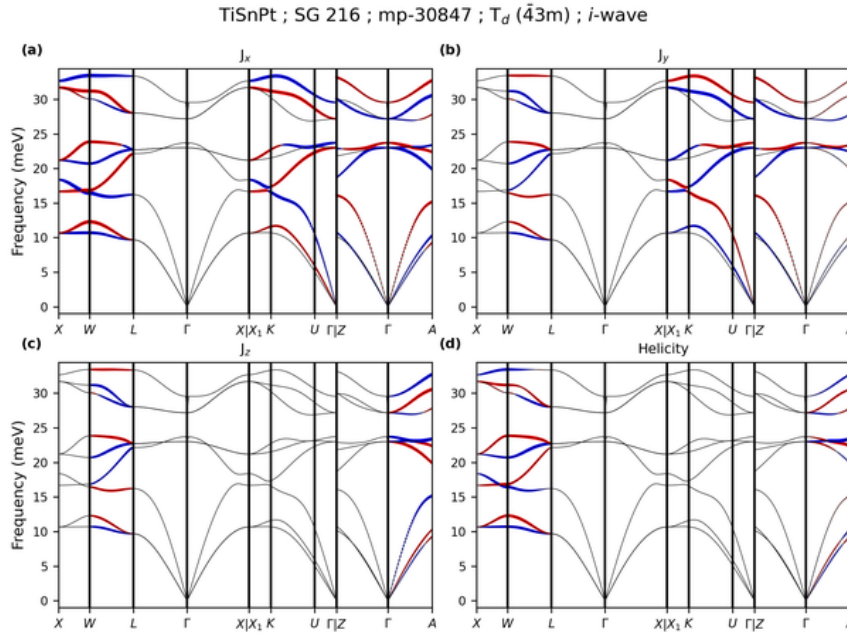


FIG. S155. Phonon dispersion of TiSnPt (mp-30847) along the specific momentum paths in the Brillouin zone of SG 216 (see Table S39). (a-c) Projections of the phonon angular momentum components J_x , J_y , and J_z onto the dispersion. (d) Projection of the phonon helicity onto the dispersion. In (a-d), red (blue) dots denote positive (negative) angular momentum or helicity, and their size is proportional to the magnitude.

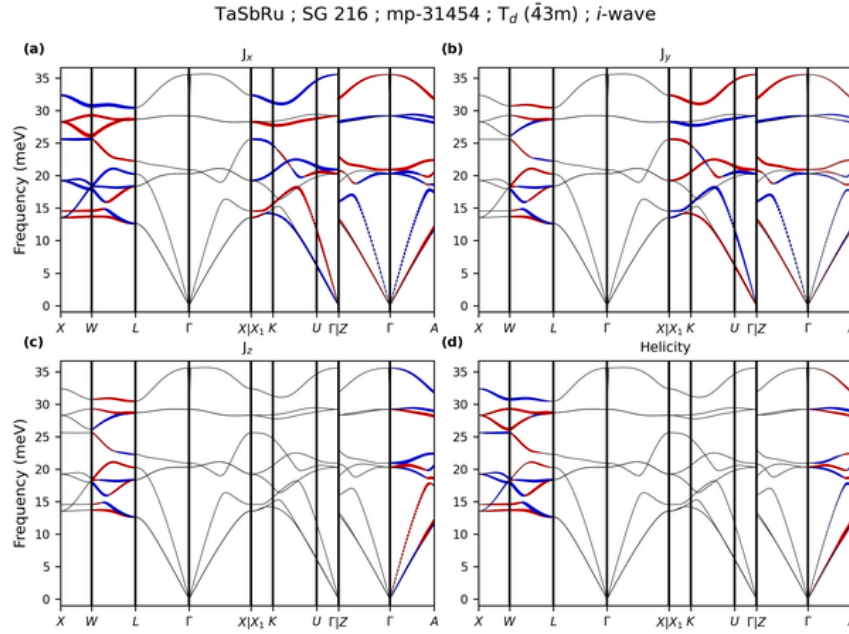


FIG. S156. Phonon dispersion of TaSbRu (mp-31454) along the specific momentum paths in the Brillouin zone of SG 216 (see Table S39). (a-c) Projections of the phonon angular momentum components J_x , J_y , and J_z onto the dispersion. (d) Projection of the phonon helicity onto the dispersion. In (a-d), red (blue) dots denote positive (negative) angular momentum or helicity, and their size is proportional to the magnitude.

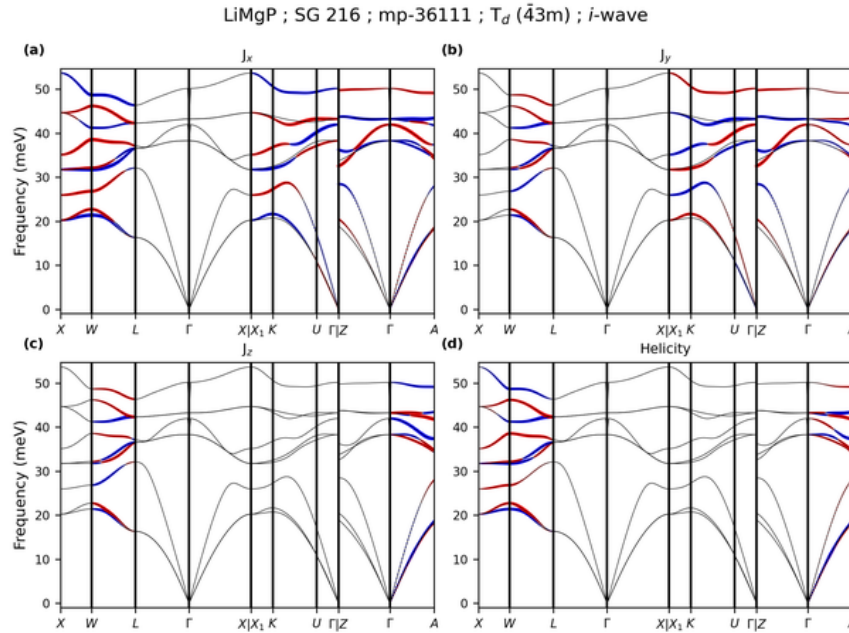


FIG. S157. Phonon dispersion of LiMgP (mp-36111) along the specific momentum paths in the Brillouin zone of SG 216 (see Table S39). (a-c) Projections of the phonon angular momentum components J_x , J_y , and J_z onto the dispersion. (d) Projection of the phonon helicity onto the dispersion. In (a-d), red (blue) dots denote positive (negative) angular momentum or helicity, and their size is proportional to the magnitude.

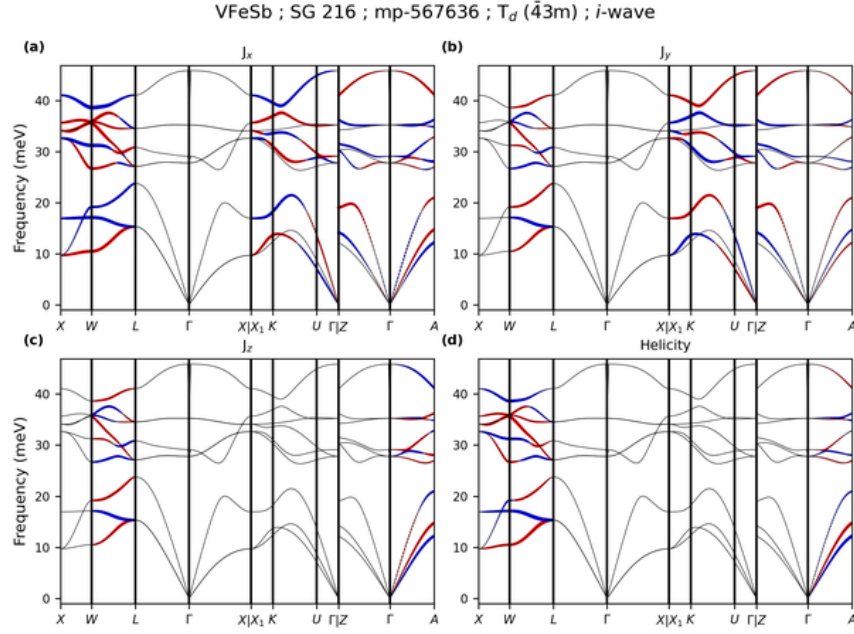


FIG. S158. Phonon dispersion of VFeSb (mp-567636) along the specific momentum paths in the Brillouin zone of SG 216 (see Table S39). (a-c) Projections of the phonon angular momentum components J_x , J_y , and J_z onto the dispersion. (d) Projection of the phonon helicity onto the dispersion. In (a-d), red (blue) dots denote positive (negative) angular momentum or helicity, and their size is proportional to the magnitude.

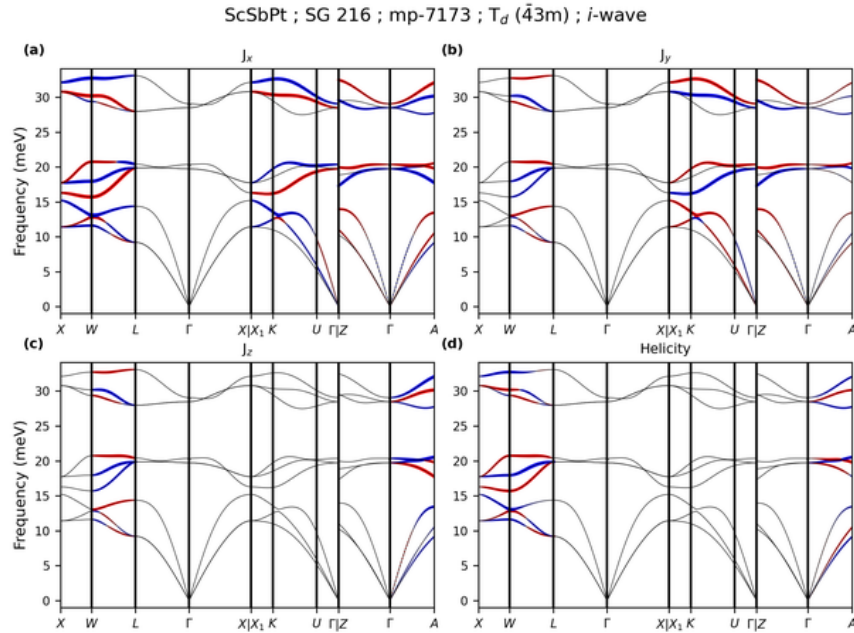


FIG. S159. Phonon dispersion of ScSbPt (mp-7173) along the specific momentum paths in the Brillouin zone of SG 216 (see Table S39). (a-c) Projections of the phonon angular momentum components J_x , J_y , and J_z onto the dispersion. (d) Projection of the phonon helicity onto the dispersion. In (a-d), red (blue) dots denote positive (negative) angular momentum or helicity, and their size is proportional to the magnitude.

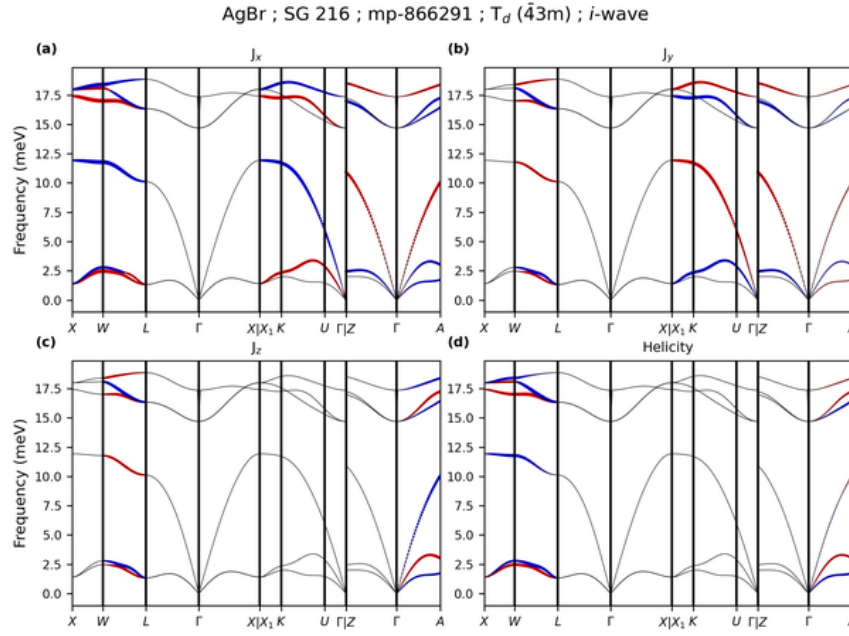


FIG. S160. Phonon dispersion of AgBr (mp-866291) along the specific momentum paths in the Brillouin zone of SG 216 (see Table S39). (a-c) Projections of the phonon angular momentum components J_x , J_y , and J_z onto the dispersion. (d) Projection of the phonon helicity onto the dispersion. In (a-d), red (blue) dots denote positive (negative) angular momentum or helicity, and their size is proportional to the magnitude.

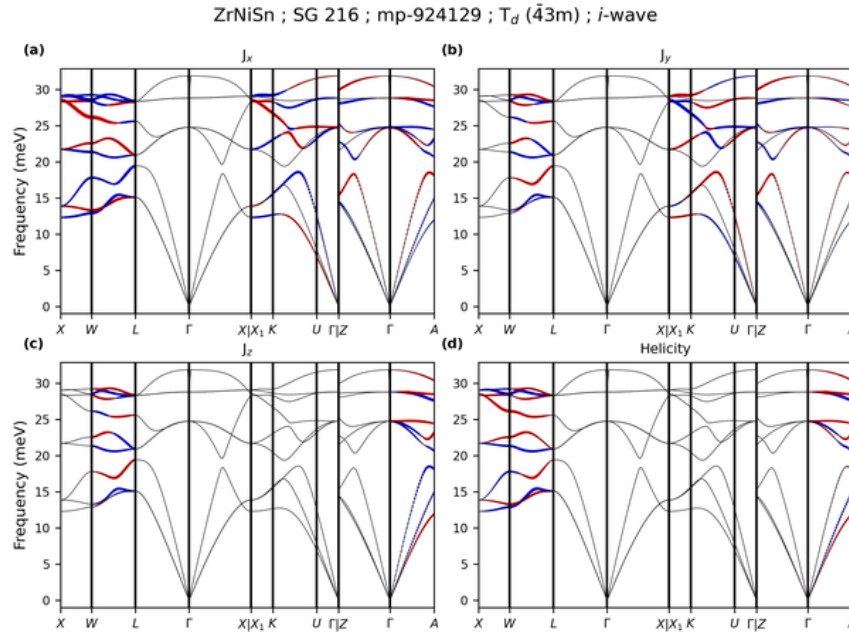


FIG. S161. Phonon dispersion of ZrNiSn (mp-924129) along the specific momentum paths in the Brillouin zone of SG 216 (see Table S39). (a-c) Projections of the phonon angular momentum components J_x , J_y , and J_z onto the dispersion. (d) Projection of the phonon helicity onto the dispersion. In (a-d), red (blue) dots denote positive (negative) angular momentum or helicity, and their size is proportional to the magnitude.

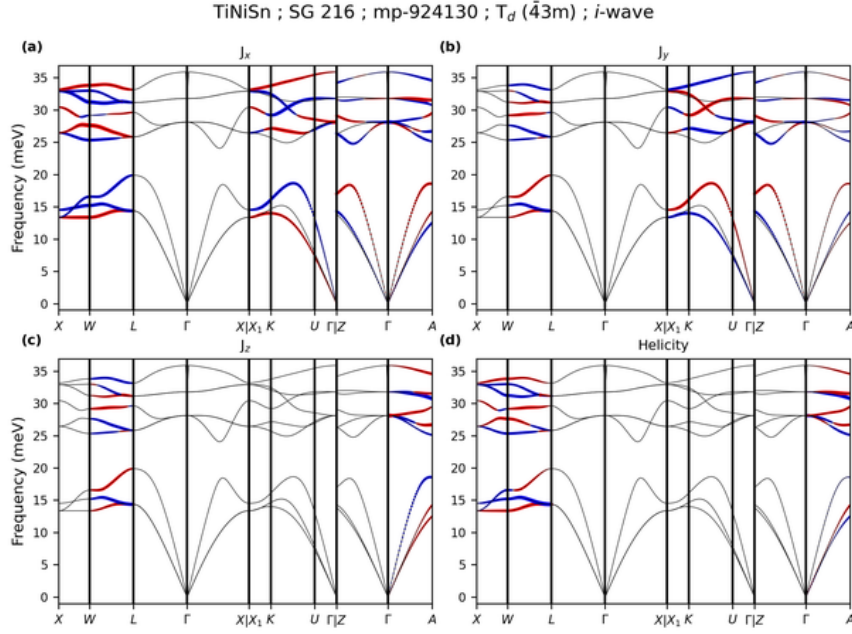


FIG. S162. Phonon dispersion of TiNiSn (mp-924130) along the specific momentum paths in the Brillouin zone of SG 216 (see Table S39). (a-c) Projections of the phonon angular momentum components J_x , J_y , and J_z onto the dispersion. (d) Projection of the phonon helicity onto the dispersion. In (a-d), red (blue) dots denote positive (negative) angular momentum or helicity, and their size is proportional to the magnitude.

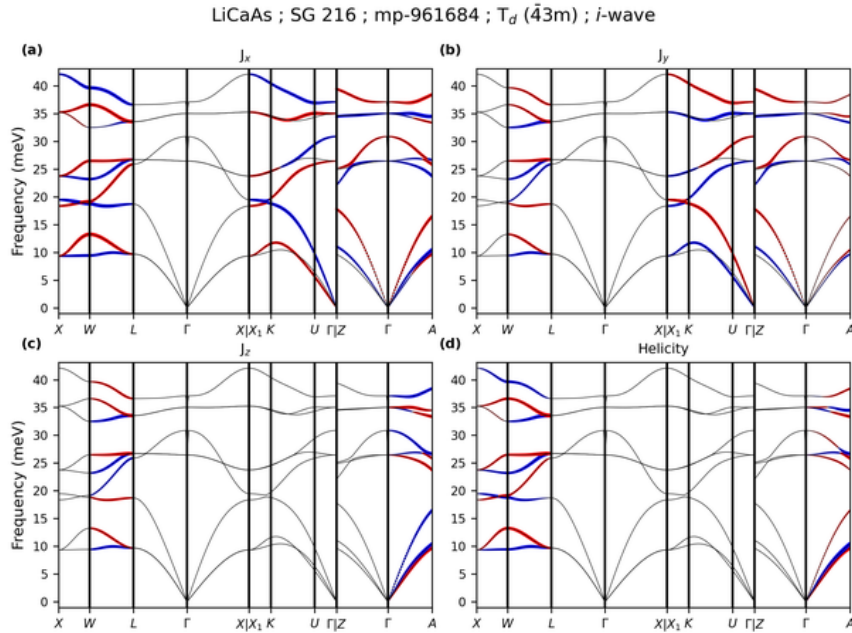


FIG. S163. Phonon dispersion of LiCaAs (mp-961684) along the specific momentum paths in the Brillouin zone of SG 216 (see Table S39). (a-c) Projections of the phonon angular momentum components J_x , J_y , and J_z onto the dispersion. (d) Projection of the phonon helicity onto the dispersion. In (a-d), red (blue) dots denote positive (negative) angular momentum or helicity, and their size is proportional to the magnitude.

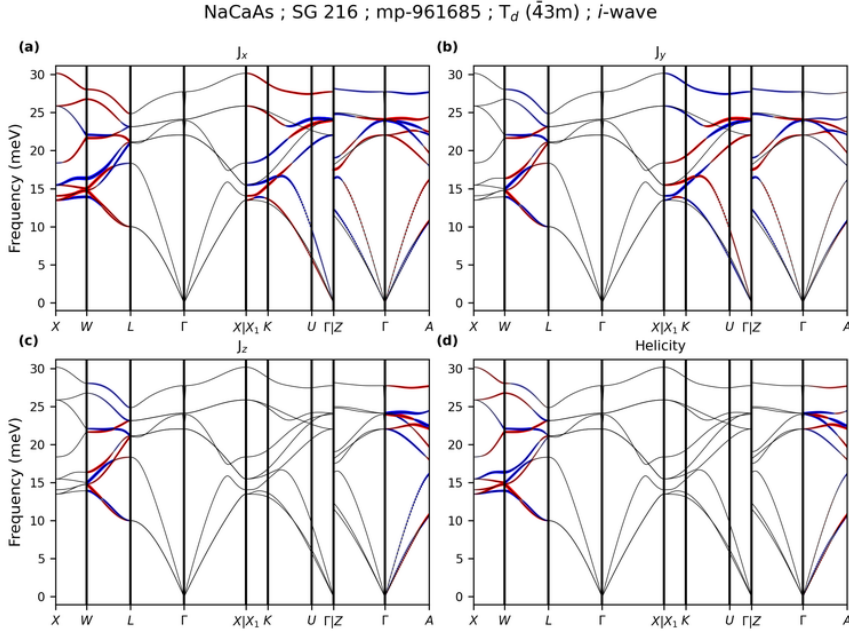


FIG. S164. Phonon dispersion of NaCaAs (mp-961685) along the specific momentum paths in the Brillouin zone of SG 216 (see Table S39). (a-c) Projections of the phonon angular momentum components J_x , J_y , and J_z onto the dispersion. (d) Projection of the phonon helicity onto the dispersion. In (a-d), red (blue) dots denote positive (negative) angular momentum or helicity, and their size is proportional to the magnitude.

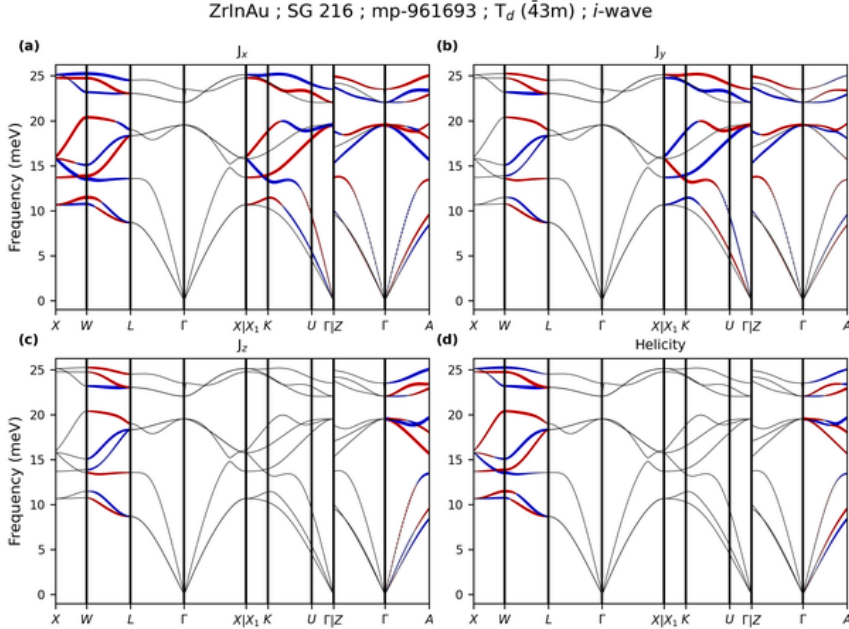


FIG. S165. Phonon dispersion of ZrInAu (mp-961693) along the specific momentum paths in the Brillouin zone of SG 216 (see Table S39). (a-c) Projections of the phonon angular momentum components J_x , J_y , and J_z onto the dispersion. (d) Projection of the phonon helicity onto the dispersion. In (a-d), red (blue) dots denote positive (negative) angular momentum or helicity, and their size is proportional to the magnitude.

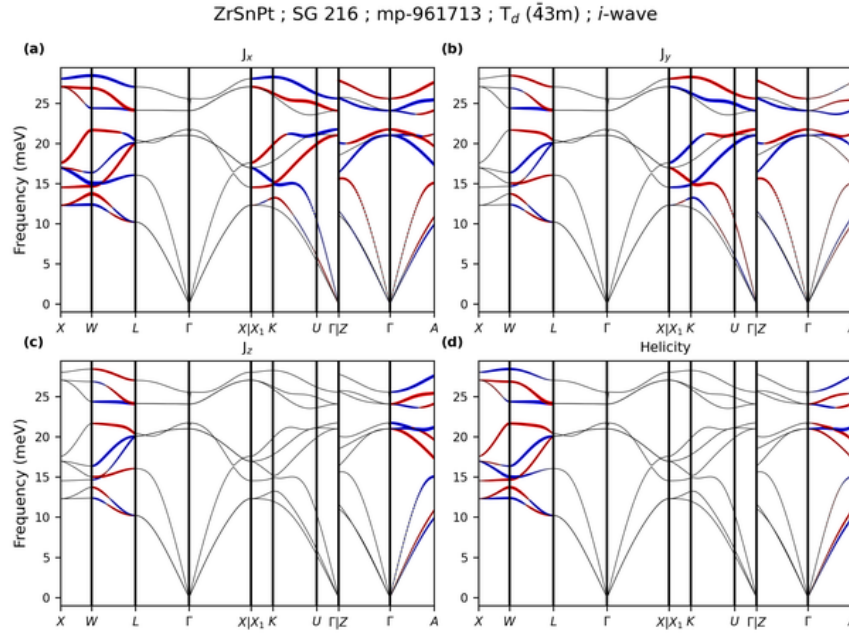


FIG. S166. Phonon dispersion of ZrSnPt (mp-961713) along the specific momentum paths in the Brillouin zone of SG 216 (see Table S39). (a-c) Projections of the phonon angular momentum components J_x , J_y , and J_z onto the dispersion. (d) Projection of the phonon helicity onto the dispersion. In (a-d), red (blue) dots denote positive (negative) angular momentum or helicity, and their size is proportional to the magnitude.

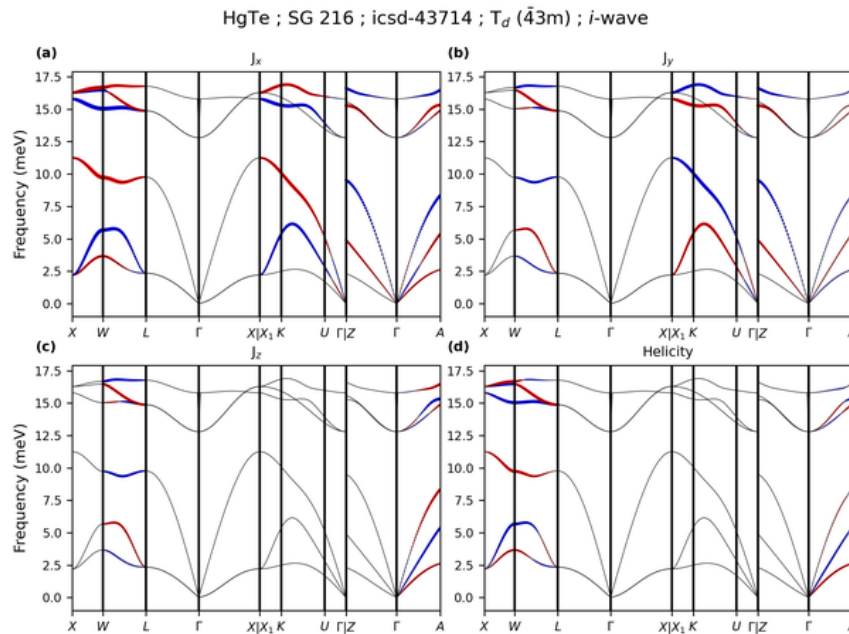


FIG. S167. Phonon dispersion of HgTe (icsd-43714) along the specific momentum paths in the Brillouin zone of SG 216 (see Table S39). (a-c) Projections of the phonon angular momentum components J_x , J_y , and J_z onto the dispersion. (d) Projection of the phonon helicity onto the dispersion. In (a-d), red (blue) dots denote positive (negative) angular momentum or helicity, and their size is proportional to the magnitude.

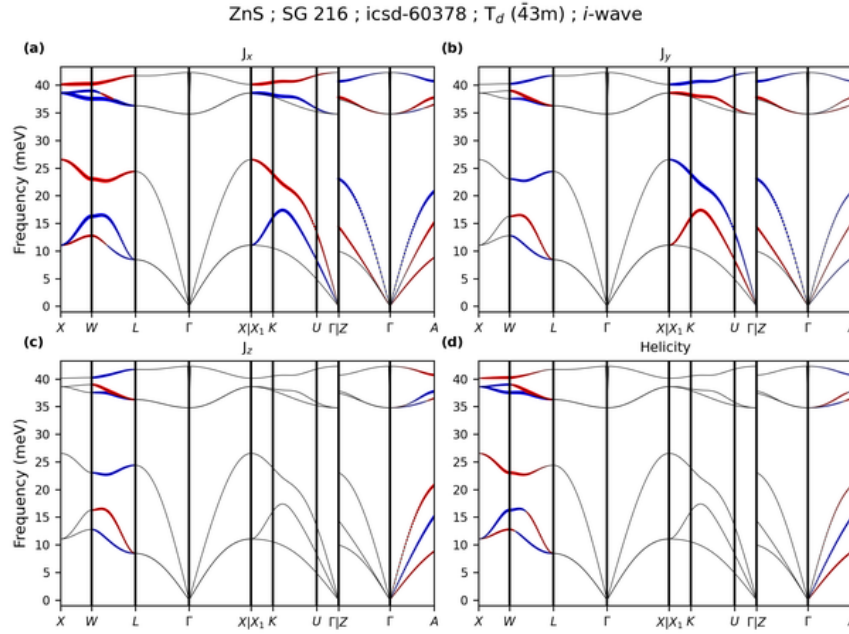


FIG. S168. Phonon dispersion of ZnS (icsd-60378) along the specific momentum paths in the Brillouin zone of SG 216 (see Table S39). (a-c) Projections of the phonon angular momentum components J_x , J_y , and J_z onto the dispersion. (d) Projection of the phonon helicity onto the dispersion. In (a-d), red (blue) dots denote positive (negative) angular momentum or helicity, and their size is proportional to the magnitude.

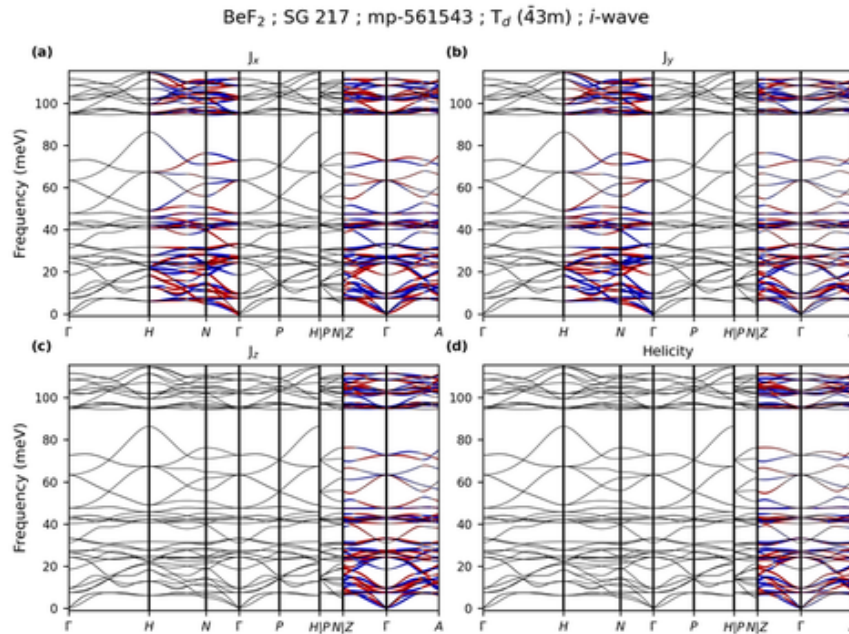


FIG. S169. Phonon dispersion of BeF₂ (mp-561543) along the specific momentum paths in the Brillouin zone of SG 217 (see Table S40). (a-c) Projections of the phonon angular momentum components J_x , J_y , and J_z onto the dispersion. (d) Projection of the phonon helicity onto the dispersion. In (a-d), red (blue) dots denote positive (negative) angular momentum or helicity, and their size is proportional to the magnitude.

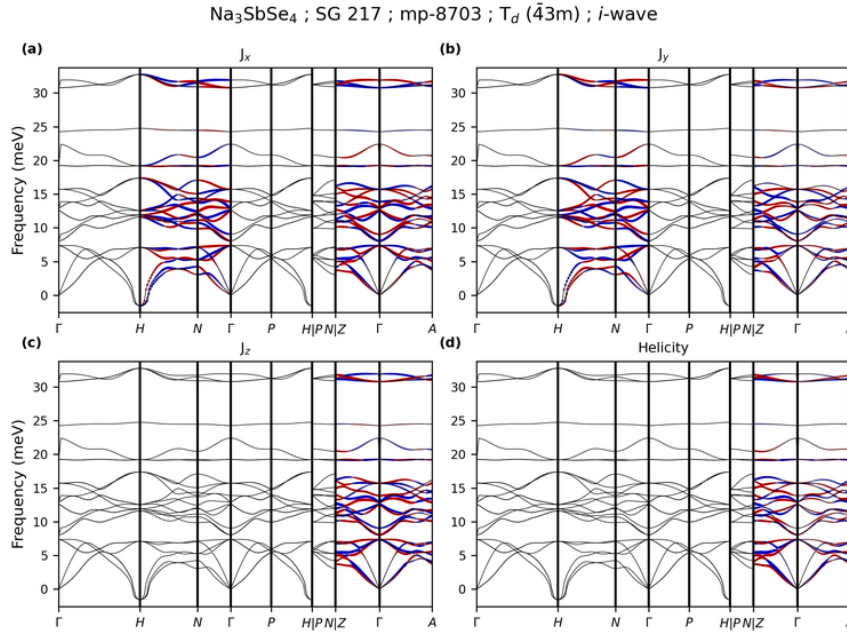


FIG. S170. Phonon dispersion of Na_3SbSe_4 (mp-8703) along the specific momentum paths in the Brillouin zone of SG 217 (see Table S40). (a-c) Projections of the phonon angular momentum components J_x , J_y , and J_z onto the dispersion. (d) Projection of the phonon helicity onto the dispersion. In (a-d), red (blue) dots denote positive (negative) angular momentum or helicity, and their size is proportional to the magnitude.

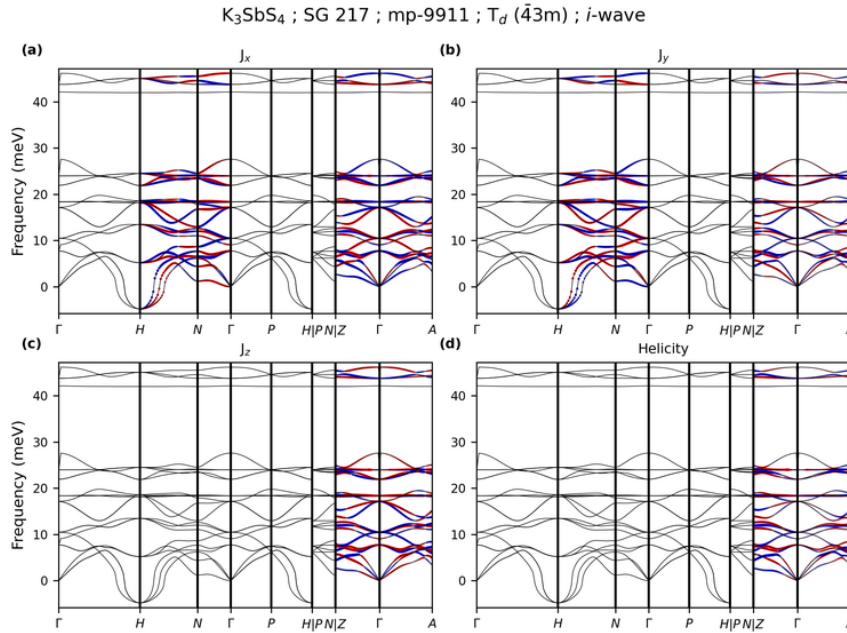


FIG. S171. Phonon dispersion of K_3SbS_4 (mp-9911) along the specific momentum paths in the Brillouin zone of SG 217 (see Table S40). (a-c) Projections of the phonon angular momentum components J_x , J_y , and J_z onto the dispersion. (d) Projection of the phonon helicity onto the dispersion. In (a-d), red (blue) dots denote positive (negative) angular momentum or helicity, and their size is proportional to the magnitude.

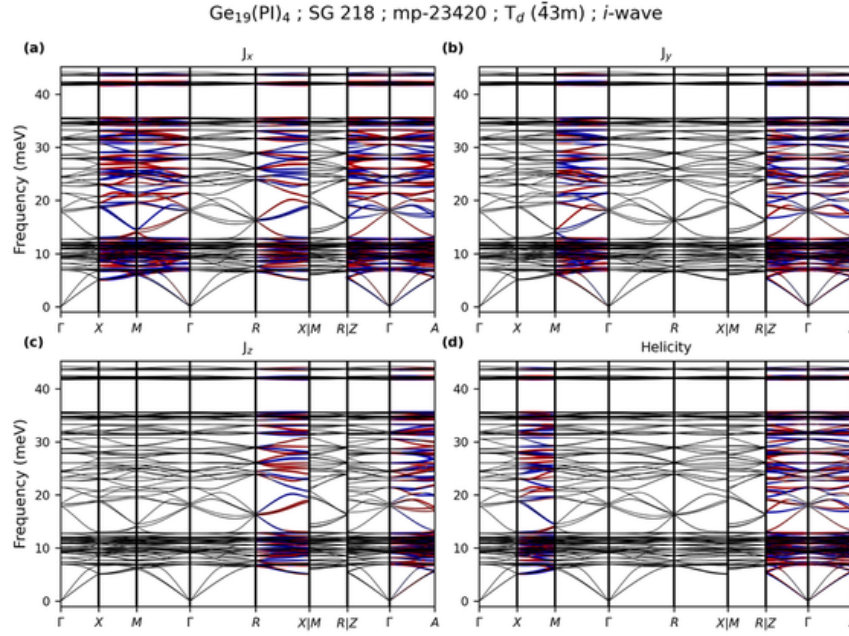


FIG. S172. Phonon dispersion of $\text{Ge}_{19}(\text{PI})_4$ (mp-23420) along the specific momentum paths in the Brillouin zone of SG 218 (see Table S41). (a-c) Projections of the phonon angular momentum components J_x , J_y , and J_z onto the dispersion. (d) Projection of the phonon helicity onto the dispersion. In (a-d), red (blue) dots denote positive (negative) angular momentum or helicity, and their size is proportional to the magnitude.

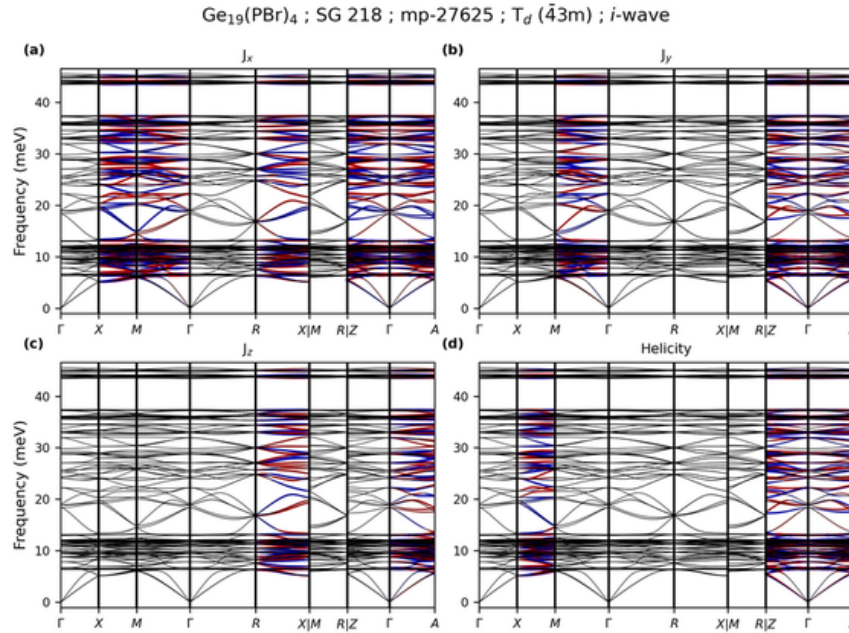


FIG. S173. Phonon dispersion of $\text{Ge}_{19}(\text{PBr})_4$ (mp-27625) along the specific momentum paths in the Brillouin zone of SG 218 (see Table S41). (a-c) Projections of the phonon angular momentum components J_x , J_y , and J_z onto the dispersion. (d) Projection of the phonon helicity onto the dispersion. In (a-d), red (blue) dots denote positive (negative) angular momentum or helicity, and their size is proportional to the magnitude.

TABLE S7: List of momentum points used for phonon spectrum plots of materials in space group 4 ($P2_1$). Coordinates are given in units of the primitive unit cell's reciprocal lattice vectors.

Symbol	E	A	Γ	B	D	C	Z	Y
Coordinates	(0.5,0.5,0.5)	(0.5,0,0.5)	(0,0,0)	(0,0,0.5)	(0,0.5,0.5)	(0.5,0.5,0)	(0,0.5,0)	(0.5,0,0)

TABLE S8: List of momentum points used for phonon spectrum plots of materials in space group 19 ($P2_12_12_1$). Coordinates are given in units of the primitive unit cell's reciprocal lattice vectors.

Symbol	Γ	X	S	Y	Z	U	R	T
Coordinates	(0,0,0)	(0.5,0,0)	(0.5,0.5,0)	(0,0.5,0)	(0,0,0.5)	(0.5,0,0.5)	(0.5,0.5,0.5)	(0,0.5,0.5)

TABLE S9: List of momentum points used for phonon spectrum plots of materials in space group 42 ($Fmm2$). Coordinates are given in units of the primitive unit cell's reciprocal lattice vectors.

Symbol	Γ	Y	T	Z	X	A_1	X_1	A	L
Coordinates	(0,0,0)	(0.5,0,0.5)	(1,0.5,0.5)	(0.5,0.5,0)	(0,0.25,0.25)	(0.5,0.25,0.75)	(1,0.75,0.75)	(0.5,0.75,0.25)	(0.5,0.5,0.5)

TABLE S10: List of momentum points used for phonon spectrum plots of materials in space group 82 ($I\bar{4}$). Coordinates are given in units of the primitive unit cell's reciprocal lattice vectors.

Symbol	P	N	Γ	M_1	M_2	X	M	X_1	R
Coordinates	(0.25,0.25,0.25)	(0,0.5,0)	(0,0,0)	(0.5,0.5,-0.5)	(-0.5,0.5,0.5)	(0,0,0.5)	(0.5,0.5,0.5)	(0,1,0.5)	(0,0.5,0.5)

TABLE S11: List of momentum points used for phonon spectrum plots of materials in space group 91 ($P4_12_2$). Coordinates are given in units of the primitive unit cell's reciprocal lattice vectors.

Symbol	Γ	X	M	Z	R	A
Coordinates	(0,0,0)	(0,0.5,0)	(0.5,0.5,0)	(0,0,0.5)	(0,0.5,0.5)	(0.5,0.5,0.5)

TABLE S12: List of momentum points used for phonon spectrum plots of materials in space group 92 ($P4_12_12$). Coordinates are given in units of the primitive unit cell's reciprocal lattice vectors.

Symbol	Γ	X	M	Z	R	A
Coordinates	(0,0,0)	(0,0.5,0)	(0.5,0.5,0)	(0,0,0.5)	(0,0.5,0.5)	(0.5,0.5,0.5)

TABLE S13: List of momentum points used for phonon spectrum plots of materials in space group 96 ($P4_32_12$). Coordinates are given in units of the primitive unit cell's reciprocal lattice vectors.

Symbol	Γ	X	M	Z	R	A
Coordinates	(0,0,0)	(0,0.5,0)	(0.5,0.5,0)	(0,0,0.5)	(0,0.5,0.5)	(0.5,0.5,0.5)

TABLE S14: List of momentum points used for phonon spectrum plots of materials in space group 97 ($I422$). Coordinates are given in units of the primitive unit cell's reciprocal lattice vectors.

Symbol	P	N	Γ	M_1	M_2	X	M	X_1
Coordinates	(0.25,0.25,0.25)	(0,0.5,0)	(0,0,0)	(0.5,0.5,-0.5)	(-0.5,0.5,0.5)	(0,0,0.5)	(0.5,0.5,0.5)	(0,1,0.5)

TABLE S15: List of momentum points used for phonon spectrum plots of materials in space group 98 ($I4_12_2$). Coordinates are given in units of the primitive unit cell's reciprocal lattice vectors.

Symbol	P	N	Γ	M_1	M_2	X	M	X_1
Coordinates	(0.25,0.25,0.25)	(0,0.5,0)	(0,0,0)	(0.5,0.5,-0.5)	(-0.5,0.5,0.5)	(0,0,0.5)	(0.5,0.5,0.5)	(0,1,0.5)

TABLE S16: List of momentum points used for phonon spectrum plots of materials in space group 100 ($P4bm$). Coordinates are given in units of the primitive unit cell's reciprocal lattice vectors.

Symbol	Γ	X	M	Z	R	A	B	C
Coordinates	(0,0,0)	(0,0.5,0)	(0.5,0.5,0)	(0,0,0.5)	(0,0.5,0.5)	(0.5,0.5,0.5)	(0.25,0.5,0.5)	(0.25,0.5,0)

TABLE S17: List of momentum points used for phonon spectrum plots of materials in space group 107 ($I4mm$). Coordinates are given in units of the primitive unit cell's reciprocal lattice vectors.

Symbol	P	N	Γ	M_1	M_2
Coordinates	(0.25,0.25,0.25)	(0,0.5,0)	(0,0,0)	(0.5,0.5,-0.5)	(-0.5,0.5,0.5)
Symbol	X	M	X_1	B	C
Coordinates	(0,0,0.5)	(0.5,0.5,0.5)	(0,1,0.5)	(0.25,0.5,0.5)	(0.25,0.5,0)

TABLE S18: List of momentum points used for phonon spectrum plots of materials in space group 109 ($I4_1md$). Coordinates are given in units of the primitive unit cell's reciprocal lattice vectors.

Symbol	P	N	Γ	M_1	M_2
Coordinates	(0.25,0.25,0.25)	(0,0.5,0)	(0,0,0)	(0.5,0.5,-0.5)	(-0.5,0.5,0.5)
Symbol	X	M	X_1	B	C
Coordinates	(0,0,0.5)	(0.5,0.5,0.5)	(0,1,0.5)	(0.25,0.5,0.5)	(0.25,0.5,0)

TABLE S19: List of momentum points used for phonon spectrum plots of materials in space group 111 ($P\bar{4}2m$). Coordinates are given in units of the primitive unit cell's reciprocal lattice vectors.

Symbol	Γ	X	M	Z	R	A
Coordinates	(0,0,0)	(0,0.5,0)	(0.5,0.5,0)	(0,0,0.5)	(0,0.5,0.5)	(0.5,0.5,0.5)

TABLE S20: List of momentum points used for phonon spectrum plots of materials in space group 121 ($I\bar{4}2m$). Coordinates are given in units of the primitive unit cell's reciprocal lattice vectors.

Symbol	P	N	Γ	M_1	M_2	X	M	X_1	R
Coordinates	(0.25,0.25,0.25)	(0,0.5,0)	(0,0,0)	(0.5,0.5,-0.5)	(-0.5,0.5,0.5)	(0,0,0.5)	(0.5,0.5,0.5)	(0,1,0.5)	(0,0.5,0.5)

TABLE S21: List of momentum points used for phonon spectrum plots of materials in space group 122 ($I\bar{4}2d$). Coordinates are given in units of the primitive unit cell's reciprocal lattice vectors.

Symbol	P	N	Γ	M_1	M_2	X	M	X_1	R
Coordinates	(0.25,0.25,0.25)	(0,0.5,0)	(0,0,0)	(0.5,0.5,-0.5)	(-0.5,0.5,0.5)	(0,0,0.5)	(0.5,0.5,0.5)	(0,1,0.5)	(0,0.5,0.5)

TABLE S22: List of momentum points used for phonon spectrum plots of materials in space group 145 ($P3_2$). Coordinates are given in units of the primitive unit cell's reciprocal lattice vectors.

Symbol	Γ	M	K	A	L	H
Coordinates	(0,0,0)	(0.5,0,0)	($\frac{1}{3}$, $\frac{1}{3}$, 0)	(0,0,0.5)	(0.5,0,0.5)	($\frac{1}{3}$, $\frac{1}{3}$, 0.5)

TABLE S23: List of momentum points used for phonon spectrum plots of materials in space group 150 ($P321$). Coordinates are given in units of the primitive unit cell's reciprocal lattice vectors.

Symbol	Γ	M	K	A	L	H

Coordinates	(0,0,0)	(0.5,0,0)	$(\frac{1}{3}, \frac{1}{3}, 0)$	(0,0,0.5)	(0.5,0,0.5)	$(\frac{1}{3}, \frac{1}{3}, 0.5)$
--------------------	---------	-----------	---------------------------------	-----------	-------------	-----------------------------------

TABLE S24: List of momentum points used for phonon spectrum plots of materials in space group 152 ($P3_121$). Coordinates are given in units of the primitive unit cell's reciprocal lattice vectors.

Symbol	Γ	M	K	A	L	H
Coordinates	(0,0,0)	(0.5,0,0)	$(\frac{1}{3}, \frac{1}{3}, 0)$	(0,0,0.5)	(0.5,0,0.5)	$(\frac{1}{3}, \frac{1}{3}, 0.5)$

TABLE S25: List of momentum points used for phonon spectrum plots of materials in space group 154 ($P3_221$). Coordinates are given in units of the primitive unit cell's reciprocal lattice vectors.

Symbol	Γ	M	K	A	L	H
Coordinates	(0,0,0)	(0.5,0,0)	$(\frac{1}{3}, \frac{1}{3}, 0)$	(0,0,0.5)	(0.5,0,0.5)	$(\frac{1}{3}, \frac{1}{3}, 0.5)$

TABLE S26: List of momentum points used for phonon spectrum plots of materials in space group 155 ($R32$). Coordinates are given in units of the primitive unit cell's reciprocal lattice vectors.

Symbol	F_1	Γ	L	T_1	T	F_2
Coordinates	(0,0.5,-0.5)	(0,0,0)	(0,0.5,0)	(0.5,0.5,-0.5)	(0.5,0.5,0.5)	(0.5,0,0.5)

TABLE S27: List of momentum points used for phonon spectrum plots of materials in space group 156 ($P3m1$). Coordinates are given in units of the primitive unit cell's reciprocal lattice vectors.

Symbol	Γ	M	K	A	L	H	C
Coordinates	(0,0,0)	(0.5,0,0)	$(\frac{1}{3}, \frac{1}{3}, 0)$	(0,0,0.5)	(0.5,0,0.5)	$(\frac{1}{3}, \frac{1}{3}, 0.5)$	(0.4166667,0.1666667,0.25)

TABLE S28: List of momentum points used for phonon spectrum plots of materials in space group 159 ($P31c$). Coordinates are given in units of the primitive unit cell's reciprocal lattice vectors.

Symbol	Γ	M	K	A	L	H	C
Coordinates	(0,0,0)	(0.5,0,0)	$(\frac{1}{3}, \frac{1}{3}, 0)$	(0,0,0.5)	(0.5,0,0.5)	$(\frac{1}{3}, \frac{1}{3}, 0.5)$	(0.4166667,0.1666667,0.25)

TABLE S29: List of momentum points used for phonon spectrum plots of materials in space group 160 ($R3m$). Coordinates are given in units of the primitive unit cell's reciprocal lattice vectors.

Symbol	F_1	Γ	L	T_1	T	F_2	C
Coordinates	(0,0.5,-0.5)	(0,0,0)	(0,0.5,0)	(0.5,0.5,-0.5)	(0.5,0.5,0.5)	(0.5,0,0.5)	(0.4166667,0.1666667,0.25)

TABLE S30: List of momentum points used for phonon spectrum plots of materials in space group 161 ($R3c$). Coordinates are given in units of the primitive unit cell's reciprocal lattice vectors.

Symbol	F_1	Γ	L	T_1	T	F_2	C
Coordinates	(0,0.5,-0.5)	(0,0,0)	(0,0.5,0)	(0.5,0.5,-0.5)	(0.5,0.5,0.5)	(0.5,0,0.5)	(0.4166667,0.1666667,0.25)

TABLE S31: List of momentum points used for phonon spectrum plots of materials in space group 169 ($P6_1$). Coordinates are given in units of the primitive unit cell's reciprocal lattice vectors.

Symbol	Γ	M	K	A	L	H
Coordinates	(0,0,0)	(0.5,0,0)	$(\frac{1}{3}, \frac{1}{3}, 0)$	(0,0,0.5)	(0.5,0,0.5)	$(\frac{1}{3}, \frac{1}{3}, 0.5)$

TABLE S32: List of momentum points used for phonon spectrum plots of materials in space group 173 ($P6_3$). Coordinates are given in units of the primitive unit cell's reciprocal lattice vectors.

Symbol	Γ	M	K	A	L	H
Coordinates	(0,0,0)	(0.5,0,0)	($\frac{1}{3}$, $\frac{1}{3}$, 0)	(0,0,0.5)	(0.5,0,0.5)	($\frac{1}{3}$, $\frac{1}{3}$, 0.5)

TABLE S33: List of momentum points used for phonon spectrum plots of materials in space group 178 ($P6_{1}22$). Coordinates are given in units of the primitive unit cell's reciprocal lattice vectors.

Symbol	Γ	M	K	A	L	H
Coordinates	(0,0,0)	(0.5,0,0)	($\frac{1}{3}$, $\frac{1}{3}$, 0)	(0,0,0.5)	(0.5,0,0.5)	($\frac{1}{3}$, $\frac{1}{3}$, 0.5)

TABLE S34: List of momentum points used for phonon spectrum plots of materials in space group 180 ($P6_{2}22$). Coordinates are given in units of the primitive unit cell's reciprocal lattice vectors.

Symbol	Γ	M	K	A	L	H
Coordinates	(0,0,0)	(0.5,0,0)	($\frac{1}{3}$, $\frac{1}{3}$, 0)	(0,0,0.5)	(0.5,0,0.5)	($\frac{1}{3}$, $\frac{1}{3}$, 0.5)

TABLE S35: List of momentum points used for phonon spectrum plots of materials in space group 186 ($P6_{3}mc$). Coordinates are given in units of the primitive unit cell's reciprocal lattice vectors.

Symbol	Γ	M	K	A	L	H	B	C
Coordinates	(0,0,0)	(0.5,0,0)	($\frac{1}{3}$, $\frac{1}{3}$, 0)	(0,0,0.5)	(0.5,0,0.5)	($\frac{1}{3}$, $\frac{1}{3}$, 0.5)	(0.41666667, 0.16666667, 0)	(0.41666667, 0.16666667, 0.25)

TABLE S36: List of momentum points used for phonon spectrum plots of materials in space group 189 ($P\bar{6}2m$). Coordinates are given in units of the primitive unit cell's reciprocal lattice vectors.

Symbol	Γ	M	K	A	L	H	B
Coordinates	(0,0,0)	(0.5,0,0)	($\frac{1}{3}$, $\frac{1}{3}$, 0)	(0,0,0.5)	(0.5,0,0.5)	($\frac{1}{3}$, $\frac{1}{3}$, 0.5)	(0.41666667, 0.16666667, 0.25)

TABLE S37: List of momentum points used for phonon spectrum plots of materials in space group 198 ($P2_{1}3$). Coordinates are given in units of the primitive unit cell's reciprocal lattice vectors.

Symbol	Γ	X	M	R
Coordinates	(0,0,0)	(0,0.5,0)	(0.5,0.5,0)	(0.5,0.5,0.5)

TABLE S38: List of momentum points used for phonon spectrum plots of materials in space group 215 ($P\bar{4}3m$). Coordinates are given in units of the primitive unit cell's reciprocal lattice vectors.

Symbol	Γ	X	M	R	Z	A
Coordinates	(0,0,0)	(0,0.5,0)	(0.5,0.5,0)	(0.5,0.5,0.5)	(0.25,0.5,0)	(0.25,0.5,0.2)

TABLE S39: List of momentum points used for phonon spectrum plots of materials in space group 216 ($F\bar{4}3m$). Coordinates are given in units of the primitive unit cell's reciprocal lattice vectors.

Symbol	X	W	L	Γ	X_1	K	U	Z	A
Coordinates	(0.5,0,0.5)	(0.5,0.25,0.75)	(0.5,0.5,0.5)	(0,0,0)	(0.5,0.5,1)	($\frac{3}{8}$, $\frac{3}{8}$, 0.75)	($\frac{1}{8}$, $\frac{1}{8}$, 0.25)	(0.25,0.5,0)	(0.25,0.5,0.2)

TABLE S40: List of momentum points used for phonon spectrum plots of materials in space group 217 ($I\bar{4}3m$). Coordinates are given in units of the primitive unit cell's reciprocal lattice vectors.

Symbol	Γ	H	N	P	Z	A
Coordinates	(0,0,0)	(0.5,0.5,0.5)	(0,0,0.5)	(0.25,0.25,0.25)	(0.25,0.5,0)	(0.25,0.5,0.2)

TABLE S41: List of momentum points used for phonon spectrum plots of materials in space group 218 ($P\bar{4}3n$). Coordinates are given in units of the primitive unit cell's reciprocal lattice vectors.

Symbol	Γ	X	M	R	Z	A
Coordinates	(0,0,0)	(0,0.5,0)	(0.5,0.5,0)	(0.5,0.5,0.5)	(0.25,0.5,0)	(0.25,0.5,0.2)

-
- [1] William Thomson Baron Kelvin, *The molecular tactics of a crystal* (Clarendon Press, 1894).
- [2] James D Watson and Francis HC Crick, “Molecular structure of nucleic acids: a structure for deoxyribose nucleic acid,” *Nature* **171**, 737–738 (1953).
- [3] William S Knowles and Milton J Sabacky, “Catalytic asymmetric hydrogenation employing a soluble, optically active, rhodium complex,” *Chemical Communications (London)* , 1445–1446 (1968).
- [4] L Horner, H Siegel, and H Büthe, “Asymmetric catalytic hydrogenation with an optically active phosphine-rhodium complex in homogeneous solution,” *Angewandte Chemie International Edition in English* **7**, 942–942 (1968).
- [5] K. v. Klitzing, G. Dorda, and M. Pepper, “New method for high-accuracy determination of the fine-structure constant based on quantized hall resistance,” *Phys. Rev. Lett.* **45**, 494–497 (1980).
- [6] Klaus von Klitzing, “The quantized hall effect,” *Rev. Mod. Phys.* **58**, 519–531 (1986).
- [7] Lifa Zhang and Qian Niu, “Angular momentum of phonons and the einstein-de haas effect,” *Physical Review Letters* **112**, 085503 (2014).
- [8] Lifa Zhang and Qian Niu, “Chiral phonons at high-symmetry points in monolayer hexagonal lattices,” *Physical review letters* **115**, 115502 (2015).
- [9] Hanyu Zhu, Jun Yi, Ming-Yang Li, Jun Xiao, Lifa Zhang, Chih-Wen Yang, Robert A Kaindl, Lain-Jong Li, Yuan Wang, and Xiang Zhang, “Observation of chiral phonons,” *Science* **359**, 579–582 (2018).
- [10] Kyosuke Ishito, Huijing Mao, Yusuke Kousaka, Yoshihiko Togawa, Satoshi Iwasaki, Tiantian Zhang, Shuichi Murakami, Jun-ichiro Kishine, and Takuya Satoh, “Truly chiral phonons in α -hgs,” *Nature Physics* **19**, 35–39 (2023).
- [11] Shuai Zhang, Zhiheng Huang, Muchen Du, Tianping Ying, Luojun Du, and Tiantian Zhang, “The chirality of phonons: Definitions, symmetry constraints, and experimental observation,” arXiv preprint arXiv:2503.22794 (2025).
- [12] Tiantian Zhang, Yizhou Liu, Hu Miao, and Shuichi Murakami, “New advances in phonons: From band topology to quasiparticle chirality,” arXiv preprint arXiv:2505.06179 (2025).
- [13] Heda Zhang, N Peshcherenko, Fazhi Yang, TZ Ward, P Raghuvanshi, L Lindsay, Claudia Felser, Y Zhang, J-Q Yan, and H Miao, “Observation of phonon angular momentum,” arXiv preprint arXiv:2409.13462 (2024).
- [14] Hao Chen, Weikang Wu, Jiaojiao Zhu, Zhengning Yang, Weikang Gong, Weibo Gao, Shengyuan A Yang, and Lifa Zhang, “Chiral phonon diode effect in chiral crystals,” *Nano Letters* **22**, 1688–1693 (2022).
- [15] Masato Hamada, Emi Minamitani, Motoaki Hirayama, and Shuichi Murakami, “Phonon angular momentum induced by the temperature gradient,” *Physical review letters* **121**, 175301 (2018).
- [16] Chao-Xing Liu, “Probing nieh-yan anomaly through phonon dynamics in the kramers-weyl semimetals of chiral crystals,” *Phys. Rev. B* **106**, 115102 (2022).
- [17] K-I Uchida, S Takahashi, K Harii, J Ieda, W Koshiba, Kazuya Ando, S Maekawa, and E Saitoh, “Observation of the spin seebeck effect,” *Nature* **455**, 778–781 (2008).
- [18] Hiroto Adachi, Ken-ichi Uchida, Eiji Saitoh, and Sadamichi Maekawa, “Theory of the spin seebeck effect,” *Reports on Progress in Physics* **76**, 036501 (2013).
- [19] Kyunghoon Kim, Eric Vetter, Liang Yan, Cong Yang, Ziqi Wang, Rui Sun, Yu Yang, Andrew H Comstock, Xiao Li, Jun Zhou, *et al.*, “Chiral-phonon-activated spin seebeck effect,” *Nature Materials* **22**, 322–328 (2023).
- [20] Jonas Fransson, “Chiral phonon induced spin polarization,” *Physical Review Research* **5**, L022039 (2023).
- [21] Xiao Li, Jinxin Zhong, Jinluo Cheng, Hao Chen, Huiqian Wang, Jun Liu, Dali Sun, Lifa Zhang, and Jun Zhou, “Chiral phonon activated spin seebeck effect in chiral materials,” *Science China Physics, Mechanics & Astronomy* **67**, 237511 (2024).
- [22] Naoki Nishimura, Takumi Funato, Mamoru Matsuo, and Takeo Kato, “Theory of chiral-phonon-activated spin seebeck effect,” arXiv preprint arXiv:2505.23083 (2025).
- [23] Ron Naaman and David H Waldeck, “Chiral-induced spin selectivity effect,” *The journal of physical chemistry letters* **3**, 2178–2187 (2012).
- [24] Ron Naaman, Yossi Paltiel, and David H Waldeck, “Chiral molecules and the electron spin,” *Nature Reviews Chemistry* **3**, 250–260 (2019).
- [25] Yizhou Liu, Jiewen Xiao, Jahyun Koo, and Binghai Yan, “Chirality-driven topological electronic structure of dna-like materials,” *Nature materials* **20**, 638–644 (2021).
- [26] Ferdinand Evers, Amnon Aharonov, Nir Bar-Gill, Ora Entin-Wohlman, Per Hedegård, Oded Hod, Pavel Jelinek, Grzegorz Kamieniarz, Mikhail Lemeshko, Karen Michaeli, *et al.*, “Theory of chirality induced spin selectivity: Progress and challenges,” *Advanced Materials* **34**, 2106629 (2022).
- [27] C Strohm, GLJA Rikken, and P Wyder, “Phenomenological evidence for the phonon hall effect,” *Physical review letters* **95**, 155901 (2005).
- [28] Yu Kagan and LA Maksimov, “Anomalous hall effect for the phonon heat conductivity in paramagnetic dielectrics,” *Physical review letters* **100**, 145902 (2008).
- [29] G Grissonnanche, S Thériault, A Gourgout, M-E Boulanger, E Lefrançois, A Ataei, F Laliberté, M Dion, J-S

- Zhou, S Pyon, *et al.*, “Chiral phonons in the pseudogap phase of cuprates,” *Nature Physics* **16**, 1108–1111 (2020).
- [30] Guohuan Xiong, Hao Chen, Dengke Ma, and Lifa Zhang, “Effective magnetic fields induced by chiral phonons,” *Physical Review B* **106**, 144302 (2022).
- [31] Yang Long, Jie Ren, and Hong Chen, “Intrinsic spin of elastic waves,” *Proceedings of the National Academy of Sciences* **115**, 9951–9955 (2018).
- [32] Jiaming Luo, Tong Lin, Junjie Zhang, Xiaotong Chen, Elizabeth R Blackert, Rui Xu, Boris I Yakobson, and Hanyu Zhu, “Large effective magnetic fields from chiral phonons in rare-earth halides,” *Science* **382**, 698–702 (2023).
- [33] R. Matthias Geilhufe and Wolfram Hergert, “Electron magnetic moment of transient chiral phonons in ktao_3 ,” *Phys. Rev. B* **107**, L020406 (2023).
- [34] Dominik M. Juraschek, Tomáš Neuman, and Prineha Narang, “Giant effective magnetic fields from optically driven chiral phonons in $4f$ paramagnets,” *Phys. Rev. Res.* **4**, 013129 (2022).
- [35] Andrey Baydin, Felix G. G. Hernandez, Martin Rodriguez-Vega, Anderson K. Okazaki, Fuyang Tay, G. Timothy Noe, Ikufumi Katayama, Jun Takeda, Hiroyuki Nojiri, Paulo H. O. Rappl, Eduardo Abramof, Gregory A. Fiete, and Junichiro Kono, “Magnetic control of soft chiral phonons in pbte ,” *Phys. Rev. Lett.* **128**, 075901 (2022).
- [36] Felix GG Hernandez, Andrey Baydin, Swati Chaudhary, Fuyang Tay, Ikufumi Katayama, Jun Takeda, Hiroyuki Nojiri, Anderson K Okazaki, Paulo HO Rappl, Eduardo Abramof, *et al.*, “Observation of interplay between phonon chirality and electronic band topology,” *Science advances* **9**, eadj4074 (2023).
- [37] Dapeng Yao and Shuichi Murakami, “Theory of spin magnetization driven by chiral phonons,” *Physical Review B* **111**, 134414 (2025).
- [38] Carl P Romao and Dominik M Juraschek, “Phonon-induced geometric chirality,” *ACS nano* **18**, 29550–29557 (2024).
- [39] Kyosuke Ishito, Huiling Mao, Yusuke Kousaka, Yoshihiko Togawa, Satoshi Iwasaki, Tiantian Zhang, Shuichi Murakami, Jun-ichiro Kishine, and Takuya Satoh, “Truly chiral phonons in α -hgs,” *Nature Physics* **19**, 35–39 (2023).
- [40] Hiroki Ueda, Mirian García-Fernández, Stefano Agrestini, Carl P Romao, Jeroen van den Brink, Nicola A Spaldin, Ke-Jin Zhou, and Urs Staub, “Chiral phonons in quartz probed by x-rays,” *Nature* **618**, 946–950 (2023).
- [41] Luojun Du, Jian Tang, Yanchong Zhao, Xiaomei Li, Rong Yang, Xuerong Hu, Xueyin Bai, Xiao Wang, Kenji Watanabe, Takashi Taniguchi, *et al.*, “Lattice dynamics, phonon chirality, and spin-phonon coupling in 2d itinerant ferromagnet fe₃gete₂,” *Advanced Functional Materials* **29**, 1904734 (2019).
- [42] Tiantian Zhang, Zhiheng Huang, Zitian Pan, Luojun Du, Guangyu Zhang, and Shuichi Murakami, “Weyl phonons in chiral crystals,” *Nano Letters* **23**, 7561–7567 (2023).
- [43] Hao Chen, Weikang Wu, Jiaojiao Zhu, Shengyuan A Yang, and Lifa Zhang, “Propagating chiral phonons in three-dimensional materials,” *Nano Letters* **21**, 3060–3065 (2021).
- [44] Sonja R Tauchert, Mikhail Volkov, Dominik Ehberger, D Kazenwadel, Martin Evers, Hannah Lange, Andreas Donges, Alexander Book, W Kreuzpaintner, U Nowak, *et al.*, “Polarized phonons carry angular momentum in ultrafast demagnetization,” *Nature* **602**, 73–77 (2022).
- [45] Kazuki Ohe, Hiroaki Shishido, Masaki Kato, Shoyo Utsumi, Hiroyasu Matsuura, and Yoshihiko Togawa, “Chirality-induced selectivity of phonon angular momenta in chiral quartz crystals,” *Phys. Rev. Lett.* **132**, 056302 (2024).
- [46] Qianqian Wang, Si Li, Jiaojiao Zhu, Hao Chen, Weikang Wu, Weibo Gao, Lifa Zhang, and Shengyuan A. Yang, “Chiral phonons in lattices with C_4 symmetry,” *Phys. Rev. B* **105**, 104301 (2022).
- [47] Mengqian Che, Jinxuan Liang, Yunpeng Cui, Hao Li, Bingru Lu, Wenbo Sang, Xiang Li, Xuebin Dong, Shuai Zhang, Tao Sun, *et al.*, “Magnetic order induced truly chiral phonons in a ferromagnetic weyl semimetal,” arXiv preprint arXiv:2411.03754 (2024).
- [48] Sinisa Coh, “Classification of materials with phonon angular momentum and microscopic origin of angular momentum,” *Phys. Rev. B* **108**, 134307 (2023).
- [49] G. Kresse and J. Furthmüller, “Efficiency of ab-initio total energy calculations for metals and semiconductors using a plane-wave basis set,” *Computational Materials Science* **6**, 15 – 50 (1996).
- [50] A Togo and I Tanaka, “First principles phonon calculations in materials science,” *Scr. Mater.* **108**, 1–5 (2015).
- [51] Yuanfeng Xu, MG Vergniory, Da-Shuai Ma, Juan L Mañes, Zhi-Da Song, B Andrei Bernevig, Nicolas Regnault, and Luis Elcoro, “Catalog of topological phonon materials,” *Science* **384**, eadf8458 (2024).
- [52] MG Vergniory, L Elcoro, Claudia Felser, Nicolas Regnault, B Andrei Bernevig, and Zhijun Wang, “A complete catalogue of high-quality topological materials,” *Nature* **566**, 480–485 (2019).
- [53] Maia G Vergniory, Benjamin J Wieder, Luis Elcoro, Stuart SP Parkin, Claudia Felser, B Andrei Bernevig, and Nicolas Regnault, “All topological bands of all nonmagnetic stoichiometric materials,” *Science* **376**, eabg9094 (2022).
- [54] Nicolas Regnault, Yuanfeng Xu, Ming-Rui Li, Da-Shuai Ma, Milena Jovanovic, Ali Yazdani, Stuart SP Parkin, Claudia Felser, Leslie M Schoop, N Phuan Ong, *et al.*, “Catalogue of flat-band stoichiometric materials,” *Nature* **603**, 824–828 (2022).

- [55] Tiantian Zhang and Shuichi Murakami, “Chiral phonons and pseudoangular momentum in nonsymmorphic systems,” *Phys. Rev. Res.* **4**, L012024 (2022).
- [56] Stefano Baroni, Stefano de Gironcoli, Andrea Dal Corso, and Paolo Giannozzi, “Phonons and related crystal properties from density-functional perturbation theory,” *Rev. Mod. Phys.* **73**, 515–562 (2001).
- [57] Mengqian Che, Jinxuan Liang, Yunpeng Cui, Hao Li, Bingru Lu, Wenbo Sang, Xiang Li, Xuebin Dong, Le Zhao, Shuai Zhang, Tao Sun, Wanjun Jiang, Enke Liu, Feng Jin, Tiantian Zhang, and Luyi Yang, “Magnetic order induced chiral phonons in a ferromagnetic weyl semimetal,” *Phys. Rev. Lett.* **134**, 196906 (2025).
- [58] R. Yang, Y.-Y. Zhu, M. Steigleider, Y.-C. Liu, C.-C. Liu, X.-G. Qiu, Tiantian Zhang, and M. Dressel, “Inherent circular dichroism of phonons in magnetic weyl semimetal $\text{Co}_3\text{Sn}_2\text{S}_2$,” *Phys. Rev. Lett.* **134**, 196905 (2025).
- [59] Markus Weißenhofer, Philipp Rieger, MS Mrudul, Luca Mikadze, Ulrich Nowak, and Peter M Oppeneer, “Truly chiral phonons arising from chirality-selective magnon-phonon coupling,” arXiv preprint arXiv:2411.03879 (2024).
- [60] P. Hohenberg and W. Kohn, “Inhomogeneous electron gas,” *Phys. Rev.* **136**, B864–B871 (1964).
- [61] W. Kohn and L. J. Sham, “Self-consistent equations including exchange and correlation effects,” *Phys. Rev.* **140**, A1133–A1138 (1965).
- [62] G. Kresse and J. Hafner, “*Ab initio* molecular dynamics for open-shell transition metals,” *Phys. Rev. B* **48**, 13115–13118 (1993).
- [63] G. Kresse and D. Joubert, “From ultrasoft pseudopotentials to the projector augmented-wave method,” *Phys. Rev. B* **59**, 1758–1775 (1999).
- [64] John P. Perdew, Kieron Burke, and Matthias Ernzerhof, “Generalized gradient approximation made simple,” *Phys. Rev. Lett.* **77**, 3865–3868 (1996).
- [65] Atsushi Togo, Laurent Chaput, Terumasa Tadano, and Isao Tanaka, “Implementation strategies in phonopy and phono3py,” *J. Phys. Condens. Matter* **35**, 353001 (2023).
- [66] Atsushi Togo, “First-principles phonon calculations with phonopy and phono3py,” *J. Phys. Soc. Jpn.* **92**, 012001 (2023).
- [67] Xavier Gonze and Changyol Lee, “Dynamical matrices, born effective charges, dielectric permittivity tensors, and interatomic force constants from density-functional perturbation theory,” *Physical Review B* **55**, 10355 (1997).
- [68] Yuedong Wang, JJ Wang, WY Wang, ZG Mei, SL Shang, LQ Chen, and ZK Liu, “A mixed-space approach to first-principles calculations of phonon frequencies for polar materials,” *Journal of Physics: Condensed Matter* **22**, 202201 (2010).